

# Eurosoil 2021: Sustainable management of soil functions as a basis to avoid, halt, and reverse land degradation

**Edited by**

Jörg Luster, Thomas Keller, Miriam Muñoz-Rojas, Lucy Crockford and Ute Wollschläger

**Published in**

Frontiers in Environmental Science



## FRONTIERS EBOOK COPYRIGHT STATEMENT

The copyright in the text of individual articles in this ebook is the property of their respective authors or their respective institutions or funders. The copyright in graphics and images within each article may be subject to copyright of other parties. In both cases this is subject to a license granted to Frontiers.

The compilation of articles constituting this ebook is the property of Frontiers.

Each article within this ebook, and the ebook itself, are published under the most recent version of the Creative Commons CC-BY licence. The version current at the date of publication of this ebook is CC-BY 4.0. If the CC-BY licence is updated, the licence granted by Frontiers is automatically updated to the new version.

When exercising any right under the CC-BY licence, Frontiers must be attributed as the original publisher of the article or ebook, as applicable.

Authors have the responsibility of ensuring that any graphics or other materials which are the property of others may be included in the CC-BY licence, but this should be checked before relying on the CC-BY licence to reproduce those materials. Any copyright notices relating to those materials must be complied with.

Copyright and source acknowledgement notices may not be removed and must be displayed in any copy, derivative work or partial copy which includes the elements in question.

All copyright, and all rights therein, are protected by national and international copyright laws. The above represents a summary only. For further information please read Frontiers' Conditions for Website Use and Copyright Statement, and the applicable CC-BY licence.

ISSN 1664-8714  
ISBN 978-2-83251-261-6  
DOI 10.3389/978-2-83251-261-6

## About Frontiers

Frontiers is more than just an open access publisher of scholarly articles: it is a pioneering approach to the world of academia, radically improving the way scholarly research is managed. The grand vision of Frontiers is a world where all people have an equal opportunity to seek, share and generate knowledge. Frontiers provides immediate and permanent online open access to all its publications, but this alone is not enough to realize our grand goals.

## Frontiers journal series

The Frontiers journal series is a multi-tier and interdisciplinary set of open-access, online journals, promising a paradigm shift from the current review, selection and dissemination processes in academic publishing. All Frontiers journals are driven by researchers for researchers; therefore, they constitute a service to the scholarly community. At the same time, the *Frontiers journal series* operates on a revolutionary invention, the tiered publishing system, initially addressing specific communities of scholars, and gradually climbing up to broader public understanding, thus serving the interests of the lay society, too.

## Dedication to quality

Each Frontiers article is a landmark of the highest quality, thanks to genuinely collaborative interactions between authors and review editors, who include some of the world's best academicians. Research must be certified by peers before entering a stream of knowledge that may eventually reach the public - and shape society; therefore, Frontiers only applies the most rigorous and unbiased reviews. Frontiers revolutionizes research publishing by freely delivering the most outstanding research, evaluated with no bias from both the academic and social point of view. By applying the most advanced information technologies, Frontiers is catapulting scholarly publishing into a new generation.

## What are Frontiers Research Topics?

Frontiers Research Topics are very popular trademarks of the *Frontiers journals series*: they are collections of at least ten articles, all centered on a particular subject. With their unique mix of varied contributions from Original Research to Review Articles, Frontiers Research Topics unify the most influential researchers, the latest key findings and historical advances in a hot research area.

Find out more on how to host your own Frontiers Research Topic or contribute to one as an author by contacting the Frontiers editorial office: [frontiersin.org/about/contact](https://frontiersin.org/about/contact)

# Eurosoil 2021: Sustainable management of soil functions as a basis to avoid, halt, and reverse land degradation

## Topic editors

Jörg Luster — Swiss Federal Institute for Forest, Snow and Landscape Research (WSL), Switzerland

Thomas Keller — Swedish University of Agricultural Sciences, Sweden

Miriam Muñoz-Rojas — University of New South Wales, Australia

Lucy Crockford — Harper Adams University, United Kingdom

Ute Wollschläger — Helmholtz Centre for Environmental Research, Helmholtz Association of German Research Centres (HZ), Germany

## Citation

Luster, J., Keller, T., Muñoz-Rojas, M., Crockford, L., Wollschläger, U., eds. (2023). *Eurosoil 2021: Sustainable management of soil functions as a basis to avoid, halt, and reverse land degradation*. Lausanne: Frontiers Media SA.  
doi: 10.3389/978-2-83251-261-6

# Table of contents

- 05 **Editorial: Eurosoil 2021: Sustainable management of soil functions as a basis to avoid, halt, and reverse land degradation**  
Jörg Luster, Lucy Crockford, Thomas Keller, Miriam Muñoz-Rojas and Ute Wollschläger
- 08 **Rewetting and Drainage of Nutrient-Poor Peatlands Indicated by Specific Bacterial Membrane Fatty Acids and a Repeated Sampling of Stable Isotopes ( $\delta^{15}\text{N}$ ,  $\delta^{13}\text{C}$ )**  
Miriam Groß-Schmolders, Kristy Klein, Axel Birkholz, Jens Leifeld and Christine Alewell
- 22 **Soil Fertility Changes With Climate and Island Age in Galápagos: New Baseline Data for Sustainable Agricultural Management**  
Matthias Strahlhofer, Martin H. Gerzabek, Nicola Rampazzo, Paulina M. Couenberg, Evelyn Vera, Xavier Salazar Valenzuela and Franz Zehetner
- 38 **Microbial Diversity of Reconstituted, Degraded, and Agricultural Soils Assessed by 16S rDNA Multi-Amplicon Sequencing**  
Laura Maretto, Saptarathi Deb, Samathmika Ravi, Claudia Chiodi, Paolo Manfredi, Andrea Squartini, Giuseppe Concheri, Giancarlo Renella and Piergiorgio Stevanato
- 49 **Soil Surface Micro-Topography by Structure-from-Motion Photogrammetry for Monitoring Density and Erosion Dynamics**  
Annelie Ehrhardt, Detlef Deumlich and Horst H. Gerke
- 63 **Mechanical Soil Database—Part I: Impact of Bulk Density and Organic Matter on Precompression Stress and Consequences for Saturated Hydraulic Conductivity**  
Richard Schroeder, Heiner Fleige, Carsten Hoffmann, Hans Joerg Vogel and Rainer Horn
- 78 **Soil Use Legacy as Driving Factor for Soil Erosion under Conservation Agriculture**  
Kathrin Grahmann, Valentina Rubio, Mario Perez-Bidegain and Juan Andrés Quincke
- 93 **Spatio-Temporal High-Resolution Subsoil Compaction Risk Assessment for a 5-Years Crop Rotation at Regional Scale**  
Michael Kuhwald, Katja Kuhwald and Rainer Duttmann
- 108 **Soil Health: New Opportunities to Innovate in Crop Protection Research and Development**  
L. W. Atwood, K. A. Racette, M. Diggelmann, C. A. Masala, S. Maund, R. Oliver, C. Screpanti, M. Wironen and S. A. Wood

- 117 **On-Farm Relationships Between Agricultural Practices and Annual Changes in Organic Carbon Content at a Regional Scale**  
Xavier Dupla, Téo Lemaître, Stéphanie Grand, Karine Gondret, Raphaël Charles, Eric Verrecchia and Pascal Boivin
- 130 **Comparing Four Indexing Approaches to Define Soil Quality in an Intensively Cropped Region of Northern India**  
Narendra Kumar Lenka, Bharat Prakash Meena, Rattan Lal, Abhishek Khandagle, Sangeeta Lenka and Abhay Omprakash Shirale
- 140 **Annual CO<sub>2</sub> Budget Estimation From Chamber-Based Flux Measurements on Intensively Drained Peat Meadows: Effect of Gap-Filling Strategies**  
Weier Liu, Christian Fritz, Stefan T. J. Weideveld, Ralf C. H. Aben, Merit van den Berg and Mandy Velthuis
- 154 **Soil Structural Quality and Relationships With Root Properties in Single and Integrated Farming Systems**  
Karina Maria Vieira Cavalieri-Polizeli, Feliciano Canequetela Marcolino, Cássio Antonio Tormena, Thomas Keller and Anibal de Moraes
- 164 **Achieving cleaner water for UN sustainable development goal 6 with natural processes: Challenges and the future**  
Lucy Crockford



## OPEN ACCESS

## EDITED AND REVIEWED BY

Yuncong Li,  
University of Florida, United States

## \*CORRESPONDENCE

Jörg Luster,  
joerg.luster@wsl.ch

## SPECIALTY SECTION

This article was submitted to Soil Processes, a section of the journal Frontiers in Environmental Science

RECEIVED 08 November 2022

ACCEPTED 10 November 2022

PUBLISHED 28 November 2022

## CITATION

Luster J, Crockford L, Keller T, Muñoz-Rojas M and Wollschläger U (2022), Editorial: Eurosoil 2021: Sustainable management of soil functions as a basis to avoid, halt, and reverse land degradation. *Front. Environ. Sci.* 10:1093226. doi: 10.3389/fenvs.2022.1093226

## COPYRIGHT

© 2022 Luster, Crockford, Keller, Muñoz-Rojas and Wollschläger. This is an open-access article distributed under the terms of the [Creative Commons Attribution License \(CC BY\)](#). The use, distribution or reproduction in other forums is permitted, provided the original author(s) and the copyright owner(s) are credited and that the original publication in this journal is cited, in accordance with accepted academic practice. No use, distribution or reproduction is permitted which does not comply with these terms.

# Editorial: Eurosoil 2021: Sustainable management of soil functions as a basis to avoid, halt, and reverse land degradation

Jörg Luster<sup>1\*</sup>, Lucy Crockford<sup>2</sup>, Thomas Keller<sup>3,4</sup>,  
Miriam Muñoz-Rojas<sup>5,6</sup> and Ute Wollschläger<sup>7</sup>

<sup>1</sup>Swiss Federal Institute for Forest, Snow and Landscape Research (WSL), Birmensdorf, Switzerland,

<sup>2</sup>Agriculture and Environment, Harper Adams University, Newport, United Kingdom, <sup>3</sup>Soil and Environment, Swedish University of Agricultural Sciences, Uppsala, Sweden, <sup>4</sup>Agroscope, Zürich, Switzerland, <sup>5</sup>Departamento de Biología Vegetal y Ecología, Facultad de Biología, Universidad de Sevilla, Sevilla, Spain, <sup>6</sup>Centre for Ecosystem Science, School of Biological, Earth and Environmental Sciences, University of New South Wales, Kensington, NSW, Australia, <sup>7</sup>UFZ-Helmholtz Centre for Environmental Research, Halle (Saale), Germany

## KEYWORDS

sustainable development goals, soil functions, land degradation, restoration, sustainable land use management, integrated water-resources management

## Editorial on the Research Topic

**Eurosoil 2021: Sustainable management of soil functions as a basis to avoid, halt, and reverse land degradation**

## Introduction

This Research Topic (RT) is related to the Eurosoil 2021 conference, focusing on the contributions of soil science to reach the targets of the UN Sustainable Development Goals SDG 6 (Clean Water and Sanitation) and SDG 15 (Life on Land). The overall aim of SDG 15 is to sustainably use and manage terrestrial ecosystems and to halt and reverse land degradation. The particular role of forests, wetlands, and mountains as water-related ecosystems makes their protection and restoration also a target of SDG 6, with the overall aim of improving the quality of drinking water resources through integrated water-resources management.

In this RT, we want to highlight the role of soil functions to achieve these targets. Soil functions (SF) are related to SDGs *via* their contributions to respective ecosystem services (ES, [Keesstra et al., 2016](#)). Soils *per se* are multifunctional and contribute to various ES. However, this multifunctionality is threatened by two main factors, leading to degradation. Firstly, the optimization and exploitation of soils for productivity compromises other SF such as water filtration, nutrient balance, C pool regulation and habitat provision ([Kopittke et al., 2021](#)). Secondly the changing climate, in

particular rising temperatures and more frequent extreme events (droughts, heavy rainfalls), affects SF directly and indirectly (Hamidov et al., 2018).

The understanding of SF and how they can be improved and maintained sustainably, how they are affected by and can be made resilient against disturbances, and how they can be restored if impaired, is key to locally adapted land-use management (Hamidov et al., 2018), e.g., for use in conservation and integrated agricultural systems (Stavi et al., 2016), or for successful nature-based catchment restoration (Keesstra et al., 2018). The quantification of SF relies on sound relations with measurable state variables and properties (e.g., Greiner et al., 2017; Vogel et al., 2019), however many of these relationships are not well established yet (Lorenz et al., 2019). The overall capacity of soils to fulfil their functions and thus to contribute to ES can be summarized in the term soil quality or soil health (e.g., Bünemann et al., 2018; Bonfante et al., 2020; Lehmann et al., 2020).

In this context, the contributions to this RT deal with various issues in quantitatively assessing SF on a local basis. They can be grouped into 1) methodological improvements of measurements and monitoring, 2) testing indicators and indices for assessment of soil degradation and restoration success, and 3) policy frameworks and case studies related to land management and soil health.

## Methodological improvements of measurements and monitoring

High-resolution monitoring of erosion dynamics, a prerequisite for establishing local soil-loss risk assessment, is difficult due to the lack of easy-to-use methods. Ehrhardt et al. successfully tested a method for the mm-scale mapping and monitoring of soil micro-topography using widely available cameras. Peatland degradation potentially contributes significantly to global warming. Carbon budgets are often based on point measurements of CO<sub>2</sub> fluxes using the closed-chamber method, and exhibit large uncertainties due to the need of gap-filling. Comparing various gap-filling techniques, Liu et al. developed a framework that can help to find the most suitable technique for a given case.

## Indicators and indices

Evaluating the degree of peatland degradation, efforts to mitigate this process, or the success of restoration, relies on suitable indicators. Comparing several undrained, drained and rewetted sites in Northern Europe, Groß-Schmolders et al. conclude that the isotopic signature of the organic matter reflects well the microbial conditions that are

characteristic for peatlands with different hydrology. Maretto et al. used microbial diversity as indicator to evaluate the success of restoring a highly degraded soil in a landfill. Soil quality indices (SQI) are widely used to evaluate locally adapted management options. Lenka et al. compared four quantitative approaches to calculate SQIs and showed that SQIs can be useful also on the scale of a larger region. One difficulty when assessing the compaction risk of soils is the large spatio-temporal dynamics of soil properties and states. Kuhwald et al. modeled the compaction risk for a 2000 km<sup>2</sup> area at high temporal and spatial resolution and were able to identify hotspots of high soil compaction risk.

## Sustainable management

Adaptation of land-use management to local soil conditions requires data on key soil properties and information on legacy-effects related to soil development and previous land-use. Compiling a large data set of mechanical and physical soil properties, Schroeder et al. revealed relations between soil texture, precompression stress and saturated hydraulic conductivity. Their findings suggest that silty soils are highly sensitive to mechanical stress. In an on-farm study including 120 farm fields, Dupla et al. measured the impact of soil management on changes in soil organic carbon contents. Their results revealed that carbon sequestration is a function of tillage intensity and the soil carbon to clay ratio. On the Galápagos islands that have been influenced by agricultural activities for only a relatively short period, Strahlhofer et al. obtained baseline data on soil fertility for soils covering wide overlapping soil age and precipitation gradients. Historical land-use is another baseline information to be considered when assessing SF. Grahmann et al. investigated how varying intensity of historic agricultural management interacts with current conservation practices. Previously intensively managed soils were clearly more susceptible to erosion than more extensively managed ones. It is often hypothesized that integrated farming systems, e.g., combining cropping and forestry, improve SF compared to single farming systems. In an experimental study, Cavalieri-Polizeli et al. could not support this hypothesis for a subtropical region but found strong positive feedbacks between soil structure, soil organic carbon content and root growth. Although substances used in crop protection are well known to potentially have adverse effects on SF, there has been little integration of pest and disease management into concepts of soil health-based agricultural management. In a policy and practice review, Atwood et al. propose a framework for aligning crop protection innovation with soil health goals.

## Conclusions

Taken together, the contributions to this RT emphasize an awareness within the soil science and related communities to translate systemic soil knowledge into information useful for practitioners and decision-makers. They also demonstrate that there are still many open issues with respect to linking soil properties and states to SF. A key question asked when setting up the program of the Eurosoil 2021 conference was whether application of relevant soil knowledge could make a significant contribution to reach the targets of the related SDGs. Considering the time constraint to do so by 2030, this application cannot only rely on studies that address soil property/state—function relationships. There is a large amount of data provided by the plethora of local-scale case studies that should be made accessible in open access data bases to be exploited in meta-analyses, statistical evaluations and systemic modelling. With such we should finally be able to quantitatively assess the site-specific impact of soil management measures on soil functions, ecosystem services and SDGs. Another issue is an adequate valuation of SF as prerequisite for funding and implementing sustainable land management options. This is emphasized in a perspectives paper by Crockford promoting integrated soil and water management to reduce the loss of soil, water, pesticides and nutrients from

agricultural fields, and clean polluted water based on natural processes (e.g., riparian zones, artificial wetlands).

## Author contributions

JL drafted a first version of this editorial. All authors contributed to the final version.

## Conflict of interest

The authors declare that the research was conducted in the absence of any commercial or financial relationships that could be construed as a potential conflict of interest.

## Publisher's note

All claims expressed in this article are solely those of the authors and do not necessarily represent those of their affiliated organizations, or those of the publisher, the editors and the reviewers. Any product that may be evaluated in this article, or claim that may be made by its manufacturer, is not guaranteed or endorsed by the publisher.

## References

- Bonfante, A., Basile, A., and Bouma, J. (2020). Targeting the soil quality and soil health concepts when aiming for the united nations sustainable development goals and the EU green deal. *Soil* 6, 453–466. doi:10.5194/soil-6-453-2020
- Bünemann, E. K., Bongiorno, G., Bai, Z., Creamer, R. E., Deyn, G., De Goede, R., et al. (2018). Soil quality – a critical review. *Soil Biol. Biochem.* 120, 105–125. doi:10.1016/j.soilbio.2018.01.030
- Greiner, L., Keller, A., Grêt-Regamey, A., and Papritz, A. (2017). Soil function assessment: Review of methods for quantifying the contributions of soils to ecosystem services. *Land Use Policy* 69, 224–237. doi:10.1016/j.landusepol.2017.06.025
- Hamidov, A., Helming, K., Bellocchi, G., Bojar, W., Dalgaard, T., Bahadur Ghaley, B., et al. (2018). Impacts of climate change adaptation options on soil functions: A review of European case-studies. *Land Degrad. Dev.* 29, 2378–2389. doi:10.1002/ldr.3006
- Keesstra, S. D., Bouma, J., Wallinga, J., Tittonell, P., Smith, P., Cerdà, A., et al. (2016). The significance of soils and soil science towards realization of the United Nations Sustainable Development Goals. *Soil* 2, 111–128. doi:10.5194/soil-2-111-2016
- Keesstra, S., Nunes, J., Novara, A., Finger, D., Avelar, D., Kalanteri, Z., et al. (2018). The superior effect of nature based solutions in land management for enhancing ecosystem services. *Sci. Total Environ.* 610–611, 997–1009. doi:10.1016/j.scitotenv.2017.08.077
- Kopittke, P. M., Berhe, A. A., Carrillo, Y., Cavagnaro, T. R., Chen, D., Chen, Q. L., et al. (2021). Ensuring planetary survival: The centrality of organic carbon in balancing the multifunctional nature of soils. *Crit. Rev. Environ. Sci. Technol.* 52, 4308–4324. doi:10.1080/10643389.2021.2024484
- Lehmann, J., Bossio, D. A., Kögel-Knabner, I., and Rillig, M. (2020). The concept and future prospects of soil health. *Nat. Rev. Earth Environ.* 1, 544–553. doi:10.1038/s43017-020-0080-8
- Lorenz, K., Lal, R., and Ehlers, K. (2019). Soil organic carbon stock as an indicator for monitoring land and soil degradation in relation to United Nations' Sustainable Development Goals. *Land Degrad. Dev.* 30, 824–838. doi:10.1002/ldr.3270
- Stavi, I., Bel, G., and Zaady, E. (2016). Soil functions and ecosystem services in conventional, conservation, and integrated agricultural systems. A review. *Agron. Sustain. Dev.* 36, 32. doi:10.1007/s13593-016-0368-8
- Vogel, H. J., Eberhardt, E., Franko, U., Lang, B., Liess, M., Weller, U., et al. (2019). Scientific data management in the age of big data: An approach supporting a resilience index development effort. *Front. Environ. Sci.* 7, 1–13. doi:10.3389/fenvs.2019.00072



# Rewetting and Drainage of Nutrient-Poor Peatlands Indicated by Specific Bacterial Membrane Fatty Acids and a Repeated Sampling of Stable Isotopes ( $\delta^{15}\text{N}$ , $\delta^{13}\text{C}$ )

Miriam Groß-Schmölbers<sup>1\*</sup>, Kristy Klein<sup>2</sup>, Axel Birkholz<sup>1</sup>, Jens Leifeld<sup>2</sup> and Christine Alewell<sup>1</sup>

<sup>1</sup>Environmental Geosciences, University of Basel, Basel, Switzerland, <sup>2</sup>Agroscope, Zürich, Switzerland

## OPEN ACCESS

### Edited by:

Miriam Muñoz-Rojas,  
University of New South Wales,  
Australia

### Reviewed by:

Jeffrey Chanton,  
Florida State University, United States  
Yansheng Li,  
Northeast Institute of Geography and  
Agroecology (CAS), China

### \*Correspondence:

Miriam Groß-Schmölbers  
miriam.gross-schmoelders@  
unibas.ch

### Specialty section:

This article was submitted to  
Soil Processes,  
a section of the journal  
Frontiers in Environmental Science

**Received:** 24 June 2021

**Accepted:** 19 August 2021

**Published:** 01 September 2021

### Citation:

Groß-Schmölbers M, Klein K,  
Birkholz A, Leifeld J and Alewell C  
(2021) Rewetting and Drainage of  
Nutrient-Poor Peatlands Indicated by  
Specific Bacterial Membrane Fatty  
Acids and a Repeated Sampling of  
Stable Isotopes ( $\delta^{15}\text{N}$ ,  $\delta^{13}\text{C}$ ).  
Front. Environ. Sci. 9:730106.  
doi: 10.3389/fenvs.2021.730106

Peatland degradation impairs soil functions such as carbon storage and the existence of biodiversity hotspots. Therefore, and in view of the ongoing climate change, an efficient method of evaluating peatland hydrology and the success of restoration efforts is needed. To understand the role of microbial groups in biogeochemical cycling, gaseous loss and isotopic fractionation that lead to specific isotopic depth patterns ( $\delta^{13}\text{C}$ ,  $\delta^{15}\text{N}$ ), we integrated previously published stable isotope data with a membrane fatty acid (mFA) analysis related to various microbial groups that are known to be common in peatlands. We performed two sampling campaigns to verify the observed stable isotope depth trends in nutrient-poor peatlands in Northern Europe. Cores were taken from adjacent drained (or rewetted) and undrained sites. Fungal-derived mFA abundance was highest in the uppermost part of the drained layer. We found increasing bacterial-derived mFA concentrations with depth peaking in the middle of the drained layers, which correlates with a  $\delta^{15}\text{N}$  peak of bulk material. The results support our hypothesis that changing peatland hydrology induce a shift in microbial community and metabolism processes and is therefore also imprinted in stable isotope values. Under waterlogged conditions overall levels of microbial-derived mFAs were generally low. Drained layers showed simultaneous changes in microbial abundance and composition and depth trends in stable isotope bulk values. Bacteria, particularly acidobacteria, can be expected to dominate increased denitrification with low oxygen saturation accompanied by increased  $\delta^{15}\text{N}$  bulk values in the remaining substrate. Interestingly, cores from recent rewetted peatlands show no depth trend of  $\delta^{15}\text{N}$  in the layers grown under rewetting conditions; this is congruent with relatively low concentrations of microbial-derived mFAs. Hence, we conclude that stable isotopes, especially  $\delta^{15}\text{N}$  values, reflect changing microbial metabolic processes, which differ between drained and undrained - and especially also for recent rewetted-peatlands. As today stable isotope measurements are routine measurements, these findings enable us to get cost- and time efficient reliable information of drainage and restoration success.

**Keywords:** peatland degradation, stable isotopes, membrane fatty acids, soil microbiology, biochemistry, element cycling

## INTRODUCTION

A unique biodiversity, slow rates of decomposition and the storage of significant quantities of carbon characterize wetland soils; this is especially true for nutrient-poor peatlands (Moore and Basiliko, 2006). The protection of biodiversity and successful peatland restoration could save 1.91 (0.31–3.38) gigatons (Gt) of CO<sub>2</sub>-equivalent greenhouse gas emissions (Leifeld and Menichetti, 2018). Furthermore, 6% of the greenhouse effect is contributed by N<sub>2</sub>O (Schulze et al., 2009), which is also released by degraded peatlands due to impaired soil functioning (Palmer and Horn, 2015). For other ecosystems, microbial communities and their major role in biochemical cycling of carbon and nitrogen in soil are well documented, but little is known of the microbial community and its function in peatlands (Elliott et al., 2015). In particular, information about microbial community structures in different layers and their influence on biochemical processes under rewetting conditions is widely unknown (Elliott et al., 2015). Thus, more reliable information about peatland degradation and restoration success is needed.

Peat soil can be divided into three layers. In the uppermost part, the acrotelm, most biological metabolism and nutrient cycling takes place (Asada et al., 2005; Artz, 2013). In the lower layer, the anaerobic, water-saturated catotelm, microbial metabolism is suppressed due to the lack of oxygen (Asada et al., 2005; Artz, 2013; Lin et al., 2014). In between, the mesotelm is characterized by a fluctuating water table and facultative anaerobic conditions, which therefore leads to shifting levels of microbial abundance and activity (Asada et al., 2005; Artz, 2013; Lin et al., 2014). Drainage of peatlands expands the mesotelm, wherein formerly preserved organic substrates can be decomposed (Zedler and Kercher, 2005). If rewetting occurs, the former mesotelm will become anaerobic again, and aerobic microbial activity will be inhibited (Asada et al., 2005; Andersen et al., 2010).

Whereas microbial metabolism of carbon is discussed in several papers (see review of Blodau (2002)), nitrogen cycling in peatlands is less well studied. Nitrogen fixation has been reported to only occur in surface layers of peat, (Lin et al., 2014). However, the N<sub>2</sub>O producing microbial mediated nitrification and denitrification of organic matter as well as other chemical processes occur also in deeper layers (Bremner, 1997; Palmer and Horn, 2015). For peatlands, Palmer et al. (2010) report denitrification of organic matter as the main N<sub>2</sub>O source. Denitrification causes a reduction of nitrate and nitrite by converting them to nitric oxide (NO) and N<sub>2</sub>O and, ultimately, to dinitrogen (N<sub>2</sub>; Novák et al., 1999). Especially for the deep, anaerobic layer, Lin et al. (2014) reported extremely low values for denitrification and other N-cycling processes and, therefore, a conservation of the substrate.

Stable isotopes of carbon and nitrogen are known indicators of peatland hydrology (Alewell et al., 2011; Krüger et al., 2016; Groß-Schmolders et al., 2020; Kohl et al., 2015). For  $\delta^{13}\text{C}$ , Alewell et al. (2011), Krüger et al. (2016), Novak et al. (1999), Hobbie et al. (2017) and Biester et al. (2014) report an enrichment of  $^{13}\text{C}$  with depth due to an increasing degree of organic matter decomposition. Substrates have a natural and specific range of

$^{13}\text{C}$  values (Lerch et al., 2011). As lignin, cellulose and lipids are known to be depleted in  $^{13}\text{C}$ , glucose, amino acids, pectin and hemicellulose are enriched in  $^{13}\text{C}$  (Lerch et al., 2011). In undrained wetlands, the combination of these substrates is mostly preserved due to the waterlogged conditions. If drainage takes place, the original bulk soil  $\delta^{13}\text{C}$  value is changed by degradation and microbial metabolism processes. Kohl et al. (2015) state that an increasing  $\delta^{13}\text{C}$  depth trend is a consequence of a switch in dominant microbial decomposition, which has stronger effects than the residual enrichment of recalcitrant compounds such as lignin. Kohl et al. (2015) stated out, that fungi are main decomposer in the uppermost soil horizons and bacteria are more prominent in deeper horizons. With this switch of dominant microbial groups, also the decomposed material switches and therefore the  $^{13}\text{C}$  bulk values change.

Additionally, a positive correlation between increased microbial metabolism and  $\delta^{15}\text{N}$  was previously presented (Groß-Schmolders et al., 2020). Fractionation of stable isotopes during microbial metabolism of nitrate and ammonium occurs, since most organisms prefer the lighter and more frequently occurring  $^{14}\text{N}$  (Kohzu et al., 2003; Robinson et al., 1998). As a result, plants in particular incorporate and translocate the lighter  $^{14}\text{N}$  upwards to stem and foliar, which leads to an enrichment of heavier  $^{15}\text{N}$  in the remaining bulk material (Högberg et al., 1996). Additionally, the mycorrhizal uptake of lighter  $^{14}\text{N}$  into plants increases the  $\delta^{15}\text{N}$  values of bulk material (Hobbie and Högberg, 2012). Furthermore, with ongoing microbial metabolic processes in peat, the  $\delta^{15}\text{N}$  values increase as long as microbial metabolism occurs, and lighter  $^{14}\text{N}$  will be leached, translocated or lost via outgassing (Novák et al., 1999; Damman, 1988; Niemen, 1998). In 2010, Goldberg et al. (2010) showed, that increasing oxygen concentrations in drained fens leads to higher N<sub>2</sub>O release by nitrification, which is followed by increasing  $\delta^{15}\text{N}$  values in the remaining substrate. Thus, microbial abundance and stable isotope ratios are closely linked, especially for some microbial groups that are more active in nitrogen cycling than others and therefore play a greater role (Tfaily et al., 2014). Fungi have a low demand for nitrogen, making them less likely to be a main driver of increasing  $\delta^{15}\text{N}$  values (Thormann, 2005). In contrast, acidobacteria are one of the main bacterial groups in peat and are highly active in nitrogen cycling; in particular, they are involved in denitrification and N fixation (Ward et al., 2009). Accordingly, their abundance can be expected to have a close link to carbon and especially nitrogen stable isotope depth trends (Weijer et al., 2010).

To examine microbial abundance, we measured the concentrations of specific membrane fatty acids (mFAs). Membrane fatty acids are valid markers to indicate the abundance of specific microbial communities. Sundh et al. (1997) and Torres and Pancost (2016) demonstrated that mFAs are persistent and, to a high degree, insoluble compounds in peat soil. Membrane fatty acids vary based on their origin (plants, specific microbial groups, etc.; Bajerski et al., 2017; Finotti et al., 1993; Piotrowska-Seget and Mroczek, 2003; Reiffarth et al., 2016; Willers et al., 2015). Therefore, based on an analysis of the quantity of mFAs present, the relative abundance

of certain microbial communities might be assessed (Piotrowska-Seget and Mrozik, 2003; Torres and Pancost, 2016). We tested the existence of four bacterial markers and one fungal marker:

- i-C15:0 and C16:1 $\omega$ 7c, which, in combination, are indicative of acidobacteria (Damast et al., 2011; Dedysh and Damsté, 2018; Myers and King, 2016);
- C14:0 and C17:0, which are generally indicative of bacteria (Willers et al., 2015; Zelles, 1997); and
- C18:2 $\omega$ 6c, which is indicative of saprotrophic fungi (Sundh et al., 1997; Elvert et al., 2003; Willers et al., 2015).

To differentiate between wetland soil functioning as carbon storage and biodiversity hotspots in undrained, rewetted and drained sites, we investigate the influence of drainage and rewetting on microbial-derived mFA abundance and stable isotopic values. We studied two peatlands with different drainage histories, using a high spatial resolution of 4 cm in the uppermost 50 cm of the peat columns. In both investigated peatlands' ditches were installed to drain the sites for agricultural use (Mikkinen et al., 1999; Nielsson et al., 2008). In Lakkasuo, Southern Finland, we located a site that had experienced continuous drainage since 1961 (Minkkinen et al., 1999). In the Swedish Degerö Stormyr, ditches were installed at the beginning of the 20th century (Nielsson et al., 2008). They have filled up naturally with sphagnum over the last 20 years and sites are thus rewetting. We compared undrained with drained sites in Lakkasuo and undrained with rewetted sites in Degerö Stormyr. Furthermore, to verify our previous results regarding stable isotopes as markers for peatland hydrology and drainage history (Minkkinen et al., 1999), we investigated depth trends at two points in time (2013 and 2017) to verify pattern stability over time.

We define a sudden directional change in the stable isotope depth patterns as "turning points," according to Alewell et al. (2011) and Groß-Schmölders et al. (2020). The  $\delta^{15}\text{N}$  turning point is located in the middle of the mesotelm, where  $\delta^{15}\text{N}$  values are highest. In contrast, the  $\delta^{13}\text{C}$  turning point marks the bottom of the mesotelm and the onset of the underlying catotelm, above which the  $\delta^{13}\text{C}$  values start to decrease continuously up to the surface.

The contribution of this paper is to examine the microbial composition of peat soil with respect to stable isotope fractionation and test the persistence of stable isotope depth trends with a repeated sampling approach.

We hypothesize the following:

- Bacterial abundance, especially that of acidobacteria, is highest in the mesotelm.
- Bacterial abundance is the main driver of the nitrogen stable isotope depth trend in nutrient-poor peatlands.
- Stable isotope depth patterns are persistent over a time span of four years (2013–2017) and are therefore reliable indicators of drainage and rewetting.

## MATERIALS AND METHODS

### Site Description

We investigated two nutrient-poor peatlands in northern Europe, both classified as fibric Histosol (HSf; IUSS, 2015; **Table 1**).

Degerö Stormyr (64°11'lat. 19°33'long.; 200 m above sea level (a.s.l.)) is situated in Northern Sweden, at the Kulbäcksliden Experimental Forest near Vindeln, between the rivers Umeälven and Vindelälven (Euroala et al., 1984). It is an acidic bog and consists of interconnected small mire patches divided by ridges of glacial till. The climate is characterized as cold with no dry seasons and cold summers (Dfc-zone after Köppen-Geiger classification; Peel et al., 2007). Mean annual temperature is +1.2°C and the annual precipitation has an average of 523 mm (Alexandersson et al., 1991). Ditches were installed in Degerö in the beginning of the 20th century but a natural reestablishment of sphagnum took place over the last few decades (>20 years). Therefore, we define this site as rewetted. In the undrained part the main moss species is *Sphagnum majus* Nielsson et al. (2008) and the water table is near the surface (**Table 1**). The humification index (HI) after von Post is low (H1-H2) and macro-residuals are highly visible (**Table 1**; Groß-Schmölders et al., 2020). Also, biochemical parameters indicate undrained conditions. The carbon:nitrogen ratio (CN) in the acrotelm is 89, and the bulk density (BD) is low (0.02 kg m<sup>-3</sup>), both is typical for undrained nutrient poor peatlands (**Table 1**; Groß-Schmölders et al., 2020). For the rewetted site the main moss species is *Sphagnum balticum* (Nielsson et al., 2008). The water table is near the surface, HI is low (H2) and macro-residuals are preserved well in the upper horizon (**Table 1**; Groß-Schmölders et al., 2020). In contrast the values of the former mesotelm indicate degradation: HI is higher (H3), less macro-residuals are visible, CN decreased to 41 and the BD increased (0.06 kg m<sup>-3</sup>; **Table 1**; Groß-Schmölders et al., 2020).

Lakkasuo (150 m a.s.l.) in Central Finland is an eccentric peatland complex with two parts. The southern part is a bog with ombrotrophic conditions; whereas the northern part is a fen (Minkkinen et al., 1999). Only samples of the ombrotrophic bog are included for this study. Lakkasuo is also located in the cold climate zone, with no dry seasons and cold summers (Dfc-zone after Köppen-Geiger classification; Peel et al., 2007). Mean annual temperature is +3°C and the average precipitation is 700 mm (Laine et al., 2004). Lakkasuo is still drained. Ditches installed in 1961 (70 cm depth, spacing of 40–60 m) affected approximately 50% of the peatland (Minkkinen et al., 1999). The main current moss species in undrained sites is *Sphagnum angustifolia* (Laine et al., 2004). HI is low (H2), a high number of macro-residuals is visible, and the water table is near the surface (<5 cm) (**Table 1**; Groß-Schmölders et al., 2020). Also, the biochemical parameters indicate undrained conditions: high CN (66) and low BD (0.02 kg m<sup>-3</sup>; **Table 1**; Groß-Schmölders et al., 2020). In the drained site *Pleurozium* spp., a moss species of drier environments, is the main moss species and a high number of pine trees is abundant. Macro-residuals are strongly affected by decomposition, HI (H3-H4) and BD (0.06 kg m<sup>-3</sup>) are high and CN (44) is low (**Table 1**; Groß-Schmölders et al., 2020).

**TABLE 1 |** Detailed information for the acrotelm/former mesotelm (only for Degerö rewetted) of the drained, rewetted and undrained sites of Degerö Stormyr and Lakkasuo at the surface (Nielsson et al., 2008; Mikkenen et al., 1999; Groß-Schmolders et al., 2020); av.: average, WT: water table below surface, C: carbon, N: nitrogen, CN: carbon: nitrogen ratio, BD bulk density [ $\text{kg m}^{-3}$ ], von Post Indices (vP).

Location	av. WT [cm]	av. pH	av. C [ $\text{kg m}^{-2}$ ]	av. N [ $\text{kg m}^{-2}$ ]	CN	BD	vP
Lakkasuo	—	—	—	—	—	—	—
undrained	5	4.1	44.8	0.7	65.6	0.02	H2
Drained	26	3.8	48.1	1.0	44.2	0.06	H3-H4
Degerö Stormyr	—	—	—	—	—	—	—
undrained	0	4.8	42.9	0.4	88.8	0.02	H1-H2
Rewetted	10	4.8	45.2	0.7	58.8/41.1	0.02/0.06	H1-H2

## Soil Sampling and Bulk Analyses

We drilled three volumetric peat cores per site in September 2013 and one in June 2017. Cores were drilled with a Russian peat corer (Eijkelkamp, Netherlands). Per site three Cores were taken (1–3). Cores were taken in the undrained parts (Degerö Stormyr (DU13<sub>1-3</sub>, DU17); Lakkasuo (LU13<sub>1-3</sub>, LU17)), and in 1-m distance to a drainage ditch (to 1-m depth) (Degerö Stormyr rewetted (DR13<sub>1-3</sub>, DR17); Lakkasuo drained (LD13<sub>1-3</sub>, LD17)). We drilled the cores in 2017 close to the location of 2013, with a GPS accuracy of 1.3 m, to monitor possible hydrology changes, which could be mirrored by stable isotope depth patterns and microbial FA abundance.

The cores were encased in hard plastic shells, stored in coolers, and transported to the laboratory. The cores were sliced in 2 cm sections for the isotope analyses. Every second section was analyzed, giving a 4 cm depth resolution. Samples were oven-dried at 40°C for 72 h, and homogenized with a vibrating ball mill (MM400, Retsch, Germany). Stable C and N isotopic signatures were measured an elemental analyzer combined with an isotope ratio mass spectrometer (EA-IRMS) (Inegra2, Sercon, Crewe, United Kingdom). Carbon isotopic composition ( $^{13}\text{C}/^{12}\text{C}$ ) was expressed relative to Vienna Pee-Dee Belemnite (VPDB) standard and reported in delta notation (‰):

$$\delta^{13}\text{C}_{\text{sample}} = \left( \frac{R_s}{R_{\text{std}}} - 1 \right) \times 100$$

$R_s$  and  $R_{\text{std}}$  are the ratios of  $^{13}\text{C}/^{12}\text{C}$  in the sample and VPDB standard ( $R_{\text{std}} = 0.011182$ ).

Nitrogen stable isotopes were expressed relative to atmospheric nitrogen and reported in delta notation (‰):

$$\delta^{15}\text{N}_{\text{sample}} = \left( \frac{R_s}{R_{\text{std}}} - 1 \right) \times 100$$

$R_s$  and  $R_{\text{std}}$  are the ratios of  $^{15}\text{N}/^{14}\text{N}$  in the sample and atmospheric nitrogen ( $R_{\text{air}} = 0.0$ ).

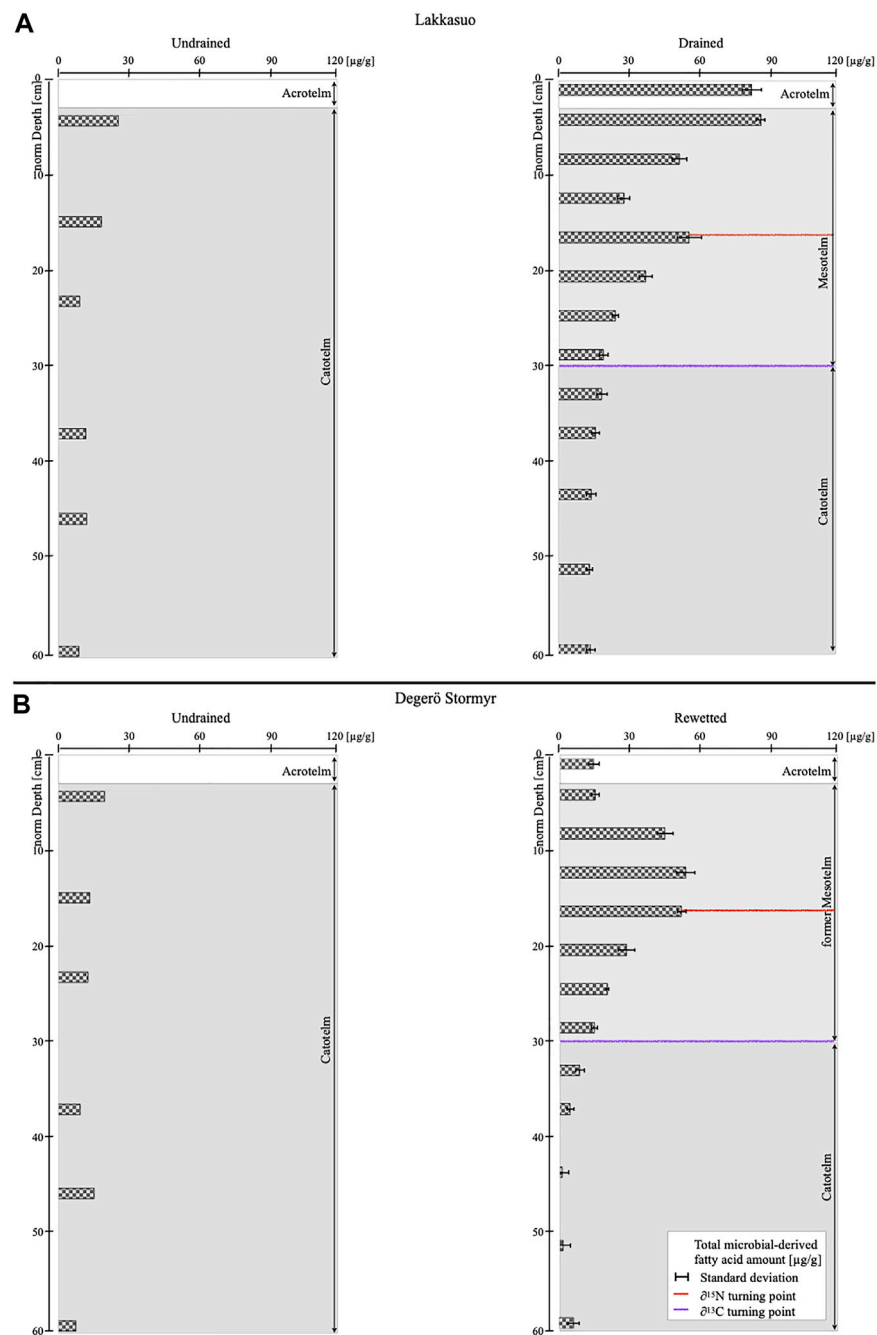
## Fatty Acid Analyses

We aimed to extract total membrane FAs to distinguish between FAs of different bacterial groups, fungi, and plants. We processed 0.2–1.1 g of sample for the lipid extraction with a mixture of  $\text{CH}_2\text{Cl}_2$ : MeOH (9:1 v/v) in an Accelerated Solvent Extractor (Dionex ASE 350). 0.1  $\mu\text{g}/\text{ml}$  of an internal standard with nonadecanoic acid was added before processing each sample.

The total lipid extracts (TLE) were saponified by adding 2 ml of KOH dissolved in MeOH (12%) and putting it in the oven for 3 h at 80°C.

Following the method of Elvert et al. (2003), the TLE were polarized with 1 ml KCl (0.1 mol), and the neutral fraction was extracted by rinsing three times with hexane, dried under a stream of  $\text{N}_2$ , and stored in the refrigerator for later analysis. We acidified the rest of the TLE with fuming hydrochloric acid to a pH of 1. The acid fraction was extracted by rinsing again three times with hexane dried under a stream of  $\text{N}_2$ . They were methylated by adding 1 ml Boron-Trifluoride ( $\text{BF}_3$ ) in MeOH (12–14%) and putting it in the oven for 1 h at 60°C. Afterwards the FA fraction was polarized with KCl (0.1 mol) and transferred in 4 ml vials by rinsing three times with hexane. After one day, in which residues could settle, we transferred the upper part with hexane in 2 ml vials to measure the FAs. The FAs were quantified with a Trace Ultra gas chromatograph (GC) equipped with a flame ionization detector (FID) (Thermo Scientific, Waltham, MA, United States). The carrier gas (helium) had a constant flow of 1.2 ml per minute and the GC-FID was set to splitless mode. Detector temperature was set to 320°C and the samples (dissolved in hexane) were injected at 300°C injector temperature. The starting temperature of the oven was 50°C and hold for 2 min. Then temperature was increased by 10°C per minute to 140°C. The temperature was held for 1 min before it was increased up to 300°C. This temperature was held for 63 min.

To identify the fungal and bacterial markers, we used the Bacterial Acid Methyl Esters standard (BAME, Supelco Mix). For bacteria, it includes the FAs C14:0 and C17:0 as general bacterial markers Zelles (1997), Willers et al. (2015)), i-C15:0 and C16:1 $\omega$ 7c for acidobacteria (Damasté et al., 2011; Dedysh and Damsté, 2018; Myers and King, 2016). The fatty acid C18:2 $\omega$ 9c was used as a marker for fungi (Andersen et al., 2010; Sundh et al., 1997; Zelles, 1997; O'Leary and Wilkinson, 1988; Vestal and White, 1989). All these markers are valid for overall membrane fatty acids and can be used to detect different microbial groups in soil (Finotti et al., 1993; Piotrowska-Seget and Mrozek, 2003; Bajerski et al., 2017). Quantification of the FAs was done using the injected internal standard C19:0 FA, after correcting for the methyl group, added during methylation reaction, normalized to dry weight of bulk material.



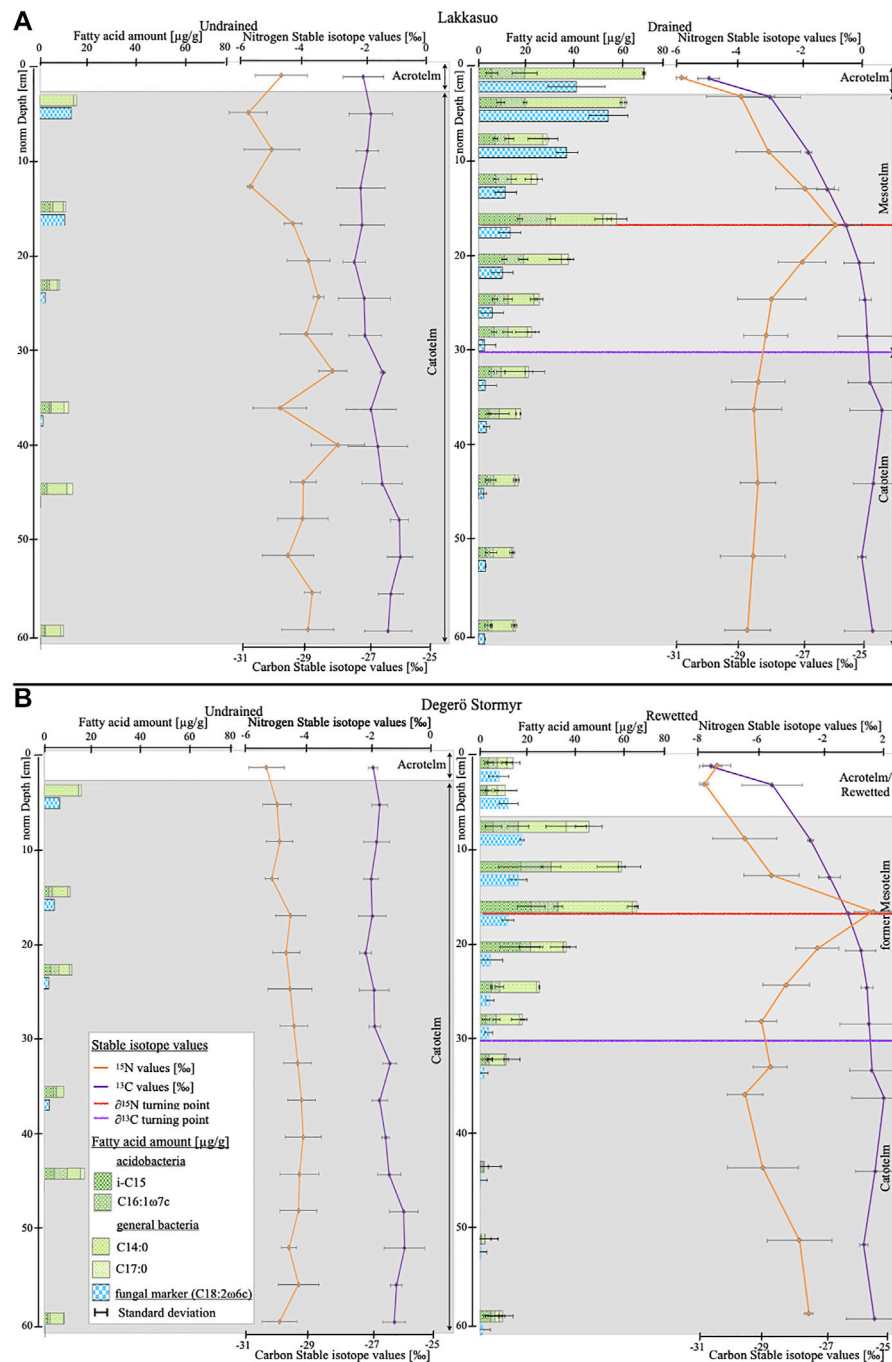
**FIGURE 1** | Average values of total microbial-derived membrane fatty acid concentrations [μg/g] **(A)** Lakkasuo: undrained (LU<sub>1-3</sub>) and drained (LD13<sub>1-3</sub>) **(B)** Degerö Stormyr: undrained (DU<sub>1-3</sub>) and rewetted (DR13<sub>1-3</sub>); Red reference line gives the  $\delta^{15}\text{N}$  turning point, violet reference line gives the  $\delta^{13}\text{C}$  turning point.

## Statistical Analysis

For the FA analysis and the comparison of spatial variations for drained vs rewetted sites, we were interested in comparing the depth trends of all single profiles with each other. This was done by using the depth of the  $\delta^{15}\text{N}$  turning point in each drained profile as the anchor point serving as normalized depth (normD) and set them to 17 cm depth (normD = 17 cm) in each single core.

Using the same procedure,  $\delta^{13}\text{C}$  trends were normalized using the same anchor point (e.g.,  $\delta^{15}\text{N}$  turning point) (for more detailed information, please see Groß-Schmolders et al., 2020).

For the cores of 2013 (3 replicates), variance, standard deviations, and spearman correlation coefficient (R) were calculated with the software R (version 1.0.153). We define an R-value above 0.4 as a strong correlation following McGrew and



**FIGURE 2 |** Stable isotope depth trends [‰] (orange:  $\delta^{15}\text{N}$ , violet:  $\delta^{13}\text{C}$ ) and fatty acids marker concentrations [μg/g], separated by different microbial groups **(A)** Lakkasuo: undrained (LU<sub>1-3</sub>) and drained (LD13<sub>1-3</sub>) **(B)** Degerö Stormyr: undrained (DU<sub>1-3</sub>) and rewetted (DR13<sub>1-3</sub>); Red reference line gives the  $\delta^{15}\text{N}$  turning point, violet reference line gives the  $\delta^{13}\text{C}$  turning point.

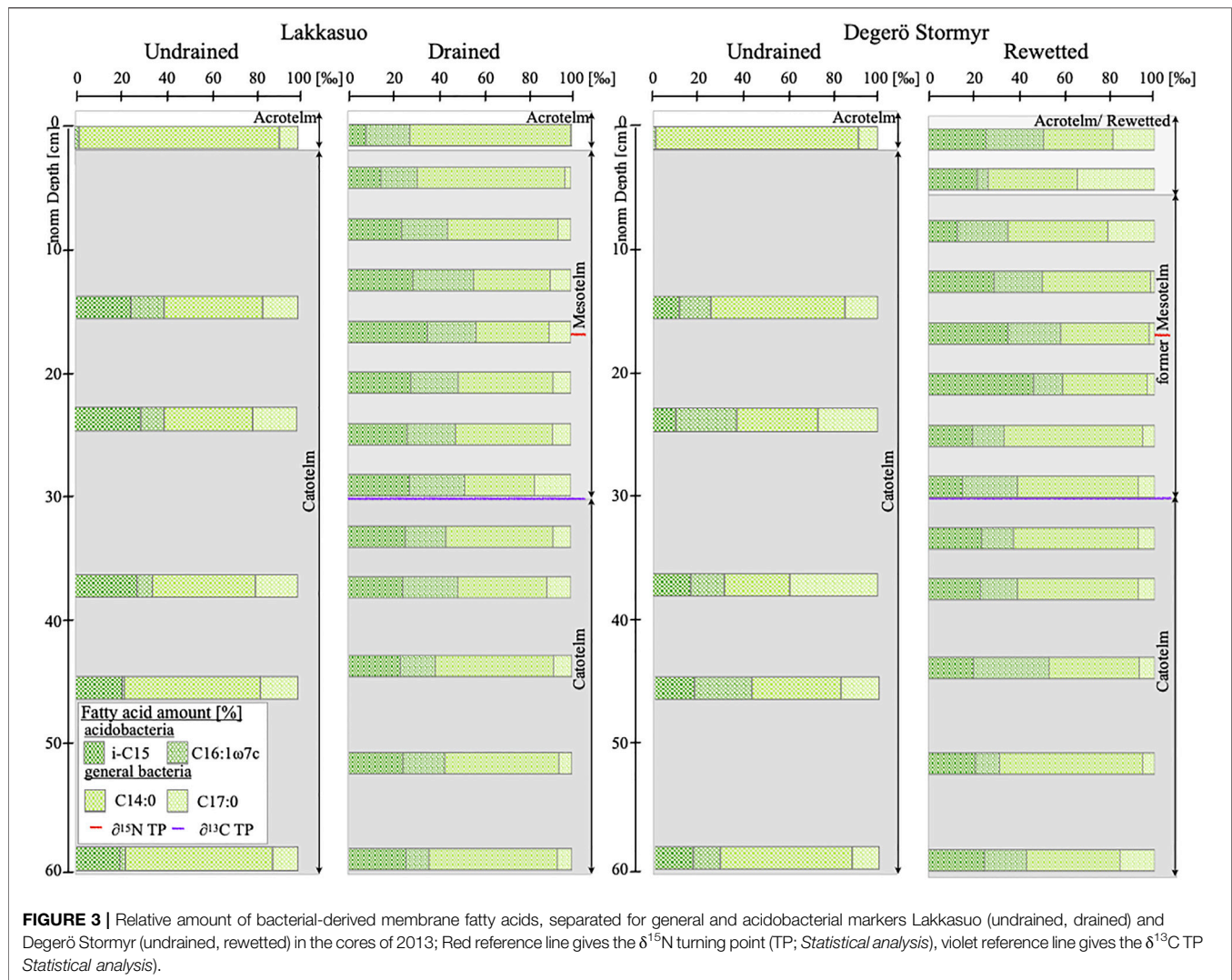
Monroe (2000) and define significance with  $p < 0.05$  (McCune and Grace, 2002).

In the following we present only the normalized data. Raw data without normalization are available in the **Supplementary Table**.

## RESULTS

### Microbial-Derived FA Quantities

Microbial-derived mFA abundance was found to be low over the whole profile in undrained sites, with an average of 16.05 μg/g



( $\pm 7.4$ ) in Lakkasuo (undrained; LU) and  $14.74 \mu\text{g/g}$  ( $\pm 4.7$ ) in Degerö Stormyr (undrained; DU). In the acrotelm, the quantity is higher (LU:  $21.8 \mu\text{g/g}$ ; DU:  $27.7 \mu\text{g/g}$ ) than in the catotelm (LU:  $13.5 \mu\text{g/g}$ ,  $\pm 4.4$ ; DU:  $13.28 \mu\text{g/g}$ ,  $\pm 3.4$ ; **Figure 1**).

In the drained site at Lakkasuo (LD), we discovered a large quantity of microbial-derived mFAs in the acrotelm {LD13<sub>1-3</sub>:  $108.7 \mu\text{g/g}$  [mean,  $\pm 5.5$  (standard deviation of  $n = 3$ ); **Figure 1**] and the mesotelm [ $62.27 \mu\text{g/g}$  ( $\pm 3.7$ ); all results from the 2013 sampling]. The highest microbial-derived mFA concentration was found at the  $\delta^{15}\text{N}$  turning point ( $73.73 \mu\text{g/g}$ ,  $\pm 6.74$ ; **Figure 1**). In the catotelm, the values of mFAs were low in the LD sites ( $21.01 \mu\text{g/g}$ ,  $\pm 2.4$ ). The concentration of fungal-derived mFAs is decreasing from  $40.33 \mu\text{g/g}$  ( $\pm 11.7$ ; **Figure 2**) in the acrotelm of LD13<sub>1-3</sub>, to very low values at the end of the mesotelm and in the catotelm ( $2.88 \mu\text{g/g}$ ,  $\pm 1.4 \mu\text{g/g}$ ; **Figure 2**). Also, the percent of fungal-derived mFAs are decreasing from 49% of all microbial-derived mFAs in the acrotelm to 14% in the catotelm. Contrary to the continually decreasing trend in depth of the fungal-derived mFAs under drained conditions, the bacterial-derived mFA concentration is highest in the middle of the

mesotelm and peaks parallel to the  $\delta^{15}\text{N}$  turning point (mean  $60.17 \mu\text{g/g}$ ,  $\pm 10.2$ ; **Figure 2**). Bacterial-derived mFAs comprise up to 85% of total microbial-derived mFAs at this depth.

For the rewetted site in Degerö Stormyr (DR13<sub>1-3</sub>), we detected low values of microbial-derived mFAs in the acrotelm and in the uppermost part of the former mesotelm [ $20.61 \mu\text{g/g}$  ( $\pm 2.6$ )]. This is expected, because of the wet conditions which are not suitable for high microbial abundance. Below, in the deeper part of the former mesotelm microbial-derived mFA quantities increases [ $53.44 \mu\text{g/g}$  ( $\pm 2.93$ )]. As in Lakkasuo, the microbial-derived mFA quantity also peaks at the  $\delta^{15}\text{N}$  turning point in the middle of the formerly drained layer ( $71.55 \mu\text{g/g}$ ,  $\pm 2.48$ ; **Figure 1**). In the below catotelm, values were low for DR sites ( $8.80 \mu\text{g/g}$ ,  $\pm 2.7$ ; **Figure 1**).

In the rewetted cores DR13<sub>1-3</sub>, we found that fungal-derived mFAs have the highest percentage of the mFAs detected in the acrotelm (35%) and in the upper part of the former mesotelm (32%, **Figure 3**). The highest total quantity of fungal-derived mFAs is in the upper mesotelm ( $16.75 \mu\text{g/g}$ ,  $\pm 3.82$ ; **Figure 2**). In the catotelm, the percentage (16%) and the total quantity of

fungal-derived mFAs ( $2.42 \mu\text{g/g}$ ,  $\pm 2.17$ ; **Figure 2/3**) is low. With decreasing fungal-derived mFA percentage, the bacterial-derived mFA percentage increases, from 65% in the acrotelm to 84% in the catotelm (**Figure 3**). Overall, bacterial-derived mFA abundance is highest at the  $\delta^{15}\text{N}$  turning point ( $62.15 \mu\text{g/g}$ ,  $\pm 5$ ) and low in the catotelm ( $7.45 \mu\text{g/g}$ ,  $\pm 3$ ; **Figure 2**).

## Stable Isotope Values

Carbon and nitrogen isotope values in undrained sites in Lakkasuo (LU13<sub>1-3</sub>, LU17) and Degerö Stormyr (DU13<sub>1-3</sub>, DU17) show no depth trend, whereas carbon isotope values vary less than nitrogen stable isotope values (**Figure 2**).

In LU13<sub>1-3</sub> and LU17, carbon isotope values range between  $-24.47\text{‰}$  and  $-28.36\text{‰}$  with a mean of  $-26.43\text{‰}$  ( $\pm 0.85$ ). Nitrogen stable isotope values in these cores are between  $0.51\text{‰}$  and  $-6.56\text{‰}$  (mean  $-3.15\text{‰}$ ,  $\pm 1.78$ ).

In DU13<sub>1-3</sub> and DU17, carbon stable isotope values are between  $-22.84\text{‰}$  and  $-27.38\text{‰}$  (mean  $-24.52\text{‰}$ ,  $\pm 0.94$ ). For nitrogen, the values range between  $-0.71\text{‰}$  and  $-9.31\text{‰}$  (mean  $-3.99$ ,  $\pm 2.27$ ).

In the drained site in Lakkasuo (LD13<sub>1-3</sub>, LD17) and the rewetted site in Degerö Stormyr (DR13<sub>1-3</sub>, DR17), values show a distinct depth pattern and vary more than in undrained sites (**Figure 2**). In both sites (LD and DR), carbon stable isotope values show a decreasing trend in the upper layers (above 30 cm normD, **Figure 2**). In LD13<sub>1-3</sub>, carbon isotope values range between  $-24.53\text{‰}$  and  $-31.04\text{‰}$  (mean  $-26.67\text{‰}$ ,  $\pm 1.23$ ), and in DR13<sub>1-3</sub>, between  $-23.30\text{‰}$  and  $-29.74\text{‰}$  (mean  $-26.33$ ,  $\pm 1.33$ ).

Nitrogen values in drained and rewetted sites show a peak in the mesotelm (17 cm normD, **Figure 2**). In LD13<sub>1-3</sub>,  $\delta^{15}\text{N}$  values are between  $0.94\text{‰}$  and  $-5.73\text{‰}$  (mean  $2.40$ ,  $\pm 1.50$ ). In DR13<sub>1-3</sub>,  $\delta^{15}\text{N}$  values are between  $1.83\text{‰}$  and  $-10.64\text{‰}$  (mean  $-3.42$ ,  $\pm 2.38$ ).

## DISCUSSION

### New Insights to Microbial Abundance in Undrained, Rewetted and Drained Sites, Identified by Membrane Fatty Acids

In the undrained sites LU and DU, microbial-derived mFA concentrations were highest in the acrotelm, which is in line with other studies (Asada et al., 2005; Artz, 2013). It is the result of environmental conditions in this layer (aerobic, rich of primary plant material). But the values of the acrotelm in the undrained sites are low compared to those of the drained sites, which is a sign of the intact carbon storage function of peat soils and could be the result of 1) the overall nutrient-poor conditions of the investigated sites Minick et al. (2019) with a reduced quantity of nutrients and 2) the incorporation of C in living vegetation (Artz et al., 2008; **Figure 1**).

The highest microbial-derived mFA concentration discovered in the drained site of Lakkasuo is in line with our previous study Groß-Schmolders et al. (2020) and Peltoniemi et al. (2009), as the facultative aerobic mesotelm, with its high content of available

organic matter, provides optimal conditions for microbial metabolism and thus contains the highest microbial-derived mFA concentrations (**Figure 1**). This is also in line with the findings of Wang et al. (2019), who showed that the mesotelm is a hot spot for microbial communities, with the highest microbial diversity.

For the rewetted site in Degerö Stormyr, we assumed that the highest mFA concentration in the former mesotelm (the newly established catotelm after rewetting; **Figure 1**) could be the result of former microbial metabolism preserved from the past aerobic conditions that occurred due to drainage. This correlation was also reported by Torres and Pancost (2016). The low microbial-derived mFA quantities in the uppermost part of DR<sub>1-3</sub>, similar to concentrations of DU (**Figure 1**) are likely a result of the recovery of undrained conditions.

Regarding microbial community assemblage, our results are congruent with previous studies (Groß-Schmolders et al. (2020), Thormann (2004)) demonstrating that fungal-derived mFA concentrations are dominant in the upper layers of drained sites (LD, **Figure 2**). This is congruent with the ecological niche for fungi being located near the surface, where there are large quantities of primary plant material and aerobic conditions (Thormann et al., 2004; Wallander et al., 2009; Strickland and Rousk, 2010). Here, fungal metabolism has a competitive advantage (De Boer et al., 2005; Thormann et al., 2003; Thormann, 2011).

In contrast to fungi, bacteria are better adapted to the facultative anaerobic conditions lower in the profile, (Winsborough and Basiliko, 2010). They are able to make use of a wider spectrum of substrates, which leads to an increase in ratios of bacterial-derived mFAs as depth increases within the mesotelm (**Figure 2**; Kohl et al., 2015).

The group of acidobacteria is of special interest here, as acidobacteria are highly abundant in soil, especially in peatlands (Hausmann et al., 2018; Damsté et al., 2015). They comprise 30% of all bacteria in nutrient-rich fens and up to 80% in pristine bogs (Serkebaeva et al., 2013). Acidobacteria are known to have a slow growth rate and are tolerant to depleted sites, which supports their abundance in nutrient-poor peatlands (Wang et al., 2019). Because of their capability to metabolize in facultative anaerobic to anaerobic conditions, acidobacteria are particularly visible in the mesotelm (Urbanova and Barta, 2014). Acidobacteria are always Gram-negative and exhibit a group of specific membrane compounds (Dedysh and Damsté, 2018). In particular acidobacteria mainly produce glycerol dialkyl glycerol tetraethers Weijers et al. (2010) and the membrane lipids i-C15:0, C16:1 $\omega$ 7c and 13,16-dimethyl octacosanedioic acid (Damsté et al., 2015; Damsté et al., 2018). The concentrations of these were linked to low pH values and decreasing oxygen availability (Weijers et al., 2010), which are typical conditions of the mesotelm. Our results are in line with these findings, as we found an increasing abundance of the mFAs i-C15:0 and C16:1 $\omega$ 7c near the  $\delta^{15}\text{N}$  turning point (**Figures 2, 3**).

### Microbial-Derived Membrane Fatty Acid Quantities and Isotopic Values

In undrained sites, we saw no depth trend in the isotopic values compared to the strong decrease of microbial-derived mFA

concentration in sublayers (**Figure 2**). We conclude that this is caused by the extreme environment of the catotelm, with low temperatures and anaerobic conditions. Hence, metabolism and decomposition processes are strongly inhibited, the mFA quantities and the isotopic fractionation rates are extremely low, and organic substrates are stored (Clymo, 1984; Frolking et al., 2001; Krüger et al., 2015).

### Microbial-Derived Membrane Fatty Acid Quantities and Carbon Isotopic Values

Carbon stable isotope values increase with depth in all investigated drained sites by  $\sim 2.48\%$  from the acrotelm to the catotelm (**Figure 2**). This increase was also found previously Alewell et al. (2011), Krüger et al. (2014) and is in the same range of what other studies have found for peatland soils (Kohl et al., 2015; Hobbie et al., 2017). Wynn et al. (2006) reported, that this trend is caused by the microbial communities involved and their preference for substrates. If more enriched substrates are degraded, the  $\delta^{13}\text{C}$  values in the remaining substrate could decrease due to the enhanced gaseous loss of  $^{13}\text{C}$  enriched  $\text{CO}_2$  (Wynn et al., 2006). For example, glucose, pectin and hemicellulose, which are enriched in  $^{13}\text{C}$ , are some of the preferred substrates for microbial metabolism and are processed in the uppermost peat soil layers. As a result,  $\delta^{13}\text{C}$  values are low in the uppermost peat layers of degraded sites, as we see in LD (**Figure 2**). In contrast to the enriched  $\delta^{13}\text{C}$  values of  $\text{CO}_2$ , methane ( $\text{CH}_4$ ) is depleted in  $\delta^{13}\text{C}$ , which could balance the effect of enriched  $\text{CO}_2$  in the remaining substrate. But as methane production mainly occurs in anerobic conditions, the effect of gaseous loss of depleted  $\text{CH}_4$  is expected to play a minor role in drained peatlands (Yang et al., 2019). In addition, Hornibrook et al. (1997) reported that the  $\delta^{13}\text{C}$  values of  $\text{CH}_4$  are increasing with decreasing depth in peatlands, which could also minor the effect of depleted  $\text{CH}_4$  in our sites. That the depleted  $\delta^{13}\text{C}$  values in top layers of peat are caused by the preferred cycling and therefore gaseous loss of heavy  $^{13}\text{C}$  isotopes can be verified by studies that reported that there is no preferred loss of lighter  $^{12}\text{C}$  during microbial metabolism (Lerch et al., 2011). Increasing values of  $\delta^{13}\text{C}$  in peat soil with depth are therefore related to a change in the processed substrates and their specific  $\delta^{13}\text{C}$  values (Kohl et al., 2015). With increasing depth, recalcitrant,  $\delta^{13}\text{C}$ -depleted substrates such as lignin are also processed, which leads to increasing mobilization of lighter  $^{12}\text{C}$  and further increasing  $\delta^{13}\text{C}$  values in the remaining bulk soil with depth (Lerch et al., 2011). Further Boström et al. (2007) assume that the  $^{13}\text{C}$  enrichment in drained soils with depth is a result of the increased contribution of microbial derived C with depth.

With regard to specific microbial groups, Kohl et al. reported in 2015 that a high fungal-to-bacterial ratio in the microbial community is negatively correlated with  $\delta^{13}\text{C}$  values in the remaining substrate; this is caused by changes in processed substrates and their carbon isotopic signals. Hence, fungal-to-bacterial ratio is decreasing, and  $\delta^{13}\text{C}$  values are increasing due to a change in microbial metabolism processes and substrates used (Kohl et al., 2015). As Kohl et al. (2015) showed, the  $\delta^{13}\text{C}$  values of bacteria ( $-40.1$  to  $-30.6\%$ ) and fungi ( $-31.1$  to  $-24.6\%$ ) stay the same in different depths of peat, but their ratios are changing,

and with them, the  $\delta^{13}\text{C}$  values of the bulk material. This is in line with our data of a decreasing fungal-to-bacterial ratio and increasing  $\delta^{13}\text{C}$  values with depth (**Figure 2**).

With regard to acidobacteria, Weijers et al. (2010) found that acidobacterial-derived mFAs have enriched  $\delta^{13}\text{C}$  values compared to plants and in the same range then bulk. The reason for that could be the preferred cycling of glucose and pectin, which are enriched in  $\delta^{13}\text{C}$  (Pankratov et al., 2008; Lerch et al., 2011). As the highest quantity of acidobacterial-derived mFAs is found in the mesotelm (**Figures 2, 3**), we found that the increasing metabolism rate of acidobacteria could be linked to the increasing  $\delta^{13}\text{C}$  values (**Figure 2**). An increase in acidobacterial-derived mFAs is expected because acidobacteria are known to be autotrophs and are therefore able to assimilate  $\text{CO}_2$  from the soil (Wiesenberg et al., 2008). As soil  $\text{CO}_2$  is enriched in  $^{13}\text{C}$  Wiesenberg et al. (2008), the increasing metabolism by acidobacteria increases the  $\delta^{13}\text{C}$  values in the remaining substrate further.

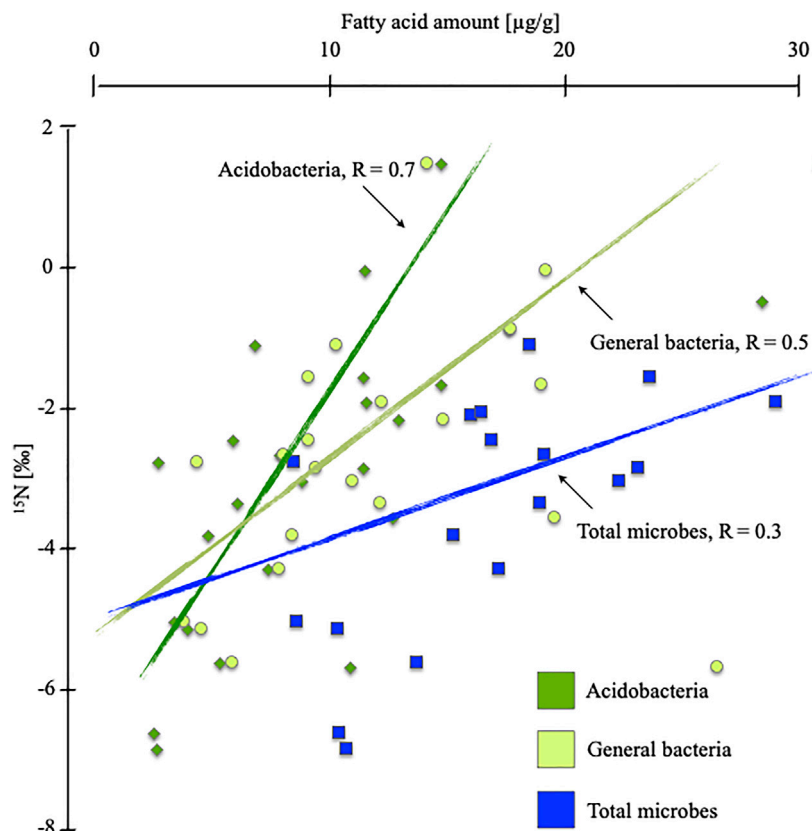
### Microbial-Derived Membrane Fatty Acid Quantities and Nitrogen Isotopic Values

Considering the parallel depth trend of the concentrations of bacterial-derived mFAs and  $\delta^{15}\text{N}$  values (**Figure 4**), we conclude that nitrogen stable isotope values appear to be linked more closely to bacterial abundance than to overall microbial abundance. This interpretation is supported by a higher Spearman correlation index of  $R = 0.54$  for bacteria compared to  $R = 0.30$  for all microbes. Peaks in bacterial-derived mFA abundance and at  $\delta^{15}\text{N}$  values occur in tandem and are visible for both sites investigated (**Figure 2**). The correlation is clear if we consider that the quantity of N in microbial biomass is a substantial part of N in bulk substrate of poor peatlands Lin et al. (2014), and thus, isotopic fractionation by microbes will influence the bulk isotopic value significantly.

We differentiated between acidobacterial and general bacterial markers. For both bacterial groups, the mFA concentrations increased towards the  $\delta^{15}\text{N}$  turning point and were lowest in the catotelm (**Figure 2**).

For both peatland sites, we found the highest concentration of acidobacterial-derived mFAs reaching approximately 50% of all bacterial-derived mFAs in the mesotelm (**Figure 3**). In the upper mesotelm and the catotelm, the percentage is approximately 40% (**Figure 3**). Hence, our results are congruent with the results of Artz in 2013, which point to a characteristic depth trend with a peak in the mesotelm of acidobacterial populations in nutrient-poor peatlands (**Figures 2, 3**).

Acidobacteria are closely involved in nitrogen cycling (Urbanova and Barta, 2014; Eichhorst et al., 2018; Kalam et al., 2020). For example, they are involved in denitrification processes (Urbanova and Barta, 2014). They reduce nitrate, nitrite and possibly nitric oxide (Ward et al., 2009; Eichhorst et al., 2018; Kalam et al., 2020). As Eichhorst et al. (2018) reported, there are also evidence for the mobilization of ammonium by acidobacteria and the gaseous loss of  $\text{N}_2\text{O}$ . All these cycling processes are known to increase  $\delta^{15}\text{N}$  values in bulk material Denk et al. (2017) and are observed predominantly in the mesotelm (Palmer and Horn, 2015; Oshiki et al., 2016). Thus, acidobacteria could be the key to forming the  $\delta^{15}\text{N}$  depth trends



**FIGURE 4 |** Spearman correlation index (R) and correlation of  $\delta^{15}\text{N}$  [‰] and microbial, general bacterial and acidobacterial membrane fatty acid marker amount [ $\mu\text{g/g}$ ], for the rewetted site in Degerö Stormyr and the drained site in Lakkasuo.

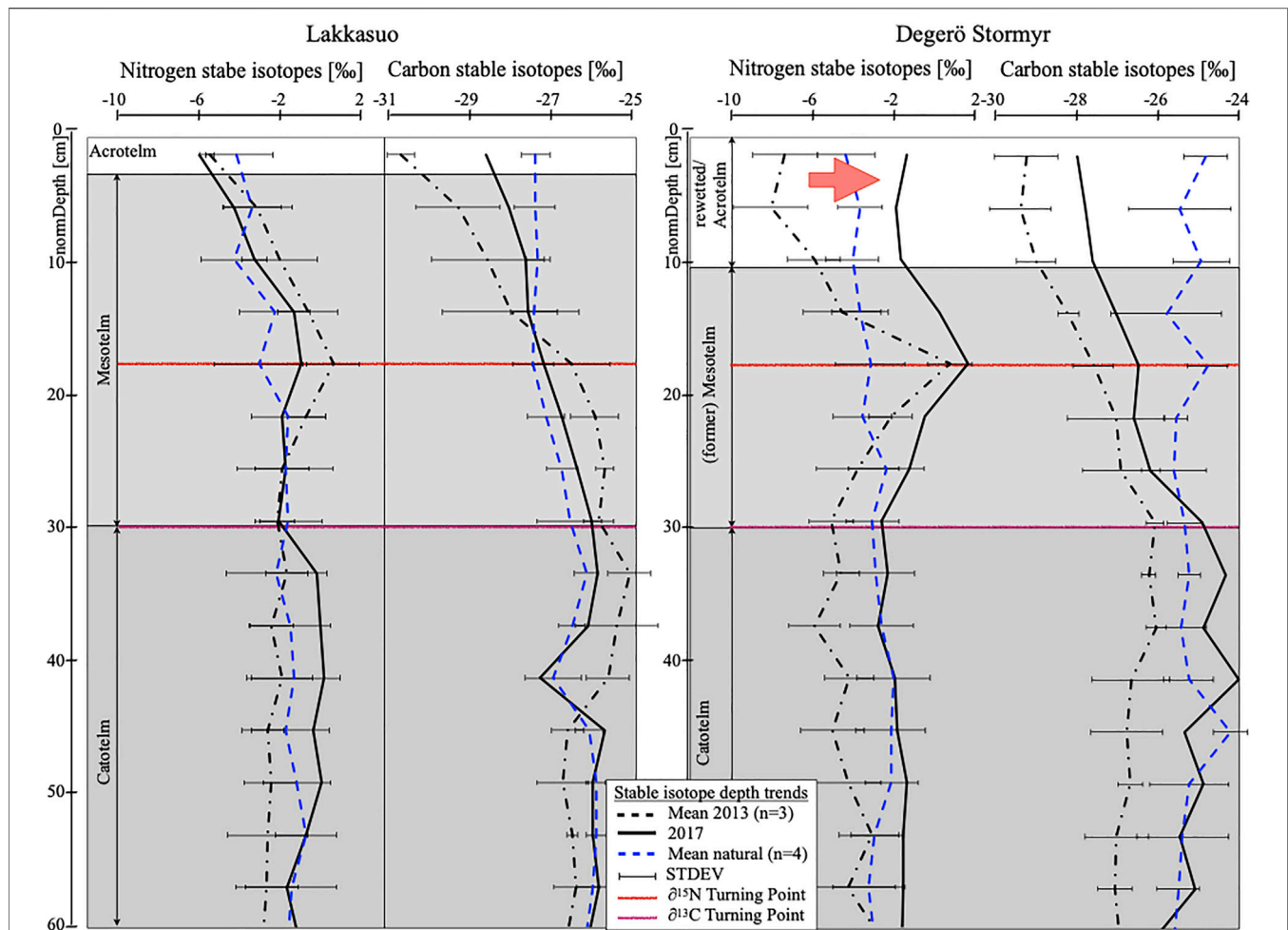
in nutrient-poor peatlands. We assume that as the occurrence of acidobacteria increases, more nitrogen will be processed. Lighter  $^{14}\text{N}$  will be released in a gaseous state, leached or mineralized and then incorporated by plants and translocated upwards within the plants. These processes should lead to increasing  $\delta^{15}\text{N}$  values in the remaining substrate (Hausmann et al., 2018). This correlation is illustrated by our data. Acidobacterial-derived mFA markers, shown in absolute concentrations (Figure 2) and in relation to other microbial markers, are highest at the  $\delta^{15}\text{N}$  turning point (Figures 2, 3). At the  $\delta^{15}\text{N}$  turning point, the relative abundance of acidobacterial-derived mFAs in relation to all bacterial-derived mFAs is highest, with 49.92% for LD and 55.64% for DR (Figure 3). Overall investigated sites,  $\delta^{15}\text{N}$  values and the acidobacterial-derived mFAs are highly significantly correlated ( $R = 0.66$ ,  $p < 0.05$ ; Figure 4).

### Depth Trend of Stable Isotopes in Drained and Rewetted Sites

The comparison of stable isotope depth trends ( $\delta^{15}\text{N}$ ,  $\delta^{13}\text{C}$ ) revealed specific differences between undrained, drained, and rewetted sites, which remained stable over both years. Regardless of the sampling year, none of the cores of undrained sites (DN13<sub>1-3</sub>, DN17, LN13<sub>1-3</sub>, LN17) showed any depth trend of stable isotopes (Figure 5). The cores of the drained site Lakkasuo

(LD13<sub>1-3</sub>, LD17) showed trends within the drained layer (acrotelm and mesotelm).  $\delta^{13}\text{C}$  values increased throughout the drained layer, and a peak of  $^{15}\text{N}$  values (the  $\delta^{15}\text{N}$  turning point) was visible in the mesotelm, which both is indicative for the ongoing loss of typical peatland soil functioning (e.g. carbon storage). In the rewetted site Degerö Stormyr (DR13<sub>1-3</sub>, DR17), no depth trends in  $\delta^{15}\text{N}$  values were observed in the layer likely formed during rewetting conditions above the layer formed during former drainage (Figure 5). Below the rewetted layer, the  $\delta^{15}\text{N}$  depth trend of the former mesotelm was preserved in the newly established (>20 years of rewetting) catotelm. The decreasing trend of  $\delta^{13}\text{C}$  values in DR also seems to have slowed down in the rewetted core in 2017 (Figure 5).

The time-dependent sampling was devised to test the robustness of the stable isotope depth pattern as an indicator for peatland hydrology in relation to the onset, duration and ending of a drainage event. With one exception, nitrogen stable isotope depth trends in both years - 2013 and 2017 - are very similar, confirming our hypothesis (Figure 5). The exception is the  $\delta^{15}\text{N}$  depth trends in Degerö Stormyr, the site that was rewetted in recent decades, where a shift in the rewetted layer in 2017 towards more undrained depth trends compared to 2013 most likely indicates a successful restoration.



**FIGURE 5 |** Depth-normalized stable isotope trends (nitrogen, carbon) for Degerö Stormyr and Lakkasuo, separated for drained sites (2013 (black dotted) and 2017 (black)) and undrained sites (blue dotted); Red reference line gives the  $\delta^{15}\text{N}$  turning point, violet reference line gives the  $\delta^{13}\text{C}$  turning point; Note the shift between the nitrogen isotope depth trend from 2013 to 2017 in the rewetted Degerö Stormyr (marked with red arrow).

The changes in stable isotope values with rewetting occur simultaneously with changes in microbial-derived mFA quantities. This indicates that the changed environmental conditions lead to changing microbial community compositions and therefore changed metabolism processes (Asada et al., 2005). This is in line with the findings of Elliott et al. (2015), who also found distinct changes in microbial communities with rewetting. In drained peat sites, they also found increased values of acidobacteria, which we also found in our sites (Figures 2, 3). Elliott et al. (2015) also indicated that changes in microbial communities are rapid after rewetting and could therefore also indicate relatively short rewetting times and the recovery of typical peatland soil functioning.

## CONCLUSION

Our results confirm that the existence of specific microbial groups is correlated to stable isotope depth trends ( $\delta^{15}\text{N}$ ,  $\delta^{13}\text{C}$ ) of

nutrient-poor peatlands, particularly that of nitrogen isotopes. An analysis of mFA markers for general bacteria as well as specific mFA markers for acidobacteria, and fungi revealed a high abundance of fungal-derived mFAs in the aerobic acrotelm. The upper mesotelm showed a transition to decreasing fungal-derived and increasing bacterial-derived mFA abundance (especially that of acidobacteria). As such, the  $\delta^{15}\text{N}$  turning point seems to be driven in particular by the nitrogen cycling of bacterial metabolism, most prominently by acidobacteria. Downwards along the (former) mesotelm,  $\delta^{15}\text{N}$  values decreased, likely due to low microbial metabolic rates. Finally, in the permanent anaerobic catotelm, where microbial metabolism is strongly impeded,  $\delta^{15}\text{N}$  values show no further depth trend. Stable isotope depth trends ( $\delta^{15}\text{N}$ ,  $\delta^{13}\text{C}$ ) from two different years were able to confirm the persistence of these trends as indicators for ongoing drainage and therefore impaired soil functioning, e.g. as storage of carbon. Furthermore,  $\delta^{15}\text{N}$  seems to indicate former drainage followed by rewetting processes. In summary, we conclude that microbial abundance as indicated

by group specific biomarkers can be confirmed as key for stable isotope depth trends and that differences in  $\delta^{15}\text{N}$  depth profiles may be indicative for drainage and rewetting.

## DATA AVAILABILITY STATEMENT

The original contributions presented in the study are included in the article/**Supplementary Material**, further inquiries can be directed to the corresponding author.

## AUTHOR CONTRIBUTIONS

MG-S conducted the sampling, measurements, evaluation and analysis of the data and cowrote the paper with CA. AB assisted

with the measurements and helped with the analytics. KK added to the discussion. JL and CA had the project idea, supervised and added to the discussion.

## FUNDING

This research has been supported by the Swiss National Science Foundation (SNF; grant no. 169556).

## SUPPLEMENTARY MATERIAL

The Supplementary Material for this article can be found online at: <https://www.frontiersin.org/articles/10.3389/fenvs.2021.730106/full#supplementary-material>

## REFERENCES

- Alewell, C., Giesler, R., Klaminder, J., Leifeld, J., and Rollog, M. (2011). Stable Carbon Isotopes as Indicators for Environmental Change in Palsa Peats. *Biogeosciences* 8, 1769–1778. doi:10.5194/bg-8-1769-2011
- Alexandersson, H., Karlström, C., and Larsson-Mccan, S. (1991). *Temperature and Precipitation in Sweden 1961-1990. Reference Normals Meteorologi*. 81. Norrköping, Sweden: Swedish Meteorological and Hydrological Institute (SMHI).
- Andersen, R., Grasset, L., Thormann, M. N., Rochefort, L., and Francez, A.-J. (2010). Changes in Microbial Community Structure and Function Following Sphagnum Peatland Restoration. *Soil Biol. Biochem.* 42, 291–301. doi:10.1016/j.soilbio.2009.11.006
- Artz, R. R. E., Chapman, S. J., Siegenthaler, A., Mitchell, E. A. D., Buttler, A., Bortoluzzi, E., et al. (2008). Functional Microbial Diversity in Regenerating Cutover Peatlands Responds to Vegetation Succession. *J. Appl. Ecol.* 45, 1799–1809. doi:10.1111/j.1365-2664.2008.01573.x
- Artz, R. R. E. (2013). *Microbial Community Structure and Carbon Substrate Use in Northern Peatlands*. Carbon Cycling in Northern Peatlands. American Geophysical Union, 111–129. doi:10.1029/2008GM000806
- Asada, T., Warner, B. G., and Aravena, R. (2005). Nitrogen Isotope Signature Variability in Plant Species from Open Peatland. *Aquat. Bot.* 82 (4), 297–307. doi:10.1016/j.aquabot.2005.05.005
- Bajerski, F., Wagner, D., and Mangelsdorf, K. (2017). Cell Membrane Fatty Acid Composition of *Chryseobacterium Frigidisoli* PB4T, Isolated from Antarctic Glacier Forefield Soils, in Response to Changing Temperature and pH Conditions. *Front. Microbiol.* 8, 677. doi:10.3389/fmicb.2017.00677
- Biester, H., Knorr, K.-H., Schellekens, J., Basler, A., and Hermanns, Y.-M. (2014). Comparison of Different Methods to Determine the Degree of Peat Decomposition in Peat Bogs. *Biogeosciences* 11, 2691–2707. doi:10.5194/bg-11-2691-2014
- Blodau, C. (2002). Carbon Cycling in Peatlands - A Review of Processes and Controls. *Environ. Rev.* 10 (2), 111–134. doi:10.1139/a02-004
- Boström, B., Comstedt, D., and Ekblad, A. (2007). Isotope Fractionation and  $^{13}\text{C}$  Enrichment in Soil Profiles during the Decomposition of Soil Organic Matter. *Oecologia* 153, 89–98. doi:10.1007/s00442-007-0700-8
- Bremner, J. M. (1997). Sources of Nitrous Oxide in Soils. *Nutrient Cycling Agroecosystem* 49, 7–16. doi:10.1023/a:1009798022569
- Chaves Torres, L., and Pancost, R. D. (2016). Insoluble Prokaryotic Membrane Lipids in a Sphagnum Peat: Implications for Organic Matter Preservation. *Org. Geochem.* 93, 77–91. doi:10.1016/j.orggeochem.2015.12.013
- Clymo, R. S. (1984). The Limits to Peat Bog Growth. *Phil. Trans. R. Soc. Lond. B* 303, 605–654. doi:10.1098/rstb.1984.0002
- Damman, A. W. H. (1988). Regulation of Nitrogen Removal and Retention in Sphagnum Bogs and Other Peatlands. *OIKOS* 51, 291–305. doi:10.2307/3565310
- De Boer, W., and van der Wal, A. (2008). Chapter 8 Interactions between Saprotrophic Basidiomycetes and Bacteria. *Br. Mycol. Soc. Symposia Ser.* 28, 143–153. doi:10.1016/S0275-0287(08)80010-0
- Dedysh, S. N., and Sinninghe Damsté, J. S. (2018). *Acidobacteria*. eLS. Chichester: John Wiley & Sons, 1–10. doi:10.1002/9780470015902.a0027685
- Denk, T. R. A., Mohn, J., Decock, C., Lewicka-Szczebak, D., Harris, E., Butterbach-Bahl, K., et al. (2017). The Nitrogen Cycle: A Review of Isotope Effects and Isotope Modeling Approaches. *Soil Biol. Biochem.* 105, 121–137. doi:10.1016/j.soilbio.2016.11.015
- Eichorst, S. A., Trojan, D., Roux, S., Herbold, C., Rattei, T., and Woebken, D. (2018). Genomic Insights into the Acidobacteria Reveal Strategies for Their Success in Terrestrial Environments. *Environ. Microbiol.* 20 (3), 1041–1063. doi:10.1111/1462-2920.14043
- Elliott, D. R., Caporn, S. J., Nwaishi, F., Nilsson, R. H., and Sen, R. (2015). Bacterial and Fungal Communities in a Degraded Ombrotrophic Peatland Undergoing Natural and Managed Re-vegetation. *PLoS One* 10, e0124726. doi:10.1371/journal.pone.0124726
- Elvert, M., Boetius, A., Knittel, K., and Jørgensen, B. B. (2003). Characterization of Specific Membrane Fatty Acids as Chemotaxonomic Markers for Sulfate-Reducing Bacteria Involved in Anaerobic Oxidation of Methane. *Geomicrobiology J.* 20, 403–419. doi:10.1080/01490450303894
- Euroala, S., Hicks, S. T., and Kaakinen, E. (1984). “Key to Finnish Mire Types,” in *European Mires*. Editor P. D. Moore (London, Great Britain): Academic Press, 1–117. doi:10.1016/b978-0-12-505580-2.50006-4
- Finotti, E., Moretto, D., Marsella, R., and Mercantini, R. (1993). Temperature Effects and Fatty Acid Patterns in Geomyces Species Isolated from Antarctic Soil. *Polar Biol.* 13, 127–130. doi:10.1007/BF00238545
- Frolking, S., Roulet, N. T., Moore, T. R., Richard, P. J. H., Lavoie, M., and Muller, S. D. (2001). Modeling Northern Peatland Decomposition and Peat Accumulation. *Ecosystems* 4, 479–498. doi:10.1007/s10021-001-0105-1
- Goldberg, S. D., Knorr, K.-H., Blodau, C., Lischheid, G., and Gebauer, G. (2010). Impact of Altering the Water Table Height of an Acidic Fen on  $\text{N}_2\text{O}$  and  $\text{NO}$  Fluxes and Soil Concentrations. *Glob. Change Biol.* 16, 220–233. doi:10.1111/j.1365-2486.2009.02015.x
- Groß-Schmolders, M., von Sengbusch, P., Krüger, J. P., Klein, K., Birkholz, A., Leifeld, J., et al. (2020). Switch of Fungal to Bacterial Degradation in Natural, Drained and Rewetted Oligotrophic Peatlands Reflected in  $\delta^{15}\text{N}$  and Fatty Acid Composition. *Soil* 6, 299–313. doi:10.5194/soil-6-299-2020
- Hausmann, B., Pelikan, C., Herbold, C. W., Köstlbacher, S., Albertsen, M., Eichorst, S. A., et al. (2018). Peatland Acidobacteria with a Dissimilatory Sulfur Metabolism. *Isme J.* 12 (7), 1729–1742. doi:10.1038/s41396-018-0077-1
- Hobbie, E. A., Chen, J., Hanson, P. J., Iversen, C. M., McFarlane, K. J., Thorp, N. R., et al. (2017). Long-term Carbon and Nitrogen Dynamics at SPRUCE Revealed through Stable Isotopes in Peat Profiles. *Biogeosciences* 14, 2481–2494. doi:10.5194/bg-14-2481-2017

- Hobbie, E. A., and Högborg, P. (2012). Nitrogen Isotopes Link Mycorrhizal Fungi and Plants to Nitrogen Dynamics. *New Phytol.* 196, 367–382. doi:10.1111/j.1469-8137.2012.04300.x
- Högborg, P., Högborg, L., Schinkel, H., Högborg, M., Johannisson, C., and Wallmark, H. (1996).  $^{15}\text{N}$  Abundance of Surface Soils, Roots and Mycorrhizas in Profiles of European forest Soils. *Oecologia* 108, 207–214. doi:10.1007/BF00334643
- Hornibrook, E. R. C., Longstaffe, F. J., and Fyfe, W. S. (1997). Spatial Distribution of Microbial Methane Production Pathways in Temperate Zone Wetland Soils: Stable Carbon and Hydrogen Isotope Evidence. *Geochimica et Cosmochimica Acta* 61 (4), 745–753. doi:10.1016/s0016-7037(96)00368-7
- IUSS Working Group WRB (2015). "World Reference Base for Soil Resources 2014, Update 2015,". World Soil Resources Reports 106 (Rome, Italy: Food and Agriculture Organization of the United Nations).
- Kalam, S., Basu, A., Ahmad, I., Sayyed, R. Z., El-Enshasy, H. A., Dailin, D. J., et al. (2020). Recent Understanding of Soil Acidobacteria and Their Ecological Significance: A Critical Review. *Front. Microbiol.* 11, 580024. doi:10.3389/fmicb.2020.580024
- Kohl, L., Laganière, J., Edwards, K. A., Billings, S. A., Morrill, P. L., Van Biesen, G., et al. (2015). Distinct Fungal and Bacterial  $\delta^{13}\text{C}$  Signatures as Potential Drivers of Increasing  $\delta^{13}\text{C}$  of Soil Organic Matter with Depth. *Biogeochemistry* 124, 13–26. doi:10.1007/s10533-015-0107-2
- Kohzu, A., Matsui, K., Yamada, T., Sugimoto, A., and Fujita, N. (2003). Significance of Rooting Depth in Mire Plants: Evidence from Natural  $^{15}\text{N}$  Abundance. *Ecol. Res.* 18, 257–266. doi:10.1046/j.1440-1703.2003.00552.x
- Krüger, J. P., Alewell, C., Minkinen, K., Szidat, S., and Leifeld, J. (2016). Calculating Carbon Changes in Peat Soils Drained for Forestry with Four Different Profile-Based Methods. *For. Ecol. Manag.* 381, 29–36. doi:10.1016/j.foreco.2016.09.006
- Krüger, J. P., Leifeld, J., and Alewell, C. (2014). Degradation Changes Stable Carbon Isotope Depth Profiles in Peats Peatlands. *Biogeosciences* 11, 3369–3380. doi:10.5194/bg-11-3369-2014
- Krüger, J. P., Leifeld, J., Glatzel, S., Szidat, S., and Alewell, C. (2015). Biogeochemical Indicators of Peatland Degradation - a Case Study of a Temperate Bog in Northern Germany. *Biogeosciences* 12, 2861–2871. doi:10.5194/bg-12-2861-2015
- Laine, J., Komulainen, V., Laiho, R., Minkinen, K., Rasinmäki, A., Sallantus, T., et al. (2004). *Lakkasuo: A Guide to a Mire Ecosystem*. Helsinki: Department of Forest Ecology. University of Helsinki.
- Leifeld, J., and Menichetti, L. (2018). The Underappreciated Potential of Peatlands in Global Climate Change Mitigation Strategies. *Nat. Commun.* 9, 1071. doi:10.1038/s41467-018-03406-6
- Lerch, T. Z., Nunan, N., Dignac, M.-F., Chenu, C., and Mariotti, A. (2011). Variations in Microbial Isotopic Fractionation during Soil Organic Matter Decomposition. *Biogeochemistry* 106, 5–21. doi:10.1007/s10533-010-9432-7
- Lin, X., Tfaily, M. M., Green, S. J., Steinweg, J. M., Chanton, P., Imvittaya, A., et al. (2014). Microbial Metabolic Potential for Carbon Degradation and Nutrient (Nitrogen and Phosphorus) Acquisition in an Ombrotrophic Peatland. *Appl. Environ. Microbiol.* 80, 3531–3540. doi:10.1128/AEM.00206-14
- McCune, B. P., and Grace, J. B. (2002). *Analysis of Ecological Communities*. Glendened Beach, United State of America: MjM Software Design.
- McGrew, J. Jr., and Monroe, C. B. (2000). *Statistical Problem Solving in Geography*. Long Grove, United States of America: Waveland Press Inc.
- Minick, K. J., Mitra, B., Li, X., Noormets, A., and King, J. S. (2019). Water Table Drawdown Alters Soil and Microbial Carbon Pool Size and Isotope Composition in Coastal Freshwater Forested Wetlands. *Front. For. Glob. Change* 2, 7. doi:10.3389/ffgc.2019.00007
- Minkinen, K., Vasander, H., Jauhainen, S., Karsisto, M., and Laine, J. (1998). Post-drain- Age Changes in Vegetation Composition and Carbon Balance in Lakkasuo Mire, Central Finland. *Plant and Soil* 207, 107–120. doi:10.1023/A:1004466330076
- Moore, T., and Basiliko, N. (2006). "Decomposition in Boreal Peatlands," in *Boreal Peatland Ecosystems, Ecological Studies (Analysis and Synthesis)* (188. Editors R. K. Wieder and D. H. Vitt (Berlin, Heidelberg, Germany: Springer).
- Myers, M. R., and King, G. M. (2016). Isolation and Characterization of Acidobacterium Ailaui Sp. nov., a Novel Member of Acidobacteria Subdivision 1, from a Geothermally Heated Hawaiian Microbial Mat. *Int. J. Syst. Evol. Microbiol.* 66, 5328–5335. doi:10.1099/ijsem.0.001516
- Niemi, M. (1998). Changes in Nitrogen Cycling Following the Clearcutting of Drained Peatland Forests in Southern Finland. *Boreal Environ.* 31, 9–21. Available at: <http://urn.fi/URN:NBN:fi-fe2016091423744>.
- Nilsson, M., Sagerfors, J., Buffam, I., Laudon, H., Eriksson, T., Grelle, A., et al. (2008). Contemporary Carbon Accumulation in a Boreal Oligotrophic Minerogenic Mire - a Significant Sink after Accounting for All C-Fluxes. *Glob. Change Biol.* 14 (10), 2317–2332. doi:10.1111/j.1365-2486.2008.01654.x
- Novák, M., Buzek, F., and Adamová, M. (1999). Vertical Trends in  $\delta^{13}\text{C}$ ,  $\delta^{15}\text{N}$  and  $\delta^{34}\text{S}$  Ratios in Bulk Sphagnum Peat. *Soil Biol. Biochem.* 31, 1343–1346. doi:10.1016/S0038-0717(99)00040-1
- O'Leary, W. M., and Wilkinson, S. (1988). "Gram-positive Bacteria," in *Microbial Lipids*. Editors C. Ratledge and S. G. Wilkinson (London: Academic Press), 117–185.
- Oshiki, M., Satoh, H., and Okabe, S. (2016). Ecology and Physiology of Anaerobic Ammonium Oxidizing Bacteria. *Environ. Microbiol.* 18 (9), 2784–2796. doi:10.1111/1462-2920.13134
- Palmer, K., and Horn, M. A. (2015). Denitrification Activity of a Remarkably Diverse Fen Denitrifier Community in Finnish Lapland Is N-Oxide Limited. *PLoS ONE* 10, e0123123. doi:10.1371/journal.pone.0123123
- Peel, M. C., Finlayson, B. L., and McMahon, T. A. (2007). Updated World Map of the Köppen-Geiger Climate Classification. *Hydrol. Earth Syst. Sci.* 11, 1633–1644. doi:10.5194/hess-11-1633-2007
- Peltoniemi, K., Fritze, H., and Laiho, R. (2009). Response of Fungal and Actinobacterial Communities to Water-Level Drawdown in Boreal Peatland Sites. *Soil Biol. Biochem.* 41, 1902–1914. doi:10.1016/j.soilbio.2009.06.018
- Piotrowska-Seget, Z., and Mrozek, A. (2003). Signature Lipid Biomarker (SLB) Analysis in Determining Changes in Community Structure of Soil Microorganisms. *Polish J. Environ. Stud.* 12 (6), 669–675.
- Reiffarth, D. G., Petticrew, E. L., Owens, P. N., and Lobb, D. A. (2016). Sources of Variability in Fatty Acid (FA) Biomarkers in the Application of Compound-specific Stable Isotopes (CSSIs) to Soil and Sediment Fingerprinting and Tracing: A Review. *Sci. Total Environ.* 565, 8–27. doi:10.1016/j.scitotenv.2016.04.137
- Robinson, D., Handley, L. L., and Scrimgeour, C. M. (1998). A Theory for  $^{15}\text{N}$  /  $^{14}\text{N}$  Fractionation in Nitrate-Grown Vascular Plants. *Planta* 205, 397–406. doi:10.1007/s004250050336
- Schulze, E. D., Luyssaert, S., Luyssaert, S., Ciais, P., Freibauer, A., Janssens, I. A., et al. the CarboEurope Team (2009). Importance of Methane and Nitrous Oxide for Europe's Terrestrial Greenhouse-Gas Balance. *Nat. Geosci.* 2, 842–850. doi:10.1038/ngeo686
- Serkebaeva, Y. M., Kim, Y., Liesack, W., and Dedysh, S. N. (2013). Pyrosequencing-based Assessment of the Bacteria Diversity in Surface and Subsurface Peat Layers of a Northern Wetland, with Focus on Poorly Studied Phyla and Candidate Divisions. *PLoS One* 8 (5), e63994–14. doi:10.1371/journal.pone.0063994
- Sinninghe Damsté, J. S., Rijpstra, W. I. C., Hopmans, E. C., Weijers, J. W. H., Foessel, B. U., Overmann, J., et al. (2011). 13,16-Dimethyl Octacosanedioic Acid (Iso-Diabolic Acid), a Common Membrane-Spanning Lipid of Acidobacteria Subdivisions 1 and 3. *Appl. Environ. Microbiol.* 77, 4147–4154. doi:10.1128/AEM.00466-11
- Strickland, M. S., and Rousk, J. (2010). Considering Fungal:bacterial Dominance in Soils - Methods, Controls, and Ecosystem Implications. *Soil Biol. Biochem.* 42, 1385–1395. doi:10.1016/j.soilbio.2010.05.007
- Sundh, I., Nilsson, M., and Borgå, P. (1997). Variation in Microbial Community Structure in Two Boreal Peatlands as Determined by Analysis of Phospholipid Fatty Acid Profiles. *Appl. Environ. Microbiol.* 63 (4), 1476–1482. doi:10.1128/aem.63.4.1476-1482.1997
- Tfaily, M. M., Cooper, W. T., Kostka, J. E., Chanton, P. R., Schadt, C. W., Hanson, P. J., et al. (2014). Organic Matter Transformation in the Peat Column at Marcell Experimental Forest: Humification and Vertical Stratification. *J. Geophys. Res. Biogeosci.* 119, 661–675. doi:10.1002/2013JG002492
- Thormann, M. (2011). *In Vitro* decomposition of Sphagnum-Derived Acrotelm and Mesotelm Peat by Indigenous and Alien Basidiomycetous. *Mires and Peat* 8, 1–12.
- Thormann, M. N., Currah, R. S., and Bayley, S. E. (2004). Patterns of Distribution of Microfungi in Decomposing Bog and Fen Plants. *Can. J. Bot.* 82, 710–720. doi:10.1139/b04-025

- Thormann, M. N. (2006). Diversity and Function of Fungi in Peatlands: A Carbon Cycling Perspective. *Can. J. Soil Sci.* 86, 281–293. doi:10.4141/S05-082
- Urbanová, Z., and Bárta, J. (2014). Microbial Community Composition Andin Silicopredicted Metabolic Potential Reflect Biogeochemical Gradients between Distinct Peatland Types. *FEMS Microbiol. Ecol.* 90, 633–646. doi:10.1111/1574-6941.12422
- Vestal, J. R., and White, D. C. (1989). Lipid Analysis in Microbial Ecology. *BioScience* 39, 535–541. doi:10.2307/1310976
- Wallander, H., Mörrth, C.-M., and Giesler, R. (2009). Increasing Abundance of Soil Fungi Is a Driver for <sup>15</sup>N Enrichment in Soil Profiles along a Chronosequence Undergoing Isostatic Rebound in Northern Sweden. *Oecologia* 160, 87–96. doi:10.1007/s00442-008-1270-0
- Wang, M., Tian, J., Bu, Z., Lamit, L. J., Chen, H., Zhu, Q., et al. (2019). Structural and Functional Differentiation of the Microbial Community in the Surface and Subsurface Peat of Two Minerotrophic Fens in China. *Plant Soil* 437, 21–40. doi:10.1007/s11104-019-03962-w
- Ward, N. L., Challacombe, J. F., Janssen, P. H., Henrissat, B., Coutinho, P. M., Wu, M., et al. (2009). Three Genomes from the Phylum Acidobacteria Provide Insight into the Lifestyles of These Microorganisms in Soils. *Appl. Environ. Microbiol.* 75 (7), 2046–2056. doi:10.1128/AEM.02294-08
- Weijers, J. W. H., Wiesenberger, G. L. B., Bol, R., Hopmans, E. C., and Pancost, R. D. (2010). Carbon Isotopic Composition of Branched Tetraether Membrane Lipids in Soils Suggest a Rapid Turnover and a Heterotrophic Life Style of Their Source Organism(s). *Biogeosciences* 7, 2959–2973. doi:10.5194/bg-7-2959-2010
- Wiesenberger, G. L. B., Schmidt, M. W. I., and Schwark, L. (2008). Plant and Soil Lipid Modifications under Elevated Atmospheric CO<sub>2</sub> Conditions: I. Lipid Distribution Patterns. *Org. Geochem.* 39 (1), 91–102. doi:10.1016/j.orggeochem.2007.09.005
- Willers, C., Jansen van Rensburg, P. J., and Claassens, S. (2015). Phospholipid Fatty Acid Profiling of Microbial Communities-A Review of Interpretations and Recent Applications. *J. Appl. Microbiol.* 119, 1207–1218. doi:10.1111/jam.12902
- Winsborough, C., and Basiliko, N. (2010). Fungal and Bacterial Activity in Northern Peatlands. *Geomicrobiology J.* 27, 315–320. doi:10.1080/01490450903424432
- Wynn, J. G., Harden, J. W., and Fries, T. L. (2006). Stable Carbon Isotope Depth Profiles and Soil Organic Carbon Dynamics in the Lower Mississippi Basin. *Geoderma* 131, 89–109. doi:10.1016/j.geoderma.2005.03.005
- Yang, G., Tian, J., Chen, H., Jiang, L., Zhan, W., Hu, J., et al. (2019). Peatland Degradation Reduces Methanogens and Methane Emissions from Surface to Deep Soils. *Ecol. Indicators* 106, 105488. doi:10.1016/j.ecolind.2019.105488
- Zedler, J. B., and Kercher, S. (2005). WETLAND RESOURCES: Status, Trends, Ecosystem Services, and Restorability. *Annu. Rev. Environ. Resour.* 30 (1), 39–74. doi:10.1146/annurev.energy.30.050504.144248
- Zelles, L. (1997). Phospholipid Fatty Acid Profiles in Selected Members of Soil Microbial Communities. *Chemosphere* 35, 275–294. doi:10.1016/S0045-6535(97)00155-0

**Conflict of Interest:** The authors declare that the research was conducted in the absence of any commercial or financial relationships that could be construed as a potential conflict of interest.

**Publisher's Note:** All claims expressed in this article are solely those of the authors and do not necessarily represent those of their affiliated organizations, or those of the publisher, the editors and the reviewers. Any product that may be evaluated in this article, or claim that may be made by its manufacturer, is not guaranteed or endorsed by the publisher.

Copyright © 2021 Groß-Schmolders, Klein, Birkholz, Leifeld and Alewell. This is an open-access article distributed under the terms of the Creative Commons Attribution License (CC BY). The use, distribution or reproduction in other forums is permitted, provided the original author(s) and the copyright owner(s) are credited and that the original publication in this journal is cited, in accordance with accepted academic practice. No use, distribution or reproduction is permitted which does not comply with these terms.



# Soil Fertility Changes With Climate and Island Age in Galápagos: New Baseline Data for Sustainable Agricultural Management

Matthias Strahlhofer<sup>1</sup>, Martin H. Gerzabek<sup>1</sup>, Nicola Rampazzo<sup>1</sup>, Paulina M. Couenberg<sup>2</sup>, Evelyn Vera<sup>3</sup>, Xavier Salazar Valenzuela<sup>3</sup> and Franz Zehetner<sup>1,4\*</sup>

<sup>1</sup>Institute of Soil Research, University of Natural Resources and Life Sciences, Vienna, Austria, <sup>2</sup>Ministry of Agriculture and Livestock, Galápagos, Ecuador, <sup>3</sup>Central University of Ecuador, Galápagos, Ecuador, <sup>4</sup>Galápagos National Park Directorate, Galápagos, Ecuador

## OPEN ACCESS

### Edited by:

Thomas Keller,  
Swedish University of Agricultural  
Sciences, Sweden

### Reviewed by:

Jean-Thomas Cornelis,  
University of British Columbia, Canada  
Calogero Schillaci,  
Joint Research Centre (Italy), Italy

### \*Correspondence:

Franz Zehetner  
franz.zehetner@boku.ac.at

### Specialty section:

This article was submitted to  
Soil Processes,  
a section of the journal  
Frontiers in Environmental Science

**Received:** 01 October 2021

**Accepted:** 12 November 2021

**Published:** 07 December 2021

### Citation:

Strahlhofer M, Gerzabek MH,  
Rampazzo N, Couenberg PM, Vera E,  
Salazar Valenzuela X and Zehetner F  
(2021) Soil Fertility Changes With  
Climate and Island Age in Galápagos:  
New Baseline Data for Sustainable  
Agricultural Management.  
Front. Environ. Sci. 9:788082.  
doi: 10.3389/fenvs.2021.788082

While the extended absence of human influence has led to matchless natural conditions on the Galápagos archipelago, agricultural activities on the inhabited islands are increasingly affecting soil health and functioning. However, a systematic assessment of the agricultural soils on the Galápagos Islands is still absent. Plate tectonics and hotspot volcanism cause an eastward drift of the archipelago and result in a west-to-east soil age gradient from approx. 1 to 1,000 ka. In addition, precipitation regimes change from arid to humid with elevation on the higher-standing islands. The objective of this study was to investigate differences in soil fertility parameters and Mehlich (III)-extractable nutrient levels along these gradients in order to provide baseline information for sustainable agricultural management. Topsoil samples (0–20 cm) from 125 farms of the islands Isabela, Santa Cruz and San Cristóbal were analyzed. Gravel and sand content, pH, electrical conductivity, cation exchange capacity, base saturation, soil organic C and total N content tended to decrease with increasing island age, while clay content, soil macroaggregate stability, plant-available water and bulk density increased. Mehlich (III)-extractable base cations Ca, K, Mg and Na as well as P, Fe and Zn showed a decreasing tendency from the youngest to the oldest island, while Mn increased with island age. Mehlich (III)-extractable Cu and Na reached their highest levels on the most intensively farmed, intermediate-aged island Santa Cruz, likely related to anthropogenic inputs and irrigation with brackish water, respectively. Changes along the altitudinal climate gradient within the studied islands were most significant for soil pH, base saturation, and Mehlich (III)-extractable Ca and Mn. Our results highlight the importance of site-specific agricultural management to account for the strong heterogeneity in soil parameters among and within the Galápagos archipelago. The data provided herein shall serve as a baseline for targeted future management strategies to avoid soil degradation, restore and maintain soil functioning and, hence, sustain the soils' provision of ecosystem services in this unique archipelago.

**Keywords:** volcanic ash soils, pedogenesis, Mehlich(III), soil structure, soil and water management, soil functions

## INTRODUCTION

Soils play a vital role in terrestrial ecosystems, providing the basis for food and biomass production, regulating and purifying water flows as well as significantly contributing to biodiversity, among other services (Adhikari and Hartemink, 2016). Land degradation processes driven by anthropogenic impacts result in impaired soil functions and increasingly compromise ecosystem services. Owing to its remote geographical location, the Galápagos archipelago had remained untouched by human influence for a long period of time, enabling the evolution of numerous endemic species under matchless biological conditions (Tye et al., 2002). However, several of the islands are now inhabited, and agricultural activities have intensified in recent decades in efforts to meet the increasing demand for agricultural products (Watson et al., 2010). Considering the growing pressure on this unique ecosystem and the islands' local food security, a better understanding of the island's soil resources is a prerequisite for sustainable agricultural management and also represents an important contribution to the environmental research agenda for Galápagos (Izurieta et al., 2018).

The remote island chain is an extraordinary “natural laboratory,” not only for studying the evolution of plant and animal species but also to investigate how soils have formed in response to different environmental factors. Plate tectonics in combination with ongoing volcanic activity in the western part of Galápagos cause an eastward drift of the archipelago and result in a pronounced gradient of rock ages between the islands (Zehetner et al., 2020). In addition, climate and especially precipitation regimes driven by the southeast trade winds change from arid lowlands to humid highlands on the windward side of the higher-standing islands (Trueman and D'Ozouville, 2010).

Systematic information on (top)soil properties in Galápagos is still scarce, and most of the available baseline information is drawn from a geo-pedological mission in 1962 (Stoops, 2013; Taboada et al., 2016; Rial et al., 2017) with very few additional later studies (e.g., Adelinet et al., 2008). In 2016 and 2017, three soil scientific expeditions laid the foundation for further, more detailed investigations, and the present study forms part of these ongoing research efforts carried out by the University of Natural Resources and Life Sciences Vienna in cooperation with the Galápagos National Park Directorate and other partner institutions. From these recent activities, several new papers on weathering and soil formation have already been published (e.g., Candra et al., 2019; Zehetner et al., 2020), and also the agricultural soils of the archipelago have been investigated (e.g., Gerzabek et al., 2019; Dinter et al., 2020, Dinter et al., 2021). Gerzabek et al. (2019) studied the effects of agricultural land management on soil quality parameters on two of the islands (Santa Cruz and San Cristóbal) by comparing arable soils to soils under forest in adjacent Galápagos National Park areas. They found signs of soil fertility decline on both investigated arable sites such as decreased SOC and total N stocks, diminished M3-extractable nutrient levels as well as reduced microbial biomass. The publications of Dinter et al. (2020), Dinter et al. (2021) are of special interest for the present study, because they are based on the same sample set as the present study, including three islands

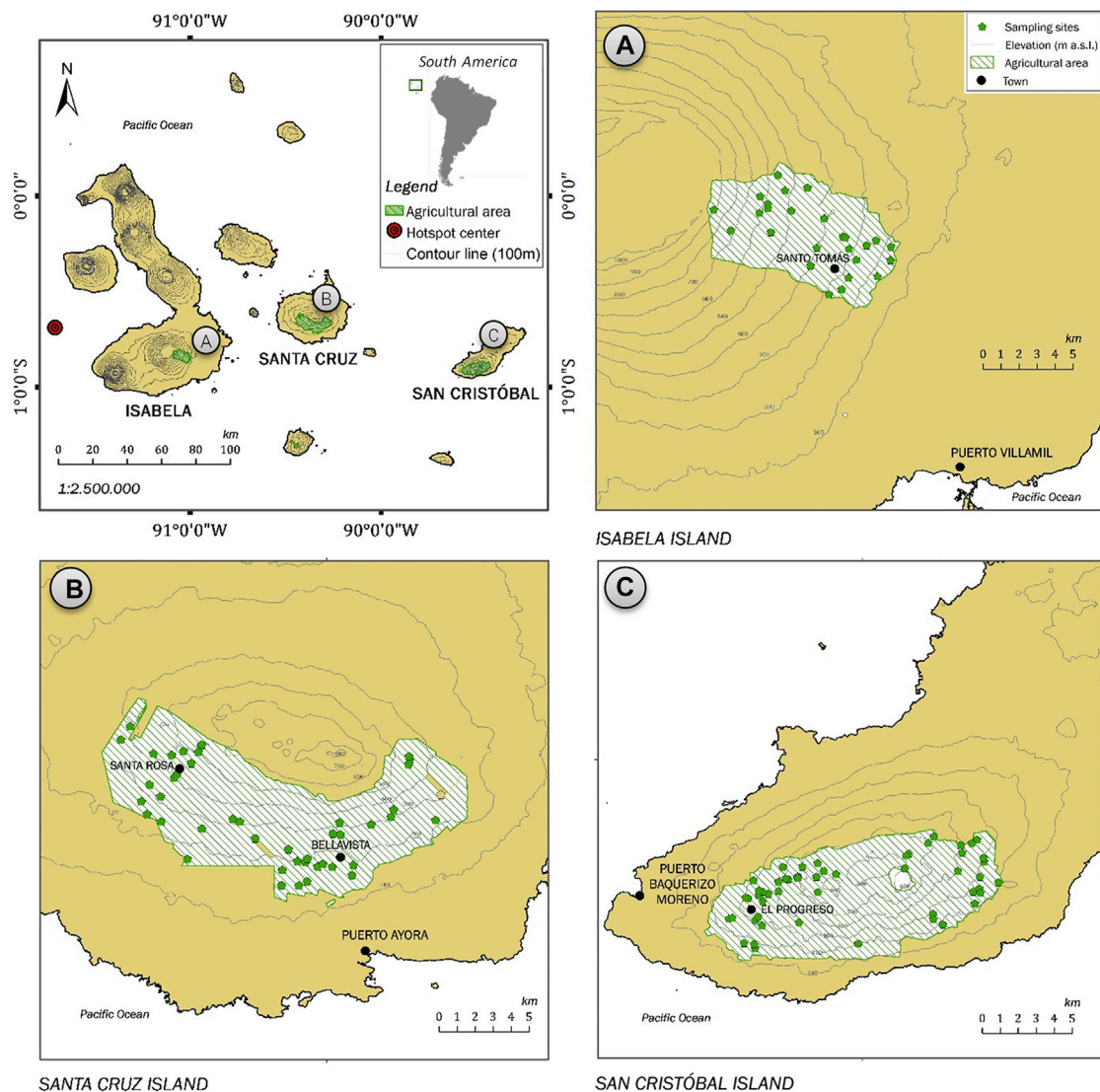
of differing ages (Isabela, Santa Cruz and San Cristóbal) and covering elevation/climate zones ranging from dry lowlands to humid highlands. Dinter et al. (2020) characterized the basic properties and nutrient reserves of agricultural soils in relation to climate and island age. They found that non-crystalline constituents and andic properties were mainly present in the young soils of Isabela Island, while the highly weathered, older soils of San Cristóbal Island were dominated by crystalline clays and iron oxides and had already lost andic properties. Furthermore, aqua regia-extractable base cations tended to decrease with increasing island age and elevation/moisture, while Al and Fe accumulated along the same gradients (Dinter et al., 2020). In Dinter et al. (2021), the focus was on trace elements, and total contents of Cd, Co, Cr, Cu, Ni and Zn were above threshold levels in many of the studied soils. The results of that study also suggest that elevated soil concentrations of Cd, Zn and Cu may be attributable to the use of agrochemicals (Dinter et al., 2021).

The present study looks more specifically into fertility parameters of arable topsoils and the resulting agricultural implications for the respective islands, considering physical and chemical indicators of soil fertility as well as Mehlich (III)-extractable (M3-extractable) nutrient levels. While Dinter et al. (2020), Dinter et al. (2021) reported on aqua regia-extractable nutrient reserves of the studied agricultural soils, our study focusses on rather bioavailable fractions of macro- and micronutrients (P, K, Ca, Mg, Na, Fe, Mn, Zn, Cu). We analyzed topsoil samples from 125 farms across three of the Galápagos islands (Isabela, Santa Cruz and San Cristóbal), which corresponds to approximately 16.5% of the agricultural production units on the archipelago (CGREG et al., 2014). The selected sites include various soil types that have formed over different durations and under different climatic regimes. Our main objectives were 1) to assess the soils fertility status in relation to soil age across the three studied islands, 2) to assess soil fertility differences between the different elevation zones within the agricultural areas of the youngest and oldest studied island, and 3) to provide baseline data for sustainable agricultural management practices on the different Galápagos islands against the background of changing environmental conditions.

## STUDY AREA

### Natural Setting and Environmental Gradients

The Galápagos archipelago is situated at the equator approx. 1,000 km west of the coast of Ecuador (**Figure 1**). The islands were formed by hotspot-induced volcanism under the Nazca tectonic plate. The estimated center of the volcanic hotspot is located southwest of Fernandina Island at the western margin of the archipelago (Hooft et al., 2003; **Figure 1**), and the Nazca plate has been moving eastward at a speed of approx. 51 km/Ma (Argus et al., 2011). This results in a pronounced age gradient of the volcanic parent materials from west to east. The western island Isabela has large areas of geologically young land surfaces (<5 ka; Reynolds et al., 1995), while the oldest dated lavas on the eastern



**FIGURE 1** | Map of the sampling locations within the agricultural areas of the three studied islands Isabela, Santa Cruz and San Cristóbal. The center of the volcanic hotspot was estimated by Hooft et al. (2003); m a.s.l. = meters above sea level.

island San Cristóbal are 2.35 Ma old (White et al., 1993). The parent materials of the studied soils cover an age range from approx. 1.5 to  $\geq 1,070$  ka and include alkali basalts and tholeiites. For more details on the geologic setting, s. Zehetner et al. (2020).

The climate of the Galápagos Islands is rather cool (mean annual temperature: 18–21°C in the highlands, where most of the agricultural area is located) and dry compared to other equatorial regions (Lasso et al., 2018), which is due to cool ocean currents and the prevailing southeast trade winds. The latter convey moisture to the windward, southeast side of the higher-standing islands, which results in a pronounced climatic gradient from arid lowlands to humid highlands, while the leeward side remains rather dry throughout (Itow, 2003). For Santa Cruz Island, median annual rainfall of 277 and 813 mm has been recorded by meteorological stations in the arid coastal zone

(2 m a.s.l.) and in the transition zone (194 m a.s.l.), respectively, while mean annual precipitation in the humid highlands has been estimated up to 1,600 mm (Trueman and D'Ozouville, 2010). For more details on the climatic conditions, s. Zehetner et al. (2020). The agricultural areas under study are located on the windward side of the three islands covering an elevation range from approx. 100–900 m a.s.l. (Figure 1). In analogy to Dinter et al. (2020), the sites of this study were grouped into three elevation zones reflecting different moisture regimes: arid, dry and transition zone (<250 m a.s.l.), humid zone (250–500 m a.s.l.) and very humid zone (>500 m a.s.l.). This classification is based on the bioclimatic zonation outlined by Rial et al. (2017), vegetation zones described by Ingala-Pronareg-Orstom. (1987) and isohyets for total seasonal rainfall developed by Trueman and D'Ozouville. (2010).

## Agriculture on Galápagos

Agriculture on the archipelago was initiated by the first colonizers during the 1800's (Perry, 1984) and has expanded over time. In 1959, the Galápagos National Park was created and 97% of the land area was declared protected national park area, with only 3% remaining for agriculture and human settlements (Guézou et al., 2010). In recent decades, agricultural land use within these 3% of land has intensified in order to meet the increasing demand for food of a growing resident population and flourishing tourism industry. Along with this, the use of mineral fertilizers and agrochemicals has increased (CGREG et al., 2014). A major challenge for agriculture on Galápagos is the limitation of freshwater during extended periods of drought, which may be further exacerbated in the future, as precipitation events governed by the *El Niño* phenomenon become increasingly irregular in response to changing global climatic patterns (Snell and Rea, 1999). Presently, a great variety of agricultural products can be encountered on the archipelago, including short cycle crops (grains and vegetables) and long cycle crops (fruits and sugarcane), along with several areas dedicated to grazing (Villa and Segarra, 2010). Most of the products are cultivated by hand without the use of heavy machinery and sold locally or grown for private consumption, aside from little exports of coffee (O'Connor Robinson et al., 2018).

## MATERIALS AND METHODS

### Soil Sampling

The 125 topsoil samples under investigation were collected in 2016 from areas designated for agricultural use (**Figure 1**) on the islands Isabela (26), Santa Cruz (46) and San Cristóbal (53). Bulk soil samples were drawn from a homogenized mixture of 15–20 subsamples per site, which were collected on a 2,500 m<sup>2</sup> plot from a depth of 0–20 cm. The bulk samples were air-dried and sieved to 2 mm. Additionally, undisturbed core samples were extracted in 250-cm<sup>3</sup> steel cylinders at approx. 10 cm soil depth at each site. The samples cover an elevation range of 146–920 m a.s.l. on Isabela, 130–572 m a.s.l. on Santa Cruz, and 176–604 m a.s.l. on San Cristóbal.

### Soil Physical Parameters

Volumetric gravel content (>2 mm) of soils with predominantly lapilli of <30 mm equivalent diameter was measured in graduated cylinders after separating the gravel from the fine earth fraction (<2 mm) by sieving. For soils with coarse fragments >30 mm, the gravel content was visually estimated in profile pits using field comparison charts. For bulk density (BD) determination, the material from the 250-cm<sup>3</sup> cylinders was weighed after oven-drying at 105°C. Soil macroaggregate stability (250–2000 µm) was tested by ultrasonic dispersion at a specific ultrasonic energy of 1500 J ml<sup>-1</sup> applied to a suspension containing 5 g of dried soil aggregates (1,000–2000 µm) in 200 ml of water. A commercial ultrasonic device (Bandelin Sonoplus HD 2200 with cylindrical ultrasonic probe V70) was used, and the degree of ultrasonic aggregate stability (USAS) was calculated according to Mentler et al. (2004) from the stable macroaggregates remaining. Water

retention at 30 and 1,500 kPa tension, respectively, was measured with a pressure membrane apparatus (Klute, 1986). Plant-available water (PAW) was calculated as the difference between the amount of water held at 30 kPa (field capacity) and 1,500 kPa (permanent wilting point), taking into account the sampling depth of 20 cm and the volumetric percentage of coarse fragments. Particle size distribution was determined using a combined sieve and pipette method as described by Soil Survey Staff. (2014). The unique nature of volcanic soils required various steps of pretreatments and dispersion techniques, which are detailed in Dinter et al. (2020).

### Soil Chemical Parameters

Electrical conductivity (EC) was measured in water extracts at a soil-to-solution ratio of 1:10, and soil pH was determined in H<sub>2</sub>O at a ratio of 1:1 and in 1 M sodium fluoride (NaF) at 1:50 (Soil Survey Staff, 2014). Total C and N was determined by dry combustion (Tabatabai and Bremner, 1991) and soil organic carbon (SOC) was calculated as the difference between total C and carbonate C determined gas-volumetrically according to Soil Survey Staff (2014). Phosphate retention was analyzed using the method of Blakemore et al. (1987). Iron contained in crystalline and non-crystalline hydrous Fe oxides was extracted using citrate-bicarbonate-dithionite (Fe<sub>c</sub>; Mehra and Jackson, 1958). Iron and aluminum associated with non-crystalline constituents was extracted using acid ammonium oxalate at pH 3 (Fe<sub>o</sub>, Al<sub>o</sub>; Schwertmann, 1964). Selected macro- and micronutrients (P, K, Ca, Mg, Na, Fe, Mn, Zn, Cu) were extracted with the Mehlich (III) method (Mehlich, 1984), and the extracted element concentrations were determined by inductively coupled plasma-optical emission spectroscopy (ICP-OES). It should be noted that the M3-extractable elements in the present study cannot be directly considered as plant-available due to the lack of on-site calibration with field experiments to determine the actual plant uptake. Nevertheless, the Mehlich (III) multiple-element extractant has proven its ability to produce relatively good correlations between extracted nutrients and plant response over a wide pH range (Zbiral, 2016). Cation exchange capacity (CEC) was estimated by summation of M3-extractable base cations plus exchangeable acidity (Ngewoh et al., 1989). Base saturation was calculated as the percentage of CEC occupied by base cations Ca<sup>2+</sup>, Mg<sup>2+</sup>, K<sup>+</sup> and Na<sup>+</sup> (Havlin, 2005). Exchangeable sodium percentage (ESP) was calculated by dividing exchangeable Na<sup>+</sup> by the sum of exchangeable cations and multiplying the result by 100 (Levy and Shainberg, 2005).

### Statistical Analyses

Statistical analyses were performed with R Studio software for Windows (version 3.4.3), except for the correlation graphs, which were elaborated in Microsoft Excel (Office 365). Descriptive statistics was displayed as boxplots showing arithmetic mean, median, upper and lower quartiles, minimum and maximum values, as well as outliers for each island separately. Principal component analysis (PCA) was carried out using the R package FactoMineR, where values were standardized prior to analysis to ensure standard deviation between 0 and 1. The factor scores of the individual islands were grouped into three elevation zones

**TABLE 1 |** Descriptive statistics (minimum, 25th percentile, median, mean  $\pm$  standard deviation, 75th percentile, maximum, skewness) of key soil properties on the three studied islands.

Island		pH in H <sub>2</sub> O	EC	BD	SOC	Al <sub>o</sub> +0.5Fe <sub>o</sub>	Fe <sub>d</sub>
		-	[ $\mu\text{S cm}^{-1}$ ]	[g cm <sup>-3</sup> ]	[%]	[%]	[g kg <sup>-1</sup> ]
Isabela (n = 26)	Min	5.7	167	0.34	4.97	2.22	13.7
	25th	6.2	314	0.38	12.11	3.51	30.8
	Median	6.5	376	0.55	16.39	4.14	42.0
	Mean $\pm$ SD	6.5 $\pm$ 0.5 c	393 $\pm$ 134 c	0.51 $\pm$ 0.12 a	15.92 $\pm$ 5.35 c	4.22 $\pm$ 1.22 c	39.7 $\pm$ 13.3 a
	75th	6.8	436	0.60	18.86	4.81	48.0
	Max	7.5	901	0.67	30.00	7.76	66.3
	Skew	0.35	2.11	-0.31	0.22	0.72	-0.07
Santa Cruz (n = 46)	Min	4.9	196	0.56	4.17	0.59	21.4
	25th	5.8	299	0.71	5.14	1.25	40.8
	Median	6.0	321	0.87	6.21	1.94	47.1
	Mean $\pm$ SD	6.0 $\pm$ 0.3 b	335 $\pm$ 73 b	0.83 $\pm$ 0.15 b	6.60 $\pm$ 2.02 b	2.36 $\pm$ 1.63 b	50.3 $\pm$ 13.4 b
	75th	6.1	374	0.94	7.41	2.78	59.8
	Max	6.9	607	1.09	12.43	8.74	75.9
	Skew	-0.35	1.19	-0.09	1.19	1.93	0.34
San Cristóbal (n = 53)	Min	3.9	105	0.62	1.83	0.29	26.0
	25th	4.8	174	0.84	4.04	0.45	53.1
	Median	5.7	206	0.90	4.35	0.58	63.6
	Mean $\pm$ SD	5.6 $\pm$ 0.8 a	221 $\pm$ 67 a	0.91 $\pm$ 0.11 c	4.49 $\pm$ 1.19 a	0.66 $\pm$ 0.36 a	62.9 $\pm$ 16.7 c
	75th	6.2	258	0.98	4.91	0.78	71.6
	Max	7.1	378	1.20	8.68	2.44	121.6
	Skew	-0.32	0.58	0.15	0.96	3.12	1.13

Island means with the same letter are not significantly different ( $\alpha = 0.05$ , ANOVA with post-hoc Tukey HSD). EC = electrical conductivity, BD = bulk density, SOC = soil organic carbon, Al<sub>o</sub>, Fe<sub>o</sub> = oxalate-extractable aluminum and iron, Fe<sub>d</sub> = dithionite-extractable iron

(<250, 250–500 and >500 m a.s.l.), as mentioned above. Many of the variables displayed a non-normal distribution and the skewness values ranged from -0.5 up to 5.3 in extreme cases, largely attributable to outliers. As outliers can convey important information about the data, we decided to keep them in the dataset and include them in all the calculations. Therefore, we used Spearman's rank correlation coefficient, which is not unduly influenced by skewness. The corresponding correlation tables are enclosed in **Supplementary Tables S3–S5**.

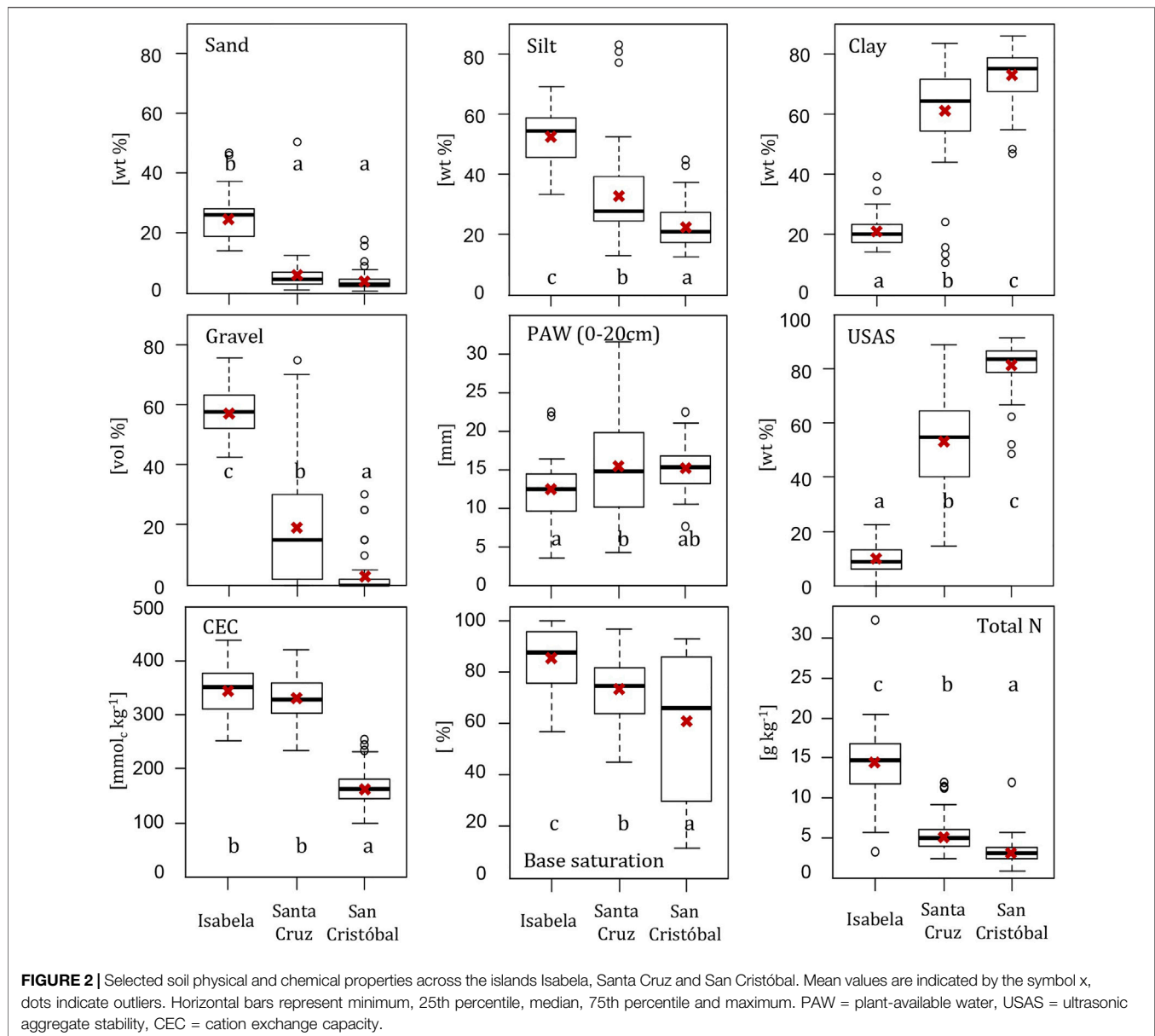
The hotspot distances of the respective sampling sites were calculated by spatial distance measurements in ArcMap 10.6.1 based on the location of the hotspot center as estimated by Hooft et al. (2003) (s. **Figure 1**). Maps displaying the spatial distribution of the analyzed soil parameters on each island are shown in **Supplementary Figures S1–S24**. These maps were elaborated using ArcMap 10.6.1 for Windows. All data displayed in the maps were classified using natural breaks.

## RESULTS

### Basic Soil Physical and Chemical Properties

The results of the physical and chemical analyses are shown in **Table 1** and **Figure 2**, with maps showing their spatial distribution on the studied islands enclosed in **Supplementary Figures S1–S15**. Descriptive statistics and Spearman's rank correlation coefficients are enclosed in **Supplementary Tables S1, S3–S5**, respectively. The soils became finer-textured with increasing island age. On the youngest studied island, Isabela, the soils had high gravel and sand contents and prevailing silt loam texture, while on the intermediate-aged and oldest studied

islands, Santa Cruz and San Cristóbal, respectively, gravel contents were much lower and the soils more clayey. Nevertheless, the existence of outliers, reflecting local heterogeneity within the islands should be noted. Soil BD increased with increasing island age from a mean of 0.51 g cm<sup>-3</sup> on the youngest island, to means of 0.83 and 0.91 g cm<sup>-3</sup> on the intermediate-aged and oldest island, respectively. Moreover, BD was negatively correlated with elevation on the youngest island, Isabela ( $r_s = -0.46$ ,  $p < 0.05$ ; **Supplementary Table S4**). Soil pH and EC decreased with increasing island age from 6.5 to 5.6 and from 393 to 221  $\mu\text{S cm}^{-1}$  (mean values), respectively. SOC varied between 5 and 30% (mean: 16%) on the youngest island, while on the oldest island, SOC was <5% for most of the tested samples. On the intermediate-aged island, Santa Cruz, we found SOC levels between 4 and 12%. Similarly, total N strongly decreased with increasing hotspot distance ( $r_s = -0.77$ ,  $p < 0.001$ , **Supplementary Table S3**), showing island means of 14.5 g kg<sup>-1</sup> on Isabela, 5.7 g kg<sup>-1</sup> on Santa Cruz and 3.3 g kg<sup>-1</sup> on San Cristóbal. PAW content of the studied topsoils (0–20 cm) increased only slightly with island age, while soil macroaggregate stability (USAS) increased strongly with hotspot distance ( $r_s = 0.79$ ,  $p < 0.001$ , **Supplementary Table S3**), from an island mean of 9.6% on Isabela to 81.2% on San Cristóbal. CEC was similar for islands Isabela (mean: 348 mmol<sub>c</sub> kg<sup>-1</sup>) and Santa Cruz (332 mmol<sub>c</sub> kg<sup>-1</sup>) but significantly lower on the oldest studied island, San Cristóbal (165 mmol<sub>c</sub> kg<sup>-1</sup>). Base saturation tended to decrease with increasing island age, although the wide interquartile range on San Cristóbal indicates a high level of heterogeneity. The andic indicator Al<sub>o</sub>+0.5Fe<sub>o</sub> decreased with increasing island age, showing mean values above the andic

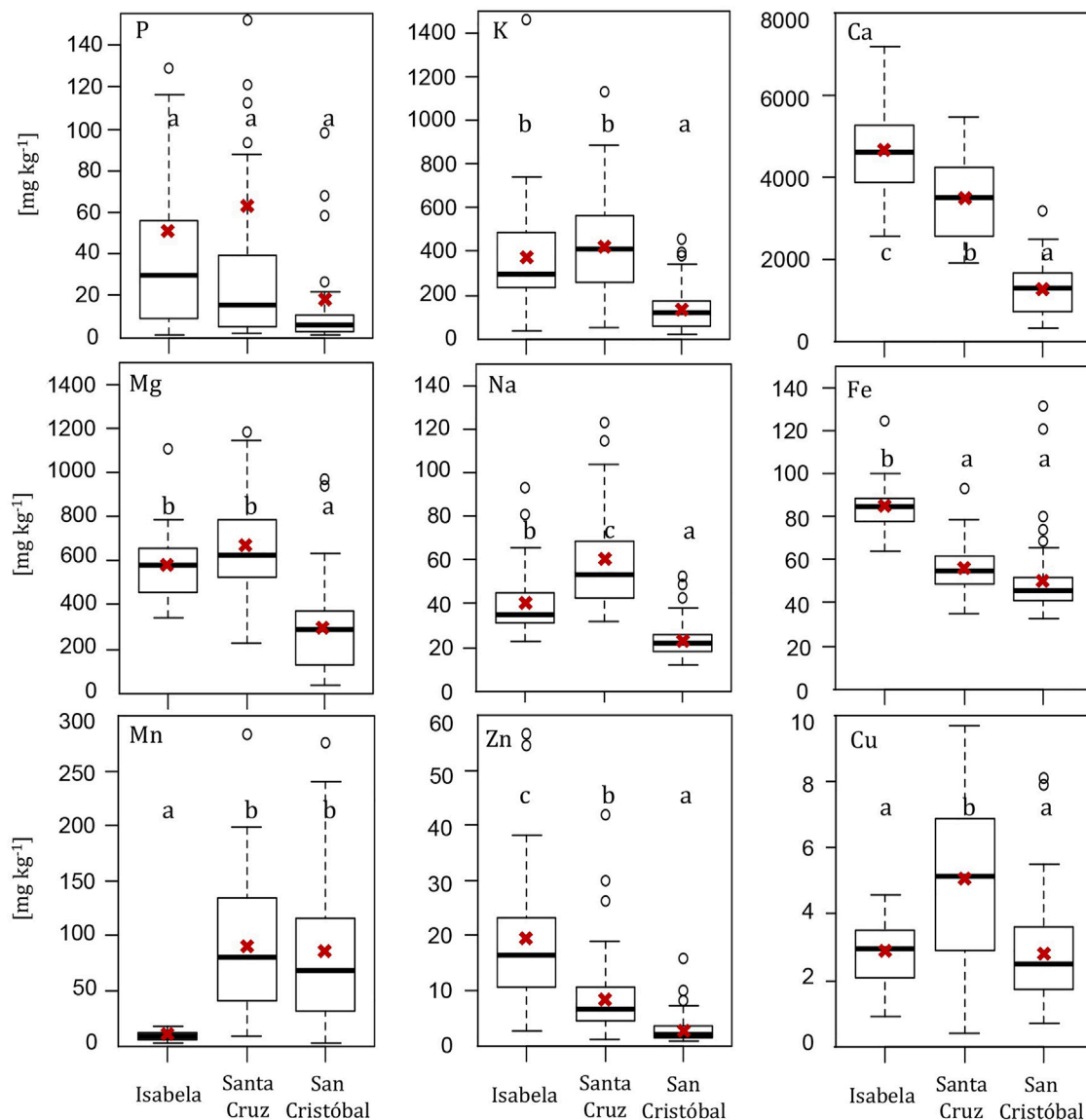


threshold level of  $\geq 2\%$  (IUSS Working Group WRB, 2015) on the youngest and intermediate-aged islands, while for the oldest studied island, San Cristóbal,  $Al_0 + 0.5Fe_0$  was clearly below this level (mean: 0.66%). Conversely, iron contained in hydrous iron oxides ( $Fe_d$ ) increased with island age, reaching a maximum of  $121.6 \text{ g kg}^{-1}$  (mean:  $62.9 \text{ g kg}^{-1}$ ) on San Cristóbal.

### Mehlich(III)-Extractable Elements

The M3-extractable concentrations of macro- and micronutrients are presented in **Figure 3**, and their spatial distribution on the studied islands is shown in **Supplementary Figures S16–S24**. Descriptive statistics and Spearman's rank correlation coefficients are enclosed in **Supplementary Tables S2, S3–S5**, respectively. The island means of K and Mg were significantly higher on Isabela and Santa Cruz compared to

San Cristóbal. M3-extractable Ca, Fe and Zn showed a decreasing trend with increasing island age (correlations with hotspot distance: Ca:  $r_s -0.74$ , Fe:  $r_s -0.64$ , Zn:  $r_s -0.63$ ;  $p < 0.001$ ; **Supplementary Table S3**), although the difference of Fe mean values for Santa Cruz and San Cristóbal was not significant (**Figure 3**). The means of M3-extractable P on the three studied islands were not significantly different from one another, and extreme outliers were detected especially on Santa Cruz Island. However, we found decreasing P median values from the youngest to the oldest studied island and a generally decreasing trend with increasing hotspot distance (P:  $r_s -0.27$ ,  $p < 0.01$ ; **Supplementary Table S3**). Although M3-extractable Na concentrations decreased between the youngest (median:  $35.0 \text{ mg kg}^{-1}$ ) and oldest (median:  $22.0 \text{ mg kg}^{-1}$ ) island, we detected highest



**FIGURE 3 |** Mehlich (III)-extractable element concentrations across the islands Isabela, Santa Cruz and San Cristóbal. Mean values are indicated by the symbol x, dots indicate outliers. Horizontal bars represent minimum, 25th percentile, median, 75th percentile and maximum. For P, five extreme outliers are not displayed in the boxplot: 423 mg kg<sup>-1</sup> on Isabela, 573 and 1,036 mg kg<sup>-1</sup> on Santa Cruz, and 213 and 222 mg kg<sup>-1</sup> on San Cristóbal.

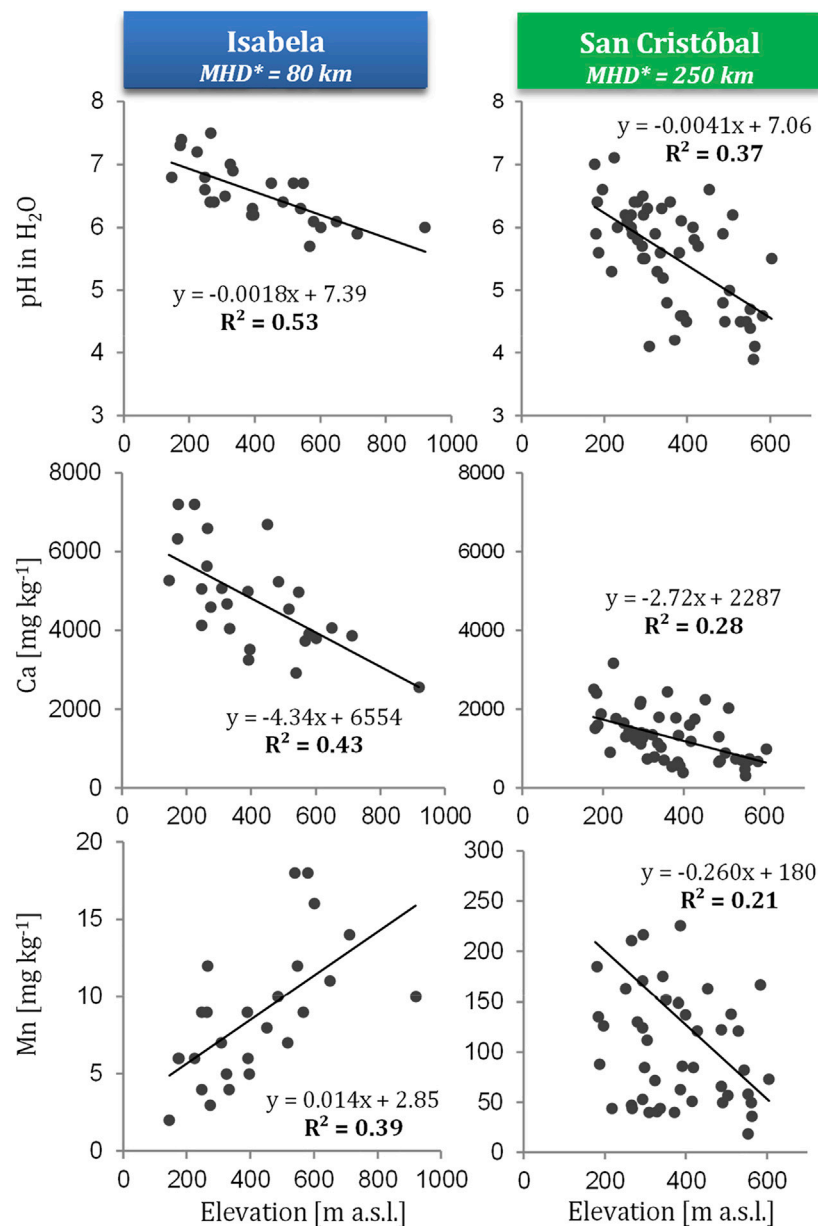
concentrations on the intermediate-aged island, Santa Cruz (median: 53.5 mg kg<sup>-1</sup>). Likewise, M3-extractable Cu was elevated on Santa Cruz Island (median: 5.2 mg kg<sup>-1</sup>, compared to 3.0 mg kg<sup>-1</sup> and 2.5 mg kg<sup>-1</sup> on the islands Isabela and San Cristóbal, respectively). By contrast, M3-extractable Mn was much lower (median: 8.5 mg kg<sup>-1</sup>) on the youngest studied island, compared to the intermediate-aged (81.5 mg kg<sup>-1</sup>) and oldest studied island (68.0 mg kg<sup>-1</sup>).

The altitudinal trends of M3-extractable Ca and Mn on the youngest and oldest studied islands are displayed along with soil pH in **Figure 4**. Correlations of all studied M3-extractable elements with elevation are shown in **Supplementary Tables S4, S5**. M3-extractable Ca followed the altitudinal trends of soil

pH and decreased with increasing elevation for both islands (Isabela:  $r_s = -0.70$ , San Cristóbal:  $r_s = -0.57$ ,  $p < 0.001$ ; **Supplementary Tables S4, S5**). Conversely, M3-extractable Mn increased with increasing elevation on the youngest island, Isabela, while it decreased on the oldest island, San Cristóbal. M3-extractable Cu decreased only slightly with increasing elevation on Isabela ( $r_s = -0.46$ ,  $p < 0.05$ ; **Supplementary Table S4**), but more strongly on San Cristóbal ( $r_s = -0.69$ ,  $p < 0.001$ ; **Supplementary Table S5**).

## Principal Component Analysis

The results of principal component analyses (PCAs) performed with the M3-extractable element data are shown in **Figure 5**.



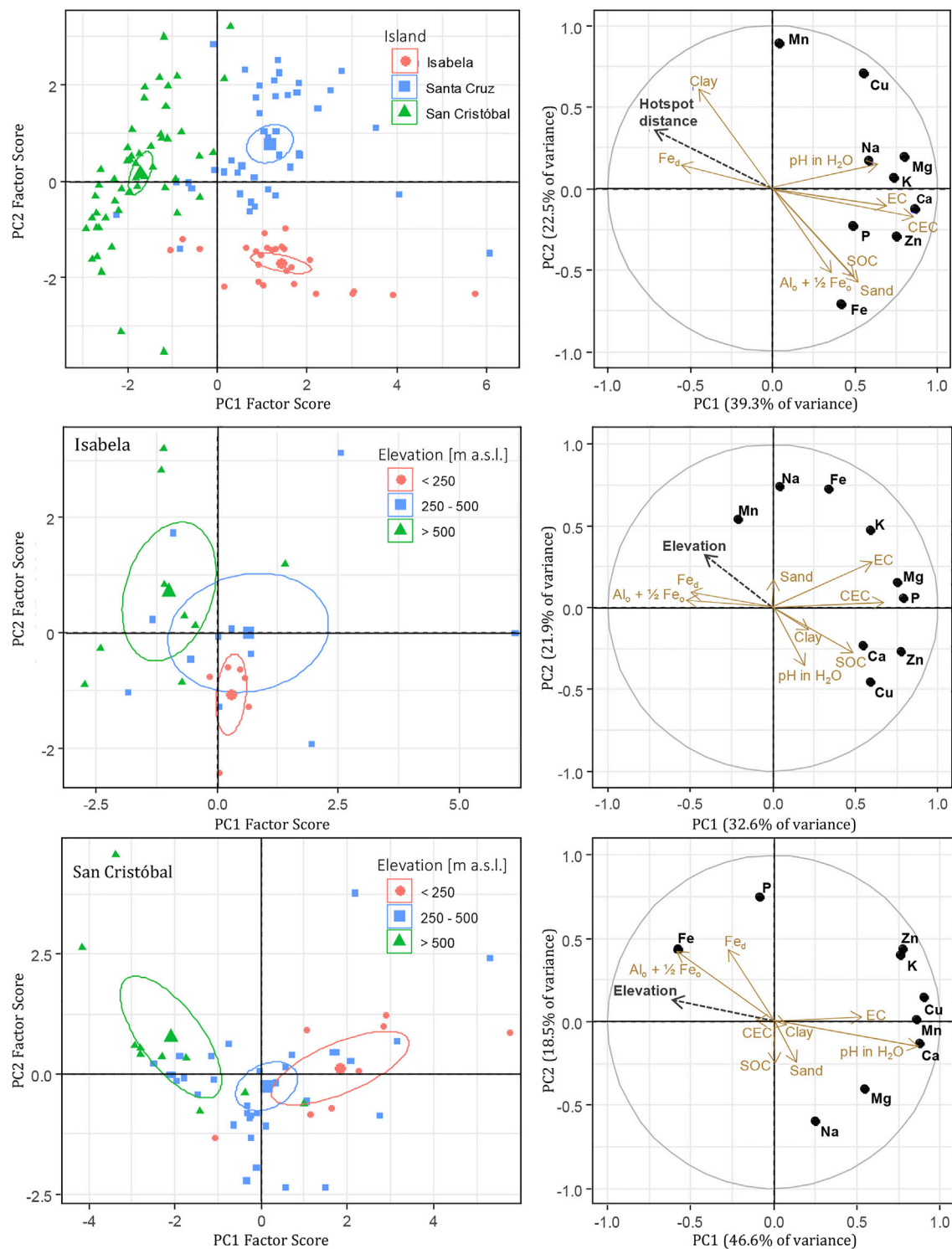
**FIGURE 4** | Altitudinal trends in soil pH and Mehlich (III)-extractable Ca and Mn for the islands Isabela and San Cristóbal. MHD = mean hotspot distance (horizontal distance of sampling points from the hotspot center as estimated by Hooft et al., 2003); m a.s.l. = meters above sea level.

Differences between the studied islands were investigated in a PCA based on element data from all islands (Figure 5, top), while trends within the youngest island, Isabela (Figure 5, middle), and the oldest island, San Cristóbal (Figure 5, bottom), were investigated in separate PCAs based on element data of the respective islands and grouping into three elevation zones. Hotspot distance, elevation and additional soil properties were included as supplementary variables to help identify potential drivers of the observed patterns.

The all-island PCA showed a segregation of the oldest island, San Cristóbal (negative scores), from the other two islands (positive scores) along PC1, and a segregation of the youngest

island, Isabela (negative scores), from the other two islands (dominantly neutral to positive scores) along PC2 (Figure 5, top left). PC1 (39.3% of variance) was directly related to soil pH, EC and CEC, and inversely related to hotspot distance and Fe<sub>d</sub>. It showed positive loadings for all studied M3-extractable elements, with particularly high loadings for Ca, Mg, K and Zn. PC2 (22.5% of variance) was directly related to clay content and inversely related to sand content, SOC and Al<sub>0</sub>+0.5Fe<sub>0</sub>. It displayed the highest positive loadings for micronutrients Mn and Cu and a high negative loading for Fe.

In the PCAs of the youngest and oldest studied islands, Isabela and San Cristóbal, respectively, the three elevation zones were



**FIGURE 5 |** Principal component analyses based on Mehlich (III)-extractable element concentrations for all studied islands (**top**), Isabela (**middle**) and San Cristóbal (**bottom**). Enlarged symbols and ellipses in the factor scores plots (**left side**) indicate means and 95% confidence intervals, respectively. The right side displays the loadings of the Mehlich (III)-extractable element concentrations (dots) and relationships with other parameters (arrows). EC = electrical conductivity, CEC = cation exchange capacity, SOC = soil organic carbon, Fe<sub>d</sub> = dithionite-extractable iron, Al<sub>o</sub> and Fe<sub>o</sub> = oxalate-extractable aluminum and iron; m a.s.l. = meters above sea level.

segregated with some overlap of their 95% confidence intervals, and their arrangement in the scores plots broadly corresponded to the direction of the factor elevation shown in the loadings plots (**Figure 5**, middle and bottom). For Isabela, PC1 (32.6% of variance) was directly related to EC and CEC, and inversely related to elevation,  $Al_o+0.5Fe_o$  and  $Fe_d$ . It showed positive loadings for most of the M3-extractable elements except for Mn. For San Cristóbal, PC1 (46.6% of variance) was directly related to soil pH and EC, and inversely related to elevation and  $Al_o+0.5Fe_o$ . It showed high positive loadings for Ca, K, Mn, Cu and Zn, and a negative loading for Fe. PC2 (21.9% of variance for Isabela, 18.5% for San Cristóbal) was little related to any of the tested supplementary variables and showed an inconsistent picture in the factor loadings for the two islands, e.g. Na had a high positive loading for Isabela and the opposite loading for San Cristóbal.

## DISCUSSION

### Trends With Island Age

Our results indicate marked pedogenic development along the studied island chain, resulting in strong differences in fertility parameters between the volcanic topsoils of our study. Soil texture and gravel content exhibited very pronounced changes, with particle sizes sharply decreasing with increasing distance from the volcanic hotspot (**Figure 2**). Soils formed on basaltic parent materials often show high concentrations of volcanic glass in the early stage and rapid neoformation of clay-sized, poorly crystalline materials in the subsequent weathering stage (e.g., Chorover et al., 2004; Mikutta et al., 2009). Similar trends of rapidly increasing clay contents with soil age have been reported by several studies on the development of volcanic soils under different climatic conditions, including Lowe (1986), Jahn et al. (1987), Delvaux et al. (1989) and Zehetner and Miller (2006). Soil BD changed from very low values (mean:  $0.51 \text{ g cm}^{-3}$ ) on the youngest studied island, Isabela, to higher values on the intermediate and oldest island (means: 0.83 and  $0.91 \text{ g cm}^{-3}$ , respectively; **Table 1**). Our findings are broadly comparable to those reported for Hawaii. For example, Chadwick et al. (2003) mainly observed low BD values ( $<0.5 \text{ g cm}^{-3}$ ) in the upper layers of soils developed on young lava flows, while higher BD values (mean:  $1.25 \text{ g cm}^{-3}$ ) have been reported for older, kaolinitic soils in Hawaii (Santo and Tsuji, 1977).

SOC and total N contents were extraordinarily high on the youngest island, Isabela (means: 15.9% and  $14.5 \text{ g kg}^{-1}$ , respectively; **Figure 2** and **Table 1**) which is characteristic of soils formed on young volcanic parent materials (Shoji et al., 1993; Nanzyo, 2002), and subsequently decreased with increasing soil age. The pronounced accumulation of soil organic matter (SOM) on Isabela Island is probably due to protective effects by non-crystalline constituents (mean  $Al_o+0.5Fe_o$ : 4.22%; **Table 1**), as pointed out by Torn et al. (1997) for Hawaiian soils. The slight increase in PAW with island age may be related to increases in clay content and Fe oxides (**Figure 2**; **Table 1**). Nevertheless, comparatively high PAW was also found in the young soils of Isabela Island (mean: 12.5 mm in 0–20 cm depth) despite

relatively low clay contents (mean: 21.4%) compared to Santa Cruz (60.7%) and San Cristóbal (72.8%). Possible explanations for this could be the aforementioned accumulation of SOM and abundance of non-crystalline materials as well as the high porosity in the young Andosols, properties that have been reported beneficial for water retention (Delmelle et al., 2015). Also, Jahn and Stahr (1996) reported higher PAW contents (20 vol%) in approx. 6-ka-old Andosols on Lanzarote Island compared to older polygenetic soils (40 ka; 10–20 vol%).

The pronounced increase in macroaggregate stability (USAS) observed in our study paralleled increasing clay and Fe oxide ( $Fe_d$ ) contents with island age, but opposed the trends observed for SOC and non-crystalline constituents ( $Al_o+0.5Fe_o$ ) across the three studied islands (**Figure 2**; **Table 1**). SOM and non-crystalline materials have been found beneficial for soil micro- and macroaggregate stability in many cases (e.g., Tisdall and Oades, 1982; Shoji et al., 1993). However, in our study, the stabilizing effects of these soil constituents could not be verified for macroaggregates (250–2000  $\mu\text{m}$ ) subjected to high ultrasonic energy levels ( $1500 \text{ J ml}^{-1}$ ). Our results rather suggest that macroaggregate stability in the studied topsoils is enhanced by bonding among and between crystalline Fe oxides and clay particles (Six et al., 2000). Indeed, we observed the formation of a pseudo-sand microstructure in soils of the oldest studied island, San Cristóbal, which is a typical feature in highly weathered, oxide-rich soils (IUSS Working Group WRB, 2015).

The significantly lower CEC levels in the soils of San Cristóbal, compared to the younger islands (**Figure 2**) could be attributable to changes in clay mineralogy from non-crystalline constituents such as allophanes to low-activity clays, notably kaolinite (Candra et al., 2021) and increasing crystallinity of Fe oxides (Dinter et al., 2020) providing less surface area (Sollins et al., 1988), in addition to decreasing pH and declining SOM contents with increasing soil age. Similarly, high CEC levels in young Andosols on Lanzarote Island have been linked to the formation of non-crystalline weathering products and the accumulation of humic substances in the early stage of soil formation (Jahn and Stahr, 1996). In our study, the soils' base saturation dropped in conjunction with pH and EC (**Figure 2**; **Table 1**), which reflects the progressive leaching of base cations with soil age and increasing hotspot distance, as also shown along component 1 in the PCA (**Figure 5**, top).

Concentrations of M3-extractable Ca decreased significantly with increasing island age (**Figure 3**), likely due to the element's high mobility and the continuous exposure to leaching processes. Rapid dissolution of non-hydrolyzing cations (e.g., Ca, Mg) in the early weathering stages of volcanic parent materials and subsequent leaching was also observed in a chronosequence in Hawaii (Chorover et al., 2004). Even though the base cations Mg, K and Na showed a decreasing tendency between the youngest and oldest island, the highest mean values were observed for the intermediate-aged island, Santa Cruz, which was most strongly pronounced (and statistically significant) for M3-extractable Na. This circumstance may be attributable to irrigation with brackish water containing high levels of dissolved salts, which is a widespread practice on that island. Also, the application of fertilizers and the common use of agrochemicals may be reflected in the

distribution of M3-extractable Mg, K, P, and especially Cu along and within the islands, showing highest mean values and considerable outliers on Santa Cruz Island. A recent census report points out that Santa Cruz is the most intensively farmed island of Galápagos, with almost twice as much annual expenditures on fertilizers and pesticides as on Isabela and San Cristóbal Island combined (CGREG et al., 2014). M3-extractable Zn showed a sharp decrease with increasing island age similar to Ca, which is probably related to the relatively high mobility and progressive leaching of Zn associated with lower soil pH values (Adriano, 2001), especially on the oldest studied island. Also M3-extractable Fe progressively decreased with increasing island age, while dithionite-extractable Fe sharply increased (**Figure 3; Table 1**). This is because the M3 reactant extracts only a fraction of Fe that corresponds to available and soluble Fe (Marcos et al., 1998) but does not extract crystalline Fe forms. The comparatively low concentrations of M3-extractable P on the oldest studied island, San Cristóbal (**Figure 3**), are probably related to its increasing occlusion in Al and Fe oxides (Walker and Syers, 1976). In addition, Rechberger et al. (2021) recently showed that increasing acidification enhanced phosphate retention in highly weathered Galápagos topsoils ( $\geq 165$  ka). In contrast to the other M3-extractable elements, the levels of Mn were very low on the youngest studied island, Isabela, probably due to the soils early weathering stage with limited release of Mn from primary minerals, while this element became more available on the older islands (**Figure 3**).

Results from PCA based on M3-extractable element data from all islands (**Figure 5**, top) further illustrate the observed trends with soil age. Notably, the factor loadings of the mobile base cations Ca, Mg, K, Na and additionally Zn were located opposite of the factor hotspot distance on PC1. Furthermore, the PCA results suggest that the observed segregation between San Cristóbal and the two younger islands on PC1 may be influenced by substantial differences in key soil properties on the oldest studied island. In particular, decreased pH and CEC levels and the transition from amorphous to crystalline Fe forms as a consequence of progressing pedogenic development may have contributed to the reduced overall nutrient availability on San Cristóbal.

## Trends With Elevation/Climate

While soil physical characteristics did not show any clear trends with elevation in the agricultural zones of the three studied islands (data not shown), soil pH (and, hence, base saturation; data not shown) and several of the M3-extractable nutrients varied significantly with altitude (**Figure 4, Supplementary Tables S4, S5**), which is likely an effect of altitudinal variations in precipitation. For all three of the studied Galápagos islands, soil pH decreased with increasing elevation, which is likely attributable to enhanced leaching of base cations and, in case of the older islands, also to the solubilization of Al, driven by the humid moisture regime in the highlands (Vitousek and Chadwick, 2013). Furthermore, enhanced soil weathering with elevation is also indicated by increasing Fe oxide content, as Dinter et al. (2020) found dithionite-extractable Fe ( $\text{Fe}_d$ ) in correspondence with the

highest elevation group ( $>500$  m a.s.l.) factor scores in their PCA of all three islands.

The elemental assemblage of a particular soil depends on the degree of soil development, the respective mobility of the elements and the specific environmental conditions (Martínez Cortizas et al., 2003), hence, a complex interplay of several factors. This was also shown in the present study when comparing the trends of M3-extractable Ca and Mn along the altitudinal gradients of the youngest and oldest studied islands, Isabela and San Cristóbal, respectively (**Figure 4, Supplementary Tables S4, S5**). M3-extractable Ca decreased with increasing elevation on both islands, which is likely reflective of its enhanced leaching owing to rising precipitation levels with altitude. Similar findings on the depletion of mobile base cations have been reported for climate gradients in New Zealand (Dixon et al., 2016) and Hawaii (Vitousek and Chadwick, 2013). By contrast, M3-extractable Mn showed very distinct patterns for Isabela and San Cristóbal. On the youngest studied island, M3-extractable Mn was at a very low level (mean:  $8.7 \text{ mg kg}^{-1}$ ) but became increasingly available with elevation and increasing precipitation likely due to weathering-induced release from primary minerals. On the oldest studied island, where primary minerals have largely been weathered, M3-extractable Mn levels were much higher (mean:  $85.8 \text{ mg kg}^{-1}$ ) but decreased with increasing elevation, likely due to long-term leaching losses under acidic conditions. On the oldest studied island, San Cristóbal, most of the M3-extractable element concentrations (K, Ca, Mg, Na, Mn, Zn and Cu) decreased significantly with increasing elevation, while M3-extractable Fe increased significantly ( $r_s$  0.68,  $p < 0.001$ ; **Supplementary Table S5**). This is probably related to the low pH values on San Cristóbal (25th percentile of soil pH in  $\text{H}_2\text{O}$ : 4.8), particularly pronounced at higher elevations (**Figure 4**). The acidic conditions in conjunction with the humid environment likely enhance the availability of (M3-extractable) Fe. Significant negative correlation between M3-extractable Fe and soil pH was also found in a series of very heterogeneous soils (pH 2.7–8.4) of northwest Spain (Marcos et al., 1998). Results from PCA based on M3-extractable element data of the individual islands (**Figure 5**, middle and bottom) highlight the different mobility of the elements across the studied elevation/climate zones. In the case of Ca, the factor loadings were opposed to the factor elevation for both islands, while the factor loadings of Mn were opposed to the factor elevation only for San Cristóbal but closely related to elevation for Isabela Island.

When investigating the effects of climate on soil formation and soil (fertility) parameters, past climate variations need to be considered, especially for the older islands Santa Cruz and San Cristóbal. Vitousek and Chadwick (2013) suggested paleoclimates to be potentially influential on observed differences in soil geochemistry on the Hawaiian archipelago. Findings from pollen analysis in sediments of El Junco crater lake on San Cristóbal suggest that the soils of the Galápagos archipelago have been subjected to long dry periods broadly corresponding to glaciation in the northern hemisphere, interrupted by moister periods during interglacial times (Colinvaux, 1972). However, in our study, differences in soil

parameters related to island age clearly outweigh climate-driven altitudinal variations within the agricultural zones.

## Implications for Soil Functioning and Sustainable Agricultural Management

In the preceding sections, we reported about pronounced soil differences depending on island age and climate zone, which affect soil functioning and entail distinct implications for agricultural management. Moreover, climate change is predicted to lead to moister conditions on the archipelago (Rial et al., 2017), probably causing a downward expansion of the humid zone into currently drier areas. Increased precipitation levels may lead to enhanced nutrient leaching, and more extreme weather events could increase the risk of drought and soil erosion. Profound knowledge of the soil properties on the different Galápagos islands is therefore essential not only to ensure the sustainability of current land management and prevent soil degradation, but also to better adapt to changing conditions in the future.

In the following sections, implications for soil functioning and sustainable agricultural management are derived from the studied soil parameters for the three islands under investigation. For M3-extractable elements, different classifications of critical concentrations of macro- and micronutrients have been proposed (e.g., Zhang et al., 2014; Zbiral, 2016). Application of such critical concentrations to the agricultural soils of Galápagos must be conducted with caution, because they may vary according to soil type, climate and crop to be grown (Zhang et al., 2014) and should ideally be calibrated with field experiments to assess plant responses. Nevertheless, they may still be useful for relative comparisons between the islands and to put the results from Galápagos into a broader context.

### Isabela Island (Young Soils)

The agricultural soils of Isabela show features commonly found in young volcanic soils and generally favorable for crop production (Wada, 1985; Shoji et al., 1993). These include high SOC contents (mean: 15.9%), silt loam texture, low BD (mean:  $0.51 \text{ g cm}^{-3}$ ) and, hence, high porosity. Topsoil PAW on Isabela Island (mean: 12.5 mm in 0–20 cm depth) was similar as for the older studied islands. However, less solum thickness (20–50 cm) compared to the other islands (Zehetner et al., 2020) may represent restrictions for water availability and agricultural production in some areas of Isabela. Nevertheless, in many cases, plant roots can reach the frequently encountered underlying paleosols for additional water and nutrient supply on this island (Zehetner et al., 2020). The high porosity of Isabela's soils implies the risk of leaching losses of nutrients as well as agrochemical residues and other contaminants. High gravel contents consisting mainly of scoriaceous lapilli (mean: 57.5%) further contribute to high hydraulic conductivity but may also reduce the risk of soil compaction (Rücknagel et al., 2013). As a consequence of the comparatively low macroaggregate stability, the agricultural soils of Isabela Island are likely more prone to erosion (by water and wind) compared to the other studied islands. This is especially important in the face of climate change with increasing magnitudes of extreme events, and calls for adaptation measures to prevent soil erosion.

Total N (mean:  $14.5 \text{ g kg}^{-1}$ ) was significantly higher on Isabela than on the other islands, probably related to the high SOC contents. However, the mineralization of organic matter and subsequent release of available N is probably limited by strong SOM stabilization due to high amounts of non-crystalline constituents in the young Andosols (Torn et al., 1997). The M3-extractable base cations Ca, Mg and K are rated high for the great majority of samples from Isabela Island according to Zhang et al. (2014). The relatively high pH (mean: 6.5 in  $\text{H}_2\text{O}$ ) and base saturation (mean: 84.9%) in conjunction with high CEC (mean:  $348 \text{ mmol}_c \text{ kg}^{-1}$ ) indicate high acid buffering and nutrient retention capacity. A decrease of soil pH along with (leaching) losses of M3-extractable Ca was observed for higher elevations on Isabela Island, while Mn became more readily available with elevation (Figure 4). Nevertheless, M3-extractable Mn is rated low in all soils of Isabela according to Zbiral (2016), while Cu levels are, on average, rated medium and Zn levels high. Interestingly, M3-extractable Fe concentrations are rated medium for all analyzed samples from Isabela (mean:  $85.1 \text{ mg kg}^{-1}$ ), but are, on average, rated low for the older studied islands. We assume that the higher availability of Fe on Isabela, in spite of comparatively high soil pH, is related to the fact that Fe occurs predominantly in amorphous oxides and organic compounds in the young Andosols of this island, while crystalline Fe oxides prevail on the older islands (Candra et al., 2021). Although strong P sorption is reported to be one of the major factors limiting plant growth in young volcanic soils (Dahlgren et al., 2004), M3-extractable P levels in the agricultural soils of Isabela are rated low for 42% of the studied soils but medium to high for the majority of the soils (Zhang et al., 2014). This is likely attributable to the relatively high pH values of these soils. Indeed, many studies reported P availability to peak at pH 6.5 (Penn and Camberato, 2019). Nevertheless, fertilization recommendations should account for potentially strong sorption of phosphate to non-crystalline materials in young volcanic soils, as recently shown by Rechberger et al. (2021) also for topsoils of Isabela Island.

### Santa Cruz Island (Intermediate-Aged Soils)

Many of the investigated soil parameters displayed relatively high variability for Santa Cruz, reflecting the island's intermediate position with volcanic deposits ranging from approx. 25 to 200 ka on the southern flank (White et al., 1993; Schwartz, 2014), where the agricultural zone is located. We found very heterogeneous soil texture, rather low BD (mean:  $0.83 \text{ g cm}^{-3}$ ), medium to high macroaggregate stability, high CEC (mean:  $332 \text{ mmol}_c \text{ kg}^{-1}$ ) and, on average, high levels of most of the studied M3-extractable nutrients (K, Ca, Mg, Zn, Cu). Topsoil PAW (mean: 15.8 mm in 0–20 cm depth) showed marked spatial variation, as displayed in **Supplementary Figure S7**, which is likely associated with the strong heterogeneity of the soil parent materials (i.e. a mosaic of different lava flows and scoria deposits of varying ages) and, hence, large variations in gravel content and soil texture on this island (Figure 2). Also, the soils macroaggregate stability varied widely, but was considerably higher than on the youngest island, indicating no imminent risk of erosion for most of the studied

soils, although the steep slopes of some highland farms near Cerro Crocker (Adelinet et al., 2008) may benefit from measures to stabilize the soil surface against erosion. SOC and total N contents (means: 6.6% and 5.7 g kg<sup>-1</sup>, respectively) as well as soil pH (mean: 6.0 in H<sub>2</sub>O) and base saturation (mean: 73.1%) were significantly lower than on Isabela Island, but still relatively high and conducive to productive agriculture.

As Santa Cruz is the agriculturally most intensively used island of the archipelago (CGREG et al., 2014), extreme outliers of M3-extractable P and Zn as well as the observed peak in M3-extractable Cu among the three islands (mean: 5.1 mg kg<sup>-1</sup>) may be related to agrochemical inputs, especially to the application of phosphate fertilizers and fungicides (Oorts, 2013; Cabral Pinto et al., 2015; Dinter et al., 2021). Elevated levels of M3-extractable Na, Mg and K, compared to the other studied islands, were observed in soils irrigated with brackish water on Santa Cruz. The highest EC values measured in the soils of Santa Cruz (max: 607  $\mu\text{S cm}^{-1}$  in 1:10 water extracts; **Table 1**) indicate a beginning threat of salinization, as EC threshold levels (in saturated soil extracts) range from 1,000 to 2,500  $\mu\text{S cm}^{-1}$  for the majority of vegetables (Almeida Machado and Serralheiro, 2017). On the other hand, the exchangeable sodium percentages in these soils (ESP max: 3.82%; **Supplementary Table S1**) do not indicate pronounced sodicity, as ESP values of >15% would be required to classify soils as sodic (USSS Staff, 1954). M3-extractable concentrations of Fe (mean: 55.7 mg kg<sup>-1</sup>, 75th percentile: 61.3 mg kg<sup>-1</sup>) were significantly lower compared to Isabela Island and are, on average, classified as low according to Zbiral (2016), which is probably related to progressing pedogenesis and crystallization of Fe oxides with island age. Moreover, levels of M3-extractable P (median: 15.5 mg kg<sup>-1</sup>) are rated low for the majority of the studied soils on Santa Cruz (Zhang et al., 2014). Hence, nutrient management strategies should especially target Fe and P in these soils. Besides their addition via fertilizers and/or manure, also mobilization strategies should be considered. Mobilization of P from inorganic compounds could be achieved, for instance, by increasing the ion competition on the sorption complex (exchangeable P) through the application of silicic acid (Schaller et al., 2020), and by cover-cropping P-capturing plants (e.g., buckwheat, lupine; Hallama et al., 2019), while biofertilization (e.g., with *Bacillus megaterium* phosphaticum) has been reported to facilitate microbial P solubilization from organic compounds (Alori et al., 2017). In addition, organic anions from dissolved organic matter can compete with phosphate ions for sorption sites and thereby increase plant-availability of P (Iyamuremye et al., 1996). Manipulating the rhizosphere (e.g. via water regulation, root fertilization) and crop management strategies such as intercropping and enhanced crop varieties may be promising measures to address Fe deficiencies in the respective soils (Zuo and Zhang, 2011).

### San Cristóbal Island (Old Soils)

The studied soils of San Cristóbal showed typical features of highly weathered soils, including clayey texture (mean clay content: 72.8%) with little gravel remaining, high macroaggregate stability, rather low pH (in H<sub>2</sub>O; mean: 5.6, 25th percentile: 4.8) and base saturation (mean: 59.3%, 25th percentile: 30.1%),

as well as lower SOC and total N contents (means: 4.5% and 3.3 g kg<sup>-1</sup>, respectively) compared to the younger and intermediate-aged islands. Soil BD was higher compared to the islands Isabela and Santa Cruz, but still predominantly <1 g cm<sup>-3</sup> and, hence, relatively low and indicative of high porosity. This, and the high macroaggregate stability (**Figure 2**) related to the commonly found pseudo-sand structure in these soils (IUSS Working Group WRB, 2015) are likely to contribute to rapid water infiltration and percolation in spite of the very high clay contents, which reduces the risk of surface runoff and soil erosion. The clayey soils of San Cristóbal Island are inherently more prone to compaction through heavy machinery or intensive grazing than the soils of the younger and intermediate-aged islands. However, such management practices are currently not common on the Galápagos Islands. The soils CEC (mean: 165 mmol<sub>c</sub> kg<sup>-1</sup>) was significantly lower than on the other studied islands, which entails reduced nutrient retention and acid buffering capacity. Aluminum toxicity in soil may occur at pH < 5.5 (Evans and Kamprath, 1970), which was found for many soils of San Cristóbal, in particular in the humid highlands of this island.

The advanced weathering stage of San Cristóbal's soils has significant implications for their nutrient status. Our results show that (M3-extractable) nutrient availability has been lowered compared to the younger studied islands, probably through progressive leaching of mobile cations in combination with low soil pH, especially in the higher-elevation zones (Dinter et al., 2021), as well as through strong bonding and occlusion of anionic nutrients like P commonly found in acidic soils rich in Al and Fe oxides (Cross and Schlesinger, 1995; Sanchez et al., 2003). Indeed, the M3-extractable P levels in the studied soils of San Cristóbal are predominantly rated low (Zhang et al., 2014), with a 75th percentile value of 11 mg kg<sup>-1</sup> (**Supplementary Table S2**). The levels of the M3-extractable base cations Ca, K and Mg are, on average, rated high according to Zhang et al. (2014), but approx. 25% of the studied samples are rated medium for Ca and low for K (25th percentile for Ca: 740 mg kg<sup>-1</sup>, and for K: 57 mg kg<sup>-1</sup>). For micronutrients, medium levels of M3-extractable Zn, Mn and Cu and low levels of Fe were, on average, found according to Zbiral (2016). Nevertheless, the M3-extractable concentrations of Zn and Cu are rated low for approx. 25% of the studied San Cristóbal soils (25th percentile for Zn: 1.3 mg kg<sup>-1</sup>, and for Cu: 1.7 mg kg<sup>-1</sup>). Many of the agricultural soils on San Cristóbal Island would benefit from measures to replenish nutrient stocks and increase SOM levels, such as the application of chicken dung (Nakamaru et al., 2000) and green manure, as well as the incorporation of crop residues and compost (Valarini et al., 2009). Liming of the low-pH soils would help to alleviate Al toxicity, to mobilize P by deprotonating variable charges on oxide surfaces and stimulating mineralization of soil organic P (Haynes, 1982), and also to restore the soils buffer-filter function.

## SUMMARY AND CONCLUSION

Our results show that the age of the individual Galápagos islands has strong bearings on the soils natural fertility. We found increasing trends of clay content and Fe oxides, BD and

macroaggregate stability with soil age, and decreasing trends of SOM, pH, CEC and base saturation. PAW contents (in 0–20 cm) were rather similar among the islands. Decreasing levels of M3-extractable base cations Ca, Mg, K and Na as well as P, Zn and Fe were observed from the youngest to the oldest studied island, while Mn concentrations increased with island age. M3-extractable Cu and Na peaked on the intermediate-aged island Santa Cruz, probably attributable to intensified agricultural activities, such as the application of agrochemicals and irrigation with brackish water, respectively. Trends along the elevation gradient within the agricultural areas of each island highlight the impact of varying precipitation regimes on soil weathering and nutrient leaching. While soil physical parameters were less influenced, pronounced changes with elevation were observed for pH, base saturation and M3-extractable nutrients.

Our study points out that the high degree of diversity in the tested soil properties and nutrient levels between and within the different Galápagos islands necessitates island-specific and climate-adapted soil management strategies to maintain soil functioning and, as a consequence, the sustainable provision of ecosystem services. A thorough account of the soils' respective pedogenic stage and associated implications for their fertility status will be decisive for future agricultural management on the inhabited islands, considering food security and the unique ecological value of the archipelago.

## DATA AVAILABILITY STATEMENT

The raw data supporting the conclusions of this article will be made available by the authors, without undue reservation.

## AUTHOR CONTRIBUTIONS

FZ and MG contributed to conception and design of the study. MS, EV and NR contributed to laboratory analyses and data

processing, and FZ validated the analytical results. MS performed the statistical analyses, visualized the results including GIS maps, and wrote the original draft of the manuscript. All authors contributed to manuscript revision, read, and approved the submitted version. FZ acquired the funding and supervised the project.

## FUNDING

This study was conducted under research permit no. PC-60-16 of the Galápagos National Park Directorate (GNPD) and supported by the Prometeo Project of Ecuador's Secretariat of Higher Education, Science, Technology and Innovation (SENESCYT).

## ACKNOWLEDGMENTS

We wish to thank the GNPD for their help, especially Jorge Carrión, the former director, for supporting our research in Galápagos. Thank you to the Ecuadorian Ministry of Agriculture and Livestock (MAG) staff members Sandra García, René Ramírez, Ángeles Prado, José Antonio Rueda, Bárbara Ordoñez, César Vinuesa, Romny Rodríguez, Hernán Simbaña, Tania Guamanquishpe and Francisco Cervantes for collecting the soil samples and completing the bulk density analysis. Thank you to the laboratory staff at BOKU University's Institute of Soil Research for assistance with the laboratory analyses.

## SUPPLEMENTARY MATERIAL

The Supplementary Material for this article can be found online at: <https://www.frontiersin.org/articles/10.3389/fenvs.2021.788082/full#supplementary-material>

## REFERENCES

- Adelinet, M., Fortin, J., d'Ozouville, N., and Violette, S. (2008). The Relationship between Hydrodynamic Properties and Weathering of Soils Derived from Volcanic Rocks, Galapagos Islands (Ecuador). *Environ. Geol.* 56, 45–58. doi:10.1007/s00254-007-1138-3
- Adhikari, K., and Hartemink, A. E. (2016). Linking Soils to Ecosystem Services - A Global Review. *Geoderma* 262, 101–111. doi:10.1016/j.geoderma.2015.08.009
- Adriano, D. C. (2001). *Trace Elements in Terrestrial Environments: Biogeochemistry, Bioavailability and Risks of Metals*. 2nd Edition. New York: Springer, 867. doi:10.1007/978-0-387-21510-5
- Alori, E. T., Glick, B. R., and Babalola, O. O. (2017). Microbial Phosphorus Solubilization and its Potential for Use in Sustainable Agriculture. *Front. Microbiol.* 8, 971. doi:10.3389/fmicb.2017.00971
- Argus, D. F., Gordon, R. G., and DeMets, C. (2011). Geologically Current Motion of 56 Plates Relative to the No-Net-Rotation Reference Frame. *Geochem. Geophys. Geosyst.* 12, Q11001. doi:10.1029/2011GC003751
- Blakemore, L. C., Searle, P. L., and Daly, B. K. (1987). *Methods for Chemical Analysis of Soils*. N.Z. Soil Bureau Scientific Report 80. New Zealand: N.Z. Soil Bureau, Lower Hutt.
- Cabral Pinto, M. M. S., Ferreira da Silva, E., Silva, M. M. V. G., and Melo-Gonçalves, P. (2015). Heavy Metals of Santiago Island (Cape Verde) Top Soils: Estimated Background Value Maps and Environmental Risk Assessment. *J. Afr. Earth Sci.* 101, 162–176. doi:10.1016/j.jafrearsci.2014.09.011
- Candra, I. N., Gerzabek, M. H., Ottner, F., Tintner, J., Wriessnig, K., and Zehetner, F. (2019). Weathering and Soil Formation in Rhyolitic Tephra along a Moisture Gradient on Alcedo Volcano, Galápagos. *Geoderma* 343, 215–225. doi:10.1016/j.geoderma.2019.01.051
- Candra, I. N., Gerzabek, M. H., Ottner, F., Wriessnig, K., Tintner, J., Schmidt, G., et al. (2021). Soil Development and Mineral Transformations along a One-million-year Chronosequence on the Galápagos Islands. *Soil Sci. Soc. Am. J.* 85, 2077–2099. doi:10.1002/saj2.20317
- CGREG, MAGAP and INEC (2014). *Censo de Unidades de Producción Agropecuaria de Galápagos*.
- Chadwick, O. A., Gavenda, R. T., Kelly, E. F., Ziegler, K., Olson, C. G., Elliott, W. C., et al. (2003). The Impact of Climate on the Biogeochemical Functioning of Volcanic Soils. *Chem. Geology*. 202, 195–223. doi:10.1016/j.chemgeo.2002.09.001
- Chorover, J., Amistadi, M. K., and Chadwick, O. A. (2004). Surface Charge Evolution of Mineral-Organic Complexes During Pedogenesis in Hawaiian Basalt. *Geochimica et Cosmochimica Acta* 68, 4859–4876. doi:10.1016/j.gca.2004.06.005

- Colinvaux, P. A. (1972). Climate and the Galapagos Islands. *Nature* 240, 17–20. doi:10.1038/240017a0
- Cross, A. F., and Schlesinger, W. H. (1995). A Literature Review and Evaluation of the Hedley Fractionation: Applications to the Biogeochemical Cycle of Soil Phosphorus in Natural Ecosystems. *Geoderma* 64 (3), 197–214. doi:10.1016/0016-7061(94)00023-4
- Dahlgren, R. A., Saigusa, M., and Ugoili, F. C. (2004). The Nature, Properties and Management of Volcanic Soils. *Adv. Agron.* 82, 113–182. doi:10.1016/S0065-2113(03)82003-5
- Delmelle, P., Opfergelt, S., Cornelis, J.-T., and Ping, C.-L. (2015). “Volcanic Soils,” in *The Encyclopedia of Volcanoes*. Editor H. Sigurdsson, et al. (Cambridge, Massachusetts: Academic Press), 1253–1264. doi:10.1016/B978-0-12-385938-9.00072-9
- Delvaux, B., Herbillon, A. J., and Vielvoye, L. (1989). Characterization of a Weathering Sequence of Soils Derived from Volcanic Ash in Cameroon: Taxonomic, Mineralogical and Agronomic Implications. *Geoderma* 45, 375–388. doi:10.1016/0016-7061(89)90017-7
- Dinter, T. C., Gerzabek, M. H., Puschenreiter, M., Strobel, B. W., Couenberg, P. M., and Zehetner, F. (2021). Heavy Metal Contents, Mobility and Origin in Agricultural Topsoils of the Galápagos Islands. *Chemosphere* 272, 129821. doi:10.1016/j.chemosphere.2021.129821
- Dinter, T. C., Gerzabek, M. H., Puschenreiter, M., Strobel, B. W., Strahlhofer, M., Couenberg, P. M., et al. (2020). Changes in Topsoil Characteristics with Climate and Island Age in the Agricultural Zones of the Galápagos. *Geoderma* 376, 114534. doi:10.1016/j.geoderma.2020.114534
- Dixon, J. L., Chadwick, O. A., and Vitousek, P. M. (2016). Climate-driven Thresholds for Chemical Weathering in Postglacial Soils of New Zealand. *J. Geophys. Res. Earth Surf.* 121, 1619–1634. doi:10.1002/2016JF003864
- Evans, C. E., and Kamprath, E. J. (1970). Lime Response as Related to Percent Al Saturation, Solution Al, and Organic Matter Content. *Soil Sci. Soc. Am. J.* 34, 893–896. doi:10.2136/sssaj1970.03615995003400060023x
- Geist, D. J., McBirney, A. R., and Duncan, R. A. (1986). Geology and Petrogenesis of Lavas from San Cristobal Island, Galapagos Archipelago. *Geol. Soc. Am. Bull.* 97, 555. doi:10.1130/0016-7606(1986)97<555:GAPOLF>2.0.CO;2
- Gerzabek, M. H., Bajraktarevic, A., Keiblinger, K., Mentler, A., Rechberger, M., Tintner, J., et al. (2019). Agriculture Changes Soil Properties on the Galápagos Islands - Two Case Studies. *Soil Res.* 57, 201. doi:10.1071/SR18331
- Guézou, A., Trueman, M., Buddenhagen, C. E., Chamorro, S., Guerrero, A. M., Pozo, P., et al. (2010). An Extensive Alien Plant Inventory from the Inhabited Areas of Galapagos. *PLOS ONE* 5, e10276. doi:10.1371/journal.pone.0010276
- Hallama, M., Pekrun, C., Lambers, H., and Kandeler, E. (2019). Hidden Miners - the Roles of Cover Crops and Soil Microorganisms in Phosphorus Cycling through Agroecosystems. *Plant Soil* 434, 7–45. doi:10.1007/s11104-018-3810-7
- Havlin, J. L. (2005). “Fertility,” in *Encyclopedia of Soils in the Environment*. Editor D. Hillel (Amsterdam: Academic Press), 2, 10–20.
- Haynes, R. J. (1982). Effects of Liming on Phosphate Availability in Acid Soils. *Plant Soil* 68, 289–308. doi:10.1007/BF02197935
- Hooff, E. E. E., Toomey, D. R., and Solomon, S. C. (2003). Anomalous Thin Transition Zone beneath the Galápagos Hotspot. *Earth Planet. Sci. Lett.* 216, 55–64. doi:10.1016/S0012-821X(03)00517-X
- INGALA-PRONAREG-ORSTOM (1987). *Islas Galápagos: Mapa de Formaciones Vegetales*. Instituto Geográfico Militar, Quito, Ecuador.
- Ito, S. (2003). Zonation Pattern, Succession Process and Invasion by Aliens in Species-Poor Insular Vegetation of the Galápagos Islands. *Glob. Environ. Res.* 7, 39–58.
- IUSS Working Group WRB (2015). “International Soil Classification System for Naming Soils and Creating Legends for Soil Maps,” in *World Soil Resources Reports*, 106. Rome, Italy: FAO.
- Iyamuremye, F., Dick, R. P., and Baham, J. (1996). Organic Amendments and Phosphorus Dynamics: III. Phosphorus Speciation. *Soil Sci.* 161, 444–451. doi:10.1097/00010694-199607000-00004
- Izurrieta, A., Delgado, B., Moity, N., Calvopiña, M., Cedeño, I., Banda-Cruz, G., et al. (2018). A Collaboratively Derived Environmental Research Agenda for Galápagos. *Pac. Conserv. Biol.* 24, 168. doi:10.1071/PC17053
- Jahn, R., and Stahr, K. (1996). Development of Soils and Site Qualities on Basic Volcanoclastics with Special Reference to the Semi-arid Environment of Lanzarote, Canary Islands, Spain. *Revista Mexicana de Ciencias Geológicas* 13, 104–112.
- Jahn, R., Zarei, M., and Stahr, K. (1987). Formation of Clay Minerals in Soils Developed from Basic Volcanic Rocks under Semi-arid Climatic Conditions in Lanzarote, Spain. *Catena* 14, 359–368. doi:10.1016/0341-8162(87)90027-0
- Klute, A. (1986). “Water Retention: Laboratory Methods,” in *Methods of Soil Analysis. Part 1. Physical and Mineralogical Methods*. Editor A. Klute. 2nd ed. (Madison, Wisconsin: ASA and SSSA), 635–660.
- Lasso, L., Espinosa, J., Espinosa, J., Moreno, J., and Bernal, G. (2018). “Soils from the Galapagos Islands,” in *The Soils of Ecuador* Editor J. Espinosa et al. World Soils Book Series (Cham, Switzerland: Springer International Publishing), 139–150.
- Levy, G. J., and Shainberg, I. (2005). “Sodic Soils,” in *Encyclopedia of Soils in the Environment*. Editor D. Hillel (Amsterdam: Academic Press), Vol. 3, 504–513. doi:10.1016/B0-12-348530-4/00218-6
- Lowe, D. J. (1986). “Controls on the Rates of Weathering and Clay Mineral Genesis in Airfall Tephra: A Review and New Zealand Case Study,” in *Rates of Chemical Weathering of Rocks and Minerals*. Editors S. M. Colman and D. P. Dethier (Orlando, FL: Academic Press), 265–330.
- Machado, R., and Serralheiro, R. (2017). Soil Salinity: Effect on Vegetable Crop Growth. Management Practices to Prevent and Mitigate Soil Salinization. *Horticulturae* 3, 30. doi:10.3390/horticulturae3020030
- Marcos, M. L. F., Alvarez, E., and Monterroso, C. (1998). Aluminum and Iron Estimated by Mehlich-3 Extractant in Mine Soils in Galicia, Northwest Spain. *Commun. Soil Sci. Plant Anal.* 29, 599–612. doi:10.1080/00103629809369970
- Martínez Cortizas, A., García-Rodeja Gayoso, E., Nóvoa Muñoz, J. C., Pontevedra Pombal, X., Buurman, P., and Terrile, F. (2003). Distribution of Some Selected Major and Trace Elements in Four Italian Soils Developed from the Deposits of the Gauro and Vico Volcanoes. *Geoderma* 117, 215–224. doi:10.1016/S0016-7061(03)00124-1
- Mehlich, A. (1984). Mehlich 3 Soil Test Extractant: A Modification of Mehlich 2 Extractant. *Commun. Soil Sci. Plant Anal.* 15, 1409–1416. doi:10.1080/00103628409367568
- Mehra, O. P., and Jackson, M. L. (1958). Iron Oxide Removal from Soils and Clays by a Dithionite-Citrate System Buffered with Sodium Bicarbonate. *Clays and Clay Minerals* 7, 317–327. doi:10.1346/ccmn.1958.0070122
- Mentler, A., Mayer, H., Straus, P., and Blum, W. E. H. (2004). Characterisation of Soil Aggregate Stability by Ultrasonic Dispersion. *Int. Agrophysics* 18, 39–45.
- Mikutta, R., Schaumann, G. E., Gildemeister, D., Bonneville, S., Kramer, M. G., Chorover, J., et al. (2009). Biogeochemistry of Mineral-Organic Associations across a Long-Term Mineralogical Soil Gradient (0.3–4100 kyr), Hawaiian Islands. *Geochimica et Cosmochimica Acta* 73, 2034–2060. doi:10.1016/j.gca.2008.12.028
- Nakamaru, Y., Nanzzyo, M., and Yamasaki, S.-i. (2000). Utilization of Apatite in Fresh Volcanic Ash by Pigeonpea and Chickpea. *Soil Sci. Plant Nutr.* 46, 591–600. doi:10.1080/00380768.2000.10409124
- Nanzzyo, M. (2002). Unique Properties of Volcanic Ash Soils. *Glob. Environ. Res.* 6, 99–112.
- Ngewoh, Z. S., Taylor, R. W., and Shuford, J. W. (1989). Exchangeable Cations and CEC Determinations of Some Highly Weathered Soils. *Commun. Soil Sci. Plant Anal.* 20, 1833–1855. doi:10.1080/00103628909368187
- O'Connor Robinson, M., Selfa, T., and Hirsch, P. (2018). Navigating the Complex Trade-Offs of Pesticide Use on Santa Cruz Island, Galapagos. *Soc. Nat. Resour.* 31, 232–245. doi:10.1080/08941920.2017.1382625
- Oorts, K. (2013). “Copper,” in *Heavy Metals in Soils, Environmental Pollution*. Editor B. J. Alloway (Dordrecht: Springer Netherlands), 367–394. doi:10.1007/978-94-007-4470-7\_13
- Penn, C., and Camberato, J. (2019). A Critical Review on Soil Chemical Processes that Control How Soil pH Affects Phosphorus Availability to Plants. *Agriculture* 9, 120. doi:10.3390/agriculture9060120
- Perry, R. (1984). “Chapter 1: The Islands and Their History,” in *Galapagos, Key Environments*. Editor R. Perry. 1st ed. (Oxford, New York: Pergamon Press in collaboration with the International Union for Conservation of Nature and Natural Resources), 1–14.
- Soil Survey Staff (2014). “Kellogg Soil Survey Laboratory Methods Manual. Soil Survey Investigations Report No. 42, ver. 5.0. National Soil Survey Center, Natural Resources Conservation Service, U.S. Department of Agriculture, Lincoln, NE.

- Rechberger, M. V., Zehetner, F., and Gerzabek, M. H. (2021). Phosphate Sorption-Desorption Properties in Volcanic Topsoils along a Chronosequence and a Climatic Gradient on the Galápagos Islands. *J. Plant Nutr. Soil Sci.* 184, 479–491. doi:10.1002/jpln.202000488
- Reynolds, R. W., Geist, D., and Kurz, M. D. (1995). Physical Volcanology and Structural Development of Sierra Negra Volcano, Isabela Island, Galápagos Archipelago. *Geol. Soc. Am. Bull.* 107, 1398–1410. doi:10.1130/0016-7606(1995)107<1398:pvasdo>2.3.co;2
- Rial, M., Martínez Cortizas, A., Taboada, T., and Rodríguez-Lado, L. (2017). Soil Organic Carbon Stocks in Santa Cruz Island, Galapagos, under Different Climate Change Scenarios. *Catena* 156, 74–81. doi:10.1016/j.catena.2017.03.020
- Rücknagel, J., Götze, P., Hofmann, B., Christen, O., and Marschall, K. (2013). The Influence of Soil Gravel Content on Compaction Behaviour and Pre-compression Stress. *Geoderma* 209–210, 226–232. doi:10.1016/j.geoderma.2013.05.030
- Sanchez, P. A., Palm, C. A., and Buol, S. W. (2003). Fertility Capability Soil Classification: A Tool to Help Assess Soil Quality in the Tropics. *Geoderma* 114, 157–185. doi:10.1016/S0016-7061(03)00040-5
- Santo, L. T., and Tsuji, G. Y. (1977). Soil Bulk Density and Water Content Measurements by Gamma-Ray Attenuation Techniques. *Tech. Bull.* 98, 1–20.
- Schaller, J., Frei, S., Rohn, L., and Gilfedder, B. S. (2020). Amorphous Silica Controls Water Storage Capacity and Phosphorus Mobility in Soils. *Front. Environ. Sci.* 8, 94. doi:10.3389/fenvs.2020.00094
- Schwartz, D. (2014). *Volcanic, Structural, and Morphological History of Santa Cruz Island, Galápagos Archipelago*. Moscow, ID: Master's Thesis, University of Idaho.
- Schwertmann, U. (1964). Differenzierung der Eisenoxide des Bodens durch Extraktion mit Ammoniumoxalat-Lösung. *Z. Pflanzenernaehr. Dueng. Bodenk.* 105, 194–202. doi:10.1002/jpln.3591050303
- Shen, J., Yuan, L., Zhang, J., Li, H., Bai, Z., Chen, X., et al. (2011). Phosphorus Dynamics: From Soil to Plant. *Plant Physiol.* 156, 997–1005. doi:10.1104/pp.111.175232
- Shoji, S., Nanzyo, M., and Dahlgren, R. (1993). Ash Soils: Genesis, Properties, and utilization. *Developments in Soil Science*. New York, Amsterdam: Elsevier.
- Six, J., Elliott, E. T., and Paustian, K. (2000). Soil Structure and Soil Organic Matter: II. A Normalized Stability Index and the Effect of Mineralogy. *Soil Sci. Soc. Am. J.* 64, 1042–1049. doi:10.2136/sssaj2000.6431042x
- Snell, H., and Rea, S. (1999). The 1997–98 El Niño in Galápagos: Can 34 Years of Data Estimate 120 Years of Pattern? *Noticias de Galápagos* 60, 11–20.
- Sollins, P., Robertson, G. P., and Uehara, G. (1988). Nutrient Mobility in Variable- and Permanent-Charge Soils. *Biogeochemistry* 6, 181–199. doi:10.1007/bf02182995
- Stoops, G. (2013). A Micromorphological Evaluation of Pedogenesis on Isla Santa Cruz (Galápagos). *Span. J. Soil Sci.* 3, 14–37. doi:10.3232/SJSS.2013.V3.N2.02
- Tabatabai, M. A., and Bremner, J. M. (1991). “Automated Instruments for Determination of Total Carbon, Nitrogen, and Sulfur in Soils by Combustion Techniques,” in *Soil Analysis*. Editor K. A. Smith (New York: Marcel Dekker), 261–286.
- Taboada, T., Rodríguez-Lado, L., Ferro-Vázquez, C., Stoops, G., and Martínez Cortizas, A. (2016). Chemical Weathering in the Volcanic Soils of Isla Santa Cruz (Galápagos Islands, Ecuador). *Geoderma* 261, 160–168. doi:10.1016/j.geoderma.2015.07.019
- Tisdall, J. M., and Oades, J. M. (1982). Organic Matter and Water-Stable Aggregates in Soils. *J. Soil Sci.* 33, 141–163. doi:10.1111/j.1365-2389.1982.tb01755.x
- Torn, M. S., Trumbore, S. E., Chadwick, O. A., Vitousek, P. M., and Hendricks, D. M. (1997). Mineral Control of Soil Organic Carbon Storage and Turnover. *Nature* 389, 170–173. doi:10.1038/38260
- Trueman, M., and D'Ozouville, N. (2010). Characterizing the Galapagos Terrestrial Climate in the Face of Global Climate Change. *Galapagos Res.* 67, 26–37.
- Tye, A., Snell, H. L., Peck, S. B., and Andersen, H. (2002). “Outstanding Terrestrial Features of the Galapagos Archipelago,” in *A Biodiversity Vision for the Galapagos Islands*. Editor R. Bensted-Smith (Puerto Ayora, Galápagos: Charles Darwin Foundation and World Wildlife Fund).
- USSL Staff (1954). *Diagnosis and Improvement of Saline and Alkali Soils*. Washington DC, USA: USDA Handbook No 60, 160.
- Valarini, P. J., Curaqueo, G., Seguel, A., Manzano, K., Rubio, R., Cornejo, P., et al. (2009). Effect of Compost Application on Some Properties of a Volcanic Soil from Central South Chile. *Chilean J. Agric. Res.* 69. doi:10.4067/S0718-58392009000300015
- Villa, Á., and Segarra, P. (2010). “Changes in Land Use and Vegetative Cover in the Rural Areas of Santa Cruz and San Cristobal,” in *Galapagos Report 2009-2010*. (Puerto Ayora, Galápagos, Ecuador. Puerto Ayora: Charles Darwin Foundation and Galápagos National Park and Governing Council of Galápagos), 85–91.
- Vitousek, P. M., and Chadwick, O. A. (2013). Pedogenic Thresholds and Soil Process Domains in Basalt-Derived Soils. *Ecosystems* 16, 1379–1395. doi:10.1007/s10201-013-9690-z
- Vitousek, P. M. (1994). Potential Nitrogen Fixation during Primary Succession in Hawai'i Volcanoes National Park. *Biotropica* 26, 234–240. doi:10.2307/2388844
- Wada, K. (1985). “The Distinctive Properties of Andosols,” in *Soil Restoration*. Editors R. Lal and B. A. Stewart (New York: Springer), 173–229. doi:10.1007/978-1-4612-5088-3\_4
- Walker, T. W., and Syers, J. K. (1976). The Fate of Phosphorus during Pedogenesis. *Geoderma* 15, 1–19. doi:10.1016/0016-7061(76)90066-5
- Watson, J., Trueman, M., Tufet, M., Henderson, S., and Atkinson, R. (2010). Mapping Terrestrial Anthropogenic Degradation on the Inhabited Islands of the Galapagos Archipelago. *Oryx* 44, 79–82. doi:10.1017/S0030605309990226
- White, W. M., McBirney, A. R., and Duncan, R. A. (1993). Petrology and Geochemistry of the Galápagos Islands: Portrait of a Pathological Mantle Plume. *J. Geophys. Res.* 98, 19533–19563. doi:10.1029/93jb02018
- Zaman, M., Shahid, S. A., and Heng, L. (2018). “Irrigation Water Quality,” in *Guideline for Salinity Assessment, Mitigation and Adaptation Using Nuclear and Related Techniques* (Cham, Switzerland): Springer International Publishing), 113–131. doi:10.1007/978-3-319-96190-3\_5
- Zbiral, J. (2016). Determination of Plant-Available Micronutrients by the Mehlich 3 Soil Extractant - a Proposal of Critical Values. *Plant Soil Environ.* 62, 527–531. doi:10.17221/564/2016-PSE
- Zehetner, F., Gerzabek, M. H., Shellnutt, J. G., Ottner, F., Lüthgens, C., Miggins, D. P., et al. (2020). Linking Rock Age and Soil Cover across Four Islands on the Galápagos Archipelago. *J. South Am. Earth Sci.* 99, 102500. doi:10.1016/j.jsames.2020.102500
- Zehetner, F., and Miller, W. P. (2006). “Toward Sustainable Crop Production in Cotacachi: An Assessment of the Soils' Nutrient Status,” in *Development with Identity: Community, Culture and Sustainability in the Andes*. Editor R. E. Rhoades (Wallingford, UK and Cambridge, MA: CABI Publishing), 177–196. doi:10.1079/9780851999494.0177
- Zhang, H., Hardy, D. H., Mylavarapu, R., and Wang, J. J. (2014). “Mehlich-3,” in *Soil Test Methods from the Southeastern United States. Southern Cooperative Series Bulletin*. Editor F. J. Sikora, 419, 101–110.
- Zuo, Y., and Zhang, F. (2011). Soil and Crop Management Strategies to Prevent Iron Deficiency in Crops. *Plant Soil* 339, 83–95. doi:10.1007/s11104-010-0566-0

**Conflict of Interest:** The authors declare that the research was conducted in the absence of any commercial or financial relationships that could be construed as a potential conflict of interest.

**Publisher's Note:** All claims expressed in this article are solely those of the authors and do not necessarily represent those of their affiliated organizations, or those of the publisher, the editors and the reviewers. Any product that may be evaluated in this article, or claim that may be made by its manufacturer, is not guaranteed or endorsed by the publisher.

Copyright © 2021 Strahlhofer, Gerzabek, Rampazzo, Couenberg, Vera, Salazar Valenzuela and Zehetner. This is an open-access article distributed under the terms of the Creative Commons Attribution License (CC BY). The use, distribution or reproduction in other forums is permitted, provided the original author(s) and the copyright owner(s) are credited and that the original publication in this journal is cited, in accordance with accepted academic practice. No use, distribution or reproduction is permitted which does not comply with these terms.



# Microbial Diversity of Reconstituted, Degraded, and Agricultural Soils Assessed by 16S rDNA Multi-Amplicon Sequencing

Laura Maretto<sup>1†</sup>, Saptarathi Deb<sup>1†</sup>, Samathmika Ravi<sup>1</sup>, Claudia Chiodi<sup>2</sup>, Paolo Manfredi<sup>3</sup>, Andrea Squartini<sup>1</sup>, Giuseppe Concheri<sup>1</sup>, Giancarlo Renella<sup>1</sup> and Piergiorgio Stevanato<sup>1\*</sup>

<sup>1</sup>Department of Agronomy, Food, Natural Resources, Animals and Environment (DAFNAE), University of Padova, Legnaro, Italy, <sup>2</sup>Crop Production and Biostimulation Laboratory (CPBL), Université Libre De Bruxelles, Bruxelles, Belgium, <sup>3</sup>MCM Ecosistemi S. r. l., Piacenza, Italy

## OPEN ACCESS

### Edited by:

Thomas Keller,  
Swedish University of Agricultural  
Sciences, Sweden

### Reviewed by:

Anna Gałazka,  
Institute of Soil Science and Plant  
Cultivation, Poland  
Magdalena Frac,  
Institute of Agrophysics (PAN), Poland

### \*Correspondence:

Piergiorgio Stevanato  
stevanato@unipd.it

<sup>†</sup>These authors have contributed  
equally to this work and share first  
authorship

### Specialty section:

This article was submitted to  
Soil Processes,  
a section of the journal  
Frontiers in Environmental Science

**Received:** 02 November 2021

**Accepted:** 13 December 2021

**Published:** 07 January 2022

### Citation:

Maretto L, Deb S, Ravi S, Chiodi C,  
Manfredi P, Squartini A, Concheri G,  
Renella G and Stevanato P (2022)  
Microbial Diversity of Reconstituted,  
Degraded, and Agricultural Soils  
Assessed by 16S rDNA Multi-  
Amplicon Sequencing.  
Front. Environ. Sci. 9:807889.  
doi: 10.3389/fenvs.2021.807889

The microbial diversity is, among soil key factors, responsible for soil fertility and nutrient biogeochemical cycles, and can be modified upon changes in main soil physicochemical properties and soil pollution. Over the years, many restoration techniques have been applied to restore degraded soils. However, the effect of these approaches on soil microbial diversity is less understood and thus requires more investigation. In this study, we analyzed the impact, on soil microbial diversity of a patented novel technology, used to restore degraded soils. Soil samples were collected from three nearby sites located in Borgotrebbe, Piacenza, Italy, and categorized as reconstituted, degraded, and agricultural soils. After total soil DNA extraction, 16S rDNA multi-amplicon sequencing was carried out using an Ion GeneStudio S5 System to compare soils' bacterial community profiles. Sequenced reads were processed to assign taxonomy and then key microbial community differences were identified across the sampling sites. Species diversity featured significant abatement at all rank levels in the degraded soil when compared to the agricultural control. The 5 year restoration technique showed full recovery of this index at the genus level but not at the phylum level, displaying a rank-dependent gradient of restored richness. In parallel, the abundance of genes involved in the nitrogen (N) biogeochemical cycle was assessed using quantitative Real-Time PCR (qPCR). Total DNA content was significantly higher ( $p < 0.05$ ) in degraded ( $\mu = 12.69 \pm 2.58 \mu\text{g g}^{-1}$ ) and reconstituted ( $\mu = 11.73 \pm 1.65 \mu\text{g g}^{-1}$ ) soil samples when compared to the agricultural soil samples ( $\mu = 2.39 \pm 0.50 \mu\text{g g}^{-1}$ ). The taxonomic diversity of each soil site was significantly different, with some instances unique of the agricultural soil even at the phylum level. The analysis of N functional genes showed that the relative abundance of bacterial *amoA* ( $p < 0.05$ ) and *nosZ* ( $p < 0.01$ ) genes were significantly lower in the agricultural than in the reconstituted and degraded soils. We concluded that the application of the soil reconstitution technique appears to enhance the active microbial community, with distinct diversity and functionality towards genes involved in N biogeochemical cycle, as compared to both the degraded and the agricultural soil.

**Keywords:** microbial diversity, next-generation sequencing, soil microbial activity, soil remediation, qPCR, soil microbial profile, 16S rDNA multi-amplicon

## INTRODUCTION

Soil originates from the weathering of parent materials under the combined action of climate, living organisms, and in function of the watershed relief and time (Jenny, 1946; Hartemink, 2016). During pedogenesis soils form complex assemblages of clay minerals (hydr-)oxides and organic matter, that result in their ultimate structure. Soil structure is responsible for soil's physical and chemical functions in the environment such as water movement and retention, and mobility and bioavailability of nutrients and pollutants (Jastrow and Miller, 1991; Gregorich et al., 1997; Robinson et al., 2009; Bünemann et al., 2018). The biotic compartment of soil, composed of interrelated communities of fungi, bacteria, archaea, viruses, protists, and other microbial eukaryotes, is also defined as the soil microbiome (Jansson and Hofmockel, 2020).

It is estimated that soil microbiome controls up to 90% of soil processes, thus it plays a fundamental role in ecosystem functioning (Gregorich et al., 1997; Nannipieri et al., 2003; Young and Crawford, 2004). Moreover, the soil microbiome influences the biogeochemical cycles of nutrients, for example, acting as source or sink of gases, it contributes to nitrogen (N) and carbon (C) rates of fixation and oxidation, and it can degrade organic pollutants (Fierer, 2017). Therefore, though only a minor portion of the available soil space is colonized by the microbial communities (Young and Crawford, 2004), the stability and the resilience of the soil system are determined by the combination of soil physical structure, nutrient availability, microbial diversity and activity (Meuer et al., 2020). The soil microbiome is impacted by human activities like agriculture, soil sealing and industrial emissions that cause environmental pollution (Roose-Amsaleg et al., 2001; Maron et al., 2011) due to the changes that these activities induce in the soil structure. Since anthropogenic activities have decreased biodiversity in soils, the assessment of the soil microbiome can be a crucial indicator of soil quality (Lehmann et al., 2020; Vieira et al., 2022).

Soil is a non-renewable natural resource, and owing to the recent increased attention to its conservation, restoration of soil quality has become a key topic in science (Qilu et al., 2017; Yan et al., 2018; Xu et al., 2019). Several techniques have been used to form a porous structure in massive non-structured soils, and those based on the amendment with organic matter, revegetation or landfarming are among the most used (Sims and Sims, 2003). However, these techniques are primarily based on the mixing of soil with organic matter that improves their texture, mineralogy, pH value and cation exchange capacity, whereas the formation of a complex structure is slow and mainly due to the action of plant roots and soil microbes over relatively longer time periods. Techniques involving physical, chemical, and biological approaches have been also used to remove or transform harmful pollutants. Among these techniques, remediation using microbial consortia is well-established and widely used due to the lack of secondary pollution, potentially rapid degradation rates, and low cost (Agamuthu et al., 2013; Hesnawi and Mogdani, 2013). However, little is known about the effect of these restoration techniques on soil microbial diversity in degraded soils that have undergone microbial

biomass loss. While microbial activity can be significantly increased by soil restoration, a steady increase of diversity of microbial communities in restored soils is more difficult to achieve, thus such techniques require a deeper investigation.

The study of soil microbiome has been constrained for a long time because only a minority of microorganisms can be cultivated using standard techniques (Robe et al., 2003; Vester et al., 2015). Amann et al. (1995) observed that the culturability of bacteria from environmental samples ranged between 0.001 and 0.3% depending on the characteristics of the matrix. High-throughput culture-unrelated techniques, like Next Generation Sequencing (NGS), have been established over time to bypass the underestimation of soil microbial diversity problem (Chiodi et al., 2020). 16S rDNA multi-amplicon metabarcoding, sequencing at the same time several hypervariable regions, can generate a substantial amount of sequences, providing crucial information for a deep characterization of the microbiome even of extremely complex natural matrices such as soils (Young et al., 2017).

In this study, combining 16S rDNA metabarcoding and qPCR analyses, we investigated soil microbiome and individual genes coding for the enzymes involved in the N biogeochemical cycle, on soils treated with a novel technology, termed soil reconstruction and patented by MCM Ecosistemi S. r. l, which aims at creating a *de novo* soil structure from the original soil solid phase.

Such in a way we aimed at filling what we perceived as a gap of knowledge. The degree of novelty of the present report being the combination of the patented novel technique and the multi-amplicon sequencing assessment of its effects on soil microbial communities.

## MATERIALS AND METHODS

### Site Location and Soil Sampling

Soil samples were collected from three sites located in Borgotrebbe, Piacenza, Italy (4503'58" N 0939'06" E, **Figure 1**). Vegetation types were mainly annual terophytes, dominated by Scotch thistle (*Onopordum acanthium* L.) (Giupponi et al., 2013; Giupponi et al., 2015).

The degraded sampling site was a closed landfill made of municipal solid wastes. The landfill, which was active from 1972 to 1985 and that was covered with a 50 cm thick layer of backfill soil, covers a 20 ha area. The reconstituted sampling site corresponded to half of the landfill that underwent a reconstruction process, becoming a technosol, operated by MCM Ecosistemi S. r. l. with a patented novel technology (Manfredi et al., 2019). The agricultural sampling site was an adjacent agricultural field under conventional maize cultivation. Sampling was carried out with the linear transect technique (Brown, 1993). From each sampling site, 12 sub-samples were collected at a 20 cm depth using a manual auger. Sub-samples triplets were mixed to obtain four main samples for each site, referred to as: Reconstituted Soil (RS) (RS1, RS2, RS3, RS4), Degraded Soil (DS) (DS1, DS2, DS3, DS4), Agricultural Soil (AS) (AS1, AS2, AS3, AS4). Composite soil samples were air-dried at room temperature for 48 h, crushed, and sieved ( $\varnothing$  0.5 mm) before the analysis.



**FIGURE 1** | Aerial photograph of the studied area located along the hydrographic right bank of the Trebbia river. Geographical coordinates: 45°03'58" N 09°39'06" E. (i) Degraded sampling site, (ii) Reconstituted sampling site, (iii) Agricultural sampling site.

## Soil Chemical Analyses

Soil pH was measured potentiometrically in ultra-pure water (ratio soil/water 1:2.5 w/v) for each of the analyzed samples. Total carbon (C) and total nitrogen (N) content was determined by dry combustion using a CNS Vario Macro elemental analyzer (Elementar, Hanau, Germany), based on the Dumas combustion method (Dumas, 1831). The calibration curve was created using a certified sulphanilamide standard. The organic carbon content of each sample was tested using the Walkley-Black method (Walkley and Black 1934), while the extractable phosphorus (P) was evaluated using the Olsen method (Olsen et al., 1954).

## Total Soil DNA Extraction, Multi-Amplicon 16S rDNA Sequencing, Analysis of Functional Genes of the N Biogeochemical Cycle

Total soil DNA was extracted from 250 mg of air-dried soil using the DNeasy PowerSoil Pro Kit (Qiagen, Germany), according to the manufacturer's instructions. Nucleic acid quantification was performed using the Qubit 3.0 fluorometer (Thermo Fisher Scientific, Carlsbad, CA) with Qubit DNA High Sensitivity Assay Kit (Thermo Fisher Scientific).

Library preparation was carried out using the 16S Ion Metagenomics Kit (Thermo Fisher Scientific) that contains two pools of primers targeting seven different hypervariable regions (V2-V4-V8 primer pool and V3-V6-V7-V9 primer pool). 16S rRNA multi-amplicon sequencing was performed using an Ion GeneStudio S5 System (Thermo Fisher Scientific).

Raw reads were trimmed for 20 nucleotides on both ends to remove primers using the *cutadapt* utility and analyzed using Quantitative Insights Into Microbial Ecology 2 (QIIME2) v2020.08 (Bolyen et al., 2019) microbiome pipeline. Imported reads were first denoised and dereplicated using the "qiime dada2" plugin followed by taxonomic classification of

Amplicon Sequence Variants (ASVs) by a "classify-consensus-blast" plugin using SILVA SSU v138.1 (Quast et al., 2012) as reference database. To check the quality of the achieved sequencing depth, alpha diversity rarefaction analysis was done using the "qiime alpha-diversity" plugin. The taxonomy abundance table at different taxonomic levels was further processed using the Calypso online suite (Zakrzewski et al., 2016) to Total Sum Scaling (TSS) normalized for library size differences. The resultant normalized table was filtered out by omitting taxa with less than the average of 10 reads across samples, and used for further diversity analysis and group comparison at different taxonomic levels. Principal component analysis was performed in Calypso using Bray-Curtis distances and the Shannon diversity index and Taxonomic Richness and community evenness were used for diversity comparisons.

The abundance of *amoA* (eubacterial, AOB), *nifH*, *nirK*, and *nosZ* bacterial genes was analyzed by quantitative Real-Time PCR (qPCR) using a QuantStudio 12K-Flex apparatus (Thermo Fisher Scientific). The 5 µL reaction mix was composed of 2.5 µL PowerUp SYBR Green Master Mix (Thermo Fisher Scientific), 0.15 µL each of forward and reverse primer (Table 1), 1.2 µL PCR-grade water, and 1 µL template DNA. A standard curve using known amounts of the target genes cloned in plasmids of known length (Chiodi et al., 2020) was obtained and data were used to calculate the copy number of the gene targets based on the Ct value.

Data analysis of gene abundance was performed using SPSS Statistics v28.0.0.0 (190) (IBM, Armonk, NY). Significant differences among the mean values were evaluated with a one-way ANOVA followed by Duncan's post hoc test. Data were expressed as mean ± standard error of the mean. A Principal Component Analysis (PCA) based on Bray-Curtis distances was performed to display the core microbiome of the three soils.

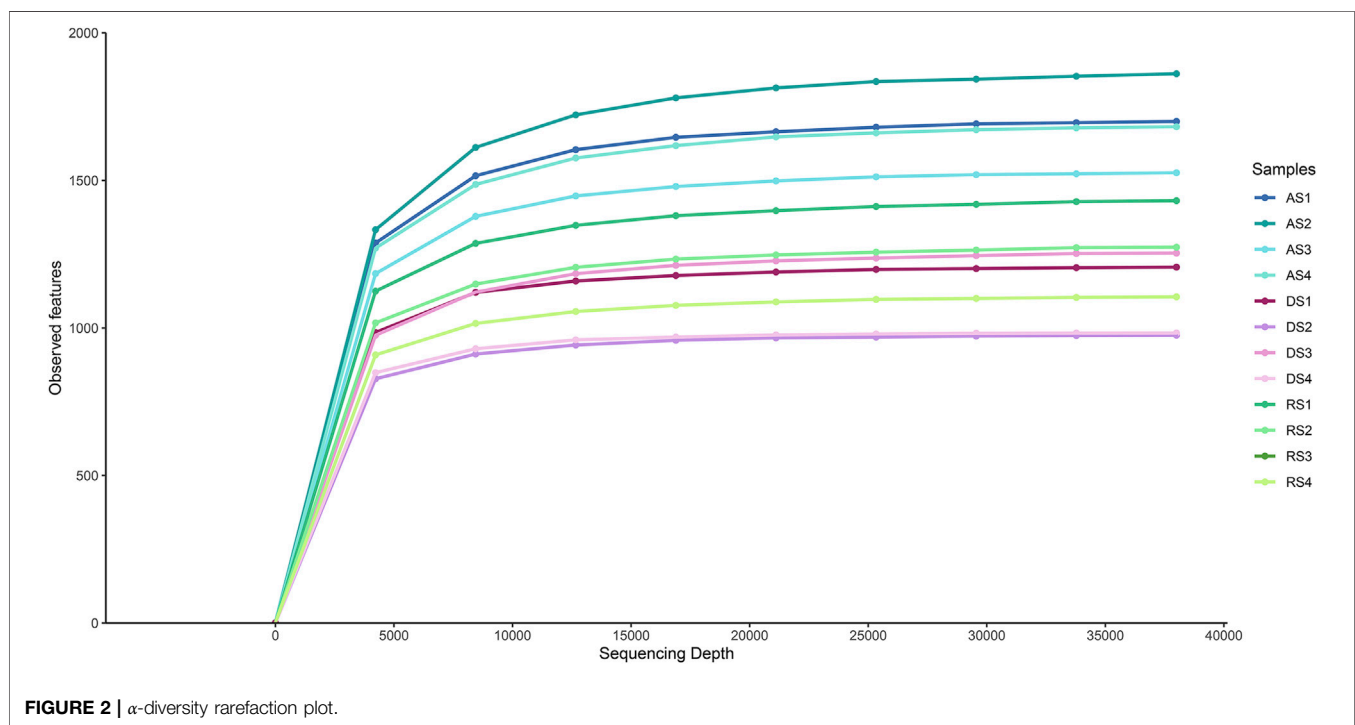
Overall data analysis, including soil chemistry, was performed using SPSS Statistics v28.0.0.0 (190) (IBM, Armonk, NY).

**TABLE 1** | Primer sequences and amplicon length.

Primer	Sequence	Amplicon length	References
<i>amoA</i> F	GGGGTTTCTACTGGTGGT	500	Rotthauwe et al. (1997)
<i>amoA</i> R	CCCCTCKGSAAGCCTTCTTC		
<i>nifH</i> F	AAAGGYGGWATCGGYAARTCCACCAC	432	Rösch et al. (2002)
<i>nifH</i> R	TTGTTSGCSGCRTACATSGCCATCAT		
<i>nosZ</i> F	CGYTGTTCMTCGACAGCCAG	706	Roesch et al. (2003)
<i>nosZ</i> R	CATGTGCAGNGCRTGGCAGAA		
<i>nirK</i> F	ATYGGCGGVCA YGGCGA	160	Henry et al. (2004)
<i>nirK</i> R	RGCTCGATCAGRTTTRTGGTT		

**TABLE 2** | Results of the chemical analyses on the soil samples at the beginning of the experiment. Means with the same letter in the vertical comparison among the sampling sites are not significantly different at S-N-K test. \*Significance level  $p < 0.05$ .

Sampling site	pH*		Total C* g·kg <sup>-1</sup>		Organic C* g·kg <sup>-1</sup>		Total N* g·kg <sup>-1</sup>		Olsen P* g·kg <sup>-1</sup>	
Agricultural	7.85 ± 0.02	b	29.98 ± 0.38	c	9.37 ± 0.32	b	1.69 ± 0.25	c	5.21 ± 1.57	b
Degraded	8.15 ± 0.03	a	41.11 ± 3.46	b	23.98 ± 4.55	b	3.07 ± 0.19	b	52.46 ± 10.67	a
Reconstituted	7.69 ± 0.04	c	66.94 ± 4.11	a	42.30 ± 2.96	a	3.98 ± 0.19	a	101.67 ± 23.02	a

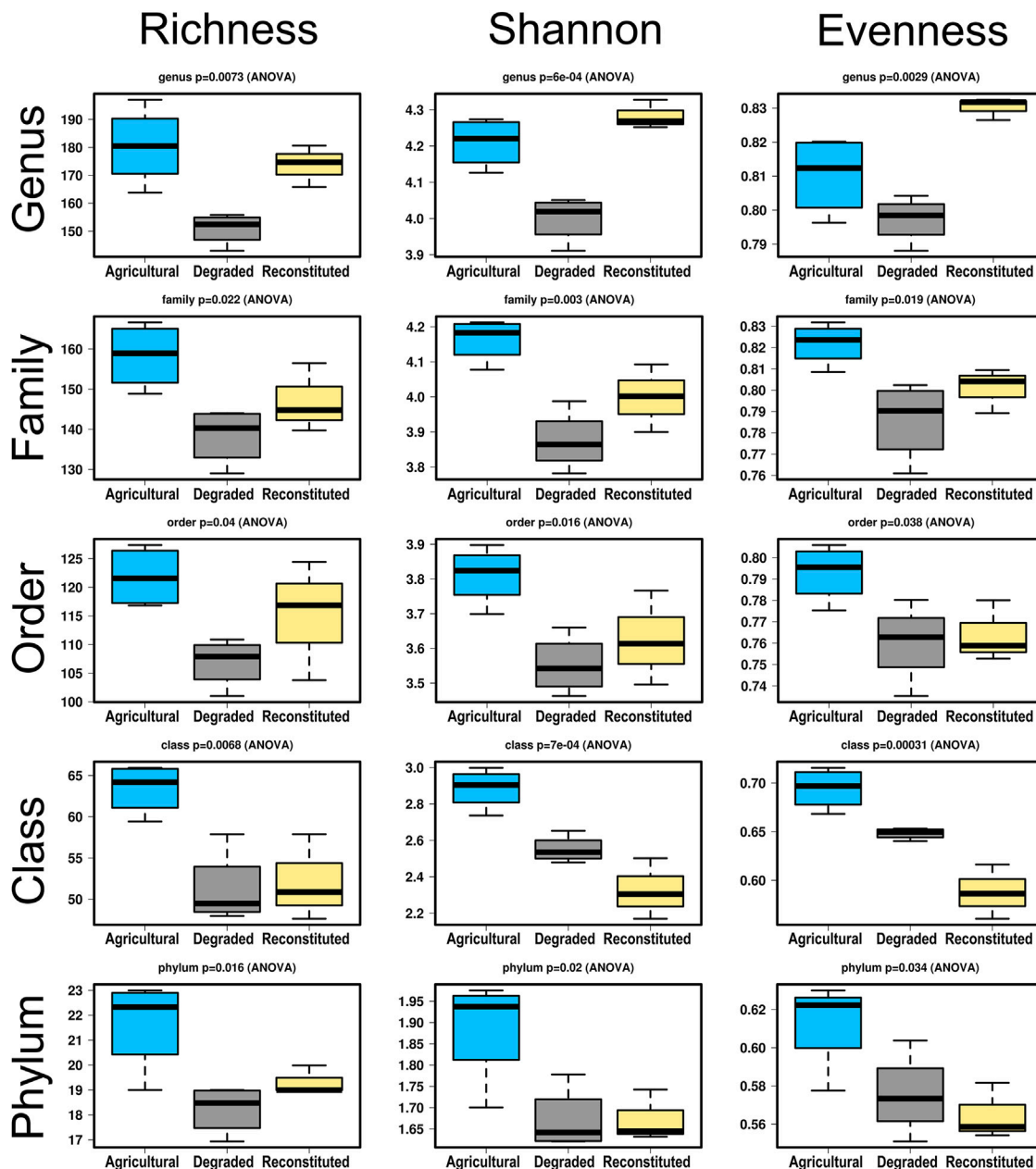
**FIGURE 2** |  $\alpha$ -diversity rarefaction plot.

Significant differences among the mean values were evaluated with a one-way analysis of variance (one-way ANOVA) followed by post hoc analysis (S-N-K test). Data are expressed as mean  $\pm$  standard error of the mean.

## RESULTS

Soil chemical analyses results are summarized in **Table 2**.

The pH value of the RS was significantly lower ( $p < 0.05$ ) than that of the DS and AS. The total C content of the AS was significantly lower ( $p < 0.05$ ) than those of the RS and DS, whereas the organic C content was significantly higher ( $p < 0.05$ ) in the RS when compared to DS and AS. Total N content was significantly higher ( $p < 0.05$ ) in the following ranking order: RS > DS > AS. Extractable Olsen P was significantly lower ( $p < 0.05$ ) in AS but no differences between DS and RS were observed.



**FIGURE 3 |** Boxplot comparisons of three ecological parameters (Taxa Richness, Shannon Index and Community Evenness) across five level of taxonomical ranks, for the bacterial communities resulting from the 16rDNA sequencing. Significance levels (ANOVA) are reported above each graph.

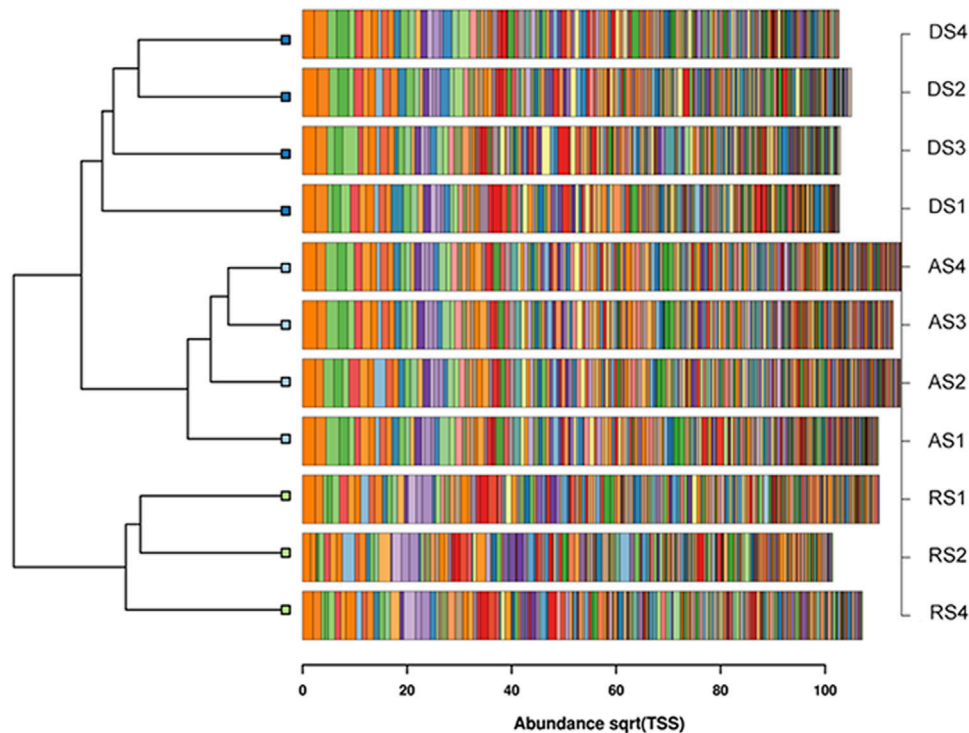
Quantification of the total soil DNA showed a significantly ( $p < 0.05$ ) higher amount of DNA in DS ( $\mu = 12.69 \pm 2.58 \mu\text{g g}^{-1}$ ) and RS ( $\mu = 11.73 \pm 1.65 \mu\text{g g}^{-1}$ ) soils compared to the AS soil ( $\mu = 2.39 \pm 0.50 \mu\text{g g}^{-1}$ ).

Bacterial 16S rDNA metabarcoding on the 12 soil samples provided a total number of 6,926,539 single-end reads, with an average length of 234 nucleotides. A total amount of 9,348 ASVs were identified and finally classified into 717 taxa. The alpha diversity rarefaction plot, corresponding to the number of observed features within samples, showed the highest number

of detected sequences in AS samples compared to DS and RS samples (Figure 2).

As regards the taxonomy depth achieved, 85.5% of the annotated sequences were classified at genus rank level, 92.7% at family level, 94.3% at order level, 95.9% at class level and 96.5% at phylum level.

Upon splitting the output of the amplified sequence variants taxonomy table in subsets relative to the five different ranks of phylum, class, order, family, genus, and summing up the numbers of each in pivot tables, the consequent diversity within each level



**FIGURE 4 |** Clustered barchart dendrogram based on the Bray-Curtis distances of the first most abundant 250 taxa for each community.

could be examined by calculating three ecological indexes assessing community richness, diversity and evenness and the results are shown in **Figure 3**.

It can be seen that for all the three parameters, and in particular for those of diversity and richness, the agricultural control sampling site presents in most cases significantly higher values than its compared degraded and reconstituted sampling sites as far as the broader systematics divisions are concerned. However, moving up to finer clades, starting from the order, and culminating in the most distinct level (genus), the rise of the values for the reconstituted sampling site is very evident and eventually yields means that become also higher than those of the agricultural sampling site. On the contrary, the values of the degraded sampling site tend to stay inferior to both other soils in almost all cases, with exceptions mainly at class level for the Shannon index and evenness values.

The relative difference of each community was further analyzed by cluster analysis and the results are shown in **Figure 4**.

The communities coming from the three soil management types are indeed partitioned accordingly in three clustered groups. The distance between the group of the agricultural soil and that of the degraded soil is shorter than the one that separates both of them from the reconstituted soil. Consistently with its nature of a reconstituted soil, the hosted bacterial communities appear thereby more distinct from those of the other origin.

Multivariate analyses were performed to further inspect the relative ordination of each of the communities and the consistency of the replicates within each group. Principal

Coordinates Analysis, Principal Component Analysis and PERMDISP2 were computed and the results are shown in **Figure 5**.

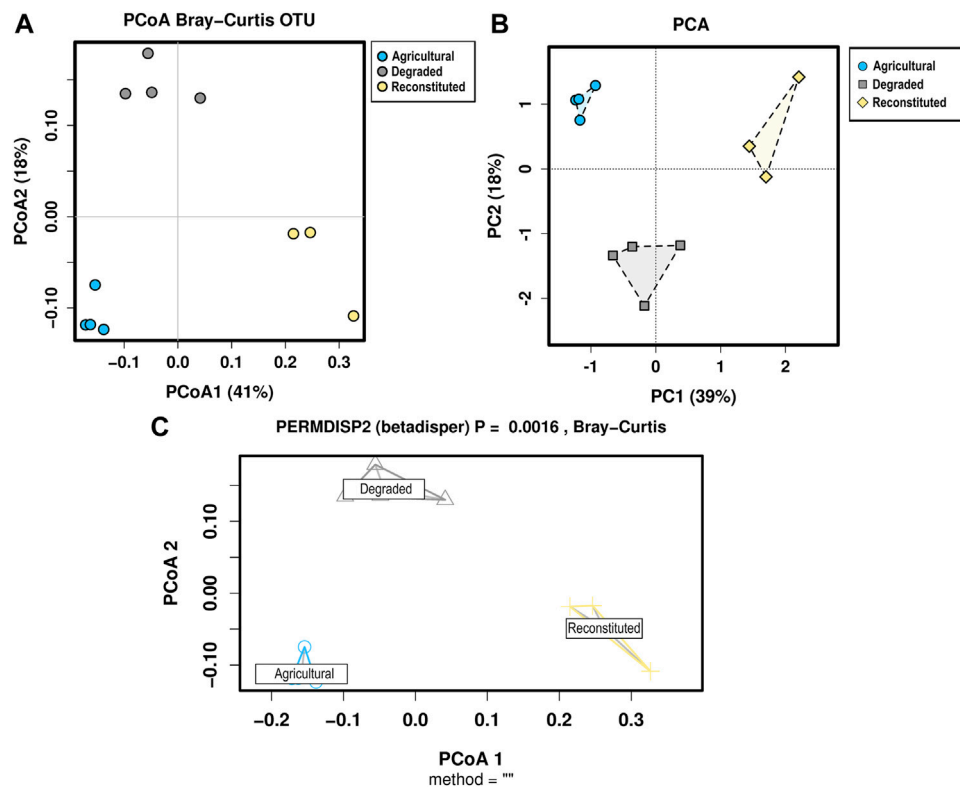
All approaches coherently separated each community on the basis of the soil management variable. The PCA showed that bacterial taxa of the three soils clustered separately with polygon's centroids significantly different (PERMANOVA  $p < 0.05$ ).

Subsequently, on the five different rank-level data subsets, an analysis of the conserved core of shared taxa and of the unique ones was carried out, yielding the results shown in **Figure 6**.

This analysis of the core versus specific sets of the microbiomes (Shade and Handelsman, 2012) showed the extent of uniqueness of taxa occurring at different ranks in each of the three management types, with the agricultural sampling site retaining the highest degrees of specificity, followed by the reconstituted sampling site and with the least number at all level the degraded sampling site. Additional information about top abundant unique taxa for each of the analysed soils, is reported in **Supplementary Table S1 (Supplementary Material S1)**.

The qPCR analyses results of the *nifH*, the bacterial *amoA*, the *nosZ*, and the *nirK* genes are compared in **Table 3**. The RS samples yielded a higher content of the *nifH* gene copies when compared to the DS samples and to the AS samples. The bacterial *amoA* gene copies were significantly ( $p < 0.05$ ) higher in the RS and in the DS samples than in AS samples.

RS samples showed the highest content of *nosZ* gene copies while DS samples showed a lower abundance and AS samples showed the lowest abundance.



**FIGURE 5** | Multivariate analyses for the bacterial communities sequencing data. **(A)** Principal Coordinate Analysis based on the Bray-Curtis distances, **(B)** Principal Component Analysis, **(C)** PERMDISP2, which visualizes the distances of each sample to the group centroid in a Principal Coordinate Analysis (PCoA) and provides a  $p$ -value for the significance of the treatments.

The *nirK* gene copies showed a significantly lower abundance ( $p < 0.01$ ) in AS samples than DS and RS samples.

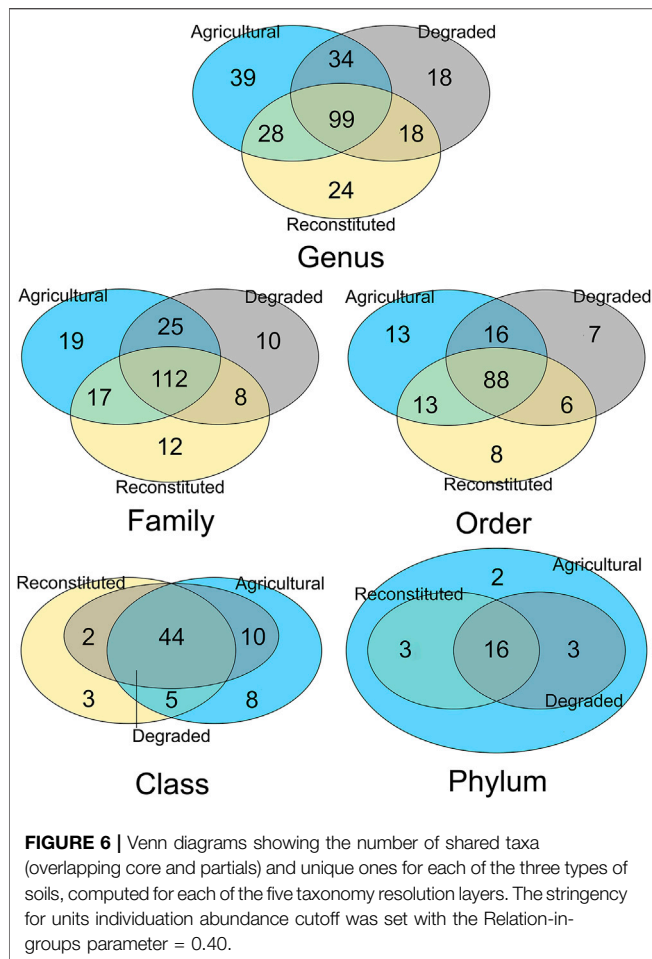
## DISCUSSION

Soils comprehend a wide range of variable conditions, including abiotic conditions, for instance, nitrogen availability and circulation, and biotic conditions that can affect the structure and the abundance of microbial communities (Islam et al., 2020). In addition, soil microbial communities are affected by anthropogenic activities like agriculture practices and environmental pollution (Fierer, 2017; Teng and Chen, 2019).

In this study we observed that, despite the lowest quantity of total soil DNA, the AS samples, under conventional management, showed higher  $\alpha$ -diversity of the bacterial community when compared to the DS samples and to the RS samples. A lack of correlation between DNA yield and bacterial diversity was previously reported by Sagova-Mareckova et al., 2008. Total soil DNA is more related to soil microbial biomass, and it is generally related to the soil pH value, the clay and organic matter content, and the vegetation cover (Burgmann et al., 2001). Thus, more microbial diversity seems to be related to long term soil activity and it is not easily reproducible with human interventions (Strickland et al., 2009). Abiotic stresses, like the discontinuous

availability of nutrients and oxygen, and biotic stresses, like the presence and the abundance of predators, exert evolutionary pressure on soil microbial communities and help to select differences among the species without affecting soil functions (Hovatter et al., 2011; Jackson and Fahrig, 2014). The increase of microbial diversity at deeper taxonomic levels in RS samples when compared to DS samples might depend on the patented reconstruction technique that consists of a chemo-mechanical process. This reconstruction technique seems to implement particle aggregation and soil porosity enhancing the exchange of gasses and liquids (Manfredi et al., 2019), leading to a more suitable environment for soil microorganisms' proliferation. The PCA plot's underlying value also confirms that the taxonomic features of each sampling site were significantly different ( $p < 0.05$ ) to cluster the analyzed soil samples. The same was confirmed by the PCoA and by the Permdisp2 analyses.

As regards details from the core vs. specific/unique microbiome analysis, at phylum level two bacterial phyla, Latescibacterota and NB1-j, were uniquely present in AS samples, although at low frequencies (both  $<1\%$ ). Those phyla are reported to be present in several environments although their function is still unknown (Jimenez et al., 2020; Dries et al., 2021; Hamdan et al., 2008; Coelho et al., 2016). At order level Chtonomonadales, a bacterial order capable to utilize different carbohydrate substrates as carbon and energy sources (Wang



et al., 2019), were almost unique in AS samples. Lactobacillales, lactic acid bacteria (Baureder and Hederstedt, 2013), and Bacteroidales, a bacterial order present in human and animal faeces (Levantesi et al., 2012), were encountered almost only in DS samples, although not in a dominant fashion. RS samples, instead featured Chlamydiales, a typical soil order reported being found in agricultural soils (Schmalenberger and Tebbe, 2002), but again not as prevailing members. In general however, it can be commented that, at each taxonomy level examined, the truly dominant members across all replicates of the three types of soils were the same, with the Proteobacteria (Gamma- and Alpha-) and Actinobacteria leading at Phylum/Class levels, the Rhizobiales and Burkholderiales at order level, the nitrifying Nitrosomonadaceae at family level. More peculiarities instead

emerged at Family and even more at Genus levels. These phenomena, besides the Venn diagram comparisons shown in **Figure 6**, are also entailed in the rank-related shifts shown for the three ecological parameters in **Figure 3**. Interestingly, the superior biodiversity values displayed by the AS samples are mostly maintained at high ranks as phylum, order, class etc., but are progressively overcome by the reconstituted restored soil, that appears to “catch up” when examined levels are unclustered in deeper and deeper ranks, culminating at genus level. In the comparison between the degraded and reconstituted soils, it is worth noticing that, while at high ranks, and particularly at class level, the Shannon index and evenness means of the reconstituted soil were lower than those of the degraded one, such is not the case for richness, which is the only index of the three, whose formula is not linked to the number of individuals found. This suggests that in both these soils numbers of individuals have an impacting effect on the ecological outcome, irrespective of the number of taxa, as long as broad categories are considered. On the contrary, when finer taxonomy resolution is the metrics (genus), the reconstituted sampling site prevails and equates the agricultural sampling site. Such sampling site can be considered to be also under a disturbance (being cropped), but with a very long history of adaptation to that predictable and recurring type of perturbation. In practice, **Figure 3** shows that the agricultural soil is both phylum-rich and genus-rich, the degraded soil is phylum-poor and genus-poor, and the reconstituted soil is phylum-poor but genus-rich. This trend is consistent with data on really undisturbed controls as climaxing forest soils (Roesch et al., 2007), in those, phylum richness resulted even higher than that of cropped soils, but their established communities had relatively less genera and species, leading to what would be the fourth of these combinations (phylum-rich and genus-poor). In practice, the reconstruction of the degraded soils shows that in a few years, such degraded soil, which is the origin of the restored one, could be rescued up to a level of microbial diversity that compares with that of the nearest agricultural soil control. Thus, the environmental carrying capacity K for possibly hosted species (Odum, 1953) and its imposed diversity ceiling appear to have been achieved by the soil reconstruction procedure, which can be seen as a rather relevant ecological goal.

The interpretation of these trends suggests an intriguing picture. The short/unpredictable/non-cyclic type of human perturbation that led to the landfill conversion (the degraded soil DS) abated community structure and led to the loss of high-ranked taxonomical divisions (phyla), whose establishment involves time. The same soil, after 5 years of restoration (the

**TABLE 3 |** Gene copy numbers resulting from the qPCR analysis conducted targeting bacterial genes involved in the nitrogen biogeochemical cycle. Means with the same letter in the vertical comparison among the sampling sites are not significantly different at Duncan's test. \*Significance level  $p < 0.05$ . \*\*Significance level  $p < 0.01$ .

Sampling site	<i>amoA</i> *		<i>nifH</i> **		<i>nosZ</i> **		<i>nirK</i> **	
	Gene copy number		Gene copy number		Gene copy number		Gene copy number	
Agricultural	$5.69 \times 10^4 \pm 5.20 \times 10^3$	b	$8.98 \times 10^5 \pm 8.37 \times 10^4$	c	$2.51 \times 10^5 \pm 4.76 \times 10^4$	c	$3.23 \times 10^3 \pm 2.02 \times 10^2$	b
Degraded	$7.91 \times 10^4 \pm 9.05 \times 10^3$	a	$9.22 \times 10^6 \pm 2.33 \times 10^6$	b	$1.51 \times 10^6 \pm 3.01 \times 10^5$	b	$1.17 \times 10^4 \pm 1.35 \times 10^3$	a
Reconstituted	$9.66 \times 10^4 \pm 8.31 \times 10^3$	a	$2.50 \times 10^7 \pm 6.50 \times 10^6$	a	$3.66 \times 10^6 \pm 4.07 \times 10^5$	a	$1.51 \times 10^4 \pm 1.86 \times 10^3$	a

RS soil) shows that, although this is too short a time to allow the return of lost phyla, it is nevertheless sufficient to drive a low-ranked diversification, leading to the recovery of diversity when measured by the genus metric. It can be also hypothesized that in fact the sudden absence of some previously present phyla, could even have left the available niches that would be then filled by the multiplying variants stemming from the remaining phyla. A scenario that, upon scaling-up of larger size and generation time, would comply to the “dinosaur-extinction/mammals radiation” model. The covariation of metabolic rate and body mass is in this sense well-demonstrated by Kleiber’s law (Kleiber, 1947). However, viewing the phenomena observed here as truly micro-evolutionary, would conflict with the notion of the 16S sequence being a molecular clock whose changes should require far longer timescales (Clark et al., 1999). Therefore, the rise of genus-level diversity in the reconstituted sampling site could be interpreted possibly as partly due to a physical recruitment (airborne immigration from other sites) and partly to a ‘technical’ recruitment, consisting in an increased detectability of reads in sequencing libraries as a consequence of the loss of other taxa that were otherwise quenching the counts of rare ones. The former mechanism (immigration) would not be sufficient by itself to explain why cells representative of missing genera should immigrate more easily than those of missing phyla and classes. But, since some phyla can encompass an extremely high diversity, while some other could be represented by even a single known species, the difference can be accounted for.

As regards the qPCR analyses of the N cycle genes, assessing the abundance of bacterial functional genes involved in nitrogen circulation is a useful tool to evaluate soil health and quality. The key steps of the nitrogen biogeochemical cycle are nitrification, the process that converts ammonium firstly in nitrite and secondly in nitrate, and denitrification, the process that reduces nitrate to molecular nitrogen (Tang et al., 2019). qPCR validated the abundance of selected microbial targets by evaluating *nifH*, bacterial *amoA*, *nosZ*, and *nirK* genes involved in the nitrogen biogeochemical cycle within the sampling sites. The degraded and the reconstituted soil samples showed a higher abundance of all the nitrogen-circulating tested genes compared to the agricultural soil samples. These disparities in gene copy numbers might be related to soils nitrogen content. Anikwe and Nwobodo (2002) reported that nitrogen content in the superficial horizon was 646–750% higher in long-term municipal waste landfill sites compared to agricultural sites. In addition, our chemical analyses results, that are in accordance with previously published results by Manfredi et al., 2019, highlighted that the reconstruction patented technique increases soils’ nitrogen content. Thus, the increased nitrogen inputs could have led to a higher nitrification and denitrification potential of degraded and restored soils. The fact that all these functional genes were found quantitatively in higher copies in the degraded and restored soil can be interpreted also in light of the above discussed result of the averagely six-fold higher content of total extractable soil DNA in both of them when compared to the agricultural cropped AS control soil. In interpreting both that difference and the ones resulting in these N-linked functional genes, it can be commented that the degraded and restored soils,

being examples of recent and non-cyclic perturbations, turning over their previous nature, can be envisaged also as the equivalent of active construction worksites, in which the microbial populations would be engaged in multiplication, new nutrient flow interception, and a number of reorganizational responses in the shifted communities, that would explain the observed higher DNA values. Nevertheless, soil total DNA could be also contributed by fungi, protists, and by the remnant material from plants and animal origin. Therefore, the active state of bacteria could not necessarily be involving all of them but more likely, some functional groups as the ones we tested by qPCR.

In conclusion, several ecological hints arose from this comparative study. It is not easy to assess whether the differences acquired by the restored soil arose by the new chances open by the perturbation as such, which modified the environmental conditions, or were more specifically due to the restoration technique itself that requires the application of non-sterile sludges coming from specific industrial processes. In addition it is still unclear if the enhanced microbial diversity in RS samples, when compared to that of the DS samples, would be temporary or permanent. It can be also underlined that, while the restoration allowed the recovery of the ecological indexes of diversity, however the resulting community profile moved even farther away from the one of the agricultural soil, as shown in the cluster dendrogram of **Figure 4**, in which the degraded and agricultural soil bacteria appear closer to each other. The effect was therefore that of a shift to a novel assemblage, whose equilibrium and fate would have to be assessed in time. Of equal importance would be to determine whether the increased gene copies of the nitrogen cycling could entail some novel environmental concerns. In highly fertilized soils, considering that, in those cases, soil microbial activity is not able to metabolize the entire amount of nitrogen (Zilio et al., 2020), leading to nitrogen leaching through the vertical profile that can potentially reach subsurface water bodies. Their N enrichment is in fact one of the main causes of eutrophication. Such environmental syndrome, consisting of nutrients enrichment of water, culminates in the large production of biomasses related to algae proliferation. The degradation of these, once their short life cycle turns them into necrotic masses, results in hypoxia or anoxia situations and, also, in toxic bacterial emissions of methane, carbon dioxide and hydrogen sulphide (Le Moal et al., 2019). On the other hand, however, three reassuring issues can be put forward against these concerns. The first is the fact that a higher content of soil DNA is also reported in literature as a positive proxy for soil equilibrium (Fusaro et al., 2018). The second is that, since the gene copies detected by qPCR increased in all targeted genes, the phenomenon could be framed within that of the overall increase of soil DNA. The third is that, among the four PCR-targeted genetic determinants, the one that increased the most, and that did so in a statistically significant manner also in the comparison between degraded and restored soil, was *nifH*, i.e. one of the structural subunits of the nitrogenase protein, to which biological nitrogen fixation from either free-living or symbiotic prokaryotes is ultimately due. Being such metabolism the main gateway for nitrogen entrance into terrestrial as well as aquatic food chains, the enhancement of

its key enzyme can be described as a positive premise in the pursuit of an improved environmental sustainability.

## DATA AVAILABILITY STATEMENT

The dataset generated for this study can be found in the European Nucleotide Archive, ID PRJEB48383, <https://www.ebi.ac.uk/ena/browser/view/PRJEB48383>.

## AUTHOR CONTRIBUTIONS

The first two authors contributed equally to this work. LM, SD, and PS made the conception, design of the study. LM, SD, GC, GR, and PM carried out the sampling. LM, SD, and CC did the sequencing. LM, SD, and SR, performed analyses. LM, SD, and AS conducted statistical analyses. LM, SD, and PS

wrote the paper. LM, SD, AS, GR, and PS contributed to critical writing and reviewing of the manuscript. All authors reviewed the manuscript and gave final approval for publication.

## FUNDING

This project was funded by the Veneto Region in the framework of the PSR 2014–2020. Author SR was supported by Cariparo Foundation (Italy).

## SUPPLEMENTARY MATERIAL

The Supplementary Material for this article can be found online at: <https://www.frontiersin.org/articles/10.3389/fenvs.2021.807889/full#supplementary-material>

## REFERENCES

- Agamuthu, P., Tan, Y. S., and Fauziah, S. H. (2013). Bioremediation of Hydrocarbon Contaminated Soil Using Selected Organic Wastes. *Proced. Environ. Sci.* 18, 694–702. doi:10.1016/j.proenv.2013.04.094
- Amann, R. L., Ludwig, W., and Schleifer, K. H. (1995). Phylogenetic Identification and *In Situ* Detection of Individual Microbial Cells without Cultivation. *Microbiol. Rev.* 59, 143–169. doi:10.1128/mr.59.1.143-169.1995
- Anikwe, M., and Nwobodo, K. C. A. (2002). Long Term Effect of Municipal Waste Disposal on Soil Properties and Productivity of Sites Used for Urban Agriculture in Abakaliki, Nigeria. *Bioresour. Technol.* 83, 241–250. doi:10.1016/S0960-8524(01)00154-7
- Baureder, M., and Hederstedt, L. (2013). Heme Proteins in Lactic Acid Bacteria. *Adv. Microb. Physiol.* 62, 1–43. doi:10.1016/B978-0-12-410515-7.00001-9
- Bolyen, E., Rideout, J. R., Dillon, M. R., Bokulich, N. A., Abnet, C. C., Al-Ghalith, G. A., et al. (2019). Reproducible, Interactive, Scalable and Extensible Microbiome Data Science Using QIIME 2. *Nat. Biotechnol.* 37 (8), 852–857. doi:10.1038/s41587-019-0209-9
- Brown, A. (1993). A Review of Soil Sampling for Chemical Analysis. *Aust. J. Exp. Agric.* 33 (8), 983. doi:10.1071/EA9930983
- Bünemann, E. K., Bongiorno, G., Bai, Z., Creamer, R. E., De Deyn, G., De Goede, R., et al. (2018). Soil Quality - A Critical Review. *Soil Biol. Biochem.* 120, 105–125. doi:10.1016/j.soilbio.2018.01.030
- Bürgmann, H., Pesaro, M., Widmer, F., and Zeyer, J. (2001). A Strategy for Optimizing Quality and Quantity of DNA Extracted from Soil. *J. Microbiol. Methods* 45, 7–20. doi:10.1016/S0167-7012(01)00213-5
- Chiodi, C., Moro, M., Squartini, A., Concheri, G., Occhi, F., Fornasier, F., et al. (2020). High-throughput Isolation of Nucleic Acids from Soil. *Soil Syst.* 4 (1), 3. doi:10.3390/soilsystems4010003
- Clark, M. A., Moran, N. A., and Baumann, P. (1999). Sequence Evolution in Bacterial Endosymbionts Having Extreme Base Compositions. *Mol. Biol. Evol.* 16(11), 1586–1598. doi:10.1093/oxfordjournals.molbev.a026071
- Coelho, F. J. R. C., Louvado, A., Domingues, P. M., Cleary, D. F. R., Ferreira, M., Almeida, A., et al. (2016). Integrated Analysis of Bacterial and Microeukaryotic Communities from Differentially Active Mud Volcanoes in the Gulf of Cadiz. *Sci. Rep.* 6, 35272. doi:10.1038/srep35272
- Dries, L., Bussotti, S., Pozzi, C., Kunz, R., Schnell, S., Löhnertz, O., et al. (2021). Rootstocks Shape Their Microbiome-Bacterial Communities in the Rhizosphere of Different Grapevine Rootstocks. *Microorganisms* 9 (4), 822. doi:10.3390/microorganisms9040822
- Dumas, J. B. A. (1831). Procédes de l'analyse organique. *Ann. Chim. Phys.* T47, 198–213.
- Fierer, N. (2017). Embracing the Unknown: Disentangling the Complexities of the Soil Microbiome. *Nat. Rev. Microbiol.* 15, 579–590. doi:10.1038/nrmicro.2017.87
- Fusaro, S., Squartini, A., and Paoletti, M. G., (2018). Functional Biodiversity, Environmental Sustainability and Crop Nutritional Properties: A Case Study of Horticultural Crops in north-eastern Italy. *Appl. Soil Ecol.* 123, 699, 708. doi:10.1016/j.apsoil.2017.06.023
- Giupponi, L., Corti, C., Manfredi, P., and Cassinari, C. (2013). Application of the Floristic-Vegetational Indexes System for the Evaluation of the Environmental Quality of a Semi-natural Area of the Po Valley (Piacenza, Italy). *Plant Sociol.* 50 (2), 47–56. doi:10.7338/pls2013502/03
- Giupponi, L., Corti, C., and Manfredi, P. (2015). The Vegetation of the Borgotrebbe Landfill (Piacenza, Italy): Phytosociological and Ecological Characteristics. *Plant Biosyst. - Int. J. Dealing all Aspects Plant Biol.* 149, 865–874. doi:10.1080/11263504.2014.945507
- Gregorich, E. G., Carter, M. R., Doran, J. W., Pankhurst, C. E., and Dwyer, L. M. (1997). "Chapter 4 Biological Attributes of Soil Quality," in *Developments in Soil Science*. Editors E. G. Gregorich and M. R. Carter (Amsterdam, Netherlands: Elsevier), 81–113. doi:10.1016/S0166-2481(97)80031-1
- Hamdan, L. J., Gillevet, P. M., Sikaroodi, M., Pohlman, J. W., Plummer, R. E., and Coffin, R. B. (2008). Geomicrobial Characterization of Gas Hydrate-Bearing Sediments along the Mid-Chilean Margin. *FEMS Microbiol. Ecol.* 65, 15–30. doi:10.1111/j.1574-6941.2008.00507.x
- Hartemink, A. E. (2016). The Definition of Soil since the Early 1800s. *Adv. Agron.* 137, 73–126. doi:10.1016/bs.agron.2015.12.001
- Henry, S., Baudoin, E., López-Gutiérrez, J. C., Martin-Laurent, F., Brauman, A., and Philippot, L. (2004). Quantification of Denitrifying Bacteria in Soils by nirK Gene Targeted Real-Time PCR. *J. Microbiol. Methods* 59 (3), 327–335. doi:10.1016/j.mimet.2004.07.002
- Hesnawi, R. M., and Mogadami, F. S. (2013). Bioremediation of Libyan Crude Oil-Contaminated Soil under Mesophilic and Thermophilic Conditions. *APCBEE Proced.* 5, 82–87. doi:10.1016/j.apcbec.2013.05.015
- Hovatter, S. R., DeJelo, C., Case, A. L., and Blackwood, C. B. (2011). Metacommunity Organization of Soil Microorganisms Depends on Habitat Defined by Presence of *Lobelia siphilitica* Plants. *Ecology* 92, 57–65. doi:10.1890/10-0332.1
- Islam, W., Noman, A., Naveed, H., Huang, Z., and Chen, H. Y. H. (2020). Role of Environmental Factors in Shaping the Soil Microbiome. *Environ. Sci. Pollut. Res.* 27, 41225–41247. doi:10.1007/s11356-020-10471-2
- Jackson, N. D., and Fahrig, L. (2014). Landscape Context Affects Genetic Diversity at a Much Larger Spatial Extent Than Population Abundance. *Ecology* 95, 871–881. doi:10.1890/13-0388.1
- Jansson, J. K., and Hofmockel, K. S. (2020). Soil Microbiomes and Climate Change. *Nat. Rev. Microbiol.* 18, 35–46. doi:10.1038/s41579-019-0265-7
- Jastrow, J. D., and Miller, R. M. (1991). Methods for Assessing the Effects of Biota on Soil Structure. *Agric. Ecosyst. Environ.* 34, 279–303. doi:10.1016/0167-8809(91)90115-E
- Jenny, H. (1946). Arrangement of Soil Series and Types According to Functions of Soil-Forming Factors. *Soil Sci.* 61 (5), 375–392. doi:10.1097/00010694-194605000-00005
- Jiménez, J. A., Novinskac, A., and Filion, M. (2020). Inoculation with the Plant-Growth-Promoting Rhizobacterium *Pseudomonas Fluorescens*

- LBUM677 Impacts the Rhizosphere Microbiome of Three Oilseed Crops. *Front. Microbiol.* 11, 569366. doi:10.3389/fmicb.2020.569366
- Kleiber, M. (1947). Body Size and Metabolic Rate. *Physiol. Rev.* 27, 511–541. doi:10.1152/physrev.1947.27.4.511
- Le Moal, M., Gascuel-Oudoux, C., Ménesguen, A., Souchon, Y., Étrillard, C., Levain, A., et al. (2019). Eutrophication: A New Wine in an Old Bottle? *Sci. Total Environ.* 651 (1), 1–11. doi:10.1016/j.scitotenv.2018.09.139
- Lehmann, J., Bossio, D. A., Kögel-Knabner, I., and Rillig, M. C. (2020). The Concept and Future Prospects of Soil Health. *Nat. Rev. Earth Environ.* 1, 544–553. doi:10.1038/s43017-020-0080-8
- Levantesi, C., Bonadonna, L., Brianco, R., Grohmann, E., Toze, S., and Tandoi, V. (2012). Salmonella in Surface and Drinking Water: Occurrence and Water-Mediated Transmission. *Food Res. Int.* 45 (2), 587–602. doi:10.1016/j.foodres.2011.06.037
- Manfredi, P., Cassinari, C., Francaviglia, R., and Trevisan, M. (2019). A New Technology to Restore Soil Fertility: Reconstitution. *Agrochimica LXIII* (3), 247–260. doi:10.12871/00021857201933
- Maron, P.-A., Mougel, C., and Ranjard, L. (2011). Soil Microbial Diversity: Methodological Strategy, Spatial Overview and Functional Interest. *Comptes Rendus Biologies* 334, 403–411. doi:10.1016/j.crv.2010.12.003
- Meurer, J., Koelbel, J., and Hoffmann, V. H. (2020). On the Nature of Corporate Sustainability. *Organ. Environ.* 33 (3), 319–341. doi:10.1177/1086026619850180
- Nannipieri, P., Ascher, J., Ceccherini, M. T., Landi, L., Pietramellara, G., and Renella, G. (2003). Microbial Diversity and Soil Functions. *Eur. J. Soil Sci.* 54, 655–670. doi:10.1111/ejss.4\_1239810.1046/j.1351-0754.2003.0556.x
- Odum, Eugene P. (1953). “Fundamentals of Ecology,” in *The Future of Nature: Documents of Global Change*. Editors Libby, Robin, Sverker. Sörlin, and Warde. Paul (New Haven: Yale University Press), 233–244. doi:10.12987/9780300188479-022
- Olsen, S. R., Cole, C. V., Watanabe, F. S., and Dean, L. A. (1954). *Estimation of Available Phosphorus in Soils by Extraction with Sodium Bicarbonate*, 939. Washington D.C.: USDA circular U.S. Gov. Print. Office.
- Qilu, C., Xueling, W., Igen, X., Hui, L., Yuhua, Z., and Qifa, Z. (2017). High-quality, Ecologically Sound Remediation of Acidic Soil Using Bicarbonate-Rich Swine Wastewater. *Sci. Rep.* 7, 11911. doi:10.1038/s41598-017-12373-9
- Quast, C., Pruesse, E., Yilmaz, P., Gerken, J., Schweer, T., Yarza, P., et al. (2012). The SILVA Ribosomal RNA Gene Database Project: Improved Data Processing and Web-Based Tools. *Nucleic Acids Res.* 41 (D1), D590–D596. doi:10.1093/nar/gks1219
- Robe, P., Nalin, R., Capellano, C., Vogel, T. M., and Simonet, P. (2003). Extraction of DNA from Soil. *Eur. J. Soil Biol.* 39, 183–190. doi:10.1016/S1164-5563(03)00033-5
- Robinson, D. A., Lebron, L., and Vereecken, H. (2009). On the Definition of the Natural Capital of Soils: A Framework for Description, Evaluation, and Monitoring. *Soil Sci. Soc. Am. J.* 73, 1904–1911. doi:10.2136/sssaj2008.0332
- Roesch, L. F. W., Fulthorpe, R. R., Riva, A., Casella, G., Hadwin, A. K. M., Kent, A. D., et al. (2007). Pyrosequencing Enumerates and Contrasts Soil Microbial Diversity. *ISME J.* 1 (4), 283–290. doi:10.1038/ismej.2007.53
- Roose-Amsaleg, C. L., Garnier-Sillam, E., and Harry, M. (2001). Extraction and Purification of Microbial DNA from Soil and Sediment Samples. *Appl. Soil Ecol.* 18, 47–60. doi:10.1016/S0929-1393(01)00149-4
- Rothauwe, J. H., Witzel, K. P., and Liesack, W. (1997). The Ammonia Monooxygenase Structural Gene *amoA* as a Functional Marker: Molecular fine-scale Analysis of Natural Ammonia-Oxidizing Populations. *Appl. Environ. Microbiol.* 63 (12), 4704–4712. doi:10.1128/aem.63.12.4704-4712.1997
- Rösch, C., Mergel, A., and Bothe, H. (2002). Biodiversity of Denitrifying and Dinitrogen-Fixing Bacteria in an Acid Forest Soil. *Appl. Environ. Microbiol.* 68 (8), 3818–3829. doi:10.1128/AEM.68.8.3818-3829.2002
- Sagova-Mareckova, M., Cermak, L., Novotna, J., Plhachova, K., Forstova, J., and Kopecky, J. (2008). Innovative Methods for Soil DNA Purification Tested in Soils with Widely Differing Characteristics. *Appl. Environ. Microbiol.* 74 (9), 2902–2907. doi:10.1128/AEM.02161-07
- Schmalenberger, A., and Tebbe, C. C. (2002). Bacterial Community Composition in the Rhizosphere of a Transgenic, Herbicide-Resistant maize (*Zea mays*) and Comparison to its Non-transgenic Cultivar Bosphore. *FEMS Microbiol. Ecol.* 40 (1), 29–37. doi:10.1111/j.1574-6941.2002.tb00933.x
- Shade, A., and Handelsman, J. (2012). Beyond the Venn Diagram: the hunt for a Core Microbiome. *Environ. Microbiol.* 14 (1), 4–12. doi:10.1111/j.1462-2920.2011.02585.x
- Sims, R. C., and Sims, J. L. (2003). “Landfarming Framework for Sustainable Soil Bioremediation,” in *Utilization Bioremediation Reduce Soil Contamination: Probl. Solutions*. NATO Sci. Ser. IV Earth Environ. Sci. Editors V. Šašek, J. A. Glaser, and Ph. Baveye (Dordrecht, Netherlands: Springer), 19, 319–334. doi:10.1007/978-94-010-0131-1\_27
- Strickland, M. S., Osburn, E., Lauber, C., Fierer, N., and Bradford, M. A. (2009). Litter Quality Is in the Eye of the Beholder: Initial Decomposition Rates as a Function of Inoculum Characteristics. *Funct. Ecol.* 23, 627–636. doi:10.1111/j.1365-2435.2008.01515.x
- Tang, J., Zhang, J., Ren, L., Zhou, Y., Gao, J., Luo, L., et al. (2019). Diagnosis of Soil Contamination Using Microbiological Indices: A Review on Heavy Metal Pollution. *J. Environ. Manage.* 242, 121–130. doi:10.1016/j.jenvman.2019.04.061
- Teng, Y., and Chen, W. (2019). Soil Microbiomes-A Promising Strategy for Contaminated Soil Remediation: A Review. *Pedosphere* 29 (3), 283–297. doi:10.1016/S1002-0160(18)60061-X
- Vester, J. K., Glaring, M. A., and Stougaard, P. (2015). Improved Cultivation and Metagenomics as New Tools for Bioprospecting in Cold Environments. *Extremophiles* 19, 17–29. doi:10.1007/s00792-014-0704-3
- Vieira, C. K., dos Anjos Borges, L. G., Bortolini, J. G., Soares, C. R. F. S., Giongo, A., and Stürmer, S. L. (2022). Does a Decrease in Microbial Biomass Alter Mycorrhizal Attributes and Soil Quality Indicators in Coal Mining Areas under Revegetation Process? *Sci. Total Environ.* 802, 149843. doi:10.1016/j.scitotenv.2021.149843
- Walkley, A., and Black, I. A. (1934). An Examination of the Degtjareff Method for Determining Soil Organic Matter, and a Proposed Modification of the Chromic Acid Titration Method. *Soil Sci.* 37 (1), 29–38. doi:10.1097/00010694-193401000-00003
- Wang, B., Wang, Y., Cui, X., Zhang, Y., and Yu, Z. (2019). Bioconversion of Coal to Methane by Microbial Communities from Soil and from an Opencast Mine in the Xilingol Grassland of Northeast China. *Biotechnol. Biofuels* 12, 236. doi:10.1186/s13068-019-1572-y
- Xu, J., Liu, C., Hsu, P.-C., Zhao, J., Wu, T., Tang, J., et al. (2019). Remediation of Heavy Metal Contaminated Soil by Asymmetrical Alternating Current Electrochemistry. *Nat. Commun.* 10, 2440. doi:10.1038/s41467-019-10472-x
- Yan, Y., Xue, F., Muhammad, F., Yu, L., Xu, F., Jiao, B., et al. (2018). Application of Iron-Loaded Activated Carbon Electrodes for Electrokinetic Remediation of Chromium-Contaminated Soil in a Three-Dimensional Electrode System. *Sci. Rep.* 8, 5753. doi:10.1038/s41598-018-24138-z
- Young, I. M., and Crawford, J. W. (2004). Interactions and Self-Organization in the Soil-Microbe Complex. *Science* 304, 1634–1637. doi:10.1126/science.1097394
- Young, J. M., Austin, J. J., and Weyrich, L. S. (2017). Soil DNA Metabarcoding and High-Throughput Sequencing as a Forensic Tool: Considerations, Potential Limitations and Recommendations. *FEMS Microbiol. Ecol.* 93 (2), fiw207. doi:10.1093/femsec/fiw207
- Zakrzewski, M., Proietti, C., Ellis, J. J., Hasan, S., Brion, M.-J., Berger, B., et al. (2016). Calypso: A User-Friendly Web-Server for Mining and Visualizing Microbiome-Environment Interactions. *Bioinformatics* 33 (5), btw725–783. doi:10.1093/bioinformatics/btw725
- Zilio, M., Motta, S., Tambone, F., Scaglia, B., Boccasile, G., Squartini, A., et al. (2020). The Distribution of Functional N-Cycle Related Genes and Ammonia and Nitrate Nitrogen in Soil Profiles Fertilized with mineral and Organic N Fertilizer. *PLoS ONE* 15 (6), e0228364. doi:10.1371/journal.pone.0228364

**Conflict of Interest:** PM is employed by MCM Ecosistemi S. r. l.

The remaining authors declare that the research was conducted in the absence of any commercial or financial relationships that could be construed as a potential conflict of interest.

**Publisher's Note:** All claims expressed in this article are solely those of the authors and do not necessarily represent those of their affiliated organizations, or those of the publisher, the editors and the reviewers. Any product that may be evaluated in this article, or claim that may be made by its manufacturer, is not guaranteed or endorsed by the publisher.

Copyright © 2022 Maretto, Deb, Ravi, Chiodi, Manfredi, Squartini, Concheri, Renella and Stevanato. This is an open-access article distributed under the terms of the Creative Commons Attribution License (CC BY). The use, distribution or reproduction in other forums is permitted, provided the original author(s) and the copyright owner(s) are credited and that the original publication in this journal is cited, in accordance with accepted academic practice. No use, distribution or reproduction is permitted which does not comply with these terms.



# Soil Surface Micro-Topography by Structure-from-Motion Photogrammetry for Monitoring Density and Erosion Dynamics

Annelie Ehrhardt\*, Detlef Deumlich and Horst H. Gerke

Research Area 1 "Landscape Functioning" Working Group "Hydropedology", Leibniz-Centre for Agricultural Landscape Research (ZALF), Müncheberg, Germany

## OPEN ACCESS

### Edited by:

Ute Wollschläger,  
Helmholtz Association of German  
Research Centres (HZ), Germany

### Reviewed by:

Rainer Duttmann,  
University of Kiel, Germany  
Thomas Keller,  
Swedish University of Agricultural  
Sciences, Sweden

### \*Correspondence:

Annelie Ehrhardt  
Annelie.Ehrhardt@zalf.de

### Specialty section:

This article was submitted to  
Soil Processes,  
a section of the journal  
Frontiers in Environmental Science

**Received:** 07 July 2021

**Accepted:** 30 November 2021

**Published:** 17 January 2022

### Citation:

Ehrhardt A, Deumlich D and Gerke HH  
(2022) Soil Surface Micro-Topography  
by Structure-from-Motion  
Photogrammetry for Monitoring  
Density and Erosion Dynamics.  
Front. Environ. Sci. 9:737702.  
doi: 10.3389/fenvs.2021.737702

Soil erosion is a major threat to soil fertility, food security and water resources. Besides a quantitative assessment of soil loss, the dynamics of erosion-affected arable soil surfaces still poses challenges regarding field methods and predictions because of scale-dependent and soil management-related complex soil-crop-atmosphere processes. The objective was to test a photogrammetric Structure-from-Motion (SfM) technique for the mm-scale mapping of the soil surface micro-topography that allows the monitoring without special equipment and with widely available cameras. The test was carried out in May 2018 on three plots of 1.5 m<sup>2</sup> (upper-, middle-, and footslope) covering surface structural features (tractor wheel lane, seed rows) along a Maize-cultivated hillslope with a coarse-textured topsoil and a runoff monitoring station. The changes in mm-scaled surface micro-topography were derived from repeatedly photographed images of the same surface area during a 2-weeks period with two rain events. A freely available SfM-program (VisualSfM) and the QGIS software were used to generate 3D-models of the surface topography. Soil cores (100 cm<sup>3</sup>) were sampled to gravimetrically determine the topsoil bulk density. The micro-topographical changes resulting from rainfall-induced soil mass redistribution within the plots were determined from the differences in SfM maps before and after rain. The largest decrease in mean soil surface elevation and roughness was observed after rain for the middle slope plot and primarily in initially less compacted regions. The spatially-distributed intra-plot changes in soil mass at the mm-scale derived from the digital micro-topography models indicated that local depressions were filled with sediments from surrounding knolls during rainfall. The estimated mass loss determined with the SfM technique decreased, if core sample-based soil settlement was considered. The effect of changes in the soil bulk density could be described after calibration also with an empirical model suggested in the Root-Zone-Water-Quality-Model. Uncertainties in the presented plot-scale SfM-technique were due to geo-referencing and the numerical limitations in the freely available SfM-software. The photogrammetric technique provided valuable information on soil surface structure parameters such as surface roughness. The successful application of SfM with widely available cameras and freely available software might stimulate the monitoring of erosion in regions with limited accessibility.

**Keywords:** deposition, compaction, soil settlement, soil consolidation, surface roughness

## INTRODUCTION

Soil loss due to erosion is a global threat to arable land, environment and agricultural productivity (e.g., Borrelli et al., 2013; Pimentel and Burgess, 2013; Sutton et al., 2016). In order to take effective erosion control measures, it is necessary to quantify the soil mass that has been translocated during erosion (García-Ruiz et al., 2015). Standard approaches include stationary sediment and run-off collectors installed at experimental hillslopes, which can operate automatically for the event-based erosion monitoring (e.g., Deumlich et al., 2017) or temporary rainfall simulation experiments (e.g., Kaiser et al., 2015). Disadvantages of these methods include the cost for installation in case of monitoring stations and the relatively small surveillance areas of rainfall simulators (Boardman, 2006). Recently, the Structure-from-Motion (SfM) photogrammetry has been developed as an alternative method (James and Robson, 2012; Eltner et al., 2016) to generate Digital Elevation Models (DEMs) in relatively high spatial resolution (Eltner et al., 2015). By combining the images taken from several cardinal points after calibration (Westoby et al., 2012), this method allows to even utilize digital images from low-cost consumer-grade cameras such as those in smart-phones (Micheletti et al., 2015; Prosdocimi et al., 2017) for the calculation of 3D DEMs. Repeated photographic imaging of the same surface at consecutive times allows to derive the DEM of Difference (DoD) for determining temporal changes in soil micro-topography (Eltner et al., 2017); a mean decrease in surface elevation is indicating a soil loss (e.g., erosion) while an increase represents a gain (e.g., sedimentation). Changes in the soil surface micro-topography have also been determined by using laser scanning (e.g., Haubrock et al., 2009; Nouwakpo et al., 2016). But in contrast to SfM, laser scanning is more expensive and not widely accessible (Nadal-Romero et al., 2015). The SfM technique has already been applied to quantify soil erosion (Di Stefano et al., 2017; Vinci et al., 2017; Meinen and Robinson, 2020) or to monitor crop growth variability (Bendig et al., 2013). It has been used to identify soil structural discrepancies between conservation and conventional agriculture (Tarolli et al., 2019), and to quantify soil roughness parameters depending on soil cultivation practices (Martínez-Agirre et al., 2020).

A major challenge not only for the SfM-based quantification of soil erosion is to distinguish between soil surface elevation changes by erosion (which can be deposition of soil material from uphill regions and soil loss towards downhill regions) and changes that could occur due to soil compaction or settlement (Hänsel et al., 2016; Kaiser et al., 2018). Freshly cultivated soils are characterized by an initially unconsolidated and relatively loose structure that can easily collapse during wetting or due to raindrop impact (e.g., Bergsma und Valenzuela, 1981). This natural soil settlement can be determined by comparing the soil bulk density before the rain storm and after the soil erosion event (Hänsel et al., 2016). Empirical model approaches to estimate the bulk density changes due to soil settlement of arable soils accounted for rain intensity and rainfall energy (e.g., Linden and van Doren, 1987; Ahuja et al., 2006); these models were

implemented, for instance, in the Root-Zone-Water-Quality-Model (RZWQM) (Ahuja et al., 2000).

The accuracy of the determination of changes in the soil surface topography obtained from 3D DEMs was found to decrease with increasing plot sizes due to limited image resolution (e.g., Kaiser et al., 2018). Thus, soil height loss analyzed by SfM-photogrammetry at smaller plots could only be qualitatively compared to data collected at hillslope scale with a sediment collector station. It is well known that an upscaling of soil loss is not possible because erosion processes are scale-dependent (Boix-Fayos et al., 2006; Parsons, 2019). Boix-Fayos et al. (2007) observed increased sediment yields at larger plots as compared to smaller scales, whereas Martínez et al. (2017) reported decreased sediment yields at larger (27 m<sup>2</sup>) as compared to smaller plots (0.7 m<sup>2</sup>). The comparison of soil erosion results obtained from differently-sized plots does not allow quantifying rates of components of the soil mass changes; but it may provide relevant qualitative information on the soil surface micro topography dynamics (Boix-Fayos et al., 2007).

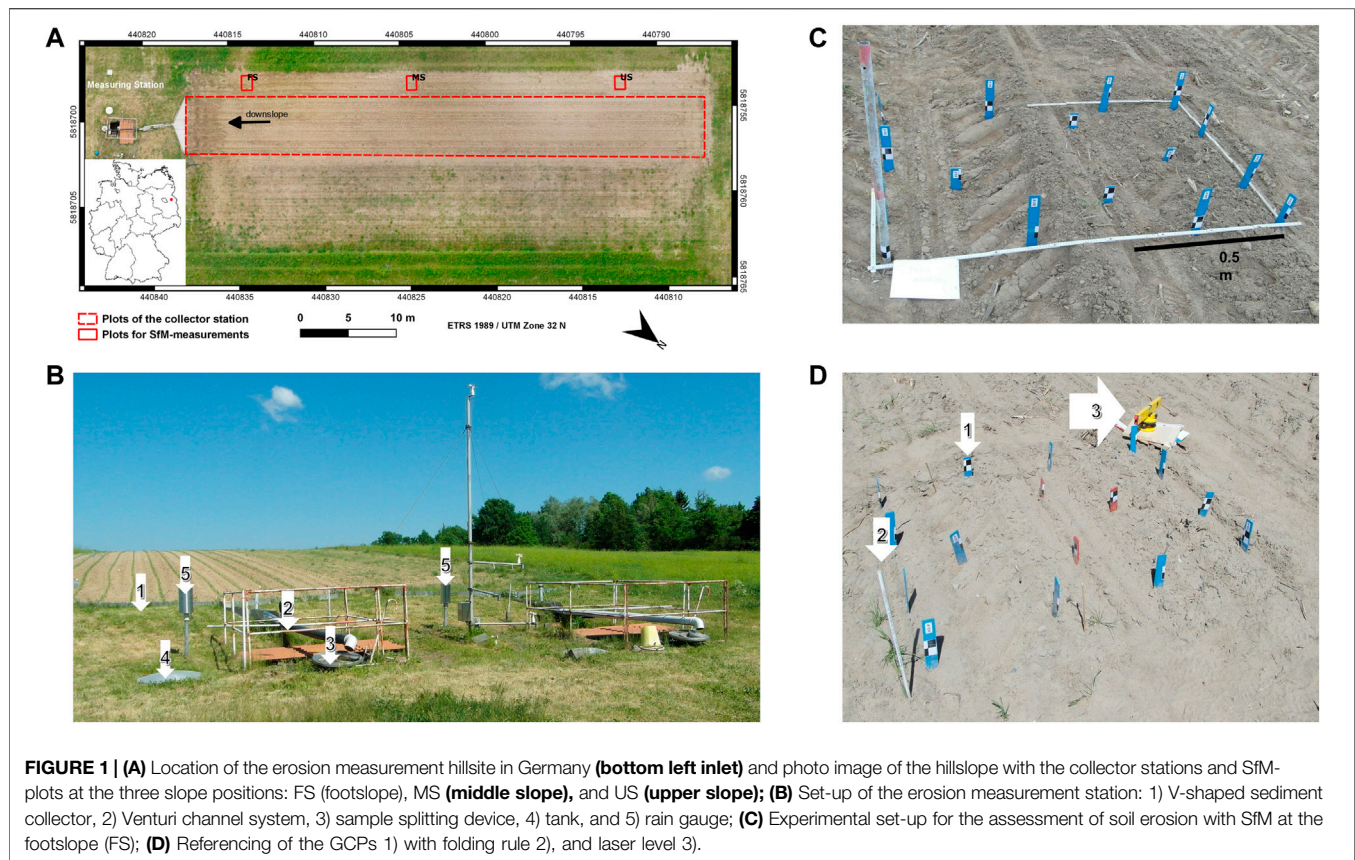
Another more technical limitation is that licensed software such as Agisoft Photoscan has been applied to generate DEMs by SfM in soil erosion studies (e.g., Prosdocimi et al., 2017; Laburda et al., 2021). Thus, SfM data processing is limited to occasions, where licensed software is affordable and available (Jiang et al., 2020). On the other hand, freely available software like VisualSfM exists (Wu, 2011):

Thus, the question arises, whether image analysis using freely available software is reasonable. Also, it still remains a challenge to distinguish between rainfall-erosion induced soil settlement and soil redistribution, deposition, or loss, when applying SfM-photogrammetry. The objective was to test a photogrammetric Structure-from-Motion (SfM) technique for the mm-scale mapping of the soil surface micro-topography that allows monitoring without special equipment and with widely available cameras. We compare two methods for the consideration of soil settlement via bulk density changes. Specific tasks were 1) to test a photogrammetric Structure-from-Motion (SfM) technique for the mm-scale mapping of the soil surface micro-topography that allows monitoring without special equipment and with widely available cameras and 2) to determine soil re-consolidation after soil tillage and sowing to analyze the effect of bulk density changes on the predicted soil mass movement. In addition 3), the changes in soil surface roughness, which can be used as parameter for soil erosion models, was determined from micro-topographical changes. For the present study, data from an experimental soil erosion hillslope were used. Observations were carried out at the same experimental field and for the same period under identical soil and crop management conditions.

## MATERIALS AND METHODS

### Experimental Hillslope and SfM Plots

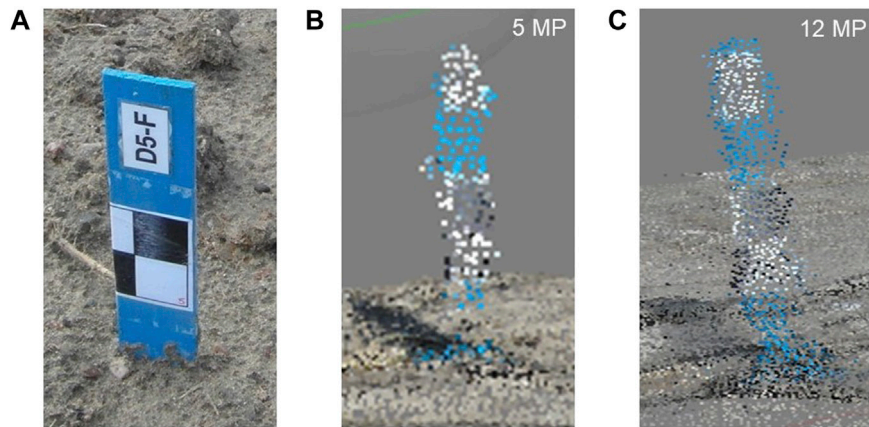
The experimental hillslope (Figure 1A) of the Leibniz-Centre of Agricultural Landscape Research (ZALF) in Müncheberg is



located in the north-eastern part of Germany (52.6°N, 14.3°E; Deumlich et al., 2017). The site is characterized by an average annual precipitation of 547 mm (1992–2019) and an annual mean temperature of 9.3°C (<https://open-research-data.zalf.de/default.aspx>, DWD-ZALF Weather Station, March 2020). The soils along the hillslope are mostly Luvisols that developed from coarse-textured glacial sediments; the topsoil consists of loamy to silty sands with about 3% clay (<0.002 mm), 16% silt (0.002–0.063 mm), 81% sand (0.063–2 mm equivalent particle diameter) and about 6 g/kg of organic carbon (Deumlich et al., 2017). The arable field of the south-east exposed hillslope (length: 53.5 m, width: 6 m) ends at the footslope in tinplate funnel for runoff and sediment collection (Figures 1A,B). Cultivation was carried out together with the sowing of corn (*Zea Maize*, L.) with a grubber-drill combination machine on April 26, 2018 (row spacing was 0.75 m); fertilizer was mechanically applied 8 days later.

The automated runoff station at the footslope of the hillslope consists of a funnel-shaped runoff collector (Figures 1B(1)), a system of pipes and channels for distributing runoff water and sediments (Figures 1B(2)), a Coshoxton-type sampler for splitting the runoff (Figures 1B(3)) with a subsurface installed automated sample collector with plastic bottles on a turntable, a runoff tank at ground level (Figures 1B(4)), for registration of the total amount of surface runoff, and a Hellmann rain gauge (Figures 1B(5)); the small tower meteorological tower was to measure wind speed, in 20, 50, 100, and 400 cm above the surface.

The plots for structure-from-motion (SfM) photogrammetry were installed on May 3, 2018, at the upper slope (US), middle slope (MS), and footslope (FS) in north-western direction on an identically-tilled area next to the large hillslope-plot (Figure 1A). Since soil erosion rates differ according to slope angle (e.g., Quan et al., 2020) these three plots were chosen for representing the different angles from 3° to 6° present at the hillslope. The potential flow lines at the soil surface of the hillslope runoff experiment determined from a digital elevation model (GlobalMapper 19.0, LiDAR, 2018; resolution: 1.2 cm × 1.2 cm, see **Supplementary Appendix SA1**) indicated that the SfM plots are not directly connected to the runoff collector at the footslope. The SfM plot size of 1 m length and 1.5 m width was selected such that all surface features (i.e., wheel track, non-compacted region, and 2 rows of corn) were included (Figure 1C) and the area was small enough to achieve mm-resolution due to SfM-processing. The distance between plots at footslope (FS) and MS was 16 m, and between plots at FS and US it was 38 m (Figure 1A). Replicates for the plots could not be identified at this field and were not required since the 3 plots at major hillslope positions could already sufficiently demonstrate the applicability of the SfM-technique and comparison of methods for soil settlement correction. The plots were marked by specially labelled sticks with black-and-white markers for ground control (GC) points (Figure 2). Sticks were driven into the ground down to at least 30 cm depth to ensure that their position was not affected by



**FIGURE 2 | (A)** Example photo of a ground control point (GCP) at the plot surface and point clouds generated by photos taken with a resolution of **(B)** 5 MP, and **(C)** 12 MP.

topsoil porosity changes. Each SfM plot received 15 sticks with GC markers, from which 3 or 4 were placed at the sides and 4 sticks were placed inside of the plot with the GC markers showing in different directions (**Figure 1C**). The local coordinates of the GC points were determined by using a ruler and a laser level (Einhell Bavaria BLW 400) relative to a reference point at the bottom left corner of each plot (**Figures 1D(2)**); UTM coordinates were obtained with GPS (Trimble Geo 7X, Handheld GNSS System, accuracy: 0.5–1.0 m) for reference points to determine the position of plots along the hillslope.

During the observation period from May 3 to May 16, 2018, two relevant rainfall events occurred on May 3 (5.8 mm) and May 15 (14.4 mm), the latter rain had the highest rain energy ( $311.5 \text{ J m}^{-2}$ ) and erosivity (EI30) of  $6 \text{ MJ mm ha}^{-1} \text{ h}^{-1}$  in terms of the maximal 30-min rain intensity (I30). The cumulative rainfall energy  $E$  of both events amounted to  $406 \text{ J m}^{-2}$ .

The bulk density,  $\rho_b$  ( $\text{kg m}^{-3}$ ) was determined gravimetrically using  $100 \text{ cm}^3$  intact soil cores (cylindrical steel cylinders of 5 cm height) by oven drying at  $105^\circ\text{C}$  for about 3 days. Samples were determined before the SfM measurements (May 3) and after the heavy rainfall (May 15) from the 1–6 cm soil depth related to the local surface elevation assuming that the value is valid initially after cultivation for most of the topsoil. The top 1 cm of soil could not be sampled without disturbance and was discarded. Since core sampling was destructive, we selected a region outside and downhill of the SfM plots for the sampling. Thus, the plot surface for SfM measurements remained intact and that the potential surface runoff from uphill was not affected by any disturbances of the soil surface. In each field campaign, 6 core samples were taken beneath each SfM plot, of which 3 samples were from the intact cultivated area and 3 soil cores from the area compacted by tractor wheels to capture the variability of soil bulk density related to visible soil structures of the plot (**Figure 1C**). The number of bulk density samples was limited because of limited soil area in the close vicinity of the SfM-plots that should remain intact for subsequent sampling and runoff observations. Note that each core sampling led to significant disturbance of the intact soil next

to the plots. Also, the soil of the larger hillslope measurements should remain intact, thus only a relatively small area for bulk density sampling was available.

The bulk density after the rainfall event on May 15 was alternatively determined from the estimated porosity  $\varphi$  (t) (Linden and van Doren, 1987) as:

$$\varphi = \varphi_i - (\varphi_i - \varphi_c)(1 - e^{(-aP-bE)}) \quad (1)$$

where  $\varphi_i$  is the initial porosity,  $\varphi_c$  the final porosity of the re-consolidated soil,  $P$  [mm] is the amount of rainfall during the event and the cumulative rainfall energy  $E$  [ $\text{J cm}^{-2}$ ]. The bulk density  $\rho_b$  is obtained by

$$\rho_b = (1 - \varphi) * \rho_s \quad (2)$$

where  $\rho_s$  is the density of the solid particles. The parameters for **Eqs. 1, 2** are defined in **Table 1**. Parameters “a” and “b” in **Eq. 1** were fitted manually. The optimization was based on the lowest root-mean-square-error (RMSE) in the mean between the measured and the calculated bulk densities inside and outside the tractor lane in the upper-, middle- and footslope.

## SfM-Photogrammetry and Image Processing

Photo images of the plots for SfM-processing were taken on a daily basis with the compact digital camera SAMSUNG WB750 in approximately 1.5 m distance from the plot’s boundaries. The camera has a locked focal length,  $f$ , of 4 mm, a maximum aperture of  $f/3.2$  (i.e., a maximum opening width of the objective lens) and a pixel size of  $1.49 \mu\text{m}$  (Samsung, 2011). The DEMs of the soil surface were generated before and after two rainfall events. Each plot was photographed 30–50-times from different perspectives to ensure a spatial overlapping of the images of at least 60% as suggested previously (Westoby et al., 2012; Kaiser et al., 2015). There was no need to adjust the camera to similar perspectives or heights for subsequent photo-sessions at different days, since the camera positions were automatically determined during the

**TABLE 1** | Original and adapted parameters for **Eq. 1**: amount of rainfall  $P$ , cumulative rainfall energy  $E$ , density of solid particles  $\rho_s$ , final bulk density  $\rho_{b,c}$ , final porosity  $\varphi_c$ , original and adapted parameters  $a$  and  $b$  and root-mean-square-error RMSE of the final measured and modelled bulk density; TL: Tractor lane.

	$P$ [mm]	$E$ [J*cm <sup>-2</sup> ]	$\rho_s$ [kg m <sup>-3</sup> ]	$\rho_{b,c}$ [kg m <sup>-3</sup> ]	$\varphi_c$ []	$a_{orig}$ []	$b_{orig}$ []	$a_{adap}$ []	$b_{adap}$ []	RMSE [kg m <sup>-3</sup> ]
within TL	20.2	0.0406	2650	1,620	0.39	0.015	1.5	0.02	1.5	75
outside TL				1,550	0.42			0.013	1.5	5

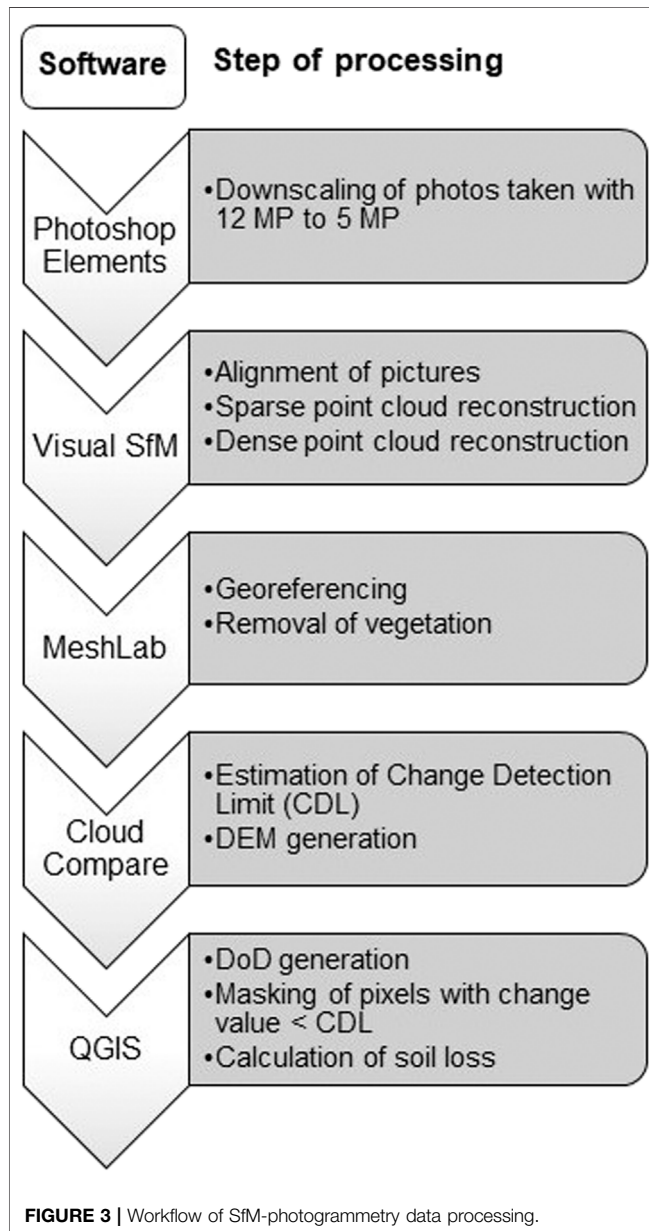


image processing, and ground control points (GCP) ensured the georeferencing of the 3D-models. This was one of the major advantages of the SfM-photogrammetry in comparison to, e.g., laser scanning. A sensor size of 5 Mega Pixel (MP) (2592 × 1944 pixels) was used for the images during the initial period (May 2 to

May 14) and a size of 12 MP (4096 × 3072 pixels) for the images taken until May 16. The 12 MP images were downscaled to a pixel sensor size of 5 MP before processing with Adobe Photoshop Elements (Adobe Systems, 2018 Adobe Photoshop Elements Version: 15.0 (20160905. m.97630) x64, operation system: Windows 8.1 64-Bit, Version: 8.1). The point cloud obtained with VisualSfM (**Figure 2**) appeared to have more evenly distributed points, as compared to a point cloud generated from original 5 MP images. This advantage of downscaling the pictures was found throughout the experimental period, such that images were only taken in 12 MP resolution at the end of the observation period.

The image processing was carried out with the freely available software VisualSfM (Wu, 2011); the workflow (**Figure 3**) depicts the applied software for each of the subsequent steps, starting with the image alignment and the reconstruction of the sparse and the dense point clouds that were combined to 3D point clouds. The sparse point cloud contains all points that are found in three or more pictures (Westoby et al., 2012). The dense point cloud contains additional points that are reconstructed by the application of the CMVS- and PMVS2-algorithms. In VisualSfM, the Scale Invariant Feature Transform (SIFT) was used to identify common points and structures in the images independent of their size, illumination, and rotation. The Bundle Block Adjustment (BBA) carried out non-linear 3D spatial optimization of camera position related to GC points (**Figure 1D**) to find the common structures on images for generation of a condensed point cloud. The Clustering View for Multi-view Stereo (CMVS) routine divided data obtained with BBA-algorithm in smaller easier to handle point cloud clusters as a first step to aggregate the combined point cloud. Finally, the Patch-based Multi-view Stereo (PMVS2) routine was applied to independently reconstruct the 3D-spatial data clusters obtained with the CMVS as the second step in point cloud aggregation.

After the Visual SfM step (**Figure 3**), georeferencing of the 3D point clouds was carried out by assigning the measured local coordinates to 4 of the reconstructed GC points (**Figure 1D**) using MeshLab software (Cignoni et al., 2008; Cignoni, 2016). All points resulting from above-ground vegetation (i.e., maize plants) were manually removed in the May 16th surface models (i.e., end of the observation period). The Level of Detection (LoD) was then estimated using CloudCompare software (Cloud Compare, 2020 CloudCompare V2, EDF R&D/TELECOM ParisTech (ENST-TSI), Paris 2016) before exporting the DEMs derived from the point clouds to QGIS software (QGIS Development Team, 2018). The DEM generated from images after a rain event was subtracted from that derived from images before the event in QGIS to create a map of the pixel-based changes in soil

surface micro-topography (for images of the workflow see **Supplementary Appendix SA4**). These DEMs of temporal Difference (DoD) were corrected for the uncertainty in the determination of the re-location of GC points by assigning a value of zero to all pixel values smaller than the LoD. Thus, we assumed that uncertainties caused by small differences in referencing the DEMs of two times were negligible. The plot-average changes in soil surface elevation,  $\overline{\Delta z}^{\Delta t}$  between two times,  $\Delta t = t_2 - t_1$  were obtained from the sum of DoD pixel values,  $\Delta z_i$  divided by the number of pixels,  $N_p = 1, \dots, i$ , as:

$$\overline{\Delta z}^{\Delta t} = \frac{1}{N_p} \sum_{i=1}^{N_p} \Delta z_i. \quad (3)$$

The LoD is defined as the smallest value of change in soil elevation that can actually be detected with SfM without being considered as noise. For the determination of the LoD only those GC points were deployed that were not used for georeferencing. For the LoD different definitions exist in the literature (e.g., Brasington et al., 2003). Here, the LoD between two measurements,  $\Delta t$ , is calculated from the differences of the x-, y-, z-coordinates (isotropic) in all directions as

$$LoD^{\Delta t} = \sqrt{\frac{1}{n \cdot k} \sum_{i=1}^n \sum_{j=1}^k \left[ \left( X_{P_{i,j}}^{t_2} - X_{P_{i,j}}^{t_1} \right)^2 \right]} \quad (4)$$

where  $X$  denotes the  $k = 3$  coordinates of the  $n = 4$  GC points ( $P_{i,j}$ ) at times  $t_1$  and  $t_2$ .

The component describing surface elevation changes due to consolidation and natural compaction (e.g., by rain impact) was considered by the mean surface elevation changes,  $\overline{\Delta z}_{cs}^{\Delta t}$  (subscript  $cs$  denotes “compacted soil”), obtained from the original ( $\bar{z}_{ts}^{t_1}$ ) mean elevation (subscript  $ts$  means “tilled soil”) and the soil bulk density relations before ( $\rho_b^{t_1}$ ) and after the rain event ( $\rho_b^{t_2}$ ) (Hänsel et al., 2016) as:

$$\bar{z}_{cs}^{t_2} = (\rho_b^{t_1} / \rho_b^{t_2}) * \bar{z}_{ts}^{t_1} \quad (5a)$$

where the thickness of tilled soil before the rain at  $t_1$  was first assumed to correspond with the height of the soil core of 5 cm. The value of  $\bar{z}_{cs}^{t_2}$  (here in mm) depends on the thickness of the cultivated soil region, considered to be affected by consolidation; here we compare the effect of a thickness of 5 cm with that of when assuming a value of  $\bar{z}_{ts}^{t_1}$  of 10 cm. Other values were not considered because major elevation changes due to consolidation during single rain events are expected to occur within the uppermost 0–10 cm layer of the topsoil (Rousseva et al., 1988). The two different thickness values were assumed as possible range, since we did not know, whether the bulk density changes occurred in the upper 5 cm of the soil or reached down to 10 cm. Different consolidation was measured outside (2/3 of the plot) and inside the tractor lane (1/3 of the plot). This was accounted for by weighing the soil surface elevation change in the different parts of the plots as:

$$\bar{z}_{cs}^{t_2} = (\rho_{b,i}^{t_1} / \rho_{b,i}^{t_2}) * \bar{z}_{ts}^{t_1} * \frac{1}{3} + (\rho_{b,o}^{t_1} / \rho_{b,o}^{t_2}) * \bar{z}_{ts}^{t_1} * \frac{2}{3} \quad (5b)$$

The subscripts “i” and “o” denote “inside” and “outside” the tractor lane, respectively.

The plot-related mean settlement-induced component of the reduction in soil surface elevation,  $\overline{\Delta z}_{cs}^{\Delta t} = (\bar{z}_{cs}^{t_2} - \bar{z}_{ts}^{t_1})$ , was subtracted from the mean changes in surface elevation obtained from either the DoD maps between the two times,  $\overline{\Delta z}^{\Delta t}$ , **Eq. 3**, to yield a corrected mean value of surface elevation changes as:

$$\overline{\Delta z}_{cor}^{\Delta t} = \overline{\Delta z}^{\Delta t} + \overline{\Delta z}_{cs}^{\Delta t} \quad (6)$$

where subscript  $cor$  denotes “corrected”.

The fraction of the area of which the soil surface elevation increased, decreased or remained unchanged was calculated for the main soil surface structural areas of the plots. The surface structures inside the tractor lane (in TL), outside the tractor lane (out TL), and the seed row (SR) were defined and manually distinguished according to the visible structures in the DoDs. The DoDs of each plot were reduced to the individual soil surface structure and pixels were classified according to increase (+), decrease (−) and no change (0) in soil height and the number of pixels in each class was summed up. The area fraction of each class of soil surface structural feature was obtained (c.f., **Eq. 3**) from the sum of pixels divided by the total number of pixels.

## Potential Errors in Data Acquisition and Processing

Throughout the process of soil loss determination by SfM several errors accumulate: 1) GC points were manually levelled, 2) the generation of the dense point clouds in Visual SfM depends on the image quality and leads in case of low quality images to a lesser point density causing errors when creating surface models 3) georeferencing errors, and 4) errors in soil loss calculation from soil elevation changes due to natural consolidation.

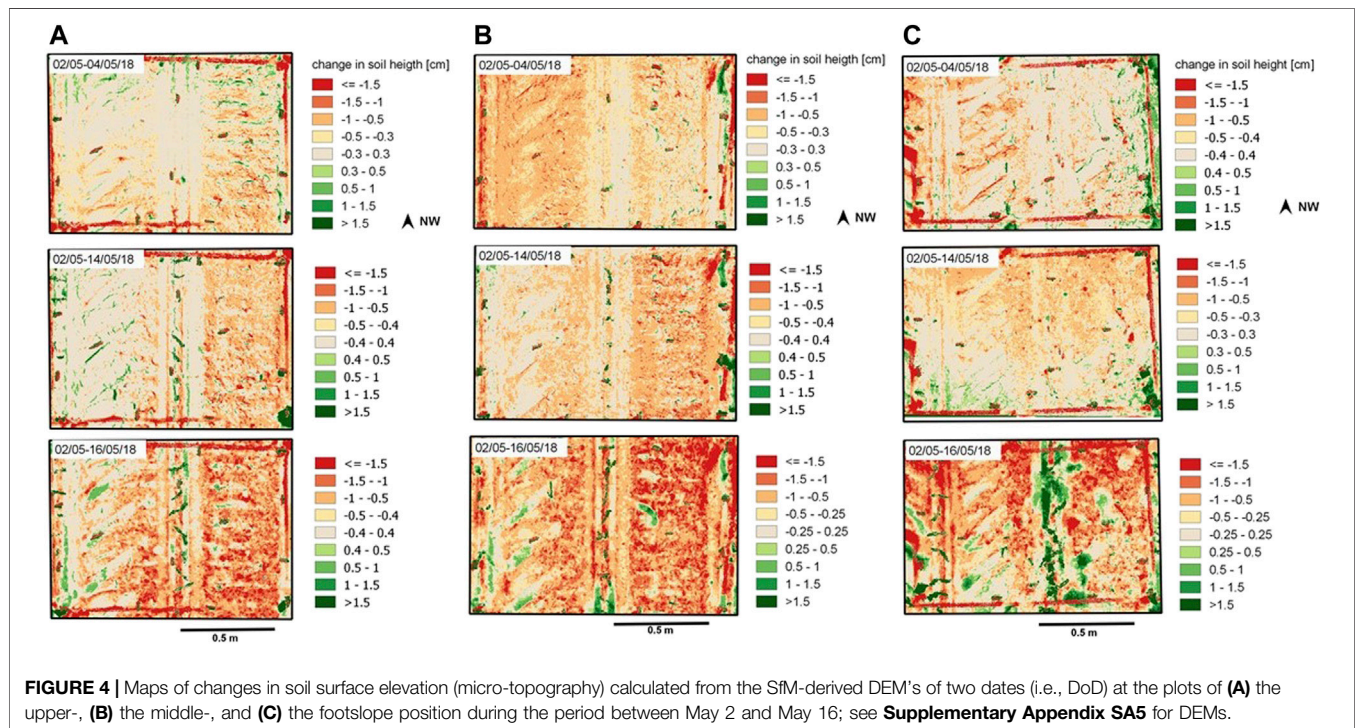
Here, the levelling the GC points with the laser level with an accuracy of  $\pm 1$  mm. The standard deviation of georeferencing the point clouds in MeshLab and the calculation of the Level of Detection (LoD) in CloudCompare amounts to 0.7 mm. For the bulk density measurements used for the correction of soil settlement, a mean standard deviation for all plots of  $70 \text{ kg m}^{-3}$  was obtained. This value resulted in an error of 0.5 mm if a 5 cm topsoil layer  $\bar{z}_{ts}^{t_1}$  and of 1.1 mm if a 10 cm topsoil layer  $\bar{z}_{ts}^{t_1}$  is assumed (**Eq. 5a**). Thus, these errors add to a maximal value of either 2.2–2.8 mm if all sources of possible inaccuracies in data acquisition and processing are considered.

## Calculation of Soil Surface Roughness

Soil surface roughness, as an important input for soil erosion models (e.g., Kaiser et al., 2015), was calculated in QGIS by employing the roughness algorithm derived from the GDAL DEM utility (QGIS Development Team 2014). This algorithm derives the roughness from the Terrain Ruggedness Index (TRI) according to Wilson et al. (2007) by averaging the absolute values of the differences in height between a pixel and its 8 neighbors. This algorithm was used because it provided a convenient and quick possibility to characterize morphologic soil surface changes within the plots. It was the only algorithm currently implemented in QGIS to determine soil roughness. In order to obtain an average roughness of the whole plot, the values of all pixels per plot were averaged.

**TABLE 2** | Surface soil (1–6 cm depth) bulk density,  $\rho_b$  ( $\text{kg m}^{-3}$ ), for the SfM-plots at the three slope positions determined from samples taken inside and outside of the wheel track of a tractor lane (TL) on May 2 and 3 and on May 22, and differences between the two times,  $\Delta$  (for statistical significant differences see boxplots in **Supplementary Appendix SA2**); mean values (MV) and standard deviation (SD) from 3 replicates. TL, Tractor lane.

Slope position	TL	May 2 and 3		May 22 (measured)			May 22 (modelled)	
		MV	SD	MV	SD	$\Delta \rho_b$		$\Delta \rho_b$
		$\rho_b$ ----- $\text{kg m}^{-3}$ -----						
foot	within	1,440	100	1,510	110	70	1,506	66
	outside	1,270	50	1,350	50	80	1,346	76
middle	within	1,480	70	1,440	150	-40	1,532	51
	outside	1,180	40	1,280	90	100	1,283	100
upper	within	1,430	80	1,410	60	-20	1,500	70
	outside	1,250	20	1,330	40	80	1,331	82



**FIGURE 4** | Maps of changes in soil surface elevation (micro-topography) calculated from the SfM-derived DEMs of two dates (i.e., DoD) at the plots of (A) the upper-, (B) the middle-, and (C) the footslope position during the period between May 2 and May 16; see **Supplementary Appendix SA5** for DEMs.

## RESULTS

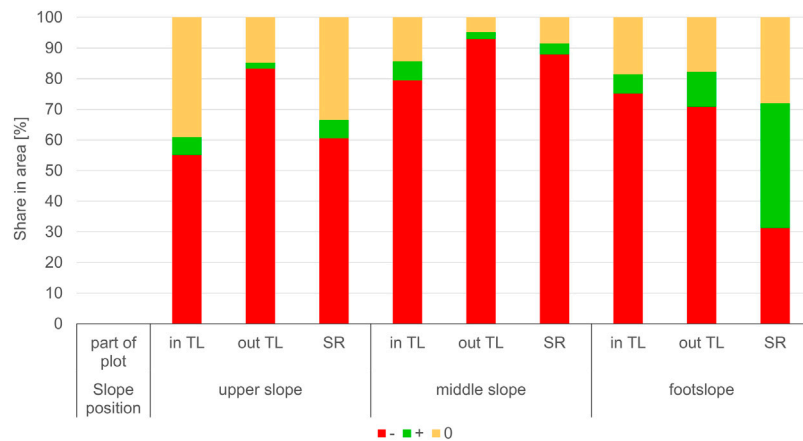
### Soil Bulk Density

Soil bulk density was initially higher in the tractor lanes ( $1,430\text{--}1,480 \text{ kg m}^{-3}$ ) than in the soil regions between tractor lanes with  $1,180\text{--}1,270 \text{ kg m}^{-3}$  (Table 2, for statistical analyses see **Supplementary Appendix SA2**). Measured soil bulk density increased within the 20 days in most plots, except for the tractor lane regions on the middle and upper slopes; however, this effect of a decrease in soil bulk density was smaller than the standard deviation and negligible. The soil outside of the tractor lanes was generally more compacted at the second date indicated by a density increase of about  $80\text{--}100 \text{ kg m}^{-3}$  as compared to the first date and the soil within tractor lanes. On the plot at the footslope position, soil regions in and outside the tractor lanes were similarly more compacted as indicated by a density increase of  $70\text{--}80 \text{ kg m}^{-3}$ . According to

statistical analysis the bulk density differences between inside and outside the tractor lane were not significant, except for the middle and upper slope on May 2, 2018 (**Supplementary Appendix SA2**). The predicted bulk density for the May 22 was similar to the measured bulk density outside the tractor lane. However, modelling showed a stronger increase in soil bulk density inside the tractor lane than the measurements suggested (Table 2).

### SfM-Measurements of Surface Structural Changes and Soil Loss

The final DoD-maps (Figure 4) show spatially-distributed patterns of increasing (green) and decreasing (red) soil surface elevations. The tractor lanes and the seed rows could be identified more clearly in the individual DEMs provided in the Appendix (**Supplementary Appendix SA5**). For the upper slope position, only relatively small



**FIGURE 5 |** Share in area that increased (+), decreased (–) or did not change (0) in the individual soil surface structural sections tractor lane (in TL), outside tractor lane (out TL) and seed row (SR) at the upper, middle and footslope from May 02 to May 16.

changes in soil surface topography are noticed during the first 2 days after the installation of the plots (**Figure 4A**, top). Settlement of the soil can be observed more in the less compacted right part of the plot as compared to the more compacted seed rows and tractor lanes. After 12 days (**Figure 4A**, centre), the settling of the soil was more pronounced (i.e., more decreasing surface elevations) also in the plot region of the initially more compacted soil. Note that the first leaves of the maize plants could be identified as spots of larger elevation increase along the seed row in the middle of the plot. After the heavy rainfall event on May 15, the increased red spots in the lowest DoD map (**Figure 4A**, bottom) indicated a larger decrease in soil surface elevation esp. in the less and more compacted regions of the plot, where more than 80% of the area was subject to soil height loss (**Figure 5**).

For the plots at the middle- (**Figure 4B**) and the footslope (**Figure 4C**) positions, the changes in soil surface topography are relatively similar during the first period between May 2, 4, and 14 (upper and central rows of the maps in **Figure 4**). An exception is the plot at the middle slope: the decrease in surface elevation was stronger in the more compacted tractor lane than in the looser region of the plot (**Figure 4B**, top). Twelve days later, the situation has changed completely: now the loose area shows higher settlement than the tractor lane (90% of the area outside the tractor lane was subject to soil height loss, **Figure 5**). This might be attributed to the different values in the level of detection, LoD, assigned to the DoDs. Changes in soil surface elevation could be masked by a higher limit used as LoD. On May 16, due to rainfall the soil surface elevation is more strongly decreasing (red spots) than increasing (green spots) especially for the plot at the middle slope (**Figure 4B**, bottom). Deposition of soil can be observed at the middle slope plot especially at the lower end of the seed row and in the imprints of the tyres. For the plot at the footslope position, the regions with an increase in surface elevation or deposition are largest and oriented along the seed row along the central part (**Figure 4C**, bottom and **Figure 5**); for this plot at the footslope, a gradient in surface elevation changes was observed ranging from decreasing elevations (erosion) in the upper to increasing elevations (deposition) in the footslope regions. Red

and green spots next to each other, especially for plots at the middle and the bottom slope position (**Figures 4B,C**, maps at the bottom), indicate a flattening of the soil surface topography due to deposition, of soil particles that were detached at the local peaks for example, within the wheel tire marks.

Between May 02 and 16, the plot at the upper slope position experienced the smallest changes in mean surface elevation. This means that here a larger area of the plot remained at the same surface elevation than at the middle slope and footslope (**Figure 5**). As observed qualitatively the middle slope had the highest surface area fraction with soil height loss in all soil surface structural regions (>80%). For the footslope, the seed row experienced the most pronounced increase in soil height, since 40% of the seed row area fraction increased in soil height (**Figure 5**).

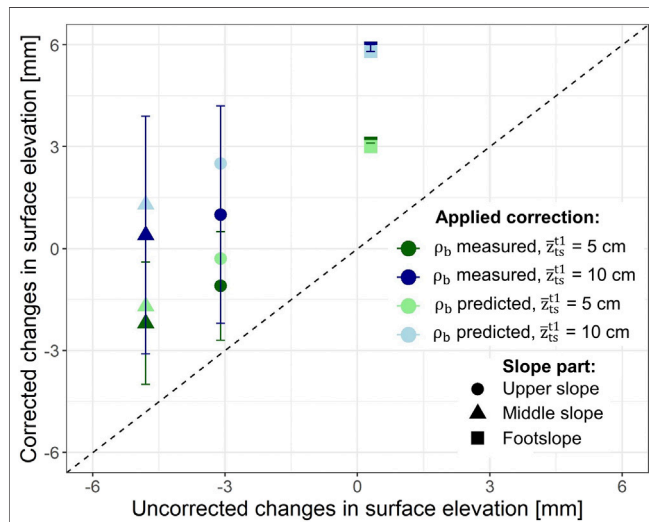
The plot-scale averages of the changes in soil surface elevation obtained from the DoD-maps between May 14 and May 16 were all larger as compared to the hillslope-related calculated soil loss of the sediment yield of the collector station (**Table 3**). The plot-scale mean elevation changes were all negative except for the plot at footslope position, if considering no soil consolidation and consolidation related to 5 cm topsoil (**Figure 6**). When consolidation was related to 10 cm topsoil, all plots (upper-, middle- and footslope) showed increase in soil surface elevation, except when no consolidation was accounted for (**Figure 6**).

The plot-scale averages of the changes in soil surface elevation depict values between –6 and –2 mm that are dependent on the slope (**Figure 7A**). One exception is the positive value found for the plot at the bottom slope position indicating predominately deposition during the rain event. The plot at the upper slope (**Figure 7A**) with the smallest inclination (6%) showed smallest elevation changes (–1.8 mm) but relatively large changes due to consolidation of approx. –5 mm (**Table 3**). The plot at the middle slope with 9% inclination experiences the most pronounced surface changes (–2.2 mm) and consolidation (up to –5.4 mm). Although the inclination was largest at the plot at the footslope (11%), only relatively small changes (–1.7 to –3.1 mm) in the mean surface elevation were observed before and deposition (+3 mm) was observed after the rainfall event on May 15 (**Table 3**). The plot

**TABLE 3 |** Weighted changes in average soil surface elevation (h), volume (V), and mass (M) at the SfM-plots along the experimental slope between May 2 and A: May 4, B: May 14, and C: May 16; D indicates changes in surface elevation and mass between May 14 and 16 after correction for soil settlement; mass, M, collected at the hillslope erosion station between May 2 and 16 (C) was used to calculate a slope-averaged value of the change in surface elevation (h) over the total hillslope.

Slope position	Compact. depth <sup>a</sup>	h [10 <sup>-3</sup> m]				V [10 <sup>-3</sup> m <sup>3</sup> ]				M [kg m <sup>-2</sup> ]			
		A	B	C	D	A	B	C	D	A	B	C	D
upper slope	5 cm	-1.8	-4.6	-3.8	-1.1	-1.7	-4.6	-3.7	-1.8	-2.35	-6.36	-5.12	-1.47
	10 cm	-1.8	-4.6	-1.7	1.0	-1.7	-4.6	-1.7	-0.1	-2.35	-6.36	-2.37	1.29
middle slope	5 cm	-4.5	-4.8	-5.1	-2.2	-5.4	-5.7	-6.2	-3.5	-5.94	-6.51	-7.19	-2.94
	10 cm	-4.5	-4.8	-2.5	0.4	-5.4	-5.7	-3.0	-1.1	-5.94	-6.51	-3.50	0.56
footslope	5 cm	-1.7	-3.1	-1.8	3.1	-1.8	-3.1	-1.9	3.0	-2.34	-4.38	-2.59	4.36
	10 cm	-1.7	-3.1	1.0	5.9	-1.8	-3.1	1.0	5.8	-2.34	-4.38	1.37	8.33
Collector Station				-0.07					-22.6			-0.097	

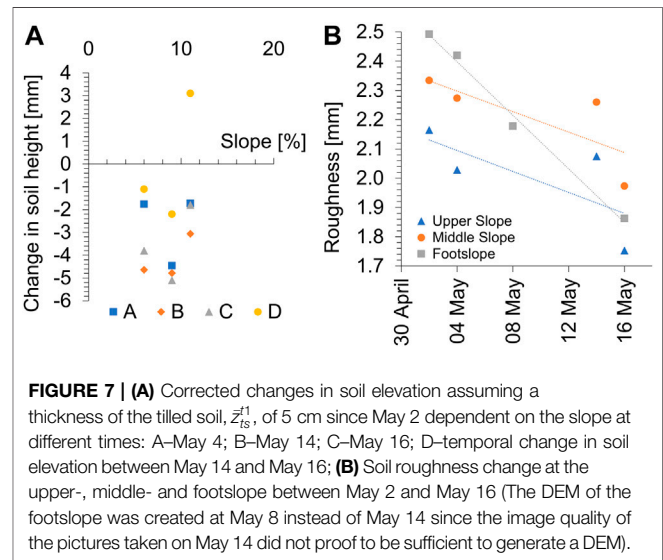
<sup>a</sup>Thickness of tilled soil,  $\bar{z}_{ts}^1$ , Eq. 5b.



**FIGURE 6 |** Uncorrected vs. corrected soil elevation changes [mm] between May 14 and May 16 in the upper slope, middle slope, footslope. The soil height elevation changes were corrected for consolidation by the measured final bulk density  $\rho_b$ , assuming a thickness of the tilled soil,  $\bar{z}_{ts}^1$ , of 5 and 10 cm and corrected for consolidation by the predicted final bulk density  $\rho_b$ , assuming a thickness of the tilled soil,  $\bar{z}_{ts}^1$ , of 5 and 10 cm.

at the middle slope shows the highest losses in surface elevation in contrast to the plots at the upper- and footslope, which corresponded with the loss in soil volume and soil mass (Table 3).

The average soil roughness in terms of the Terrain Ruggedness Index (TRI) decreased at all plots from May 2 till May 16 (Figure 7B). The plot at the footslope had the highest initial soil roughness with 2.5 mm, whereas the upper slope had the smallest initial soil roughness (2.2 mm). Throughout the observation period, the footslope position showed the strongest decrease of TRI-values from 2.5 to 1.9 mm, which corresponds to the deposition and levelling of the soil surface that was observed for the plot surface at the footslope position. At middle and upper slope positions, TRI values decreased only by approximately 0.4 mm from 2.3 to 2.0 mm and 2.1 to 1.7 mm. The soil roughness of the soil surface at the footslope position most gradually decreased (Figure 7B), while at the middle and upper slopes, the surface roughness decreased initially



**FIGURE 7 |** (A) Corrected changes in soil elevation assuming a thickness of the tilled soil,  $\bar{z}_{ts}^1$ , of 5 cm since May 2 dependent on the slope at different times: A–May 4; B–May 14; C–May 16; D–temporal change in soil elevation between May 14 and May 16; (B) Soil roughness change at the upper-, middle- and footslope between May 2 and May 16 (The DEM of the footslope was created at May 8 instead of May 14 since the image quality of the pictures taken on May 14 did not prove to be sufficient to generate a DEM).

more strongly from May 2 till May 4, remained at the same level till May 15, and decreased again after the rainfall on May 15.

## Comparison of Methods for Soil Settlement Correction and Comparison to Slope

The subplots for soil erosion assessment with SfM, installed at the upper, middle, and footslope position of the hillslope differed with respect to slope inclination. After correcting the mean soil surface elevation changes of these plots by using predicted bulk density changes, the elevation changes were generally smaller as compared to the changes obtained by using measured bulk density for the correction (Table 4). Both, measurements and predictions, resulted in an overall reduction in original mean surface elevation of the tilled soil ( $\bar{z}_{ts}^1$ ) for plots at the upper and the middle slopes. However, an increase in soil surface elevation was found for the plot at footslope position when the settlement correction was related to a 5 cm soil layer. When bulk density changes were assumed to affect a soil layer of 10 cm thickness, a net deposition was obtained for plots at the upper, middle, and footslope positions. Here, the predictions of the soil settlement

**TABLE 4 |** Slope length (L) and area (A) of the different slope sections (in m<sup>2</sup> and % of the total slope) of the total slope together with weighted changes in average soil surface elevation (h) (according the share of each slope part of in the total slope) corrected by the measured and predicted soil bulk density (Eq. 1) at the SfM-plots along the experimental slope between May 14 and 16 after correction for soil settlement;  $z_{ts}^{t1}$  denotes the applied correction value for the compaction depth of 5 and 10 cm; the weighted sum describes the average loss in soil elevation derived from the SfM-plots extrapolated to the total slope and weighted by the different area sizes.

$z_{ts}^{t1}$	L	A		h [10 <sup>-3</sup> m]			
	[M]	[m <sup>2</sup> ]	[%]	measured		Predicted	
	/	/	/	5 cm	10 cm	5 cm	10 cm
upper slope	28.5	171	54	-1.1	1.0	-0.3	2.5
middle slope	14.5	87	27	-2.2	0.4	-1.7	1.3
footslope	10	60	19	3.1	5.9	3.0	5.8
Weighted sum (US, MS, FS)				-0.60	1.74	-0.07	2.79
Total slope	53	318	100	-0.07			

correction led to larger values of the surface elevation changes as compared to the measurements (Table 4).

Although the soil loss observed by SfM at the smaller plots cannot quantitatively be compared to soil loss by surface runoff and erosion at larger slopes (Parsons, 2019, see discussion 4.4), an extrapolation may be useful to check the plausibility range of the SfM data and evaluate ranges and relative soil masses quantified with the SfM method. Still, for comparing subplot information with those of the hillslope, the soil mass changes determined at the SfM-plots need to be weighted, here according to the upper-, middle-, and footslope area fractions (Table 4). Note that the typical relations between slope lengths and relative sizes of slope sub-divisional areas (Jha et al., 2015) was modified by increasing the length of the footslope sub-division from 3 to 10 m and proportionally reducing the length of the middle slope to account for the observation of deposition along this 10 m slope region (Supplementary Appendix SA3). The soil loss measured in the collector station was in the range of SfM-measurements corrected by using the predicted bulk density changes according to Linden and van Doren (1987) when assuming a topsoil height of 5 cm. With the correction based on measured bulk density values related to a 5 cm thick topsoil, the soil loss extrapolated by the SfM-technique for the total slope was 8- to 9-times that observed at the hillslope station (Table 4). The correction of the soil settlement applied to a topsoil height of 10 cm led to an increase in soil surface elevation after the erosion event for all plots (Figure 6 and Table 4).

## DISCUSSION

### Soil Loss and Surface Structural Changes Obtained by SfM

Soil surface structural changes due to raindrop impact could be quantified with the SfM-technique at the three hillslope positions. The plot located near the footslope received more sediments than were eroded (Table 3) because in these regions, any surface runoff coming from upper slope regions is saturated with sediments and cannot take up more soil particles (Schmidt, 1996). For plots at middle and upper slope positions, surface runoff only locally affected the surface roughness (Figure 7B, Supplementary Appendix SA5) and probably generated not sufficient kinetic energy for initiating larger-scale erosion under the present conditions and slope angles. The observed internal distribution of the soil within one SfM-plot

with similar slope angle (10%) was also found in the study by Quan et al. (2020) with soil elevation increase at the lower end of the plot. Kaiser et al. (2018) and Hänsel et al. (2016) reported similar local redistribution of soil from the exposed higher elevated plot regions into the depressions and lower elevated regions.

Between May 02 and 16, the plots show a decrease in soil surface elevation in all surface structural units (Figure 5). In the plot at upper slope position, larger area fractions remained unaffected from these changes than in the plots at middle and footslope positions. Since soil erosion is unlikely to occur so far upslope due to insufficient kinetic energy of the runoff (Schmidt, 1996) and according to visual inspection, soil consolidation must have been the main reason for soil surface elevation reduction. Note that the area fraction for which elevation changes were observed with SfM for the soil surface structural regions is not directly related to the amount of soil erosion in the plot. Relatively small areas of the plot with relatively large elevation changes could have affected the overall plot scale mass changes.

The decline in soil surface roughness (Figure 7B) could be attributed to the collapse of soil aggregates. Mechanisms for aggregate breakdown have been attributed to contractive forces of water in menisci between soil particles (Hartge et al., 2014), the decrease in structural stability of soil aggregates during wetting (Bergsma und Valenzuela, 1981), the destruction of soil aggregates by rain drop impact (Bolt and Koenigs, 1972) and the subsequent transport of smaller particles into larger pores (Schmidt, 1988). The soil surface maps at the footslope position with the strongest decrease in soil roughness supported the observation that soil particles were deposited in the local depressions leading to a levelling of the profile (Figures 4, 5, 7B). The small effect of slope inclination on soil surface dynamics was probably related to relatively high infiltration rates at the upper and middle slope positions, and the focused surface runoff on cultivation-induced features such as wheel tracks and plant rows (Supplementary Appendix SA3).

### Comparison and Limitations of Techniques for Soil Consolidation Estimation

Soil loss estimated by SfM-photogrammetry was smaller when soil consolidation was accounted for either by bulk density measurements or predictions (Eq. 1) according to Linden and van Doren (1987) (Table 4). This seems more plausible because

the overall soil loss of the total slope was significantly smaller than those derived from plot-scale data (Table 3). Soil consolidation needs to be considered as an important source for soil elevation decrease of a freshly cultivated soil in temperate climate zones (Schmidt, 1988).

When comparing the measurement with the prediction of soil settlement correction, similar trends for the overall change in soil height of the plots can be found: A decrease in soil height for the upper and middle slopes and increase (i.e., net deposition) for the footslope position (Table 4). The prediction method has the advantage that no elaborate bulk density measurements are needed after each precipitation event. Measurement errors of the soil bulk density can lead to larger errors, so a lot of soil samples need to be taken and larger soil areas need to be disturbed for the sampling. In case of the bulk density prediction, however, site-specific characteristics cannot directly be included in the analysis. Additionally, data of bulk density changes as determined here by core sampling, cannot clearly distinguish between natural soil settlement and erosion or deposition (e.g., Knapen et al., 2008). Both processes might lead to a change in bulk density in addition to natural consolidation due to raindrop impact. An alternative approach in this case would be to determine the bulk density changes in a levelled area (i.e., control plot) that is not subject to soil erosion but only to natural soil consolidation via rainfall. However, this plot would have to be located in the vicinity to the sloped plot, to ensure comparable raindrop impact and soil conditions. To install such a control plot in the field, might be challenging; and could be only tested under simulated rainfall and in the laboratory (e.g., Kaiser et al., 2018). The settlement prediction considers bulk density changes only due to raindrop impact for levelled plots and thus predicts final bulk densities without the impact. The advantage of the prediction over the direct measurements is that the model could be calibrated by fitting parameters “a” and “b” to site-specific bulk density changes observed when erosion impact could be excluded.

## Limitations Caused by SfM-Data Processing

Besides deviations caused by conditions in the field, uncertainties might occur also throughout the SfM-processing due to low precision in georeferencing of the 3D point clouds in MeshLab. Because of limited computational power, dense point clouds were not generated for every single part of the plots. In most cases, the centre of the GCPs was not exactly represented by a single point but was rather located in between two points. Consequently, throughout the georeferencing process only one of the points located a certain distance away from the actual GCP centre could be chosen for georeferencing leading to a deviation from the real coordinates. The described georeferencing error has been accounted for by considering a detection level, LoD (Figure 7, legends).

Between the points of the 3D point cloud, an interpolation was carried out in areas with a low point density during DEM generation in CloudCompare. This is the case especially in the regions close to the plot boundaries, where the coverage with images was lower than in the plot centre. For every time step,

VisualSfM produced different point clouds depending on the photo images. This was also the case, when two 3D models of the same object were generated from a different set of pictures. Hence, for both 3D models, different point clouds existed as a template for the DEM generation so that interpolation between the points was different leading to differences in the DEMs of the same object. This interpolation error increased with the complexity of an object's surface. Since soil surfaces were rather heterogeneous, this error was probably important. A possible solution could be to use pictures with a higher image resolution (Figure 2; i.e., from 5 to 12 MP). Unfortunately, VisualSfM software was unable to process such highly resolved data. By the use of downscaled pictures from 12 MP to 5 MP in Photoshop Elements, the point cloud density was not increased but the points were more evenly distributed throughout the point cloud. Other software such as PhotoScan (Agisoft, 2018) would be better able to handle a variable amount of data points (Jiang et al., 2020). However, this software was not available and required more computational power.

Challenges of small-scale erosion quantification by SfM and future needs.

The SfM-photogrammetry proved to be a useful tool to observe small scale soil surface micro-topography and structural changes at three plots or subplots along a hillslope. The advantage of our case study carried out in combination with the hillslope erosion experiment was that the same agricultural management was carried out uniformly over the whole field and that the basic conditions, soil, crop, tillage, and weather information could be directly used and compared with the complete hillslope. However, the soil loss found at the SfM-plots could not be related to that measured at the hillslope collector station for several reasons: For a start, the origin of the sediments collected at the footslope is uncertain, and according to the surface flow lines, sediments may have also passed the funneled collector (c.f. **Supplementary Appendix SA1**). It is not clear, where the sediment in the collector station might have come from. Travel distances of particles is finite and small (Parsons et al., 2010), thus the small plots can only estimate local redistribution. Also, the suggested approach to relate soil surface elevation changes of a smaller slope to the average soil surface elevation changes of a larger slope (Table 4) is dependent on the empirically adjusted slope length among other factors. Thus, this approach is site specific and cannot be transferred to other areas. Similar comparisons of smaller plots to larger slopes (Chaplot and Poesen, 2012) gave considerably higher sediment delivery rates from 1 m<sup>2</sup> plots as compared to hillslope-scale (899 versus 4.3 g m<sup>-2</sup> y<sup>-1</sup>). These authors attributed this discrepancy to splash erosion being the dominant sediment detachment and transport mechanism at hillslopes. Martinez et al. (2017) also found lower sediment yields at larger plots (27 m<sup>2</sup>) as compared to smaller plots (0.7 m<sup>2</sup>). In contrast, Boix-Fayos et al. (2007) found higher sediment concentrations at larger plots (30 m<sup>2</sup>) than in 1 m<sup>2</sup>-sized plots.

Thus, the observed discrepancies between the different soil loss estimation techniques in this study can be attributed to the smaller size of the plots used for the SfM-measurements (1.5 m<sup>2</sup>) in contrast to the collector station that accumulates the eroded sediment from a 318 m<sup>2</sup> hillslope. The SfM-plots reveal the local deposition and erosion processes and do not allow estimating

processes between plots (Parsons et al., 2010). Any comparison would improve, if DoD maps of the hillslope were generated provided the SfM-technique could be applied to the total area. Unfortunately, the resolution of the DoDs for a larger area would still be too coarse, the identification of effects of rain events on surface structure dynamics is limited (Kaiser et al., 2018). On the other hand, one could separate larger hillslopes into smaller areas (1–3 m<sup>2</sup>) that are each observed in detail with SfM and finally merged into a large DoD maps.

The SfM measurements basically provide quantitative and spatially-distributed information on the surface topography; it is not possible to distinguish between deposition of soil from uphill and erosion of soil that left the plot and the settlement. Furthermore, the change in the surface micro-topography includes the decline in surface roughness after rain. This may be considered as a kind of local erosion and deposition, which makes it difficult to separate between the deposition from uphill and local processes. The separation between input and output from changes in mean surface elevation requires additional assumptions that could be based on observations at the neighboring hillslope as follows:

Upper slope position: Based on observations it may be assumed that here the deposition from above was negligibly small such that the changes in surface elevation can be explained by runoff soil loss and by settlement.

The soil surface at the middle slope is in a through-flux position and has both deposition from above and soil loss towards downhill positions. Soil settlement could be the main unknown when assuming that lateral inputs equal outputs of soil mass. At the footslope position, there is clearly more deposition than erosion such it is assumed that the surface elevation changes account for net accumulation and some settlement.

Note that the observations do not allow to exactly quantify the rates of the different components of the soil mass changes but we can provide information on potentially relevant limits by making estimates when assuming minimal and maximal ranges limits from the comparison with the data obtained at the complete hillslope.

## CONCLUSION

The application of SfM-photogrammetry on a bare soil allowed quantifying differences in soil surface elevation and structure dynamics due to the impact of rainfall, erosion, and consolidation on soils freshly sowed with Maize. Maps of local or micro-topographic changes were generated for plots at three hillslope positions.

The results of testing different soil consolidation rates in form of soil bulk density changes in topsoil layers indicated that it would be necessary to better account for the structure dynamics in the entire topsoil volume when trying to estimate the elevation changes caused by natural consolidation. The results of the comparisons between data and regression approach suggest that the relatively simple regression after calibration can be useful to correct soil surface elevation changes induced by rain for natural soil settlement.

The results of the soil mass balancing of the plots from the difference between SfM surface elevation maps before and after a

rain event revealed also uncertainties that resulted from georeferencing and computation limits of the used software.

The SfM technique designed for the non-destructive and repeated monitoring of soil surface structural dynamics under field conditions, provided valuable information on soil structure parameters such as surface roughness. Improvements could be achieved by using higher resolution images and expanding the SfM-application to the hillslope.

The results suggest that the use of widely available cameras and application of freely available software for processing photos and DEMs is possible. This may stimulate the application and monitoring of erosion-affected soil surface changes in many arable soil landscapes and regions with limited accessibility. Further improvements of the standardized application, the accuracy, and the calibration of empirical bulk density models are still necessary.

## DATA AVAILABILITY STATEMENT

The original contributions presented in the study are included in the article/**Supplementary Material**, further inquiries can be directed to the corresponding author.

## AUTHOR CONTRIBUTIONS

AE: Conceptualization; Data curation; Formal analysis; Investigation; Methodology; Software; Validation; Visualization; Writing-original draft; Writing-review and editing. HG: Conceptualization; Methodology; Supervision; Validation; Writing-review and editing. DD: Resources; Methodology; Supervision

## FUNDING

The research was funded by the Leibniz Centre for Agricultural Landscape Research (ZALF), which is a research institution of the Leibniz Association in the legal form of a non-profit registered association. ZALF is financed in equal parts by the Federal Ministry of Food and Agriculture (BMEL) and the Ministry for Science, Research and Culture of the State of Brandenburg (MWFK).

## ACKNOWLEDGMENTS

We thank Anette Eltner (Technical University Dresden) and Phoebe Hänsel (Technical University Bergakademie Freiberg) for support in handling or application of the SfM-technique and software and Lidia Völker (ZALF Müncheberg) for plotting surface flow maps of the hillslope.

## SUPPLEMENTARY MATERIAL

The Supplementary Material for this article can be found online at: <https://www.frontiersin.org/articles/10.3389/fenvs.2021.737702/full#supplementary-material>

## REFERENCES

- Adobe Systems (2018). Adobe Photoshop Elements. Available at: <https://www.adobe.com/de/products/photoshop-elements.html> 10 (Access date: 19, 2018).
- Agisoft (2018). PhotoScan. Available at: <https://www.agisoft.com/03> Access date: 21, 2020).
- Ahuja, L. R., Ma, L., and Timlin, D. J. (2006). Trans-Disciplinary Soil Physics Research Critical to Synthesis and Modeling of Agricultural Systems. *Soil Sci. Soc. Am. J.* 70 (2), 311–326. doi:10.2136/sssaj2005.0207
- Ahuja, L. R., Rojas, K. W., Hanson, J. D., Shaffer, M. D., and Ma, L. (2000). *Root Zone Water Quality Model: Modeling Management Effects on Water Quality and Crop Production*. Highland Ranch, CO: Water Resources Pub., LLC.
- Bendig, J., Bolten, A., and Bareth, G. (2013). Monitoring des Pflanzenwachstums mit Hilfe multitemporaler und hoch auflösender Oberflächenmodelle von Getreidebeständen auf Basis von Bildern aus UAV-Befliegungen. *pfg* 2013, 551–562. Available at: <https://kups.ub.uni-koeln.de/20608/>. doi:10.1127/1432-8364/2013/0200
- Bergsma, E., and Valenzuela, C. R. (1981). Drop Testing Aggregate Stability of Some Soils Near Merida, Spain. *Earth Surf. Process. Landforms* 6, 309–318. doi:10.1002/esp.3290060310
- Boardman, J. (2006). Soil Erosion Science: Reflections on the Limitations of Current Approaches. *CATENA* 68 (2-3), 73–86. doi:10.1016/j.catena.2006.03.007
- Boix-Fayos, C., Martínez-Mena, M., Arnau-Rosalén, E., Calvo-Cases, A., Castillo, V., and Albaladejo, J. (2006). Measuring Soil Erosion by Field Plots: Understanding the Sources of Variation. *Earth-Science Rev.* 78 (3-4), 267–285. doi:10.1016/j.earscirev.2006.05.005
- Boix-Fayos, C., Martínez-Mena, M., Calvo-Cases, A., Arnau-Rosalén, E., Albaladejo, J., and Castillo, V. (2007). Causes and Underlying Processes of Measurement Variability in Field Erosion Plots in Mediterranean Conditions. *Earth Surf. Process. Landforms* 32 (1), 85–101. doi:10.1002/esp.1382
- Bolt, G. H., and Koenigs, F. F. (1972). Physical and Chemical Aspects of the Stability of Soil Aggregates. *Ghent Rijksfac Landbouwetensch Meded* 29, 955–973.
- Borrelli, P., Robinson, D. A., Fleischer, L. R., Lugato, E., Ballabio, C., Alewell, C., et al. (2013). An Assessment of the Global Impact of 21st century Land Use Change on Soil Erosion. *Nat. Commun.* 8 (1), 2013. doi:10.1038/s41467-017-02142-7
- Brasington, J., Langham, J., and Rumsby, B. (2003). Methodological Sensitivity of Morphometric Estimates of Coarse Fluvial Sediment Transport. *Geomorphology* 53 (3-4), 299–316. doi:10.1016/S0169-555X(02)00320-3
- Chaplot, V., and Poesen, J. (2012). Sediment, Soil Organic Carbon and Runoff Delivery at Various Spatial Scales. *CATENA* 88 (1), 46–56. doi:10.1016/j.catena.2011.09.004
- Cignoni, P. (2016). MeshLab: an Open-Source Mesh Processing Tool. Online Available. Available at: <http://www.meshlab.net/04> (Access date: 29, 2018).
- Cignoni, P., Callieri, M., Corsini, M., Dellepiane, M., Ganovelli, F., and Ranzuglia, G. (2008). “MeshLab: an Open-Source Mesh Processing Tool,” in Proceedings of the Eurographics Italian Chapter Conference, Salerno, Italy, July 2008 (Geneva, Switzerland: The Eurographics Association).
- Cloud Compare (2016). CloudCompare V2. Edition 2.7.0. Available at: <http://www.cloudcompare.org> 04 (Access date: 28, 2018).
- Deumlich, D., Jha, A., and Kirchner, G. (2017). Comparing Measurements, <sup>7</sup>Be Radiotracer Technique and Process-Based Erosion Model for Estimating Short-Term Soil Loss from Cultivated Land in Northern Germany. *Soil Water Res.* 12 (No. 3), 177–186. doi:10.17221/124/2016-SWR
- Di Stefano, C., Ferro, V., Palmeri, V., and Pampaloni, V. (2017). Measuring Rill Erosion Using Structure from Motion: A Plot experiment. *CATENA* 156, 383–392. doi:10.1016/j.catena.2017.04.023
- Eltner, A., Baumgart, P., Maas, H.-G., and Faust, D. (2015). Multi-temporal UAV Data for Automatic Measurement of Rill and Interrill Erosion on Loess Soil. *Earth Surf. Process. Landforms* 40, 741–755. doi:10.1002/esp.3673
- Eltner, A., Kaiser, A., Abellan, A., and Schindewolf, M. (2017). Time Lapse Structure-From-Motion Photogrammetry for Continuous Geomorphic Monitoring. *Earth Surf. Process. Landforms* 42, 2240–2253. doi:10.1002/esp.4178
- Eltner, A., Kaiser, A., Castillo, C., Rock, G., Neugirg, F., and Abellán, A. (2016). Image-based Surface Reconstruction in Geomorphometry - Merits, Limits and Developments. *Earth Surf. Dynam.* 4, 359–389. doi:10.5194/esurf-4-359-2016
- García-Ruiz, J. M., Beguería, S., Nadal-Romero, E., González-Hidalgo, J. C., Lana-Renault, N., and Sanjuán, Y. (2015). A Meta-Analysis of Soil Erosion Rates across the World. *Geomorphology* 239 (1–2), 160–173. doi:10.1016/j.geomorph.2015.03.008
- Hänsel, P., Schindewolf, M., Eltnner, A., Kaiser, A., and Schmidt, J. (2016). Feasibility of High-Resolution Soil Erosion Measurements by Means of Rainfall Simulations and SfM Photogrammetry. *Hydrology* 3 (4), 38. doi:10.3390/hydrology3040038
- Hartge, K. H., Horn, R., Bachmann, J., and Peth, S. (2014). *Einführung in die Bodenphysik: Mit 24 Tabellen*. 4th ed. Stuttgart: Schweizerbart.
- Haubrock, S.-N., Kuhnert, M., Chabrilat, S., Güntner, A., and Kaufmann, H. (2009). Spatiotemporal Variations of Soil Surface Roughness from In-Situ Laser Scanning. *CATENA* 79 (2), 128–139. doi:10.1016/j.catena.2009.06.005
- James, M. R., and Robson, S. (2012). Straightforward Reconstruction of 3D Surfaces and Topography with a Camera: Accuracy and Geoscience Application. *J. Geophys. Res.* 117 (F3), a–n. doi:10.1029/2011JF002289
- Jha, A., Schkade, U., and Kirchner, G. (2015). Estimating Short-Term Soil Erosion Rates after Single and Multiple Rainfall Events by Modelling the Vertical Distribution of Cosmogenic <sup>7</sup>Be in Soils. *Geoderma* 243–244, 149–156. doi:10.1016/j.geoderma.2014.12.020
- Jiang, S., Jiang, C., and Jiang, W. (2020). Efficient Structure from Motion for Large-Scale UAV Images: A Review and a Comparison of SfM Tools. *ISPRS J. Photogrammetry Remote Sensing* 167 (7), 230–251. doi:10.1016/j.isprsjprs.2020.04.016
- Kaiser, A., Erhardt, A., and Eltnner, A. (2018). Addressing Uncertainties in Interpreting Soil Surface Changes by Multitemporal High-Resolution Topography Data across Scales. *Land Degrad. Dev.* 29 (8), 2264–2277. doi:10.1002/ldr.2967
- Kaiser, A., Neugirg, F., Schindewolf, M., Haas, F., and Schmidt, J. (2015). Simulation of Rainfall Effects on Sediment Transport on Steep Slopes in an Alpine Catchment. *Proc. IAHS* 367, 43–50. doi:10.5194/piahs-367-43-2015
- Knapen, A., Poesen, J., and Baets, S. D. (2008). Rainfall-induced Consolidation and Sealing Effects on Soil Erodibility during Concentrated Runoff for Loess-Derived Topsoils. *Earth Surf. Process. Landforms* 33 (3), 444–458. doi:10.1002/esp.1566
- Laburda, T., Krása, J., Zúmr, D., Devátý, J., Vrána, M., Zambon, N., et al. (2021). SfM-MVS Photogrammetry for Splash Erosion Monitoring under Natural Rainfall. *Earth Surf. Process. Landforms* 46 (5), 1067–1082. doi:10.1002/esp.5087
- Linden, D. R., and van Doren, D. M., Jr (1987). “Simulation of Interception, Surface Roughness, Depression Storage, and Soil Settling,” in *NTRM, A Soil Crop Simulation Model for Nitrogen, Tillage and Crop-Residue Management. Conservation Research Report. Vol. 34-1*. Editors M. J. Shaffer and W. E. Larson (Washington, DC: USDA-ARS), 90–93.
- Martinez, G., Weltz, M., Pierson, F. B., Spaeth, K. E., and Pachepsky, Y. (2017). Scale Effects on Runoff and Soil Erosion in Rangelands: Observations and Estimations with Predictors of Different Availability. *CATENA* 151, 161–173. doi:10.1016/j.catena.2016.12.011
- Martinez-Agirre, A., Álvarez-Mozos, J., Milenković, M., Pfeifer, N., Giménez, R., Valle, J. M., et al. (2020). Evaluation of Terrestrial Laser Scanner and Structure from Motion Photogrammetry Techniques for Quantifying Soil Surface Roughness Parameters over Agricultural Soils. *Earth Surf. Process. Landforms* 45 (3), 605–621. doi:10.1002/esp.4758
- Meinen, B. U., and Robinson, D. T. (2020). Where Did the Soil Go? Quantifying One Year of Soil Erosion on a Steep Tile-Drained Agricultural Field. *Sci. Total Environ.* 729, 138320. doi:10.1016/j.scitotenv.2020.138320
- Micheletti, N., Chandler, J. H., and Lane, S. N. (2015). Investigating the Geomorphological Potential of Freely Available and Accessible Structure-From-Motion Photogrammetry Using a Smartphone. *Earth Surf. Process. Landforms* 40 (4), 473–486. doi:10.1002/esp.3648
- Nadal-Romero, E., Revuelto, J., Errea, P., and López-Moreno, J. I. (2015). The Application of Terrestrial Laser Scanner and SfM Photogrammetry in Measuring Erosion and Deposition Processes in Two Opposite Slopes in a Humid Badlands Area (central Spanish Pyrenees). *SOIL* 1 (2), 561–573. doi:10.5194/soil-1-561-2015
- Nouwakpo, S. K., Weltz, M. A., and McGwire, K. (2016). Assessing the Performance of Structure-From-Motion Photogrammetry and Terrestrial

- LiDAR for Reconstructing Soil Surface Microtopography of Naturally Vegetated Plots. *Earth Surf. Process. Landforms* 41 (3), 308–322. doi:10.1002/esp.3787
- Parsons, A. J. (2019). How Reliable Are Our Methods for Estimating Soil Erosion by Water?. *Sci. Total Environ.* 676, 215–221. doi:10.1016/j.scitotenv.2019.04.307
- Parsons, A. J., Wainwright, J., Fukuwara, T., and Onda, Y. (2010). Using Sediment Travel Distance to Estimate Medium-Term Erosion Rates: a 16-year Record. *Earth Surf. Process. Landforms* 35 (14), 1694–1700. doi:10.1002/esp.2011
- Pimentel, D., and Burgess, M. (2013). Soil Erosion Threatens Food Production. *Agriculture* 3 (3), 443–463. doi:10.3390/agriculture3030443
- Prosdocimi, M., Burguet, M., Di Prima, S., Sofia, G., Terol, E., Rodrigo Comino, J., et al. (2017). Rainfall Simulation and Structure-From-Motion Photogrammetry for the Analysis of Soil Water Erosion in Mediterranean Vineyards. *Sci. Total Environ.* 574, 204–215. doi:10.1016/j.scitotenv.2016.09.036
- QGIS Development Team (2018). QGIS Geographic Information System: Open Source Geospatial Foundation Project. Available at: <https://qgis.org/en/site/>
- QGIS Development Team (2014). QGIS User Guide. Available at: [https://docs.qgis.org/2.8/en/docs/user\\_manual/index.html](https://docs.qgis.org/2.8/en/docs/user_manual/index.html) (Accessed July 15, 2019).
- Quan, X., He, J., Cai, Q., Sun, L., Li, X., and Wang, S. (2020). Soil Erosion and Deposition Characteristics of Slope Surfaces for Two Loess Soils Using Indoor Simulated Rainfall experiment. *Soil Tillage Res.* 204, 104714. doi:10.1016/j.still.2020.104714
- Rousseva, S. S., Ahuja, L. R., and Heathman, G. C. (1988). Use of a Surface Gamma-Neutron Gauge for *In Situ* Measurement of Changes in Bulk Density of the Tilled Zone. *Soil Tillage Res.* 12 (3), 235–251. doi:10.1016/0167-1987(88)90014-1
- Samsung (2011). *Samsung WB750 User Manual*. South Korea: Samsung.
- Schmidt, J. (1996). *Entwicklung und Anwendung eines physikalisch begründeten Simulationsmodells für die Erosion geneigter landwirtschaftlicher Nutzflächen: 34 Tabellen*. Institut für Geographische Wissenschaften. Berlin: ISBN. 3880090629 (Development and application of a physically based simulation model for soil erosion along sloped agricultural areas).
- Schmidt, J. (1988). “Wasserhaushalt und Feststofftransport an geneigten, landwirtschaftlich bearbeiteten Nutzflächen,”. Dissertation. na (Berlin: Free University), 86. Water budget and solid matter transport in sloped agricultural areas.
- Sutton, P. C., Anderson, S. J., Costanza, R., and Kubiszewski, I. (2016). The Ecological Economics of Land Degradation: Impacts on Ecosystem Service Values. *Ecol. Econ.* 129 (3), 182–192. doi:10.1016/j.ecolecon.2016.06.016
- Tarolli, P., Cavalli, M., and Masin, R. (2019). High-resolution Morphologic Characterization of Conservation Agriculture. *CATENA* 172, 846–856. doi:10.1016/j.catena.2018.08.026
- Vinci, A., Todisco, F., Brigante, R., Mannocchi, F., and Radicioni, F. (2017). A Smartphone Camera for the Structure from Motion Reconstruction for Measuring Soil Surface Variations and Soil Loss Due to Erosion. *Hydrol. Res.* 48 (3), 673–685. doi:10.2166/nh.2017.075
- Westoby, M. J., Brasington, J., Glasser, N. F., Hambrey, M. J., and Reynolds, J. M. (2012). ‘Structure-from-Motion’ Photogrammetry: A Low-Cost, Effective Tool for Geoscience Applications. *Geomorphology* 179, 300–314. doi:10.1016/j.geomorph.2012.08.021
- Wilson, M. F. J., O’Connell, B., Brown, C., Guinan, J. C., and Grehan, A. J. (2007). Multiscale Terrain Analysis of Multibeam Bathymetry Data for Habitat Mapping on the Continental Slope. *Mar. Geodesy* 30, 3–35. doi:10.1080/01490410701295962
- Wu, C. (2011). VisualSFM: A Visual Structure from Motion System. Available at: <http://ccwu.me/vsfm/04> (Access date: 29, 2018).

**Conflict of Interest:** The authors declare that the research was conducted in the absence of any commercial or financial relationships that could be construed as a potential conflict of interest.

**Publisher’s Note:** All claims expressed in this article are solely those of the authors and do not necessarily represent those of their affiliated organizations, or those of the publisher, the editors and the reviewers. Any product that may be evaluated in this article, or claim that may be made by its manufacturer, is not guaranteed or endorsed by the publisher.

Copyright © 2022 Ehrhardt, Deumlich and Gerke. This is an open-access article distributed under the terms of the Creative Commons Attribution License (CC BY). The use, distribution or reproduction in other forums is permitted, provided the original author(s) and the copyright owner(s) are credited and that the original publication in this journal is cited, in accordance with accepted academic practice. No use, distribution or reproduction is permitted which does not comply with these terms.



# Mechanical Soil Database—Part I: Impact of Bulk Density and Organic Matter on Precompression Stress and Consequences for Saturated Hydraulic Conductivity

Richard Schroeder<sup>1\*</sup>, Heiner Fleige<sup>1</sup>, Carsten Hoffmann<sup>2</sup>, Hans Joerg Vogel<sup>3</sup> and Rainer Horn<sup>1</sup>

## OPEN ACCESS

### Edited by:

Thomas Keller,  
Swedish University of Agricultural  
Sciences, Sweden

### Reviewed by:

Mario Rolim,  
Federal Rural University of  
Pernambuco, Brazil  
Miriam Fernanda Rodrigues,  
Federal Technological University of  
Paraná Dois Vizinhos, Brazil

### \*Correspondence:

Richard Schroeder  
r.schroeder@soils.uni-kiel.de

### Specialty section:

This article was submitted to  
Soil Processes,  
a section of the journal  
Frontiers in Environmental Science

**Received:** 12 October 2021

**Accepted:** 14 January 2022

**Published:** 14 February 2022

### Citation:

Schroeder R, Fleige H, Hoffmann C,  
Vogel HJ and Horn R (2022)  
Mechanical Soil Database—Part I:  
Impact of Bulk Density and Organic  
Matter on Precompression Stress and  
Consequences for Saturated  
Hydraulic Conductivity.  
Front. Environ. Sci. 10:793625.  
doi: 10.3389/fenvs.2022.793625

<sup>1</sup>Institute for Plant Nutrition and Soil Science, Christian-Albrechts-University Kiel, Kiel, Germany, <sup>2</sup>Leibniz Centre for Agricultural Landscape Research (ZALF) e. V., Müncheberg, Germany, <sup>3</sup>Department Soil System Science Helmholtz Centre for Environmental Research—UFZ, Halle, Germany

The mechanical strength of agricultural soils depends on many soil properties and functions. The database, “soil strength and consequences for sustainable land use and soil management SOILMECHDAT-Kiel”, originates from the “Horn Research Group” includes analyses of undisturbed soil samples taken from more than 460 profiles in and is developed in collaboration with BONARES, a funding initiative of the German Federal Ministry for Education and Research that focuses on the sustainable use of soils. For over 40 years, over 42 different authors recorded 59 physical and 29 chemical parameters for complete soil profiles. In order to the aim of the initial analyses of this data is to determine the influence of bulk density (BD) organic matter (OM) and time (year) on precompression stress (Pc) and saturated hydraulic conductivity (ks) as a function of Pc. Three main textural groups sand, loam, and silt for both topsoils and subsoils (SS) were studied. In loamy and silty subsoils BD and OM are not related to Pc ( $R^2 = 0.17$  and  $R^2 = 0.25$ ). OM and bulk density are more related to Pc in sandy soils ( $R^2 = 0.55$ – $0.59$ ). The link between ks and Pc showed that sandy soils have a significantly higher Pc ( $>150$  kPa) and conductivities did not change much. In loamy soils, with a Pc  $>90$  kPa, 50% of the ks fell below the critical value of  $10 \text{ cm d}^{-1}$ . For silty soils, at a Pc of 60 kPa, 50% of the data fall below the critical value of ks. These findings suggest that the stability of loamy and silty soils not only depends on OM and BD, but requires further data to explain the variation in the measurements. With respect to ks, the results show that fertile silty soils are more sensitive than formerly defined.

**Keywords:** database, stress strain, precompression stress, saturated hydraulic conductivity, bulk density, organic matter, ecological properties, undisturbed soil profiles

## INTRODUCTION

Soil compaction, especially subsoil compaction, is one of the major threats of soil degradation globally (Bridges and Oldeman, 1999). The European Soil Framework Directive (2006) stated that soil compaction, along with erosion by water and wind, is one of the main physical processes that severely threatens soil and causing degradation. It is estimated that 32% of the subsoils (SS) in Europe are highly degraded and 18% are moderately vulnerable to compaction and soil degradation, caused by too heavy agricultural and forestry machinery. The machinery is responsible for the degradation of an area of 330,000 km<sup>2</sup> (Soane and van Ouwerkerk, 1995; Fraters, 1996), and the affected area increases continuously (Keller et al., 2017, 2019).

The main reasons for the increase in compaction, arable or forest soils are the ever-increasing weight of the machines and the increased frequency of wheeling under unfavorable (high moisture) soil conditions. This statement is repeatedly mentioned by Horn (1983), Håkansson et al. (1987), Lebert (1989), Alakukku (1996), Kühner (1997), Wiermann et al. (2000), Arvidsson et al. (2001), Horn and Fleige (2003); Horn and Fleige, (2009), Keller et al. (2004), Horn and Smucker, 2005, Zink et al. (2010), Riggert (2015), Keller et al. (2019), and Horn (2021). But the consequences are most often underestimated although well defined (Arvidsson and Håkansson, 1996; Zink et al., 2010). Although many farmers do care on these threats, visible and measurable effects (e.g., yield decline or increased probability of flooding even during the growing season) have often resulted in minor changes in land management. However, soil degradation occurs generally in all soils, even if the intensity and the consequences differ depending on the internal soil properties as well as the kind and frequency of stress application. The latter has increased over the last decades (Arvidsson and Håkansson, 1996; Zink, 2009; Duttman et al., 2014; Hartge and Horn, 2016; Horn et al., 2017; Keller et al., 2019). The consequences of land management and tillage, needs to be analyzed, because saturated hydraulic conductivity ( $k_s$ ) also depends on shear- and vibration-induced soil deformation interactions. These interactions enhance the degradation of soil properties, especially if the soil water content is high and the internal soil strength is low (Huang et al., 2021a, b). Furthermore, intense animal trampling often in combination with induced overgrazing of moist to wet pastures, causes soil compression and leads to a reduction of coarse pores with smaller continuity. Even if soil horizons are still structured after stress application, the trampling will lead to a compacted platy structure in the topsoil and changes down to deep depths (Fazekas and Horn, 2005).

The reduction of pore space and especially of macropores, along with the conversion of three-dimensionally uniform pore systems to completely horizontal anisotropic conditions in platy structured soil horizons by compaction must be regarded as harmful. Thus, compaction may cause severe consequences for hydraulic, gas, and heat transport, as well as for nutrient storage and uptake by plants, if the stresses exceed the internal soil strength (Horn et al., 2019). By 2050, food production must increase by + 70% to nourish the nine billion people on earth

(Horn and Blum, 2020). In addition, climate change will affect precipitation frequency and intensity and the temperature. Consequently, soil structure changes need to be studied to gain insight into basic soil physical and mechanical properties and how they change over time. These interactions are seldom published for whole soil profiles but for only single soil horizons as well as their time dependent changes.

The “Horn Research Group” has studied for over 40 years the topic of soil strength for soil profiles with different geological substrates, climatic boundary conditions, and different land uses and the relation to sustainable land use and soil management. The compiled a database: SOILMECHDAT-Kiel, which includes these physical and mechanical properties. With coordinates available, this database can be used to develop, at various scales (farm level to country to continent), soil maps showing strength or stress distribution based on wheeling experiments and consecutive analyses of stress distribution patterns at given mechanical soil properties.

The precompression stress (= internal soil strength,  $P_c$ ) is a sensitive and scale-spanning parameter that defines the rigidity of the soil structure. It indicates the current state of compaction, as a result of all previous physical, chemical, or biological compressive and stabilizing processes as well as natural decompression (loosening such as bioturbation). It is derived from stress-strain curves and is the transition from the recompression to the virgin compression range. It depends on the matric potential, as well as former pedo- and anthropogenic processes (Mordhorst et al., 2020). The higher the soil strength, the lower is the likelihood for additional mechanical stress and long-term degradation of soil structure (Horn and Dexter 1989; Horn et al., 1991a; Kirby 1991b; Van den Akker et al., 1999; Trautner et al., 2003; Horn and Fleige, 2009; Keller et al., 2019). The values for  $P_c$  also document the range of resilience (recompression range) while in the virgin compression stress range it declines due to plastic deformation (Horn and Blum 2020).

The  $P_c$  value is often related to soil conditions in early spring at matric potential values of pF 1.8 (–60 hPa) or when the soil is drying due to evapotranspiration and the soil water content is reduced to values such as pF 2.5 (–300 hPa) matric potential. The drier the soil is, the more negative is the pore water pressure and the soil structure solidifies. Relationships between matric potential and internal soil strength can be described by the effective stress equation (Bishop 1959) which enable to quantify the effective stresses between particles or aggregates and the stabilizing or weakening effects of the pore water pressure. Besides the soil strength change with matric potential can also the impact of the chi factor at given total stresses for the effective stresses be quantified. Besides landuse and soil management can also geogenic impacts for given soil types be quantified in order to classify mechanical properties of soils from farm to country or continental scale or with respect to tentative effects for given land use managements. In order to optimize the analysis purpose, the following properties that affect soil strength are included in the database: texture, structure, clay mineralogy, organic matter (OM), bulk density (BD), chemical composition, and negative pore water pressure (= matric potential) (for more

details see also Larson et al., 1980; Horn, 1981; McBride, 1989; Soane, 1990; O'Sullivan, 1992; Watts and Dexter, 1997; Zhang et al., 1997; Paz and Guérif, 2000; Keller et al., 2011; Baumgartl and Horn, 2013).

Shear strength, determines the binding forces between particles (texture) or the ability of soil aggregates to withstand the rearrangement (= strain) against smearing (also defined as slip). The shear parameters defined by the Mohr Coulomb equation are the angle of internal friction and cohesion, and they define the slope and the intercept of the linear regression equation between shear resistance as dependent variable and normal stress for a given matric potential, of a structured soil horizon.

Soil physical properties affected by soil deformation are the  $k_s$  and air permeability ( $k_l$ ), which show a dependency on the internal soil strength. Both the  $k_s$  and unsaturated hydraulic conductivity ( $k_u$ ) as well as  $k_l$  as a function of matric potential represent the functional quality of soil structure and pore continuity as they define the air and water fluxes within the soil. (Arthur et al., 2012; Berisso et al., 2012). but the rigidity of the structured pore system is limited to the recompression stress range while within the virgin compression stress range decrease these values intensely and cause a decrease of continuity of the pore network (Hamamoto et al., 2011; Horn 2021). The same would be in addition true for gas diffusivity, which, however, was not always analysed during the research activities. If pores lose their continuity (blocked pores) and diameter fluxes are reduced and in the worst case also the liquefaction increase with more intense impacts or an increased rigidity change (Huang et al., 2021a). Blocked pores are affected by soil management including shearing (Dörner and Horn 2006) and can be related to soil deformation processes if the history as well as the registered management of the analysed soils are regarded.

Organic matter (OM) does not only increase the water storage in soils, but also the hydraulic or pneumatic functions which helps to define structure properties (Piccolo et al. (1997); IPCC, 2003; Janssens et al., 2005; Jones et al., 2005; Smith et al., 2005; Stolbovoy et al., 2007; Saha et al., 2011). Feller and Beare (1997) substantiated the physical interactions between clay particles and OM and showed that, with increasing humus content, the structural stability of the soil improved. Specifically, the clay particles and OM should be in proportion to each other to form organic carbon complexes (Dexter et al., 2008; Horn and Blum, 2020).

The objectives of this first paper are the following:

- In cooperation with BONARES, a funding initiative of the German Federal Ministry for Education and Research, we want to create a database to document and statistically evaluate the soil strength of structured and pre-drained soils under agricultural use.
- To determine the link between the  $P_c$  and OM, BD and  $k_s$  for the three soil classes (sand, loam, and silt) and time depending changes separated in top- and subsoils.
- The aim of this project is to elaborate scenarios how to at least maintain for the present soil structural properties as a sustainable soil management, according to an initiative of

the German Federal Ministry of Education and Research (BMBF).

## MATERIALS AND METHODS

The origin database is composed of three Excel tables (not shown in this paper), which inform about the soil profiles that were studied using the three German Soil Mapping Instructions (AG Bodenkunde, 1982; AG Boden, 1994; Ad-hoc-AG Boden, 2005) over the last 40 years. Each table is divided into metadata and physical/chemical parameters. The measured values are assigned to their respective parameter sheets. These include parameters of "Chemical properties", "Water retention", "Saturated hydraulic conductivity", "Air conductivity", " $P_c$ " and "Shear resistance". The complete description of the database will be part of the finalizing PhD thesis while at present some general information about parameters needed to detect and to quantify soil properties and functions will be given.

### Origin Data

Mechanical data originate from master's and PhD publications and other projects from the Institute of Soil Science of CAU in Kiel, Germany. More than 70% of the soil samples analysed originate from Germany (Figure 1) and will be completely available for further analyses within the BONARES database following the finished PhD Thesis in 2022 of R. Schroeder.

Further sampling took place in Switzerland, Estonia, Norway, Finland, Great Britain, Brazil, Chile, and China. The database includes up to 59 physical/mechanical and 29 chemical parameters and consider amongst others texture, structure, BD, OM pore size distribution, soil strength parameters and hydraulic as well as pneumatic functions as well as pH etc. The analyses recorded are from a period between 1979 and 2019, with over 460 profiles, 588 Topsoil-horizons (TS), 974 Subsoil-horizons (SS), and 225 underground horizons quantified and available for statistical analysis. TS horizons are defined as all mineral horizons with the main symbol "A" and with their TS horizon limit between 0 and 30 cm. The SS horizons are identified according to the German classification system: B, P, T, S, G, M, E, R, and Y with an upper horizon limit of >0 cm und mineral surface. Subsurface mineral horizons (not/less weathered) ( $n = 225$ ) are defined by the symbol "C"/"-C" as parent material. The variable number of the three horizon groups is due to different sampling depths and sampling strategies. The SS horizons include also those with OM > 1%, which result from former deeper ploughing strategies (35–40 cm) from early 1970th/80th. Because the later ploughing was limited to 25–30 cm, these deeper parts of A-horizons are defined as "buried" and SS horizons.

### Documentation of Soil Use

The database allows a categorization of the investigated areas with respect to their use, properties, and functions. Different types of land use were included and categorized amongst others as "peatland", "grassland", "forest", and "arable land".



**FIGURE 1** | Location of the documented soil profiles (red dots). source: r studio, package: ggplot2.

The peatland area share (4.3%) includes areas that are difficult or impossible to use and are not under agricultural use. This proportion includes bog areas (Histosols) with more than 30 cm organic cover (>30% OM) and “subhydric areas”. Bog areas also include fallow areas (share: < 1%). The data share for grassland is 28% and includes (mowed) pastures, all types of grasslands, parks, and cultivated moors. “Forest” with 10% includes woodlands, as well as mixed coniferous and deciduous forests. 62% of the profiles are under conventional (86%) or conservation (14%) agricultural use. Conventionally farmed areas are characterized by regular ploughing (p) operations of the TS (Ap-horizon), with tillage depth varying between 25–30 cm. Areas with conservation tillage are not ploughed or have minor or no tillage.

## Database Structure and Processing

For each soil mapping manual: AG Bodenkunde (1982) AG Boden (1994) and Ad-hoc-AG Boden (2005) an Excel spreadsheet (Excel 2016) was created. The spreadsheets for each Excel spreadsheet are divided into the sections: *profile*, *horizon*, *chemical properties*, *water retention*, *hydraulic conductivity*, *precompression stress* and *shearing* (Table 1). This allows a systematic transfer of the profile data from the publications and other sources into the database. The entries are made by means of free text or a predefined drop-down menu. The parameters of the *profile* and *horizon* listed represent elementary basic information of the sample sites,

which are considered as a minimum requirement for inclusion in the database. Table 1 give an overview about the main sections of the construction of the data basis and the given parameter.

## Section Profile

The profile number 1) is generated individually for each profile in the database. It is used as a reference for the chemical and physical parameters, and it ensures an exact assignment of the laboratory analyses to the respective profile metadata. It is composed of the four initial letters of the author and the number of the profile as a digit.

In case of further publications by an author, further consecutive profile numbers are added. For further classification, the project name (3). 3–17 are directly oriented to the title data of the respective mapping manual (AG Bodenkunde, 1982; AG Boden, 1994; Ad-hoc-AG Boden, 2005) and are further defined there.

## Section Horizon

In the “Section Horizon”, the profile number 1) already described is placed in front of the soil parameters as a profile reference. Together with the horizon number 2) as horizon reference, they form the link between the profile reference and the measurement results. The information on points one0–17 is also defined according to the respective soil mapping instructions and further described there.

**TABLE 1** | Structure of each Excel spreadsheet of the soil data base with the main sections: Profile, Horizon, precompression stress (Pc), shearing, chemical properties and texture with several given parameters (0–30).

Profile	Horizon	Precompression Stress	Shearing	Chemical Properties and texture
Profile_No (1)	Profile_No (1)	Profile_No (1)	Profile_No (1)	Profile_No (1)
Horizon_No (2)	Horizon_No (2)	Horizon_No (2)	Horizon_No (2)	Horizon_No (2)
Project remark (3)	Horizon upper limit (10)	Treatment_ID_pv (18)	Treatment_ID_shearing (18)	CaCO <sub>3</sub> (26)
Date of recording (4)	Horizon lower limit (11)	Method_ID_pv (19)	Method_ID_shearing (19)	pH (CaCl <sub>2</sub> ) (27)
Easting (5)	Horizon symbol (12)	Matrix potential (20)	Matrix potential (20)	Organic carbon (28)
Northing (6)	Humus content (13)	Precompression stress (21)	Normal stress (23)	Organic matter (29)
Type of use/sealing (7)	Substrate type (14)	Bulk density (22)	Cohesion (24)	Texture (30)
Soil type short (8)	Substrate genesis (16)	—	Angle of internal friction (25)	
Soil subtype (9)	Texture group (17)	—	—	

**TABLE 2** | Classification of the precompression stress (Pc), bulk density  $\rho$  and organic matter (OM) according to DVWK 1997, Horn/Fleige 2003 and Ad-Hoc AG Boden 2005.

Level	Precompression Stress Pc (kPa)	Bulk density $\rho$ (g cm <sup>-3</sup> )	Organic matter (mass%)
Very Low	<30 (p1)	<1.2 (p1)	0 (h0)
Low	30–60 (p2)	1.2–< 1.4 (p2)	<1 (h1)
Mean	60–90 (p3)	1.4–< 1.6 (p3)	1–< 2 (h2)
High	90–120 (p4)	1.6–< 1.8 (p4)	2–< 4 (h3)
Very High	120–150 (p5)	> 1.8 (p5)	4–< 8 (h4)
Extremely High	>150 (p6)	—	8–< 15 (h5)

**TABLE 3** | Critical values to verify harmful subsoil compaction by precompression stress (Pc) (low indication) and saturated hydraulic conductivity (ks) (high indication) for different texture groups according to (Horn and Fleige 2009) and critical ks value according to UBA, 2004a.

Parameter		Horn and Fleige (2009)	Dimension
—	Silt	>70	kPa
Precompression stress Pc	Loam	>90	kPa
	Sand	>130	kPa
Sat. hydraulic conductivity	Any texture group	<10	cm d <sup>-1</sup>

## Section Precompression Stress

Methodologies for the physical and chemical soil parameters are noted in the appendix of the database and assigned to the corresponding parameters as numerical codes. Throughout the entire period, the physical and chemical analyses of the disturbed and undisturbed soil samples were performed with identical methods according to Schlichting et al. (1966), Schlichting et al. (1995), Hartge (1978), Hartge and Horn (1992, 2009, 2016), and Blume et al. (2011). detailed information on the measurements can be found in the respective publications.

All strength data in the database is determined for undisturbed cylinder specimens (236 cm<sup>3</sup>) by means of uniaxial compression tests (oedometer), and they were calculated using the method of Casagrande (1936). Further information can be found in Hartge and Horn (2009, 2016), Scheffer and Schachtschabel (2018) and Horn (1980). For an adequate evaluation of the Pc values, additional data are necessary. The *treatment\_ID\_pv* 18) and the *method\_ID\_pv* 19) refer by numerical code to treatment

measures, which were carried out during the test. Each Pc, BD and OM value 21) is classified as defined in DVWK (1997), Horn and Fleige (2003); Horn and Fleige (2009) and Ad-Hoc AG Boden 2005 (Table 2). It is also often stated that BD may have an influence on soil strength. Thus, it is used as a guiding parameter for the derivation of the Pc.

Table 3 shows the limits for Pc of the main textural groups (MTG) according to DVWK (1997) and Horn and Fleige (2009).

## Section Shearing

Prediction of the Pc (= internal soil strength) and the parameters of the shear resistance need to be determined. To get values of shear resistance, the Mohr Coulomb equation (Eq. (1)) was used:

$$\tau = \sigma_n \cdot \tan \phi + c \quad (1)$$

where  $c$  as the cohesion (kPa),  $\phi$  as the angle of internal friction (°) and  $\sigma_n$  as vertical compression stress (kPa) results in  $\tau$  as shear resistance (kPa).

**TABLE 4 |** Soils according to the German classification system (Ad-Hoc-AG Boden 2005, in parentheses) and WRB (2014),  $n = 150$ .

Terrestrial soils (91.4 %)	Semiterrestrial soils (8.6 %)
[BB] Cambisol (40)	[AQ] Fluvisol Gleysol (7)
[CF] Rendzic Leptosol (1)	[GG] Gleysol (9)
[DD] Vertic Cambisol (1)	[MC] Calcaric Fluvisol Gleysol (1)
[LL] Luvisol (25)	[MN] Eutric Fluvisol Gleysol (1)
[PP] Podzol (10)	—
[RZ] Calcaric Regosol (2)	—
[SS] Stagnosol (29)	—
[TT] Chernozem (3)	—
[YE] Plaggic Anthrosol (1)	—
[YK] Soil derived from colluvic material (18)	—

The effects of soil structure, texture, OM, and water content are linked and can be applied to explain soil strength and changes in soil functions (Zhang et al., 1997; Huang et al., 2021a, b). The structure of this section follows the pattern of those described earlier. Matric potential determined pre-drainage (20) affects items 24 and 25, which relate to the shear resistance.

## Section Chemical Properties and Texture

Due to the heterogeneous objectives of the publications included, the data base is diverse. The OM is calculated by a factor of 1.72 from organic carbon. All other chemical analyses in the database, as well as calculations, are based on identical methods described in Schlichting et al. (1966), Schlichting et al. (1995), and Blume et al. (2011). The classification of OM follows the recommendations of AG Bodenkunde, 1982, AG Boden, 1994, Ad-hoc-AG Boden, 2005 (Table 2).

## Data Selection and Preparation of Analysis

In this first paper, we have chosen to document Pc as a function of the OM and the BD for various texture classes. The chemical data OM, texture as well as BD are generally available for almost all profiles. The classification into MTG, according to Ad-hoc-AG Boden, 2005, is intended to show the influence of texture, and the differences in susceptibility to over-compaction and the resulting ks (for more details: Larson et al., 1980; Horn, 1981; Hettiaratchi, 1987; Batey and McKenzie, 2006). Furthermore, the influence of OM on soil strength will be dealt with in this paper as it is often mentioned by Feller and Beare, (1997); Alekseeva and Alekseev, (1999); Alakukku et al. (2003). Furthermore, we have considered the specific pre-drainage, since, as already mentioned, the matrix potential plays a major role in soil stability.

The following pre-settings were chosen:

- Conventional management (includes Ap-horizon).
- Pre-drainage: pF 1.8
- $OM \leq 5\%$
- $BD > 1 \text{ g cm}^{-3}$
- Specification of texture classes (sand, silt and loam)
- Indication of Pc and/or cohesion (c).

The pre-drainage of pF 1.8 was chosen to define the weakest (most moist condition in spring) soil conditions. Only TS and SS were selected for each profile, without any further horizon

differentiation of the SS. A TS horizon with a designated platy structure (pla) was added to SS, because the formation of a platy structure in the TS is rather unlikely with regular ploughing. The pre-settings resulted in 150 profiles from six countries: China (4), Estonia (2), Germany (121), Great Britain (3), Norway (17), and Switzerland (3). Terrestrial soils dominate conventionally farmed agricultural land, account for over 91%, and are represented by eleven different soil types (Table 4).

Four semi-terrestrial soil types (ground water affected soil types) are also represented and account for about 9%. Cambisols are the most represented (30%), followed by Stagnosols (22%) and soils derived from colluvic material (14%).

From soil types with corresponding specifications, there are a total of 348 analyzed soil horizons with Pc data (Table 5).

Overall, loam (36%) and silt (31%) are the most represented soil texture. The percentage of sandy soils is 20.1%. When considering the soil types with respect to the grain size distribution (Figure 2), a total of 25 different soil texture classes can be defined. The most common soil texture class is medium loamy sands (SL3) with 17% and strong loamy sands (SL4) with 15%, which corresponds to one third of the horizons. A second concentration of soil texture classes is observed in the medium clayey silt (Ut3), with 12% and in the strong clayey silt (Ut4) with 10%.

## Statistical Evaluation

Statistical analysis of the data was done using the statistical program R 4.0.3 (R Core Team, 2020). For processing, tables in AG Bodenkunde, 1982, AG Boden, 1994, Ad-hoc-AG Boden, 2005 are linked in R to form a main table using R package called *dplyr* to allow uniform statistical analyses of all profiles.

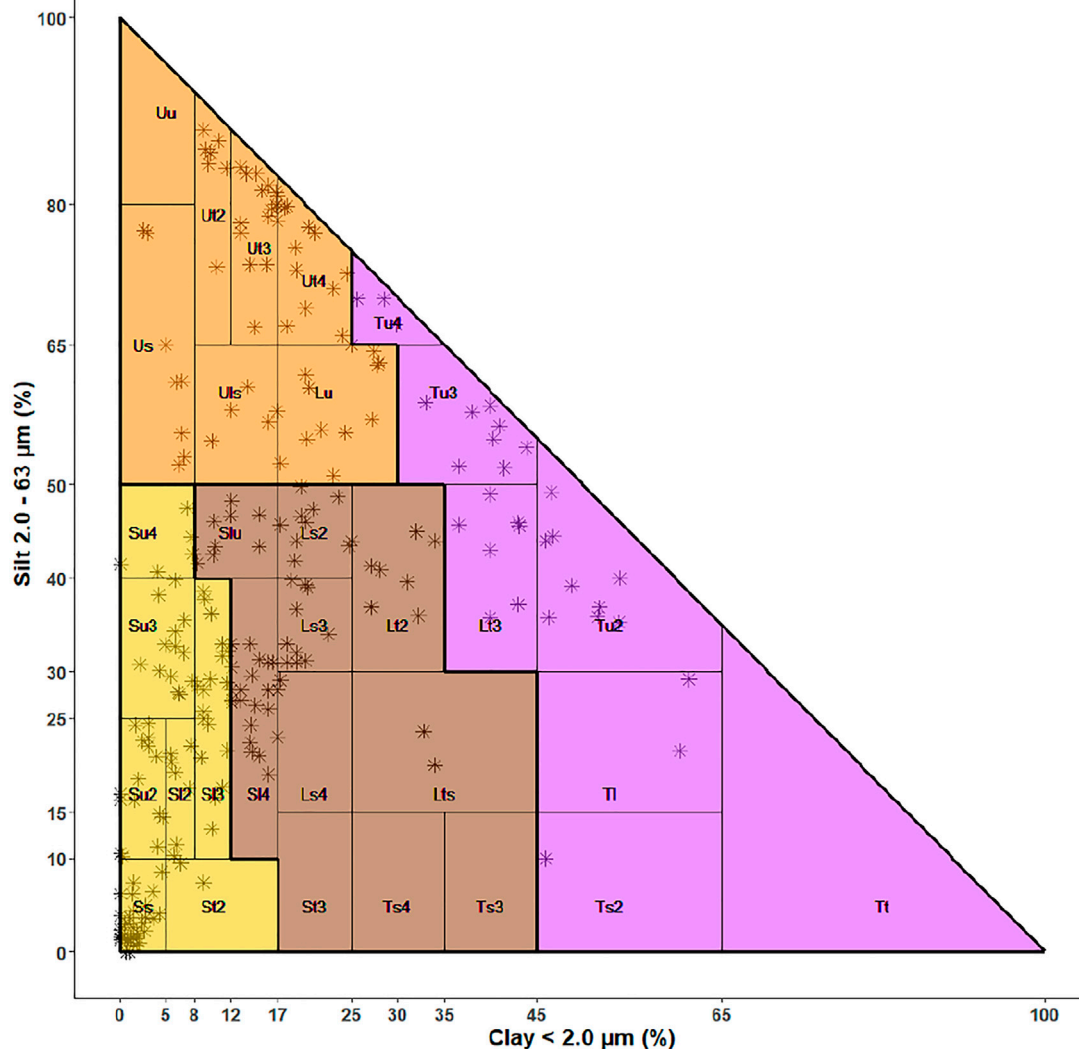
Time series have been established on 35% of the studied plots. For this reason, the “date” was considered as a parameter for sampling. Multiple linear regression analysis was performed according to Chambers (1992) and Wickham et al. (2021). In the computational model (Eq. (2)), the precompression stress ( $y$  (Pc)) is described as a dependent variable to the independent variables of organic matter ( $\chi_1(OM)$ ), bulk density ( $\chi_2(BD)$ ), and the year of sampling ( $\chi_3$  (year)).  $\epsilon$  is the level of variance in the error term or residuals of multi linear regression model.

$$y(Pc) = \beta_1\chi_1(OM) + \beta_2\chi_2(BD) + \beta_3\chi_3(\text{year}) + \epsilon \quad (2)$$

Statistically significant differences between samples were determined by using Wilcoxon and T-tests. The results were classified as statistically significance level (\*\*\*)  $p < 0.001$  (\*\*)  $p < 0.01$  [\*]  $p < 0.05$ , []  $p > 0.05$  and is given in each Equation (Eq. 3–8). Furthermore, all laboratory analyses were readjusted to the

**TABLE 5 |** Topsoils ( $n = 153$ ) and subsoils ( $n = 179$ ) of conventionally farmed land and their classification into main soil texture classes: sands ( $n = 73$ ), silts ( $n = 111$ ), clays ( $n = 39$ ) and loams ( $n = 109$ ), absolute values of the main texture groups (BHG) are given in parentheses ( $n = 348$ ).

Topsoils (48.3 %)	Subsoils (51.7 %)
Sand (26)	Sand (41)
Silts (52)	Silts (50)
Clays (11)	Clays (32)
Loams (64)	Loams (56)



**FIGURE 2 |** Texture classes (according to Ad-Hoc AG Boden 2005) from the selected 138 profiles with precompression (Pc) values and Saturated hydraulic conductivity (ks) values, star = topsoil (n = 142), square = subsoil (n = 147), n = 289.

standard of Ad-hoc-AG Boden (2005), based on raw data, to create comparability among profiles or horizons.

## RESULTS

## Main Soil Properties and Precompression Stress Ranges in Top- and Subsoils

The following graphs are subdivided into the MTG of sand, loam, and silt, and Pc values as a function of OM (%) and BD ( $\text{g cm}^{-3}$ ) for the TS and SS (**Figure 3-5**). For the linear regression equations **Eq. 3-8**, the unit for OM is also % and for BD is  $\text{g cm}^{-3}$ .

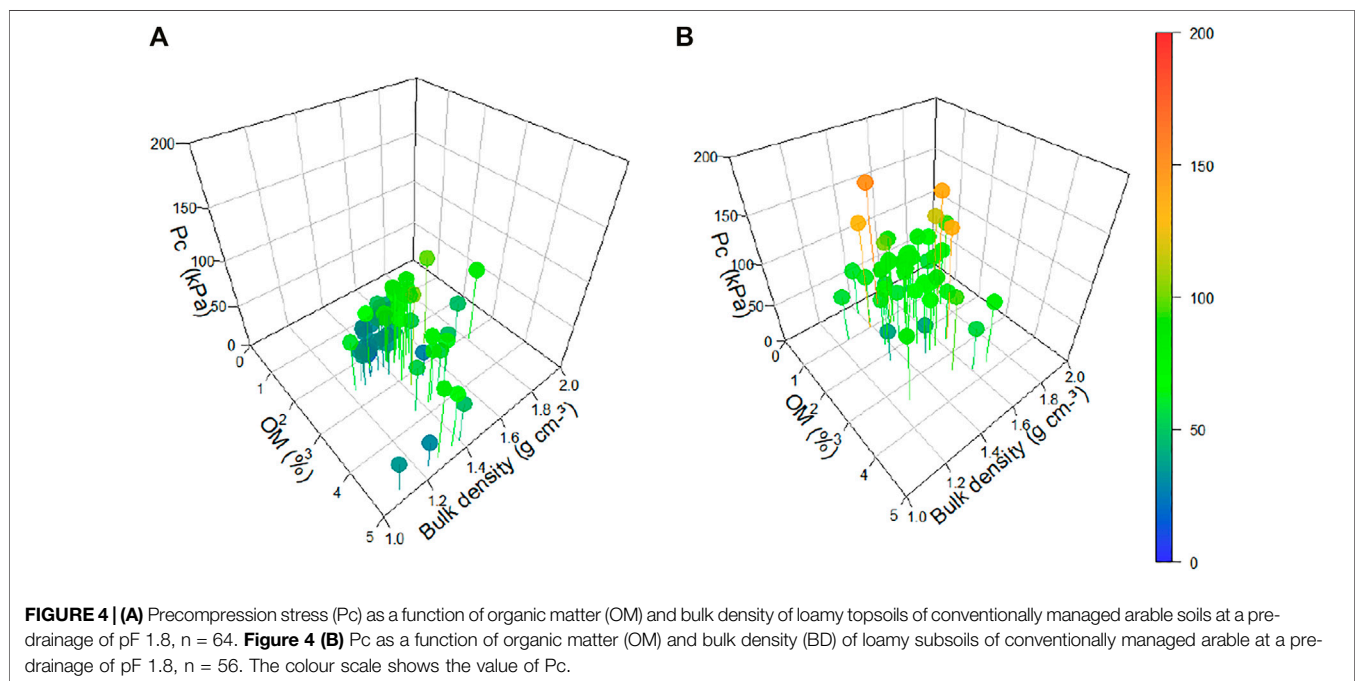
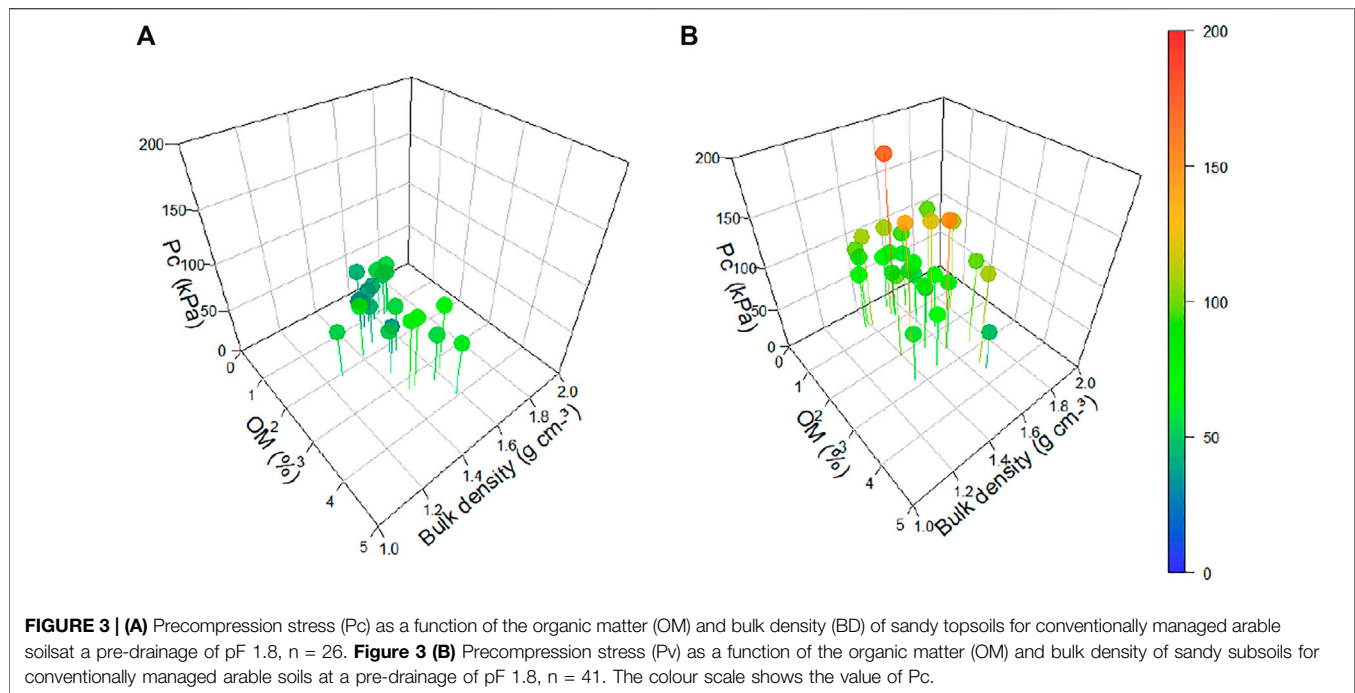
**Sand**

Sandy soils samples were taken between 1991 and 2013. The minimum BD value range from  $1.27 \text{ g cm}^{-3}$  to  $1.84 \text{ g cm}^{-3}$  54%

of the horizons had a mean BD between 1.4 and 1.6 g cm<sup>-3</sup>. The OM range from 0.2 to 3.9%, while the average Pc was 76 kPa, reaching a maximum value of 170 kPa at a BD of 1.62 g cm<sup>-3</sup> and OM of 0.21%. The lowest Pc values, between 30 and 39 kPa, were observed at BD of 1.52–1.58 g cm<sup>-3</sup> and an OM between 1 and 2% (**Figure 3**).

A large amount of reclaimed and colluviated horizons were noted between 2002 and 2013 and are characterized by very low Pc values in both TS and SS. This circumstance leads to a significant decrease in Pc as a function of time and must be considered (Eq. (3) and (4)).

In sandy horizons, neither the carbonate nor the clay content (<12%) in the available data reached values that could lead to separated aggregates like (sub)angular blocky structure. When considering the TS (**Figure 3A**), an average Pc of 51 kPa was measured and the OM was on average 2.0%. There was only one value with <1% (n = 1).



The regression analysis for the TS showed a positive correlation between OM ( $p < 0.05$ ) and  $P_c$  (Eq. (3)).

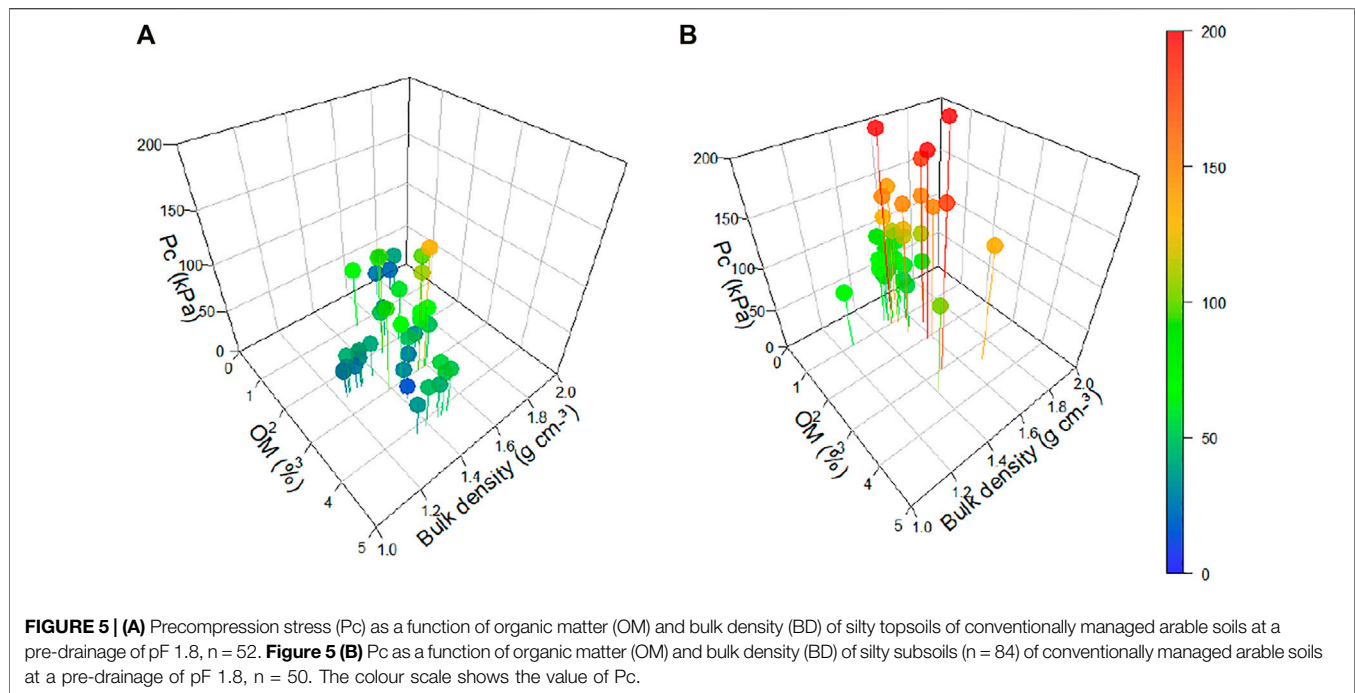
In the SS (Figure 3B), compared to the TS, the average  $P_c$  increased by 74%–94 kPa. The OM showed a 12% decrease to 1.4%. In comparison, the average BD of  $1.58 \text{ g cm}^{-3}$  was increased by 3%. (Eq. (4)).

$$P_c(TS) = 7.9(\pm 3.1)OM[*] + (18.5)(\pm 25.4)BD + (-0.4)(\pm 0.3)year + 1179.7$$

$$R^2 = 0.55, p < 0.05 \quad (3)$$

$$P_c(SS) = 3.5(\pm 4.1)OM + 45(\pm 34.2)BD + (-3.8)(\pm 0.6)year[***] + 7585.3$$

$$R^2 = 0.59, p < 0.001 \quad (4)$$



Neither in TS nor in SS BD have a significant effect on Pc. However, the year of sampling had a significant influence on Pc in SS. Pc decreased as a function of time, for the sandy SS ( $p < 0.01$ ) which consists mainly of Stagnosols (28%) and soils derived from colluvic material (18.5%) in the later decades with low Pc values.

### Loam

Loamy soils samples were taken between 1979 and 2019. Most of the conventionally farmed profiles in the database are loamy soils. The main soil types are classified as Cambisol (48%), followed by Stagnosol (30%). The ranges of values for OM (0.3–4.8%) and for BD (1.2–1.86 g cm<sup>-3</sup>) are wider in loamy soils (Figure 4) compared to the sandy ones (Figure 3). The average Pc of the soils with loamy texture is 67 kPa and is 12 kPa smaller than the Pc of sandy soils. However, their scattering is larger, ranging from 21 to 160 kPa.

There is a high amount of OM in loamy SS. Due to their pedogenesis and management methods over the last decades, a large number of the soil types (Cambisol, Luvisol, Stagnosol) show increasing OM in SS. On average, the OM of the loamy TS (Figure 4A) is 2.8%, with 50.9% of those classified as medium humous (h3) and 23.6% as weak humous (h2). The BD ranges from ρ 2 (1.1 g cm<sup>-3</sup>) to ρ 5 (1.81 g cm<sup>-3</sup>) with the maximum Pc of 113 kPa. Significances in the loamy TS is observed for BD ( $p < 0.01$ ) and year ( $p < 0.001$ ) with an  $R^2 = 0.45$ . However, OM ( $p > 0.05$ ) has no statistical effect on Pc at all.

$$Pc(TS) = -0.1 (\pm 2.9)OM + 57.8 (\pm 19.6)BD^{**} + (-1.0) (\pm 0.2)year^{***} + 2050.9$$

$$R^2 = 0.45, p < 0.001 \quad (5)$$

$$Pc(SS) = -0.8 (\pm 4.2)OM + 62.1 (\pm 30.5)BD^{*} + (-1.4) (\pm 5.3)year^{**} + 2880.2$$

$$R^2 = 0.17, p < 0.05 \quad (6)$$

In the loamy SS (Figure 4B), a larger scatter is observed for OM and BD ( $R^2 = 0.17$ ). The average Pc is 84 kPa, which is 66% more compared to that of TS. For OM < 1%, as well as for BD > 1.7 g cm<sup>-3</sup>, Pc values exceed 120 kPa mostly for Cambisol and Stagnosol. BD ( $p < 0.05$ ) have a significant influence of Pc in both TS and SS. Normally, the SS, in contrast to the TS, has strongly reduced OM. For loamy SS 30% M-Horizons with high OM content and a slightly decrease of Pc over years was observed ( $p < 0.01$ ).

### Silt

Silty soils samples were taken between 1979 and 2019 and have the highest Pc (200 kPa in SS). They represent very low to high OM content (h0 - h4) and low to very high BD values (ρ 2—ρ 5). In silty TS a direct effect of OM nor BD on Pc is not detectable ( $R^2 = 0.26$ ). Due to mechanical tillage under conventional management, the mechanical strength ( $p < 0.05$ ) decline significantly over years (Eq. (7)). The average Pc and OM are 49 kPa and 2.6%, respectively. The BD varies from low (ρ 2) to very high (ρ 4) due to different mechanical tillage methods and sampling times. Sampling with the highest BD took place direct after wheeling experiments.

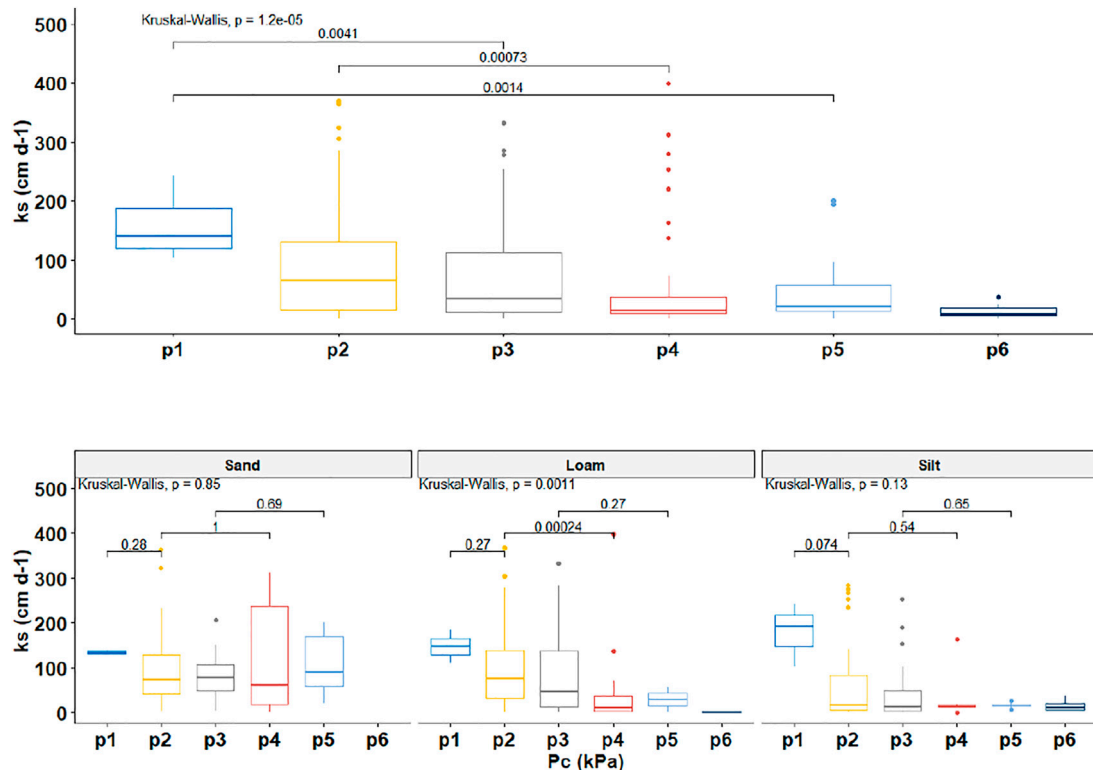
$$Pc(TS) = 2.5 (\pm 3.8)OM + 50.9 (\pm 29.1)BD + (-0.6) (\pm 0.3)year^{*} + 1179.7$$

$$R^2 = 0.26, p < 0.005 \quad (7)$$

$$Pc(SS) = 29 (\pm 7.6)OM^{***} + 72.7 (\pm 72.1)BD + (-0.5) (\pm 0.6)year + 993.1$$

$$R^2 = 0.25, p < 0.005 \quad (8)$$

In the silty SS (Figure 5A), a significantly lower humus content and a 220% increase in average Pc (up to 114 kPa) compared to TS



**FIGURE 6 |** Saturated hydraulic conductivity ( $k_s$ ) to precompression stress ( $P_c$ ) divided into groups p1 (0–30 kPa),  $n = 10$ , p2 (30–60 kPa),  $n = 96$ , p3 (60–90 kPa),  $n = 94$ , p4 (90–120 kPa),  $n = 55$ , p5 (120–150 kPa),  $n = 20$ , and p6 (>150 kPa),  $n = 14$ , terrestrial soils in total (top) and divided into the main soil texture classes (BHG) (bottom),  $n = 289$ .

can be observed. In the SS with  $P_c > 100$  kPa, platy structures are found almost exclusively, accounting for 28.1% of the silty SS. Further, no colluvic material was detected in silty SS. Only OM have a significant effect on  $P_c$  ( $p < 0.001$ ) but BD are not related to  $P_c$  at all ( $R^2 = 0.25$ ). Between 1981 and 1997, a steady increase in the  $P_c$  in the SS from 40 to over 200 kPa was also observed for identical silty plots. In addition, increased platy structures occurred, which were first used agriculturally since 1995.

## Saturated Hydraulic Conductivity

In **Figure 6** (top)  $k_s$  in  $\text{cm d}^{-1}$  is shown as a function of  $P_c$  divided into classification groups (p1 – p6) for all soil profiles. **Figure 6** (bottom) show the profile horizons which are subdivided into the MTG. For better comparability with the results of Horn and Fleige (2009) in **Table 2**, to evaluate the impact of  $P_c$  on  $k_s$ .

With increasing  $P_c$   $k_s$  decreases significantly over all three MTG ( $p < 0.01$ ) (**Figure 6** top). From  $P_c$  group p2 (30–60 kPa) to group p4 (90–120 kPa),  $k_s$  decreases by 72%, falling from  $50 \text{ cm d}^{-1}$ – $13.8 \text{ cm d}^{-1}$  ( $p < 0.05$ ). In p3 (60–90 kPa), 75% of the values are still above the critical value of  $10 \text{ cm d}^{-1}$ , with a median of  $26.6 \text{ cm d}^{-1}$ . Even at a  $P_c$  of 90–120 kPa, 50% of the soil horizons have a value of  $<14 \text{ cm d}^{-1}$ . In group p6 (>150 kPa), >50% of the measurements are below  $10 \text{ cm d}^{-1}$ , with the median dropping further to  $8.3 \text{ cm d}^{-1}$ .

Sandy soils from p3–p5 have the highest  $k_s$  values with no significant decrease of  $k_s$  ( $p = 0.7$ ) between the  $P_c$  groups (**Figure 6** bottom). The median for the groups p2–p5 is between 40 and  $100 \text{ cm d}^{-1}$  and shows no critical  $k_s$  value up to 150 kPa. In loamy soils a pronounced decline of the  $k_s$  occurs with increasing  $P_c$ . Up to 90 kPa, 75% of the conductivities are above  $10 \text{ cm d}^{-1}$ , but experience a significant reduction from p2 to p4 to  $11.2 \text{ cm d}^{-1}$  ( $p < 0.01$ ). Nearly 50% of the  $k_s$  of loamy soils with  $P_c$  between 90 and 120 kPa are below  $10 \text{ cm d}^{-1}$  and are reduced by a factor of 10 as the  $P_c$  increases to 120–150 kPa. The  $k_s$  of silty soils is more sensitive to  $P_c$  compared to sandy and loamy soils. Between group p1 and p2 the  $k_s$  is reduced by 75% and drops from  $69 \text{ cm d}^{-1}$ – $17 \text{ cm d}^{-1}$  ( $p = 0.07$ ). As  $P_c$  continues to increase beyond 60 kPa, conductivity remains consistently low and varying between 11 and  $16 \text{ cm d}^{-1}$ . If the  $P_c$  of 150 kPa is exceeded, all  $k_s$  are smaller than the critical value of  $10 \text{ cm d}^{-1}$ .

## DISCUSSION

### Bulk Density, Organic Matter, and Soil Structure

The evaluation of physical and mechanical parameters of undisturbed soil samples is a time-consuming, but necessary, approach to document the natural behaviour of soils. This approach is even the more urgent today, because only by

compilation of the data already collected can undisturbed soil samples be evaluated statistically and analysed to develop advanced pedotransfer functions. Also, changes over years can be documented. A section of the database presented in this paper allows differentiation of soil horizons using chemical and physical parameters. In addition, the changes of the parameters over time can help to elucidate alterations due to soil management - e.g., the long-term consequences of high axial loads on agricultural soils.

The very low  $P_c$  values in the TS of the conventionally farmed areas (78%) is due to continuous tillage, which repeatedly homogenizes the existing aggregates. Hartge and Horn (2016), Zheng et al. (2018) and Chellappa et al. (2021), showed that, compared to conservation soil management, conventional soil management homogenizes and destroys soil structure by reducing the number of macroaggregates ( $>1$  mm), and it makes soils more susceptible to soil deformation. Furthermore, the database contains data for samples that were collected during spring to autumn, which furthermore will affect the soil strength. These interactions will be subject to further analyses. Kay et al. (1987), Ehlers et al. (2000) and Horn and Smucker (2005) described seasonal changes from the homogenization due to tillage and a small increase in soil strength throughout the year. They observed that, over time, conservation or no tillage resulted in a higher soil strength which comes along with a quasi-dynamic equilibrium at smallest free entropy and optimized accessibility of particle surfaces (for more details see also Hartge and Horn 2016). However, reduced stability in the TS of all MTG results in enhanced water erosion, loss of OM and following retarded structure formation and strengthening due to glueing etc. as well as an enhanced methane or  $N_2O$  emission to the atmosphere (Puget and Lal, 2005; Mishra et al., 2010; Du et al., 2013; Haas et al., 2016; Zheng et al., 2018). Finally, it also causes an increase in dispersed clay in the soil solution (Watts and Dexter, 1997).

There is nearly an inverse relationship in the SS below the plough depth ( $>25$ – $30$  cm) and the TS, when BD, OM, and soil strength are considered. The lack of soil loosening on arable land combined with the rapid increase in axle loads of agricultural machinery by about 65% between 1989 and 2009 (Schjønning et al., 2015; Keller et al., 2019) should lead to a strong increase in  $P_c$  with a coinciding worsening of  $k_s$  and air permeability. Keller et al. (2019) concluded that high axle loads and driving in the plough furrow directly provoked SS over-compaction. This result can partial be confirmed for SS from the database. 20% of loamy SS and 62% of silty SS show platy structures at  $P_c$  of  $>140$  kPa and a significant relation to BD in silty and loamy SS. This development increases the penetration resistance for plant roots and reduces accessibility of particle surfaces and exchange places for nutrient storage and availability (Jansson and Johansson, 1998; Bygdén et al., 2004). At  $OM < 1\%$ , Bt and Bw-horizons with polyhedral and platy structures dominate and indicate a strong increase in soil strength. The influence of BD also has an impact on the composition of the soil horizons, and results for BD are similar to the horizons with  $OM < 1\%$ . Again, the Bt- and Bw-horizons have both the highest  $P_c$  (by low  $OM < 1\%$ ) and  $BD > 1.5$  g cm $^{-3}$ . Our results confirm the model predictions of Hartmann et al. (2012) concerning reduced

aeration and plant available water storage in combination with soil compaction effects.

On the other hand, proportion of stagnic M-horizons of colluvic material (17%) and buried A-horizons for loamy and silty soils are particularly high, which were recorded between the 80s and 00's. Thus, we explain the strong presence of OM in the SS with colluvial materials, which also have the lowest  $P_c$ . This observation is consistent with the conclusions of Blanco-Canqui et al. (2009). This circumstance lead to the fact that in unstructured sandy and loamy SS with high OM values ( $>1\%$ ) decreasing values of  $P_c$  over years ( $p < 0.05$ ) are observed. This unnatural increase of OM in SS thus causes a stronger slope of the regression line in the sandy and loamy soils and leads to implausible values outside the given time frame in years. For further considerations, especially OM contents have to be looked at more closely under the aspect of soil genesis on agricultural soils.

Further, the reduced number, deformation and destruction of soil aggregates by ploughing (Horn and Fleige, 2003; Six et al., 2004; Arvidsson and Keller, 2007; Page-Dumroese et al., 2006; Imhoff et al., 2015) and the increasing axle loads (Schjønning et al., 2015), result not only in higher stress induced strains and soil shearing in the TS but also in the SS with low OM content. This deformation due to compaction and shearing cannot be explained by the densification of the soil with increasing BD which confirm the findings of Huang et al. (2021a, b), who showed that different forms of stress (static or cyclic loading) application resulted in variable internal soil processes, including a loosening, irrespective of high stresses applied. These relations also confirmed that the primary classification based on soil texture is not sufficient to document general differences in soil strength, if soils as three-phase-systems are considered. OM and the matric potential in each case are the main factors influencing soil stability in highly disturbed agricultural TS and SS, since natural structuring by swelling and shrinkage and following strengthening by organic compounds like acids, exudates etc. can only occur in very short time frames before the next destruction due to repeated tillage, seedbed preparation followed by wheeling throughout the season due to spraying and fertiliser applications occurs. These impacts result in a continuous arrangement of particles, changes in pore continuity and coinciding altered up to short term positive pore water pressure. All this makes the predictions using texture dependencies less reliable and does not allow long-term predictions (Horn et al., 2019a).

Arable soils with reduced stability due tillage are much more susceptible to over-compaction (Arvidsson and Hakansson, 1996) and this is evident because excessive  $P_c$  ( $>150$  kPa) especially of silty soils results in poor ecological properties like  $k_s$ . This observation leads to the assumption that MTG, depending on the structuring and matric potential, have different  $P_c$  ranges in which sufficient soil strength with good ecological parameters are given.

Soil structure down to deeper depths needs to be linked with soil strength data and soil functions. At a given matric potential down to depth are structured soils the stronger the more developed are the aggregates (Horn, 1981) which results in

minor or no changes in hydraulic conductivity or air permeability (Hartge and Horn, 1989; Wiermann, 1998; Zink et al., 2010; Horn et al., 2018). This observation can be one of the main reasons for the low  $R^2$  between  $P_c$ , OM and BD in the three MTG under consideration. Horn (1981) arranged various aggregate types according to increasing soil strength starting with coherent-prismatic-blocky, subangular blocky, and finally crumbly structure. However, due to the today's stresses applied will the aggregate dependent  $P_c$  values of such structures be exceeded by anthropogenic (tillage, wheeling etc.) and geological processes (ice pressure), and form flats which prevent not only an easy deep rooting and high accessibility of particle surfaces for nutrient storage etc., but even more important is the newly formed horizontal anisotropy for fluxes (Horn et al., 2019a). The link between these aggregate types and soil mechanical properties is essential to know for a reliable prediction as it was already published by Fleige et al. (2002) and Horn and Fleige, (2009) for smaller datasets. Thus, the low  $R^2$  is due to the extreme highly variable OM contents (0–4%) in SS.

In further papers we will compare selected data (based on soil type and perennial sampling) over time, because it would prove and enlarge the findings of Ehlers et al. (1983) that soil strength is one of the most important factors for root growth and that over time the over-compaction status of soils reaches deeper soil layers. The consequences of the more compacted soil horizons can be also derived from the delayed root growth down to depth (Keller et al., 2019) which especially concerning the necessary nutrient and water uptake by plant roots will cause yield loss besides increasing soil loss due to water and wind erosion.

### Saturated Hydraulic Conductivity

It is important to determine when detrimental degradation of the soil occurs. The concept of  $P_c$ , according to Horn et al. (1991b) and Lebert and Horn (1991), describes the mechanical strength of soil structure against vertical compressive stresses. If the mean normal stress ( $\sigma_n$ ) is smaller than the  $P_c$ , the soil retains its physical integrity and no changes occur with respect to pore volume, pore connectivity, and continuity. If  $\sigma_n$ , however, exceeds the  $P_c$ , i.e. ( $P_c/\sigma_n < 1$ ), irreversible changes result, including reduced gas diffusion, hydraulic conductivity, and negatively altered pore size distribution. The DVWK (1997) documents the link between  $P_c$  and limiting soil properties like  $k_s$  (Table 3), which is based on the new database.

In sandy soils, the single grain structure is almost exclusively present, according to the results the primary pore size distribution allows a high  $k_s$  to be measured even beyond the critical stress value of >150 kPa.

However, loamy soils are much more sensitive to elevated  $P_c$ . Nearly 50% of the measured  $k_s$  are below the critical value of  $10 \text{ cm d}^{-1}$  (UBA, 2004a) at  $P_c$  between 90 and 120 kPa. According to Horn and Fleige (2009) the limit of 90 kPa for over-compression threat at 1.8 pF can thus be confirmed for loamy soils. Given the average  $P_c$  values of loamy (84 kPa) and silty (114 kPa) SS, we can assume that the recorded soils under agricultural use of the last 40 years show critical  $k_s$  values. Between 30 and 150 kPa, silty soils have lower  $k_s$  than loamy

and sandy soils. A total of 27% of silty SS fall below the critical value, which is an indicator of the sensitivity of these soils. Although silty soils are among the most productive soils also in Germany and have been intensively used for agriculture for decades or even centuries, no restriction values regarding maximum allowed stress application have been defined. According to the studies of Imhoff et al. (2015) and Díaz-Zorita and Grosso (1999), soil vulnerability increases with increasing silt content and humid conditions (precipitation > evaporation), which confirms the results in this study.

### Final Remarks

The data presented in this first paper indicate that soil strength or remained constant but the coinciding ecological soil functions of arable soils decreased and can confirm the analyses of Keller et al. (2019). The dataset can be the basis for predictions how soil management can limit soil type and structure dependent sustainability if applied stresses exceed the internal soil strength and following changes in plant growth, fluxes including groundwater recharge, surface runoff and carbon sequestration. It is irrefutable, that soil deformation processes and intensities depend on texture in combination with soil aggregation which require corresponding and varying threshold values to avoid further soil degradation and preserve the actual soil properties for further generations.

### CONCLUSION

Agricultural soils are anthropogenically influenced and differ from natural sites in terms of their mechanical properties. For the derivation of valid mechanical soil models, the development of a soil database, such as the one presented in this paper, is essential to estimate the consequences of mechanical cultivation. The data show that the three MTG (sand, loam, and silt) have different  $P_c$  values as a consequence of long-term agricultural soil management. The factors BD and OM of the TS and SS alone do not characterize sufficiently the  $P_c$ , because the latter depends on soil structure and pore water pressure, too. Within the scope of this project, these connections for the entire soil profile data are described in the following papers with detailed analyses.

The link and comparison between the  $P_c$ , and the limiting soil ecological functions can be the basis for soil type specific management recommendations as they are defined in the German soil Protection law (BBodSchG, 1998) by means of the actual, precaution and activity values to avoid further irreversible soil degradation.

### DATA AVAILABILITY STATEMENT

The original contributions presented in the study are included in the article/supplementary material, further inquiries can be directed to the corresponding author.

## AUTHOR CONTRIBUTIONS

HF supervises my dissertation work. CH collaborated on the structure of the database. RH, as a former prof, is reviewing the research.

## REFERENCES

- Ad-hoc AG Boden (2005). *Bodenkundliche Kartieranleitung*. 5. Aufl. Stuttgart: Schweizerbart'sche Verlag, 438
- AG Boden (1994). *Bodenkundliche Kartieranleitung*. 4. Aufl. Nachdr. Stuttgart: Schweizerbart'sche Verlag, 392pp.
- AG Bodenkunde (1982). *Bodenkundliche Kartieranleitung*. 3. Aufl. Stuttgart: Schweizerbart'sche Verlag, 331.
- Alakukku, L., Weisskopf, P., Chamen, W. C. T., Tijink, F. G. J., van der Linden, J. P., Pires, S., et al. (2003). Prevention Strategies for Field Traffic-Induced Subsoil Compaction: a Review. *Soil Tillage Res.* 73, 145–160. doi:10.1016/S0167-1987(03)00107-7
- Alakukku, L. (1996). Persistence of Soil Compaction Due to High Axle Load Traffic. I. Short-Term Effects on the Properties of clay and Organic Soils. *Soil Tillage Res.* 37, 211–222. doi:10.1016/0167-1987(96)01016-1
- Alekseeva, T., and Alekseev, A. (1999). Factors Affecting the Structural Stability of Three Contrasting Soils of China. *Catena* 38, 45–64. doi:10.1016/S0341-8162(99)00055-7
- Arthur, E., Schjønning, P., Moldrup, P., and de Jonge, L. W. (2012). Soil Resistance and Resilience to Mechanical Stresses for Three Differently Managed sandy Loam Soils. *Geoderma* 173–174, 50–60. doi:10.1016/j.geoderma.2012.01.007
- Arvidsson, J., and Hakansson, I. (1996). Do effects of Soil Compaction Persist after Ploughing? Results from 21 Long-Term Field Experiments in Sweden. *Soil Tillage Res.* 39, 175–197. doi:10.1016/S0167-1987(96)01060-4
- Arvidsson, J., and Keller, T. (2007). Soil Stress as Affected by Wheel Load and Tyre Inflation Pressure. *Soil Tillage Res.* 96, 284–291. doi:10.1016/j.still.2007.06.012
- Arvidsson, J., Trautner, A., Van Den Akker, J. J. H., and Schjønning, P. (2001). Subsoil Compaction Caused by Heavy Sugarbeet Harvesters in Southern Sweden II. *Soil Tillage Res.* 60, 79–89. doi:10.1016/S0167-1987(01)00168-4
- Batey, T., and McKenzie, D. C. (2006). Soil Compaction: Identification Directly in the Field. *Soil Use Manage.* 22, 123–131. doi:10.1111/j.1475-2743.2006.00017.x
- Baumgartl, W., and Horn, R. (2013). “Assessing Soil Degradation by Using a Scale-Spanning Soil Mechanical Approach: A Review. Soil Degradation 1–61,” in *Advances in Geocology* (Catena Verlag), 42. 978-3-923381-59-3.
- BBodSchG (1998). *Gesetz zum Schutz des Bodens vom 17.03.1998*. Germany: The Federal Ministry of Justice and Consumer Protection, 502. BGBl. I S.
- Berisso, F. E., Schjønning, P., Keller, T., Lamandé, M., Etana, A., de Jonge, L. W., et al. (2012). Persistent Effects of Subsoil Compaction on Pore Size Distribution and Gas Transport in a Loamy Soil. *Soil Tillage Res.* 122, 42–51. doi:10.1016/j.still.2012.02.005
- Bishop, A. W. (1959). The Principle of Effective Stress. *Teknisk Ukeblad* 106 (39), 859–863.
- Blanco-Canqui, H., Stone, L. R., Schlegel, A. J., Lyon, D. J., Vigil, M. F., Mikha, M., et al. (2009). No-till Induced Increase in Organic Carbon Reduces Maximum Bulk Density of Soils. *Soil Sci. Soc. Am. J.* 73, 1871–1879. doi:10.2136/sssaj2008.0353
- Blume, H. P., Stahr, K., and Leinweber, P. (2011). *Bodenkundlichen Praktikum*. Heidelberg: Spektrum Verlag, 255. 978-3-8274-1553-0.
- Bridges, E. M., and Oldeman, L. R. (1999). Global Assessment of Human-Induced Soil Degradation. *Arid Soil Res. Rehabil.* 13 (4), 319–325. doi:10.1080/089030699263212
- Bygdén, G., Eliasson, L., and Wästerlund, I. (2003). Rut Depth, Soil Compaction and Rolling Resistance when Using Bogie Tracks, *J. Terramechanics* 40, 179–190. doi:10.1016/j.jterra.2003.12.001
- Casagrande, A. (1936). “The Determination of Pre-consolidation Load and its Practical Significance,” in Proc. Int. Conf. Soil Mech. Found. Eng. Harvard University Cambridge, 60–64.
- Chambers, J. M. (1992). “Linear Models,” in *Chapter 4 of Statistical Models in S*. Editors J. M. Chambers and T. J. Hastie (Wadsworth & Brooks/Cole).
- Chellappa, J., Sagar, K. L., Sekaran, U., Kumar, S., and Sharma, P. (2021). Soil Organic Carbon, Aggregate Stability and Biochemical Activity under Tilled and No-Tilled Agroecosystems. *J. Agric. Food Res.* 4, 100139. doi:10.1016/j.jafr.2021.100139
- Dexter, A. R., Richard, G., Arrouays, D., Czyż, E. A., Jolivet, C., and Duval, O. (2008). Complexed Organic Matter Controls Soil Physical Properties. *Geoderma* 144 (Issues 3–4), 620–627. doi:10.1016/j.geoderma.2008.01.022
- Díaz-Zorita, M., and Grosso, G. A. (1999). Effect of Soil Texture, Organic Carbon and Water Retention on the Compactability of Soils from the Argentinean Pampas. *Soil Tillage Res.* 54, 121–126.
- Dörner, J., and Horn, R. (2006). Anisotropy of Pore Functions in Structured Stagnic Luvisols in the Weichselian Moraine Region in N Germany. *Z. Pflanzenernähr. Bodenk.* 169, 213–220. doi:10.1002/JPLN.200521844
- Du, Z.-L., Ren, T.-s., Hu, C.-s., Zhang, Q.-z., and Blanco-Canqui, H. (2013). Soil Aggregate Stability and Aggregate-Associated Carbon under Different Tillage Systems in the North China Plain. *J. Integr. Agric.* 12, 2114–2123. doi:10.1016/S2095-3119(13)60428-1
- Duttmann, R., Schwanebeck, M., Nolde, M., and Horn, R. (2014). Predicting Soil Compaction Risks Related to Field Traffic during Silage Maize Harvest. *Soil Sci. Soc. America J.* 78 (2), 408–421. doi:10.2136/sssaj2013.05.0198
- DVWK (1997). *Soil Strength in Structured Unsaturated Soils. Part II Physical Soil Properties (In German, with English Summary and Captures) Gefügestabilität Ackerbaulich Genutzter Mineralböden. Teil II: Ableitung Physikalischer Bodenkenngößen. Merkblätter 235, Wirtschafts- und Verlagsges. Bonn: Gas und Wasser.*
- Ehlers, W., Kopke, U., Hesse, F., and Bohm, W. (1983). Penetration Resistance and Root Growth of Oats in Tilled and Untilled Loess Soil. *Soil Tillage Res.* 3, 261–275. doi:10.1016/0167-1987(83)90027-2
- Ehlers, W., Werner, D., and Mähner, T. (2000). Wirkung mechanischer Belastung auf Gefüge und Ertragsleistung einer Löss-Parabraunerde mit zwei Bearbeitungssystemen. *J. Plant Nutr. Soil Sci.* 163, 321–333. doi:10.1002/1522-2624(200006)163:3<321::aid-jpln321>3.0.co;2-y
- Fazekas, O., and Horn, R. (2005). Zusammenhang zwischen hydraulischer und mechanischer Bodenstabilität in Abhängigkeit von der Belastungsdauer. *Z. Pflanzenernähr. Bodenk.* 168, 60–67. doi:10.1016/j.geoderma.2011.02.006
- Feller, C., and Beare, M. H. (1997). Physical Control of Soil Organic Matter Dynamics in the Tropics. *Geoderma* Vol. 79 (Issues 1–4), 69–116. doi:10.1016/S0016-7061(97)00039-6
- Fleige, H., Horn, R., and Stange, F. (2002). Soil Mechanical Parameters Derived from the CA-database on Subsoil Compaction. *Adv. GeoEcology* 35, 359–366. doi:10.1016/j.still.2011.04.004
- Fraters, B. (1996). *Generalized Soil Map of Europe. Aggregation of the FAO-UNESCO Soil Units Based on the Characteristics Determining the Vulnerability to Degradation Processes*. Bilthoven, Netherlands: National Institute of Public Health and the Environment, 67.
- Haas, C., Holthusen, D., Mordhorst, A., Lipiec, J., and Horn, R. (2016). Elastic and Plastic Soil Deformation and its Influence on Emission of Greenhouse Gases. *Int. Agrophys.* 30, 173–184. doi:10.1515/intag-2015-0088
- Håkansson, I., Voorhees, W. B., Elonen, P., Raghavan, G. S. V., Lowery, B., Van Wijk, A. L. M., et al. (1987). Effect of High Axle-Load Traffic on Subsoil Compaction and Crop Yield in Humid Regions with Annual Freezing. *Soil Tillage Res.* 10 (3), 259–268. doi:10.1016/0167-1987(87)90032-8
- Hamamoto, S., Moldrup, P., Kawamoto, K., Wollesen de Jonge, L., Schjønning, P., and Komatsu, T. (2011). Two-Region Extended Archie's Law Model for Soil Air Permeability and Gas Diffusivity. *Soil Sci. Soc. America J.* 75, 795–806. doi:10.2136/sssaj2010.0207
- Hartge, K. H., and Horn, R. (1989). *Die physikalische Untersuchung von Boden*. 2.ed. Stuttgart: Enke Verlag.

## ACKNOWLEDGMENTS

The authors are highly indebted to Prof. M.B. Kirkham United States (Kansas State University) for her very valuable English language corrections and intense discussion contributions.

- Hartge, K. H., and Horn, R. (1992). *Die physikalische Untersuchung von Boden*. 3.ed. Stuttgart: Enke Verlag.
- Hartge, K. H., and Horn, R. (2009). *Die physikalische Untersuchung von Böden*. Stuttgart 4. Schweitzerbart'sche Verlagsbuchhandlung. 978-3-510-65246-4.
- Hartge, K. H., and Horn, R. (2016). *Essential Soil Physics*. Stuttgart: Schweizerbart Science Publisher. 978-3-510-65288-4.
- Hartge, K. H. (1978). *Einführung in die Bodenphysik*, 364 Seiten, Ferd. Stuttgart: Enke Verlag. 3-432-89682-4. doi:10.1002/jpln.19811440222
- Hartmann, P., Zink, A., Fleige, H., and Horn, R. (2012). Effect of Compaction, Tillage and Climate Change on Soil Water Balance of Arable Luvisols in Northwest Germany. *Soil Tillage Res.* 124, 211–218. doi:10.1016/j.still.2012.06.004
- Hettiaratchi, D. R. P. (1987). A Critical State Soil Mechanics Model for Agricultural Soils. *Soil Use Manage.* 3, 94–105. doi:10.1111/j.1475-2743.1987.tb00718.x
- Horn, R., and Blum, W. E. H. (2020). Effect of Land-Use Management Systems on Coupled Physical and Mechanical, Chemical and Biological Soil Processes: How Can We Maintain and Predict Soil Properties and Functions? *Front. Agr. Sci. Eng.* 7 (3), 243. Article Number 104709. doi:10.15302/J-FASE-2020334
- Horn, R., and Dexter, A. R. (1989). Dynamics of Soil Aggregation in an Irrigated Desert Loess. *Soil Tillage Res.* 13 (3), 253–266. doi:10.1016/0167-1987(89)90002-0
- Horn, R., and Fleige, H. (2009). Risk Assessment of Subsoil Compaction for Arable Soils in Northwest Germany at Farm Scale. *Soil Tillage Res.* 102, 201–208. doi:10.1016/j.still.2008.07.015
- Horn, R., and Smucker, A. (2005). Structure Formation and its Consequences for Gas and Water Transport in Unsaturated Arable and forest Soils. *Soil Tillage Res.* 82 (1), 5–14. doi:10.1016/j.still.2005.01.002
- Horn, R., Baumgartl, T., Kühner, S., Lebert, M., and Kayser, R. (1991a). Zur Bedeutung des Aggregierungsgrades für die Spannungsverteilung in strukturierten Böden. *Z. Pflanzenernähr. Bodenk.* 154, 21–26. doi:10.1002/jpln.19911540106
- Horn, R., Lebert, M., and Burger, N. (1991b). "Vorhersage der mechanischen Belastbarkeit von Böden als Pflanzenstandort auf der Grundlage von Labor- und In Situ-Messungen," in *Materialien 73: Mechanische Belastbarkeit von Böden Bayerns*. Bayerisches Staatsministerium für Landesentwicklung und Umweltfragen München. doi:10.1016/j.jenvman.2005.11.022
- Horn, R., Fleige, H., and Zimmermann, I. (2017). "Soil Texture and Structure: Role in Soil Health," in *Managing Soil Health for Sustainable Agriculture, Volume 1: Fundamentals*. Editor D. Reicosky (Cambridge, UK: Burleigh Dodds Science Publishing). 978 1 78676 188 0. doi:10.1016/j.geodrs.2021.e00398
- Horn, R., Fleige, H., Lal, R., and Zimmermann, I. (2018). "Soil Health and Functions as a Basic Requirement for Advancing the SDG's, 52–60," in *Soils and Sustainable Development Goals. GeoEcology Essay. Catena Soil Sciences*. Editors R. Lal, R. Horn, and T. Kosaki (Stuttgart. 978-3-510-65425-3.
- Horn, R., Mordhorst, A., Fleige, H., Zimmermann, I., Burbaum, B., Filipinski, M., et al. (2019a). Soil Type and Land Use Effects on Tensorial Properties of Saturated Hydraulic Conductivity in Northern Germany. *Eur. J. Soil Sci.* 71, 179–189. doi:10.1111/ejss.12864
- Horn, R. (1980). Die Ermittlung der vertikalen Druckfortpflanzung im Boden mit Hilfe von Dehnungsmeßstreifen. *Z. Kulturtechnik Flugbereinigung* 21, 343–349.
- Horn, R. (1981). "Die Bedeutung der Aggregierung von Böden für die mechanische Belastbarkeit." in *Schriftenreihe TU Berlin*. 200. 3-7983-0792-X
- Horn, R. (1983). Die Bedeutung der Aggregierung für die Druckfortpflanzung im Boden. *Z. Kulturtechnik Flugbereinigung* 24, 238–249.
- Horn, R., and Fleige, H. (2003). A Method for Assessing the Impact of Load on Mechanical Stability and on Physical Properties of Soils. *Soil and Tillage Research* 73, 89–99. doi:10.1016/S0167-1987(03)00102-8
- Horn, R., Mordhorst, A., Fleige, H., Zimmermann, I., Burbaum, B., and Filipinski, M. (2019). Soil Type and Management Effects on Organic Carbon Stocks and Soil Structure Quality in North Germany. *Bulgarian Journal of Soil Science* 4.
- Horn, R. (2021). "Soils in Agricultural Engineering: Effect of Land-Use Management Systems on Mechanical Soil Processes," in *Hydrogeology, Chemical Weathering, and Soil Formation*. Editors A. Hunt, M. Egli, and B. Faybishenko (Hoboken, NJ, USA: Wiley & Sons), 187–199. 978-1-119-56396-9. Chapter 10A.
- Huang, X., Horn, R., and Ren, T. (2021a). Deformation and Pore Water Pressure Change during Static and Cyclic Loading with Subsequent Shearing on Soils with Different Textures and Matric Potentials. *Soil Tillage Res.* 209, 104909. doi:10.1016/j.still.2020.104909
- Huang, X., Horn, R., and Ren, T. (2021b). *Soil Structure Effects on Deformation, Pore Water Pressure, and Consequences for Air Permeability during Compaction and Subsequent Shearing*. Geoderma in press.
- Imhoff, S., Pires da Silva, A., Ghiberto, P. J., Tormena, C. A., Pilatti, M. A., and Libardi, P. L. (2015). Physical Quality Indicators and Mechanical Behavior of Agricultural Soils of Argentina. *PLoS ONE* 11 (4), e0153827. doi:10.1371/journal.pone.0153827
- IPCC (2003). *Good Practice Guidance for Land Use, Land-Use Change and Forestry*. Geneva: Intergovernmental Panel on Climate Change IPCC. 4-88788-003-0.
- Janssens, I. A., Freibauer, A., Schlamadinger, B., Ceulemans, R., Ciais, P., Dolman, A. J., et al. (2005). The Carbon Budget of Terrestrial Ecosystems at Country-Scale - a European Case Study. *Biogeosciences* 2, 15–26. doi:10.5194/bg-2-15-2005
- Jansson, K.-J., and Johansson, J. (1998). *Soil Changes after Traffic with a Tracked and a Wheeled forest Machine: A Case Study on a silt Loam in Sweden*. S-750 07 Uppsala, Sweden: Swedish University of Agricultural Sciences, Department of Operational Efficiency.
- Jones, R. J. A., Hiederer, R., Rusco, E., and Montanarella, L. (2005). Estimating Organic Carbon in the Soils of Europe for Policy Support. *Eur. J. Soil Sci.* 56, 655–671. doi:10.1111/j.1365-2389.2005.00728.x
- Kay, B. D., Groenevelt, P. H., Angers, D. A., and Baldock, J. A. (1988). Quantifying the Influence of Cropping History on Soil Structure. *Can. J. Soil Sci.* 68, 359–368. doi:10.4141/cjss88-033
- Keller, T., Arvidsson, J., Dawidowski, J. B., and Koolen, A. J. (2004). Soil Precompression Stress. *Soil Tillage Res.* 77, 97–108. doi:10.1016/j.still.2003.11.003
- Keller, T., Lamandé, M., Schjønning, P., and Dexter, A. R. (2011). Analysis of Soil Compression Curves from Uniaxial Confined Compression Tests. *Geoderma* 163, 13–23. doi:10.1016/j.geoderma.2011.02.006
- Keller, T., Colombi, T., Ruiz, S., Manalili, M. P., Rek, J., Stadelmann, V., et al. (2017). Long-term Soil Structure Observatory for Monitoring post-compaction Evolution of Soil Structure. *Vadose Zone J.* 16, vzj2016.11.0118. doi:10.2136/vzj2016.11.0118
- Keller, T., Sandin, M., Colombi, T., Horn, R., and Or, D. (2019). Historical Increase in Agricultural Machinery Weights Enhanced Soil Stress Levels and Adversely Affected Soil Functioning. *Soil Tillage Res.* 194, 104293. doi:10.1016/j.still.2019.104293
- Kirby, J. M. (1991b). Strength and Deformation of Agricultural Soil: Measurement and Practical Significance. *Soil Use Manage.* 7 (4), 223–229. doi:10.1111/j.1475-2743.1991.tb00878.x
- Kühner, S. (1997). *Simultane Messung Von Spannungen Und Bodenbewegungen Bei Statischen Und Dynamischen Belastungen Zur Abschätzung Der Dadurch Induzierten Bodenbeanspruchung*. PhD Thesis. Germany: Christian-Albrechts-Universität zu Kiel, Schriftenreihe Institut für Pflanzenernährung und Bodenkunde. Band 39.
- Larson, W. E., Gupta, S. C., and Useche, R. A. (1980). Compression of Agricultural Soils from Eight Soil Orders. *Soil Sci. Soc. Am. J.* 44, 450–457. doi:10.2136/sssaj1980.03615995004400030002x
- Lebert, M., and Horn, R. (1991). A Method to Predict the Mechanical Strength of Agricultural Soils. *Soil Tillage Res.* 19, 275–286. doi:10.1016/0167-1987(91)90095-F
- Lebert, M. (1989). Beurteilung und Vorhersage der mechanischen Belastbarkeit von Ackerboden. *Bayreuther bodenkundliche Berichte* 12, 131.
- McBride, R. A. (1989). Estimation of Density-Moisture-Stress Functions from Uniaxial Compression of Unsaturated, Structured Soils. *Soil Tillage Res.* 13, 383–397. doi:10.1016/0167-1987(89)90045-7
- Mishra, U., Lal, R., Liu, D., and Van Meirvenne, M. (2010). Predicting the Spatial Variation of the Soil Organic Carbon Pool at a Regional Scale. *Soil Sci. Soc. Am. J.* 74, 906–914. doi:10.2136/sssaj2009.0158
- Mordhorst, A., Fleige, H., Burbaum, B., Filipinski, M., and Horn, R. (2020). Natural and Anthropogenic Compaction in North Germany (Schleswig-Holstein): Verification of Harmful Subsoil Compactions. *Soil Use Manage* 37, 556–569. doi:10.1111/sum.12631
- O'Sullivan, M. F. (1992). Uniaxial Compaction Effects on Soil Physical Properties in Relation to Soil Type and Cultivation. *Soil Tillage Res.* 24, 257–269. doi:10.1016/0167-1987(92)90091-O
- Page-Dumroese, D. S., Jurgensen, M. F., Tiarks, A. E., Ponder, Jr., F., Jr., Sanchez, F. G., Fleming, R. L., et al. (2006). Soil Physical Property Changes at the North

- American Long-Term Soil Productivity Study Sites: 1 and 5 Years after Compaction. *Can. J. For. Res.* 36 (3), 551–564. doi:10.1139/x05-273
- Paz, A., and Guérif, J. (2000). Influence of Initial Packing Density, Water Content and Load Applied during Compaction on Tensile Strength of Dry Soil Structural Units. *Adv. Geocol.* 32, 22–31.
- Piccolo, A., Pietramellara, G., and Mbagwu, J. S. C. (1997). Use of Humic Substances as Soil Conditioners to Increase Aggregate Stability. *Geoderma* 75, 267–277. doi:10.1016/S0016-7061(96)00092-4
- Puget, P., and Lal, R. (2005). Soil Organic Carbon and Nitrogen in a Mollisol in central Ohio as Affected by Tillage and Land Use. *Soil Tillage Res.* 80, 201–213. doi:10.1016/j.still.2004.03.018
- R Core Team (2020). *R: A Language and Environment for Statistical Computing*. Vienna, Austria: R Foundation for Statistical Computing. URL: <https://www.R-project.org/>.
- Riggert, R. (2015). *Spannungseinträge unter Holzerntemaschinen und Auswirkungen auf bodenphysikalische Parameter*. Dissertation. Germany: Institut für Pflanzenernährung und Bodenkunde der CAU Kiel. Band 107.
- Saha, D., Kukal, S. S., and Sharma, S. (2011). Landuse Impacts on SOC Fractions and Aggregate Stability in Typic Ustochrepts of Northwest India. *Plant Soil* 339, 457–470. doi:10.1007/s11104-010-0602-0
- Scheffer, F., and Schachtschabel, P. (2018). *Lehrbuch der Bodenkunde*. Auflage 17. Heidelberg: Akademischer Verlag.
- Schjonning, P., Stettler, M., Keller, T., Lassen, P., and Lamandé, M. (2015). Predicted Tyre-Soil Interface Area and Vertical Stress Distribution Based on Loading Characteristics. *Soil Tillage Res.* 152, 52–66. doi:10.1016/j.still.2015.03.002
- Schlichting, E., Blume, H.-P., and Stahr, K. (1966). *Bodenkundliches Praktikum*. Hamburg: Parey Verlag. doi:10.1002/jpln.19671160209
- Schlichting, E., Blume, H.-P., and Stahr, K. (1995). *Bodenkundliches Praktikum*. Berlin, Wien: Blackwell Wissenschafts-Verlag. 978-3-8274-2733-5.
- Six, J., Bossuyt Degryze, H. S., Degryze, S., and Deneff, K. (2004). A History of Research on the Link between (Micro)aggregates, Soil Biota, and Soil Organic Matter Dynamics. *Soil Tillage Res.* 79 (1), 7–31. doi:10.1016/j.still.2004.03.008
- Smith, J., Smith, P., Wattenbach, M., Zaehle, S., Hiederer, R., Jones, R. J. A., et al. (2005). Projected Changes in mineral Soil Carbon of European Croplands and Grasslands, 1990–2080. *Glob. Change Biol.* 11, 2141–2152. doi:10.1111/j.1365-2486.2005.001075.x
- Soane, B. D., and van Ouwerkerk, C. (1995). Implications of Soil Compaction in Crop Production for the Quality of the Environment. *Soil Tillage Res.* 35, 5–22. doi:10.1016/0167-1987(95)00475-8
- Soane, B. D. (1990). The Role of Organic Matter in Soil Compactibility: A Review of Some Practical Aspects. *Soil Tillage Res.* 16, 179–201. doi:10.1016/0167-1987(90)90029-D
- Stolbovoy, V., Montanarella, L., Filippi, N., Jones, A., Gallego, J., and Grassi, G. (2007). *Soil Sampling Protocol to Certify the Changes of Organic Carbon Stock in Mineral Soil of the European Union*. Luxembourg: Office for Official Publications of the European Communities.
- The European Soil Framework Directive (2006). *The European Soil Framework Directive*. (Brussels: Commission of the European Communities). Available at: [https://www.euronatur.org/fileadmin/migration/uploads/media/Info43\\_EU-Bodenschutzrichtlinie.pdf](https://www.euronatur.org/fileadmin/migration/uploads/media/Info43_EU-Bodenschutzrichtlinie.pdf) (Accessed September 22, 2006).
- Trautner, A., van den Akker, J. J. H., van den Akker, J. J. H., Fleige, H., Arvidsson, J., and Horn, R. (2003). A Subsoil Compaction Database: its Development, Structure and Content. *Soil Tillage Res.* 73, 9–13. doi:10.1016/S0167-1987(03)00095-3
- UBA (2004a). *Ableitung von Kriterien zur Charakterisierung einer schädlichen Bodenveränderung, entstanden durch nutzungsbedingte Verdichtung von Böden/Regelungen zur Gefahrenabwehr*. Berlin: Umweltbundesamt Hrsg., Texte 46/04, 122.
- Van den Akker, J. J. H., Arvidsson, J., and Horn, R. (1999). “Experiences with the impact and prevention of subsoil compaction in the European Community,” in Proceedings of the first workshop of the Concerted Action ‘Experiences with the impact of subsoil compaction on soil, crop growth and environment and ways to prevent subsoil compaction (Wageningen, The Netherlands), 28–30. May 1998,
- Watts, C. W., and Dexter, A. R. (1997). The Influence of Organic Matter in Reducing the Destabilization of Soil by Simulated Tillage. *Soil Tillage Res.* 42, 253–275. doi:10.1016/S0167-1987(97)00009-3
- Wickham, H., François, R., Henry, L., and Müller, K. (2021). *Dplyr: A Grammar of Data Manipulation*. R package version 1.0.3. Available at: <https://CRAN.R-project.org/package=dplyr>.
- Wiermann, C., Werner, D., Horn, R., Rostek, J., and Werner, B. (2000). Stress/strain Processes in a Structured Unsaturated Silty Loam Luvisol under Different Tillage Treatments in Germany. *Soil Tillage Res.* 53, 117–128. doi:10.1016/S0167-1987(99)00090-2
- Wiermann, C. (1998). *Auswirkungen Differenzierter Bodenbearbeitungen Auf Die Bodenstabilität Und Das Regenerationsvermögen Losburtiger Ackerstandorte*. PhD Thesis. Kiel: Christian-Albrechts-Universität zu Kiel, Schriftenreihe Institut für Pflanzenernährung und Bodenkunde. Band 45.
- WRB (2014). *IUSS Working Group World Reference Base for Soil Resources, Update 2015: International Soil Classification System for Naming Soils and Creating Legends for Soil Maps*. FAO, Rome: World Soil Resources Reports.
- Zhang, H., Hartge, K. H., and Ringe, H. (1997). Effectiveness of Organic Matter Incorporation in Reducing Soil Compactibility. *Soil Sci. Soc. Am. J.* 61, 239–245. doi:10.2136/sssaj1997.03615995006100010033x
- Zheng, H., Liu, W., Zheng, J., Luo, Y., Li, R., Wang, H., et al. (2018). Effect of Long-Term Tillage on Soil Aggregates and Aggregate-Associated Carbon in Black Soil of Northeast China. *PLoS One* 13, e0199523. doi:10.1371/journal.pone.0199523
- Zink, A., Fleige, H., and Horn, R. (2010). Load Risks of Subsoil Compaction and Depths of Stress Propagation in Arable Luvisols. *Soil Sci. Soc. Am. J.* 74 (5), 1733–1742. doi:10.2136/sssaj2009.0336
- Zink, A. D. (2009). *Bodenstabilität und Auswirkungen dynamischer Lasteneinträge auf physikalische Eigenschaften von Ackerböden unter konservierender und konventioneller Bodenbearbeitung*. Dissertation. Deutschland: Agrar- und Ernährungswissenschaftliche Fakultät der CAU Kiel. Band 84.

**Conflict of Interest:** The authors declare that the research was conducted in the absence of any commercial or financial relationships that could be construed as a potential conflict of interest.

**Publisher’s Note:** All claims expressed in this article are solely those of the authors and do not necessarily represent those of their affiliated organizations, or those of the publisher, the editors and the reviewers. Any product that may be evaluated in this article, or claim that may be made by its manufacturer, is not guaranteed or endorsed by the publisher.

Copyright © 2022 Schroeder, Fleige, Hoffmann, Vogel and Horn. This is an open-access article distributed under the terms of the Creative Commons Attribution License (CC BY). The use, distribution or reproduction in other forums is permitted, provided the original author(s) and the copyright owner(s) are credited and that the original publication in this journal is cited, in accordance with accepted academic practice. No use, distribution or reproduction is permitted which does not comply with these terms.



# Soil Use Legacy as Driving Factor for Soil Erosion under Conservation Agriculture

Kathrin Grahmann<sup>1,2\*</sup>, Valentina Rubio<sup>3,4</sup>, Mario Perez-Bidegain<sup>5</sup> and Juan Andrés Quincke<sup>3</sup>

<sup>1</sup>Leibniz Centre for Agricultural Landscape Research (ZALF), Resource-Efficient Cropping Systems, Research Area 2 "Land Use and Governance", Müncheberg, Germany, <sup>2</sup>Leibniz Centre for Agricultural Landscape Research (ZALF), Data Dimensionality, Research Platform "Data Analysis & Simulation", Müncheberg, Germany, <sup>3</sup>Instituto Nacional de Investigación Agropecuaria (INIA), Programa de Producción y Sustentabilidad Ambiental, Estación Experimental INIA La Estanzuela, Colonia, Uruguay, <sup>4</sup>Instituto Nacional de Investigación Agropecuaria (INIA), Programa de Cultivos de Secano, Estación Experimental INIA La Estanzuela, Colonia, Uruguay, <sup>5</sup>Universidad de la República, Facultad de Agronomía, Departamento de Suelos y Aguas, Montevideo, Uruguay

## OPEN ACCESS

### Edited by:

Miriam Muñoz-Rojas,  
University of New South Wales,  
Australia

### Reviewed by:

Ademir De Oliveira Ferreira,  
Federal Rural University of  
Pernambuco, Brazil  
Jiban Shrestha,  
Nepal Agricultural Research Council,  
Nepal  
Ruixing Hou,  
Institute of Geographic Sciences and  
Natural Resources Research (CAS),  
China

### \*Correspondence:

Kathrin Grahmann  
Kathrin.Grahmann@zalf.de

### Specialty section:

This article was submitted to  
Soil Processes,  
a section of the journal  
Frontiers in Environmental Science

**Received:** 26 November 2021

**Accepted:** 28 January 2022

**Published:** 28 February 2022

### Citation:

Grahmann K, Rubio V,  
Perez-Bidegain M and Quincke JA  
(2022) Soil Use Legacy as Driving  
Factor for Soil Erosion under  
Conservation Agriculture.  
Front. Environ. Sci. 10:822967.  
doi: 10.3389/fenvs.2022.822967

Water erosion can cause irreversible depletions in soil quality and crop productivity. The susceptibility of the soil to erosion is affected by current and historical management practices. Historical soil management practices like ploughing or subsoil loosening may lead to irreversible degradations of soils, which in turn increases soil erosion risk. Six "Wischmeier" plots under conservation agriculture, but with different historic treatments regarding soil use and management, were evaluated. These plots were installed in 1984 in Colonia del Sacramento, Uruguay on a Vertic Argiudoll. The objective of this study was to quantify how changes in soil quality, generated by different historical soil use and management over the last 35 years, contribute to current runoff and soil erosion in a cropping system under soil conservation practices using no-till, residue retention and cover crops. Considering differences in soil legacy effects of previous land use, plots were grouped in three treatments with contrasting historic index of agricultural intensification (IAI). The IAI was developed combining the duration of land use under agricultural production and the number and intensity of tillage activity resulting in the treatments: tillage with crop-pasture rotation (TIL\_CP), no-tillage under several rotations (NT\_Mix) and tillage with continuous cropping (TIL\_CROP) with an increasing IAI of 3.5, 7.1 and 11.8, respectively. Rainfall events, runoff water and total, fixed and volatile solids were studied from 2017 to 2019. Soil physical (bulk density, penetration resistance, infiltration rate, aggregate stability), chemical (soil organic carbon (SOC), pH, phosphorous (P-Bray)) and biological properties (particulate organic matter (POM), potentially mineralizable nitrogen (PMN)) were assessed in 2019. Yearly average runoff amounted 209, 579 and 320 mm in 2017, 2018 and 2019, respectively. Yearly average soil losses were 233, 805 and 139 kg/ha with significant differences among years. The lowest soil losses were observed in TIL\_CP (231, 615 and 146 kg/ha in 2017, 2018 and 2019, respectively) with lowest IAI of 3.5. Infiltration rate was the lowest in plots with highest IAI. Soil bulk density was highest (1.3 g/cm<sup>3</sup>) in plots with high IAI. SOC and PMN were lowest in TIL\_CROP (3.0% SOC and 34 mg/kg PMN), holding the highest IAI of 11.8. Conservation agriculture minimized soil erosion losses in all plots and years, and erosion was much lower than the maximum tolerable threshold of 7,000 kg/ha for this particular soil. However, in historically intensively tilled and cropped soils,

soil quality showed long-term adverse effects pointing towards a reduced resilience of the agricultural system.

**Keywords:** *RUSLE, Uruguay, long-term experiment, soil degradation, intensification index, sediments, runoff*

## INTRODUCTION

Soil erosion remains a major challenge worldwide, being the greatest threat for sustainable soil management and subsequent food production (Rickson et al., 2015). Soil erosion, its control and remediation practices are related to nine out of 15 sustainable development goals defined by the United Nations (FAO, 2019). This highlights the worldwide preoccupation about soil loss and its immediate and indirect consequences fueling the sustainability discussion. Changes in land use and cover generated by the disturbance of natural grasses are the main factor leading to accelerated soil erosion (Borrelli et al., 2017). In Uruguay, land use changes occurred since the early 2000s in form of agricultural intensification shifting towards continuous, annual cropping systems and simplified rotations which led to fresh water pollution and soil quality deterioration (Carrasco-Letelier and Beretta-Blanco, 2017; Ernst et al., 2018). Furthermore, Uruguay is affected by climate change, mainly shown by increasing precipitation rates and extreme weather events that directly alter water erosion risks (Munka et al., 2007; PNUD (Programa de las Naciones Unidas para el Desarrollo) Uruguay, 2007). The combination of deteriorated soils with more intense rainfall events increases the risk of soil erosion compromising soil and water quality.

Soil organic carbon (SOC) losses have been reported as a result of agricultural intensification increase in Uruguay (Beretta-Blanco et al., 2019; Grahmann et al., 2020) which could be related to incessant soil losses by erosion although soil conservation practices were implemented by law. SOC is the main determinant of aggregate stability of Mollisols (Novelli et al., 2013; Rubio et al., 2019), the most important agricultural soil type in Uruguay. Added to this, water erosion preferentially removes the light organic fraction of low density and therefore contributes to SOC pool depletion (Lal, 2003) and atmospheric CO<sub>2</sub> emissions (Lal, 2019). Soil erosion is strongly coupled with other nutrients' runoff like nitrogen (N) which has consequences for freshwater and marine ecosystems leading to contamination, algae growth and overall biodiversity decline (De Vries et al., 2013). The particulate organic matter (POM) and potentially mineralizable N (PMN) were found to be sensitive indicators to detect the vulnerability for water erosion and overall soil degradation (Wander et al., 1998; Fabrizzi et al., 2003). Other parameters to monitor soil quality decrease and nutrient losses via erosion are total, fixed and volatile suspended solids and the carbon (C) and N enrichment ratios of the transported sediments (Palis et al., 1990; Holz and Augustin, 2021).

Conservation agriculture with its three principles of minimum soil tillage, crop rotation and residue retention is an often reported management system to effectively reduce soil erosion (Ernst and Siri-Prieto, 2009; Willett et al., 2019). To minimize soil erosion, soil cover must be coupled with a stable soil structure. As

the basic unit of soil structure, stable aggregates are key for soil quality, soil fertility, and resistance to degradation (Le Bissonnais, 1996). A stable soil structure is crucial for maintaining soil porosity, gas exchange, water infiltration, erosion resistance, and SOC sequestration (Six et al., 2004; Morris et al., 2019). A reduction in tillage intensity increases soil structural stability, improves aggregate distribution and enhances soil porosity and therefore infiltration, thus decreasing soil erodibility, improving soil fertility and improving overall agronomic productivity (Azooz and Arshad, 2011; Verhulst et al., 2011; Palm et al., 2014). Straw residues on the soil surface act like barriers that prevent the soil from receiving directly the high kinetic energy of raindrops during heavy rainfalls (Turtola et al., 2007), hence reducing surface soil dispersion and crust formation. In addition to this direct effect of residue retention on soil infiltration, conservation agricultural practices also contribute indirectly through improved structural stability, bulk density and pore structure (Kumar and Goh, 1999; Zhang et al., 2007; Ranaivoson et al., 2017).

Long-term experiments are important to understand how conservation agriculture modifies the dynamics in biochemical and geophysical processes over decades, which in consequence affect soil erodibility (Richter et al., 2007; Johnston and Poulton, 2018; Grahmann et al., 2020). As for surface runoff and erosion determination, surface runoff plots that count with a predefined, surrounded area and water collection tanks, so called "Wischmeier" plots are required (Kinnell, 2016). Experimental facilities of long-term surface runoff plots are used to document the effects of conservation agriculture on soil erosion providing a valuable, but seldom available experimental data set.

Since 2013, it is mandatory for Uruguayan farms larger than 50 ha to present a land use and management plan that ensures an estimated average soil erosion rate smaller than a previously defined soil-specific tolerance threshold (MGAP, 2013). The application of this law, which was updated lastly in 2018, aims to promote conservation agriculture practices reducing the risk of soil erosion in cropping systems based on the Revised Universal Soil Loss Equation (RUSLE) (Pérez-Bidegain et al., 2018; Zurbriggen et al., 2020). The RUSLE model was calibrated and validated for Uruguay and available in an adapted software tool (EROSION 6.0) (Renard et al., 1997; García Prechac et al., 2017; Pérez-Bidegain et al., 2017). Hereof, it is important to emphasize that the current K factors of the Uruguayan RUSLE, which indicates how susceptible a soil is to water detachment, was calculated by Puentes (1981) based on soil characteristics determined in a soil sampling campaign conducted in 1976 (MGAP-DSA, 1976).

While the use of simulation models to predict soil erosion has been widely applied in the country, the actual state of soil quality was not considered yet. As the supposedly stable K factor was defined in the 1980s and was calculated considering soil texture,

total soil carbon content and two classification factors associated to soil structure and permeability, this might lead to an underestimation of erosion in today's degraded soils and does not consider the dynamics of soil aggregate stability, the history of land use and the subsequent SOC losses at the regional scale (Alewell et al., 2019). The deterioration of soil properties caused by their past use and management, and particularly tillage, can have a great impact on erosion (Beniston et al., 2015) and has rarely been studied in a remediation context. Soil management practices, like deep ploughing or subsoil loosening lead to irreversible soil structure changes, which in turn affect soil quality over many decades (Schneider et al., 2017) and cause persistent soil legacy effects of previous land use. This may also account for the cover management factor (C factor), which is directly influenced by the vegetation type, growth stage of the vegetation and root mass, not only from a yearly perspective, but over a longer period of time (Gyssels et al., 2005; Panagos et al., 2015a). In the current study, the history of soil use and crop management intensity for each experimental unit was transformed to a newly developed index of agricultural intensification (IAI) combining the number of years under tillage activities and crop production with the length of agricultural production periods (intensification sequence index, Caviglia and Andrade, 2010; Martinez et al., 2020).

The objectives of this study were 1) to quantify surface runoff, soil and nutrient losses in a continuous cropping system under conservation agriculture implemented in long-term surface runoff plots and 2) to determine the variability in physical, chemical and hydraulic soil properties due to soil use and management history. We hypothesized that current conservation practices reduce soil losses to a minimum and assumed that differences in physical and chemical soil parameters between plots were existent and generated by differences in historical land use management which in turn explains the variability of soil losses between the plots nowadays. Furthermore, this paper provides starting points to discuss an update of the erodability factor K that might be affected by previous tillage and crop management through effects on SOC and soil structure.

## MATERIALS AND METHODS

### Experimental Site

The study was conducted at INIA La Estanzuela, Uruguay (lat. 34°20'S, long 57°41'W, 66 m a.s.l.), in a soil classified as Vertic Argiudoll (USDA Soil Taxonomy; Soil Survey Staff, 2014). The site has a warm temperate climate with annual rainfall of 1,125 mm and an annual reference evapotranspiration of about 1,180 ( $\pm 143$ ) mm over 55 years (Grahmann et al., 2020). Maximum monthly mean temperature ranges from 15°C in the winter to 28°C in the summer, and the minimum monthly mean temperature varies from 6°C in the winter to 17°C in the summer (Baethgen et al., 2021). Available water holding capacity was 92.7 mm in 0–56 cm depth for undisturbed soil (Hill et al., 2008). In 0–15 cm soil depth, the particle size fraction contains 178 g/kg sand, 450 g/kg silt, and 372 g/kg clay and soil organic

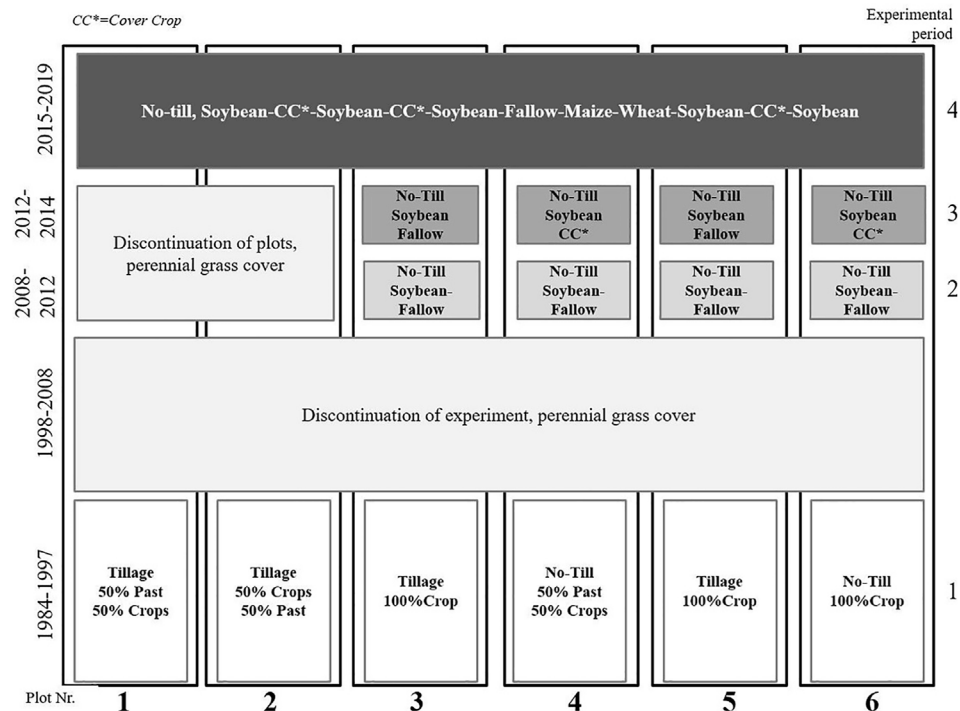
carbon (SOC) averaged 2.93% ( $\pm 0.09$ ) in 0–7.5 cm soil depth for the experimental site in 2019.

### Long-Term Wischmeier Plots

The long-term experiment was installed in 1984 when six Wischmeier runoff plots were built with a size of 22.1 m length and 3.5 m width along an agricultural field's slope side. The difference in height between top and bottom end of each plot was measured by means of an automatic level and level staff in 2020, and the resulting slope ranged between 4.3 and 4.7%. Each plot was completely surrounded by a metal border of 10 cm height of which 5 cm were inserted into the soil. The lower side ended up in a funnel system which transported the runoff water to a first cement tank of 750 L capacity embedded in the soil. During extreme rainfall events, the overflow system led through a fractionator, with one seventh (1/7) of water passing to a second tank of 1000 L capacity. The total runoff water storage capacity captured up to 100 mm runoff events in each plot.

A schematic overview of the historical treatments and land use changes for each experimental period and plot can be found in **Figure 1**. Since the beginning of the experiment, four experimental periods were distinguished. In the first experimental period (1984–1997), half of the plots were managed with conventional tillage using a chisel plough to 10–15 cm soil depth. Additionally, two different crop rotations were investigated: continuous cropping and crop-pasture rotations. The treatments were randomly distributed. The data of this experimental period were used to validate the USLE model for contrasting soil use systems (García-Préchac, 1992). Between 1998 and 2008, the experiment was discontinued due to financial constraints, leaving the plots without any use under perennial grass cover. Since 2008, the second experimental period, four of the plots were recovered to test a soybean (*Glycine max*)–fallow rotation under no-till management focusing on the assessment of the environmental impact of agrochemicals. In the third experimental period, cover crops rotating with soybean were incorporated in half of the plots from 2012 to 2014 and the research focus was set on phosphorus runoff (Lizarralde et al., 2015). In the fourth experimental period which started in 2015, two more plots were taken into operation with continuous crop rotation of soybean – cover crop (Black oats (*Avena strigosa*))—soybean – cover crop (Ryegrass (*Lolium multiflorum*))—soybean – fallow – maize (*Zea mays*)—wheat (*Triticum aestivum* L.)—soybean – cover crop (Rye (*Secale cereale*) and vetch (*Vicia villosa*))—soybean. Since 2015, all six plots were used and managed uniformly (“uniformity trial”) with best soil conservation practices using no-till, residue retention and cover crops.

Sowing and harvest operations were conducted with experimental agricultural machinery, pesticide applications were conducted manually according to best management practice. The cover crop mix of rye and hairy vetch was sown in May 2019 and roller-crimped in November 2019, while the previous cover crops were terminated with glyphosate. Fertilizer application in form of solid urea and diammonium phosphate during the last six study years was



**FIGURE 1 |** Experimental design of the Wischmeier plots and their history of soil use and management since the experimental onset in 1984.

**TABLE 1 |** Planting and harvest dates and average fertilizer rates per year and crop since uniform management started in 2014 (CC: cover crop).

Crop	Planting	Harvest/Termination	Fertilizer kg/ha	
			N	P
Soybean	30 January 2014	20 May 2014		
Ryegrass (CC)	14 May 2014	8 October 2014	10.5	26.2
Soybean	28 November 2014	27 April 2015		
Oats (CC)	10 April 2015	4 September 2015		
Soybean	24 November 2015	1 May 16		
Ryegrass (CC)	26 April 2016	15-Sep 2016		
Soybean	30 November 2016	23 May 2017		
Maize	8 November 2017	23 May 2018	94.4	16.1
Wheat	29 June 2018	23 December 2018	189.6	18.1

identical in each of the plots and was applied according to previous soil tests (Table 1).

## Index of Agricultural Intensification

Information regarding crop rotation and tillage intensity for each plot since 1984 were used to estimate an index of agricultural intensification (IAI), a way of classified scoring for historical soil use intensity. The IAI is estimated as the product of two indices, one accounting for cropping sequence intensification (ISI) and the second one for tillage intensification (ITI). Land use intensity is estimated using the index of sequence intensification (ISI) and is calculated on a yearly basis to account for the number of crops with active plant growth during the study period (Caviglia and Andrade, 2010; Novelli et al., 2013). The index enlarges with an increasing

number of crops planted per year. To account for the reported beneficial effects on soil quality and structure through pasture incorporation into crop rotation (Studdert et al., 1997; Ernst et al., 2018), a coefficient of 0.5 was applied during the first experimental phase to the cropping sequence length when pastures were included (Wischmeier and Smith, 1978).

$$ISI = \sum \left( \frac{(\text{weighting factor (pasture)}) \times \text{total number of crops}}{\text{cropping sequence length}} \right) \quad (1)$$

Tillage intensity was evaluated using a specifically developed index of tillage intensification (ITI). This index evaluates the total number of tillage events and weights them based on the C tillage factors provided by Panagos et al. (2015b). A weighting factor of 1 was applied to conventional tillage (conform to the C factor for tilled bare soil in the RUSLE, Renard et al., 1997); 0.25 for no-till

**TABLE 2 |** Land use history expressed as index of agricultural intensification per plot and experimental period (ISI: index of sequence intensification, ITI: index of tillage intensification, IAI: index of agricultural intensification).

Treatment	TIL_CP	TIL_CP	NT_Mix	NT_Mix	TIL_CROP	TIL_CROP
Plot	1	2	4	6	3	5
			Index of sequence intensification (ISI)			
1984–1997	1.1	1.2	1.1	1.3	1.3	1.4
2008–2011			1.1	1.1	1.1	1.1
2012–2014			2.0	2.0	1.0	1.0
2015–2019	1.8	1.8	1.8	1.8	1.8	1.8
			Index of tillage intensification (ITI)			
1984–1997	0.8	0.9	0.2	0.3	1.3	1.4
2008–2011			0.3	0.3	0.3	0.3
2012–2014			0.3	0.3	0.3	0.3
2015–2019	0.4	0.4	0.4	0.4	0.4	0.4
			Index of agricultural intensification (IAI)			
1984–1997	0.8	1.1	0.2	0.4	1.7	1.9
2008–2011			0.3	0.3	0.3	0.3
2012–2014			0.5	0.5	0.3	0.3
2015–2019	0.6	0.6	0.6	0.6	0.6	0.6

**TABLE 3 |** Treatment groups according to their multiplier IAI criteria based on the summed experimental period averages of the index of sequence intensification (ISI) and the index of tillage intensification (ITI).

Plots	Abbreviation	Description	ISI	ITI	IAI
1,2	TIL_CP	Tillage and crop pasture rotation	3.0	1.2	3.5
4,6	NT_Mix	No-Till under several rotations	6.2	1.2	7.1
3,5	TIL_CROP	Tillage and continuous cropping	5.3	2.2	11.8

and 0.01 for broadcast sowing of cover crops by hand causing minimal soil disturbance.

$$ITI = \sum \left( \frac{\text{weighting factor} \times \text{total number of tillage events}}{\text{total sequence length (years)}} \right) \quad (2)$$

The IAI was calculated for each of the four experimental periods and accounted for fallow time when certain plots were discontinued (**Table 2**). The discontinuation period of all plots between 1998 and 2008 was not included in the IAI determination. The second and fourth experimental phases have identical IAI for all plots as they were managed uniformly over the respective periods. **Table 2** demonstrates that the ISI had a higher weight than the ITI due to intensive cropping with up to two crops per year. To strengthen index interactions and its hazard effects on soil quality, ISI and ITI were multiplied (IAI, **Table 2**) as undertaken in the Soil Quality Rating (SQR) procedures presented by Mueller et al. (2007). Otherwise using sums, NT\_Mix and TIL\_CROP would have led to a similar IAI, although their soil use history was disparate. Especially during the first experimental period between 1984 and 1997, IAI differed between plots with lowest IAI in plot 4 and 6 and highest in plot 3 and 5.

Due to the limited number of long-term Wischmeier plots, two plots with similar land use history and IAI were grouped into

three treatment groups (**Table 3**). The no-till treatment group NT\_Mix had differences in historical cropping intensity with crop-pasture rotation in plot 4 and continuous cropping in plot 6.

## Continuous Measurements

Daily and 10 min record precipitation data were provided by the Research Unit of Climate and Geographic Systems, GRAS, INIA, Uruguay to calculate rainfall intensity parameters during 2017–2019 (available at <http://www.inia.uy/gras>). Meteorological data were obtained from an automated weather station (Campbell Scientific, Inc, Logan, UT, United States) equipped with pluviograph and pluviometer located approximately 700 m from the experimental site. According to Sasal et al. (2010), daily rainfall events were classified into three groups: small (< 40 mm), intermediate (41–69 mm) and large (>70 mm). After each rainfall event, the amount of precipitation and the volume of runoff water per plot were recorded. The water height in the tank was recorded and the volume of runoff water was calculated using previously calibrated conversion factors for each tank and plot. The calibration was carried out yearly, filling the tanks with a rising, precise amount of water and simultaneously recording the water table height in each of the six tanks. The runoff coefficient was determined for each rainfall event as the ratio of runoff per rainfall.

Historical data on water runoff, sediment losses, and SOC were continuously measured since the installation in 1984 and available for the present study. Between 2017 and 2019, water samples were taken after each runoff event to evaluate the amount of fixed (mineral material), volatile (organic material) and total suspended solids with the gravimetric method Nr. 2540 of the American Public Health Association (APHA et al., 2012). For this, the runoff water was homogenized in the tank and a maximum 1,000 ml water sample was taken; for small rainfall events, a smaller sample proportion was available. In the laboratory, 100 ml sample were added to previously

washed and dried glass microfiber filters <0,2 µm (934-AH Whatman™; Little Chalfont, United Kingdom) using a Büchner funnel and a vacuum pump with an adjusted pressure between 10 and 20 mbar. Total solids were determined by drying the filter at 105°C for 4 h and weighed afterwards with an analytical precision balance. In a subsequent step, the same filter was incinerated at 550°C for 2 h, and after cooling to room temperature, weighed a second time to determine fixed suspended solids. Volatile suspended solids were calculated as the difference between total and fixed solids. Method quality of each batch was controlled by using a total of three control samples of a 25 and 100 mg/L kaolin solution and distilled water blanks.

For the soil loss (ERO) calculations on a hectare basis per runoff event, the following equation was used.

$$ERO = TSS \left( \frac{mg}{L} \right) \times RUN (L) / 1000000 / (A (m^2) \times 10000) \quad (3)$$

where TSS is the amount of total suspended solids in mg per liter, RUN is the total amount of water in the tank in liter and A is the Wischmeier plot area in m<sup>2</sup>.

In four occasions of high runoff water collection during spring 2019 (9<sup>th</sup> of September, 2<sup>nd</sup> of October, 11<sup>th</sup> of October, 13<sup>th</sup> of October), sediments were collected through 10 L runoff samples and water evaporated gently over 48 h at 50°C. Sediment samples were subsequently analyzed for total carbon (C) and N<sub>tot</sub> by LECO. Data were used to calculate the sediment nutrient enrichment for C and N as the ratio of nutrient concentration in eroded sediment to that of soil samples taken in October 2019 in 0–7.5 cm soil depth (Palis et al., 1990).

Crop yield was determined manually for two subsamples per plot, cutting two crop rows per 4 linear meters.

## Soil Measurements

### Field Sampling

Historical sampling campaigns for SOC were carried out with a soil auger taking one composite sample per plot in 0–20 cm soil depth in the years 1984, 1986, 1987, 1989–1996, and in 0–15 cm soil depth in the years 2011, 2014–2016.

On 27<sup>th</sup> of December 2018, all plots were sampled for one composite soil sample at three depths (0–7.5, 7.5–15, 15–30 cm) and on 25<sup>th</sup> of October 2019, all plots were sampled for two composite samples at five depths (0–7.5, 7.5–15, 15–30, 30–45, 45–60 cm).

### Soil Chemical Analysis

SOC and total N (N<sub>tot</sub>) were analyzed by dry combustion at 900°C followed by infrared detection (LECO Truespec; Wright and Bailey (2001)). Before 2011, SOC samples were analyzed with the Tinsley method (heated dichromate/titration), therefore SOC values obtained since 2011 were converted using a previous determined factor of 0.81 (Grahmann et al., Forthcoming 2022; in press).

Soil pH was determined potentiometrically (1:2.5 soil/distilled water suspension; Beretta-Blanco et al., 2014). Phosphorus was measured colorimetrically by the Bray-1 method using a

1:10 (w/v) soil/solution ratio and an extraction time of 5 min (Bray and Kurtz, 1945). Cation exchange capacity was analyzed by extracting the exchangeable cations Ca, Na, Mg and K with 1 M ammonium acetate (NH<sub>4</sub>OAc) at pH 7, and reading the extract by atomic emission (K and Na) according to Jackson (1964) and atomic absorption (Ca and Mg) or by atomic emission with ICP-OES equipment.

### Soil Physical Properties

Undisturbed soil samples were taken for the determination of bulk density in December 2018 and December 2019 for two depth increments (0–7.5, 7.5–15 cm). Three sites located at the upper, middle and lower part of each plot were selected. Samples were taken using a soil probe with a cylinder volume of 98.2 cm<sup>3</sup> and samples dried for 48 h at 105°C. Penetration resistance was measured from 0 to 80 cm soil depth with a hand held Penetrologger (Eijelkamp, Giesbeek, Netherlands, cone base area 1 cm<sup>2</sup>) at 4 days (13<sup>th</sup> of September, 19<sup>th</sup> of September, 30<sup>th</sup> of October and 23<sup>rd</sup> of December) in 2019. Resistance measurements were executed according to the manufacturer's instructions by applying the electronic penetrometer together with a datalogger, allowing for immediate storage and processing of the data in the datalogger. In parallel, soil moisture was measured volumetrically in 6 cm soil depth.

Three soil blocks were sampled in April 2019 in the upper, middle and lower part of each plot (15 cm × 15 cm × 20 cm). From those samples, a visual evaluation of soil structure (VESS) was conducted in the field as described by Guimarães et al. (2011). The samples were then air dried for the determination of four indicators of aggregate stability in the laboratory. The stability of aggregates to quantify the main processes of aggregate breakdown associated with water stress were assessed as proposed by Le Bissonnais (1996). This methodology evaluates three mechanisms of aggregate breakdown: 1) Aggregate slaking due to fast wetting (Treatment 1); 2) Differential swelling (Treatment 2) and 3) Mechanic breakdown (Treatment 3). Three 5 g samples of 3–5 mm aggregates were taken for the determination of aggregate stability for each of the treatments. For treatment 1, the aggregates were immersed in 250 ml of distilled water for 10 min. For treatment 2, the aggregates were capillary rewetted on a tension table at 3 cm tension for 30 min before their immersion in water. For treatment 3, the aggregates were rewetted in ethanol, then immersed in water (to avoid fast wetting) and mechanically agitated 10 times using a Feodoroff agitator. Each one of these treatment samples was gently transferred to a 50 µm sieve, previously immersed in ethanol. Fragments greater than 50 µm were oven-dried at 40°C and dry-sieved through seven different sieve sizes (3,000, 2,000, 1,000, 500, 250, 100, and 50 µm). The aggregate stability for each treatment was expressed as the normalized mean weight diameter for each individual treatment, and the mean aggregate diameter of all treatments (MWD<sub>LeBissonnais</sub>) is evaluated.

The fourth evaluated indicator corresponds to the USDA wet aggregate stability (Aggregates<sub>USDA</sub>; method 1B1b2a1 in USDA-NRCS, 2004), that follows a disruption of an initially 3 g air dried sample of 1–2 mm soil aggregates by submerging and wet sieving in distilled water through a 0.5 mm sieve. A following dispersion

in sodium hexametaphosphate solution (Calgon) is performed for determining >0.5 mm sand mass. Sand mass is subtracted from both the initial mass (i.e., 3 g) and the mass retained after sieving in water. Aggregate stability is computed as the ratio between the latter and former dry sand-free soil masses.

### Soil Hydrological Measurements

Infiltration rates were determined by double-ring infiltrometers (Eijkelkamp, Giesbeek, Netherlands) in May 2019 in five selected sites per plot according to the Eijkelkamp user manual (Eijkelkamp, 2018). Two rings were installed in non-disturbed rows and three rings in the planting rows. Philip's infiltration equation was applied for steady state infiltration rates (Philip, 1957). Surface saturated hydraulic conductivity ( $K_s$ ) was estimated through the measurement of steady-state infiltration, solving Wooding equation (Wooding, 1968), using the White and Sully method (White and Sully, 1987; Logsdon and Jaynes, 1993; Angulo-Jaramillo et al., 2000).

### Soil Biological Properties

Particulate organic matter (POM) fractions of 212  $\mu\text{m}$ , 53  $\mu\text{m}$  and <53  $\mu\text{m}$  (mineral-associated organic matter, MAOM) were separated by an adapted method of Cambardella and Elliott (1992) using 6.66 g of dry, 2 mm sieved soil and 20 ml of calgon (5% sodium hexametaphosphate). After drying, each fraction was analyzed for SOC.

Potentially mineralizable nitrogen (PMN) was measured in three occasions in 2019 by anaerobic incubation of fresh soil samples over 7 days and subsequent determination of the produced ammonium ( $\text{NH}_4$ ) by colorimetry (Waring and Bremner, 1964; Bundy and Meisinger, 1994). Analyzed samples were from identical origin as samples used to determine aggregate stability (see above). Details for POM and PMN analysis are reported in (Fabrizzi et al., 2003).

### Soil Erosion Modeling and Statistical Analysis

The Revised Universal Soil Loss Equation (RUSLE) is the mostly used, widespread model to predict average annual soil losses resulting from rainfall erosion of cropland (Renard et al., 1997; Tang et al., 2015). The estimation of soil erosion with this model is defined by six factors: R is a runoff-rainfall erosivity factor; K is a soil erodibility factor; LS is a topographic factor combining slope length (L) and slope steepness (S); C is a cover-management factor and P is a supporting practices factor. RUSLE was used to model the corresponding annual long-term erosion losses for the three treatment groups. The RUSLE factors R (rainfall erosivity), L (slope length factor) and S (slope steepness factor) did not change within the experimental site. The same applied for the P factor (support practice factor) as all plots were managed identically. The 30-years R factor for this region was 4248 MJ mm/ha/h/yr (Pérez-Bidegain et al., 2017) and the K factor was 0.023 t ha h/MJ/ha/mm (Puentes, 1981). The three treatment groups differed in the C factor (cover-management factor), which ranged between 0.06 and 0.3 (Clerici and García Préchac, 2001; Hill et al., 2008).

A widespread weakness of long-term runoff plots is their unreplicated nature (Packer et al., 1992; Williams et al., 2009; Ramos-Scharrón and Figueroa-Sánchez, 2017) which can result in an unbalanced experimental design during their long-term history which is why in this study, plots were grouped as pairs per treatment. However, repeated measures over time for continuous variables and pseudo-replicated point measurements within each plot did not allow an analysis of variance. Therefore, with acknowledgement of pseudoreplication (Davies and Gray, 2015), data were analyzed using descriptive statistics, paired "t" tests (Microsoft Office Excel 2010), a general linear model (SAS Version 9.4; PROC GLM) (SAS Institute, Cary, United States, NC) and correlation analysis to evaluate this comprehensive data set.

## RESULTS

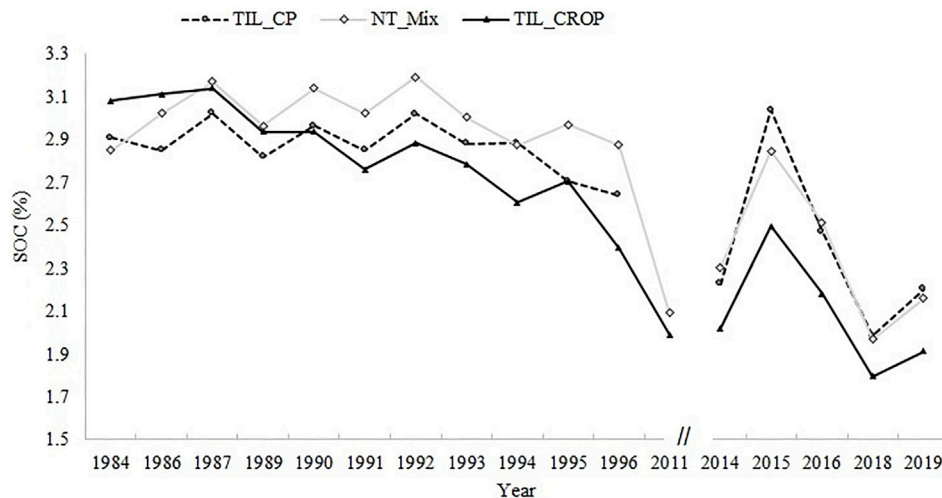
### Evolution of Soil Organic Carbon

SOC decreased continuously in the first experimental period until 1996 and tended to slightly increase in the study years. In June 2015, SOC reached a high level in all treatment groups after soybean harvest. In April 2015, Black oats were sown broadcast and high root biomass was present during sampling. A sharp decrease in all treatments was recorded in December 2018 when maize and wheat were cropped within the same calendar year. TIL\_CROP had lowest SOC content in most of the measured years and showed a sharp SOC depletion during the first experimental period. TIL\_CP was 6 years longer under fallow and had the lowest IAI, showing higher SOC in most sampling events after conservation agriculture was applied in all plots (Figure 2).

Soybean yields ranged from 1,322 kg/ha in 2014–5,472 kg/ha in 2017. NT\_Mix and TIL\_CROP were most intensively cropped, having three times more grain extracted compared with TIL\_CP over the last 10 years (Supplementary Table S1). In the last experimental period between 2015 and 2019, lowest crop yields were obtained in plot 3 (TIL\_CROP), and for soybean also in plot 1 (TIL\_CP) and highest yields were observed in plot 2 (TIL\_CP) and plot 6 (NT\_Mix).

### Soil Chemical and Biological Properties

SOC was the lowest in both years and most depths in TIL\_CROP and increased for all treatments in the second year (Supplementary Table S2). The opposite happened for  $N_{\text{tot}}$  which was lower in 2019, having lowest content for both years in TIL\_CROP in the first 30 cm soil depth. Soil pH was slightly acidic in the top soil for all treatments and increased with decreasing soil depth, in many occasions pH was lowest in NT\_Mix. Particulate organic matter (POM) averaged 0.08 g/100 g soil for coarse POM (>212  $\mu\text{m}$ ) and 0.09 g/100 g soil for fine POM (53–212  $\mu\text{m}$ ), while mineral-associated organic matter (MAOM, <53  $\mu\text{m}$ ) averaged 2.49 g/100 g soil. Significantly highest POM was measured in the TIL\_CP with lowest IAI and 6 years longer fallow period. Potentially mineralizable nitrogen (PMN) averaged 47, 37 and 42 mg/kg in 0–7.5 cm and 3, 10 and 16 mg/kg in



**FIGURE 2 |** Topsoil carbon content (SOC in %) for each treatment group (fallow period between 1997 and 2010 was excluded) since the onset of the experiment in 1984 until 2019.

7.5–15 cm soil depth for the sampling dates 25<sup>th</sup> October, 11<sup>th</sup> November and 29<sup>th</sup> November 2019, respectively. Lowest PMN was measured on two occasions in TIL\_CROP (data not shown).

### Soil Physical and Hydrological Properties

The average infiltration rate for all treatments was 27.5 mm/h. Infiltration rate was highest with NT\_Mix and lowest in TIL\_CROP, the same was true for saturated hydraulic conductivity ( $K_s$ ) which averaged 22.4 mm/h. Both parameters were significantly lowest in plot 3 and highest in plot 6 ( $p = 0.0011$  and  $0.0018$ , respectively; **Table 4**). Bulk density averaged  $1.35 \text{ g/cm}^3$  in both depths (0–7.5, 7.5–15 cm) in 2018 and  $1.22 \text{ g/cm}^3$  in 7.5 and  $1.26 \text{ g/cm}^3$  in 15 cm soil depth in 2019 and was lowest in both years in plots with lowest IAI in TIL\_CP and increased with higher IAI due to historical tillage intervention and longer continuous cropping. Penetration resistance in 0–15 cm soil depth was 1,482, 1,382 and 1,646 kPa for TIL\_CP, NT\_Mix and TIL\_CROP, respectively averaged over four measurement days. It was significantly highest in three out of four measurement days in TIL\_CROP ( $p = 0.0059$ ).

Treatments had no statistically significant effect on  $\text{Aggregates}_{\text{USDA}}$  and the VESS index. Nevertheless, TIL\_CP had higher  $\text{Aggregates}_{\text{USDA}}$  and an “intact” soil structure score (VESS index 2 with high aggregate porosity) whereas NT\_Mix and TIL\_CROP obtained VESS scores of three and more (firm structure with low aggregate porosity). For measured aggregate stability according to USDA and Le Bissoinai, mean weight diameter of soil aggregates was lowest in TIL\_CROP, having the highest IAI (**Table 4**).

Most pronounced differences in soil quality parameters caused by different soil use and management history were found for infiltration rate (Infil\_mm/h), saturated hydraulic conductivity ( $K_s$ \_mm/h) and PMN in 7.5 cm soil depth (**Figure 3**). Although

not statistically substantiated, relative differences in VESS and SOC in 7.5 cm soil depth between treatments groups were recognized.

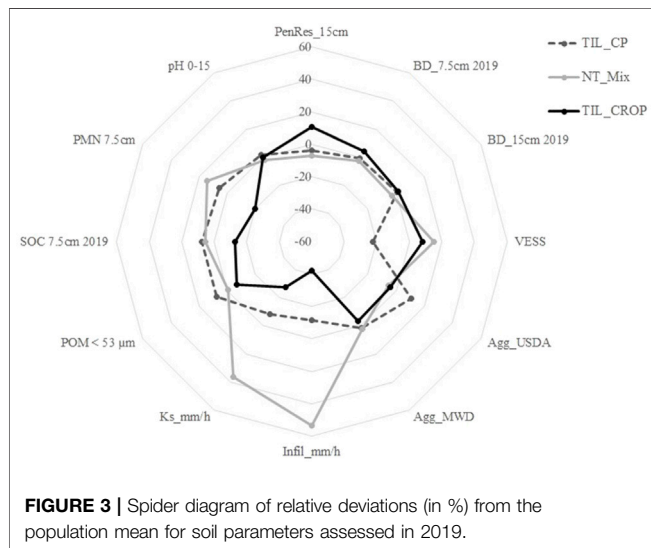
### Soil Erosion, Runoff and Nutrient Losses

Yearly average runoff was 2.7 times greater in 2018 than 2017 while the runoff coefficient was 2.5 times greater in 2018 (**Table 5**).

Yearly average soil losses amounted 233, 805 and 139 kg/ha for the three respective study years with highest erosion rates in 2018 in all treatment groups. Yearly differences can mostly be explained by climatic variability. The higher erosion was due to more intense rainfall events and about 100 mm more rainfall in 2018 compared with the other two studied years. Also, the number of high, intensive rainfall events above 40 mm was the highest in 2018 (6), but only 2 and 3 events were recorded in 2017 and 2019, respectively (**Table 5**). Overall, rainfall occurred in about a third of each calendar year. A power regression and moderate correlation was found between rainfall and surface runoff for 98 events during 2017 and 2019 ( $R^2 = 0.53$ ;  $y = 0.0013x^{2.1045}$ ). Few rainfall events above the 1:1 line caused higher runoff than the actual amount of rainfall of the corresponding event and was influenced by the actual state of soil moisture saturation and hence, previous rainfall events (data not shown). We found overall higher erosion rates in the NT\_Mix and lowest in the TIL\_CP to sustain our hypothesis that a smaller IAI score is condensed in soil erosion rates due to historical intensive cropping and tillage (**Figure 4**). As soil and crop management was similar in the last five study years, measured differences in runoff and erosion between plots were elicited by soil management legacy or due to natural spatial variability between plots. The coefficient of variation (CV) among Wischmeier plots was high and between 52% (8<sup>th</sup> October) and 120% (3<sup>rd</sup> September) in 2017 for soil erosion events

**TABLE 4 |** Treatment averages for physical and chemical soil properties measured in 2019 (GLM-SAS: capital letters indicate evidence of significant different treatment groups ( $p < 0.05$ ); MWD-mean weight diameter, SOC-soil organic carbon, PMN-potentially mineralizable nitrogen, POM-C-particulate organic matter carbon).

Parameter	Unit	TIL_CP	NT_Mix	TIL_CROP	p-value
Infiltration rate	mm/h	24.2 B	42.2 A	15.9 B	0.0011
Bulk density (0–7.5 cm)	g/cm <sup>3</sup>	1.2 A	1.2 A	1.3 B	0.0326
Penetration Res (15 cm, 4 dates)	kPa	1,428 A	1,382 A	1,646 B	0.0059
VESS	Index	2.1	3.2	3.0	0.1541
Aggregates <sub>USDA</sub>	%	53.8	46.1	46.8	0.1712
MWD <sub>LeBissoin</sub>	mm	2.4 A	2.4 A	2.3 B	0.0001
SOC (0–7.5 cm)	%	3.7	3.6	3.0	0.0647
PMN (0–7.5 cm, 3 dates)	mg/kg	44.4	48.0	33.6	0.1558
POM-C (MOAM, < 53 µm)	g/kg	26.8 A	24.8 AB	23.2 B	0.0404

**FIGURE 3 |** Spider diagram of relative deviations (in %) from the population mean for soil parameters assessed in 2019.

of more than 5 kg/ha. In 2018, CV increased between 23% (16<sup>th</sup> December) to 145% (29<sup>th</sup> May) and in 2019, CV between plots was between 45% (26<sup>th</sup> July) and 74% (30<sup>th</sup> January) for soil erosion events with more than 5 kg/ha average soil loss.

The estimated long-term soil erosion rate with RUSLE was 1,000 kg/ha, 1,600 kg/ha, and 2,100 kg/ha for NT\_Mix, TIL\_CP, and TIL\_CROP, respectively.

In 2019, volatile solids corresponded to one third of total soil losses, representing mainly the removal of straw residues and decomposing material on the soil surface (Table 6). The share of fixed material increased with increasing total soil loss. Moderate to high correlations were found between the amount of lost volatile solids and maximum rainfall intensity ( $R^2 = 0.64$  for NT-Mix;  $R^2 = 0.70$  for TIL\_CP;  $R^2 = 0.45$  for TIL\_CROP) and

between the fixed and volatile solid ratio and the respective runoff for each treatment group ( $R^2 = 0.70$  for NT\_Mix;  $R^2 = 0.60$  for TIL\_CP;  $R^2 = 0.45$  for TIL\_CROP).

Peaks of intense runoff events mostly coincided with high rainfall, however not all recorded rainfall events over 70 mm resulted in erosion (eg., May 2019, Figure 5). The plots were permanently covered and cropped during the monitoring period. Not for all reordered erosion events, rainfall intensity was the relevant factor. There was only one exceptional erosion event during the study period in NT\_Mix in July 2018, leading to more than 350 kg/ha soil loss within 1 month. On 30<sup>th</sup> of June, wheat was planted and hence soil was disturbed by the planter disks. Due to heavy rainfall the days before and after planting, wheat emergence was reduced and crop establishment was poor and soil was not covered properly. Although it was an exceptional erosion event in NT\_Mix, the overall magnitude of erosion was much lower than the tolerable threshold.

The enrichment ratio showed that SOC was 6.8 times higher in the sediment eroded in TIL\_CROP than contained in the topsoil, this carbon enrichment ratio was even higher in NT\_Mix and lowest with the lowest IAI in TIL\_CP (Table 7). The nutrient loss through runoff was slowed down with lowest IAI which in turn is related to the higher SOC in the topsoil observed in the latest study years (Figure 2). Highest sediment enrichment for C and N in NT\_Mix did not lead to lowest SOC content in the top soil and is explained by the overall management effect of straw retention and no-tillage over several decades in this treatment group.

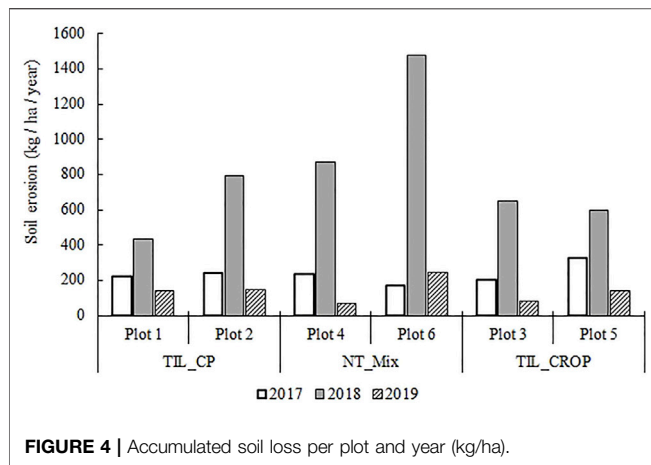
## DISCUSSION

### Historical Land Use and Current Soil Quality

During the first experimental period (1984–1997), which represented 55% of the total running time since the

**TABLE 5 |** Rainfall classification and average annual runoff information for the study period.

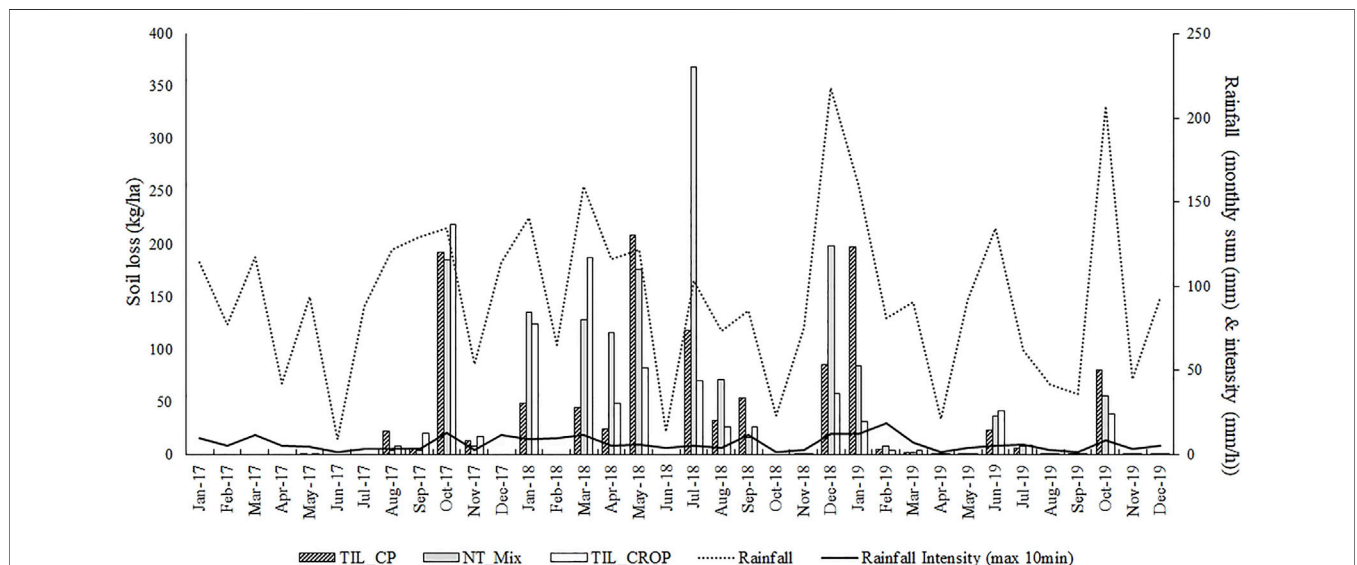
	Number of rainfall events				Total rainfall (mm/year)	Number of runoff events				Total runoff (mm/year)	Annual runoff coefficient
	< 40 mm	41–69 mm	> 70 mm	Total		< 40 mm	41–69 mm	> 70 mm	Total		
2017	127	1	1	129	1,095	29	2	0	31	209	0.19
2018	116	4	2	122	1,197	23	7	2	32	579	0.48
2019	130	3	0	133	1,064	32	2	1	35	320	0.30



**FIGURE 4 |** Accumulated soil loss per plot and year (kg/ha).

installation of the evaluated experiment, a generalized depletion of SOC was observed in all evaluated plots (**Figure 2**). This depletion was greater in TIL\_CROP systems where SOC in 1996 represented 81% of the initial SOC content whereas in TIL\_CP and NT\_Mix, the average losses were 10 and 3%. When compared to no-till systems, intensive tillage can promote C mineralization by breaking soil aggregates and therefore increasing the access of soil microorganisms to previously protected C pools (Six et al., 1999, 2000). Additionally, tillage can promote soil erosion losses (Verhulst et al., 2010). Despite that, after 1997 all plots received the same tillage management until 2019, but SOC levels in TIL\_CROP treatments remained below the C levels observed for the other two treatments during the evaluated period. The observed differences in near-surface SOC levels generated in early stages of the experiment can be related to the positive effects of historical no-tillage in NT\_Mix on soil physical indicators, like penetration resistance, aggregate stability, bulk density, and

available water capacity (Blanco-Canqui and Ruis, 2018), that were not eliminated with later changes in tillage (**Table 4; Figure 3**). Similar reverse effects on the decline in soil fertility and soil aggregation were found in a 20 year old grass pasture site with a prior history of cropping activity (Jones et al., 2016). There, the loss of SOC under pasture increased with greater years under cropping and soil aggregation and mineralizable N did not improve with perennial pastures. The same was true for TIL\_CROP with highest cropping activity where most of the measured soil quality parameters did not recover at the same level as for TIL\_CP or NT\_Mix. The TIL\_CP treatment which incorporated pastures in the rotation and had a longer discontinuation period, counted with only three soybean harvests and extracted 10 Mg of grain/ha. However, in the NT-Mix and TIL\_CROP treatments 33 Mg of grain/ha were harvested over ten harvest years (**Supplementary Table S1**). As expected, the combination of lower C and nutrient extraction with the lower tillage intensities in TIL\_CP maintain an overall higher soil quality when compared to more extractive and tillage intensive systems (Amsili et al., 2021). The observed soil degradation in TIL\_CROP is consistent with that reported for continuous annual cropping systems in the Pampas region where a continuous nutrient extraction combined with relatively low mineral fertilizer inputs (**Table 1**) might explain the historical decline of SOC (**Figure 2**). The observed depletions in SOC can significantly deplete obtainable yields (Ernst et al., 2020; Rubio et al., 2021a). When short-term management strategies such as increasing crop fertilization and mechanical soil decompaction have been proven insufficient to remediate yield depletion (Ernst et al., 2020; Rubio et al., 2021b), our results indicate that 5 years of conservation agriculture do not compensate for the degradation of soils generated by previous land use history. Significant differences in several soil properties confirm our hypothesis that the soil



**FIGURE 5 |** Monthly pattern of soil erosion for the respective treatment groups in relation to climatic variables of monthly rainfall and highest monthly 10-min rainfall intensity.

**TABLE 6** | Fixed and volatile solids in kg/ha/day for selected soil erosion events in 2019, sorted from shortest to longest rainfall duration per rainfall event.

	kg/ha						mm					
	Fixed solids			Volatile solids			Ratio			Runoff		
	TIL_CP	NT_Mix	TIL_CROP	TIL_CP	NT_Mix	TIL_CROP	TIL_CP	NT_Mix	TIL_CROP	TIL_CP	NT_Mix	TIL_CROP
12-Feb-19	1.9	1.9	1.6	0.5	0.7	0.5	3.6	2.6	3.5	3.3	1.7	3.0
13-Oct-19	35.2	22.9	15.1	4.1	4.2	2.4	8.6	5.5	6.3	95.5	94.6	79.3
30-Jan-19	59.6	67.0	20.3	18.2	13.8	8.6	3.3	4.9	2.4	70.3	82.9	43.7
18-Jun-19	8.2	13.9	26.4	1.9	3.8	4.6	4.4	3.7	5.7	35.1	34.3	47.5
12-Mar-19	0.8	1.0	3.1	0.4	0.4	0.8	2.1	2.3	3.9	4.0	2.4	7.2
23-Feb-19	1.2	1.6	1.0	0.4	1.0	1.0	2.7	1.7	1.0	3.8	4.1	5.7
16-Jan-19	1.8	2.8	1.8	1.0	1.1	1.2	1.7	2.6	1.5	7.2	7.7	8.3
26-Jul-19	3.6	4.0	5.5	1.3	1.0	2.8	2.9	3.8	2.0	31.7	33.7	31.7
17-Jun-19	10.3	8.5	9.1	3.1	3.9	1.1	3.3	2.2	8.2	49.5	52.9	51.3

**TABLE 7** | Sediment enrichment ratio for carbon (SOC) and nitrogen ( $N_{tot}$ ) in surface runoff samples ( $n = 4$ , SD = standard deviation).

	TIL_CP	SD	NT_Mix	SD	TIL_CROP	SD
SOC	5.2	1.7	7.4	1.3	6.8	0.7
$N_{tot}$	4.4	1.3	7.1	1.7	6.3	1.6

management legacy still lingers on the current state of soil (Table 4). Further studies are needed to determine the amount of time needed to recover soil health and yield in degraded areas. The intensification of agricultural production, in the form of historical cropping sequence and tillage activity, was represented by the study's treatment groups. However, it should be avoided to generalize that higher cropping intensity automatically leads to worse soil conditions and hence to higher erosion rates. This depends on the management practice at the cropping system level and on multiple options and combinations cropping intensification is realized (Mouratiadou et al., 2021). Permanent cover, growing roots and continuous N and C input may also lead to beneficial effects on soil quality which highly depends on the management (crop rotation, tillage, cover crops, etc) (Xiong et al., 2019; Cassman and Grassini, 2020). However, sustainable intensification as a condition to avoid soil deterioration was not given in the current study with simplified and soybean focused crop rotation in the second and third experimental period.

## Historical Land use and Current Soil Erosion

The distinction between volatile and fixed suspended solids in water samples is done to determine total mineral soil loss and additional removal of organic material, most present as SOC, by water erosion. According to Lal (2019), there is a big lack of research in this area showing that particulate organic carbon or POM are related to losses of volatile solids. In 2019, higher POM was found in treatments with higher volatile solid losses. The annual losses of volatile solids in 2019 increased with decreasing IAI averaging 84 kg/ha in TIL\_CP, 58 kg/ha in NT-Mix and only 40 kg/ha in TIL\_CROP showing the opposite pattern of POM ( $TIL\_CROP < NT\_Mix < TIL\_CP$ ). Highest losses of volatile solids in TIL\_CP were also measured in 2017 (148 kg/ha in TIL\_CP, 106 kg/ha in TIL\_CROP and 74 kg/ha in NT-Mix), however no POM was assessed for the other 2 years.

Several studies reported that the soil removed by erosion is 1.3–5 times richer in organic matter than the remaining soil (Bagarello and Ferro, 2017) which was even higher in NT-Mix and TIL\_CROP (Table 7). In line with our results, Bertol et al. (2007) analyzed organic carbon in runoff sediments under soybean cropping and found higher losses in no-till compared with conventional tillage, but overall C enrichment ratio was much smaller (between 1.00 and 1.17) than in the current study. Sediment ratios did not follow a certain treatment tendency for the selected rainfall events (Table 6). But higher SOC combined with improved soil structure indices in TIL\_CP may lead to the assumption that SOC was tighter bound to MAOM and hence less prone to get lost as fixed solids (attached to sediments, Holz and Augustin, 2021).

As discussed in the previous section, historical land use had a legacy effect on soil quality parameters, several of which

reportedly may control soil erodibility (Victoria et al., 2001; Taleshian Jeloudar et al., 2018; Alaboz et al., 2021). However, the soil loss data of the present study do not support a corresponding effect of historical land use on soil erosion. An explanation to the relatively low erosion rates measured across the 3 years of study (Figure 4) is found in the no-tillage practices that were implemented in 2009, 12 years after the end of the initial experimental period (Figure 1). Cover crops were later consistently incorporated in all plots and possibly further improving soil conservation. Soil quality parameters might be responding to this management, although noticeable effects are largely limited to the surface soil layers (Liebig et al., 2004) and only gradually reach deeper soil. Another finding that supports this explanation is small differing ratio of fixed:volatile sediments across historic use treatments for several sampling days in 2019 (Table 6). Consequently, in spite of the latest conservation practices, soil quality parameters are still exhibiting the legacy effects, while erosion losses can be mitigated substantially through enhanced soil cover. As proposed recently by (Willett et al., 2019), no-tillage with residue cover is a functioning soil conservation practice to prevent nutrient losses as shown in the current study by reduced soil erosion and subsequent minimal C and N loss during the experimental period.

Infiltration rate, saturated hydraulic conductivity and PMN were the soil quality parameters more affected by the soil use history (Figure 3). Infiltration rate and saturated hydraulic conductivity are key soil hydrologic properties that affect soil water dynamics, hence soil water erosion (Toy et al., 2002). RUSLE allows for estimating long-term soil erosion average rates, hence its results cannot be compared with yearly measurements of sediment losses over the three study years. Nevertheless, RUSLE can be used as an indicator of sustainability. Erosion estimations were based on the nationally calibrated RUSLE/USLE model and assumed a scenario of continuing soil use and management in each of the treatment groups. This resulted in relatively high soil loss rates (i.e. between 1,000 and 2,100 kg/ha/yr), but still well below the tolerable soil loss threshold of 7,000 kg/ha/yr. The lowest modelled erosion was obtained for NT\_Mix, as a consequence of using a lower C-factor to account for improved soil cover from remaining crop or pasture residues. Although it was not the purpose of this paper to validate the RUSLE model, the modelled erosion rate of 1,000 kg/ha/yr in NT\_Mix performed averagely in the range between 71 and 1,478 kg/ha/yr for the measured yearly rates (Figure 4), but the model obtained much higher rates for the remaining treatments TIL\_CP and TIL\_CROP. However, Knapen et al. (2008) and Blanco-Canqui et al. (2009) showed that conservation tillage practices may also contribute to reduced erosion through a smaller erodibility factor K. Therefore, if the erodibility factor is modified in response to soil use (or soil quality parameters), modelled and observed erosion rates could perform better. We therefore propose that these measured soil legacy effects in soil properties should be reflected in changes of the RUSLE soil K factor, which cannot be static but dynamic due to ongoing, permanent processes that affect soil quality (Alewell et al., 2019). The runoff plots have existed since 1984, which implied considerably changes in treatments and different land use

management over time. Overall, TIL\_CROP showed a noticeable degradation pattern compared with the other two treatment groups which should be translated into a higher erodibility. Although Sasal et al. (2010) reported a linear regression between ISI and cumulative runoff, this was not confirmed with the applied IAI in the current study. Runoff was lowest in all 3 years in TIL\_CP, but highest in NT\_Mix whereas the treatment with the highest IAI, TIL\_CROP, had medium runoff rates for all 3 years. Hence, increasing historical soil use and management intensity does not automatically lead to higher runoff rates, but rather depends on a complex combination of cropping and tillage management factors and subsequent soil process effects.

## CONCLUSION

Over the study period, conservation agriculture controlled soil erosion and soil loss was minimal and far below the national threshold of 7,000 kg/ha. Historical soil use and management caused significant long-term effects on soil properties leading to adverse effects in soil quality in historically intensively tilled and cropped soils. We found significant differences, especially for soil physical parameters between the soil legacy treatments which were mainly due to the historical management conducted during the first experimental period from 1984 to 1997. Five years of conservation agriculture with year-around soil cover did not remediate soil degradation caused by continuous cropping and ploughing. The agricultural intensification index was sensible to detect cumulative treatment differences due to previous soil and land use. The legacy of soil use and management affected the resilience of current sustainable cropping systems. This study found evidence that soil erodibility is affected by cropping management changes over time, and requires an adjustment of the K factor when crop and tillage activity had historical modifications. However, it seems that surface cover during the study period offsets the importance of soil quality status regarding the proneness to soil loss. Conservation agriculture compensated for reduced soil quality in the short-term and protected TIL\_CROP in order to avoid soil erosion.

## DATA AVAILABILITY STATEMENT

The raw data supporting the conclusion of this article will be made available by the authors on request, without undue reservation.

## AUTHOR CONTRIBUTIONS

KG and VR conducted the samplings and measurements, KG was responsible for evaluation and analysis of the data. KG did the writing of the original draft and the visualization, MP-B assisted with the RUSLE modelling and added to the discussion. JQ added to the discussion. KG and VR had the project idea, supervised and added to the discussion.

## FUNDING

This study has been financially supported by the National Institute of Agricultural Research (INIA), Uruguay (Grant number N-23622).

## ACKNOWLEDGMENTS

We thank Jorge Sawchik for the re-installation of this experiment. We thank Wilfredo Mesa, Emiliano Barolín, Héctor Vergara,

Gualberto Soulier, Leonardo Silva, Nicolás Leiva and Marcelo Schusselin for trial maintenance; Carolina Lizarralde for previous trial analysis and Henning Schwalm for the analysis of suspended solids in the laboratory.

## SUPPLEMENTARY MATERIAL

The Supplementary Material for this article can be found online at: <https://www.frontiersin.org/articles/10.3389/fenvs.2022.822967/full#supplementary-material>

## REFERENCES

- Alaboz, P., Dengiz, O., Demir, S., and Şenol, H. (2021). Digital Mapping of Soil Erodibility Factors Based on Decision Tree Using Geostatistical Approaches in Terrestrial Ecosystem. *Catena* 207, 105634. doi:10.1016/j.catena.2021.105634
- Alewell, C., Borrelli, P., Meusburger, K., and Panagos, P. (2019). Using the USLE: Chances, Challenges and Limitations of Soil Erosion Modelling. *Int. Soil Water Conservation Res.* 7, 203–225. doi:10.1016/j.iswcr.2019.05.004
- Amsili, J. P., van Es, H. M., and Schindelbeck, R. R. (2021). Cropping System and Soil Texture Shape Soil Health Outcomes and Scoring Functions. *Soil Security* 4, 100012. doi:10.1016/j.soisec.2021.100012
- Angulo-Jaramillo, R., Vandervaere, J.-P., Roullet, S., Thony, J.-L., Gaudet, J.-P., and Vauclin, M. (2000). Field Measurement of Soil Surface Hydraulic Properties by Disc and Ring Infiltrimeters. A Review and Recent Developments. *Soil Tillage Res.* 55, 1–29. doi:10.1016/S0167-1987(00)00098-2
- APHAWWAWPCF (2012). *Standard Methods for the Examination of Water and Wastewater*. Washington: American Public Health Association.
- Azooz, R. H., and Arshad, M. A. (2011). Soil Infiltration and Hydraulic Conductivity under Long-Term No-Tillage and Conventional Tillage Systems. *Can. J. Soil Sci.* 76, 143–152. doi:10.4141/cjss96-021
- Baethgen, W. E., Parton, W. J., Rubio, V., Kelly, R. H., and Lutz, S. S. M. (2021). Ecosystem Dynamics of Crop-Pasture Rotations in a Fifty-Year Field experiment in Southern South America: Century Model and Field Results. *Soil Sci. Soc. Am. J.* 85, 423–437. doi:10.1002/saj2.20204
- Bagarello, V., and Ferro, V. (2017). “Measuring Soil Loss and Subsequent Nutrient and Organic Matter Loss on Farmland,” in *Oxford Research Encyclopedias*. Oxford University Press. doi:10.1093/acrefore/9780199389414.013.189
- Beniston, J. W., Shipitalo, M. J., Lal, R., Dayton, E. A., Hopkins, D. W., Jones, F., et al. (2015). Carbon and Macronutrient Losses during Accelerated Erosion under Different Tillage and Residue Management. *Eur. J. Soil Sci.* 66, 218–225. doi:10.1111/ejss.12205
- Beretta-Blanco, A., Bassahum, D., Musselli, R., Beretta-Blanco, A., Bassahum, D., Musselli, R., et al. (2014). Medir el pH del suelo en la mezcla suelo: agua en reposo o agitando? *Agrociencia Uruguay* 18, 90–94. doi:10.2477/vol18iss2pp90-94
- Beretta-Blanco, A., Pérez, O., and Carrasco-Letelier, L. (2019). Soil Quality Decrease over 13 Years of Agricultural Production. *Nutr. Cycl Agroecosyst* 114, 45–55. doi:10.1007/s10705-019-09990-3
- Bertol, I., Engel, F. L., Mafra, A. L., Bertol, O. J., and Ritter, S. R. (2007). Phosphorus, Potassium and Organic Carbon Concentrations in Runoff Water and Sediments under Different Soil Tillage Systems during Soybean Growth. *Soil Tillage Res.* 94, 142–150. doi:10.1016/j.still.2006.07.008
- Blanco-Canqui, H., Mikha, M. M., Benjamin, J. G., Stone, L. R., Schlegel, A. J., Lyon, D. J., et al. (2009). Regional Study of No-Till Impacts on Near-Surface Aggregate Properties that Influence Soil Erodibility. *Soil Sci. Soc. Am. J.* 73, 1361–1368. doi:10.2136/sssaj2008.0401
- Blanco-Canqui, H., and Ruis, S. J. (2018). No-Tillage and Soil Physical Environment. *Geoderma* 326, 164–200. doi:10.1016/j.geoderma.2018.03.011
- Borrelli, P., Robinson, D. A., Fleischer, L. R., Lugato, E., Ballabio, C., Alewell, C., et al. (2017). An Assessment of the Global Impact of 21st Century Land Use Change on Soil Erosion. *Nat. Commun.* 8, 2013. doi:10.1038/s41467-017-02142-7
- Bray, R. H., and Kurtz, L. T. (1945). Determination of Total, Organic, and Available Forms of Phosphorus in Soils. *Soil Sci.* 59, 39–46. doi:10.1097/00010694-194501000-00006
- Bundy, L. G., and Meisinger, J. J. (1994). “Nitrogen Availability Indices,” in *Methods of Soil Analysis, Part 2. Microbiological and Biochemical Properties* (London: Macmillan Education UK), 951–984. doi:10.2136/sssabookser5.2.c41
- Cambardella, C. A., and Elliott, E. T. (1992). Particulate Soil Organic-Matter Changes across a Grassland Cultivation Sequence. *Soil Sci. Soc. Am. J.* 56, 777–783. doi:10.2136/sssaj1992.03615995005600030017x
- Carrasco-Letelier, L., and Beretta-Blanco, A. (2017). Erosión hídrica del suelo estimada para 99 cuencas uruguayas. *Ciencia e investigación agraria* 44, 184–194. doi:10.7764/rcia.v44i2.1717
- Cassman, K. G., and Grassini, P. (2020). A Global Perspective on Sustainable Intensification Research. *Nat. Sustain.* 3, 262–268. doi:10.1038/s41893-020-0507-8
- Caviglia, O., and Andrade, F. (2010). Sustainable Intensification of Agriculture in the Argentinean Pampas: Capture and Use Efficiency of Environmental Resources. *Am. J. Plant Sci. Biotechnol.* 3, 1–8. doi:10.1016/j.fcr.2003.10.002
- Clerici, C., and García Préchac, F. (2001). Miscelanea Aplicaciones Del Modelo USLE/RUSLE para estimar las pérdidas de erosión en Uruguay y la región del sur de la cuenca del Río de la Plata. *Agrociencia* 1, 92–103.
- Davies, G. M., and Gray, A. (2015). Don't Let Spurious Accusations of Pseudoreplication Limit Our Ability to Learn from Natural Experiments (And Other Messy Kinds of Ecological Monitoring). *Ecol. Evol.* 5, 5295–5304. doi:10.1002/ece3.1782
- De Vries, W., Kros, J., Kroeze, C., and Seitzinger, S. P. (2013). Assessing Planetary and Regional Nitrogen Boundaries Related to Food Security and Adverse Environmental Impacts. *Curr. Opin. Environ. Sustainability* 5, 392–402. doi:10.1016/j.cosust.2013.07.004
- Eijkelkamp (2018). *Manual Double Ring Infiltrometer. M-0904E*. Netherlands: Eijkelkamp Soil & Water, Giesbeek.
- Ernst, O. R., Dogliotti, S., Cadenazzi, M., and Kemanian, A. R. (2018). Shifting Crop-Pasture Rotations to No-Till Annual Cropping Reduces Soil Quality and Wheat Yield. *Field Crops Res.* 217, 180–187. doi:10.1016/j.fcr.2017.11.014
- Ernst, O. R., Kemanian, A. R., Mazzilli, S., Siri-Prieto, G., and Dogliotti, S. (2020). The Dos and Don'ts of No-Till Continuous Cropping: Evidence from Wheat Yield and Nitrogen Use Efficiency. *Field Crops Res.* 257, 107934. doi:10.1016/j.fcr.2020.107934
- Ernst, O., and Siri-Prieto, G. (2009). Impact of Perennial Pasture and Tillage Systems on Carbon Input and Soil Quality Indicators. *Soil Tillage Res.* 105, 260–268. doi:10.1016/j.still.2009.08.001
- Fabrizzi, K. P., Morón, A., and García, F. O. (2003). Soil Carbon and Nitrogen Organic Fractions in Degraded vs. Non-Degraded Mollisols in Argentina. *Soil Sci. Soc. Am. J.* 67, 1831–1841. doi:10.2136/sssaj2003.1831
- FAO (2019). Global Symposium on Soil Erosion. Outcome Doc. Available at: <http://www.fao.org/3/ca5697en/ca5697en.pdf> (Accessed February 9, 2022).
- García Prechac, F., Terra, J., Sawchik, J., and Pérez Bidegain, M. (2017). Mejora de las estimaciones con USLE/ RUSLE empleando resultados de parcelas de escurrimiento para considerar el efecto del agua del suelo. *Agrociencia Uruguay* 21 (2), 100–104. doi:10.2477/vol21iss2pp100-104

- García-Préchac, F. (1992). Propiedades físicas y erosión en rotaciones de cultivos y pasturas. *Rev. Inia-uruguay Inv. Agr.* 1, 127–140.
- Grahmann, K., Rubio Dellepiane, V., Terra, J. A., and Quincke, J. A. (2020). Long-Term Observations in Contrasting Crop-Pasture Rotations over Half a century: Statistical Analysis of Chemical Soil Properties and Implications for Soil Sampling Frequency. *Agric. Ecosyst. Environ.* 287, 106710. doi:10.1016/j.agee.2019.106710
- Grahmann, K., Terra, J. A., Ellerbrock, R., Rubio, V., Barro, R., Caamaño, A., et al. (Forthcoming 2022). Data Accuracy and Method Validation of Chemical Soil Properties in Long-Term Experiments: Standard Operating Procedures for a Non-Certified Soil Laboratory in Latin America. *Geoderma Regional*, e00487. doi:10.1016/j.geodrs.2022.e00487
- Guimarães, R. M. L., Ball, B. C., and Tormena, C. A. (2011). Improvements in the Visual Evaluation of Soil Structure. *Soil Use Manag.* 27, 395–403. doi:10.1111/j.1475-2743.2011.00354.x
- Gyssels, G., Poesen, J., Bochet, E., and Li, Y. (2005). Impact of Plant Roots on the Resistance of Soils to Erosion by Water: A Review. *Prog. Phys. Geogr. Earth Environ.* 29, 189–217. doi:10.1191/0309133305pp443ra
- Hill, M., García Préchac, F., Terra, J. A., and Sawchik, J. (2008). Incorporación del efecto del contenido de agua en el suelo en el modelo USLE/ RUSLE para estimar erosión en Uruguay [Soil water content effect in the USLE/ RUSLE model to estimate erosion in Uruguay]. *Agrociencia Uruguay* 19 (1), 94–101. doi:10.2477/vol19iss1pp94-101
- Holz, M., and Augustin, J. (2021). Erosion Effects on Soil Carbon and Nitrogen Dynamics on Cultivated Slopes: A Meta-Analysis. *Geoderma* 397, 115045. doi:10.1016/j.geoderma.2021.115045
- Jackson, M. L. (1964). *Análisis Químico de Suelos*. Barcelona: Ediciones Omega S.A.
- Johnston, A. E., and Poulton, P. R. (2018). The Importance of Long-term Experiments in Agriculture: Their Management to Ensure Continued Crop Production and Soil Fertility; the Rothamsted Experience. *Eur. J. Soil Sci.* 69, 113–125. doi:10.1111/ejss.12521
- Jones, A. R., Orton, T. G., and Dalal, R. C. (2016). The Legacy of Cropping History Reduces the Recovery of Soil Carbon and Nitrogen after Conversion from Continuous Cropping to Permanent Pasture. *Agric. Ecosyst. Environ.* 216, 166–176. doi:10.1016/j.agee.2015.09.029
- Kinnell, P. I. A. (2016). A Review of the Design and Operation of Runoff and Soil Loss Plots. *Catena* 145, 257–265. doi:10.1016/j.catena.2016.06.013
- Knapen, A., Poesen, J., Govers, G., and De Baets, S. (2008). The Effect of Conservation Tillage on Runoff Erosivity and Soil Erodibility during Concentrated Flow. *Hydrol. Process.* 22, 1497–1508. doi:10.1002/hyp.6702
- Kumar, K., and Goh, K. M. (1999). Crop Residues and Management Practices: Effects on Soil Quality, Soil Nitrogen Dynamics, Crop Yield, and Nitrogen Recovery. *Adv. Agron.* 68, 197–319. doi:10.1016/S0065-2113(08)60846-9
- Lal, R. (2019). Accelerated Soil Erosion as a Source of Atmospheric CO<sub>2</sub>. *Soil Tillage Res.* 188, 35–40. doi:10.1016/j.still.2018.02.001
- Lal, R. (2003). Soil Erosion and the Global Carbon Budget. *Environ. Int.* 29, 437–450. doi:10.1016/S0160-4120(02)00192-7
- Le Bissonnais, Y. (1996). Aggregate Stability and Assessment of Soil Crustability and Erodibility: I. Theory and Methodology. *Eur. J. Soil Sci.* 47, 425–437. doi:10.1111/j.1365-2389.1996.tb01843.x
- Liebig, M. A., Tanaka, D. L., and Wienhold, B. J. (2004). Tillage and Cropping Effects on Soil Quality Indicators in the Northern Great Plains. *Soil Tillage Res.* 78, 131–141. doi:10.1016/j.still.2004.02.002
- Lizarralde, C., Baethgen, W., Cadenaz, M., Capurro, C., and Sawchik, J. (2015). “Phosphorus Runoff in a Non-Fertilized Soybean Production System of SW Uruguay,” in ABSTRACT – Conference on Land and Water Challenges “Tools for development”, 24. doi:10.2477/VOL19ISS3PP24
- Logsdon, S. D., and Jaynes, D. B. (1993). Methodology for Determining Hydraulic Conductivity with Tension Infiltrometers. *Soil Sci. Soc. America J.* 57, 1426–1431. doi:10.2136/sssaj1993.03615995005700060005x
- Martínez, J. P., Crespo, C., Sainz Rozas, H., Echeverría, H., Studdert, G., Martínez, F., et al. (2020). Soil Organic Carbon in Cropping Sequences with Predominance of Soya Bean in the Argentinean Humid Pampas. *Soil Use Manag.* 36, 173–183. doi:10.1111/sum.12547
- MGAP (2013). Ministerio de Ganadería, Agricultura y Pesca Resolución N° 74/013 de DGRN - 18/01/2013 - Resolución Ministerial - Planes de Uso. Obligatoriedad de la presentación de planes de uso, manual de medidas exigibles para todos los cultivos. Available at: <https://www.gub.uy/ministerio-ganaderia-agricultura-pesca/institucional/normativa/resolucion-n-74013-dgrn-18012013-resolucion-ministerial-planes-uso>.
- MGAP-DSA (1976). *Descripción de las unidades de suelos, Min. de Agric. Y Pesca / Dirección de Suelos y Fertilizante*. Montevideo, Uruguay.
- Morris, E. K., Morris, D. J. P., Vogt, S., Gleber, S.-C., Bigalke, M., Wilcke, W., et al. (2019). Visualizing the Dynamics of Soil Aggregation as Affected by Arbuscular Mycorrhizal Fungi. *ISME J.* 13, 1639–1646. doi:10.1038/s41396-019-0369-0
- Mouratiadou, I., Latka, C., van der Hilst, F., Müller, C., Berges, R., Bodirsky, B. L., et al. (2021). Quantifying Sustainable Intensification of Agriculture: The Contribution of Metrics and Modelling. *Ecol. Indicators* 129, 107870. doi:10.1016/j.ecolind.2021.107870
- Mueller, L., Schindler, U., Behrendt, A., and Eulenstein, F. (2007). The Muencheberg Soil Quality Rating (SQR): Field Manual for Detecting and Assessing Properties and Limitations of Soils for Cropping and Grazing. Muencheberg, Germany. Available at: [https://www.zalf.de/de/forschung\\_lehre/publikationen/Documents/Publikation\\_Mueller\\_L/field\\_mueller.pdf](https://www.zalf.de/de/forschung_lehre/publikationen/Documents/Publikation_Mueller_L/field_mueller.pdf) (Accessed February 9, 2022).
- Munka, C., Cruz, G., and Caffera, R. M. (2007). Long Term Variation in Rainfall Erosivity in Uruguay: A Preliminary Fournier Approach. *Geojournal* 70, 257–262. doi:10.1007/s10708-008-9139-7
- Novelli, L. E., Caviglia, O. P., Wilson, M. G., and Sasal, M. C. (2013). Land Use Intensity and Cropping Sequence Effects on Aggregate Stability and C Storage in a Vertisol and a Mollisol. *Geoderma* 195–196, 260–267. doi:10.1016/j.geoderma.2012.12.013
- Packer, I., Hamilton, G., and Koen, T. (1992). Runoff, Soil Loss and Soil Physical Property Changes of Light Textured Surface Soils from Long Term Tillage Treatments. *Soil Res.* 30, 789–806. doi:10.1071/SR9920789
- Palis, R., Okwach, G., Rose, C., and Saffigna, P. (1990). Soil Erosion Processes and Nutrient Loss. 1. The Interpretation of Enrichment Ratio and Nitrogen Loss in Runoff Sediment. *Soil Res.* 28, 623–639. doi:10.1071/SR9900623
- Palm, C., Blanco-Canqui, H., DeClerck, F., Gatere, L., and Grace, P. (2014). Conservation Agriculture and Ecosystem Services: An Overview. *Agric. Ecosyst. Environ.* 187, 87–105. doi:10.1016/j.agee.2013.10.010
- Panagos, P., Borrelli, P., Meusburger, K., Alewell, C., Lugato, E., and Montanarella, L. (2015a). Estimating the Soil Erosion Cover-Management Factor at the European Scale. *Land use policy* 48, 38–50. doi:10.1016/j.landusepol.2015.05.021
- Panagos, P., Policy, E. S., Environ, B., Policy, S., Panagos, P., Borrelli, P., et al. (2015b). The New Assessment of Soil Loss by Water Erosion in Europe. *Environ. Sci. Pol.* 54, 438–447. doi:10.1016/j.envsci.2015.08.012
- Pérez-Bidegain, M., Hill, M., Clerici, C., Terra, J. A., Sawchik, J., and García-Préchac, F. (2018). “Regulatory Utilization of USLE/RUSLE Erosion Rate Estimates in Uruguay: a Policy Coincident with the UN Sustainable Development Goals,” in *Soil and Sustainable Development Goals Chapter*. Editors R. Lal, R. Horn, and T. Kosaki (Stuttgart: Catena Soil Sciences - Schweizerbart.), 82–91.
- Pérez-Bidegain, M., Piaggio, J. M., Baethgen, W. E., and García Préchac, F. (2017). Rainfall Erosivity Factor Update in Uruguay. *Agrociencia* 21 (3), 91–99. doi:10.31285/AGRO.21.2.11
- Philip, J. R. (1957). The Theory of Infiltration: 4. Sorptivity and Algebraic Infiltration Equations. *Soil Sci.* 84, 257–264. doi:10.1097/00010694-195709000-00010
- PNUD (Programa de las Naciones Unidas para el Desarrollo) Uruguay (2007). Uruguay: El Cambio Climático Aquí Y Ahora. Material complementario del Informe Mundial Sobre Desarrollo Humano 2007-2008, 39.
- Puentes, R. (1981). A Framework for the Use of the Universal Soil Loss Equation in Uruguay. M.Sci. Thesis. Texas, United States: Texas A&M University.
- Ramos-Scharrón, C. E., and Figueroa-Sánchez, Y. (2017). Plot-, Farm-, and Watershed-Scale Effects of Coffee Cultivation in Runoff and Sediment Production in Western Puerto Rico. *J. Environ. Manage.* 202, 126–136. doi:10.1016/j.jenvman.2017.07.020
- Ranaivosoa, L., Naudin, K., Ripoché, A., Affholder, F., Rabeharisoa, L., and Corbeels, M. (2017). Agro-Ecological Functions of Crop Residues under Conservation Agriculture. A Review. *Agron. Sustain. Dev.* 37, 26. doi:10.1007/s13593-017-0432-z
- Renard, K., Foster, G., Weesies, G., McCool, D., and Yoder, D. (1997). Predicting Soil Erosion by Water: A Guide to Conservation Planning with the Revised

- Universal Soil Loss Equation (RUSLE). Available at: [http://www.ars.usda.gov/SP2UserFiles/Place/64080530/RUSLE/AH\\_703.pdf](http://www.ars.usda.gov/SP2UserFiles/Place/64080530/RUSLE/AH_703.pdf) (Accessed February 9, 2022).
- Richter, D. d., Hofmockel, M., Callahan, M. A., Powlson, D. S., and Smith, P. (2007). Long-Term Soil Experiments: Keys to Managing Earth's Rapidly Changing Ecosystems. *Soil Sci. Soc. Am. J.* 71, 266–279. doi:10.2136/sssaj2006.0181
- Rickson, R. J., Deeks, L. K., Graves, A., Harris, J. A. H., Kibblewhite, M. G., and Sakrabani, R. (2015). Input Constraints to Food Production: The Impact of Soil Degradation. *Food Sec.* 7, 351–364. doi:10.1007/s12571-015-0437-x
- Rubio, V., Diaz-Rossello, R., Quincke, J. A., and van Es, H. M. (2021a). Quantifying Soil Organic Carbon's Critical Role in Cereal Productivity Losses under Annualized Crop Rotations. *Agric. Ecosyst. Environ.* 321, 107607. doi:10.1016/j.agee.2021.107607
- Rubio, V., Pérez-Bidegain, M., Beretta, A., Barolin, E., and Quincke, A. (2019). Impacto de propiedades físico-químicas en la estabilidad estructural de Molisoles. *Cienc. Del. Suelo* 37, 367–371.
- Rubio, V., Quincke, A., and Ernst, O. (2021b). Deep Tillage and Nitrogen Do Not Remediate Cumulative Soil Deterioration Effects of Continuous Cropping. *Agron J* 113, 5584–5596. doi:10.1002/agrj.2.20927
- Sasal, M. C., Castiglioni, M. G., and Wilson, M. G. (2010). Effect of Crop Sequences on Soil Properties and Runoff on Natural-Rainfall Erosion Plots under No Tillage. *Soil Tillage Res.* 108, 24–29. doi:10.1016/j.still.2010.03.010
- Schneider, F., Don, A., Hennings, I., Schmittmann, O., and Seidel, S. J. (2017). The Effect of Deep Tillage on Crop Yield - What Do We Really Know? *Soil Tillage Res.* 174, 193–204. doi:10.1016/j.still.2017.07.005
- Six, J., Elliott, E. T., and Paustian, K. (1999). Aggregate and Soil Organic Matter Dynamics under Conventional and No-Tillage Systems. *Soil Sci. Soc. Am. J.* 63, 1350–1358. doi:10.2136/sssaj1999.6351350x
- Six, J., Ogle, S. M., Breidt, F. J., Conant, R. T., Mosier, A. R., and Paustian, K. (2004). The Potential to Mitigate Global Warming with No-Tillage Management Is Only Realized when Practised in the Long Term. *Glob. Chang. Biol.* 10, 155–160. doi:10.1111/j.1529-8817.2003.00730.x
- Six, J., Paustian, K., Elliott, E. T., and Combrink, C. (2000). Soil Structure and Organic Matter I. Distribution of Aggregate-Size Classes and Aggregate-Associated Carbon. *Soil Sci. Soc. Am. J.* 64, 681–689. doi:10.2136/sssaj2000.642681x
- Soil Survey Staff (2014). Keys to Soil Taxonomy. Available at: [http://www.nrcs.usda.gov/Internet/FSE\\_DOCUMENTS/nrcs142p2\\_051546.pdf](http://www.nrcs.usda.gov/Internet/FSE_DOCUMENTS/nrcs142p2_051546.pdf) (Accessed February 9, 2022).
- Studdert, G. A., Echeverría, H. E., and Casanovas, E. M. (1997). Crop-Pasture Rotation for Sustaining the Quality and Productivity of a Typic Argiudoll. *Soil Sci. Soc. America J.* 61, 1466–1472. doi:10.2136/sssaj1997.03615995006100050026x
- Taleshian Jeloudar, F., Ghajar Sepanlou, M., and Emadi, S. M. (2018). Impact of Land Use Change on Soil Erodibility. *Glob. J. Environ. Sci. Manag.* 4, 59–70. doi:10.22034/gjesm.2018.04.01.006
- Tang, Q., Xu, Y., Bennett, S. J., and Li, Y. (2015). Assessment of Soil Erosion Using RUSLE and GIS: A Case Study of the Yangou Watershed in the Loess Plateau, China. *Environ. Earth Sci.* 73, 1715–1724. doi:10.1007/s12665-014-3523-z
- Toy, T. J., Foster, G. R., and Renard, K. G. (2002). *Soil Erosion : Processes, Prediction, Measurement, and Control*. New York, United States: John Wiley & Sons, 338, 352.
- Turtola, E., Alakukku, L., Uusitalo, R., and Kaseva, A. (2007). Surface Runoff, Subsurface Drainflow and Soil Erosion as Affected by Tillage in a Clayey Finnish Soil. *Agric. Food Sci.* 16, 332–351. doi:10.2137/145960607784125429
- USDA-NRCS (2004). Soil Survey Laboratory Methods Manual. Soil Survey Investigations Report No. 42, Version 4.0. Available at: [https://www.nrcs.usda.gov/wps/portal/nrcs/detail/soils/ref/?cid=nrcs142p2\\_054247](https://www.nrcs.usda.gov/wps/portal/nrcs/detail/soils/ref/?cid=nrcs142p2_054247)
- Verhulst, N., Govaerts, B., Verachtert, E., Castellanos-Navarrete, A., Mezzalama, M., Wall, P. C., et al. (2010). "Conservation Agriculture, Improving Soil Quality for Sustainable Production Systems," in *Advances in Soil Science: Food Security and Soil Quality*. Editors R. Lal and B. A. Stewart (Boca Raton, FL, USA: CRC Press), 137–208. doi:10.1201/ebk1439800577-7
- Verhulst, N., Kienle, F., Sayre, K. D., Deckers, J., Raes, D., Limon-Ortega, A., et al. (2011). Soil Quality as Affected by Tillage-Residue Management in a Wheat-maize Irrigated Bed Planting System. *Plant Soil* 340, 453–466. doi:10.1007/s11104-010-0618-5
- Victoria, C., Kacevas, A., and Fiori, H. (2001). "Assessment of Erodibility, Runoff and Infiltration in a Uruguayan Vertisol," in *Sustain. Glob. Farm. Sel. Pap. from 10th Int. Soils Conserv. Organ. Meet.*, 807–811.
- Wander, M. M., Bidart, M. G., and Aref, S. (1998). Tillage Impacts on Depth Distribution of Total and Particulate Organic Matter in Three Illinois Soils. *Soil Sci. Soc. America J.* 62, 1704–1711. doi:10.2136/sssaj1998.03615995006200060031x
- Waring, S. A., and Bremner, J. M. (1964). Ammonium Production in Soil under Waterlogged Conditions as index of Nitrogen Availability. *Nature* 201, 464–466. Available at: <https://www.nature.com/articles/201464a0.pdf>. doi:10.1038/201951a0
- White, I., and Sully, M. J. (1987). Macroscopic and Microscopic Capillary Length and Time Scales from Field Infiltration. *Water Resour. Res.* 23, 1514–1522. doi:10.1029/WR023i008p01514
- Willett, W., Rockström, J., Loken, B., Springmann, M., Lang, T., Vermeulen, S., et al. (2019). Food in the Anthropocene: the EAT-Lancet Commission on Healthy Diets from Sustainable Food Systems. *Lancet* 393, 447–492. doi:10.1016/S0140-6736(18)31788-4
- Williams, J. D., Gollany, H. T., Siemens, M. C., Wuest, S. B., and Long, D. S. (2009). Comparison of Runoff, Soil Erosion, and winter Wheat Yields from No-Till and Inversion Tillage Production Systems in Northeastern Oregon. *J. Soil Water Conservation* 64, 43–52. doi:10.2489/jswc.64.1.43
- Wischmeier, W. H., and Smith, D. D. (1978). *Predicting Rainfall Erosion Losses: A Guide to Conservation Planning*. Agricultural Handbook No. 537. Washington, DC, United States: U.S. Department of Agriculture, Science and Education Administration. doi:10.1128/AAC.03728-14
- Wooding, R. A. (1968). Steady Infiltration from a Shallow Circular Pond. *Water Resour. Res.* 4, 1259–1273. doi:10.1029/WR004i006p01259
- Wright, A. F., and Bailey, J. S. (2001). Organic Carbon, Total Carbon, and Total Nitrogen Determinations in Soils of Variable Calcium Carbonate Contents Using a Leco CN-2000 Dry Combustion Analyzer. *Commun. Soil Sci. Plant Anal.* 32, 3243–3258. doi:10.1081/CSS-120001118
- Xiong, M., Sun, R., and Chen, L. (2019). A Global Comparison of Soil Erosion Associated with Land Use and Climate Type. *Geoderma* 343, 31–39. doi:10.1016/j.geoderma.2019.02.013
- Zhang, G., Chan, K., Oates, A., Heenan, D., and Huang, G. (2007). Relationship between Soil Structure and Runoff/soil Loss after 24 Years of Conservation Tillage. *Soil Tillage Res.* 92, 122–128. doi:10.1016/j.still.2006.01.006
- Zurbriggen, C., González-Lago, M., Baraibar, M., Baethgen, W., Mazzeo, N., and Sierra, M. (2020). Experimentation in the Design of Public Policies: The Uruguayan Soils Conservation Plans. *Iberoam. - Nord. J. Lat. Am. Caribb. Stud.* 49, 52–62. doi:10.16993/iberoamericana.459

**Conflict of Interest:** The authors declare that the research was conducted in the absence of any commercial or financial relationships that could be construed as a potential conflict of interest.

**Publisher's Note:** All claims expressed in this article are solely those of the authors and do not necessarily represent those of their affiliated organizations, or those of the publisher, the editors, and the reviewers. Any product that may be evaluated in this article, or claim that may be made by its manufacturer, is not guaranteed or endorsed by the publisher.

Copyright © 2022 Grahmann, Rubio, Perez-Bidegain and Quincke. This is an open-access article distributed under the terms of the Creative Commons Attribution License (CC BY). The use, distribution or reproduction in other forums is permitted, provided the original author(s) and the copyright owner(s) are credited and that the original publication in this journal is cited, in accordance with accepted academic practice. No use, distribution or reproduction is permitted which does not comply with these terms.



# Spatio-Temporal High-Resolution Subsoil Compaction Risk Assessment for a 5-Years Crop Rotation at Regional Scale

Michael Kuhwald<sup>1\*</sup>, Katja Kuhwald<sup>2</sup> and Rainer Duttman<sup>1</sup>

<sup>1</sup>Department of Geography, Landscape Ecology and Geoinformation Science, Kiel University, Kiel, Germany, <sup>2</sup>Department of Geography, Earth Observation and Modelling, Kiel University, Kiel, Germany

## OPEN ACCESS

### Edited by:

Thomas Keller,  
Swedish University of Agricultural  
Sciences, Sweden

### Reviewed by:

Cássio Tormena,  
Universidade Estadual de Maringá,  
Brazil

Miriam Muñoz-Rojas,  
University of New South Wales,  
Australia

### \*Correspondence:

Michael Kuhwald  
kuhwald@geographie.uni-kiel.de

### Specialty section:

This article was submitted to  
Soil Processes,  
a section of the journal  
Frontiers in Environmental Science

**Received:** 26 November 2021

**Accepted:** 22 February 2022

**Published:** 09 March 2022

### Citation:

Kuhwald M, Kuhwald K and  
Duttman R (2022) Spatio-Temporal  
High-Resolution Subsoil Compaction  
Risk Assessment for a 5-Years Crop  
Rotation at Regional Scale.  
Front. Environ. Sci. 10:823030.  
doi: 10.3389/fenvs.2022.823030

Soil compaction results whenever applied soil stress by machinery exceed the soil strength. Both, soil strength and stress, are spatially and temporally highly variable, depending on the weather situation, the current crop type, and the machinery used. Thus, soil compaction risk is very dynamic, changes from day to day and from field to field. The objective of this study was to analyze the spatio-temporal dynamics of soil compaction risk and to identify hot-spot areas of high soil compaction risk at regional scale. Therefore, we selected a study area (~2,000 km<sup>2</sup>) with intensive arable farming in Northern Germany, having a high share of cereals, maize and sugar beets. Sentinel-2 images were used to derive the crop types for a 5-years crop rotation (2016–2020). We calculated the soil compaction risk using an updated version of the SaSCiA-model (Spatially explicit Soil Compaction risk Assessment) for each single day of the period, with a spatial resolution of 20 m. The results showed the dynamic changes of soil compaction risk within a year and throughout the entire crop rotation. The relatively dry years 2016 and 2018–2020 reduced the soil compaction risk even at high wheel loads applied to soil during maize and sugar beet harvest. Contrary, high precipitation in 2017 increased the soil compaction risk considerably. Focusing on the complete 5-year period, 2.7% of the cropland area was identified as hot-spots of soil compaction risk, where the highest soil compaction risk class (“extremely high”) occurred every year. Additionally, 39.8% of the cropland was affected by “extremely high” soil compaction at least in one of the 5 years. Although the soil compaction risk analysis does not provide information on the actual extent of the compacted area, the identification of risk areas within a period may contribute to understand the dynamics of soil compaction risk in crop rotation at regional scale and provide advice to mitigate further soil compaction in areas classified as high risk.

**Keywords:** soil degradation, sustainable management, modelling, field traffic, SaSCiA-model

## INTRODUCTION

Soil compaction is one of the main soil degradation processes on agricultural land worldwide (FAO, 2015). This degradation process is expected to continue in the coming centuries due to intensive field traffic activities with heavy machinery (Keller et al., 2017; Keller et al., 2019; Tehen et al., 2020). Continued soil compaction, however, contradicts the sustainable development goal 15 (SDG15),

**TABLE 1 |** Common spatial models and spatial approaches in soil compaction research (according to Kuhwald (2019).

Reference	Aim/focus/product	Used method
Horn et al. (2002)	- Maps for Germany: precompression stress, changes in air capacity and air conductivity by applied stress	- Application of Lebert and Horn (1991), DVWK 234 (1995)
Jones et al. (2003)	- Map of subsoil susceptibility for soil compaction for Europe	- Application of Jones et al. (2003)
van den Akker (2004)	- Wheel load bearing capacity map of the Netherlands	- Used SOCOMO van den Akker (2004)
Horn et al. (2005)	- Precompression stress, contact area stress (and their relationship) and change in air conductivity	- Application of Lebert and Horn (1991), DVWK 234 (1995), Horn and Fleige (2003)
	- Soil maps for Europe, Germany and for a farm	
Horn and Fleige (2009)	- Maps of precompression, change in air capacity	- Application of Lebert and Horn (1991), DVWK 234 (1995), Horn and Fleige (2003)
	- Subsoil stress of 60 and 90 kPa (40 cm)	
Kroulik et al. (2009)	- Mapping spatial pattern of traffic intensity	- GPS tracking and tire measurements (tire width)
	- Wheel track area and wheel passages for entire cropping season	
Lebert (2010)	- Maps of susceptibility to soil compaction for varying field capacities for entire Germany	- Application of Lebert and Horn (1991), DVWK 234 (1995), Horn and Fleige (2003), DIN V 19688 (2011)
	- Assumption of the same field capacities for entire Germany	
van den Akker and Hoogland (2011)	- Calculating the soil vulnerability and susceptibility to soil compaction in the Netherlands	- Application of Jones et al. (2003) and van den Akker (2004)
	- Calculating the soil strength and the allowable wheel load for the Netherlands	
Duttmann et al. (2013)	- Modelling and mapping of wheel passages, wheel load, mean ground contact pressure for maize harvest	- Application of Diserens (2002), Diserens (2009)
		- Recorded GPS-data and time stamps
Duttmann et al. (2014)	- Modelling and mapping of wheel passages, wheel load, mean ground contact pressure, soil strength, soil stress (2D and 3D) for maize harvest	- Application of Diserens (2002), Diserens (2009), Horn and Fleige (2003)
		- Recorded GPS-data and time stamps
D'Or and Destain (2014)	- Calculation of precompression stress maps and soil compaction risk maps for Belgium	- Application of Horn and Fleige (2003), Keller (2005), Schjønning et al. (2008)
Schjønning et al. (2015a)	- Mapping wheel load carrying capacity for Europe	- Application of Terranimo (Stettler et al., 2014) algorithm
	- For a tire with a diameter of 800 mm, soil depth of 25 cm and traffic at a matric potential of - 300hPa	
Lamandé et al. (2018)	- Mapping wheel load carrying capacity for Europe (for rubber tracks and wheels)	- Application of Frida (Schjønning et al., 2008; Schjønning et al., 2015a) and Schjønning and Lamandé (2018) for soil strength calculation
	- Tire: 1050/50R32, at a depth of 35 cm	
	- Matric potential of -50 hPa	
Kuhwald et al. (2018)	- Mapping daily soil compaction risk at regional scale with high spatial resolution (20 m*20 m)	- SaSCiA-model, incorporates Horn and Fleige (2003), DIN V 19688 (2011), Nendel et al. (2011), Rücknagel et al. (2012, 2013, 2015)
Ledermüller et al. (2018)	- Mapping soil compaction risk for a feral state (Lower Saxony) in Germany	- Application of Lorenz et al. (2016)
Augustin et al. (2020)	- Modelling spatial pattern of traffic intensity for an entire crop rotation for one field	- Application of FITraM (Augustin et al., 2019), which incorporates Koolen et al. (1992)
	- Maps of wheel passages, maximum wheel load, maximum mean ground contact pressure for maize harvest	
Duttmann et al. (2021)	- modelling of soil compaction risk beneath the wheel tracks of a complete maize season	- Application of FITraM and SaSCiA (Kuhwald et al., 2018; Augustin et al., 2019)

which aims to achieve land degradation neutrality by sustainable land use management. Reducing soil compaction is therefore necessary to achieve the SDG 15 and to enable a sustainable soil use.

Soil compaction is defined as an increase of bulk density while pore volume decreases (Horn et al., 1995). Compared to an uncompacted soil, compacted soils have a lower air capacity, reduced water infiltration, lower air permeability, lower biological activity, reduced root and plant growth (e.g., Horn et al., 1995; Weisskopf et al., 2010; Destain et al., 2016; Szatanik-Kloc et al., 2018). Therefore, compacted soils are more susceptible to surface water runoff and soil erosion (Alaoui et al., 2018; Keller et al., 2019). In addition, soil compaction results often in lower yields (Arvidsson and Håkansson, 2014; Daigh et al., 2020). As soil compaction is persistent (Keller et al., 2017; Seehusen et al., 2021), especially in the subsoil, the environmental effects are present in the long term. As exemplarily shown by Graves et al. (2015) for

England and Wales, the total economic costs of soil degradation caused by soil compaction can be three times that of soil erosion. Thus, quantifying and localizing already compacted soils is as important as identifying areas where the risk of soil compaction is increased to prevent further soil degradation.

Calculating area percentages is challenging as soil compaction on arable land is a spatio-temporal highly dynamic process (Schjønning et al., 2015b), because crop type, soil, weather and used machinery interact (Kuhwald et al., 2018). Comparing soil strength against soil stress is the most common approach to evaluate whether soil compaction may occur during wheeling (Horn and Fleige, 2003; Horn et al., 2005). Soil strength results from soil texture, carbon content, soil structure and soil moisture (Horn et al., 1995; Horn and Fleige, 2003; Rücknagel et al., 2012; Gut et al., 2015). Soil stress depends on the wheel load, tire inflation pressure, contact area and amount of wheel passes (Horn, 2003; Horn et al., 2003; Arvidsson and Keller, 2007;

Botta et al., 2009; Schjønning et al., 2012). Several studies exist that analyzed the various effects of wheeling on stress propagation and distribution inside the soil as on physical soil properties as well (e.g., Gebhardt et al., 2009; Lamandé and Schjønning, 2011; Hartmann et al., 2012; Keller et al., 2012; Berisso et al., 2013; Seehusen et al., 2019).

From field and laboratory experiments, numerous functions were derived to calculate e.g. the contact area, the soil strength at a certain soil moisture state or the stress distribution while wheeling (Keller et al., 2007; Schjønning et al., 2008; Diserens, 2009; Rücknagel et al., 2012). These functions, incorporated into more complex assessment models, allow to estimate soil compaction behavior at different spatial scales. **Table 1** lists common spatial approaches and models in soil compaction research.

The growing availability of high resolute data from global navigation satellite systems (GNSS) received and recorded by modern farm vehicles enables to precisely predict traffic intensity (e.g., Kroulík et al., 2009; Duttman et al., 2013) and traffic related compaction effects at field scale (e.g., Duttman et al., 2014; Augustin et al., 2020; Duttman et al., 2021).

From field to larger scales, the pre-compression (or pre-consolidation stress)-concept (e.g., Lebert and Horn, 1991) has been applied in various studies (e.g., Horn et al., 2002; Horn et al., 2005; Horn and Fleige, 2009; Lebert, 2010; Destain et al., 2016). The results are maps showing the susceptibility to soil compaction (Jones et al., 2003; Lebert, 2010), the soil compaction risk (D'Or and Destain, 2014) or, by using further equations, changes in air conductivity and air capacity (Horn et al., 2002; Horn et al., 2005; Horn and Fleige, 2009). Furthermore, the wheel load carrying capacity can be derived by calculating the soil strength and setting threshold values for soil stress. Examples are given by van den Akker (2004) for the Netherlands and by Schjønning et al. (2015b) and Lamandé et al. (2018) for Europe.

One limitation of all these large scale predictions is the assumption of static conditions, either for the soil or for the used machinery data or for both. Dynamic changes of soil stress and soil strength in space and time were rarely considered.

Newer approaches try to consider the dynamics of soil stress and soil strength in soil compaction risk modelling at regional scale (Kuhwald et al., 2018; Ledermüller et al., 2018). The approach of Ledermüller et al. (2018) uses available soil moisture information at a spatial resolution of 1\*1 km<sup>2</sup> provided by the German weather service (DWD) and land use data from the Integrated Administration and Control System (IACS) to calculate soil compaction risk according to Lorenz et al. (2016). This method aims at a long-term assessment of topsoil compaction risk, which can support farmers in decision making.

Kuhwald et al. (2018) developed a different approach to calculate soil compaction risk, called “SaSCiA” (Spatially explicit Soil Compaction risk Assessment). The raster-based model incorporates spatial information of the soil and current crop types and calculates the daily soil strength depending on actual soil moisture. For the calculation of soil stress, the current

crop type, the actual soil moisture, crop-dependent used machinery and field traffic days are considered. The modelling results are daily maps of soil compaction risk at a spatial resolution of 20 m. As shown in a first study by Kuhwald et al. (2018), the SaSCiA-model was successfully used to simulate the daily changes of soil compaction risk, separated by different soil depths (20, 35 and 50 cm), within 1 year for two study areas. Among other aspects, the high variability of soil compaction risk within a year was evident, confirming the significant influence of the actual weather conditions in a respective region. However, Kuhwald et al. (2018) analyzed only 1 year for each study area. Therefore, variations between years for a specific study area could not be accounted for.

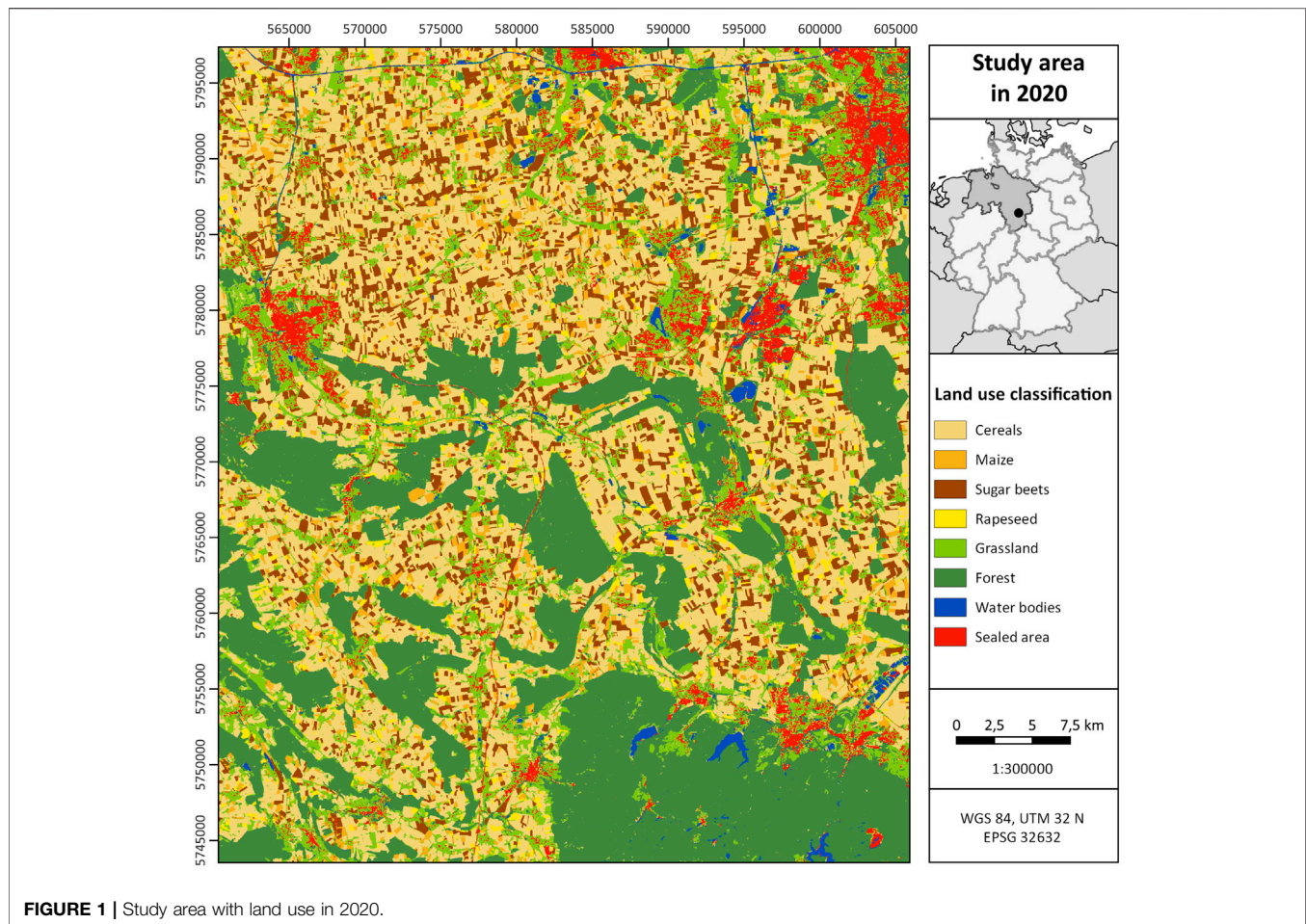
Thus, the following research questions arise for this study: (i) whether and to what extent does soil compaction risk vary between individual years, and (ii) does a continuous calculation of soil compaction risk over a longer period enable the detection of areas within the region that are more often affected by high soil compaction risk than other areas? To answer both questions, we analyzed the soil compaction risk for a 5-year period for an intensively cropped region using an updated version of the SaSCiA-model. The objectives of this study are (i) to model and analyze the variation of soil compaction risk within the individual years and within the 5-years period (2016–2020), and (ii) to identify areas with recurring patterns of high soil compaction risk within this period. We hypothesize that (i) the variation in soil compaction risk between the single years will be strong depending on actual weather conditions, but that (ii) classes of higher soil compaction risk can be observed for the same areas in each year, which enables to delineate “hot-spot” areas of increased soil compaction risk.

This study focusses on a perennial analysis of soil compaction risk dynamics at regional scale to understand the spatio-temporal characteristics of soil compaction. Furthermore, identifying areas of different soil compaction risk during a crop rotation enables selective and specific intervention through soil management to mitigate potential soil compaction. In this way, this study may support to a more sustainable soil use as envisaged by the SDG 15.

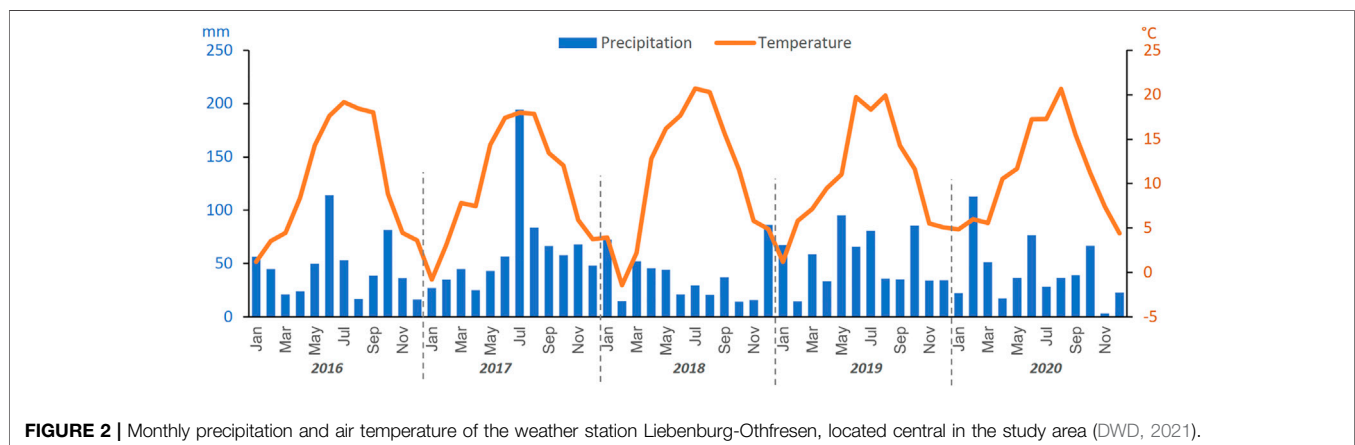
## MATERIALS AND METHODS

### Study Area

A 2,000 km<sup>2</sup> region in Lower Saxony (Germany) near the city of Hildesheim was selected as study area (**Figure 1**). Intensive agricultural use characterizes this region. Most important crop types are winter wheat (*Triticum aestivum*), sugar beets (*Beta vulgaris*), silage maize (*Zea mays*) and rapeseed (*Brassica napus*). The study area is part of the Lower Saxony Loess Hill Country. The geology of the region is complex, resulting in diversely distributed soil parent material. Deeply weathered loess predominates along the hill slopes, while loamy deposits occur in the valleys. Shallow layers of sandy and clayey weathered materials are mostly found at the hilltops. Typical soil types at the hill slopes and valleys are Luvisols (often stagnic) and Cambisols, while Leptosols and Regosols (FAO, 2014) occur at the hilltops. Forests cover the hilly areas and the areas



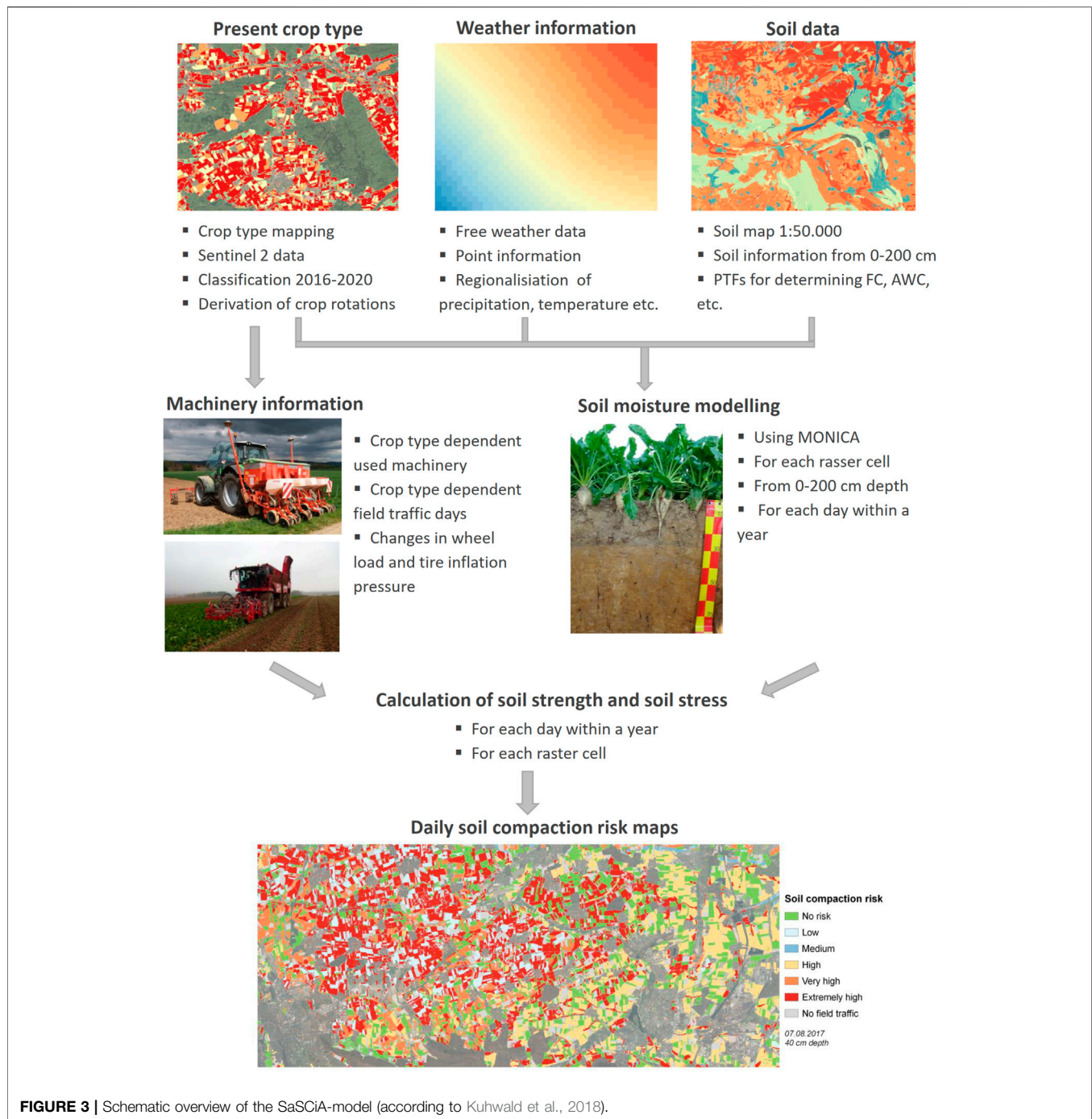
**FIGURE 1 |** Study area with land use in 2020.



with shallow soil development. The climate is humid with a mean annual precipitation of 649 mm and mean annual temperature of 10.0°C (weather station Liebenburg-Othfresen; DWD, 2021). The weather conditions for the investigated period are exemplarily shown for the weather station “Liebenburg-Othfresen,” which is centrally located in the study area (**Figure 2**).

## Modelling, Model Structure and Input Data

The SaSCiA-model (Spatially explicit Soil Compaction risk Assessment) was used for the 5-years analysis. The freely available study by Kuhwald et al. (2018) describes the model and its components in detail. Here, we briefly explain the model and highlight the changes in the model and the used input data.



The SaSciA-model incorporates crop type data, weather information, soil data, machinery information, the crop model “MONICA” and various pedotransfer functions (e.g., Horn and Fleige, 2003; Nendel et al., 2011; Rücknagel et al., 2012; Rücknagel et al., 2013; Rücknagel et al., 2015). Based on these components, it calculates the daily soil compaction risk for each raster cell within a selected area (Figure 3). In this study, we modelled and analyzed the subsoil compaction risk at a soil depth of 40 cm. Since this depth will not be reached by regular primary tillage and related loosening effects, soil compaction

persists (Keller et al., 2017; Keller et al., 2021) and may not recover in short-term.

### Crop Types and Crop Rotations

The crop types and crop rotations for the period (2016–2020) were derived by land use mapping and land use classification. During each summer (July–September) of the investigation period, we mapped crop types in the study area for ground control. Field mapping data encompassed the following target classes: cereals (e.g., winter wheat, rye, barley), maize, winter

rapeseed, sugar beets and grassland. Google Earth imagery supported the identification of less changing land cover classes such as water bodies, evergreen/deciduous forest and sealed areas. The mapped data formed the basis for a remote sensing approach to obtain spatially continuous maps of cultivated crop types at 20 m spatial resolution.

To this end, we selected 20 cloud-free or almost cloud-free Sentinel-2 scenes, which were acquired during the vegetation periods 2016–2020 (**Supplementary Table S1**). Since its launch in 2015, Sentinel-2 data are widely used and established for crop type mapping (e.g., Immitzer et al., 2016). To ensure data comparability, we downloaded atmospherically corrected (Sen2Cor (Müller-Wilm, 2016); Level-2A products from the Copernicus Open Access Hub (<https://scihub.copernicus.eu/>). Crop types were classified by using a random forest classification algorithm implemented as QGIS plugin (dzetsaka classification; Karasiak, 2016). The random forest algorithm is a supervised ensemble classifier and well known for crop type classification. To learn the spectral signatures of the target classes (training), the classifier requires georeferenced data on known crop types (Belgiu and Drăguț, 2016). For this purpose, we used the crop types mapped annually in the study area. The Sentinel-2 bands 2–7, 8A, 11 and 12 (20 m spatial resolution) of all selected scenes from a year served as spectral input, whereas we excluded cloudy pixels based on the standard cloud mask of the Level-2A products.

Speckle in the crop type maps was reduced by using a  $3 \times 3$  pixel median filter. Here, speckle means natural classification noise. At field borders, for instance, different land cover are represented within one  $20 \text{ m} \times 20 \text{ m}$  large pixel (e.g., the crop type, field path and hedgerow or crop type of adjacent field). The result are single, erroneously classified pixels and a grainy appearing land cover map. Filtering is a common post-classification tool to refine and smoothen the map. Furthermore, we applied the IRSeL tool (Rathjens et al., 2014). IRSeL is a post-classification tool for refining remote sensing based land cover maps (e.g., interpolation of no data gaps, reduction of misclassifications between crop types and less dynamic classes; Kandziora et al., 2014; Rathjens et al., 2014). Accuracy assessment followed the suggestions by Foody (2002) using independent field mapping data, which were not used for classifier training (**Supplementary Table S2**).

Subsequently, the received crop types were used to calculate soil moisture, to select the machinery employed for crop-specific field traffic activities and to define time periods for these activities.

## Weather Data

The weather data is used to calculate the soil moisture within the crop model MONICA. Required weather information are temperature (minimum, maximum, average), precipitation, relative humidity, Sun duration and wind speed. In the original SaSCiA-version, only one weather station was used for deriving weather information for an entire region. As weather is highly variable in space, one station may not adequately represent the weather conditions within a region of  $2,000 \text{ km}^2$ . For this reason, we newly incorporated regionalized weather data in the model. In a first step, all available weather stations within the

federal state “Lower Saxony” were identified and the available data automatically downloaded using the R-package “papro” (Hamer, 2019). Afterwards the data were processed in R (version 4.1.0; R Core Team, 2020) to generate regionalized weather information for each day for each of the required weather variable. From these grids, the weather input-files for each crop-soil grid cell were automatically generated. As a result, the spatial variation of weather can be considered in the calculation of soil compaction risk.

## Soil Data

Soil data was extracted from the digital soil map BK 50 (scale 1: 50,000) provided by the federal state agency of Lower Saxony (LBEG, 2020). The BK 50 contains information of e.g., soil type, soil horizons, soil depths, soil texture class, carbon content, gravel content and dry bulk density class, which were used for modelling. Further information about air capacity, field capacity, available field capacity and wilting point were derived according to Wessolek et al. (2009). In total, 1,800 different soil profiles were located within the study area and used for further soil compaction analysis.

## Machinery Data

The study area represents a region with highly mechanized agriculture, i.e., nearly all field processes are conducted with heavy machinery. The SaSCiA-model considers the used machinery based on the present crop type. For each crop type, a machinery with fixed wheel load and tire inflation pressure is defined and the periods for potential field traffic (**Supplementary Table S3**; cf. Kuhwald et al., 2018). For instance, it is assumed that the winter wheat is harvested between the first and 15th of August each year using a 220 kw combine harvester (max wheel load: 8,200 Mg, tire inflation pressure: 2.0 bar). We used the same machinery setups and field traffic days as selected by Kuhwald et al. (2018).

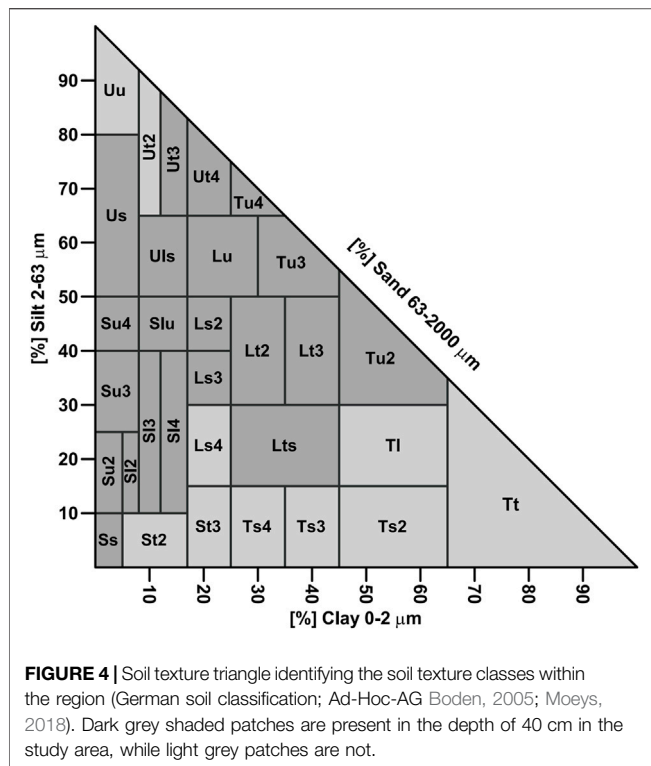
## Soil Moisture Modelling

Soil moisture is calculated from the present crop type, weather information and soil data for each day for each grid cell using the MONICA-model (Nendel et al., 2011). Among others, the model provides the soil moisture in 10 cm intervals for the depth between 0 and 200 cm (cf. Kuhwald et al., 2018).

## Calculation of Soil Strength, Soil Stress and Soil Compaction Risk

The soil strength is calculated by the static soil properties (e.g., soil texture, gravel content) in combination with the modelled soil moisture by the MONICA-model using the pedotransfer functions of Horn and Fleige (2003), DIN V 19688 (2011), Rücknagel et al. (2012), Rücknagel et al. (2013) and Rücknagel et al. (2015). The result is a dynamic change of soil strength on a daily basis, depending on present crop type, weather situation and soil properties.

The soil strength is compared against the soil stress caused by the used machinery. The latter depends on the present crop type and time of year. The soil stress is calculated by the pedotransfer function from Koolen et al. (1992) and Rücknagel et al. (2015).



Input data is the wheel load, the tire inflation pressure and the desired depth of risk analyses.

The comparison of soil strength and soil stress results in the soil compaction index (Rücknagel et al., 2015). The index is divided into five classes ranging from “no risk” (value <0) to “extremely high” (value >0.4) soil compaction risk. Though, the final result is a soil compaction risk class for each grid cell for each day within a year.

## Spatio-Temporal Analysis and Hot-Spots Detection

The temporal analysis of soil compaction risk within a year was performed by stringing together the daily results for the investigated period.

For the analyses of recurring patterns, all grid cells of 1 year with the class “extremely high” soil compaction risk were summed up. The results were summed raster for each year showing the areas of the highest soil compaction risk class. By summarizing and counting these five grids, we can identify the hot-spots of extremely high soil compaction risk and areas, that were never affected by such a high soil compaction risk class.

## RESULTS

### Spatial Characterization of the Study Area

The total size of the study area is 2,000 km<sup>2</sup>. The cover by arable land had a share of 50.2%, followed by forest (27.2%), grassland (16.0%), sealed area (5.4%) and water bodies (1.2%; **Supplementary Table S2**).

Organic soils cannot be processed by the SaSCiA-model since the incorporated functions (Horn and Fleige, 2003; Rücknagel et al., 2015) are invalid for soil with organic matter content >30%. Therefore, 1,562 of the originally 1,800 soil profiles could be used for soil compaction risk analysis, representing 116,309 ha under arable use.

At the desired depth of 40 cm, a wide range of soil texture classes occurred (**Figure 4**). Soil texture classes having high clay (Tt, Tl, Ts) and silt content (Uu, Ut2) were absent, as were those with low silt but high sand content (St2, St3, Ls4, Ts4, Ts3; according to the German classification scheme; Ad-Hoc-AG Boden, 2005).

Within the 116,309 ha area, cereals share ranged from 54 to 68% and was the predominating crop type in all years, while rapeseed always had the lowest share (4–12%; **Table 2**).

### Spatial Distribution of Soil Compaction Risk

**Figure 5** exemplarily shows the spatial distribution of soil compaction risk on 07 August 2017 for the depth of 40 cm. On this date, all soil compaction risk classes (“no risk” to “extremely high risk”) occurred in the study area, each with varying percentages of area (**Table 3**). In total, one quarter of the cropland area was not affected by field traffic, while another quarter revealed no soil compaction risk. The remaining area was distributed among the classes “low” to “extremely high” soil compaction risk, with the “extremely high” class having the highest share at 19.3%.

No field traffic occurred for maize and rapeseed as no field traffic was assumed for these crop types on this date. The plant height of maize prevents any field traffic without damaging the plants; rapeseed has already been harvested and the sowing of a subsequent crop is too early in the year. For sugar beet, the class “no risk” dominated (19.1%), while 2.9% of the sugar beet area had a “low” soil compaction risk. Thus, the risk classes “medium” to “extremely high” referred to the crop type cereals on this date.

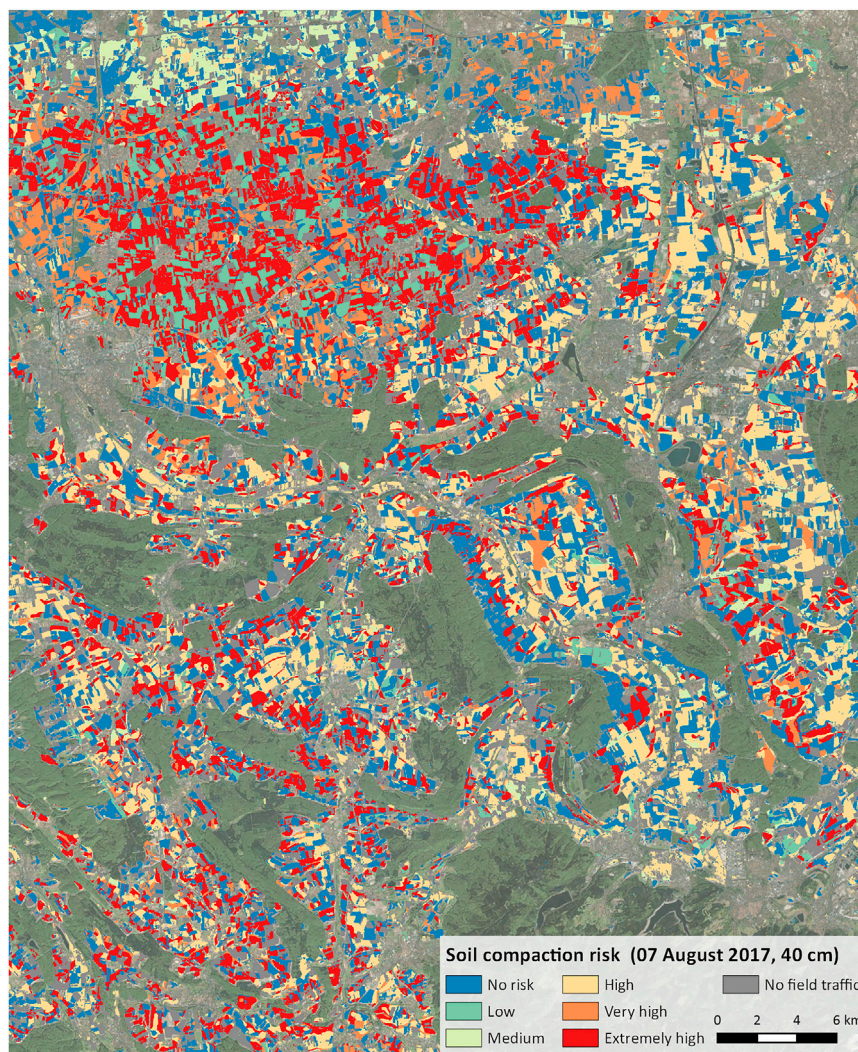
### Temporal Variation of Soil Compaction Risk

Summarizing all daily soil compaction risk maps of a year and calculating the area shares of each soil compaction risk class, results in a temporal overview of soil compaction risk (**Figures 6A–E**). Focusing on all years, there were periods without soil compaction risk, e.g., December and January. Here, no field traffic was assumed, thus no soil compaction could occur. During the rest of the year, the percentage of arable land, which was potentially affected by soil compaction, varies from 10 to 100%. Autumn was the period with most field traffic activities. The risk class “no risk” predominates in all years. The highest risk class “extremely high” mainly occurred in spring. From February to mid of June, all soil compaction risk classes occurred in all years, which was not the case in summer and autumn.

Comparing the years with each other, 2017 showed a distinctly different distribution of soil compaction risk. In particular from mid of July to November, the soil compaction risk was much higher than in all other years. For instance, the classes “high” to “extremely high” accounted for 43.6% of the arable land in mid of August. At the same time the year before and the years after, this

**TABLE 2 |** Absolute and percentage area of the classified crop types for the single years between 2016 and 2020.

Crop type	2016		2017		2018		2019		2020	
	ha	%	ha	%	ha	%	ha	%	ha	%
Cereals	77,155	66.3	62,880	54.1	76,065	65.4	62,594	53.8	78,722	67.7
Maize	14,312	12.3	16,805	14.4	12,308	10.6	17,754	15.3	9,843	8.5
Sugar beets	15,042	12.9	25,590	22.0	19,022	16.4	22,430	19.3	22,866	19.7
Rapeseed	9,800	8.4	11,034	9.5	8,914	7.7	13,530	11.6	4,878	4.2

**FIGURE 5 |** Spatial distribution of soil compaction risk on 07 August 2017 at a depth of 40 cm.

percentage ranged between 0.0 and 10.0%; the “extremely high risk” class was absent in August in any other year than 2017.

### Hot-Spots of Soil Compaction Risk Within the Region

Focusing on the class “extremely high” soil compaction risk enables the detection of areas that are mostly at risk for soil

compaction within the region. In a first step, all daily soil compaction risk maps with the class “extremely high” risk were summarized for each year (**Supplementary Figures S1–S5**). This yielded in the amount of days, on which a certain area/raster cell falls into the highest compaction risk class within 1 year. In 2016 and 2018–2020, the highest soil compaction risk class is absent in more than 90% of the cropland area. In 2017, however, only 60.3% of the area were

**TABLE 3** | Absolute and percentage area of soil compaction risk classes for the four crop types on 07 August 2017 at a depth of 40 cm.

Risk class	Cereals		Maize		Sugar beet		Rapeseed		Total	
	ha	%	ha	%	ha	%	ha	%	ha	%
No field traffic	0	0.0	16,805	14.4	0	0	11,034	9.5	27,839	23.9
No risk	6,435	5.5	0	0	22,197	19.1	0	0	28,632	24.6
Low	1,322	1.1	0	0	3,392	2.9	0	0	4,714	4.1
Medium	4,080	3.5	0	0	0	0	0	0	4,080	3.5
High	21,388	18.4	0	0	0	0	0	0	21,388	18.4
Very high	7,190	6.2	0	0	0	0	0	0	7,190	6.2
Extremely high	22,466	19.3	0	0	0	0	0	0	22,466	19.3

not at “extremely high” risk (**Table 4**). Additionally, the number of days with “extremely high” soil compaction risk is increased in 2017 compared to the four other years, e.g., 21,985 ha with 11–20 days of “extremely high” soil compaction risk **Table 4**.

In a second step, all soil compaction risk maps of the 5 years (= 1,827 days) with the class “extremely high” were summarized to identify the area of highest soil compaction risk (**Figure 7**). It showed that 39.8% of the cropland was exposed to “extremely high” soil compaction risk at least once during the entire study period (**Table 5**). Overall, 2.7% of the area revealed an “extremely high” soil compaction risk in each year. The areas, which were never or only once affected by “extremely high” soil compaction risk, were heterogeneously distributed across the study area. The north-western part of the study area showed a remarkable cluster with increased soil compaction risk.

Analyzing the 2.7% area exposed to “extremely high” soil compaction risk in all 5 years in more detail revealed that a high percentage of this area (40.3–86%) corresponds to the crop type cereals (**Table 6**), followed by maize with a share ranging between 12.0 and 28.7%. An exception was 2017, where cereals (40.3%) and sugar beets (39.1%) reached similar area percentages.

Focusing on the soil characteristics of the 2.7% area showed that the soil texture class “Ut4” (German classification scheme; clay content: 17–25%, silt content: 65–83%) predominated this area with 3,055 ha. Further affected soil texture classes were Sl2, Lt2 and Lu. However, almost all soil texture classes (Ls2, Lt2, Lt3, Lts, Lu, Sl2, Ss, Su3, Su4, Tu2, Tu3, Tu4, Uls, Us, Ut3, Ut4) occurred at the areas exposed to “extremely high” soil compaction risk in at least 1 year.

## DISCUSSION

### Spatio-Temporal Variation of Soil Compaction Risk

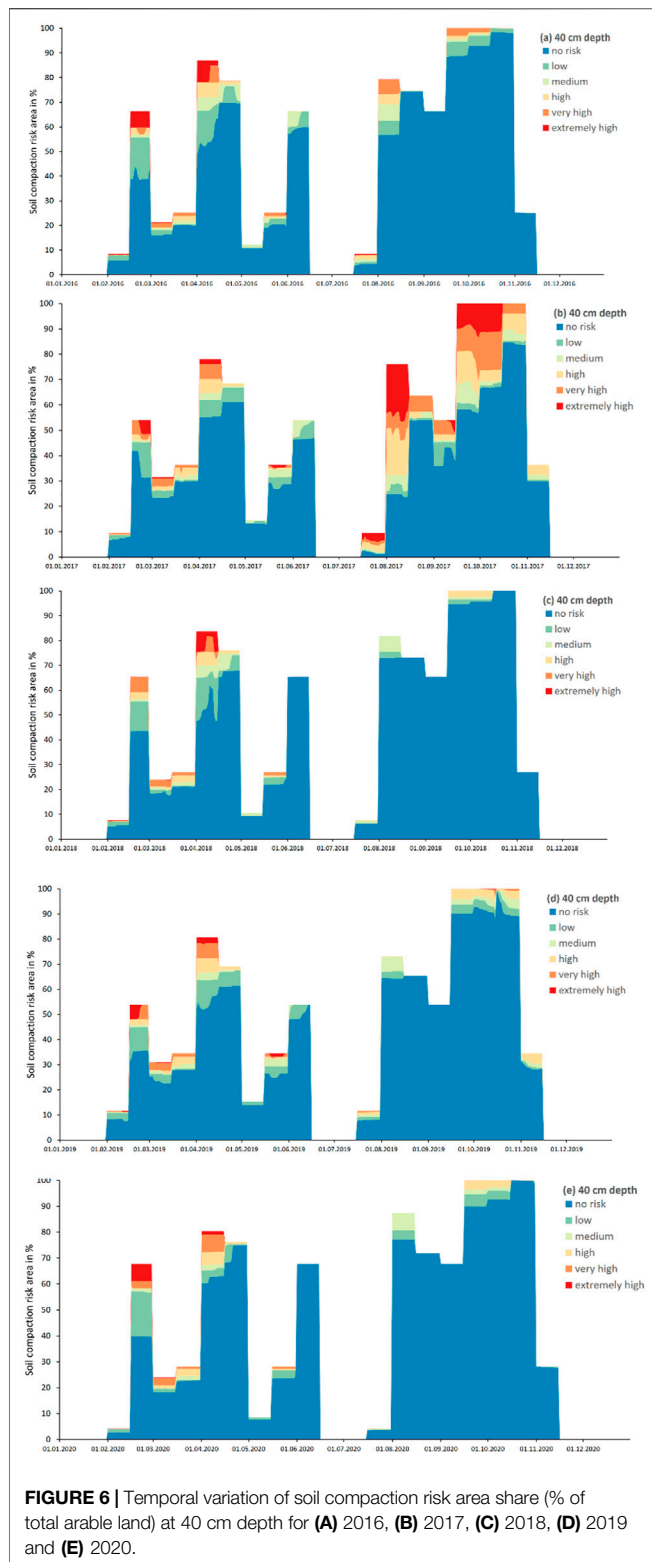
Our study showed the high spatio-temporal variation of soil compaction risk within a region. This applies to the annual changes in the same way as to the changes between the individual years.

These variations result from the interaction of actual soil strength and soil stress, which was calculated from the present crop type, soil data, weather data, machinery characteristics and field traffic days. The combination and interaction of these factors

resulted in a heterogenous distribution of soil compaction risk across the region (exemplarily shown in **Figure 5**). Cereals harvest with wheel loads of 8.2 Mg (**Supplementary Table S3**) and relatively wet soil conditions in 2017 (discussion below) resulted in an increased share of high to “extremely high” soil compaction risk at that date. The areas with sugar beets were less affected, as only spraying operation with wheel loads of 1.1/2.4 Mg were assumed, causing only “low” soil compaction risk (**Table 3**). The selected wheel loads represent typical ones for the study area. However, as wheel loads continuously increase in intensive agriculture (Keller et al., 2019; Kuhwald, 2019), higher wheel loads will frequently occur in the study area as well, resulting in higher soil stress and thus in higher soil compaction risk.

Weather is one highly variable and strongly influencing factor affecting variation of soil compaction risk, which exerts a large influence both within a year and between years. Within a year, spring is the period with the highest soil compaction risk in all years. The reason is a decreased evapotranspiration during winter, while precipitation is at a high level (**Figure 2**). Both factors increase soil moisture until spring. Generally, an increase in soil moisture leads to a decrease in soil strength (Rücknagel et al., 2012; Gut et al., 2015; Edwards et al., 2016). Thus, the soil strength is decreased to a minimum when field traffic activities occur in spring, usually in March and at the beginning of April. Consequently, it can be assumed that a high share of field traffic activities occurring at this time are associated with an increased soil compaction risk. Many field studies investigated the negative effects of field traffic in spring under wet soil conditions on soil functions (e.g., Schjønning et al., 2016; Pulido-Moncada et al., 2019; Ren et al., 2019).

During summer, evapotranspiration increases. The soils may become drier, which generally results in higher soil strength and lower soil compaction risk in general, as seen for the years 2016 and 2018–2020. In contrast, precipitation was higher in 2017. The mean annual precipitation was 750 mm this year, while it ranged between 454 and 641 mm in the other 4 years (DWD, 2021). Especially in July and August, the precipitation was significantly higher amounting to 278 mm in 2017 compared to 50–117 mm as registered for 2016 and 2018–2020 (**Figure 2**; **Supplementary Table S4**). The high amount of precipitation in summer increased the soil moisture even in the subsoil. Thus, the soil strength was reduced and the soil compaction risk noticeably increased in 2017 during cereal harvest. The effects of increased soil moisture were



also evident in autumn for 2017, where the soil compaction risk remained at a high level during maize and sugar beet harvest. The harvest of maize and sugar beets are accompanied with high wheel loads, resulting in high soil stress and increased soil

compaction risk (e.g., Peth et al., 2006; Barik et al., 2014; Duttman et al., 2014; Destain et al., 2016; Götze et al., 2016). Thus, an increased susceptibility to soil compaction can generally be expected for maize and sugar beet.

Nevertheless, modelled soil compaction risk was relatively low during autumn in 2016 and 2018–2020. These years were extremely dry (e.g., Zscheischler and Fischer, 2020; Kowalski et al., 2022), especially in the summer months. The dryness increased soil strength and resulted in a reduced soil compaction risk even for the heavy machineries used for maize and sugar beet harvest. Thus, an increased soil compaction risk in autumn can be expected for “normal” years, during which the precipitation is around the long-term average.

Overall, analyses of the spatio-temporal dynamics revealed that 1 year with increased precipitation can considerably affect the soil compaction risk. This is particularly problematic as soil compaction, especially subsoil compaction, can be persistent for many years (Etana et al., 2013; Keller et al., 2017; Keller et al., 2021; Seehusen et al., 2021). Thus, 1 year of increased soil compaction risk accompanied by unsuited field traffic activities can be sufficient to affect soil functions and soil health in the long term.

### Hot-Spots of Soil Compaction Risk

The hot-spot analysis revealed an area share of 2.7% that was exposed to the highest soil compaction risk class (“extremely high”) in each year of the 5-years period. From the perspective of sustainable soil use and soil protection, these areas are suggested to be the most endangered ones. In order to prevent harmful soil changes, they have to be managed carefully.

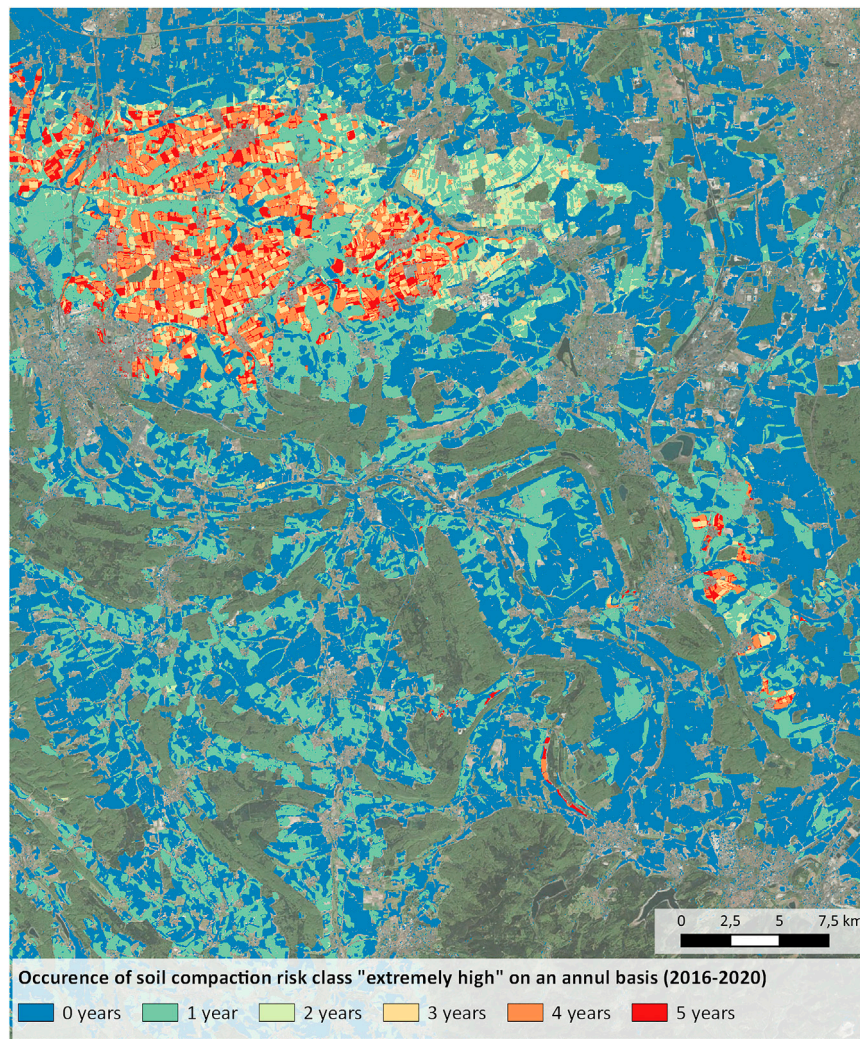
The soil texture class “Ut4” dominated the 2.7% area. Generally, silty clay soils are highly susceptible to soil compaction compared to other soil texture classes (Lorenz et al., 2016). In the study area, 260 soil profiles are characterized by the soil texture class “Ut4” at the investigated depth, representing an area of 39,574 ha. Out of these, only 54 soil profiles were part of the 2.7% hot-spot area. Thus, soil texture of “Ut4” is not necessarily associated with the highest soil compaction risk.

Focusing on the area that is affected at least in 1 year by the highest soil compaction risk class revealed an area share of 39.8%. The majority of these area is affected in 1 year (Table 5). As described above, soil compaction, especially subsoil compaction, is persistent and hardly to recover. Thus, even a one-time increased soil compaction risk can result in soil compaction that persists for many years if field traffic is conducted with machinery unsuitable for the current situation. In practice, this will not be the case for the entire 39.8% area; however, the analysis showed the high area share that is potentially affected.

As described above, the 5-years period was characterized by mainly dry years. The mean annual precipitation between 2016 and 2020 was 582 mm, while it was 680 mm between the years 2005 and 2015 (Supplementary Table S4). Lower precipitation and soil desiccation during the investigated period compared to previous years resulted in a potentially

**TABLE 4** | Absolute and percentage area of days with the class “extremely high” soil compaction risk summarized for each year (2016–2020).

Days	2016		2017		2018		2019		2020	
	ha	%	ha	%	ha	%	ha	%	ha	%
0	105,207	90.5	70,047	60.3	106,291	91.4	106,088	91.2	106,915	91.9
1–10	402	0.3	5,891	5.1	6,953	6.0	7,068	6.1	104	0.1
11–20	2,633	2.3	22,060	18.9	2,969	2.6	1,459	1.3	9,127	7.8
21–30	7,641	6.6	16,247	14.0	56	0.0	1,691	1.5	145	0.1
31–40	35	0.0	1,457	1.3	36	0.0	3	0.0	17	0.0
>40	391	0.3	607	0.5	4	0.0	0	0.0	0	0.0

**FIGURE 7** | Spatial location of hot-spots (class “extremely high” soil compaction risk) of soil compaction risk on an annual basis for the period 2016–2020.

underestimated hot-spot area. Thus, we assume that the area percentage of the highest risk class would have been larger when the weather and soil moisture conditions of a longer period would have been considered. However, it remains to be seen whether drier conditions will be the new “normal” in the study area.

The potential area exposed to high soil compaction risk will further increase when changing the definition of “hot-spot”. The presented hot-spot analysis was conducted for the “extremely high” soil compaction risk class. When considering the two highest classes (“very high” and “extremely high”), the hot-spot area increased considerably

**TABLE 5 |** Absolute and percentage area of hot-spots (containing only the class “extremely high” soil compaction risk) of soil compaction risk, grouped by number of years of their occurrence.

	Occurrence of class “extremely high” soil compaction risk in					
	0 years	1 year	2 years	3 years	4 years	5 years
Area share (in %)	60.2	26.8	2.1	2.5	5.7	2.7
Total area (in ha)	69,977	31,220	2,475	2,854	6,649	3,134

**TABLE 6 |** Absolute and percentage crop type area of the areas with every year soil compaction risk class “extremely high”.

	2016		2017		2018		2019		2020	
	ha	%	ha	%	ha	%	ha	%	ha	%
Cereals	2,487	79.4	1,263	40.3	2,199	70.2	1,906	60.8	2,696	86.0
Maize	50	16.2	503	16.0	844	26.9	899	28.7	376	12.0
Sugar beet	6	0.2	1,224	39.1	2	0.1	97	3.1	9	0.3
Rapeseed	134	4.3	143	4.6	88	2.8	231	7.4	52	1.7

**TABLE 7 |** Absolute and percentage area of hot-spots (containing the classes “very high” and “extremely high” soil compaction risk) of soil compaction risk, grouped by number of years of their occurrence.

	Occurrence of classess “very high” and “extremely high” soil compaction risk in					
	0 years	1 year	2 years	3 years	4 years	5 years
Area share (in %)	40.1	42.4	2.7	1.8	1.8	11.1
Total area (in ha)	46,678	49,369	3,185	2,076	2,145	12,854

(Table 7). The area share affected at least one time every year by “very high” and/or “extremely high” soil compaction risk was at 11.1%. Only 40% of the study area were never affected by “very high” and/or “extremely high” soil compaction risk.

The definition of the term “hot-spot” is therefore very important to provide information on the spatial extent of critical soil compaction risk. This also raises the question of how to assess the respective risk classes. The used approach classifies the soil compaction risk in five classes (Rücknagel et al., 2015; Götze et al., 2016). Terranimo, for instance, uses only three classes (Stettler et al., 2014), while Jones et al. (2003) uses four classes. It remains unclear, however, how these classes are to be evaluated. Is a “medium” soil compaction risk tolerable, or will it result in severe soil compaction? Thus, an evaluation of the calculated soil compaction risk is necessary, as exemplarily shown by Götze et al. (2016), in order to derive the critical risk classes.

## Advances and Limitations of the Soil Compaction Risk Analysis

Generally, it must be kept in mind that the used SaSCiA-model calculates the risk of soil compaction. Thus, the model does not predict the real occurrence and distribution of soil compaction, but indicates where soil compaction is likely to occur. Furthermore, the SaSCiA-model has some limitations, which are discussed in detail by Kuhwald et al. (2018). An

important limitation is that the wheel pass frequency is not considered in the SaSCiA-model, although the amount of wheel passes has an impact on soil compaction (e.g., Botta et al., 2009; Pulido-Moncada et al., 2019). Another limitation is associated with the raster approach, which leads to the fact that the entire raster cell is always affected by field traffic. This results in an overestimation of the risk area, since almost never all parts of a field are wheeled during one field traffic activity (except for sugar beet harvest with a self-propelled harvester; Augustin et al., 2020).

However, two limitations of the original SaSCiA-version were addressed in the present study. The first one was the use of all available weather stations (a total of 55 stations) within the federal state to regionalize the weather information; in the original approach, only one weather station was used (cf. Kuhwald et al., 2018). Thus, spatial variations, e.g., in precipitation, could be accounted for in the 5-years analysis. The second one was the use of a soil map at a scale of 1:50.000 instead of a soil map of 1:200.000 (Kuhwald et al., 2018), which increased the accuracy of the spatial representation of soil characteristics. However, even a soil map of at a scale of 1:50.000 shows a relatively coarse spatial resolution compared to a Sentinel 2-pixel size of 20 m. Therefore, a higher spatial resolution soil map is needed to increase the reliability of the soil compaction risk assessment, but is not yet available for the region.

Independent on model limitations, the model approach and model results may be useful to support sustainable soil use and soil protection.

## CONCLUSION

This study modelled the spatio-temporal soil compaction risk on a daily basis for 5 years for a region. Thus, for the first time, it was feasible to analyze and show how the dynamic characteristic of soil compaction risk vary in space and time over such a long period of time with high spatial (20 m) and temporal (daily) resolution.

One main result of this analysis is that 1 year of increased precipitation can contribute to a tremendous increase in soil compaction risk, which was the case in this study in 2017. Another important finding was that 2.7% of the area exhibited the highest soil compaction risk class (“extremely high”) in each year of the study period. Looking at the areas that were affected by “extremely high” soil compaction risk at least once, this percentage increased to 39.8%.

As discussed above, soil compaction is persistence and many years are required to reach the pre-soil compaction state, if it is achievable at all. Assuming a share of nearly 40% of compacted soil in the study area would therefore have strong environmental effects and will reduce the yield substantially. However, the modelled results show the risk of soil compaction, not the actual state. But by identifying the risk, the extent of possible soil degradation becomes apparent.

Thus, this study may contribute to increased awareness of soil compaction risk dynamics in order to mitigate further soil degradation. In this sense, a next step must be the integration of weather forecast to enable the prediction of soil compaction risk for the following days. This prediction will enable to decide on which day a field might be trafficked by identifying the day with the lowest soil compaction risk.

## DATA AVAILABILITY STATEMENT

The data analyzed in this study is subject to the following licenses/restrictions: - The soil map used (BK 50) must be paid for use. - The weather data used is free available ([https://opendata.dwd.de/climate\\_environment/CDC/](https://opendata.dwd.de/climate_environment/CDC/))—The satellite

data used is free available (Sentinel 2; <https://scihub.copernicus.eu/>). Requests to access these datasets should be directed to [https://opendata.dwd.de/climate\\_environment/CDC/](https://opendata.dwd.de/climate_environment/CDC/); <https://scihub.copernicus.eu/>.

## AUTHOR CONTRIBUTIONS

MK designed the study, conducted the modelling, analyzed the data and wrote the majority of the text. KK prepared the satellite data, conducted the crop type classification and contributed to the text. RD contributed in reviewing and finalizing the manuscript.

## FUNDING

The Federal Ministry of Education and Research (BMBF) supported this study within the framework of the BonaRes-initiative (Grant No.: 031B1065C). We acknowledge financial support for publications cost by Land Schleswig-Holstein within the funding programme Open Access Publikationsfonds.

## ACKNOWLEDGMENTS

We are grateful to the Rebecca Kessler, Franziska Wagner, Frida Schneeberg and Celina Thomas, who conducted the crop type mapping in the field. We thank the reviewers who improved the manuscript with helpful comments.

## SUPPLEMENTARY MATERIAL

The Supplementary Material for this article can be found online at: <https://www.frontiersin.org/articles/10.3389/fenvs.2022.823030/full#supplementary-material>

## REFERENCES

- Alaoui, A., Rogger, M., Peth, S., and Blöschl, G. (2018). Does Soil Compaction Increase Floods? A Review. *J. Hydrol.* 557, 631–642. doi:10.1016/j.jhydrol.2017.12.052
- Arvidsson, J., and Håkansson, I. (2014). Response of Different Crops to Soil Compaction-Short-Term Effects in Swedish Field Experiments. *Soil Tillage Res.* 138, 56–63. doi:10.1016/j.still.2013.12.006
- Arvidsson, J., and Keller, T. (2007). Soil Stress as Affected by Wheel Load and Tyre Inflation Pressure. *Soil Tillage Res.* 96, 284–291. doi:10.1016/j.still.2007.06.012
- Augustin, K., Kuhwald, M., Brunotte, J., and Duttman, R. (2019). FiTraM: A Model for Automated Spatial Analyses of Wheel Load, Soil Stress and Wheel Pass Frequency at Field Scale. *Biosyst. Eng.* 180, 108–120. doi:10.1016/j.biosystemseng.2019.01.019
- Augustin, K., Kuhwald, M., Brunotte, J., and Duttman, R. (2020). Wheel Load and Wheel Pass Frequency as Indicators for Soil Compaction Risk: A Four-Year Analysis of Traffic Intensity at Field Scale. *Geosciences* 10, 292. doi:10.3390/geosciences10080292
- Barik, K., Aksakal, E. L., Islam, K. R., Sari, S., and Angin, I. (2014). Spatial Variability in Soil Compaction Properties Associated with Field Traffic Operations. *CATENA* 120, 122–133. doi:10.1016/j.catena.2014.04.013
- Belgiu, M., and Drăguț, L. (2016). Random forest in Remote Sensing: A Review of Applications and Future Directions. *ISPRS J. Photogrammetry Remote Sensing* 114, 24–31. doi:10.1016/j.isprsjprs.2016.01.011
- Berisso, F. E., Schjonning, P., Lamandé, M., Weisskopf, P., Stettler, M., and Keller, T. (2013). Effects of the Stress Field Induced by a Running Tyre on the Soil Pore System. *Soil Tillage Res.* 131, 36–46. doi:10.1016/j.still.2013.03.005
- Boden, Ad-Hoc-A. G. (2005). *Bodenkundliche Kartieranleitung*. 5. Stuttgart: Aufl.Hannover. Schweizbart.
- Botta, G. F., Becerra, A. T., and TournBellora, F. B. (2009). Effect of the Number of Tractor Passes on Soil Rut Depth and Compaction in Two Tillage Regimes. *Soil Tillage Res.* 103, 381–386. doi:10.1016/j.still.2008.12.002
- D’Or, D., and Destain, M.-F. (2014). Toward a Tool Aimed to Quantify Soil Compaction Risks at a Regional Scale: Application to Wallonia (Belgium). *Soil Tillage Res.* 144, 53–71. doi:10.1016/j.still.2014.06.008
- Daigh, A. L. M., DeJong-Hughes, J., and Acharya, U. (2020). Projections of Yield Losses and Economic Costs Following Deep Wheel-traffic Compaction during the 2019 Harvest. *Agric. Environ. Lett.* 5, e20013. doi:10.1002/ael2.20013
- Destain, M.-F., Roisin, C., Dalcq, A.-S., and Mercatoris, B. C. N. (2016). Effect of Wheel Traffic on the Physical Properties of a Luvisol. *Geoderma* 262, 276–284. doi:10.1016/j.geoderma.2015.08.028

- DIN V 19688 (2011). *Soil Quality - Determination of Compactibility Risk of mineral Sub-soils Based on the Assessed Preconsolidation Stress*.
- Diserens, E. (2009). Calculating the Contact Area of Trailer Tyres in the Field. *Soil Tillage Res.* 103, 302–309. doi:10.1016/j.still.2008.10.020
- Diserens, E. (2002). Ermittlung der Reifen-Kontaktfläche im Feld mittels Rechenmodell: Eine wichtige Voraussetzung, um die Bodenbeanspruchung im Ackerbau zu beurteilen. *FAT Berichte* 1–11.
- Duttman, R., Augustin, K., Brunotte, J., and Kuhwald, M. (2021). *Modeling of Field Traffic Intensity and Soil Compaction Risks in Agricultural Landscapes*. (accepted).
- Duttman, R., Brunotte, J., and Bach, M. (2013). Spatial Analyses of Field Traffic Intensity and Modeling of Changes in Wheel Load and Ground Contact Pressure in Individual fields during a Silage maize Harvest. *Soil Tillage Res.* 126, 100–111. doi:10.1016/j.still.2012.09.001
- Duttman, R., Schwanebeck, M., Nolde, M., and Horn, R. (2014). Predicting Soil Compaction Risks Related to Field Traffic during Silage maize Harvest. *Soil Sci. Soc. America J.* 78, 408–421. doi:10.2136/sssaj2013.05.0198
- DVWK 234 (1995). *Gefügestabilität Ackerbaulich Genutzter Mineralböden - Teil 1: Mechanische Belastbarkeit*.
- DWD (2021). *Climate Data Center (CDC)*.
- Edwards, G., White, D. R., Munkholm, L. J., Sørensen, C. G., and Lamandé, M. (2016). Modelling the Readiness of Soil for Different Methods of Tillage. *Soil Tillage Res.* 155, 339–350. doi:10.1016/j.still.2015.08.013
- Etana, A., Larsbo, M., Keller, T., Arvidsson, J., Schjønning, P., Forkman, J., et al. (2013). Persistent Subsoil Compaction and its Effects on Preferential Flow Patterns in a Loamy till Soil. *Geoderma* 192, 430–436. doi:10.1016/j.geoderma.2012.08.015
- FAO (2015). Status of the World's Soil Resources. Main Report.
- FAO (2014). *World Reference Base for Soil Resources. International Soil Classification System for Naming Soils and Creating Legends for Soil Maps*. Rome: World Soil Resources Report 106.
- Food, G. M. (2002). Status of Land Cover Classification Accuracy Assessment. *Remote Sensing Environ.* 80, 185–201. doi:10.1016/S0034-4257(01)00295-4
- Gebhardt, S., Fleige, H., and Horn, R. (2009). Effect of Compaction on Pore Functions of Soils in a Saalean Moraine Landscape in North Germany. *Z. Pflanzenernähr. Bodenk.* 172, 688–695. doi:10.1002/jpln.200800073
- Götze, P., Rücknagel, J., Jacobs, A., Märländer, B., Koch, H.-J., and Christen, O. (2016). Environmental Impacts of Different Crop Rotations in Terms of Soil Compaction. *J. Environ. Manage.* 181, 54–63. doi:10.1016/j.jenvman.2016.05.048
- Graves, A. R., Morris, J., Deeks, L. K., Rickson, R. J., Kibblewhite, M. G., Harris, J. A., et al. (2015). The Total Costs of Soil Degradation in England and Wales. *Ecol. Econ.* 119, 399–413. doi:10.1016/j.ecolecon.2015.07.026
- Gut, S., Chervet, A., Stettler, M., Weisskopf, P., Sturny, W. G., Lamandé, M., et al. (2015). Seasonal Dynamics in Wheel Load-Carrying Capacity of a Loam Soil in the Swiss Plateau. *Soil Use Manage* 31, 132–141. doi:10.1111/sum.12148
- Hamer, W. (2019). *Whamer/papros: Papros-Pathogen PROgnosis System*.
- Hartmann, P., Zink, A., Fleige, H., and Horn, R. (2012). Effect of Compaction, Tillage and Climate Change on Soil Water Balance of Arable Luvisols in Northwest Germany. *Soil Tillage Res.* 124, 211–218. doi:10.1016/j.still.2012.06.004
- Horn, R., Domżał, H., Słowińska-Jurkiewicz, A., and van Ouwerkerk, C. (1995). Soil Compaction Processes and Their Effects on the Structure of Arable Soils and the Environment. *Soil Tillage Res.* 35, 23–36. doi:10.1016/0167-1987(95)00479-C
- Horn, R., and Fleige, H. (2003). A Method for Assessing the Impact of Load on Mechanical Stability and on Physical Properties of Soils. *Soil Tillage Res.* 73, 89–99. doi:10.1016/S0167-1987(03)00102-8
- Horn, R., Fleige, H., Richter, F.-H., Czyz, E. A., Dexter, A., Diaz-Pereira, E., et al. (2005). SIDASS Project. *Soil Tillage Res.* 82, 47–56. doi:10.1016/j.still.2005.01.007
- Horn, R., and Fleige, H. (2009). Risk Assessment of Subsoil Compaction for Arable Soils in Northwest Germany at Farm Scale. *Soil Tillage Res.* 102, 201–208. doi:10.1016/j.still.2008.07.015
- Horn, R., Simota, C., Fleige, H., Dexter, A., Rajkai, K., and de la Rosa, D. (2002). Prognose der mechanischen Belastbarkeit und der auflastabhängigen Änderung des Lufthaushaltes in Ackerböden anhand von Bodenkarten. *Z. für Pflanzenernährung Bodenkunde* 165, 235–239. doi:10.1002/1522-2624(200204)165:2<235::aid-jpln235>3.0.co;2-h
- Horn, R. (2003). Stress-strain Effects in Structured Unsaturated Soils on Coupled Mechanical and Hydraulic Processes. *Geoderma* 116, 77–88. doi:10.1016/S0016-7061(03)00095-8
- Horn, R., Way, T., and Rostek, J. (2003). Effect of Repeated Tractor wheeling on Stress/strain Properties and Consequences on Physical Properties in Structured Arable Soils. *Soil Tillage Res.* 73, 101–106. doi:10.1016/S0167-1987(03)00103-X
- Immitzer, M., Vuolo, F., and Atzberger, C. (2016). First Experience with Sentinel-2 Data for Crop and Tree Species Classifications in Central Europe. *Remote Sensing* 8, 166. doi:10.3390/rs8030166
- Jones, R. J. A., Spoor, G., and Thomasson, A. J. (2003). Vulnerability of Subsoils in Europe to Compaction: a Preliminary Analysis. *Soil Tillage Res.* 73, 131–143. doi:10.1016/S0167-1987(03)00106-5
- Kandziora, M., Dörnhöfer, K., Oppelt, N., and Müller, F. (2014). Detecting Land Use and Land Cover Changes in Northern German Agricultural Landscapes to Assess Ecosystem Service Dynamics. *Landscape Online* 1–24. doi:10.3097/lo.201435
- Karasiak, N. (2016). *Dzetsaka Qgis Classification Plugin*.
- Keller, T. (2005). A Model for the Prediction of the Contact Area and the Distribution of Vertical Stress below Agricultural Tyres from Readily Available Tyre Parameters. *Biosyst. Eng.* 92, 85–96. doi:10.1016/j.biosystemseng.2005.05.012
- Keller, T., Arvidsson, J., Schjønning, P., Lamandé, M., Stettler, M., and Weisskopf, P. (2012). *In Situ* Subsoil Stress-Strain Behavior in Relation to Soil Precompression Stress. *Soil Sci.* 177, 490–497. doi:10.1097/SS.0b013e318262554e
- Keller, T., Colombi, T., Ruiz, S., Manalili, M. P., Rek, J., Stadelmann, V., et al. (2017). Long-Term Soil Structure Observatory for Monitoring Post-Compaction Evolution of Soil Structure. *Vadose Zone J.* 16. doi:10.2136/vzj2016.11.0118
- Keller, T., Colombi, T., Ruiz, S., Schymanski, S. J., Weisskopf, P., Koestel, J., et al. (2021). Soil Structure Recovery Following Compaction: Short-term Evolution of Soil Physical Properties in a Loamy Soil. *Soil Sci. Soc. Am. J.* 85, 1002–1020. doi:10.1002/saj2.20240
- Keller, T., Défossez, P., Weisskopf, P., Arvidsson, J., and Richard, G. (2007). SoilFlex: A Model for Prediction of Soil Stresses and Soil Compaction Due to Agricultural Field Traffic Including a Synthesis of Analytical Approaches. *Soil Tillage Res.* 93, 391–411. doi:10.1016/j.still.2006.05.012
- Keller, T., Sandin, M., Colombi, T., Horn, R., and Or, D. (2019). Historical Increase in Agricultural Machinery Weights Enhanced Soil Stress Levels and Adversely Affected Soil Functioning. *Soil Tillage Res.* 194, 104293–104312. doi:10.1016/j.still.2019.104293
- Koolen, A. J., Lerink, P., Kurstjens, D. A. G., van den Akker, J. J. H., and Arts, W. B. M. (1992). Prediction of Aspects of Soil-Wheel Systems. *Soil Tillage Res.* 24, 381–396. doi:10.1016/0167-1987(92)90120-Z
- Kowalski, K., Okujeni, A., Brell, M., and Hostert, P. (2022). Quantifying Drought Effects in Central European Grasslands through Regression-Based Unmixing of Intra-annual Sentinel-2 Time Series. *Remote Sensing Environ.* 268, 112781. doi:10.1016/j.rse.2021.112781
- Kroulik, M., Kumbhála, F., Hula, J., and Honzik, I. (2009). The Evaluation of Agricultural Machines Field Trafficking Intensity for Different Soil Tillage Technologies. *Soil Tillage Res.* 105, 171–175. doi:10.1016/j.still.2009.07.004
- Kuhwald, M. (2019). *Detection and Modelling of Soil Compaction of Arable Soils: From Field Survey to Regional Risk Assessment*, 1–108.
- Kuhwald, M., Dörnhöfer, K., Oppelt, N., and Duttman, R. (2018). Spatially Explicit Soil Compaction Risk Assessment of Arable Soils at Regional Scale: The SaSCiA-Model. *Sustainability* 10, 1618–1629. doi:10.3390/su10051618
- Lamandé, M., Greve, M. H., and Schjønning, P. (2018). Risk Assessment of Soil Compaction in Europe - Rubber Tracks or Wheels on Machinery. *CATENA* 167, 353–362. doi:10.1016/j.catena.2018.05.015
- Lamandé, M., and Schjønning, P. (2011). Transmission of Vertical Stress in a Real Soil Profile. Part I: Site Description, Evaluation of the Söhne Model, and the Effect of Topsoil Tillage. *Soil Tillage Res.* 114, 57–70. doi:10.1016/j.still.2011.05.004
- LBEG (2020). *Bodenkarte 1:50.000 (BK 50). Landesamt für Bergbau, Energie und Geologie (LBEG)*. Hannover, Germany.

- Lebert, M. (2010). Entwicklung eines Prüfkonzepthes zur Erfassung der tatsächlichen Verdichtungsgefährdung landwirtschaftlich genutzter Böden. *UBA-Texte*, 1–96.
- Lebert, M., and Horn, R. (1991). A Method to Predict the Mechanical Strength of Agricultural Soils. *Soil Tillage Res.* 19, 275–286. doi:10.1016/0167-1987(91)90095-F
- Ledermüller, S., Lorenz, M., Brunotte, J., and Fröba, N. (2018). A Multi-Data Approach for Spatial Risk Assessment of Topsoil Compaction on Arable Sites. *Sustainability* 10, 2915–2922. doi:10.3390/su10082915
- Lorenz, M., Brunotte, J., Vorderbrügge, T., Brandhuber, R., Koch, H.-J., Senger, M., et al. (2016). Adaptation of Load Input by Agricultural Machines to the Susceptibility of Soil to Compaction - Principles of Soil Conserving Traffic on Arable Land. *Appl. Agric. For. Res.*, 101–144. doi:10.3220/LBF1473334823000
- Moeys, J. (2018). *Soiltexture: Functions for Soil Texture Plot, Classification and Transformation*.
- Müller-Wilm, U. (2016). *S2PAD SEN2COR 2.2.0 -Readme, S2PAD-VEGA-SRN-0001*.
- Nendel, C., Berg, M., Kersebaum, K. C., Mirschel, W., Specka, X., Wegehenkel, M., et al. (2011). The MONICA Model: Testing Predictability for Crop Growth, Soil Moisture and Nitrogen Dynamics. *Ecol. Model.* 222, 1614–1625. doi:10.1016/j.ecolmodel.2011.02.018
- Peth, S., Horn, R., Fazekas, O., and Richards, B. G. (2006). Heavy Soil Loading its Consequence for Soil Structure, Strength, Deformation of Arable Soils. *Z. Pflanzenernähr. Bodenk.* 169, 775–783. doi:10.1002/jpln.200620112
- Pulido-Moncada, M., Munkholm, L. J., and Schjønning, P. (2019). Wheel Load, Repeated wheeling, and Traction Effects on Subsoil Compaction in Northern Europe. *Soil Tillage Res.* 186, 300–309. doi:10.1016/j.still.2018.11.005
- R Core Team (2020). *R: A Language and Environment for Statistical Computing*. Vienna, Austria: R foundation for Statistical Computing.
- Rathjens, H., Dörnhöfer, K., and Oppelt, N. (2014). IRSel-An Approach to Enhance Continuity and Accuracy of Remotely Sensed Land Cover Data. *Int. J. Appl. Earth Observation Geoinformation* 31, 1–12. doi:10.1016/j.jag.2014.02.010
- Ren, L., D'Hose, T., Ruysschaert, G., De Pue, J., Meftah, R., Cnudde, V., et al. (2019). Effects of Soil Wetness and Tyre Pressure on Soil Physical Quality and maize Growth by a Slurry Spreader System. *Soil Tillage Res.* 195, 104344. doi:10.1016/j.still.2019.104344
- Rücknagel, J., Christen, O., Hofmann, B., and Ulrich, S. (2012). A Simple Model to Estimate Change in Precompression Stress as a Function of Water Content on the Basis of Precompression Stress at Field Capacity. *Geoderma* 178, 1–7. doi:10.1016/j.geoderma.2012.01.035
- Rücknagel, J., Götze, P., Hofmann, B., Christen, O., and Marschall, K. (2013). The Influence of Soil Gravel Content on Compaction Behaviour and Pre-compression Stress. *Geoderma* 209, 226–232. doi:10.1016/j.geoderma.2013.05.030
- Rücknagel, J., Hofmann, B., Deumelandt, P., Reinicke, F., Bauhardt, J., Hülsbergen, K.-J., et al. (2015). Indicator Based Assessment of the Soil Compaction Risk at Arable Sites Using the Model REPRO. *Ecol. Indicators* 52, 341–352. doi:10.1016/j.ecolind.2014.12.022
- Schjønning, P., Lamandé, M., Keller, T., Pedersen, J., and Stettler, M. (2012). Rules of Thumb for Minimizing Subsoil Compaction. *Soil Use Manag.* 28, 378–393. doi:10.1111/j.1475-2743.2012.00411.x
- Schjønning, P., and Lamandé, M. (2018). Models for Prediction of Soil Precompression Stress from Readily Available Soil Properties. *Geoderma* 320, 115–125. doi:10.1016/j.geoderma.2018.01.028
- Schjønning, P., Lamandé, M., Munkholm, L. J., Lyngvig, H. S., and Nielsen, J. A. (2016). Soil Precompression Stress, Penetration Resistance and Crop Yields in Relation to Differently-Trafficked, Temperate-Region sandy Loam Soils. *Soil Tillage Res.* 163, 298–308. doi:10.1016/j.still.2016.07.003
- Schjønning, P., Lamandé, M., Tøgersen, F. A., Arvidsson, J., and Keller, T. (2008). Modelling Effects of Tyre Inflation Pressure on the Stress Distribution Near the Soil-Tyre Interface. *Biosyst. Eng.* 99, 119–133. doi:10.1016/j.biosystemseng.2007.08.005
- Schjønning, P., Stettler, M., Keller, T., Lassen, P., and Lamandé, M. (2015a). Predicted Tyre-Soil Interface Area and Vertical Stress Distribution Based on Loading Characteristics. *Soil Tillage Res.* 152, 52–66. doi:10.1016/j.still.2015.03.002
- Schjønning, P., van den Akker, J. J. H., Keller, T., Greve, M. H., Lamandé, M., Simojoki, A., et al. (2015b). “Driver-Pressure-State-Impact-Response (DPSIR) Analysis and Risk Assessment for Soil Compaction-A European Perspective,” in *Advances in Agronomy*. Editor D. L. Sparks, 183–237. doi:10.1016/bs.agron.2015.06.001
- Seehusen, T., Mordhorst, A., Riggert, R., Fleige, H., Horn, R., and Riley, H. (2021). Subsoil Compaction of a clay Soil in South-East Norway and its Amelioration after 5 Years. *Int. Agrophys.* 35, 145–157. doi:10.31545/intagr/135513
- Seehusen, T., Riggert, R., Fleige, H., Horn, R., and Riley, H. (2019). Soil Compaction and Stress Propagation after Different wheeling Intensities on a silt Soil in South-East Norway. *Acta Agriculturae Scand. Section B - Soil Plant Sci.* 69, 343–355. doi:10.1080/09064710.2019.1576762
- Stettler, M., Keller, T., Weisskopf, P., Lamandé, M., Lassen, P., and Schjønning, P. (2014). Terranimo- a Web-Based Tool for Evaluating Soil Compaction. *Landtechnik* 69 (3), 132–138.
- Szatanik-Kloc, A., Horn, R., Lipiec, J., Siczek, A., and Szerement, J. (2018). Soil Compaction-Induced Changes of Physicochemical Properties of Cereal Roots. *Soil Tillage Res.* 175, 226–233. doi:10.1016/j.still.2017.08.016
- Techen, A.-K., Helming, K., Brüggemann, N., Veldkamp, E., Reinhold-Hurek, B., Lorenz, M., et al. (2020). “Soil Research Challenges in Response to Emerging Agricultural Soil Management Practices,” in *Advances in Agronomy*. Editor D. L. Sparks (Amsterdam: Academic Press), 179–240. doi:10.1016/bs.agron.2020.01.002
- van den Akker, J. J. H., and Hoogland, T. (2011). Comparison of Risk Assessment Methods to Determine the Subsoil Compaction Risk of Agricultural Soils in The Netherlands. *Soil Tillage Res.* 114, 146–154. doi:10.1016/j.still.2011.04.002
- van den Akker, J. J. H. (2004). SOCOMO: a Soil Compaction Model to Calculate Soil Stresses and the Subsoil Carrying Capacity. *Soil Tillage Res.* 79, 113–127. doi:10.1016/j.still.2004.03.021
- Weisskopf, P., Reiser, R., Rek, J., and Oberholzer, H.-R. (2010). Effect of Different Compaction Impacts and Varying Subsequent Management Practices on Soil Structure, Air Regime and Microbiological Parameters. *Soil Tillage Res.* 111, 65–74. doi:10.1016/j.still.2010.08.007
- Wessolek, G., Kaupenjohann, M., and Renger, M. (2009). *Bodenökologie und Bodengenese*. Bodenphysikalische Kennwerte und Berechnungsverfahren für die Praxis
- Zscheischler, J., and Fischer, E. M. (2020). The Record-Breaking Compound Hot and Dry 2018 Growing Season in Germany. *Weather Clim. Extremes* 29, 100270. doi:10.1016/j.wace.2020.100270

**Conflict of Interest:** The authors declare that the research was conducted in the absence of any commercial or financial relationships that could be construed as a potential conflict of interest.

**Publisher's Note:** All claims expressed in this article are solely those of the authors and do not necessarily represent those of their affiliated organizations, or those of the publisher, the editors, and the reviewers. Any product that may be evaluated in this article, or claim that may be made by its manufacturer, is not guaranteed or endorsed by the publisher.

Copyright © 2022 Kuhwald, Kuhwald and Duttman. This is an open-access article distributed under the terms of the Creative Commons Attribution License (CC BY). The use, distribution or reproduction in other forums is permitted, provided the original author(s) and the copyright owner(s) are credited and that the original publication in this journal is cited, in accordance with accepted academic practice. No use, distribution or reproduction is permitted which does not comply with these terms.



# Soil Health: New Opportunities to Innovate in Crop Protection Research and Development

L. W. Atwood<sup>1†</sup>, K. A. Racette<sup>1†</sup>, M. Diggelmann<sup>2</sup>, C. A. Masala<sup>2</sup>, S. Maund<sup>2\*</sup>, R. Oliver<sup>3</sup>, C. Screpanti<sup>2</sup>, M. Wironen<sup>1</sup> and S. A. Wood<sup>1,4</sup>

<sup>1</sup>The Nature Conservancy, Arlington, VA, United States, <sup>2</sup>Syngenta, Basel, Switzerland, <sup>3</sup>Syngenta, Jealott's Hill, United Kingdom, <sup>4</sup>Yale School of the Environment, New Haven, CT, United States

## OPEN ACCESS

### Edited by:

Lucy Crockford,  
Harper Adams University,  
United Kingdom

### Reviewed by:

Cristina Lazcano,  
University of California, Davis,  
United States  
Yansheng Li,  
Northeast Institute of Geography and  
Agroecology (CAS), China

### \*Correspondence:

K. A. Racette  
kelly.racette@tnc.org  
S. Maund  
steve.maund@syngenta.com

<sup>†</sup>These authors share first authorship

### Specialty section:

This article was submitted to  
Soil Processes,  
a section of the journal  
Frontiers in Environmental Science

**Received:** 24 November 2021

**Accepted:** 09 February 2022

**Published:** 09 March 2022

### Citation:

Atwood LW, Racette KA,  
Diggelmann M, Masala CA, Maund S,  
Oliver R, Screpanti C, Wironen M and  
Wood SA (2022) Soil Health: New  
Opportunities to Innovate in Crop  
Protection Research  
and Development.  
Front. Environ. Sci. 10:821742.  
doi: 10.3389/fenvs.2022.821742

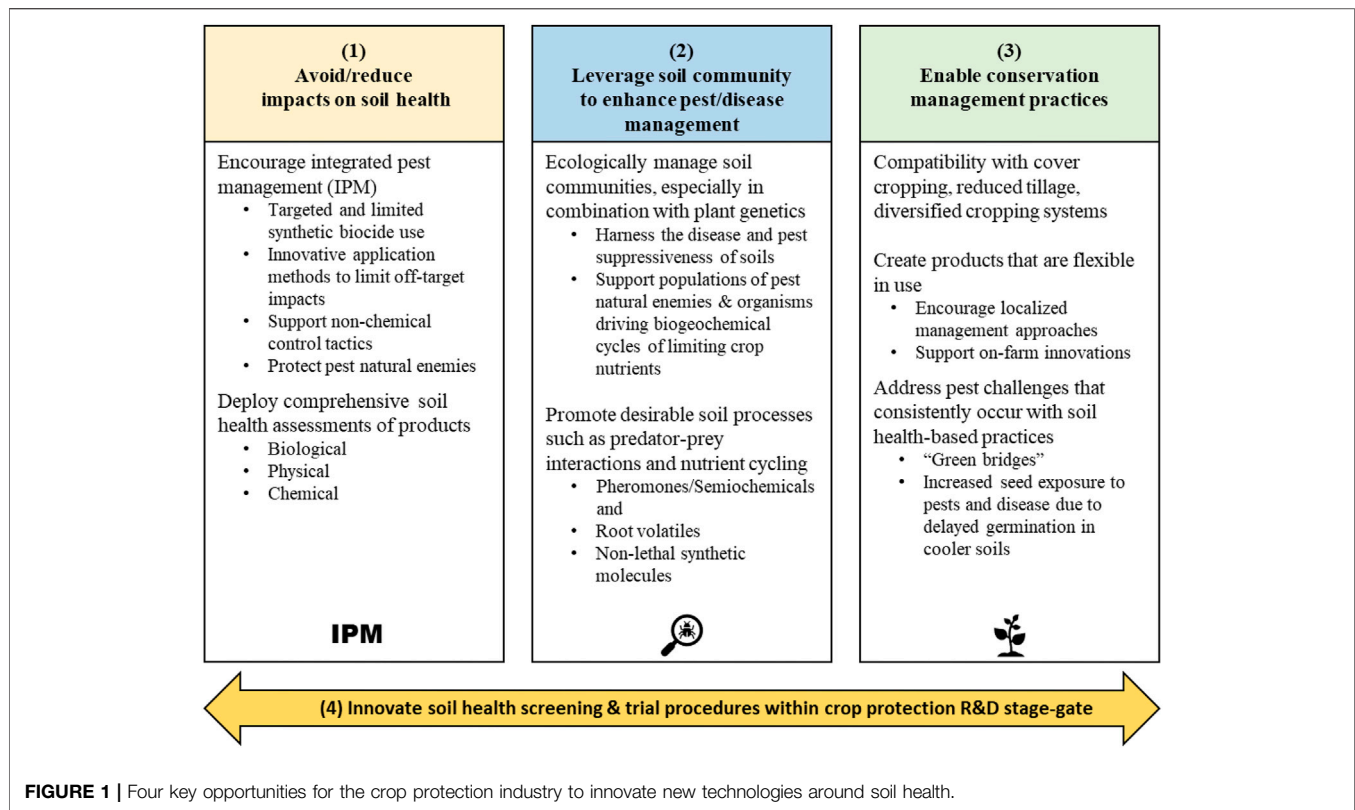
Soil health-based agricultural management practices are widely promoted to reduce erosion, increase nutrient use efficiency, improve soil structure, and sustain or increase yields. Pest and disease management are less frequently considered as components of a soil health management system. We present a framework for how the crop protection industry can advance soil health by developing systems of crop protection innovation that simultaneously target soil health outcomes, either through direct impact on soil or by enabling practices that promote soil health outcomes. Such an approach could lead to cross-sectoral, integrated agricultural solutions that achieve agronomic, environmental, and economic goals.

**Keywords:** soil health, crop protection, research and development, sustainable agriculture, innovation framework, ecological pest management

## INTRODUCTION

The concept of soil health has united farmers, researchers, government agencies, non-profits, and the private sector around the possibility that management of agroecosystems can meaningfully contribute to solving major environmental challenges. Soil health is a multi-dimensional concept that refers to the ability of soil to serve as an ecosystem that sustains plants and animals while supporting human uses such as agriculture and forestry (Lehmann et al., 2020). Decades of evidence has illustrated the agronomic and environmental benefits of agricultural practices such as cover cropping, reduced tillage, and diversified crop rotations (Atwood and Wood, 2021). These soil health practices align with the principles of conservation agriculture: maintain living plant cover, reduce disturbance, and diversify crop rotations. While the benefits of these practices on soil-derived ecosystem services can vary (Palm et al., 2014), there is considerable opportunity to increase the adoption, and thus the benefits, of agronomic practices that reduce erosion and nutrient loss, rebuild soil carbon, and sustain agronomic production.

Pest management is an important component of agriculture, with most farmers relying on multiple pest management practices, including insecticides, fungicides, and herbicides. Many of the available chemical, biological, and genetic crop protection solutions maximize short-term benefits by avoiding pest damage within a season without targeting long-term soil health outcomes creating unintentional trade-offs and highlighting the need for innovation. This includes the drastic rise in biological resistance to chemical crop protection products that results from poor product stewardship and costs farmers billions of U.S. dollars per year (Mortensen et al., 2012; Perotti et al., 2020). Still, the relationship between crop protection innovation and soil health is rarely discussed. An exception to this is weed management, for two reasons: reverting to tillage to manage



herbicide resistant weeds would directly reduce soil health (Nunes et al., 2020; Van Deynze et al., 2021) and practices that promote soil health can positively contribute to weed management, e.g., cover cropping (Osipitan et al., 2018).

Historically soil health and crop protection have taken seemingly incompatible approaches, but the future is still unfolding and there is time for evolution within the industry that improves the complementarity between these management strategies and amplifies their agri-environmental benefits. On one hand, the crop protection industry has traditionally taken a more reactive approach to pest threats where management occurs after infestation. Soil health, alternatively, has taken a more preventative approach with a goal of avoiding pest establishment and reducing the need for curative intervention. It is conceivable to envision a future where ecological interactions in the soil are protected and fostered by crop protection innovations, improving soil health and preventing pests from economically damaging crops. This evolution of crop protection is also being supported by remarkable advances in complementary disciplines (e.g., digital technology). Novel imaging-based diagnostic tools, new equipment for precision application of agricultural inputs, and improved predictive algorithms for abiotic and biotic stresses all allow the offer of more targeted crop protection programs (Abit et al., 2018). The transition to this future would also align with and contribute to society's broader vision for sustainability across sectors, which is outlined in international policies and initiatives like the European Green Deal (European Union, 2019) and the United Nations' 2030 Agenda for Sustainable Development (United Nations,

2015). Through the establishment of the Coalition of Action 4 Soil Health (CA4SH), the crop protection industry and other relevant stakeholders have demonstrated their intention to act collaboratively to remove barriers to sustainable agricultural systems that promote soil health.

Moving to a system of crop protection that promotes soil health is an underexplored pathway to achieve long-term, agricultural sustainability and productivity. This will require methods of pest management that are compatible with specific soil health practices and also do not degrade the functional capacity of soil communities. To this end, we present three key research and development priorities the crop protection community should pursue simultaneously: 1) innovate products and application methods that avoid or reduce impacts on soil health; 2) innovate products that, alone or in combination with plant genetics, leverage soil functions and communities to enhance pest and disease management and/or biogeochemical nutrient cycling and enable reduced input use; and 3) innovate products that enable management practices that benefit soil health, while minimizing tradeoffs. Achieving these three opportunities requires a fourth innovation: 4) develop new soil health screening and field trial procedures along the crop protection research and development (R&D) stage-gate process (Figure 1). All four of these innovation opportunities are necessary to capitalize on the potential of soil health to deliver long-term agronomic and environmental benefits. We recognize that the economic impacts and feasibility of new technologies developed under this framework will undoubtedly influence adoption, but due to their novelty, the necessary data for

economic analyses do not currently exist and remain out of scope of the current discussion.

## CROP PROTECTION INNOVATION SHOULD CAPITALIZE ON THE ROLE OF SOIL IN PEST REGULATION

The functioning of soil biological communities is a key feature of soil health (Lehmann et al., 2020). Soil-based agroecosystem services important for crop health, like pest management and nutrient cycling, depend on biological interaction (Delgado-Baquerizo et al., 2020). Although the relationship between soil biodiversity and agroecosystem services is both complex and context-dependent (Bradford et al., 2014; Wagg et al., 2014; Gamfeldt and Roger, 2017; Fanin et al., 2018; Delgado-Baquerizo et al., 2020), supporting and protecting soil organisms generally enhances their contributions to agroecosystem services (Tooker et al., 2020).

Microbial and invertebrate biomass and activity, and often biodiversity, tend to increase with soil health practices compared to conventional management practices (Tsiafouli et al., 2015; Atwood and Wood, 2021; Carlos et al., 2021). As the soil environment becomes more competitive, rates of crop infection commonly decrease because pathogenic microbes must increasingly compete for resources and overcome interactions with antagonistic and interfering non-pathogenic microbes (Abawi and Widmer, 2000; de Faria et al., 2021). Additionally, biological pest control generally increases with improved soil health due to appreciable predator-prey interactions among invertebrates (Neher and Barbercheck, 2019; Alyokhin et al., 2020). This increase in biological control can result in direct economic benefits for farmers. In Sweden, for example, it is estimated that soil dwelling predators contribute €41 ha<sup>-1</sup> yr<sup>-1</sup> by controlling a single pest and increasing spring barley yields 303 kg ha<sup>-1</sup> (Östman et al., 2003). There are, however, potential tradeoffs associated with increased soil biodiversity including, but not limited to, increased predation of alternate prey opposed to target pests due to predators' preferences for alternate prey (Lynch et al., 2022). Such potential tradeoffs are generally outweighed by the agroecosystem service benefits associated with supporting and protecting soil organisms (Tooker et al., 2020).

In many agricultural systems, soil-derived crop protection services are masked, limited, and/or disrupted by management practices, resulting in an increased reliance on pesticides. Simplified crop rotations, frequent or extensive tillage, and the inadequate or inappropriate use of fertilizers and manure have all been correlated with increased incidence or severity of soil-borne pathogens and pests (Peters et al., 2003), despite that mechanisms of soil suppressiveness appear to be well conserved across a wide range of soil-pathogen combinations (van Agtmaal et al., 2018). The relationship between soil management and suppressiveness is explained by the fact that the latter is a process that is mediated by soil communities (Weller et al., 2002; Campos et al., 2016) - any practice that directly or indirectly alters soil community composition,

diversity, or activity could have an effect on soils' natural ability to regulate pest populations. Conventional tillage or plowing practices and the removal of crop residues have both been demonstrated to reduce the quantity and quality of soil organic matter and thereby reduce soil suppressiveness to multiple types of crop pests and pathogens (Kremer and Li, 2003; Fang et al., 2012; Bongiorno et al., 2019; Palojarvi et al., 2020). The effects of other practices that are commonly described as beneficial for soil health, such as diversified crop rotations (Congreves et al., 2015), are not as clear. A comprehensive review by Rusch et al. (2010) posited that crop monocultures create environments that cannot support soil-mediated crop protection services due to inadequate resource availability. Still, meta-analysis reveals this may not hold true in up to 48% of scenarios (Rusch et al., 2010), as is the case in the development of soils highly suppressive to *Fusarium* wilt following the long-term, continuous monoculture of strawberry (Cha et al., 2016). A thorough understanding of the mechanisms of soil-mediated crop protection and their interaction with conservation management strategies is therefore critical to realizing crop protection systems that deliver opportunities (1) and (2) of the proposed framework (Figure 1). Furthermore, there is potential to innovate chemical products or plant genetics (for use alone or in combination with improved soil management) that regenerate soil-derived crop protection services by cultivating and protecting soil community function. Innovations could promote or enhance suppression of invertebrate and weed pests via predator-prey interactions (Sanchez-Morena and Ferris, 2007), suppression of soil-borne pathogens via soil microorganisms (Cha et al., 2016), fortification of plant health with nutrient cycling (Campos et al., 2016; Neher and Barbercheck, 2019), and attraction of predators to pest outbreaks with plant volatiles and exudates (Turlings and Erb, 2018).

The use of plant-derived volatile organic compounds is one example of how the role of chemical signaling in plant and invertebrate interactions could be leveraged for crop protection innovation. Evidence has established that plants have the ability to influence soil communities in beneficial ways (Hiltbold and Turlings, 2012). For instance, herbivory by the cabbage root fly (*Delia radicum*) elicits the release of a volatile compound, dimethyl disulfide, from cabbage roots (Danner et al., 2012), simultaneously inhibiting the fly's reproductive behavior and attracting its natural predators (Ferry et al., 2009). Similarly, more than 74 different root exudates have been described as driving factors of host plant location in belowground insect herbivores (Johnson and Nielsen, 2012), either recruiting beneficial species to the rhizosphere (Williams and Vries, 2020) or repelling harmful ones (Xu et al., 2015). Identification of individual compounds contributing to dynamic plant-pest interactions could enable the development and optimization of natural or close semiochemical derivatives for use in novel push-pull systems of pest control (Werle et al., 2019). By definition, push-pull systems capitalize on the abilities of plants to manipulate pests, integrating stimuli that make the crop unattractive to the pest (push) with those that make non-cropped areas attractive (pull) (Cook et al., 2007). Recent research

examining the chemical basis of nematode herbivory in *Capsicum* spp (Kihika et al., 2017) illustrates the potential of using this strategy for belowground pests, though there are many more examples of modulating behavior of pests aboveground through push-pull systems (Cook et al., 2007; Xu et al., 2018; Rivera et al., 2020). Beyond “push-pull” systems there are numerous opportunities to innovate novel methods of pest control—that regulate soil communities using root exudate chemistries (Chaparro et al., 2012), plant-microbe or other symbioses, (Mercado-Blanco and Bakker, 2007; Borghi et al., 2021), mediation of tri-trophic interactions, (Helmberger et al., 2017), and improved cycling of crop limiting nutrients (Moreau et al., 2019)—and reach soil health goals.

While the implications of pesticide driven changes in soil biological communities are still under investigation (Nettles et al., 2016; Storck et al., 2018; Hage-Ahmed et al., 2019) development of new crop protection products should safeguard the continuation of ecosystem services by avoiding or reducing impacts on soil biological communities. The desire to avoid impacts that are not well understood has driven increasing attention within both the policy and R&D communities on technologies that decrease reliance on chemical pest control methods and reduce inputs. This includes strategies to elicit natural plant defenses and immune responses through priming (Worrall et al., 2011), advanced breeding techniques/genetic modification (Bruce, 2012), or plant- or microbe-derived molecules (Wiesel et al., 2014), including plant hormones (De Mesmaeker et al., 2019). One novel approach for eliciting or enhancing plant defenses is through the use of RNA (host-induced sRNA, dsRNA, or RNAi) for targeted gene silencing in fungal pathogens (Niu et al., 2021). RNA-based crop protection technologies can prevent colonization and infection of crop species by fungal pathogens [e.g., of *Sclerotinia sclerotiorum*, the causal agent of white stem rot in canola (McLoughlin et al., 2018)] and, in some cases, directly reduce the virulence of fungal pathogens [e.g., of *Botrytis cinerea*, which causes gray mold (Cai et al., 2018)]. However, to determine any technology’s suitability for conserving soil health while simultaneously delivering effective crop protection, the innovation will need to undergo a comprehensive assessment that includes its impacts on soil biological, physical, and chemical properties. Such assessments are therefore a critical first step towards effectively implementing emerging policies that aim to protect and reverse degradation of soil resources for agriculture, nature, and climate, for example, those that comprise the European Union Soil Strategy for 2030. (European Union, 2021).

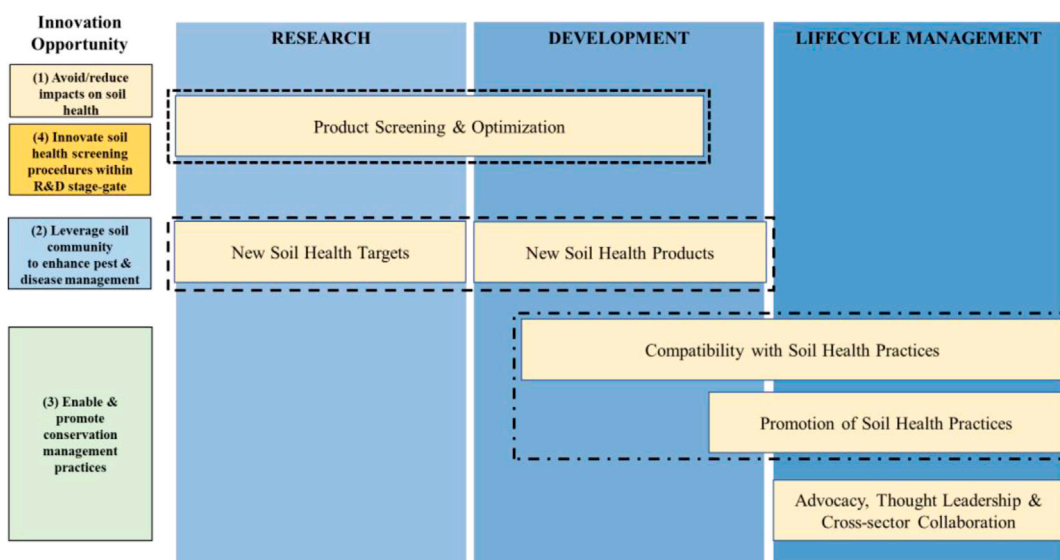
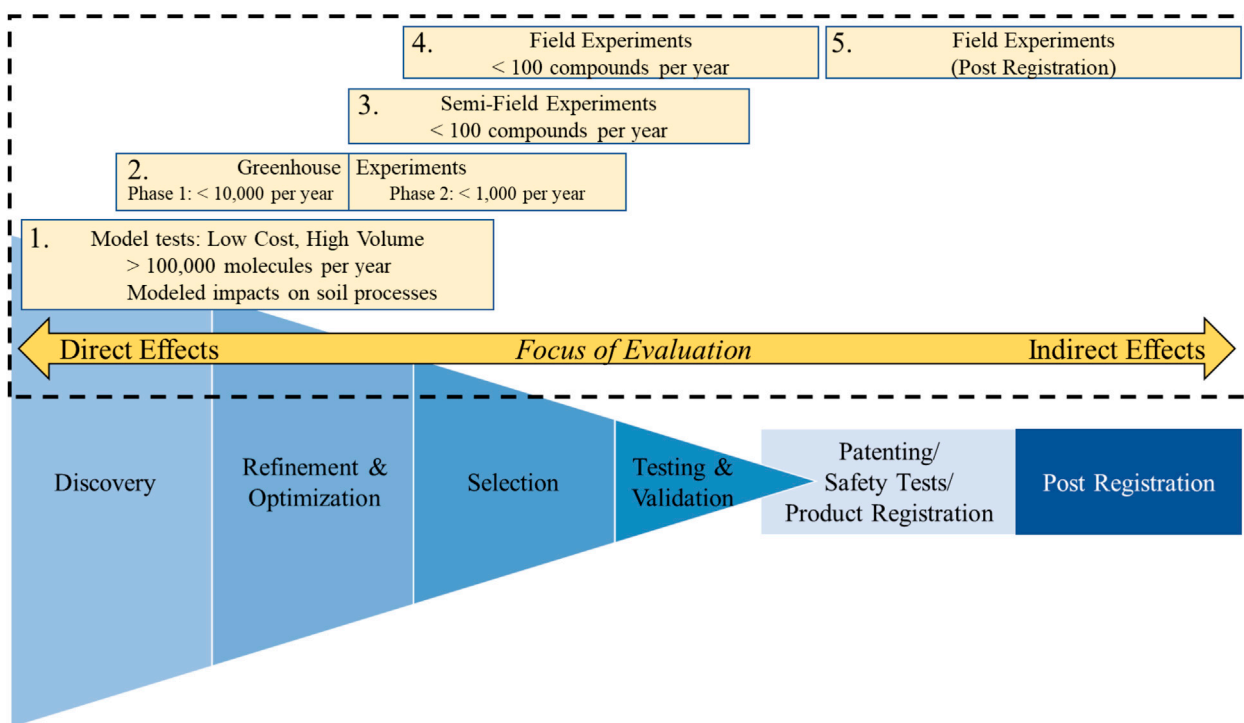
## CROP PROTECTION INNOVATION SHOULD ENABLE CONSERVATION MANAGEMENT PRACTICES

Structuring new innovations and application methods into an integrated pest management (IPM) approach (i.e., a coordinated management strategy that utilizes a diverse set of prevention, cultural, biological, mechanical, and chemical tactics based on cost-benefit analyses (Kogan, 1998)) will not only help to

conserve soil health, but also reduce the incidence of chemical resistance. Indeed, addressing the root causes of the evolution of chemical resistant pest species can be considered a primary principle of IPM (Barzman et al., 2015) and this outcome underpins many existing policy initiatives, such as Directive 2009/128/EC of the European Parliament that outlines the framework for the sustainable use of pesticides within the European Union (European Union, 2009). Even with growing consensus that IPM effectively protects crops, the environment, and soil health and is critical to sustainable agricultural systems (Anderson et al., 2019), it is not yet widely adopted, largely because of perceived risks and intensive knowledge requirements (Parsa et al., 2014; Bakker et al., 2021). By integrating the principles of IPM into the targeting, design and promotion of novel technologies, the crop protection industry can support IPM adoption and ensure the longevity of their innovations.

Regardless of the availability of innovative crop protection products that support soil health, implementation of conservation practices can vary substantially based on location, farm size, and farmer knowledge and perceptions, all of which influence the management approach (Scopel et al., 2013; Hermans et al., 2021). For increased impact on soil health at scale, crop protection innovations should aim to support localized management approaches for farms of all sizes, across a wide variety of cropping systems and environmental contexts. Innovating for a wider range of scenarios would enable the adoption of more diverse or complex cropping systems, while expanding the potential market for new solutions. Encouraging crop diversification benefits the crop protection industry directly because diversified rotations boost biological control and decrease the probability of developing resistant populations (Harker et al., 2016; Isbell et al., 2017), thus protecting the longevity of new products. Technological innovations, including useful decision support tools, are also needed within this context to alleviate the knowledge burden that accompanies management of complex systems. With interest in diversifying rotations growing (Runck et al., 2014), moving beyond monocultures of blockbuster crops towards lesser-researched crops will support the next frontier of sustainable agriculture.

Another opportunity for innovation is to focus on crop protection challenges that consistently occur when soil health practices are implemented. For example, surface residue retention protects soil organisms, maintains soil moisture (Turmel et al., 2015), and suppresses weeds (Mobli and Chauhan, 2020), but can also exacerbate waterlogging and result in lower yields in areas experiencing high rainfall (Rusinamhodzi et al., 2011). If it rains just before or during planting, lowering soil temperatures, seeds may remain quiescent in the soil and be more vulnerable to pathogens and invertebrates (Gamfeldt and Roger, 2017). Prophylactic seed treatments are currently the primary practice for managing this challenge, but potential off-target soil health impacts associated with some insecticide-fungicide seed treatments demonstrate the need for soil health compatible alternatives (Douglas and Tooker, 2015). Relevant innovations could include the development of products that can be used for seed priming or enhance seed or seedling defenses, competitive abilities, or vigor in suboptimal conditions. The types of

**A****B**

**FIGURE 2 |** Schematic of **(A)** major activities supporting innovation opportunities along the crop protection research and development (R&D) and lifecycle management timelines and **(B)** R&D pipeline with opportunities to screen for soil health impacts highlighted with dashed (---) box. The focus of the soil health evaluations will phase from potential direct effects of compounds on soil functions or soil health parameters in the early stages to indirect effects of compounds on soil health in later stages. Number of compounds evaluated in each phase is aspirational and may not reflect actual number of compounds currently undergoing evaluation.

vulnerabilities that accompany conservation agriculture are prime foci for innovative crop protection products. They also offer an opportunity for innovation in other sectors, such as

breeding cover crops that are tailored to expected climate change and creating farm equipment that enables practices like early seeding of cover crops alongside cash crops.

## SCREENING FOR SOIL HEALTH IMPACTS IN THE R&D PIPELINE

The integration of additional soil health measures into the crop protection R&D pipeline is critical for determining each potential crop protection product's compatibility with soil health (Figure 2A). This would have two benefits: first, ensuring that new compounds do not directly contribute to the deterioration of important soil community functions; second, providing criteria for optimizing new compounds that target soil health. The need to define effective and feasible screening methods for soil health impacts within crop protection R&D has become even more urgent in light of updates to the European Union's Chemicals Strategy for Sustainability. (European Union, 2020). An emerging initiative under this strategy, Safe- and Sustainable-by-Design, is intended to serve as a guiding principle for future regulation of chemicals to catalyze the transition towards chemicals, materials, and products that are designed to be inherently safe and sustainable. In the short period since the introduction of Safe- and Sustainable-by-design, it has already become clear that appropriate criteria and assessment tools will be foundational to its success (Mech et al., 2022).

R&D follows a stage-gate process, in which innovations are subjected to evaluations and risk assessments specific to each stage, presenting the potential to integrate soil health measures at multiple scales—from lab assays, to microcosms, to field trials. However, migrating the indicators and evaluations developed for field trials into the lab, or vice versa, is not straightforward. Many relevant soil properties change on the scale of years or are the result of complex biotic and abiotic interactions that are difficult to replicate in controlled environments. Similarly, high-throughput assays are, by nature, simplifications of soil ecosystems and can be challenging to translate to the field-scale. Thus, new methods, indicators, and approaches need to be innovated to align soil health screening with the existing R&D process (Figure 2B).

In particular, biological indicators will be crucial in testing the compatibility of new products with soil health during the stage-gate process. Biological indicators, such as nitrogen- or phosphorus-mineralizing enzyme activity, comprise the smallest proportion of indicators (20%) used in current soil health assessments despite the important role of soil biology in determining the overall health of a soil. (Lehmann et al., 2020). The lack of uptake of biological indicators is largely due to the difficulty in interpreting them, which limits their utility in selecting and monitoring strategies to improve soil health. (Fierer et al., 2021). This presents opportunities to identify new biological indicators of soil health that are both meaningful and compatible with high-throughput screening. Such innovative measures, whether biological or otherwise, should serve as proxies of longer-term dynamics in soil health (Fierer et al., 2021) if they are to be used successfully in early-stage R&D.

The later stages of product development—where experiments are conducted in greenhouse microcosms and fields—are better suited for ecological evaluations because the experimental system

can include multiple interacting components (Figure 2B). The opportunity to innovate and test new measures of soil health tailored to different stages means that there will need to be flexibility built into R&D processes to allow adjustment of procedures based on forthcoming knowledge. This will enable continual improvements in matching the assessments with the desirable function(s) the product intends to support.

Ultimately the acceptance of soil health-oriented crop protection innovations, particularly among practitioners of sustainable agriculture and the environmental community, will depend on the industry's ability to establish a credible product evaluation process. That is, one with scientifically robust criteria that demonstrate product compatibility with and support of sustainability-focused systems. The implementation of appropriate screening procedures should be complimented by transparent efforts to support voluntary and regulatory efforts that are part of a shift towards more complex agroecosystems that support long-term sustainability. This includes defining processes for collaborating on and sharing learning from the development of criteria and assessment tools with policymakers and other stakeholders to contribute to the refinement of policies like Safe- and Sustainable-by-design.

## CONCLUSION

Increased pesticide resistance has cost millions of dollars in damages, highlighting the need for innovation in the crop protection sector. Efforts to promote soil health and conservation agriculture are largely occurring independent of crop protection innovation. Our framework highlights a way to align the need for crop protection innovation with the broader goals of soil health, revealing potentially fruitful avenues for research and innovation. Achieving this alignment requires new crop protection solutions that benefit soil health directly and indirectly by enabling other soil health practices. Developing these innovations requires new approaches to R&D in the crop protection sector. Greater collaboration between the crop protection sector, the public sector, and civil society can help ensure that agronomic and environmental targets are aligned and achieved together.

## ONE SENTENCE SUMMARY

Innovative crop protection solutions that deliver agronomic and environmental targets require new approaches to R&D that integrate soil health goals.

## AUTHOR CONTRIBUTIONS

Conceptualization: LA, KR, MD, CM, SM, RO, CS, MW, and SW  
Visualization: LA, KR, and MW  
Writing – original draft: LA and KR  
Writing – review and editing: LA, KR, MD, CM, SM, RO, CS, MW and SW.

## REFERENCE

- Abawi, G. S., and Widmer, T. L. (2000). Impact of Soil Health Management Practices on Soilborne Pathogens, Nematodes and Root Diseases of Vegetable Crops. *Appl. Soil Ecol.* 15 (1), 37–47. doi:10.1016/s0929-1393(00)00070-6
- Abit, M. J. M., Brian Arnall, D., and Phillips, S. B. (2018). "Environmental Implications of Precision Agriculture," in *Precision Agriculture Basics*. Editors D. K. Shannon, D. E. Clay, and N. R. Kitchen (Madison, WI: American Society of Agronomy, Crop Science Society of America, and Soil Science Society of America). doi:10.2134/precisionagbasics.2017.0035
- Alyokhin, A., Nault, B., and Brown, B. (2020). Soil Conservation Practices for Insect Pest Management in Highly Disturbed Agroecosystems - a Review. *Entomol. Exp. Appl.* 168 (1), 7–27. doi:10.1111/eea.12863
- Anderson, J. A., Ellsworth, P. C., Faria, J. C., Head, G. P., Owen, M. D. K., Pilcher, C. D., et al. (2019). Genetically Engineered Crops: Importance of Diversified Integrated Pest Management for Agricultural Sustainability. *Front. Bioeng. Biotechnol.* 7, 24. doi:10.3389/fbioe.2019.00024
- Atwood, L. W., and Wood, S. (2021). AgEvidence: Agro-Environmental Responses of Conservation Agricultural Practices in the US Midwest Published from 1980 to 2020. *Knowl. Netw. Biocomplexity*. doi:10.5063/Z31X15
- Bakker, L., Sok, J., Van Der Werf, W., and Bianchi, F. J. J. A. (2021). Kicking the Habit: What Makes and Breaks Farmers' Intentions to Reduce Pesticide Use? *Ecol. Econ.* 180, 106868. doi:10.1016/j.ecolecon.2020.106868
- Barzman, M., Bärberi, P., Birch, A. N. E., Boonekamp, P., Dachbrodt-Saaydeh, S., Graf, B., et al. (2015). Eight Principles of Integrated Pest Management. *Agron. Sustain. Dev.* 35, 1199–1215. doi:10.1007/s13593-015-0327-9
- Bongiorno, G., Postma, J., Bünemann, E. K., Brussaard, L., de Goede, R. G. M., Mäder, P., et al. (2019). Soil Suppressiveness to *Pythium Ultimeum* in Ten European Long-Term Field Experiments and its Relation with Soil Parameters. *Soil Biol. Biochem.* 133, 174–187. doi:10.1016/j.soilbio.2019.03.012
- Borghi, L., Screpanti, C., Lumbroso, A., Lachia, M., Gubeli, C., and De Mesmaeker, A. (2021). Efficiency and Bioavailability of New Synthetic Strigolactone Mimics with Potential for Sustainable Agronomical Applications. *Plant and Soil* 465, 109–123. doi:10.1007/s11104-021-04943-8
- Bradford, M. A., Wood, S. A., Bardgett, R. D., Black, H. I. J., Bonkowski, M., Eggers, T., et al. (2014). Discontinuity in the Responses of Ecosystem Processes and Multifunctionality to Altered Soil Community Composition. *Proc. Natl. Acad. Sci. USA* 111 (40), 14478–14483. doi:10.1073/pnas.1413707111
- Bruce, T. J. A. (2012). GM as a Route for Delivery of Sustainable Crop protection. *J. Exp. Bot.* 63 (2), 537–541. doi:10.1093/jxb/err281
- Cai, Q., Qiao, L., Wang, M., He, B., Lin, F. M., Palmquist, J., et al. (2018). Plants Send Small RNAs in Extracellular Vesicles to Fungal Pathogen to Silence Virulence Genes. *Science* 360, 63931126–63931129. doi:10.1126/science.aar4142
- Campos, S. B., Lisboa, B. B., Camargo, F. A. O., Bayer, C., Sczyrba, A., Dirksen, P., et al. (2016). Soil Suppressiveness and its Relations with the Microbial Community in a Brazilian Subtropical Agroecosystem under Different Management Systems. *Soil Biol. Biochem.* 96, 191–197. doi:10.1016/j.soilbio.2016.02.010
- Carlos, F. S., Schaffer, N., Marcolin, E., Fernandes, R. S., Mariot, R., Mazzurana, M., et al. (2021). A Long-term No-tillage System Can Increase Enzymatic Activity and Maintain Bacterial Richness in Paddy fields. *Land Degrad. Dev.* 32 (6), 2257–2268. doi:10.1002/ldr.3896
- Cha, J.-Y., Han, S., Hong, H.-J., Cho, H., Kim, D., Kwon, Y., et al. (2016). Microbial and Biochemical Basis of a Fusarium Wilt-Suppressive Soil. *Isme J.* 10, 119–129. doi:10.1038/ismej.2015.95
- Chaparro, J. M., Sheflin, A. M., Manter, D. K., and Vivanco, J. M. (2012). Manipulating the Soil Microbiome to Increase Soil Health and Plant Fertility. *Biol. Fertil. Soils* 48, 489–499. doi:10.1007/s00374-012-0691-4
- Congreves, K. A., Hayes, A., Verhallen, E. A., and Van Eerd, L. L. (2015). Long-term Impact of Tillage and Crop Rotation on Soil Health at Four Temperate Agroecosystems. *Soil Tillage Res.* 152, 17–28. doi:10.1016/j.still.2015.03.012
- Cook, S. M., Khan, Z. R., and Pickett, J. A. (2007). The Use of Push-Pull Strategies in Integrated Pest Management. *Annu. Rev. Entomol.* 52, 375–400. doi:10.1146/annurev.ento.52.110405.091407
- Danner, H., Samudrala, D., Cristescu, S. M., and Van Dam, N. M. (2012). Tracing Hidden Herbivores: Time-Resolved Non-invasive Analysis of Belowground Volatiles by Proton-Transfer-Reaction Mass Spectrometry (PTR-MS). *J. Chem. Ecol.* 38, 785–794. doi:10.1007/s10886-012-0129-3
- de Faria, M. R., Costa, L. S. A. S., Chiamonte, J. B., Bettiol, W., and Mendes, R. (2021). The Rhizosphere Microbiome: Functions, Dynamics, and Role in Plant Protection. *Trop. Plant Pathol.* 46 (1), 13–25. doi:10.1007/s40858-020-00390-5
- De Mesmaeker, A., Screpanti, C., Fonné-Pfister, R., Lachia, M., Lumbroso, A., and Bouwmeester, H. (2019). Design, Synthesis and Biological Evaluation of Strigolactone and Strigolactam Derivatives for Potential Crop Enhancement Applications in Modern Agriculture. *Chimia (Aarau)* 73 (7–8), 549–560. doi:10.2533/chimia.2019.549
- Delgado-Baquerizo, M., Reich, P. B., Trivedi, C., Eldridge, D. J., Abades, S., Alfaro, F. D., et al. (2020). Multiple Elements of Soil Biodiversity Drive Ecosystem Functions across Biomes. *Nat. Ecol. Evol.* 4, 210–220. doi:10.1038/s41559-019-1084-y
- Douglas, M. R., and Tooker, J. F. (2015). Large-Scale Deployment of Seed Treatments Has Driven Rapid Increase in Use of Neonicotinoid Insecticides and Preemptive Pest Management in U.S. Field Crops. *Environ. Sci. Technol.* 49, 5088–5097. doi:10.1021/es506141g
- European Union (2021). *Communication from the Commission to the European Parliament, the Council, the European Economic and Social Committee and the Committee of the Regions EU Soil Strategy for 2030 Reaping the Benefits of Healthy Soils for People, Food, Nature and Climate. COM/2021/699 Final*. Brussels: European Union.
- European Union (2020). *Communication from the Commission to the European Parliament, the European Council, the Council, the European Economic and Social Committee and the Committee of the Regions A New Industrial Strategy for Europe. COM/2020/102 Final*. Brussels: European Union.
- European Union (2019). *Communication from the Commission to the European Parliament, the European Council, the Council, the European Economic and Social Committee and the Committee of the Regions the European Green Deal. COM/2019/640 Final*. Brussels: European Union.
- European Union (2009). Directive 2009/128/EC of the European Parliament and of the Council of 21 October 2009 Establishing a Framework for Community Action to Achieve the Sustainable Use of Pesticides. *Off. J. Eur. Union* 309, 71.
- Fang, X., You, M. P., and Barbeti, M. J. (2012). Reduced Severity and Impact of Fusarium Wilt on Strawberry by Manipulation of Soil pH, Soil Organic Amendments and Crop Rotation. *Eur. J. Plant Pathol.* 134, 619–629. doi:10.1007/s10658-012-0042-1
- Fanin, N., Gundale, M. J., Farrell, M., Ciobanu, M., Baldock, J. A., Nilsson, M.-C., et al. (2018). Consistent Effects of Biodiversity Loss on Multifunctionality across Contrasting Ecosystems. *Nat. Ecol. Evol.* 2 (2), 269–278. doi:10.1038/s41559-017-0415-0
- Ferry, A., Le Tron, S., Dugravot, S., and Cortesero, A. M. (2009). Field Evaluation of the Combined Deterrent and Attractive Effects of Dimethyl Disulfide on *Delia Radicum* and its Natural Enemies. *Biol. Control.* 49, 219–226. doi:10.1016/j.biocontrol.2009.01.013
- Fierer, N., Wood, S. A., and Bueno de Mesquita, C. P. (2021). How Microbes Can, and Cannot, Be Used to Assess Soil Health. *Soil Biol. Biochem.* 153, 108111. doi:10.1016/j.soilbio.2020.108111
- Gamfeldt, L., and Roger, F. (2017). Revisiting the Biodiversity-Ecosystem Multifunctionality Relationship. *Nat. Ecol. Evol.* 1 (7), 168. doi:10.1038/s41559-017-0168
- Hage-Ahmed, K., Rosner, K., and Steinkellner, S. (2019). Arbuscular Mycorrhizal Fungi and Their Response to Pesticides. *Pest Manag. Sci.* 75, 583–590. doi:10.1002/ps.5220
- Harker, K. N., O'Donovan, J. T., Turkington, T. K., Blackshaw, R. E., Lupwayi, N. Z., Smith, E. G., et al. (2016). Diverse Rotations and Optimal Cultural Practices Control Wild Oat (*Avena Fatua*). *Weed Sci.* 64 (1), 170–180. doi:10.1614/ws-d-15-00133.1
- Helmberger, M. S., Shields, E. J., and Wickings, K. G. (2017). Ecology of Belowground Biological Control: Entomopathogenic Nematode Interactions with Soil Biota. *Appl. Soil Ecol.* 121, 201–213. doi:10.1016/j.apsoil.2017.10.013
- Hermans, T. D. G., Dougill, A. J., Whitfield, S., Peacock, C. L., Eze, S., and Thierfelder, C. (2021). Combining Local Knowledge and Soil Science for Integrated Soil Health Assessments in Conservation Agriculture Systems. *J. Environ. Manage.* 286, 112192. doi:10.1016/j.jenvman.2021.112192
- Hiltbold, I., and Turlings, T. C. J. (2012). Manipulation of Chemically Mediated Interactions in Agricultural Soils to Enhance the Control of Crop Pests and to

- Improve Crop Yield. *J. Chem. Ecol.* 38, 641–650. doi:10.1007/s10886-012-0131-9
- Isbell, F., Adler, P. R., Eisenhauer, N., Fornara, D., Kimmel, K., Kremen, C., et al. (2017). Benefits of Increasing Plant Diversity in Sustainable Agroecosystems. *J. Ecol.* 105, 871–879. doi:10.1111/1365-2745.12789
- Johnson, S. N., and Nielsen, U. N. (2012). Foraging in the Dark - Chemically Mediated Host Plant Location by Belowground Insect Herbivores. *J. Chem. Ecol.* 38, 604–614. doi:10.1007/s10886-012-0106-x
- Kihika, R., Murungi, L. K., Coyne, D., Ng'ang'a, M., Hassanali, A., Teal, P. E. A., et al. (2017). Parasitic Nematode *Meloidogyne incognita* Interactions with Different Capsicum Annum Cultivars Reveal the Chemical Constituents Modulating Root Herbivory. *Sci. Rep.* 7, 2903. doi:10.1038/s41598-017-02379-8
- Kogan, M. (1998). Integrated Pest Management: Historical Perspectives and Contemporary Developments. *Annu. Rev. Entomol.* 43 (1), 243–270. doi:10.1146/annurev.ento.43.1.243
- Kremer, R. J., and Li, J. (2003). Developing weed-suppressive Soils through Improved Soil Quality Management. *Soil Tillage Res.* 72, 193–202. doi:10.1016/s0167-1987(03)00088-6
- Lehmann, J., Bossio, D. A., Kögel-Knabner, I., and Rillig, M. C. (2020). The Concept and Future Prospects of Soil Health. *Nat. Rev. Earth Environ.* 1, 544–553. doi:10.1038/s43017-020-0080-8
- Lynch, C. A., Olivia, M. S., Chapman, E. G., Crossley, M. S., Crowder, D. W., Fu, Z., et al. (2022). Alternative Prey and Farming System Mediate Predation of Colorado Potato Beetles by Generalists. *Pest Manage. Sci.* doi:10.1002/ps.6553
- McLoughlin, A. G., Wytinck, N., Walker, P. L., Girard, I. J., Rashid, K. Y., de Kievit, T., et al. (2018). Identification and Application of Exogenous dsRNA Confers Plant protection against *Sclerotinia sclerotiorum* and *Botrytis Cinerea*. *Sci. Rep.* 8, 7320. doi:10.1038/s41598-018-25434-4
- Mech, A., Gottardo, S., Amenta, V., Amodio, A., Belz, S., Bøwadt, S., et al. (2022). Safe- and Sustainable-By-Design: The Case of Smart Nanomaterials. A Perspective Based on a European Workshop. *Regul. Toxicol. Pharmacol.* 128, 105093. doi:10.1016/j.yrtph.2021.105093
- Mercado-Blanco, J., and Bakker, P. A. H. M. (2007). Interactions between Plants and Beneficial *Pseudomonas* spp.: Exploiting Bacterial Traits for Crop protection. *Antonie van Leeuwenhoek* 92 (4), 367–389. doi:10.1007/s10482-007-9167-1
- Mobli, A., and Chauhan, B. S. (2020). Crop Residue Retention Suppresses Seedling Emergence and Biomass of winter and Summer Australian weed Species. *Weed Biol. Manag.* 20 (3), 118–128. doi:10.1111/wbm.12208
- Moreau, D., Bardgett, R. D., Finlay, R. D., Jones, D. L., and Philippot, L. (2019). A Plant Perspective on Nitrogen Cycling in the Rhizosphere. *Funct. Ecol.* 33, 540–552. doi:10.1111/1365-2435.13303
- Mortensen, D. A., Egan, J. F., Maxwell, B. D., Ryan, M. R., and Smith, R. G. (2012). Navigating a Critical Juncture for Sustainable weed Management. *BioScience* 62 (1), 75–84. doi:10.1525/bio.2012.62.1.12
- Neher, D., and Barbercheck, M. (2019). Soil Microarthropods and Soil Health: Intersection of Decomposition and Pest Suppression in Agroecosystems. *Insects* 10 (12), 414. doi:10.3390/insects10120414
- Nettles, R., Watkins, J., Ricks, K., Boyer, M., Licht, M., Atwood, L. W., et al. (2016). Influence of Pesticide Seed Treatments on Rhizosphere Fungal and Bacterial Communities and Leaf Fungal Endophyte Communities in maize and Soybean. *Appl. Soil Ecol.* 102, 61–69. doi:10.1016/j.apsoil.2016.02.008
- Niu, D., Hamby, R., Sanchez, J. N., Cai, Q., Yan, Q., and Jin, H. (2021). RNAs - a New Frontier in Crop protection. *Curr. Opin. Biotechnol.* 70, 204–212. doi:10.1016/j.copbio.2021.06.005
- Nunes, M. R., Karlen, D. L., Veum, K. S., Moorman, T. B., and Cambardella, C. A. (2020). Biological Soil Health Indicators Respond to Tillage Intensity: A US Meta-Analysis. *Geoderma* 369, 114335. doi:10.1016/j.geoderma.2020.114335
- Osipitan, O. A., Dille, J. A., Assefa, Y., and Knezevic, S. Z. (2018). Cover Crop for Early Season Weed Suppression in Crops: Systematic Review and Meta-Analysis. *Agron.j.* 110, 2211–2221. doi:10.2134/agronj2017.12.0752
- Östman, Ö., Ekblom, B., and Bengtsson, J. (2003). Yield Increase Attributable to Aphid Predation by Ground-Living Polyphagous Natural Enemies in spring Barley in Sweden. *Ecol. Econ.* 451, 149–158. doi:10.1016/s0921-8009(03)00007-7
- Palm, C., Blanco-Canqui, H., DeClerck, F., Gatere, L., and Grace, P. (2014). Conservation Agriculture and Ecosystem Services: An Overview. *Agric. Ecosyst. Environ.* 187, 87–105. doi:10.1016/j.agee.2013.10.010
- Palojarvi, A., Kellock, M., Parikka, P., Jauhiainen, L., and Alakukku, L. (2020). Tillage System and Crop Sequence Affect Soil Disease Suppressiveness and Carbon Status in Boreal Climate. *Front. Microbiol.* 11, 534786. doi:10.3389/fmicb.2020.534786
- Parsa, S., Morse, S., Bonifacio, A., Chancellor, T. C. B., Condori, B., Crespo-Pérez, V., et al. (2014). Obstacles to Integrated Pest Management Adoption in Developing Countries. *Proc. Natl. Acad. Sci. USA* 111 (10), 3889–3894. doi:10.1073/pnas.1312693111
- Perotti, V. E., Larran, A. S., Palmieri, V. E., Martinatto, A. K., and Permingeat, H. R. (2020). Herbicide Resistant Weeds: A Call to Integrate Conventional Agricultural Practices, Molecular Biology Knowledge and New Technologies. *Plant Sci.* 290, 110255. doi:10.1016/j.plantsci.2019.110255
- Peters, R. D., Sturz, A. V., Carter, M. R., and Sanderson, J. B. (2003). Developing Disease-Suppressive Soils through Crop Rotation and Tillage Management Practices. *Soil Tillage Res.* 72, 181–192. doi:10.1016/s0167-1987(03)00087-4
- Rivera, M. J., Martini, X., Conover, D., Mafrá-Neto, A., Carrillo, D., and Stelinski, L. L. (2020). Evaluation of Semiochemical Based Push-Pull Strategy for Population Suppression of Ambrosia Beetle Vectors of laurel Wilt Disease in Avocado. *Sci. Rep.* 10, 2670. doi:10.1038/s41598-020-59569-0
- Runck, B. C., Kantar, M. B., Jordan, N. R., Anderson, J. A., Wyse, D. L., Eckberg, J. O., et al. (2014). The Reflective Plant Breeding Paradigm: a Robust System of Germplasm Development to Support Strategic Diversification of Agroecosystems. *Crop Sci.* 54 (5), 1939–1948. doi:10.2135/cropsci2014.03.0195
- Rusch, A., Valantin-Morison, M., Sarthou, J. P., and Roger-Estrade, J. (2010). "Integrating Crop and Landscape Management into New Crop protection Strategies to Enhance Biological Control of Oilseed Rape Insect Pests," in *Biocontrol-based Integrated Management of Oilseed Rape Pests* (Dordrecht: Springer), 415–448. doi:10.1007/978-90-481-3983-5\_17
- Rusinamhodzi, L., Corbeels, M., van Wijk, M. T., Rufino, M. C., Nyamangara, J., and Giller, K. E. (2011). A Meta-Analysis of Long-Term Effects of Conservation Agriculture on maize Grain Yield under Rain-Fed Conditions. *Agron. Sustain. Dev.* 31, 657–673. doi:10.1007/s13593-011-0040-2
- Sanchez-Morena, S., and Ferris, H. (2007). Suppressive Service of the Soil Food Web: Effects of Environmental Management. *Agric. Ecosyst. Environ.* 119, 75–87. doi:10.1016/j.agee.2006.06.012
- Scopel, E., Triomphe, B., Affholder, F., Da Silva, F. A. M., Corbeels, M., Humberto J., et al. (2013). Conservation Agriculture Cropping Systems in Temperate and Tropical Conditions, Performances and Impacts: A Review. *Agron. Sust. Dev.* 33 (1), 113–130. doi:10.1007/s13593-012-0106-9
- Storck, V., Nikolaki, S., Perruchon, C., Chabanis, C., Sacchi, A., Pertile, G., et al. (2018). Lab to Field Assessment of the Ecotoxicological Impact of Chlorpyrifos, Isoproturon, or Tebuconazole on the Diversity and Composition of the Soil Bacterial Community. *Front. Microbiol.* 9, 1412. doi:10.3389/fmicb.2018.01412
- Tooker, J. F., O'Neal, M. E., and Rodriguez-Saona, C. (2020). Balancing Disturbance and Conservation in Agroecosystems to Improve Biological Control. *Annu. Rev. Entomol.* 65, 81–100. doi:10.1146/annurev-ento-011019-025143
- Tsiafouli, M. A., Thébault, E., Sgardelis, S. P., de Ruiter, P. C., van der Putten, W. H., Birkhofer, K., et al. (2015). Intensive Agriculture Reduces Soil Biodiversity across Europe. *Glob. Change Biol.* 21 (2), 973–985. doi:10.1111/gcb.12752
- Turling, T. C. J., and Erb, M. (2018). Tritrophic Interactions Mediated by Herbivore-Induced Plant Volatiles: Mechanisms, Ecological Relevance, and Application Potential. *Annu. Rev. Entomol.* 63 (1), 433–452. doi:10.1146/annurev-ento-020117-043507
- Turling, M.-S., Speratti, A., Baudron, F., Verhulst, N., and Govaerts, B. (2015). Crop Residue Management and Soil Health: a Systems Analysis. *Agric. Syst.* 134, 6–16. doi:10.1016/j.agry.2014.05.009
- United Nations (2015). *General Assembly Resolution A/RES/70/1. Transforming Our World, the 2030 Agenda for Sustainable Development. Distr.: General 70/1.* New York, NY: United Nations.
- van Agtmaal, M., Straathof, A. L., Termorshuizen, A., Lievens, B., Hoffland, E., and de Boer, W. (2018). Volatile-mediated Suppression of Plant Pathogens Is Related to Soil Properties and Microbial Community Composition. *Soil Biol. Biochem.* 117, 164–174. doi:10.1016/j.soilbio.2017.11.015
- Van Deynze, B., Swinton, S. M., and Hennessy, D. A. (2021). Are Glyphosate-Resistant Weeds a Threat to Conservation Agriculture? Evidence from Tillage Practices in Soybean. *Am. J. Agric. Econ.* 104 (2), 1–28. doi:10.1111/ajae.12243

- Wagg, C., Bender, S. F., Widmer, F., and van der Heijden, M. G. A. (2014). Soil Biodiversity and Soil Community Composition Determine Ecosystem Multifunctionality. *Proc. Natl. Acad. Sci.* 111 (14), 5266–5270. doi:10.1073/pnas.1320054111
- Weller, D. M., Raaijmakers, J. M., Gardener, B. B. M., and Thomashow, L. S. (2002). Microbial Populations Responsible for Specific Soil Suppressiveness to Plant Pathogens. *Annu. Rev. Phytopathol.* 40, 309–348. doi:10.1146/annurev.phyto.40.030402.110010
- Werle, C. T., Ranger, C. M., Schultz, P. B., Reding, M. E., Addesso, K. M., Oliver, J. B., et al. (2019). Integrating Repellent and Attractant Semiochemicals into a Push-Pull Strategy for Ambrosia Beetles (Coleoptera: Curculionidae). *J. Appl. Entomol.* 143, 333–343. doi:10.1111/jen.12594
- Wiesel, L., Newton, A. C., Elliott, I., Booty, D., Gilroy, E. M., Birch, P. R. J., et al. (2014). Molecular Effects of Resistance Elicitors from Biological Origin and Their Potential for Crop protection. *Front. Plant Sci.* 5, 655. doi:10.3389/fpls.2014.00655
- Williams, A., and Vries, F. T. (2020). Plant Root Exudation under Drought: Implications for Ecosystem Functioning. *New Phytol.* 225, 1899–1905. doi:10.1111/nph.16223
- Worrall, D., Holroyd, G. H., Moore, J. P., Glowacz, M., Croft, P., Taylor, J. E., et al. (2011). Treating Seeds with Activators of Plant Defence Generates Long-lasting Priming of Resistance to Pests and Pathogens. *New Phytol.* 193, 770–778. doi:10.1111/j.1469-8137.2011.03987.x
- Xu, Q., Hatt, S., Lopes, T., Zhang, Y., Bodson, B., Chen, J., et al. (2018). A Push-Pull Strategy to Control Aphids Combines Intercropping with Semiochemical Releases. *J. Pest Sci.* 91, 93–103. doi:10.1007/s10340-017-0888-2
- Xu, Z., Zhao, Y.-Q., Yang, D.-J., Sun, H.-J., Zhang, C.-L., and Xie, Y.-P. (2015). Attractant and Repellent Effects of Sweet Potato Root Exudates on the Potato Rot Nematode, *Ditylenchus Destructor*. *Nematol* 17, 117–124. doi:10.1163/15685411-00002856

**Conflict of Interest:** Authors MD, CM, SM, RO, and CS were employed by Syngenta.

The remaining authors declare that the research was conducted in the absence of any commercial or financial relationships that could be construed as a potential conflict of interest.

**Publisher's Note:** All claims expressed in this article are solely those of the authors and do not necessarily represent those of their affiliated organizations or those of the publisher, the editors, and the reviewers. Any product that may be evaluated in this article, or claim that may be made by its manufacturer, is not guaranteed or endorsed by the publisher.

Copyright © 2022 Atwood, Racette, Diggelmann, Masala, Maund, Oliver, Screpanti, Wironen and Wood. This is an open-access article distributed under the terms of the Creative Commons Attribution License (CC BY). The use, distribution or reproduction in other forums is permitted, provided the original author(s) and the copyright owner(s) are credited and that the original publication in this journal is cited, in accordance with accepted academic practice. No use, distribution or reproduction is permitted which does not comply with these terms.



# On-Farm Relationships Between Agricultural Practices and Annual Changes in Organic Carbon Content at a Regional Scale

Xavier Dupla<sup>1,2\*</sup>, Téo Lemaître<sup>1</sup>, Stéphanie Grand<sup>2</sup>, Karine Gondret<sup>1</sup>, Raphaël Charles<sup>3</sup>, Eric Verrecchia<sup>2</sup> and Pascal Boivin<sup>1</sup>

<sup>1</sup>University of Applied Sciences of Western Switzerland, HES-SO, HEPIA-Agronomy, Geneva, Switzerland, <sup>2</sup>University of Lausanne, FGSE-IDYST, Lausanne, Switzerland, <sup>3</sup>Research Institute of Organic Agriculture FiBL, Lausanne, Switzerland

## OPEN ACCESS

### Edited by:

Jörg Luster,  
Swiss Federal Institute for Forest,  
Switzerland

### Reviewed by:

Marjin Van De Broek,  
ETH Zürich, Switzerland  
Mirjam Helfrich,  
Thünen Institut of Climate-Smart  
Agriculture, Germany

### \*Correspondence:

Xavier Dupla  
xavier.dupla@unil.ch

### Specialty section:

This article was submitted to  
Soil Processes,  
a section of the journal  
Frontiers in Environmental Science

**Received:** 12 December 2021

**Accepted:** 11 March 2022

**Published:** 24 March 2022

### Citation:

Dupla X, Lemaître T, Grand S,  
Gondret K, Charles R, Verrecchia E  
and Boivin P (2022) On-Farm  
Relationships Between Agricultural  
Practices and Annual Changes in  
Organic Carbon Content at a  
Regional Scale.  
Front. Environ. Sci. 10:834055.  
doi: 10.3389/fenvs.2022.834055

Both soil quality degradation and climate change mitigation issues emphasize the need to increase, or at least stabilize, the topsoil organic carbon content (wt%) in arable land. This on-farm study aimed at measuring the impact of agricultural practices on changes in soil organic carbon (SOC) content over 10 years. A total of 120 fields belonging to 120 farms representative of the cropping systems and soil properties in Western Switzerland (Lake Geneva region) was randomly selected. The field 0–20 cm topsoil was sampled at a 10-years interval, and the corresponding cropping practices were gathered using farmer's interviews and the mandatory records of yearly practices at field level in Swiss-farms. Only 1) organic matter inputs and 2) cover-crop intensity were significantly correlated to SOC increase while 3) the soil tillage intensity and 4) the soil saturation in carbon expressed as a SOC to clay content ratio were correlated to SOC decrease. Among others, temporary meadows were not correlated to changes in SOC content mainly due to increased tillage and decreased cover-crops between meadows. Organic farming did not correlate either with SOC changes due to the large tillage intensity applied for weed control. The observed SOC content changes ranged from –56‰ to +74‰ and were well explained by a linear regression model with additive effect of the four identified SOC change factors. The additivity of these factors means that farmers can emphasize the methods of their choice when regenerating their soils. This study advocates that strict no-till is not required at low carbon saturation level (small SOC:Clay ratio). However, as carbon saturation increases, conservation tillage and then no-till practices become necessary to further increase SOC contents. These findings are in accordance with previous studies showing that since 2015 SOC is increasing at more than +4‰ on average in the region and provide practical insights to further manage the transition of farming systems towards soil regeneration.

**Keywords:** soil organic carbon, soil organic matter, carbon content change, tillage, cover-crop, organic amendments, meadow, on-farm results

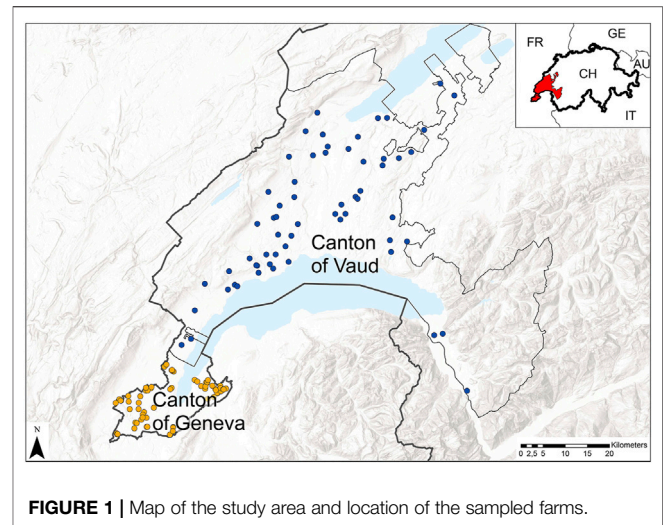
**Abbreviations:** AMG, model from Andriulo, Mary and Guerif on soil carbon dynamics (Andriulo et al., 1999); ANOVA, Analysis of Variance; ISMO, stability index of organic matter; LTE, Long Term Experiment; OM, Organic Matter; PCA, Principal Component Analysis; SEM, Standard Error of the Mean; SOC, Soil Organic Carbon; STIR, Soil Tillage Intensity Rating; STIRAC, Soil Tillage Intensity Rating calculated over annual crops' duration.

# 1 INTRODUCTION

According to Olson et al., 2014, carbon sequestration is “the process of transferring CO<sub>2</sub> from the atmosphere into the soil of a land unit, through plants, plant residues and other organic solids which are stored or retained in the unit as part of the soil organic matter (humus).” A sequestration for at least 20 years is often chosen as a criterion (IPCC, 2006). The 4-per-mille initiative (Minasny et al., 2017) has raised high hopes on the potential of this Negative Emission Technology (NET) to contribute to ecological transition by mitigating the increase in atmospheric CO<sub>2</sub> due to fossil energy consumption. Briefly, it suggests that increasing by a factor of 1.004 every year the soil organic carbon (SOC) stocks in the soil upper layer would significantly reduce the CO<sub>2</sub> concentration in the atmosphere. The feasibility of this initiative has been highly disputed (Powlson et al., 2011; Baveye et al., 2018; De Vries, 2018; Minasny et al., 2018; White et al., 2018; Chenu et al., 2019; Rumpel et al., 2020). The potential of this NET in agricultural soils, however, was underlined by two assessment reports of European Academies Science Advisory Council (EASAC, 2018, 2019). Consequently, much of the literature has been devoted to seeking methods achieving this objective (Dignac et al., 2017; Zomer et al., 2017; Chenu et al., 2019; Rumpel et al., 2020). These studies have mainly highlighted the potential of agricultural practices belonging to the pillars of Conservation Agriculture (Hobbs et al., 2008), i.e., continuous soil cover by plants and residues, limited tillage and diversification of crop rotation.

Regardless of climate issues, SOC is a major factor of topsoil fertility (Bünemann et al., 2018; King et al., 2020). In the second half of the 20th century, intensified agriculture caused a sharp decrease in topsoil SOC content (wt%) (McLauchlan, 2006), estimated at 50–70% of initial topsoil SOC content (Kucharik et al., 2001; Lal, 2004; Sanderman et al., 2017). This decrease was attributed to intense soil disturbance, shortening of the rotation lengths and export of the crop residues (West and Post, 2002; Reicosky, 2003; McLauchlan, 2006; Smith et al., 2012). Therefore, considerations including decline of soil quality and provision of ecosystem services are put forward to call for restoration of the SOC content in arable land (Swinton et al., 2007; Power, 2010; Blanco-Canqui et al., 2013), rather than focusing on carbon sequestration alone which may lead to hazardous practices for soil quality (Baveye et al., 2020). Moreover, the desirable SOC content in cropland was often related to the concept of clay complexation and saturation with organic carbon. This concept is expressed as a SOC:Clay ratio (Dexter et al., 2008; Johannes et al., 2017; Prout et al., 2020) that can be used to calculate carbon sequestration potential (Merante et al., 2017; Chen et al., 2019; Dupla et al., 2021).

Whether increasing the SOC content and SOC stock of the topsoil in cropland is an achievable objective is still highly disputed (e.g., Chambers et al., 2016; Baveye et al., 2018; White et al., 2018; Chenu et al., 2019; Paustian et al., 2019; Amelung et al., 2020; Giller et al., 2021). Highly contrasting conclusions are reported, particularly with respect to the potential of no-till practices and their influence on SOC loss (Dimassi et al., 2014;



**FIGURE 1 |** Map of the study area and location of the sampled farms.

Powlson et al., 2014; Haddaway et al., 2017). However, most of these results were obtained on long term experiments (LTE).

A recent study performed on the Swiss long-term experiments reported negative annual change rates in SOC content of the 0–20 cm topsoil for all the LTEs regardless of the cropping system (Keel et al., 2019). Conversely, in another large scale on-farm study conducted in the Lake Geneva region, Dupla et al. (2021) showed that the SOC content of the cropland 0–20 cm topsoil was increasing on average, with annual SOC change rates ranging from less than –30‰ to more than +30‰. With a cropland mean SOC annual change rate increasing from –5‰ at the end of the 20th century to more than +5‰ at present, this study contradicted Keel et al. (2019) findings, though performed under the same climate and soil conditions. Consequently Dupla et al. (2021) concluded that LTE results cannot be extrapolated to farm fields, as already underlined by previous studies (Govaerts et al., 2009; Cook et al., 2013).

Based on the findings of Dupla et al. (2021), this study was performed in the same geographical area, namely in the Vaud and Geneva cantons—Switzerland. Here, we explored the relationships between the observed SOC content annual change rates in the 0–20 cm topsoil and the cropping practices, over the past 10 years, for 120 fields and farms representative of the soils and cropping systems of this region. Special attention was given to the practices commonly recognized as possible SOC content change factors such as cover crops and green manure, organic manure application, soil tillage intensity and temporary meadow.

## 2 MATERIALS AND METHODS

### 2.1 Study Area

This study was conducted on 120 farms from Western Switzerland (Lake Geneva region), namely Geneva and Vaud cantons, western Switzerland (Figure 1). The climate is oceanic (Cfb) in the plains according to Köppen-Geiger climate types (Peel et al., 2007). The dominant soil type is Cambi-Luvisol (IUSS

**TABLE 1 |** Distribution of soil organic carbon (SOC) (%), clay (%), SOC to clay ratio (%), SOC:Clay ratio (%) and annual SOC change rates (‰) for Geneva and Vaud croplands.

Region	Parameter	n (fields)	Min	Max	Median	Mean (SE)
Canton of Geneva	SOC (% g g <sup>-1</sup> )	1'206	0.58	2.49	1.45	1.49 (0.35)
	Clay (% g g <sup>-1</sup> )	493	11.00	39.08	23.20	23.43 (5.37)
	SOC:Clay ratio (%)	493	2.94	13.04	6.24	6.57 (1.74)
	SOC change rate (‰)	184	-28.95	+28.04	+1.74	+2.01 (11.71)
Canton of Vaud	SOC (% g g <sup>-1</sup> )	12'108	0.060	3.48	1.62	1.74 (0.57)
	Clay (% g g <sup>-1</sup> )	1'265	7.40	35.70	19.60	20.28 (5.34)
	SOC:Clay ratio (%)	1'265	3.05	13.73	7.94	8.13 (2.02)
	SOC change rate (‰)	754	-30.16	+32.60	+3.41	+3.72 (11.59)

Working Group WRB, 2014), developed on calcareous Pleistocene moraines mixed with some Tertiary molasse fragments (local parent rock). Other soil types were not considered, and only farms with annual crops in the rotation were included (livestock farms relying exclusively on permanent meadows were not considered).

To receive ecological subsidies, Swiss farmers are required to analyze a topsoil (0–20 cm) composite sample from each of their field in a certified laboratory at least every 10 years. This sampling method was assessed as an unbiased and reliable method to determine SOC annual change rates at farm scale (Deluz et al., 2020). The corresponding database contains more than 35'000 soil analyses from 1993 to present and was used by Dupla et al. (2021) to determine the regional SOC annual change rate distribution and its change with time. The corresponding parameters are summarized in Table 1.

## 2.2 Farm Selection and Data Collection

The 120 farms were randomly selected using the regional farming directory. One field per farm was randomly selected and the mandatory information recorded by farmers in their logbooks over the past 10 years was used to describe the farming practices conducted on the field. These include the different operations conducted on each field (soil preparation, fertilization, treatments, yield, cover-crops, and rotation) with the date and quantity of each product used or harvested. One-to-one in-depth interviews were conducted with the 120 farmers to validate their practices and complete them in case of missing information in the logbook. The survey included the different farming types in the region, such as organic, conventional, presence or absence of livestock.

We focused on the cropping practices potentially impacting SOC content changes, namely temporary meadow duration, cover-crop properties, organic matter application, soil tillage intensity and rotation diversity. These factors are described below and summarized in Table 2.

### 2.2.1 Cover-Crops

The numbered cover-crops only included green-manure, i.e., cover-crops whose residues are left on the field. Harvested or grazed cover-crops were considered as standard crops. The cover-crop biomass was not recorded in the past-ten years; however, we could calculate 1) the number

**TABLE 2 |** Main cropping practices considered in the study.

Cropping Practice	Description
Temporary meadow	Fraction of temporary meadow cover, averaged over 10 years in %
Spring crops	Number of spring crops
Cover-crop species	Mean number of species in the cover-crops
Fallow periods	Number of uncovered periods over the annual crop duration normalized to a 10-year period
Organic matter input	Mean input of humified organic matter in t.ha <sup>-1</sup> over 10 years
Rotation species	Mean number of species in the rotation
Soil tillage intensity rating	Mean soil tillage intensity rating per year (STIR)
Soil tillage intensity rating over the annual crop duration	Mean soil tillage intensity rating per year of annual cropping (excluding periods in temporary meadow) over 10 years (STIR <sub>AC</sub> )

and duration of long-lasting cover-crops (between summer harvest and a spring crop seeding); 2) the number and duration of short cover-crops (between a summer harvest and an autumn-crop seeding); and 3) the number of species in the cover-crops.

However, there is an obvious relationship between the number of cover-crops and the temporary meadow duration. Therefore, to better account for the efforts of the farmer to cover the soil independently from the proportion of temporary meadow in the rotation, an uncovered soil score was created to quantify cover-cropping missed opportunities. Over the rotation, the number of fallow periods longer than 6 weeks and not covered with a cover-crop was divided by the number of annual crops and then normalized to a 10-year period. For instance, in a 6-years rotation made of 4 annual crops and 2 years of temporary meadows, a farmer who has missed 2 opportunities to use cover crops would get a score of  $2 \times 10/4 = 5$  equivalent to 5 cover-cropping missed opportunities over a 10-years rotation made only of annual crops.

### 2.2.2 Organic Matter Application

Organic amendments were standardized as humified organic matter inputs in t.ha<sup>-1</sup> over the 10-year period. The amount of organic matter application (manure, slurry, digestate, and compost) was transformed to humified organic matter inputs depending on the organic amendment nature and form using the coefficients of specific stability index of organic matter (ISMO)

**TABLE 3 |** Summary of the main soil properties and cropping practices. Soil organic carbon content (SOC) (%) and clay content (%) at the beginning of the 10-year period and their ratio (SOC:Clay ratio) (%). Rate of SOC annual change (‰). Share of temporary meadows in 10 years (%). Share of spring crops in 10 years (%). Mean number of species in the cover-crops. Number of fallow periods in 10 years. Cumulated organic matter amendments in humified organic matter in tons per 10 years. Number of species in the rotation. STIR: Mean Soil Tillage Intensity Rating per year over the 10-year period. STIR<sub>AC</sub>: Mean Soil Tillage Intensity Rating per year over the 10-year period.

Canton	Variables	Minimum	Maximum	Median	Mean	SEM
Geneva	SOC (% g g <sup>-1</sup> )	0.81	2.97	1.51	1.52	0.06
	Clay (% g g <sup>-1</sup> )	10.85	54.50	23.15	24.65	0.96
	SOC:Clay ratio (%)	3.33	12.01	6.45	6.41	0.22
	SOC change rate (‰)	-56.28	73.73	0.00	2.29	2.47
	Temporary meadow (%)	0.00	70.00	0.00	8.00	0.02
	Spring crops (%)	0.00	60.00	20.00	23.00	0.02
	Cover-crop species	0.00	10.30	5.00	5.10	0.40
	Fallow periods	0.00	10.00	3.65	3.72	0.34
	OM input (t.ha <sup>-1</sup> .10 years <sup>-1</sup> )	0.00	64.69	0.00	4.74	1.33
	Rotation species	3.00	7.00	5.00	5.03	0.14
	STIR	6.00	208.57	111.50	97.31	7.55
	STIR <sub>AC</sub>	6.00	255.50	118.00	102.09	7.88
Vaud	SOC (% g g <sup>-1</sup> )	0.87	3.19	1.57	1.68	0.07
	Clay (% g g <sup>-1</sup> )	8.90	41.00	18.20	20.01	0.73
	SOC:Clay ratio (%)	4.38	16.34	8.12	8.67	0.34
	SOC change rate (‰)	-39.34	66.79	8.48	8.04	2.56
	Temporary meadow (%)	0.00	63.00	12.00	19.00	0.03
	Spring crops (%)	0.00	90.00	25.00	30.00	0.03
	Cover-crop species	0.00	10.43	3.00	3.12	0.30
	Fallow periods	0.00	7.86	2.93	2.65	0.26
	OM input (t.ha <sup>-1</sup> .10 years <sup>-1</sup> )	0.00	69.71	16.64	17.87	1.75
	Rotation species	3.00	9.00	5.00	4.67	0.15
	STIR	6.77	195.70	117.01	107.77	5.80
	STIR <sub>AC</sub>	7.12	245.28	121.95	118.10	6.62
Vaud and Geneva	SOC (% g g <sup>-1</sup> )	0.81	3.19	1.51	1.60	0.04
	Clay (% g g <sup>-1</sup> )	8.90	54.50	21.05	22.33	0.64
	SOC:Clay ratio (%)	3.33	16.34	7.20	7.54	0.23
	SOC change rate (‰)	-56.28	73.73	0.00	5.16	1.79
	Temporary meadow (%)	0.00	70.00	0.00	13.00	0.02
	Spring crops (%)	0.00	90.00	25.00	26.00	0.02
	Cover-crop species	0.00	10.43	3.55	4.11	0.26
	Fallow periods	0.00	10.00	3.00	3.19	0.22
	OM input (t.ha <sup>-1</sup> .10 years <sup>-1</sup> )	0.00	69.71	6.59	11.31	1.25
	Rotation species	3.00	9.00	5.00	4.85	0.10
	STIR	6.00	208.57	114.50	102.54	4.76
	STIR <sub>AC</sub>	6.00	255.50	121.43	110.10	5.18

(Bouthier et al., 2014) used in the AMG model (Andriulo et al., 1999; Levavasseur et al., 2020).

### 2.2.3 Soil Tillage Intensity Rating

The index of Soil Tillage Intensity Rating (STIR) (USDA, 2003) was used to estimate overall soil disturbance based on specific standardized scores attached to soil management practices. A single tillage operation to 23 cm depth gives for instance a score of 74, while direct seeding would give a score of 4. For each investigated field, all soil management practices over the last 10 years were considered to calculate STIR values. The cumulated values were then divided by ten to obtain the variable subsequently referred to as STIR.

Like cover-crops, the average tillage intensity over 10 years is highly influenced by the share of temporary meadow. To take into account the soil tillage intensity applied on annual crops regardless of temporary meadow duration in the rotation, a second index

denoted STIR<sub>AC</sub> was also calculated over the annual crops duration in the rotation and then normalized to 10 years.

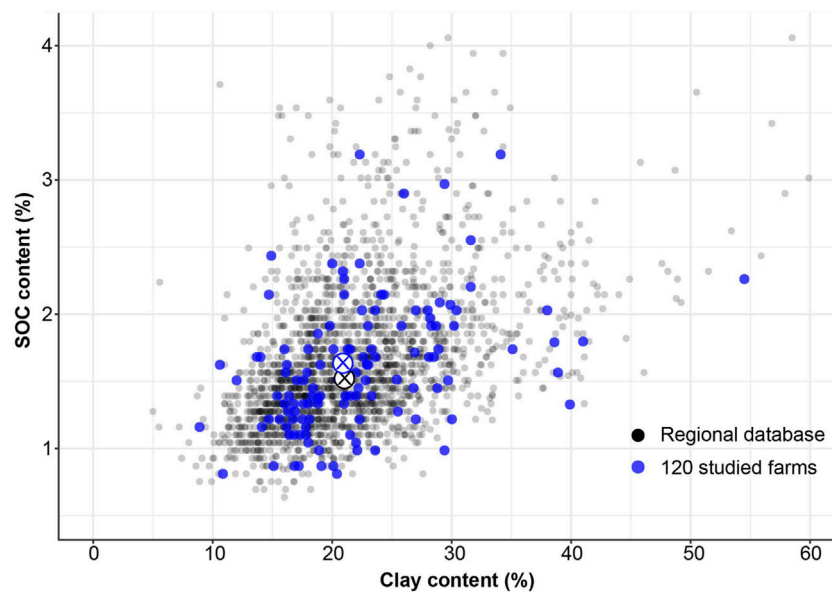
### 2.2.4 Temporary Meadow

Temporary meadow duration was expressed as percentage over the 10-year period.

## 2.3 Soil Sampling and Analysis

The selected fields were sampled at the beginning and the end of the 10-years interval by collecting 15 to 20 aliquots along the field diagonals at 0–20 cm depth to obtain a composite sample (Deluz et al., 2020). SOC and clay contents (wt%) were analyzed using Walkley-Black (Nelson and Sommers, 1983) and pipette methods (Jennings et al., 1922; Robinson, 1922), respectively.

This allowed the SOC:Clay ratio of the field to be calculated. The 10-years mean SOC annual change rate (‰) of each field



**FIGURE 2 |** SOC vs. clay contents (circles) and respective centroids (circled X) of soil samples from the regional Geneva and Vaud database (grey) and from sampled fields of the 120 surveyed farms (blue).

being the equivalent of the common ratio in a geometric sequence, it was calculated using **Eq. 1** (see **Supplementary Material** for additional computational explanations).

$$\text{SOC annual change rate (\%)} = 1000 \times \left( \left( \frac{\text{SOC}_2}{\text{SOC}_1} \right)^{\frac{1}{n}} - 1 \right) \quad (1)$$

with  $\text{SOC}_1$  and  $\text{SOC}_2$  being the SOC contents of the soil at the beginning ( $\text{SOC}_1$ ) and end ( $\text{SOC}_2$ ) of the period, and  $n$  the number of years between the two analyses ( $n = 10$ ).

## 2.4 Statistical Analysis and Modelling

All statistical analyses and modelling were performed with R (v 4.0.3, R Development Core Team 2020). Variables of interest included the SOC annual change rate, the clay content, the initial SOC content, the initial SOC:Clay ratio and eight cropping practices averaged over the 10 years (**Table 2**). All variables were quantitative. For each cropping practice, we also created a class variable which was subsequently used in an analysis of covariance (see below).

For each quantitative variable, the mean and median were calculated to represent the central tendency and the minimum, maximum and standard error of the mean (SEM) to represent dispersion. Linear models (simple and multiple regressions, analyses of variance and analyses of covariance—see details below) were then used to investigate relationships between the SOC annual change rate, soil properties, cropping practices and cantons. The  $\alpha$  level for model and effect significance was set at 0.05 unless stated otherwise. Approximate normality and homogeneous variance of model residuals were assessed on residual plots.

A one-way analysis of variance (ANOVA) was conducted to test for differences in the SOC annual change rate, soil properties

and cropping practices between the two cantons. We investigated bivariate linear relationships between quantitative variables by calculating Pearson's correlation coefficients (see **Supplementary Table S1**). Significant correlations between the SOC annual change rate and other variables were further described with simple linear regressions.

A multiple regression analysis was subsequently conducted to account for the cumulative effect of soil properties and cropping practices on the SOC annual change rate (McCullagh and Nelder, 1989). The dependent variable was the SOC annual change rate, and predictors were selected among variables representing cropping practices and the initial SOC:Clay ratio. To maximize validity, reliability and parsimony (Chatfield, 1995), the regression analysis was not performed on the maximum model (the model containing all the potential predictors). Unimportant variables were first discarded during a model selection process consisting of a stepwise selection using an  $\alpha$  level of 0.15 for both variable entry and variable removal. A permissive alpha level of 0.15 was used to make sure that any predictor potentially influencing the response variable remained included in the model. The multiple regression analysis was then conducted on the resulting model; the significance of predictors was from here on assessed using the regular alpha level of 0.05. To reduce model instability arising from variable collinearity, we excluded moderately to highly correlated predictors, defined here as variables having absolute correlation coefficients greater than 0.3. Multi-collinearity was low, and partial least square or ridge regression approaches did not yield any improvement.

To check for the robustness of the multiple regression result, we repeated the analysis using a covariance model, with the SOC annual change rate as dependent variable, the SOC:Clay ratio as a covariate, and cropping practices as class effects. Models using class variables as predictors are generally more robust to potential

**TABLE 4 |** Pearson correlation coefficients and *p*-value of the significant correlations between rates of SOC annual change, cropping practices, and soil properties. SOC refers to the soil organic carbon content at the beginning of the 10-year period.

Variable	Variable	Pearson Correlation	<i>p</i> -value
SOC change rate (‰)	Number of cover-crop species	0.18	0.050
SOC change rate (‰)	Fallow periods	−0.30	0.001
SOC change rate (‰)	OM input (t.ha <sup>−1</sup> )	0.31	0.001
SOC change rate (‰)	STIR <sub>AC</sub>	−0.27	0.002
SOC change rate (‰)	STIR	−0.30	0.001
SOC change rate (‰)	SOC:Clay (%)	−0.27	0.003
SOC:Clay (%)	Temporary meadow share (%)	0.22	0.018
SOC:Clay (%)	Number of cover-crop species	−0.27	0.003
SOC:Clay (%)	OM input (t.ha <sup>−1</sup> )	0.20	0.026
Temporary meadow share (%)	Spring crops share (%)	−0.26	0.004
Temporary meadow share (%)	Number of cover-crop species	−0.28	0.002
Temporary meadow share (%)	STIR <sub>AC</sub>	0.26	0.004
Temporary meadow share (%)	STIR	−0.24	0.009
Cover-crop species	STIR <sub>AC</sub>	−0.44	<0.001
Cover-crop species	STIR	−0.32	<0.001
Cover-crop species	Number of species in rotation	0.20	0.030
Fallow periods	STIR <sub>AC</sub>	0.23	0.012
Fallow periods	STIR	0.23	0.011
Fallow periods	Spring crops share (%)	−0.48	<0.001
Fallow periods	Number of species in rotation	−0.19	0.041
STIR	STIR <sub>AC</sub>	0.85	<0.001
STIR	Spring crops share (%)	0.25	0.006

collinearity effect. Results were similar to what was obtained using multiple regression approaches and are presented in the Supplementary Material (see **Supplementary Table S2**). Due to the relatively high number of predictors, interaction effects could not robustly be assessed.

We used a Principal Component Analysis (PCA) (Wold et al., 1987) based on the correlation matrix to illustrate the relationship between the significant agricultural practices related to SOC annual change rates.

### 3 RESULTS

#### 3.1 Properties of the Sampled Fields and Surveyed Cropping Practices

The selected farms have a mean cultivated surface area of 50 ha, which is slightly above the mean size observed in the region (36 ha) and 15% of the farms were under Swiss organic farming label, which is slightly above the regional mean (11%). 48% of the farms had no livestock, and the average livestock units in the other farms was 10 which lies in the mean regional range (5.8–20.5).

The properties of the studied fields and the related cropping practices averaged on the 10-year period are reported in **Table 3**. Due to differences in agriculture management history, the cropping systems in the two cantons showed some differences. Livestock was more developed in Vaud farms than in Geneva farms. Geneva canton subsidizes cover crops of short fallow periods (e.g., from barley to colza) contrary to Vaud, and the

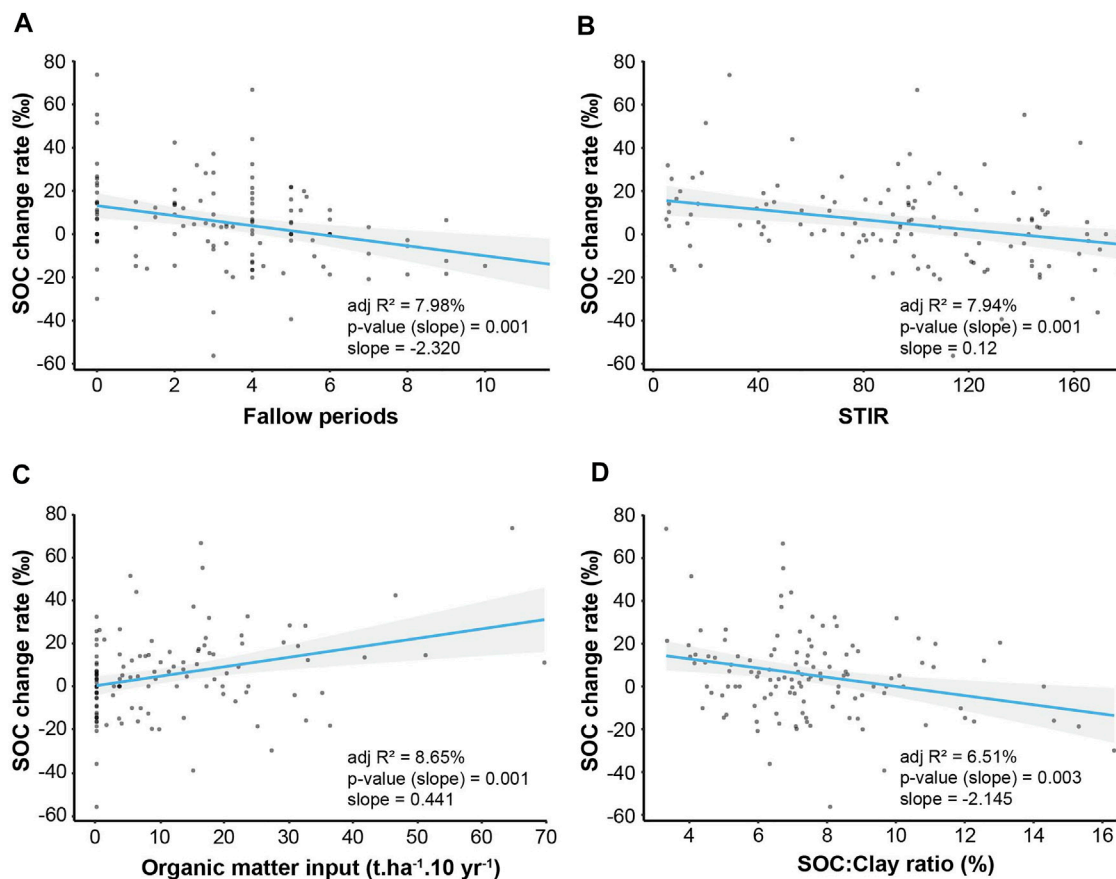
rotations show little variation in spring crop frequency in Geneva compared to Vaud, which explains the differences in the corresponding cover-crop properties. However, the canton effect was not significant on the SOC annual change rate and its relationships with other variables.

The distributions of initial SOC and clay contents are presented in **Figure 2**, together with the values observed in the regional data base used in Dupla et al. (2021). As can be seen from their centroid and their distribution, the sampled fields from the 120 farms are representative of the regional SOC and clay contents, and SOC:Clay ratio distribution.

The observed rates of SOC annual change show a median value of 0 and ranged from −56‰ to +74‰. These change rates display a similar pattern to the rates found at the regional scale by Dupla et al. (2021) (**Table 1** and **Table 3**) despite a higher dispersion compared with the minimum and maximum rates (−30.12 and +32.47‰, respectively) in both cantons. According to ANOVA, the soils from Vaud had significantly less clay and a higher SOC:Clay ratio than in Geneva, but the SOC change rate was not significantly different between cantons, which is similar to the observations of the regional database study.

#### 3.2 Pearson Correlations and Linear Regressions

Significant Pearson correlation coefficients between the observed rates of SOC annual change, the soil analyses, and the investigated cropping practices are presented in **Table 4**.



**FIGURE 3** | Linear regressions between SOC annual change rates (%) and cropping practices **(A)**: fallow periods, **(B)**: Soil Tillage Intensity (STIR) and **(C)**: organic matter input) and between SOC annual change rates (%) and initial SOC:Clay ratio (%) **(D)**.

Among the cropping practices, only the cover-crop related properties, STIR, and OM inputs showed significant correlation with the SOC annual change rate. Among the cover-crop properties, the number of fallow periods showed the largest and most significant correlation to SOC change rate ( $-0.3$ ,  $p$ -value =  $0.0009$ ) and was, therefore, used in the multivariate analysis. The number of species in the cover-crops showed a positive effect on the SOC change rate ( $0.18$ ,  $p$ -value =  $0.0496$ ). The STIR ( $-0.3$ ,  $p$ -value =  $0.001$ ) and the STIR<sub>AC</sub> ( $-0.27$ ,  $p$ -value =  $0.002$ ) were negatively correlated to the SOC change rate. Due to its stronger significance, the STIR rather than the STIR<sub>AC</sub> was used in the multivariate analysis. The organic matter input was positively correlated to SOC change rates ( $0.26$ ,  $p$ -value =  $0.0042$ ). Interestingly, neither the proportion of temporary meadow in the rotation nor the crop rotation diversity had a significant effect on the SOC annual change rate. The linear regressions between SOC annual change rates, SOC:Clay ratios and cropping practices are presented in **Figure 3**.

Among the soil properties, the SOC content and SOC:Clay ratio at the beginning of the 10-year period showed a negative correlation with the SOC annual change rate, namely  $-0.26$  ( $p$ -value =  $0.004$ ) and  $-0.27$  ( $p$ -value =  $0.003$ ), respectively. The correlations with the annual change rates and the other SOC

change factors were more significant when using SOC:Clay ratio rather than with SOC alone (see **Supplementary Table S1**).

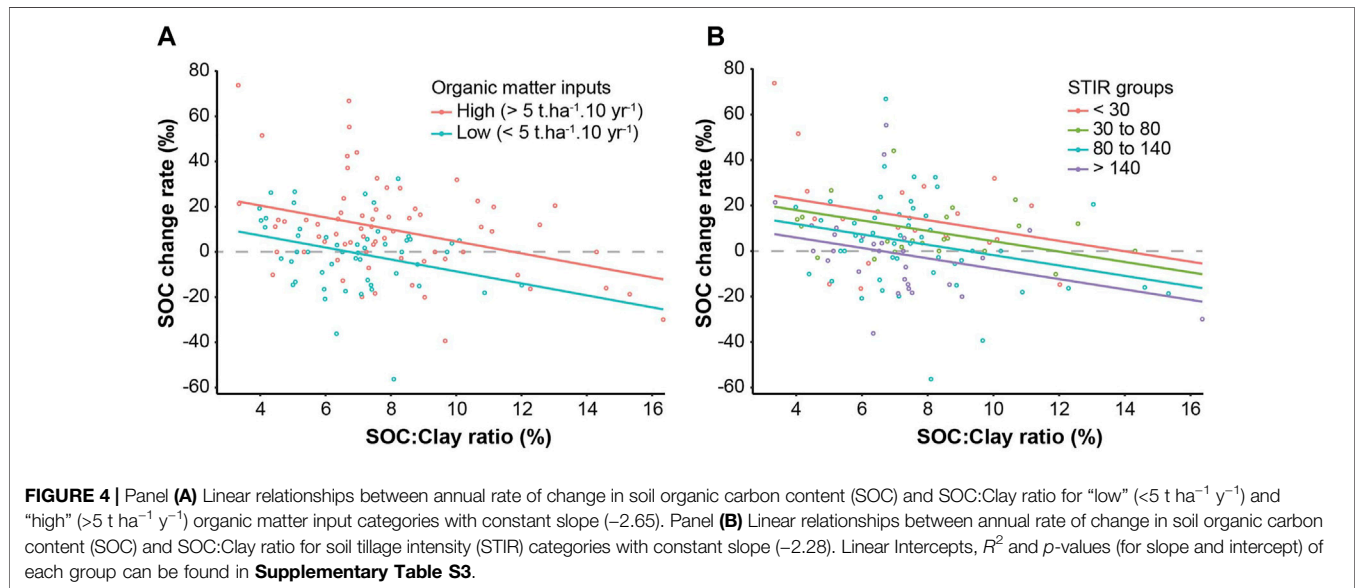
Some practices were significantly cross correlated. The STIR showed negative correlation to the cover-crops related indexes, such as number of species ( $-0.32$ ,  $p$ -value <  $0.001$ ) and fallow periods ( $0.23$ ,  $p$ -value =  $0.01$ ), as well as with temporary meadow duration ( $-0.24$ ,  $p$ -value =  $0.009$ ) and spring crops share ( $0.25$ ,  $p$ -value =  $0.006$ ). STIR<sub>AC</sub> showed similar correlations than STIR to all practices except spring crops (no correlation). Moreover, it showed a positive correlation to temporary meadow share ( $0.26$ ,  $p$ -value =  $0.004$ ), contrary to STIR. Organic matter input was positively correlated to temporary meadow duration ( $0.21$ ,  $p$ -value =  $0.0236$ ), and negatively correlated to the number of species in the cover-crops ( $-0.21$ ,  $p$ -value =  $0.0222$ ) and fallow periods ( $-0.25$ ,  $p$ -value =  $0.006$ ). This latter was negatively correlated to temporary meadow duration ( $-0.3$ ,  $p$ -value =  $0.0008$ ).

### 3.3 Multivariate Analysis

According to stepwise regression, the independent variables that showed significant contribution to SOC change rates were the SOC:Clay ratio at the beginning of the period, fallow periods,

**TABLE 5 |** General linear model of SOC annual change rates as a function of farming practices and soil properties.

Variable	Parameter Estimate	Standard Error	Pr >  t	Model Adj. $R^2$
Intercept	37.03	5.83	<0.001	—
Organic matter input	0.53	0.11	<0.001	0.086
SOC:Clay ratio	-2.95	0.61	<0.001	0.196
STIR	-0.12	0.03	<0.001	0.311
Fallow periods	-1.26	0.62	0.043	0.329



STIR, and OM inputs. Since the covariance model with practices as class effects provided similar results to the linear regression model, we only present results from the latter (see **Supplementary Table S2** for covariance results).

The results of the stepwise regression are presented in **Table 5**. All variables left in the model, namely the initial SOC:Clay ratio, fallow periods, STIR, and OM inputs, are significant at the 0.05 level. No other variable met this significance level for entry into the model. Introducing organic farming yielded no significant effect as well.

According to stepwise regression analysis, OM input had a positive influence on SOC change rates while the initial SOC:Clay ratio, the proportion of fallow periods, and the tillage intensity had a negative influence. Other predictors such as meadow and spring crop share were not significant. The ranking of the relative effects, based on the partial  $R^2$ , was not performed because of small effects and some collinearity among predictors. The corresponding model was additive and accounted for 33% variance of the annual SOC change rate.

The combined effect of the practices was illustrated by representing the linear relationships between SOC change rates and SOC:Clay ratios for different categories of OM input (**Figure 4A**) and STIR (**Figure 4B**). In both cases, the interaction between the categories and the slopes were not significant. Therefore, we kept a constant slope for the categories. **Figure 4A** shows that the larger the SOC:Clay

ratio, the smaller the annual SOC change rate for a given OM input, with neutral SOC change rates on average at a SOC:Clay ratios of 7 and 12% for OM input categories of <5 t ha<sup>-1</sup> y<sup>-1</sup> and >5 t ha<sup>-1</sup> y<sup>-1</sup>, respectively.

**Figure 4B** illustrates the role of the initial clay saturation status (SOC:Clay ratio) with respect to SOC increase and tillage intensity. Positive SOC change rates with large tillage intensities are mostly observed at small SOC:Clay ratios and more generally, the higher the SOC:Clay ratio, the lower the STIR needs to be to allow for a SOC increase. In other words, no-till becomes increasingly necessary at large SOC content, but is not required to increase SOC content at low clay saturation level.

## 4 DISCUSSION

### 4.1 Significant Predictors Influencing Soil Organic Carbon Annual Change Rates

The correlations between the cropping practices depict different cropping systems that can be summarized as follows. The proportion of temporary meadow is largely varying between farms and between cantons. The larger this proportion, the higher the organic matter input, the initial SOC:Clay ratio, the STIR<sub>AC</sub>, the proportion of fallow periods corresponding to cover-cropping missed opportunities in the rotation, the spring crops share, and the lower the cover-crop

diversity. Moreover, regardless of temporary meadow duration, STIR was highly variable, and the use of cover-crops (duration and diversity) was inversely proportional to the mechanical intensity (see **Supplementary Figure S1**). This means that 1) farmers having livestock and temporary meadow tend to apply high mechanical intensity and neglect cover-crops while applying more OM inputs; that 2) mechanical intensity in general jeopardizes cover-crop intensification; and that 3) farmers having no temporary meadows tend to reduce soil tillage intensity and to grow cover-crops to regenerate effective soil quality losses due to decades of intensive agriculture.

Data analysis shows that the only factors influencing significantly rates of SOC annual change are the cover-crops (intensity and diversity, positive effect), organic matter inputs (positive effect), and the mechanical intensity applied to the annual crops (negative effect). They represent, therefore, the pillars of SOC increase. Organic farming, temporary meadow duration as well as rotation diversity showed no significant effect, though often referred-to in the literature as soil regenerating and/or carbon sequestration factors (Fließbach et al., 2007; Senapati et al., 2014; Autret et al., 2016; Blanco-Canqui et al., 2017; Chenu et al., 2019; Colombi et al., 2019). Rotation diversity did not vary on a large range in this survey (**Table 3**). Moreover, longer rotations corresponded to contrasting strategies. In some cases, it corresponded to the addition of a “cash-crop,” namely potatoes or sugar-beet, while the longer rotation was also negatively correlated to fallow periods, thus corresponding to an increased use of the cover-crops and decreased tillage intensity.

Organic matter application and cover-crops intensity and diversity are highlighted in many studies as factors of SOC increase (Maltas et al., 2013; O’Connell et al., 2015; Ruis and Blanco-Canqui, 2017; Büchi et al., 2018; Wendling et al., 2019). Their significant effect is particularly remarkable in this survey because the cover-crop biomass was not available, though it is assumed to be a key factor (Blanco-Canqui et al., 2015; Poeplau and Don, 2015) and should be even more strongly correlated to SOC change rates than our available information. However, the decreasing number of fallow periods and the number of species in the cover-crops can be considered as indicators of farmers motivation, thus increasing the likelihood of higher biomass of cover-crops. This is a common observation made by the authors and the advising services in the region (Wendling et al., 2017).

## 4.2 Impact of Temporary Meadows and Organic Farming

The non-significant effect of the proportion of temporary meadow on SOC change rates (see **Supplementary Figure S2**), despite its large range (from 0 to 70% of the past 10-years rotations in this survey, **Table 3**), is particularly surprising with respect to the common acknowledgment that temporary meadow may be a guarantee of sustainable soil management in agriculture. However, temporary meadow duration was positively correlated to factors associated with SOC decrease (namely the STIR<sub>AC</sub> applied on the annual crops in the rotation, the number of fallow periods, and the SOC:Clay ratio), whereas

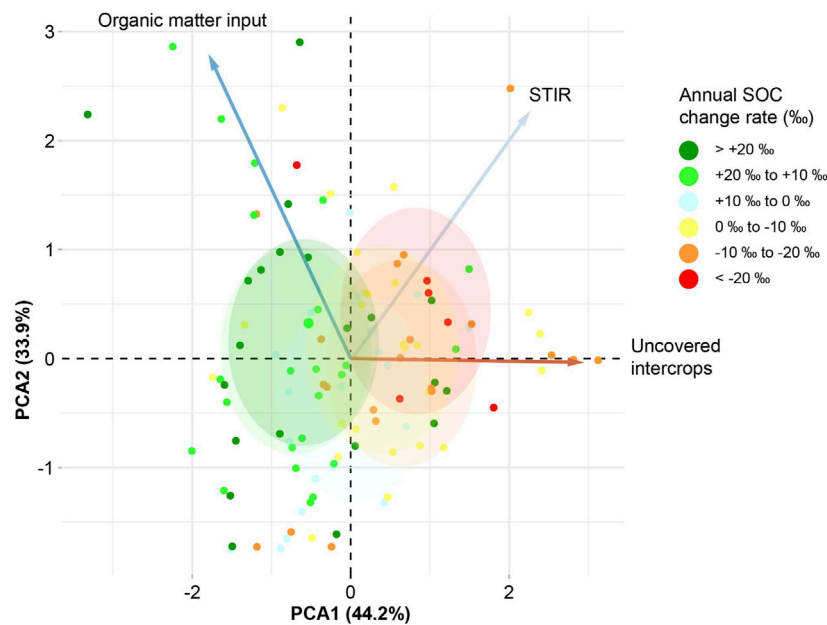
it was negatively correlated to the number of species in the cover-crops which is considered as a key factor of SOC increase (e.g., Ranaldo et al., 2020). Moreover, there was no correlation between temporary meadow and OM inputs, which might be due to increased liquid manure and digestate application with increasing temporary meadow share, which is growingly observed. Temporary meadows, therefore, are not conducive to increasing the SOC content, especially when SOC:Clay ratio was already high. From this point of view 1) the larger SOC:Clay ratio observed with temporary meadows appears to be inherited from the past and is decreasing and 2) this should be mitigated by increasing OM inputs and/or decreasing tillage intensity and increasing cover-crop intensity on the annual crops.

Organic farming had no significant effect on SOC change rates as a predictor (see **Supplementary Figure S3**). It performed according to the intensity of application of the SOC increase factors. Organic farming is often associated with livestock and manure application but also to a high STIR for weed control, which is the case in this data set (see **Supplementary Figure S4**).

## 4.3 Soil Tillage is the Only Significant Factor Decreasing Soil Organic Carbon Annual Change Rates

The only practice accounting for SOC content decrease was the mechanical intensity. This may appear contradictory to some findings, such as Dimassi et al. (2014) or Powlson et al. (2014), who reported limited or no effect of tillage compared with no-till practices. However, these results were obtained in LTEs. They were observed under constant treatment over a long time, with site-specific SOC:Clay ratio, cropping practices and climate conditions, and with tillage as unique difference between the treatments. Such research is designed to quantify the potential SOC mineralization by tillage. Conversely, our observations cover a large range of soil conditions and practices interacting in the cropping systems. In particular, **Table 4** shows that the Pearson correlation coefficient between STIR and fallow periods was positive (0.31,  $p$ -value = 0.0006). This can be related to a well-known observation that working the soil after a summer harvest not only delays the seeding of the cover-crop, but also dries out the soil down to the tillage limit, thus retarding seed emergence until significant rainfall events, usually occurring during fall in this region (Büchi et al., 2018). As a result, many farmers choose not to seed cover-crops in such conditions, or the seeded cover-crop shows a late development and reaches small biomass. Therefore, although the present on-farm results cannot adjudicate on the precise impact of soil tillage on SOC mineralization, they show that in a systemic perspective, soil tillage compromises the main SOC increase factor, namely cover-crops.

Additionally, threshold values of mechanical intensity can be derived from **Figure 4B**. Fields with conventional tillage (STIR > 140), conservation tillage (80 > STIR > 140) or no-till (STIR < 30) display positive SOC change rates up to SOC:Clay ratios of 7, 10 and 14% on average, respectively. These latter SOC:Clay ratios coincide with the soil structure vulnerability thresholds for poor, acceptable and optimal soil structures, respectively, (Johannes



**FIGURE 5 |** PCA biplot of the 120 studied fields together with the agricultural practices retained in the linear model projected on plane of the first two principal components (variance in %). Each field is colored according to its annual SOC change rate (‰). Euclidean concentration ellipses follow the same color scale.

et al., 2017; Prout et al., 2020), thus confirming the relevance of these thresholds for SOC management.

#### 4.4 Multivariate Analysis and Insights for Soil Organic Carbon Content Management

Stepwise regression analysis provides additional information to the Pearson correlations. The model accounts for 33% of the variance of the SOC annual change rate, which may be considered small. However, there are many reasons for this limited  $R^2$ , because 1) the independent variables were collected from farmers and averaged over 10 years, which does not mean that they were constant during this period since cropping systems are continuously changing; 2) the climate conditions were different each year, with alternating wet and dry conditions in spring and autumn, thus sharply modifying the harvest dates and the cover-crops development conditions; and 3) the cover-crop biomass was not known though most likely representing the key information, which could be assessed by simulating the cover-crop biomass with the collected information and meteorological data. **Figure 5** presents the distribution of the fields with respect to the two first principal components of the retained three agricultural practices accounting for SOC content change. The more intensely one practice was used, the more towards the practice's arrowhead each field would be positioned. Conversely, if one practice was avoided (e.g., no-till for the STIR parameter) then the field would be located at the opposite end of the practice's arrow in the PCA biplot. The SOC change rate categories display a gradual shift of concentration ellipses towards higher STIR, organic matter inputs and fallow period values as SOC change rates decrease. This gradual distribution casts light on the beneficial impact of low tillage intensity, organic

amendments and intense cover-cropping on SOC content change.

The absence of clear statistical interactions implies that the roles of the different factors are additive. If so, farmers may select which SOC increase factors to emphasize when adapting their system. However, the higher the clay saturation by SOC, the more intense the use of the different factors should be, as illustrated for instance with tillage intensity in **Figure 4B**. Therefore, farmers could select the intensity to apply on the different SOC increase factors depending 1) on their cropping system, 2) whether they are in a regeneration strategy or not, and 3) their SOC:Clay ratio.

The observed SOC annual change rates are consistent with the regional study of Dupla et al. (2021). Contrary to findings in Swiss LTEs (Keel et al., 2019) many Swiss farms do increase their SOC content at a larger rate than 4‰ and the factors seem clearly identified. However, large negative SOC change rates are also observed, which could be corrected in the future by applying the corresponding changes in the cropping practices.

#### 4.5 Implications for Soil Research

Together with the study of Dupla et al. (2021), these results may seem very contradictory with previous findings on SOC dynamics in arable land. The impact of tillage on SOC dynamics is considered negligible by Powlson et al. (2014) or Dimassi et al. (2014) while its strong negative effect appears in this on-farm study. In Swiss LTEs, all cropping practices, including conservation agriculture, induced a decrease in SOC according to the study by Keel et al. (2019) while high rates of SOC content increase are found on-farm. Experimental conditions in LTEs can deviate significantly from on-farm conditions, as illustrated in this study. On-farm practices are the result of systemic decisions

considering different factors that co-evolve from year to year, whereas in LTEs we aim to quantify mechanistic processes by comparing the effects of single factors over the long term from a unique research perspective. For example, our results show that the higher the SOC:Clay ratio, the more detrimental the mechanical intensity can be to the SOC content, whereas in a field experiment dealing with this issue, only a narrow range of SOC:Clay ratios can be considered, thus excluding the observation of this effect. Furthermore, we have highlighted the negative interaction between tillage and cover crops, which is the result of systemic constraints and farmers' choices, another effect that will not be revealed in the LTE.

These observations call for a thorough reflection when selecting research strategies, with a clear distinction between objectives. Experimentation under controlled conditions is of paramount importance to decipher mechanisms and quantify processes. In addition, field trials can provide useful demonstrations and stimulate farmer innovation. However, the transfer of these results to the farm may not be straightforward and may even lead to misinterpretation. On-farm soil quality management clearly requires systemic research, especially for key issues such as carbon sequestration and the preservation of soil functions.

## 5 CONCLUSION

In 120 farms representative of Western Switzerland (Lake Geneva region) agricultural sector, the most significant factors for SOC content increase or decrease corresponded to the mechanical intensity applied on annual crops (negative effect), the organic matter inputs (positive effect), and the frequency and diversity of non-harvested cover-crops (positive effect). The temporary meadow duration had no effect on the SOC content change, due to adverse practices on the annual crops of the corresponding rotations, namely larger mechanical intensity and lower cover crop frequency with increasing meadow duration. Moreover, organic matter application did not increase with temporary meadow. Therefore, the larger SOC to clay ratios observed with temporary meadow were interpreted as inherited from the past. In such a case, temporary meadows do not guarantee sustainable soil quality management.

The factors for SOC increase or decrease were additive. Clay saturation by SOC decreased the positive effects of organic matter inputs and cover-crops and increased the negative effects of tillage intensity. The cover-crop intensity and diversity were negatively correlated to tillage intensity, which may explain the significant negative effect of tillage intensity contrary to what was reported in

some field experiments. This is consistent with a common on-farm observation that tilling the soil before seeding a cover-crop jeopardizes the chances to yield high biomass cover-crops, thus discouraging many farmers to seed expensive multi-species cover-crops especially during summer short fallow periods.

The observed SOC increases are consistent with the regional study of Dupla et al. (2021). In contrast with the results obtained in the Swiss LTEs (Keel et al., 2019), Swiss farms can increase their SOC content at a rate greater than 4‰, although large negative change rates can also be found, which can be corrected in the future by applying changes in cropping practices. These results define a roadmap for SOC-increasing cropping systems in the region. The roadmap is based on progressive changes in the intensity of the different SOC content levers, depending on the current SOC:Clay ratio of the fields.

## AUTHOR CONTRIBUTIONS

XD, TL and KG collected the data under the supervision of PB. SG performed the analytic calculations and statistical modelling. XD and PB wrote the manuscript with support from SG, EV and RC. All authors provided critical feedback and helped shape the content of this study.

## FUNDING

Open access funding provided by University of Lausanne.

## ACKNOWLEDGMENTS

The authors thank Sebastien Gassmann, Soil Protection Division, Geneva, and François Füllemann, Soil Protection Division, Vaud, Nicolas Courtois, Agrigenève agricultural advisory association, Geneva and Andy Gray, English editor, for facilitating this work.

## SUPPLEMENTARY MATERIAL

The Supplementary Material for this article can be found online at: <https://www.frontiersin.org/articles/10.3389/fenvs.2022.834055/full#supplementary-material>

## REFERENCES

- Amelung, W., Bossio, D., de Vries, W., Kögel-Knabner, I., Lehmann, J., Amundson, R., et al. (2020). Towards a Global-Scale Soil Climate Mitigation Strategy. *Nat. Commun.* 11, 5427. doi:10.1038/s41467-020-18887-7
- Andriulo, A., Mary, B., and Guerif, J. (1999). Modelling Soil Carbon Dynamics with Various Cropping Sequences on the Rolling Pampas. *Agronomie* 19, 365–377. doi:10.1051/agro:19990504
- Autret, B., Mary, B., Chenu, C., Balabane, M., Girardin, C., Bertrand, M., et al. (2016). Alternative Arable Cropping Systems: A Key to Increase Soil Organic Carbon Storage? Results from a 16 Year Field experiment. *Agric. Ecosyst. Environ.* 232, 150–164. doi:10.1016/j.agee.2016.07.008
- Baveye, P. C., Berthelin, J., Tessier, D., and Lemaire, G. (2018). The “4 Per 1000” Initiative: A Credibility Issue for the Soil Science Community? *Geoderma* 309, 118–123. doi:10.1016/j.geoderma.2017.05.005
- Baveye, P. C., Schnee, L. S., Boivin, P., Laba, M., and Radulovich, R. (2020). Soil Organic Matter Research and Climate Change: Merely Re-storing Carbon versus Restoring Soil Functions. *Front. Environ. Sci.* 8. doi:10.3389/fenvs.2020.579904
- Blanco-Canqui, H., Francis, C. A., and Galusha, T. D. (2017). Does Organic Farming Accumulate Carbon in Deeper Soil Profiles in the Long Term? *Geoderma* 288, 213–221. doi:10.1016/j.geoderma.2016.10.031

- Blanco-Canqui, H., Shapiro, C. A., Wortmann, C. S., Drijber, R. A., Mamo, M., Shaver, T. M., et al. (2013). Soil Organic Carbon: The Value to Soil Properties. *J. Soil Water Conservation* 68, 129A–134A. doi:10.2489/jswc.68.5.129A
- Blanco-Canqui, H., Shaver, T. M., Lindquist, J. L., Shapiro, C. A., Elmore, R. W., Francis, C. A., et al. (2015). Cover Crops and Ecosystem Services: Insights from Studies in Temperate Soils. *Agron. J.* 107, 2449–2474.
- Bouthier, A., Duparque, A., Mary, B., Sagot, S., Trochard, R., Levert, M., et al. (2014). Adaptation et mise en œuvre du modèle de calcul de bilan humique à long terme AMG dans une large gamme de systèmes de grandes cultures et de polyculture-élevage. *Innov. Agronomiques* 34, 125–139.
- Büchi, L., Georges, F., Walder, F., Banerjee, S., Keller, T., Six, J., et al. (2019). Potential of Indicators to Unveil the Hidden Side of Cropping System Classification: Differences and Similarities in Cropping Practices between Conventional, No-Till and Organic Systems. *Eur. J. Agron.* 109, 125920. doi:10.1016/j.eja.2019.125920
- Büchi, L., Wendling, M., Amossé, C., Necpalova, M., and Charles, R. (2018). Importance of Cover Crops in Alleviating Negative Effects of Reduced Soil Tillage and Promoting Soil Fertility in a winter Wheat Cropping System. *Agric. Ecosyst. Environ.* 256, 92–104. doi:10.1016/j.agee.2018.01.005
- Bünemann, E. K., Bongiorno, G., Bai, Z., Creamer, R. E., De Deyn, G., de Goede, R., et al. (2018). Soil Quality - A Critical Review. *Soil Biol. Biochem.* 120, 105–125. doi:10.1016/j.soilbio.2018.01.030
- Chambers, A., Lal, R., and Paustian, K. (2016). Soil Carbon Sequestration Potential of US Croplands and Grasslands: Implementing the 4 Per Thousand Initiative. *J. Soil Water Conservation* 71, 68A–74A. doi:10.2489/jswc.71.3.68A
- Chatfield, C. (1995). Model Uncertainty, Data Mining and Statistical Inference. *J. R. Stat. Soc. Ser. A (Statistics Society)* 158, 419–466. doi:10.2307/2983440
- Chen, S., Arrouays, D., Angers, D. A., Martin, M. P., and Walter, C. (2019). Soil Carbon Stocks under Different Land Uses and the Applicability of the Soil Carbon Saturation Concept. *Soil Tillage Res.* 188, 53–58. doi:10.1016/j.still.2018.11.001
- Chenu, C., Angers, D. A., Barré, P., Derrien, D., Arrouays, D., and Balesdent, J. (2019). Increasing Organic Stocks in Agricultural Soils: Knowledge Gaps and Potential Innovations. *Soil Tillage Res.* 188, 41–52. doi:10.1016/j.still.2018.04.011
- Colombi, T., Walder, F., Büchi, L., Sommer, M., Liu, K., Six, J., et al. (2019). On-farm Study Reveals Positive Relationship between Gas Transport Capacity and Organic Carbon Content in Arable Soil. *SOIL* 5, 91–105. doi:10.5194/soil-5-91-2019
- Cook, S., Cock, J., Oberthür, Th., and Fisher, M. (2013). On-Farm Experimentation. *Better Crops* 97, 17–20.
- De Vries, W. (2018). Soil Carbon 4 Per Mille: a Good Initiative but Let's Manage Not Only the Soil but Also the Expectations. *Geoderma* 309, 124–129. doi:10.1016/j.geoderma.2017.05.026
- Deluz, C., Nussbaum, M., Sauzet, O., Gondret, K., and Boivin, P. (2020). Evaluation of the Potential for Soil Organic Carbon Content Monitoring with Farmers. *Front. Environ. Sci.* 8, 113. doi:10.3389/fenvs.2020.00113
- Dexter, A. R., Richard, G., Arrouays, D., Czyż, E. A., Jolivet, C., and Duval, O. (2008). Complexed Organic Matter Controls Soil Physical Properties. *Geoderma* 144, 620–627. doi:10.1016/j.geoderma.2008.01.022
- Dignac, M.-F., Derrien, D., Barré, P., Barot, S., Cécillon, L., Chenu, C., et al. (2017). Increasing Soil Carbon Storage: Mechanisms, Effects of Agricultural Practices and Proxies. A Review. *Agron. Sustain. Dev.* 37, 14. doi:10.1007/s13593-017-0421-2
- Dimassi, B., Mary, B., Wylleman, R., Labreuche, J., Couture, D., Piraux, F., et al. (2014). Long-term Effect of Contrasted Tillage and Crop Management on Soil Carbon Dynamics during 41 Years. *Agric. Ecosyst. Environ.* 188, 134–146. doi:10.1016/j.agee.2014.02.014
- Dupla, X., Gondret, K., Sauzet, O., Verrecchia, E., and Boivin, P. (2021). Changes in Topsoil Organic Carbon Content in the Swiss Leman Region Cropland from 1993 to Present. Insights from Large Scale On-Farm Study. *Geoderma* 400, 115125. doi:10.1016/j.geoderma.2021.115125
- EASAC (2019). *Forest Bioenergy, Carbon Capture and Storage, and Carbon Dioxide Removal: An Update*. Halle: German National Academy of Sciences Leopoldina.
- EASAC (2018). *Negative Emission Technologies: What Role in Meeting Paris Agreement Targets?*. Halle: German National Academy of Sciences Leopoldina.
- Fließbach, A., Oberholzer, H.-R., Gunst, L., and Mäder, P. (2007). Soil Organic Matter and Biological Soil Quality Indicators after 21 Years of Organic and Conventional Farming. *Agric. Ecosyst. Environ.* 118, 273–284. doi:10.1016/j.agee.2006.05.022
- Giller, K. E., Hijbeek, R., Andersson, J. A., and Sumberg, J. (2021). Regenerative Agriculture: An Agronomic Perspective. *Outlook Agric.* 50, 13–25. doi:10.1177/0030727021998063
- Govaerts, B., Verhulst, N., Castellanos-Navarrete, A., Sayre, K. D., Dixon, J., and Dendooven, L. (2009). Conservation Agriculture and Soil Carbon Sequestration: Between Myth and Farmer Reality. *Crit. Rev. Plant Sci.* 28, 97–122. doi:10.1080/07352680902776358
- Haddaway, N. R., Hedlund, K., Jackson, L. E., Kätterer, T., Lugato, E., Thomsen, I. K., et al. (2017). How Does Tillage Intensity Affect Soil Organic Carbon? A Systematic Review. *Environ. Evid.* 6, 1–48. doi:10.1186/s13750-017-0108-9
- Hobbs, P. R., Sayre, K., and Gupta, R. (2008). The Role of Conservation Agriculture in Sustainable Agriculture. *Phil. Trans. R. Soc. B* 363, 543–555. doi:10.1098/rstb.2007.2169
- IPCC (2006). *2006 IPCC Guidelines for National Greenhouse Gas Inventories. Prepared by the National Greenhouse Gas Inventories Programme*. Editor H. S. Eggleston, L. Buendia, K. Miwa, T. Ngara, and K. Tanabe (Japan: IGES).
- IUSS Working Group WRB (2014). International Soil Classification System for Naming Soils and Creating Legends for Soil Maps. *Update 2015 World Soil Resour. Rep. No.* 106, 192.
- Jennings, D. S., Gardner, W., and Gardner, W. (1922). A New Method of Mechanical Analysis of Soils. *Soil Sci.* 14, 485–499. doi:10.1097/00010694-192212000-00011
- Johannes, A., Matter, A., Schulin, R., Weisskopf, P., Baveye, P., and Boivin, P. (2017). Optimal Organic Carbon Values for Soil Structure Quality of Arable Soils. Does clay Content Matter? *Geoderma* 302, 21. doi:10.1016/j.geoderma.2017.04.021
- Keel, S. G., Anken, T., Büchi, L., Chervet, A., Fließbach, A., Flisch, R., et al. (2019). Loss of Soil Organic Carbon in Swiss Long-Term Agricultural Experiments over a Wide Range of Management Practices. *Agric. Ecosyst. Environ.* 286, 106654. doi:10.1016/j.agee.2019.106654
- King, A. E., Ali, G. A., Gillespie, A. W., and Wagner-Riddle, C. (2020). Soil Organic Matter as Catalyst of Crop Resource Capture. *Front. Environ. Sci.* 8, 50. doi:10.3389/fenvs.2020.00050
- Kucharik, C. J., Brye, K. R., Norman, J. M., Foley, J. A., Gower, S. T., and Bundy, L. G. (2001). Measurements and Modeling of Carbon and Nitrogen Cycling in Agroecosystems of Southern Wisconsin: Potential for SOC Sequestration during the Next 50 Years. *Ecosystems* 4, 237–258. doi:10.1007/s10021-001-0007-2
- Lal, R. (2004). Soil Carbon Sequestration Impacts on Global Climate Change and Food Security. *Science* 304, 1623–1627. doi:10.1126/science.1097396
- Levassasseur, F., Mary, B., Christensen, B. T., Duparque, A., Ferchaud, F., Kätterer, T., et al. (2020). The Simple AMG Model Accurately Simulates Organic Carbon Storage in Soils after Repeated Application of Exogenous Organic Matter. *Nutr. Cycl. Agroecosyst.* 117, 215–229. doi:10.1007/s10705-020-10065-x
- Maltas, A., Charles, R., Jeangros, B., and Sinaj, S. (2013). Effect of Organic Fertilizers and Reduced-Tillage on Soil Properties, Crop Nitrogen Response and Crop Yield: Results of a 12-year experiment in Changins, Switzerland. *Soil Tillage Res.* 126, 11–18. doi:10.1016/j.still.2012.07.012
- McCullagh, P., and Nelder, J. A. (1989). *Generalized Linear Models*. London: CRC Press.
- McLauchlan, K. (2006). The Nature and Longevity of Agricultural Impacts on Soil Carbon and Nutrients: A Review. *Ecosystems* 9, 1364–1382. doi:10.1007/s10021-005-0135-1
- Merante, P., Dibari, C., Ferrise, R., Sánchez, B., Iglesias, A., Lesschen, J. P., et al. (2017). Adopting Soil Organic Carbon Management Practices in Soils of Varying Quality: Implications and Perspectives in Europe. *Soil Tillage Res.* 165, 95–106. doi:10.1016/j.still.2016.08.001
- Minasny, B., Arrouays, D., McBratney, A. B., Angers, D. A., Chambers, A., Chaplot, V., et al. (2018). Rejoinder to Comments on Minasny et al., 2017 Soil carbon 4 per mille. *Geoderma* 292, 59–86. *Geoderma* 309, 124–129. doi:10.1016/j.geoderma.2017.05.026
- Minasny, B., Malone, B. P., McBratney, A. B., Angers, D. A., Arrouays, D., Chambers, A., et al. (2017). Soil Carbon 4 Per Mille. *Geoderma* 292, 59–86. doi:10.1016/j.geoderma.2017.01.002

- Nelson, D. W., and Sommers, L. (1983). Total Carbon, Organic Carbon, and Organic Matter. *Methods Soil Analysis. Part 2. Chem. Microbiol. properties* 9, 539–579. doi:10.2134/agronmonogr9.2.2ed.c29
- O'Connell, S., Grossman, J. M., Hoyt, G. D., Shi, W., Bowen, S., Marticorena, D. C., et al. (2015). A Survey of Cover Crop Practices and Perceptions of Sustainable Farmers in North Carolina and the Surrounding Region. *Renew. Agric. Food Syst.* 30, 550–562. doi:10.1017/S1742170514000398
- Olson, K. R., Al-Kaisi, M. M., Lal, R., and Lowery, B. (2014). Experimental Consideration, Treatments, and Methods in Determining Soil Organic Carbon Sequestration Rates. *Soil Sci. Soc. America J.* 78, 348–360. doi:10.2136/sssaj2013.09.0412
- Paustian, K., Larson, E., Kent, J., Marx, E., and Swan, A. (2019). Soil C Sequestration as a Biological Negative Emission Strategy. *Front. Clim.* 1. doi:10.3389/fclim.2019.00008
- Peel, M. C., Finlayson, B. L., and McMahon, T. A. (2007). Updated World Map of the Köppen-Geiger Climate Classification. *Hydrol. Earth Syst. Sci.* 11, 1633–1644. doi:10.5194/hess-11-1633-2007
- Poeplau, C., and Don, A. (2015). Carbon Sequestration in Agricultural Soils via Cultivation of Cover Crops - A Meta-Analysis. *Agric. Ecosyst. Environ.* 200, 33–41. doi:10.1016/j.agee.2014.10.024
- Power, A. G. (2010). Ecosystem Services and Agriculture: Tradeoffs and Synergies. *Phil. Trans. R. Soc. B* 365, 2959–2971. doi:10.1098/rstb.2010.0143
- Powlson, D. S., Stirling, C. M., Jat, M. L., Gerard, B. G., Palm, C. A., Sanchez, P. A., et al. (2014). Limited Potential of No-Till Agriculture for Climate Change Mitigation. *Nat. Clim Change* 4, 678–683. doi:10.1038/nclimate2292
- Powlson, D. S., Whitmore, A. P., and Goulding, K. W. T. (2011). Soil Carbon Sequestration to Mitigate Climate Change: a Critical Re-examination to Identify the True and the False. *Eur. J. Soil Sci.* 62, 42–55. doi:10.1111/j.1365-2389.2010.01342.x
- Prout, J. M., Shepherd, K. D., McGrath, S. P., Kirk, G. J. D., and Haefele, S. M. (2020). What Is a Good Level of Soil Organic Matter? an index Based on Organic Carbon to clay Ratio. *Eur. J. Soil Sci.* 72, 2493–2503. doi:10.1111/ejss.13012
- Ranaldo, M., Carlesi, S., Costanzo, A., and Barberi, P. (2020). Functional Diversity of Cover Crop Mixtures Enhances Biomass Yield and weed Suppression in a Mediterranean Agroecosystem. *Weed Res.* 60, 96–108. doi:10.1111/wre.12388
- Reicosky, D. C. (2003). "Tillage-Induced CO<sub>2</sub> Emissions and Carbon Sequestration: Effect of Secondary Tillage and Compaction," in *Conservation Agriculture: Environment, Farmers Experiences, Innovations, Socio-Economy, Policy*. Editors L. García-Torres, J. Benites, A. Martínez-Vilela, and A. Holgado-Cabrera (Dordrecht: Springer Netherlands), 291–300. doi:10.1007/978-94-017-1143-2\_35
- Robinson, G. W. (1922). A New Method for the Mechanical Analysis of Soils and Other Dispersions. *J. Agric. Sci.* 12, 306–321. doi:10.1017/s0021859600005360
- Ruis, S. J., and Blanco-Canqui, H. (2017). Cover Crops Could Offset Crop Residue Removal Effects on Soil Carbon and Other Properties: A Review. *Agron.j.* 109, 1785–1805. doi:10.2134/agronj2016.12.0735
- Rumpel, C., Amiraslani, F., Chenu, C., Garcia Cardenas, M., Kaonga, M., Koutika, L.-S., et al. (2020). The 4p1000 Initiative: Opportunities, Limitations and Challenges for Implementing Soil Organic Carbon Sequestration as a Sustainable Development Strategy. *Ambio* 49, 350–360. doi:10.1007/s13280-019-01165-2
- Sanderman, J., Hengl, T., and Fiske, G. J. (2017). Soil Carbon Debt of 12,000 Years of Human Land Use. *Proc. Natl. Acad. Sci. U.S.A.* 114, 9575–9580. doi:10.1073/pnas.1706103114
- Senapati, N., Chabbi, A., Gastal, F., Smith, P., Mascher, N., Loubet, B., et al. (2014). Net Carbon Storage Measured in a Mowed and Grazed Temperate Sown Grassland Shows Potential for Carbon Sequestration under Grazed System. *Carbon Manage.* 5, 131–144. doi:10.1080/17583004.2014.912863
- Smith, W. N., Grant, B. B., Campbell, C. A., McConkey, B. G., Desjardins, R. L., Kröbel, R., et al. (2012). Crop Residue Removal Effects on Soil Carbon: Measured and Inter-model Comparisons. *Agric. Ecosyst. Environ.* 161, 27–38. doi:10.1016/j.agee.2012.07.024
- Swinton, S. M., Lupi, F., Robertson, G. P., and Hamilton, S. K. (2007). *Ecosystem Services and Agriculture: Cultivating Agricultural Ecosystems for Diverse Benefits*. Elsevier.
- USDA (2003). Publication : USDA ARS. Available at: <https://www.ars.usda.gov/research/publications/publication/?seqNo115=158750> (Accessed November 21, 2021).
- Wendling, M., Büchi, L., Amossé, C., Jeangros, B., Walter, A., and Charles, R. (2017). Specific Interactions Leading to Transgressive Overyielding in Cover Crop Mixtures. *Agric. Ecosyst. Environ.* 241, 88–99. doi:10.1016/j.agee.2017.03.003
- Wendling, M., Charles, R., Herrera, J., Amossé, C., Jeangros, B., Walter, A., et al. (2019). Effect of Species Identity and Diversity on Biomass Production and its Stability in Cover Crop Mixtures. *Agric. Ecosyst. Environ.* 281, 81–91. doi:10.1016/j.agee.2019.04.032
- West, T. O., and Post, W. M. (2002). Soil Organic Carbon Sequestration Rates by Tillage and Crop Rotation. *Soil Sci. Soc. Am. J.* 66, 1930–1946. doi:10.2136/sssaj2002.1930
- White, R. E., Davidson, B., Lam, S. K., and Chen, D. (2018). A critique of the paper 'Soil carbon 4 per mille' by Minasny et al. (2017). *Geoderma* 309, 115–117. doi:10.1016/j.geoderma.2017.05.025
- Wold, S., Esbensen, K., and Geladi, P. (1987). Principal Component Analysis. *Chemometrics Intell. Lab. Syst.* 2, 37–52. doi:10.1016/0169-7439(87)80084-9
- Zomer, R. J., Bossio, D. A., Sommer, R., and Verchot, L. V. (2017). Global Sequestration Potential of Increased Organic Carbon in Cropland Soils. *Sci. Rep.* 7, 15554–15558. doi:10.1038/s41598-017-15794-8

**Conflict of Interest:** The authors declare that the research was conducted in the absence of any commercial or financial relationships that could be construed as a potential conflict of interest.

**Publisher's Note:** All claims expressed in this article are solely those of the authors and do not necessarily represent those of their affiliated organizations, or those of the publisher, the editors and the reviewers. Any product that may be evaluated in this article, or claim that may be made by its manufacturer, is not guaranteed or endorsed by the publisher.

Copyright © 2022 Dupla, Lemaitre, Grand, Gondret, Charles, Verrecchia and Boivin. This is an open-access article distributed under the terms of the Creative Commons Attribution License (CC BY). The use, distribution or reproduction in other forums is permitted, provided the original author(s) and the copyright owner(s) are credited and that the original publication in this journal is cited, in accordance with accepted academic practice. No use, distribution or reproduction is permitted which does not comply with these terms.



# Comparing Four Indexing Approaches to Define Soil Quality in an Intensively Cropped Region of Northern India

Narendra Kumar Lenka<sup>1\*</sup>, Bharat Prakash Meena<sup>1</sup>, Rattan Lal<sup>2</sup>, Abhishek Khandagle<sup>1</sup>, Sangeeta Lenka<sup>1\*</sup> and Abhay Omprakash Shirale<sup>1</sup>

<sup>1</sup>Indian Institute of Soil Science, Bhopal, India, <sup>2</sup>CFAES Rattan Lal Center for Carbon Management and Sequestration, The Ohio State University, Columbus, OH, United States

## OPEN ACCESS

### Edited by:

Jörg Luster,  
Swiss Federal Institute for Forest,  
Snow and Landscape Research  
(WSL), Switzerland

### Reviewed by:

Ruhollah Taghizadeh,  
University of Tübingen, Germany  
Mojtaba Zeraatpisheh,  
Henan University, China  
Agnieszka Klimkowicz-Pawlas,  
Institute of Soil Science and Plant  
Cultivation, Poland

### \*Correspondence:

Narendra Kumar Lenka  
nklenka74@gmail.com  
Sangeeta Lenka  
sangeeta\_2@rediffmail.com

### Specialty section:

This article was submitted to  
Soil Processes,  
a section of the journal  
Frontiers in Environmental Science

**Received:** 29 January 2022

**Accepted:** 07 March 2022

**Published:** 31 March 2022

### Citation:

Lenka NK, Meena BP, Lal R, Khandagle A, Lenka S and Shirale AO (2022) Comparing Four Indexing Approaches to Define Soil Quality in an Intensively Cropped Region of Northern India. *Front. Environ. Sci.* 10:865473. doi: 10.3389/fenvs.2022.865473

The usefulness of the soil quality index (SQI) as a tool to evaluate management options has mostly been studied within the boundaries of a crop or experimental field, calling for the need to enhance its utility in regional-scale soil health assessment. Thus, four quantitative approaches for computing the SQI were evaluated with samples collected from 0 to 15 and 15 to 30 cm depths at 156 points from the Trans-Gangetic Plains of North India. Principal component analysis (PCA) and soil function (SF)-based approaches were used to select the minimum dataset from 18 soil parameters and assign weights to key indicators. In both approaches, two different data transformation methods were followed: 1) routine method with maximum or minimum values of indicator parameters and 2) percentile method with the 90th or 10th percentile value as the denominator or numerator for “more is better” and “less is better” scoring functions, respectively. The PCA output with factor loadings from the varimax rotation showed six principal components accounting for 75% of the total variance, with PC1 explaining the highest variance (26.8%) followed by PC2 (16%). The SF-based approach was better than PCA in terms of a higher correlation of SQI with rice and wheat yields. The percentile method showed a higher correlation in both PCA and SF methods. The SQI computed from 0 to 30 cm soil data did not show any superiority over that from 0 to 15 cm soil. Thus, the soil function-based approach with the percentile method of data transformation proved better to compute the SQI and establish a relationship with production function.

**Keywords:** soil quality index, soil management assessment framework, soil productivity, soil ecosystem services (ES), quantification of soil functions, soil capital, regenerative agriculture

## 1 INTRODUCTION

Globally, soil-based production systems are showing signs of fatigue with an ever-increasing need for production intensification as most of the growth in agricultural production has to come from enhanced productivity from existing or shrinking agricultural land resources (Shah and Wu, 2019). The need to produce more food for a burgeoning population puts tremendous pressure on our production systems and natural resource base. Thus, scientific management for maintaining soil quality remains the key to ensuring global food security (Subba Rao and Lenka, 2020; Çelik et al., 2021; Janků et al., 2022). The soil quality index (SQI) approach has been used as a quantitative tool to establish linkage between soil health encompassing physical, chemical, and biological properties of soil and a management goal (Andrews et al., 2002; Abdollahi et al., 2015; Nakajima et al., 2015; Haney

et al., 2018; Vasu et al., 2021). However, the usefulness of SQI as a tool to evaluate management options has mostly been studied within the boundaries of a crop or experimental field (Sharma et al., 2005; Masto et al., 2007; Stott et al., 2011; Vasu et al., 2021). A few studies are available where the SQI approach has been used on a regional scale (Vasu et al., 2016).

As there is no direct method to measure soil quality, its assessment is attempted only through monitoring changes in specific soil quality indicators over time or comparing them over best management practices (Mukherjee and Lal, 2014; Nakajima et al., 2015; Zeraatpisheh et al., 2020; Çelik et al., 2021; Janků et al., 2022). Among the several soil quality evaluation procedures, the soil quality assessment framework (Andrews et al., 2004) involving normalization techniques and linear or non-linear scoring procedures has been used to evaluate the effect of management on soil health. In this framework, identifying soil quality indicators and assigning weights to each indicator parameter are critical in developing a robust SQI that can correlate well with a specific soil function (Amorim et al., 2020). Techniques such as expert opinion or statistical tools such as principal component analysis (PCA) have often been used to form a minimum database.

The SQI computed employing the PCA approach suffers from a significant limitation that only the principal components explaining at least 5% of the variation in the data and with eigenvalue > 1.0 are taken into account. In this process, some critical and vital parameters for a given management goal are sometimes excluded (Vasu et al., 2016). Next, the PCA-derived indicators change with time, and the weights of each indicator may be different in different management zones. On the contrary, a soil function-based approach involving expert opinion can be a less tedious and more reliable approach for use on a regional scale provided the computed SQI is validated with the parameter defined for the specific management goal (Fernandes et al., 2011).

In either of these methods, data transformation is done using linear or non-linear scoring techniques. Most of the indexing methods have used three scoring functions, viz., “more is better,” “less is better,” or “optimum is better,” as per the type of indicator parameter and its importance to the soil function under study (Karlen et al., 2013; Lenka et al., 2014; Nakajima et al., 2015; Vasu et al., 2021). In this method, the maximum or minimum of the parameter value is taken as the denominator or numerator, respectively, to transform the parameter values to unitless scores as per the scoring function chosen (more is better, less is better, or optimum is better). A single value of maximum or minimum to transform the data is suitable in small experimental field studies. However, when the SQI is used on a regional scale, the values of maxima or minima for data transformation can be exceptionally high or low and thus may bring in error in the computation of indicator scores. Instead, the 90th percentile value for “more is better” and the 10th percentile value for “less is better” type of indicator can more appropriately represent the highest or lowest class of the indicator parameter. However, all previous attempts to compute the SQI are based on the maximum or minimum value for data transformation. No study has been available showing the parameter values of the highest or the lowest group being used

for data transformation. Furthermore, it is argued that the SQI computed using soil profile data (0–30 cm or 0–60 cm depth) may be better correlated with crop yield than that calculated from the surface soil data (Mukherjee and Lal, 2014; Vasu et al., 2016). However, some other studies report a different trend of results (Karlen et al., 2013).

Keeping the above in view, the objectives of this study were 1) to compare the PCA-based approach with the soil function-based approach for the computation of SQI on a regional scale, 2) to compare the two data transformation procedures, viz., the routine method vs. the percentile method, and 3) to compare the SQI computed from the surface soil (0–15 cm soil depth) data with that computed from the 0–30 cm data. This study is based on the following three hypotheses: the computed SQI would be more relevant and better correlate with the production goal 1) if the parameters of the MDS adequately represent the soil functions, 2) if the data transformation procedure is not based on a single extreme parameter value, rather than based on a class of values, and 3) if soil data of a profile or greater depth is used than the surface layer or 0–15 cm depth data.

## 2 MATERIALS AND METHODS

### 2.1 Study Region

The Udham Singh Nagar district, with a geographical area of 3,055 km<sup>2</sup> in the state of Uttarakhand, India, is the study region. The district is a part of the Trans-Gangetic Plains of India and is intensively cultivated (cropping intensity of about 212%), with rice (*Oryza sativa*) and wheat (*Triticum aestivum*) being the major crops. It is one of India's highest chemical fertilizer-consuming regions per the Fertilizer Use Statistics (Fertilizer Association of India, 2017), with an average consumption of 545 kg ha<sup>-1</sup> of N + P<sub>2</sub>O<sub>5</sub> + K<sub>2</sub>O. The district is considered the food bowl of the Uttarakhand state and lies between 28°43' N and 31°27' N latitude and between 77°34' E and 81°02' E longitude. The climate of the study district is sub-tropical sub-humid with 1,433 mm of annual average rainfall. The annual maximum temperature goes up to 42°C during the summer months, and the minimum temperature varies between 1°C and 4°C. Inceptisols and Entisols are the major soil types, with Udifluventic Ustochrepts, Typic Ustipsamments, Udic Ustochrepts, Udic Haplusterts, and Typic Ustochrepts being the major soil classes (Soil Survey Staff, 2014).

### 2.2 Soil Sampling and Analysis

Georeferenced soil samples were collected during the months of May to June in the year 2019 from 0 to 15 cm and 15 to 30 cm depths after the harvest of the winter season crop. From the study district, samples were collected at 10 km grid points. For identifying grid points, the Toposheet of Survey of India was used. Each grid point represented either one village or a village cluster within a 5 km distance. From each grid village or village cluster, 2–4 farmers representing a small/medium and a large farmer category were selected. Soil samples were collected by making composite samples from 5 to 7 auger points from each sampling farmer. In total, samples were collected from 156

locations. The samples were air-dried and sieved for laboratory analysis for 18 parameters, including physical, chemical, and biological soil properties. The sample passing through a 0.5 mm sieve was used for estimating organic carbon. In contrast, soil samples passing through 2 mm sieves were used for the remaining soil quality parameters. The physical parameters were bulk density and soil moisture retention at 33 and 1,500 kPa in Pressure Plate Apparatus, and chemical parameters were pH, electrical conductivity (EC), available N (N), available P (P), available K (K), cation exchange capacity (CEC), available sulfur (S),  $\text{KMnO}_4$  oxidizable carbon, and the soil organic carbon fractions (very labile, labile, and less labile fractions distinguished on the basis of the chemical oxidation method). The biological parameters were the dehydrogenase assay (DHA), fluorescein diacetate (FDA), soil respiration, and acid phosphatase activity. Standard analytical protocols Lenka et al. (2019) were used for estimating the 18 soil quality parameters (Supplementary Table S1).

Yield data of rice and wheat crops for the five previous years were collected from individual farm holders through a questionnaire. The average of five-year yield data was used for regressing with SQI values.

## 2.3 Minimum Dataset Selection

### 2.3.1 Principal Component Analysis Method

The PCA method is a dimension reduction approach in which the number of variables of the dataset is reduced by retaining most of the original variability in the dataset. Principal components (PCs) with high eigenvalues are considered best representatives explaining the variability (Mukherjee and Lal, 2014; Zeraatpisheh et al., 2020). The PCA in this study was carried out for the 18 soil parameters. The PCs with eigenvalues  $\geq 1$  were selected, as they described more data variability. The retained PCs were subjected to varimax rotation to maximize the correlation between each PC and soil properties by distributing the variance. Under each PC, highly weighted variables were selected as critical soil quality indicators for the computation of SQI. Multivariate correlation coefficients were used to check for redundancy and correlation between the variables. If the variables are well-correlated ( $r \geq 0.70$ ), then the variable having the highest factor loading (absolute value) was retained as an indicator among the well-correlated variables. In case of a non-significant correlation between the highly weighted variables, reflecting their independent functioning, all the variables were retained in the minimum dataset (Vasu et al., 2016). The variables selected from this procedure formed the MDS and were termed the “key indicators” and were considered for computation of SQI.

### 2.3.2 Soil Function–Based Approach

In this approach, primary soil functions were defined based on expert opinion with regard to their established role in the soil production function, similar to the “Soil Management Assessment Framework” suggested by Andrews et al. (2004) and Wienhold et al. (2009). Indicators under the four soil functions, viz., 1) soil structure and water storage, 2) nutrient supply function, 3) soil biological activity, and 4) soil basic characteristics having the potential to limit soil use for

production, were selected based on expert opinion, previous literature, and facts about the edaphic conditions of the study area (Table 1). The appropriate scoring functions for each parameter are shown in Table 1.

## 2.4 Data Transformation

### 2.4.1 Linear Scoring With a Single Value of Maximum or Minimum

The selected indicators in the MDS in both PCA and SF approaches were transformed into dimensionless values ranging from 0 to 1 using the linear scoring method (Stott et al., 2011; Amorim et al., 2020). Indicators were ranked in ascending or descending order depending on whether a higher value was considered “good” or “bad” in terms of soil function. For “more is better” indicators, each indicator value was divided by the highest value (maximum) such that the highest value received a score of 1.0. For “less is better” indicators, the lowest value (minima) was divided by the indicator value such that the lowest value received a score of 1.0. The “optimum is better” function was considered for some indicators like pH. The “more is better” function was considered up to a threshold range (pH of 6.5–7.5), after which the “lower is better” function was used as described above (Sharma et al., 2005; Zeraatpisheh et al., 2020). The indicator score was calculated as per the following formula:

$$\text{Score} = \frac{\text{Parameter value}}{\text{Maxima (highest value) of the dataset}} \quad (\text{For 'more is better' indicators}) \quad (1)$$

$$\text{Score} = \frac{\text{Minima (lowest value of the database)}}{\text{Parameter value}} \quad (\text{For 'less is better' indicators}) \quad (2)$$

### 2.4.2 Linear Scoring With Percentile Value as Maximum or Minimum

In this method, the 90th percentile value of a particular indicator parameter was considered the maximum value for the “more is better” type of indicator, whereas the 10th percentile value of the indicator parameter was taken as the minimum value for the “less is better type” of parameter. The other procedures were similar to those described in Section 2.4.1. If the computed score was higher than 1.0, it was restricted to a maximum value of 1.0. The indicator score was calculated using the following formula:

$$\text{Score} = \frac{\text{Parameter value}}{\text{90th percentile value of the dataset}} \quad (\leq 1.0) \quad (\text{For 'more is better' indicators}) \quad (3)$$

$$\text{Score} = \frac{\text{10th percentile value of the dataset}}{\text{Parameter value}} \quad (\leq 1.0) \quad (\text{For 'less is better' indicators}) \quad (4)$$

**TABLE 1** | Soil functions, their indicators, and assigned weights.

Function	Weight	Function indicators	Weight	Scoring function
Maintaining soil structure and water storage	0.35	Soil organic carbon	0.20	More is better
		Available water capacity	0.10	More is better
		Bulk density	0.05	Less is better
Nutrient supply function	0.25	KMnO <sub>4</sub> oxidizable C	0.05	More is better
		Available N	0.05	More is better
		Available P	0.05	More is better
		Available K	0.05	More is better
		Available S	0.05	More is better
Soil biological activity	0.20	Soil respiration	0.10	More is better
		Dehydrogenase	0.05	More is better
		Fluorescein diacetate	0.05	More is better
Soil basic properties, potential to limit production	0.20	pH	0.10	Optimum is better
		EC	0.10	Less is better

## 2.5 Assigning Weights

The next step in SQI calculation was assigning weights to each indicator parameter selected under the MDS. In the PCA approach, the selected indicators in the MDS were given weights using the PCA output. Each PC explained a certain percentage of variability in the total dataset. The percentage of variance explained by each indicator under a particular PC, when divided by the cumulative percentage of variance explained by all PCs with eigenvectors > 1, gave the weight for the indicator(s) selected under a given PC.

In the SF-based approach, weights were assigned first to the major soil functions (Table 1). In the second level, the weights of each soil function were further sub-divided to the indicator parameters as per the relative importance of the particular indicator, assessed by expert opinion and as per the literature survey (Fernandes et al., 2011; Vasu et al., 2016).

## 2.6 SQI Calculation

The indicators were assigned weights so that the sum of weights of all factors is unity. The weighted MDS indicator scores for each observation were summed up using the following function:

$$SQI = \sum_{i=1}^{i=n} Wi.Si \quad (5)$$

where  $Wi$  = weight assigned to each selected indicator and  $Si$  = score of each indicator.

The SQI, as discussed above, was computed using the soil data of two different depths, viz., 0–15 cm and 0–30 cm data.

## 2.7 Statistical Analysis

The dimension reduction of the data was performed through principal component analysis to select the minimum dataset. The normality of the data was checked by the Shapiro–Wilk test at  $p < 0.05$ , and the data were found to be normally distributed. Pearson's correlation coefficient was used as the indicator to evaluate the statistical correlation between the SQI and the crop yield. The significance of the correlation was tested by Student's  $t$ -test at  $p < 0.05$ . The statistical analysis was carried out using the statistical software SPSS Version 21.0.

## 3 RESULTS

### 3.1 Descriptive Statistics of Soil Properties

The soil samples were analyzed for 18 parameters covering important physical, chemical, and biological properties. The data on soil properties (Table 2) showed soils of the study region were mostly neutral in reaction with the average pH of 7.26 (varying from 5.39 to 8.54). The soils were mostly non-saline (average EC of 0.17 dS m<sup>-1</sup>), good in soil organic carbon content (average SOC of 0.80%), and moderate in AWC (average value of 28.84%) despite variations in the samples. The average CEC was 15.25 cmol (p<sup>+</sup>) kg<sup>-1</sup>, BD was 1.45 Mg m<sup>-3</sup>, soil respiration was 4.94 mg CO<sub>2</sub>/100g/day, and KMnO<sub>4</sub> oxidizable C was 564 mg kg<sup>-1</sup>. The data indicated higher lability of SOC as observed from the values of very labile fraction and the KMnO<sub>4</sub> oxidizable C. The physical parameters were less variable with a lower coefficient of variation (CV) value than chemical and biological parameters. The most variable parameters (CV > 0.35) were available P, K, and S, CEC, EC, FDA, soil respiration, and the carbon fractions (labile, less labile, and very labile) (Wilding, 1985). Compared to the carbon fractions, SOC and KMnO<sub>4</sub> oxidizable carbon showed less variability. In terms of available nutrients, the plant available N was mostly in the low range (average of 226 kg ha<sup>-1</sup>), but available P and K were in the range of high availability (average values of P and K were 67 and 238 kg ha<sup>-1</sup>, respectively). The moderately variable (CV, 0.15–0.35) parameters were available N, AWC, SOC, dehydrogenase, and acid phosphatase. However, pH and BD were the least variable (CV < 0.15) parameters. The skewness of most of the parameters was within the range of -0.5 to + 0.5, indicating a reasonably symmetrical distribution. Data of available K and less labile C fraction were positively skewed. The data distribution of available K and less labile C fraction was leptokurtic with kurtosis values greater than 3.0, indicating more outliers. However, distributions of other monitored parameters were platykurtic with kurtosis values lower than 3.0 and indicating fewer extreme values (Table 2).

**TABLE 2 |** Descriptive statistics of soil properties of 0–15 cm depth used for soil quality assessment ( $n = 156$ ).

Soil property	Min.	Max.	Mean	90th percentile	10th percentile	Median	SD	Skewness	Kurtosis	CV (%)
pH	5.39	8.54	7.26	8.28	5.85	7.34	0.80	−0.59	−0.34	11.02
EC	0.07	0.37	0.17	0.28	0.09	0.16	0.07	0.92	0.49	42.63
Bulk density ( $\text{Mg m}^{-3}$ )	1.13	1.72	1.45	1.62	1.25	1.45	0.14	−0.25	−0.40	9.48
Available water capacity (% v/v)	8.89	42.57	28.84	38.87	18.59	29.82	8.10	−0.51	−0.10	28.08
Cation exchange capacity ( $\text{C mol kg}^{-1}$ )	6.70	30.43	15.25	23.21	8.19	14.48	5.61	0.66	0.15	36.81
Soil organic carbon (%)	0.20	1.44	0.80	1.19	0.51	0.76	0.27	0.33	−0.15	33.61
Very labile carbon ( $\text{mg kg}^{-1}$ )	1515	9796	4460	6690	2400	4112	1671	0.70	0.70	37.5
Labile carbon ( $\text{mg kg}^{-1}$ )	261	4592	2218	3506	758	2283	1022	0.06	−0.34	46.1
Less labile carbon ( $\text{mg kg}^{-1}$ )	182	6958	1300	2321	493	1062	1048	3.48	16.54	80.5
Soil respiration ( $\text{mg CO}_2/100 \text{ g/day}$ )	1.05	8.38	4.94	7.33	2.62	4.71	1.90	−0.03	−1.05	38.48
$\text{KMnO}_4$ oxidizable C ( $\text{mg kg}^{-1}$ )	285	793	564	736	363	559	129	−0.33	−0.41	22.9
Available N ( $\text{kg ha}^{-1}$ )	134	370	226	263	174	227	42	0.92	2.93	18.9
Available P ( $\text{kg ha}^{-1}$ )	21.40	132.90	66.87	107.42	35.69	60.45	28.02	0.63	−0.45	41.90
Available K ( $\text{kg ha}^{-1}$ )	63	987	238	385	92	194.32	175.90	2.61	8.34	73.77
Available S ( $\text{kg ha}^{-1}$ )	1.86	88.27	26.45	74.09	4.54	17.40	24.84	1.26	0.48	93.89
Dehydrogenase activity ( $\mu\text{g TPF g}^{-1} 24 \text{ hr}^{-1}$ )	76	304	151	212	96	134	50	0.69	0.25	32.83
Fluorescein diacetate activity ( $\mu\text{g fluorescein g soil}^{-1} \text{ hr}^{-1}$ )	10	94	49	73	22	49	19	0.10	0.39	38.34
Acid phosphatase activity ( $\mu\text{g PNP g soil}^{-1} \text{ hr}^{-1}$ )	226	548	403	489	326	396	68	−0.09	0.50	16.95

SD, standard deviation; CV, coefficient of variation.

**TABLE 3 |** Output of principal component analysis with eigenvalue, variance, and factor loadings of component matrix variables ( $n = 156$ ).

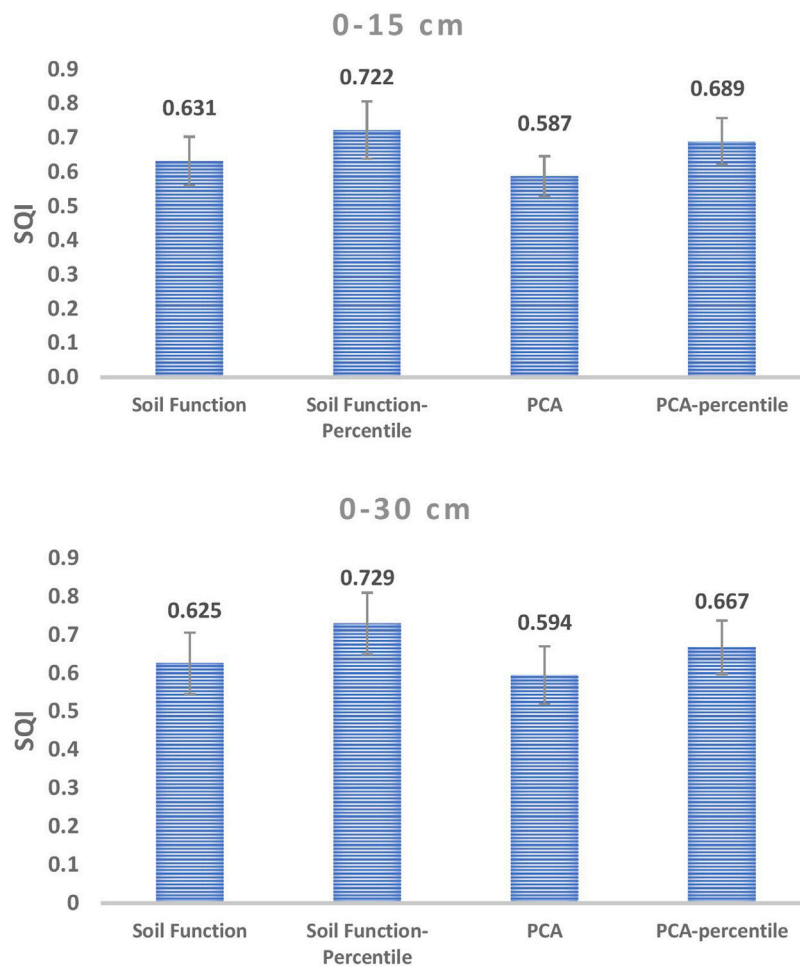
Principal components	PC1	PC2	PC3	PC4	PC5	PC6
Eigenvalue	4.817	2.888	1.912	1.568	1.299	1.072
% variance	26.763	16.043	10.623	8.711	7.215	5.954
% cumulative variance	26.763	42.806	53.429	62.140	69.355	75.309
Weightage assigned	35.537	21.303	14.106	11.567	9.581	7.906
<b>Factor loadings (rotated component matrix)</b>						
pH	0.180	−0.239	0.011	<b>0.758</b>	0.295	−0.227
EC	0.518	<b>−0.640</b>	−0.345	0.207	0.136	−0.161
Dehydrogenase	−0.329	0.483	0.220	0.524	0.181	0.109
Fluorescein diacetate	0.340	0.423	0.386	−0.289	0.278	0.451
Acid phosphatase	−0.090	0.524	−0.209	0.083	0.032	0.056
Soil organic C	<b>0.928</b>	−0.142	0.157	0.190	−0.002	−0.161
Very labile C	<b>0.862</b>	−0.123	0.239	0.142	0.107	−0.149
Labile C	<b>0.625</b>	−0.400	0.127	−0.201	0.060	−0.307
Less labile C	0.480	0.263	−0.104	0.546	−0.268	0.142
$\text{KMnO}_4$ oxidizable C	0.530	0.301	0.559	−0.202	−0.194	−0.154
Available N	<b>0.779</b>	0.137	−0.046	−0.069	−0.138	0.211
Available K	<b>0.694</b>	0.025	0.075	0.091	0.460	0.192
Available P	0.124	<b>0.758</b>	0.041	−0.060	0.133	−0.099
Available S	0.024	0.175	−0.082	0.135	<b>0.805</b>	−0.144
Bulk density	−0.039	−0.051	<b>0.797</b>	0.008	0.416	0.122
Cation exchange capacity	0.426	0.084	0.508	0.244	−0.221	−0.375
Soil respiration	−0.045	−0.012	0.083	−0.029	−0.122	<b>0.818</b>
Available water capacity	0.129	−0.095	<b>0.712</b>	0.032	−0.177	0.101

The values of factor loadings in Bold letter were highly weighted variables. The underlined ones are variables retained in the MDS.

### 3.2 Principal Component Analysis

The PCA output showed six PCs with eigenvalue  $>1$ , accounting for 75% of the variance (Table 3). PC1 explained the highest variance (26.76%) followed by PC2 (16%), PC3 (10%), PC4 (8.7%), PC5 (7.2%), and PC6 (5.95%). The factor loadings resulting from the varimax rotation showed SOC, very labile C, labile C, available N, and available K to be the factors under PC1. However, multiple regression indicated SOC was highly

correlated with labile C and very labile C (Supplementary Table S2). Hence under PC1, SOC, available N, and available K were retained as the indicator parameters for MDS. Under PC2, higher values of factor loadings were for EC and available P. The multiple correlation values showed EC and available P to be weakly correlated (Supplementary Table S3). Hence, both EC and available P were retained under PC2 for MDS formation. Similarly, BD was retained under PC3 (Supplementary Table



**FIGURE 1** | Soil quality index (SQI) of 0–15 cm and 0–30 cm soil under four indexing procedures ( $n = 156$ ). Error bars indicate standard deviation.

S4). For PC4, PC5, and PC6, only single parameters showed factor loadings greater than 0.60. Hence, pH, available S, and soil respiration were included for MDS under PC4, PC5, and PC6, respectively.

### 3.3 Indicator Weights and Weighted Scores

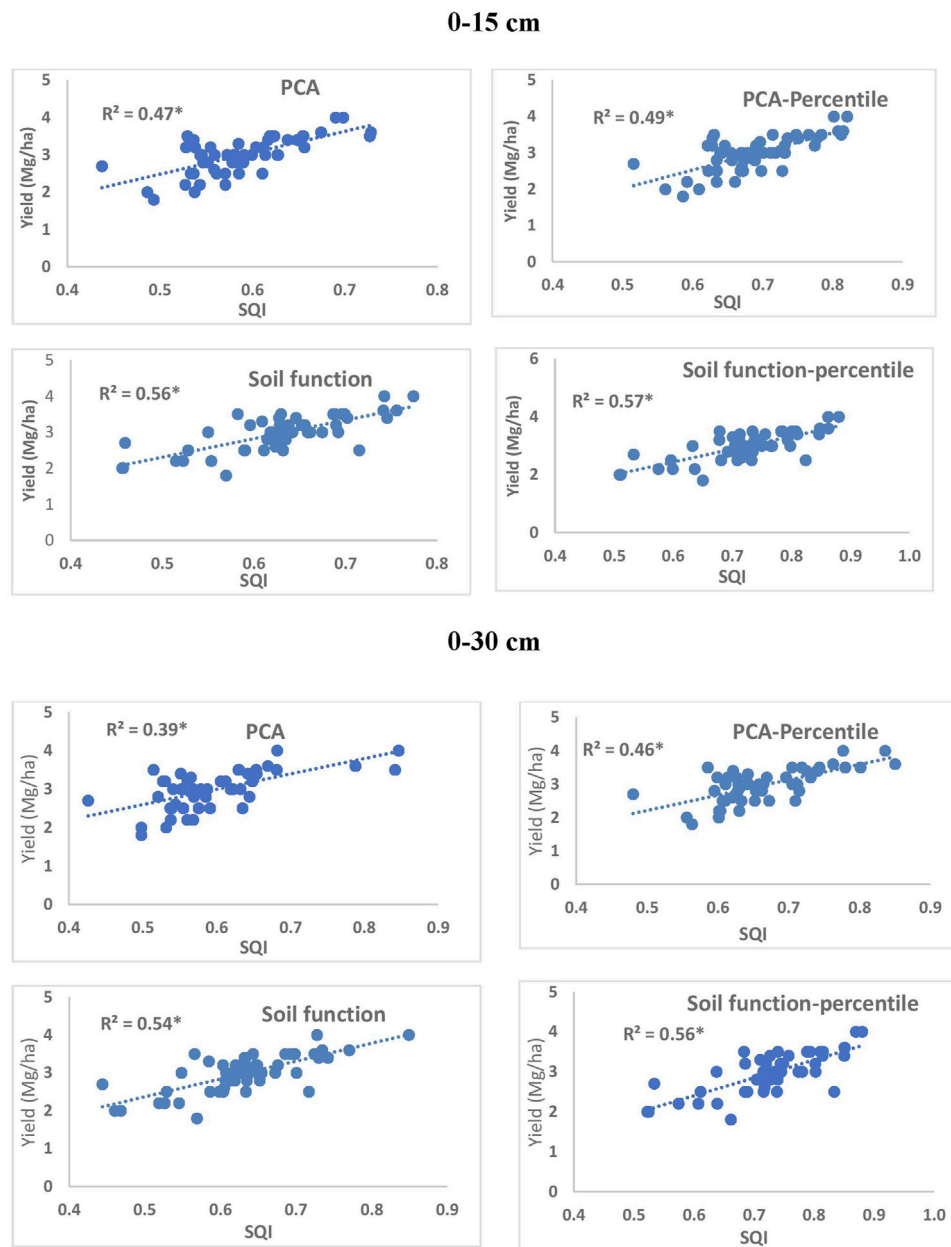
In the PCA approach, weights were assigned to the nine selected indicators as per the percentage of variance explained by selected indicators in each PC (Table 3). For instance, the variance explained by PC1 was divided among three indicators, viz., SOC, available N, and available K. Thus, SOC, available N, and available K received a weight of 11.8% each. The bulk density (BD) was the only physical parameter under the MDS and received a score of 14%. In contrast, soil respiration (SR) was the only biological parameter and received a score of 8%. The average weighted scores were higher when the percentile values were used as numerators or denominators than when the routinely used maximum or minimum values were used (Supplementary Figure S1). Among parameters, the weighted score was higher for SOC and BD. Despite an equal weight assigned to SOC, available N, and available K, the average weighted score of available N and available K was lower than that of SOC in both the

scoring techniques (PCA and PCA-percentile). This trend was observed due to uniformly distributed parameter values in SOC compared to the maximum or 90th percentile values. On the contrary, due to high fertilizer application in the study region, few values were much higher than their corresponding population in the case of nutrient elements such as available N, P, and K, thus reducing their weighted scores.

In the SF method, 13 parameters were selected covering physical, chemical, and biological properties (Table 1). SOC was given a score of 20%, considering its role in multiple soil functions. The physical parameters, viz., BD and AWC, were jointly assigned a score of 15%. Like the PCA method, the average weighted scores were higher when the percentile values were used as numerators or denominators than when the routinely used maximum or minimum values were used (Supplementary Figure S2).

### 3.4 Soil Quality Index

The average SQI values computed using the four methods for the two sets of soil data (0–15 cm and 0–30 cm) are shown in Figure 1. In both the datasets, the SQI value in the PCA



**FIGURE 2 |** Correlation of soil quality index (SQI) derived from the soil data of 0–15 cm and 0–30 cm with rice yield under the four different indexing methods ( $n = 52$ ).

method was the lowest (**Figure 1**), whereas the highest SQI values were observed in the SF-percentile method. When percentile values were used as numerators or denominators for transforming data to unitless scores, the computed SQI values increased in the PCA and SF methods. The average SQI values of the 0–15 cm soil were 0.587, 0.631, 0.689, and 0.722 under PCA, PCA-percentile, SF, and SF-percentile methods (**Figure 1**; **Supplementary Table S5**). In all the indexing methods, SQI values of the 0–30 cm soil were similar to the corresponding SQI of the 0–15 cm soil. The SQI of the 0–15 cm soil varied from 0.44 to 0.73 under PCA, 0.46 to 0.77 under SF, 0.52 to 0.82 under

PCA-percentile, and 0.51 to 0.88 under SF-percentile methods (**Supplementary Table S5**). The range of SQI in the 0–30 cm soil was slightly higher than that in 0–15 cm soil.

### 3.5 Regression of SQI With Crop Yield

The SQI computed using the four methods was correlated with rice and wheat yield (**Figure 2**; **Supplementary Figure S3**). In all cases, the correlation was significant between SQI and crop yield at  $p < 0.05$ . In both the crops and in both the computing methods (PCA and SF), the correlation ( $r^2$ ) values were higher in the percentile technique. Furthermore, for any data transformation

technique, the  $r^2$  values were higher in the SF than in the PCA method. The SQI correlated better with rice yield (**Figure 2**) than with wheat yield (**Supplementary Figure S3**). For any crop and indexing method, the correlation between SQI and yield was better when the SQI was computed using soil data from 0 to 15 cm soil depth than that from 0 to 30 cm soil data. For instance, the  $r^2$  value between SQI and rice yield in the PCA method was 0.47 when the SQI was computed using the 0–15 cm soil data (**Figure 2**). However, a lower correlation ( $r^2 = 0.39$ ) was observed when the soil data of 0–30 cm (average of 0–15 and 15–30 cm depths) were used (**Figure 2**).

## 4 DISCUSSION

### 4.1 Method for Selection of Indicators: PCA vs. SF (Expert Opinion) Approach

Our results showed that the soil function-based approach (based on expert opinion and representing the major soil functions) resulted in a better correlation of SQI with yields of both the test crops (rice and wheat), thus indicating the first hypothesis set in this study. We termed it the “soil function-based method” in place of “expert opinion” to highlight the role of soil functions in deciding the management goal. One of the reasons for higher correlation under the SF-based approach was the inclusion of representative variables in the MDS covering physical, chemical, and biological parameters. The indicators chosen under the SF-based approach covered the four major soil functions, viz., soil structure and water storage, nutrient supply, soil biological activity, and the basic soil properties limiting production (**Table 1**). Also under these broad soil functions, key parameters were considered as per expert opinion. On the contrary, nine indicators were part of the MDS in the PCA method where only single parameters were covered under physical (BD) and biological (soil respiration) properties. Similar to our study, Gelaw et al. (2015) included SOC, water stable aggregation, total porosity, total N, microbial biomass carbon, and CEC as the parameters covering four soil functions, viz., 1) accommodating water entry, 2) facilitating water movement and availability, 3) resisting degradation, and 4) supplying nutrients for plant growth and estimating SQI using a soil management assessment framework for four land uses in smallholder farm situations in Ethiopia. Such an approach based on soil functions was also attempted by Fernandes et al. (2011) for soil quality evaluation under different tillage practices in Brazil. Amorim et al. (2020) took seven soil quality indicators and evaluated the effect of long-term conservation cropping on soil quality using a linear scoring technique. On a regional scale similar to our study, Vasu et al. (2016) reported the SQI computed by the expert opinion method to be better correlated with crop yield than PCA one.

### 4.2 Data Transformation Procedure

As expected, the percentile method of data transformation showed a higher correlation in both the test crops (**Figure 2**; **Supplementary Figure S3**) and in both the SF and PCA methods than the routinely followed method, thus conforming to the

second hypothesis. Most studies on the SQI have used linear scoring techniques for data transformation to unitless scores (Andrews et al., 2004; Masto et al., 2007; Mukherjee and Lal, 2014; Klimkiewicz-Pawlas et al., 2019; Amorim et al., 2020). The routinely followed procedure has been to divide the parameter value by the highest parameter value of the dataset (maximum) in the “more is better” type of indicator, such as SOC. In the “less is better” type of indicator such as BD, the lowest value (minimum) is used as the numerator and the parameter value as the denominator. However, as previously explained, this procedure is beset with a good chance of error when we go for SQI assessment on a regional scale, as few outlier values of maxima or minima in the entire dataset can alter the score of the individual parameters. Thus, the approach of taking the 90th percentile value as the maximum and the 10th percentile value as the minimum for data transformation as designed in this study is the first of its kind in the SQ assessment research. The higher weighted scores (**Supplementary Figures S1, S2**) and higher SQI values (**Figure 1**) in the percentile method resulted from minimization of error and reduction of chance of extremity, otherwise caused when a maximum or minimum value is used. Therefore, the percentile method is more suitable to broad-base the utility of SQI in regional-scale soil quality assessment and defining management goals.

### 4.3 Role of Soil Sampling Depth in SQI Computation

This study compared the SQI computed from 0 to 15 cm soil data with that computed from mean data of 0–15 cm and 15–30 cm (0–30 cm) soil data. The results showed the former better correlated with crop yield than the latter (**Figure 2**; **Supplementary Figure S3**), which was against our set hypothesis. The range (minimum to maximum) of SQI values was higher in the 0–30 cm soil dataset (**Supplementary Table S5**) due to masking of extreme values in either depth during averaging of parameter values. The average SQI values of both the datasets (0–15 cm and 0–30 cm) were similar (**Figure 1**). This indicates crop yield is more regulated by the parameters of the surface soil layer. Our findings conform to those of Amorim et al. (2020). The SQI values of the surface layer are expected to be higher than those of the 15–30 cm soil layer, primarily due to better SOC and associated physical and fertility parameters such as lower BD, better aggregation, and higher nutrient availability in the surface layer. The surface soil layer or the plow layer is the dynamic layer primarily contributing to plant nutrition. In their study, Amorim et al. (2020) reported soil quality at 0–15 and 15–30 cm soil depths corresponding to 74.7 and 64% of their potential, respectively. A similar observation was also made by Karlen et al. (2013) from a study in Central Iowa, United States, showing near-surface soil functioning at 82–85% of potential and at a lower capacity at lower depths. Thus, when the SQI is computed from the data averaged over soil depth (in this case, an average of 0–15 and 15–30 cm soil data), the correlation between SQI and crop yield was lower. However, our findings are in contrast to the reports of Vasu et al. (2016), where the SQI from 0 to 100 cm soil data provided better correlation than the

SQI computed from the 0 to 15 cm soil layer. Such different trends might be possible due to a semiarid climate and rainfed situation in their study region, where root growth might be deeper, and thus, deeper layer soil conditions regulate the crop growth. On the contrary, our study was undertaken in an alluvial soil characterized by highly intensive cropping, heavy chemical fertilizer application, and provision of good irrigation, which might have restricted the root growth zone to upper layers of soil.

## CONCLUSION

The utility of soil quality indexing as a tool for soil health monitoring and to evaluate land management practices needs to go beyond the farm plots and experimental fields to a broader regional scale. This study provided a new approach for data transformation when the SQI is used on a regional scale. As suggested in this study, the percentile method for data transformation proved better in terms of correlation with yields of rice and wheat crops. Secondly, the dataset of 0–15 cm soil depth can provide optimum information for routine soil quality monitoring, which thus can save resources by avoiding sampling from deeper soil layers. Thirdly, the superiority of the soil function–based approach over PCA implied that an agro-ecological region–specific minimum dataset could be formed for long-term soil health monitoring on a regional or country scale to maintain optimum soil productivity.

## DATA AVAILABILITY STATEMENT

The original contributions presented in the study are included in the article/**Supplementary Material**, further inquiries can be directed to the corresponding author.

## REFERENCES

- Abdollahi, L., Hansen, E. M., Rickson, R. J., and Munkholm, L. J. (2015). Overall Assessment of Soil Quality on Humid Sandy Loams: Effects of Location, Rotation and Tillage. *Soil Tillage Res.* 145, 29–36. doi:10.1016/j.still.2014.08.009
- Amorim, H. C. S., Ashworth, A. J., Wienhold, B. J., Savin, M. C., Allen, F. L., Arnold, M., et al. (2020). Soil Quality Indices Based on Long-Term Conservation Cropping Systems Management. *Agrosystems, Geosciences Environ.* 3, e20036. doi:10.1002/agg2.20036
- Andrews, S. S., Karlen, D. L., and Cambardella, C. A. (2004). The Soil Management Assessment Framework: A Quantitative Soil Quality Evaluation Method. *Soil Sci. Soc. Am. J.* 68, 1945–1962. doi:10.2136/sssaj2004.1945
- Andrews, S. S., Karlen, D. L., and Mitchell, J. P. (2002). A Comparison of Soil Quality Indexing Methods for Vegetable Production Systems in Northern California. *Agric. Ecosyst. Environ.* 90, 25–45. doi:10.1016/s0167-8809(01)00174-8
- Çelik, I., Günel, H., Acir, N., Barut, Z. B., and Budak, M. (2021). Soil Quality Assessment to Compare Tillage Systems in Cukurova Plain, Turkey. *Soil Tillage Res.* 208, 104892. doi:10.1016/j.still.2020.104892
- Fernandes, J. C., Gamero, C. A., Rodrigues, J. G. L., and Mirás-Avalos, J. M. (2011). Determination of the Quality Index of a Paleudult under Sunflower Culture and Different Management Systems. *Soil Tillage Res.* 112, 167–174. doi:10.1016/j.still.2011.01.001

## AUTHOR CONTRIBUTIONS

NL and SL conceived the study. BM carried out the sampling. NL, AK, SL, and AS carried out the laboratory analysis and data analysis. NL and RL prepared the manuscript. All authors checked and approved the manuscript.

## FUNDING

This research was funded by a competitive extramural research grant from the Science and Engineering Research Board (SERB) under the Department of Science and Technology, Government of India, vide Grant No. EMR/2017/005542.

## ACKNOWLEDGMENTS

The cooperation by farmers of the study region in providing crop and nutrient management information and soil samples is duly acknowledged.

## SUPPLEMENTARY MATERIAL

The Supplementary Material for this article can be found online at: <https://www.frontiersin.org/articles/10.3389/fenvs.2022.865473/full#supplementary-material>

**Supplementary Figure S1 | (A)** Parameter weights as derived from the PCA output and the weighted scores of parameters under **(B)** routinely followed and **(C)** percentile methods of data transformation in the PCA method.

**Supplementary Figure S2 | (A)** Parameter weights and the weighted scores of parameters under **(B)** routinely followed and **(C)** percentile methods of data transformation in the soil function (SF) method.

**Supplementary Figure S3 |** Correlation of soil quality index (SQI) derived from the soil data of 0–15 cm and 0–30 cm with wheat yield under the four different indexing methods ( $n = 52$ ).

- Fertilizer Association of India (2017). *Fertilizer and Agriculture Statistics – Northern Region*. New Delhi: FAI House.
- Gelaw, A., Singh, B., and Lal, R. (2015). Soil Quality Indices for Evaluating Smallholder Agricultural Land Uses in Northern Ethiopia. *Sustainability* 7, 2322–2337. doi:10.3390/su7032322
- Haney, R. L., Haney, E. B., Smith, D. R., Harmel, R. D., and White, M. J. (2018). The Soil Health Tool-Theory and Initial Broad-Scale Application. *Appl. Soil Ecol.* 125, 162–168. doi:10.1016/j.apsoil.2017.07.035
- Janků, J., Kosánová, M., Kozák, J., Herza, T., Jehlička, J., Maitah, M., et al. (2022). Using of Soil Quality Indicators to Assess Their Production and Ecological Functions. *Soil Water Res.* 17, 45–58. doi:10.17221/146/2021-SWR
- Karlen, D. L., Cambardella, C. A., Kovar, J. L., and Colvin, T. S. (2013). Soil Quality Response to Long-Term Tillage and Crop Rotation Practices. *Soil Tillage Res.* 133, 54–64. doi:10.1016/j.still.2013.05.013
- Klimkowicz-Pawlas, A., Ukalska-Jaruga, A., and Smreczak, B. (2019). Soil Quality Index for Agricultural Areas under Different Levels of Anthropopressure. *Int. Agrophys.* 33, 455–462. doi:10.31545/intagr/113349
- Lenka, N. K., Mandal, D., and Sudhishri, S. (2014). Permissible Soil Loss Limits for Different Physiographic Regions of West Bengal. *Curr. Sci.* 107, 665–670.
- Lenka, N. K., Thakur, J. K., and Lenka, S. (2019). *Soil Health Analysis*. New Delhi: New India Publication Agency, 112.
- Masto, R. E., Chhonkar, P. K., Singh, D., and Patra, A. K. (2007). Soil Quality Response to Long-Term Nutrient and Crop Management on a Semi-Arid

- Inceptisol. *Agric. Ecosyst. Environ.* 118, 130–142. doi:10.1016/j.agee.2006.05.008
- Mukherjee, A., and Lal, R. (2014). Comparison of Soil Quality Index Using Three Methods. *PLoS ONE* 9 (8), e105981. doi:10.1371/journal.pone.0105981
- Nakajima, T., Lal, R., and Jiang, S. (2015). Soil Quality Index of a Crosby Silt Loam in Central Ohio. *Soil Tillage Res.* 146, 323–328. doi:10.1016/j.still.2014.10.001
- Shah, F., and Wu, W. (2019). Soil and Crop Management Strategies to Ensure Higher Crop Productivity within Sustainable Environments. *Sustainability* 11, 1485. doi:10.3390/su11051485
- Sharma, K. L., Mandal, U. K., Srinivas, K., Vittal, K. P. R., Mandal, B., Grace, J. K., et al. (2005). Long-Term Soil Management Effects on Crop Yields and Soil Quality in a Dryland Alfisol. *Soil Tillage Res.* 83, 246–259. doi:10.1016/j.still.2004.08.002
- Soil Survey Staff (2014). *Keys to Soil Taxonomy*. 12th ed. Washington, DC, USA: USDA-Natural Resources Conservation Service.
- Stott, D. E., Cambardella, C. A., Tomer, M. D., Karlen, D. L., and Wolf, R. (2011). A Soil Quality Assessment within the Iowa River South Fork Watershed. *Soil Sci. Soc. Am. J.* 75, 2271–2282. doi:10.2136/sssaj2010.0440
- Subba Rao, A., and Lenka, N. K. (2020). Developments on Soil Health Management in India as Mirrored through Sustained Researches and Policy Interventions. *Indian J. Fert.* 16, 1230–1242.
- Vasu, D., Singh, S. K., Ray, S. K., Duraisami, V. P., Tiwari, P., Chandran, P., et al. (2016). Soil Quality Index (SQI) as a Tool to Evaluate Crop Productivity in Semi-Arid Deccan Plateau, India. *Geoderma* 282, 70–79. doi:10.1016/j.geoderma.2016.07.010
- Vasu, D., Tiwari, G., Sahoo, S., Dash, B., Jangir, A., Sharma, R. P., et al. (2021). A Minimum Data Set of Soil Morphological Properties for Quantifying Soil Quality in Coastal Agroecosystems. *Catena* 198, 105042. doi:10.1016/j.catena.2020.105042
- Wienhold, B. J., Karlen, D. L., Andrews, S. S., and Stott, D. E. (2009). Protocol for Indicator Scoring in the Soil Management Assessment Framework (SMAF). *Renew. Agric. Food Syst.* 24, 260–266. doi:10.1017/s1742170509990093
- Wilding, L. P. (1985). “Spatial Variability: its Documentation, Accommodation, and Implication to Soil Surveys,” in *Soil Spatial Variability*. Editors D.R. Nielsen and J. Bouma (Netherlands: Wageningen).
- Zeraatpisheh, M., Bakhshandeh, E., Hosseini, M., and Alavi, S. M. (2020). Assessing the Effects of Deforestation and Intensive Agriculture on the Soil Quality through Digital Soil Mapping. *Geoderma* 363, 114139. doi:10.1016/j.geoderma.2019.114139

**Conflict of Interest:** The authors declare that the research was conducted in the absence of any commercial or financial relationships that could be construed as a potential conflict of interest.

**Publisher’s Note:** All claims expressed in this article are solely those of the authors and do not necessarily represent those of their affiliated organizations, or those of the publisher, the editors, and the reviewers. Any product that may be evaluated in this article, or claim that may be made by its manufacturer, is not guaranteed or endorsed by the publisher.

Copyright © 2022 Lenka, Meena, Lal, Khandagale, Lenka and Shirale. This is an open-access article distributed under the terms of the Creative Commons Attribution License (CC BY). The use, distribution or reproduction in other forums is permitted, provided the original author(s) and the copyright owner(s) are credited and that the original publication in this journal is cited, in accordance with accepted academic practice. No use, distribution or reproduction is permitted which does not comply with these terms.



# Annual CO<sub>2</sub> Budget Estimation From Chamber-Based Flux Measurements on Intensively Drained Peat Meadows: Effect of Gap-Filling Strategies

Weier Liu<sup>1\*</sup>, Christian Fritz<sup>1,2\*</sup>, Stefan T. J. Weideveld<sup>2</sup>, Ralf C. H. Aben<sup>2</sup>, Merit van den Berg<sup>2,3</sup> and Mandy Velthuis<sup>2</sup>

<sup>1</sup>Integrated Research on Energy, Environment and Society (IREES), University of Groningen, Groningen, Netherlands, <sup>2</sup>Aquatic Ecology and Environmental Biology, Radboud Institute for Biological and Environmental Sciences (RIBES), Radboud University, Nijmegen, Netherlands, <sup>3</sup>Department of Earth Sciences, Vrije Universiteit Amsterdam, Amsterdam, Netherlands

## OPEN ACCESS

### Edited by:

Jörg Luster,  
Swiss Federal Institute for Forest,  
Snow and Landscape Research  
(WSL), Switzerland

### Reviewed by:

Mathias Hoffmann,  
Leibniz Center for Agricultural  
Landscape Research (ZALF), Germany  
Martin Maier,  
Forstliche Versuchs-und  
Forschungsanstalt Baden-  
Württemberg (FVA), Germany

### \*Correspondence:

Weier Liu  
weier.liu@rug.nl  
liuweier2@hotmail.com  
Christian Fritz  
Christian.fritz@ru.nl

### Specialty section:

This article was submitted to  
Soil Processes,  
a section of the journal  
Frontiers in Environmental Science

**Received:** 28 October 2021

**Accepted:** 04 March 2022

**Published:** 02 May 2022

### Citation:

Liu W, Fritz C, Weideveld STJ,  
Aben RCH, van den Berg M and  
Velthuis M (2022) Annual CO<sub>2</sub> Budget  
Estimation From Chamber-Based Flux  
Measurements on Intensively Drained  
Peat Meadows: Effect of Gap-  
Filling Strategies.  
Front. Environ. Sci. 10:803746.  
doi: 10.3389/fenvs.2022.803746

Estimating annual CO<sub>2</sub> budgets on drained peatlands is important in understanding the significance of CO<sub>2</sub> emissions from peatland degradation and evaluating the effectiveness of mitigation techniques. The closed-chamber technique is widely used in combination with gap-filling of CO<sub>2</sub> fluxes by parameter fitting empirical models of ecosystem respiration ( $R_{eco}$ ) and gross primary production (GPP). However, numerous gap-filling strategies are available which are suitable for different circumstances and can result in large variances in annual budget estimates. Therefore, a need for guidance on the selection of gap-filling methodology and its influence on the results exists. Here, we propose a framework of gap-filling methods with four Tiers following increasing model complexity at structural and temporal levels. Tier one is a simple parameter fitting of basic empirical models on an annual basis. Tier two adds structural complexity by including extra environmental factors such as grass height, groundwater level and drought condition. Tier three introduces temporal complexity by separation of annual datasets into seasons. Tier four is a campaign-specific parameter fitting approach, representing highest temporal complexity. The methods were demonstrated on two chamber-based CO<sub>2</sub> flux datasets, one of which was previously published. Performance of the empirical models were compared in terms of error statistics. Annual budget estimates were indirectly validated with carbon export values. In conclusion, different gap-filling methodologies gave similar annual estimates but different intra-annual CO<sub>2</sub> fluxes, which did not affect the detection of the treatment effects. The campaign-wise gap-filling at Tier four gave the best model performances, while Tier three seasonal gap-filling produced satisfactory results throughout, even under data scarcity. Given the need for more complete carbon balances in drained peatlands, our four-Tier framework can serve as a methodological guidance to the handling of chamber-measured CO<sub>2</sub> fluxes, which is fundamental in understanding emissions from degraded peatlands and its mitigation. The performance of models on intra-annual data should be validated in future research with continuous measured CO<sub>2</sub> flux data.

**Keywords:** closed-chamber methods, drained peatland, carbon dioxide, CO<sub>2</sub> flux modeling, data interpolation

# 1 INTRODUCTION

Covering only 3% of the global land surface, peatland contains over 600 Gt of carbon, which is nearly 30% of all global soil carbon (Parish et al., 2008; Yu et al., 2010). However, centuries of peatland drainage for agriculture and forestry have changed large peatland areas from carbon sinks into sources. At present, around 10% of global peatland is degraded due to drainage or exploitation (Joosten, 2010). Drained peatlands are estimated to annually emit 1.91 Gt CO<sub>2</sub>-equivalents without further exploitation (Leifeld and Menichetti, 2018). This comprises an estimated 12–41% of the greenhouse gas (GHG) emission budget for keeping global warming below +1.5 to +2°C (Leifeld et al., 2019). Given the importance of emissions from degraded peatlands, numerous studies have focused on the measurement of the net ecosystem exchange (NEE), and, subsequently, estimation of the annual CO<sub>2</sub> budgets. These studies helped understanding the magnitude of emissions among different peatland systems (Campbell et al., 2014; Tiemeyer et al., 2016), influences of environmental factors (Järveoja et al., 2016; Hoyt et al., 2019), effects of land use and management (Beetz et al., 2013; Günther et al., 2015; Renou-Wilson et al., 2016), and peatland's contribution to large-scale CO<sub>2</sub> emission inventories (Wilson et al., 2016a; Tiemeyer et al., 2020). Annual CO<sub>2</sub> budgets provide straightforward information that could be easily adopted in policy- or decision-making regarding peatland degradation.

Closed-chamber methods represent an inexpensive and easy-to-use technique that is suitable for use on a wide range of ecosystems (Heng, 2021). At larger scale, however, estimation of annual CO<sub>2</sub> budgets is heavily dependent on spatial and temporal interpolation, i.e., gap-filling of chamber measurement data. The most frequently-used gap-filling methodologies include parameter fitting of empirical models, such as the simple temperature and PAR (photosynthetically active radiation) dependent functions of ecosystem respiration ( $R_{eco}$ ) and gross primary production (GPP), respectively. The most frequently used relations are the Arrhenius-type  $R_{eco}$  relation (Lloyd and Taylor, 1994) and rectangular hyperbolic light response equation of GPP (Michaelis and Menten, 1913).

A wide variety of models with different complexity can be applied for better interpretation of the processes. In model structure, various environmental factors can be incorporated to improve model performance. For example, hydrological regimes (e.g., soil moisture content, groundwater level) regulates  $R_{eco}$  by establishing aerobic and anaerobic zones within the soil profile (Juszczak et al., 2013). Plant composition, biomass and phenology can reflect the temporal variations on the contributions from microbial heterotrophic and plant autotrophic respiration to  $R_{eco}$  (Järveoja et al., 2020) and the photosynthesis capacity of the plants to GPP (Peichl et al., 2018). An extensive summary of commonly used model structures and environmental factors are presented in **Supplementary Table S1**. Parameter fitting of these models are applied with time scales from campaign-specific (e.g., Beetz et al., 2013) to seasonal (Waddington and Roulet, 2000) or annual (Wilson et al., 2016b), adding a temporal dimension of the model's complexity.

Such diversity of gap-filling methodology creates variations in the annual CO<sub>2</sub> budget estimation, which may lead to uncertainties on the ability of the methodology to reach budget estimates closest to the real CO<sub>2</sub> fluxes. Such uncertainties affect upscaling of the CO<sub>2</sub> emission and conclusions in field trials and comparative studies (Hoffmann et al., 2015). Huth et al. (2017) found strongly diverse CO<sub>2</sub> budgets (−7.3 to 15.6 t ha<sup>−1</sup>) across gap-filling options with different pooling methods of measured data (temporal complexity). Karki et al. (2019) calculated widely variable NEE estimates, ranging from −9.35 to −2.08 t ha<sup>−1</sup> yr<sup>−1</sup> on one plot, when combining eight  $R_{eco}$  and eight GPP models (structural complexity). Previous studies attempted to mitigate such uncertainties by standardizing the data acquisition and processing approaches. Hoffmann et al. (2015) proposed a standardized automatic data processing algorithm for campaign-specific modeling. Huth et al. (2017) provided options of the timing of the flux measurements, strategies of data pooling and methods of flux partitioning. However, the methodological diversity of gap-filling and the subsequent uncertainties still complicates the application and interpretation of chamber-based flux data.

Manual closed chamber measurements require human resources to carry out the measurements. Which makes that the current state of the method may be limited due to practical issues, such as accessibility of the sites, equipment deficiency, and/or unexpected influence from management or weather events (e.g., in Weideveld et al., 2021), resulting in flux datasets with potentially low measurement frequency, prolonged data gaps, and/or large variations. The standard campaign-specific method may not be possible under such circumstances, requiring additional procedures in the gap-filling data processing and modeling.

The above-mentioned methodological challenges regarding diversity of the methods, uncertainties, and data deficiency confounds the handling of chamber-measured flux data, as well as the subsequent data analysis of comparative studies or field trials. A streamlined framework for the gap-filling strategy is timely needed that contributes to the current methodological standards. The main objectives of this study are: 1) present a systematic framework of gap-filling methodologies following a gradient of structural and temporal model complexity; 2) demonstrate and compare the statistical performances of the gap-filling methods using multiple datasets; 3) investigate the potential influence of gap-filling method selection on the detection of treatment effects in a field trial.

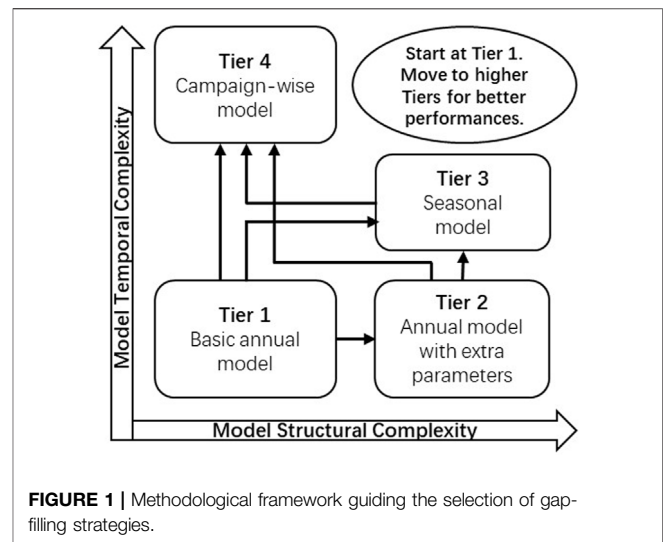
## 2 MATERIALS AND METHODS

### 2.1 CO<sub>2</sub> Flux Dataset

Selected gap-filling methodologies were tested on an existing chamber-based CO<sub>2</sub> flux dataset from the province of Friesland, the Netherlands, published in Weideveld et al. (2021). CO<sub>2</sub> exchanges were monitored from January 2017 till December 2018 at four farms. All farm locations have large fields with deep drainage (ditch water levels from 60 to 90 cm below surface)

and intensive fertilization ( $>230 \text{ kg N ha}^{-1} \text{ yr}^{-1}$ ). The peat soils have a thickness of 0.8–2.0 m, some of which are covered with a carbon-rich clay layer of 20–40 cm. The grasslands are dominated by *Lolium perenne*. Each farm was set up with a control site containing traditional drainage and infiltration ditches, and a treatment site containing sub-soil irrigation (SSI) drains. The SSI system functions by installing permeable drainage/irrigation pipes at around 10 cm below ditch water level. It was proposed to elevate groundwater level in the dry summer season to reduce CO<sub>2</sub> emissions, while fulfilling a drainage function when the groundwater level is above the ditch water level (van den Akker et al., 2010; Querner et al., 2012 as cited in; Weideveld et al., 2021).

CO<sub>2</sub> fluxes were measured on all four farms twice a month during the growing season (April–September) and once a month during the rest of the year. On each site, three 15 cm-deep soil collars for flux measurements with chambers ( $80 \times 80 \times 50 \text{ cm}$ ) were installed as replicates. An opaque (dark) chamber was used to measure ecosystem respiration ( $R_{\text{eco}}$ ) and a transparent (light) chamber for the measurement of net ecosystem exchange (NEE). Gross primary production (GPP) was directly derived from NEE using measured daytime  $R_{\text{eco}}$ , which could avoid propagating  $R_{\text{eco}}$  modeling errors into GPP models (Huth et al., 2017), while light and dark measurements were performed in sequence to minimize errors due to deviations in temperature over time. During each campaign, per field flux measurements were performed from sunrise to noon, or from noon to sunset. Depending on the duration of sunlight, an average of nine light and 10 dark measurements during winter, and 18 light and 20 dark measurements were achieved. An average of 383 measured CO<sub>2</sub> fluxes were collected per site and year (Weideveld et al., 2021; **Supplementary Table S2**). Grass height and groundwater table (GWT) were measured at the start of every field campaign. Photosynthetically active radiation (PAR) and soil temperature at 5 and 10 cm depth were measured during the campaigns. PAR, soil temperature and air temperature were also continuously recorded every 5 min during and between field campaigns. The recorded data was allocated into hourly averages to simplify the computation in the following gap-filling extrapolation. According to Hoffmann et al. (2015), the use of hourly average PAR and temperature could induce systematic bias in the gap-filled annual budget estimates. The positively skewed distribution pattern of the GPP functions could result in an overestimation of over  $1 \text{ t CO}_2 \text{ ha}^{-1} \text{ yr}^{-1}$  in the GPP estimates (Hoffmann et al., 2015). Meanwhile, bias in the  $R_{\text{eco}}$  estimates in our case was presumably small since soil temperature as the driving environmental factor for the  $R_{\text{eco}}$  functions changes slower than air temperature. Grass yield inside soil collars was harvested eight times in 2017 and five times in 2018. Total carbon was measured in dry plant material ( $\text{t C ha}^{-1} \text{ yr}^{-1}$ ) to determine C-export via harvest. Slurry manure was applied four times per year at rates of  $119\text{--}181 \text{ kg N ha}^{-1} \text{ yr}^{-1}$  with a C/N ratio of  $16.3 \pm 1.3$  (mean $\pm$ SD) to simulate C-import via farm management. Export and import of carbon were converted from carbon content to CO<sub>2</sub> for calculating the CO<sub>2</sub> balance. More details on the experimental design, flux measurements and data treatment are available in Weideveld et al. (2021).



In the previous analysis in Weideveld et al. (2021), a campaign-wise gap-filling strategy was applied and no effect from the SSI technique was detected. In 2018, the experimental farms suffered from an extreme drought. Parameter fitting of the data therefore faced difficulties and led to uncertainties in the CO<sub>2</sub> budget estimates, which was presumably due to drought effect that could not be explained by the measured environmental factors such as soil moisture and GWT. This extensive dataset combining multiple years and locations with the unexpected drought events provided opportunities to test the performances of gap-filling strategies and exemplify their differences.

## 2.2 Gap-Filling Methodological Tiers

A framework of four Tiers of gap-filling methodologies was constructed (Figure 1). A Tier represents a level of methodological complexity, which has been used in the IPCC GHG inventory reporting methods (IPCC, 2019). Tier 1 is the basic method applying the original form of the empirical models without extra independent variables on annual datasets. Higher Tiers are more demanding in terms of model complexity and data requirements. Within each Tier, the most commonly used empirical models of  $R_{\text{eco}}$  and GPP were selected from **Supplementary Table S1**. Parameter fitting was performed using non-linear least square (NLS) models with the R package *lme4* (Bates et al., 2015). Model complexity was determined by two aspects: model structure and temporal scale. Structural complexity was increased by adding extra parameters to the basic empirical models. Temporal complexity was increased by shortening modeling periods by separating the dataset according to seasonality or applying campaign-specific models. For both  $R_{\text{eco}}$  and GPP, multiple model structures were tested at each Tier. Significance of the parameters was determined by the *p*-value and *t*-statistic of the parameter estimate from the NLS model. Models that performed poorly (non-converging regressions, insignificant/abnormal parameter values, etc.) were discarded while the best

**TABLE 1** | Equations of the empirical models selected for the gap-filling framework.

	<b>R<sub>eco</sub></b>	<b>GPP</b>
Tier 1–BASIC	<b>ARR</b> : $R_{ref} \times e^{E_0 \times (\frac{1}{T_{ref}-T_0} - \frac{1}{T-T_0})}$ (1) <b>Exp</b> : $A \times e^{bT}$ (2)	<b>MM</b> : $\frac{GPP_{max} \times \alpha \times PAR}{GPP_{max} + \alpha \times PAR}$ (3) <b>SMT</b> : $\frac{GPP_{max} \times \alpha \times PAR}{\sqrt{GPP_{max}^2 + (\alpha \times PAR)^2}}$ (4) <b>MIT</b> : $GPP_{max} \times (1 - e^{-\frac{\alpha \times PAR}{GPP_{max}}})$ (5)
Tier 2–PARA	<b>ARR – D</b> : $R_{ref} \times e^{E_0 \times (\frac{1}{T_{ref}-T_0} - \frac{1}{T-T_0})} + a \times DI$ (6)	<b>MM – G</b> : $\frac{GPP_{max} \times GH \times \alpha \times PAR}{(GPP_{max} \times GH) + \alpha \times PAR}$ (7) <b>MM – GT</b> : $\frac{GPP_{max} \times GH \times \alpha \times PAR}{(GPP_{max} \times GH) + \alpha \times PAR} \times Ft$ (8) <b>MM – GTD</b> : $\frac{GPP_{max} \times GH \times \alpha \times PAR}{(GPP_{max} \times GH) + \alpha \times PAR} \times Ft + a \times DI$ (9)
Tier 3–SS	<b>Non-drought: Eq. 1</b> <b>Drought: Eq. 6</b> (Linear $a \times T + b \times DI + c$ (10) <sup>a</sup> )	<b>Non-drought: Eq. 8</b> <b>Drought: Eq. 9</b>
Tier 4–CW	<b>Eq. 1</b>	<b>Eq. 3</b>

**Abbreviations:** BASIC, basic annual models; PARA, annual models with extra parameters; SS, seasonal gap-filling; CW, campaign-wise gap-filling; ARR, Lloyd-Taylor modified Arrhenius model; EXP, Van't Hoff exponential model; MM, Michaelis-Menten/SMT, Smith's/MIT, Mitscherlich's light response curve; -D, with drought index; -G, with grass height; -T, with temperature function (Ft).

<sup>a</sup>A linear model was used for the drought season in 2017, where ARR-D did not result in acceptable performance.

performing model combinations (see **Section 2.3**) were selected to be used in the next Tiers and for further statistical analysis.

### 2.2.1 Tier One: Basic Annual Models

From **Supplementary Table S1**, the most widely-used empirical models were selected as the basic annual models. For R<sub>eco</sub>, temperature-dependent functions including the Lloyd-Taylor modified Arrhenius (**Table 1, Eq. 1**) and Van't Hoff exponential (**Table 1, Eq. 2**) models were selected. Air temperature, soil temperature at 5 and 10 cm depth were tested in the parameter fitting. Soil temperature at 5 cm depth consistently provided better performances in different models and was therefore selected to be used in other Tiers. For GPP, rectangular hyperbolic functions including the Michaelis-Menten's (**Table 1, Eq. 3**), Smith's (**Table 1, Eq. 4**) and Mitscherlich's (**Table 1, Eq. 5**) light response curves were selected. For the parameter fitting, flux measurement data was pooled over the entire year. The Lloyd-Taylor modified Arrhenius and Michaelis-Menten's hyperbolic functions were selected to be used in the higher Tiers.

### 2.2.2 Tier Two: Annual Models With Extra Parameters

#### 2.2.2.1 Inclusion of Extra Environmental Factors

Extra environmental factors were introduced into the Tier one models for an increased model structural complexity. Multiple mathematical forms of the environmental factors were tested and compared for the best model performance (**Supplementary Table S1B**). Grass height was used as a vegetation index since it is correlated to a wide range of vegetation indexes, such as Normalized Difference Vegetation Index (NDVI), Leaf Area Index (LAI) and Difference Vegetation Index (DVI) (Payero et al., 2004), although rarely used directly. The GPP model with grass height modified GPP<sub>max</sub> (Karki et al., 2019, **Table 1, Eq. 7**) was selected for further calculations. R<sub>eco</sub> models with grass height were not included due to frequently

insignificant parameter fitting, indicating a weak correlation. A temperature function (**Supplementary Table S1B**) was introduced to the GPP function with grass height (Karki et al., 2019, **Table 1, Eq. 8**) to account for the influence of low temperature during winter and spring (Yamori et al., 2014). Groundwater table, although frequently used in other studies (see references in **Supplementary Table S1B**), was discarded from the models due to its generally poor model performance in this study. Soil moisture was not tested due to lack of continuous measurements.

#### 2.2.2.2 Introducing a Drought Index

In order to describe the contrasting climate conditions in the studied years, a drought index was defined based on drought events (any period with more than three consecutive days without precipitation, Jassey and Signarbieux, 2019) and the cumulative atmospheric water flux (precipitation minus evapotranspiration, P-ET, Stagge et al., 2015). The daily precipitation and evapotranspiration data were collected from the nearest official KNMI weather station (weather station Leeuwarden, 18–30 km distance from research sites, Weideveld et al., 2021). The accumulated P-ET was reset to zero at the beginning of both years. Pulses of water from small precipitation events can stimulate the carbon flux (Munson et al., 2010; Shen et al., 2015). Munson et al. (2010) found on a semiarid grassland that water is less limiting to carbon fluxes after rain events above 5 mm. No such study was found for peat meadows. Therefore, we reset the accumulated P-ET also after rain events above 5 mm, assuming a reduced drought effect. The drought index was then calculated as absolute values of the accumulated P-ET that remained negative with resets after rain events (**Supplementary Figure S1**). The drought index was then tested in different forms and included as a residual term in both the R<sub>eco</sub> and GPP models (**Table 1, Eqs 6, 9**) as only this form resulted in significant model parameters.

**TABLE 2 |** Summary of the analysis of variance (ANOVA) for the mixed-effects models fitted on the gap-filled NEE for each gap-filling strategy. Year, treatment and their interaction are independent variables, and farm location is included as a random effect.

Model combination	Independent variable	Sum of squares	F~F <sub>1, 16</sub>	p value
Tier 1—BASIC	Year	4.50	0.06	0.8150
	Treatment	11.79	0.15	0.7053
	Year × Treatment	162.57	2.04	0.1721
Tier 2—PARA	Year	466.00	6.07	0.0255 (*)
	Treatment	41.51	0.54	0.4730
	Year × Treatment	168.68	2.20	0.1578
Tier 3—SS	Year	1,013.59	14.85	0.0014 (**)
	Treatment	0.28	0.00	0.9496
	Year × Treatment	176.82	2.59	0.1270
Tier 4—CW	Year	182.93	1.86	0.1913
	Treatment	0.39	0.00	0.9505
	Year × Treatment	40.64	0.41	0.5292

BASIC, annual basic model; PARA, model with extra parameters; SS, seasonal; CW, Campaign-wise.

Significance is indicated in brackets behind the p-value, with \*p < 0.05, \*\*p < 0.01.

### 2.2.3 Tier Three: Seasonal Gap-Filling

The annual flux datasets were split into two seasonal subsets, adding a level of temporal complexity. Here, seasonality was defined based on drought conditions, whereas a drought season had a positive drought index, and non-drought seasons had a drought index equal to zero. The best performing Tier one and Tier two models were tested in the parameter fitting of two seasonal data sets. For non-drought periods, an Arrhenius  $R_{eco}$  model was combined with a Michalis-Menten GPP model with grass height and temperature function. For drought periods, both models were applied with addition of a drought index. The drought period covered only 37 days in 2017 (151 days in 2018), which led to insufficient data points for the model fitting. Therefore, linear regressions were applied to the modeled  $R_{eco}$  for the drought period in 2017 (Table 1, Eq. 10); and the parameter of light response function adopted fixed  $GPP_{max}$  and  $\alpha$  from the annually fitted Tier two models.

### 2.2.4 Tier Four: Campaign-Wise Gap-Filling

Campaign-wise gap-filling refers to parameter fitting of flux data measured on an individual measurement date. The modeling and gap-filling procedure is adopted from Weideveld et al. (2021): Per campaign, Arrhenius and Michalis-Menten functions were fitted for  $R_{eco}$  and GPP, respectively. Pooling of data from two or more adjacent campaigns was applied when the range of PAR did not cover a complete light response curve including the light-limited part and after the light saturation point. This occurred in both years during winter from January to March, and occasionally in 2017 during summer from June to September when data was collected on rainy and cloudy days (see campaign-wise parameters in **Supplementary Dataset**). Gap-filling between two adjacent campaigns are averages of the CO<sub>2</sub> flux estimates from these two campaign-wise models, weighted by the temporal distances of the gap-filled moment to each of the measurements.

## 2.3 Model Performance

Performances of the fitted models were evaluated by comparing measured and modeled values based on a series of model

indicators following Moriasi et al. (2007) as used by Hoffmann et al. (2015). Mean absolute error (MAE), RMSE (root mean square error)—observations standard deviation ratio (RSR), coefficient of determination ( $r^2$ ), modified index of agreement (md), and Nash–Sutcliffe's model efficiency (NSE) were calculated for each model. Goodness of the fit was determined on a set of thresholds rating the indicators (Hoffmann et al., 2015).

## 2.4 Gap-Filling and Validation

Hourly CO<sub>2</sub> fluxes ( $R_{eco}$ , GPP and NEE) were calculated by feeding the environmental variables (hourly average soil temperature at 5 cm depth, air temperature, PAR, and interpolated grass height) to the selected gap-filling models. Grass height was linearly interpolated between measurement campaigns using the R package zoo (Zeileis and Grothendieck, 2005). More accurate interpolation was not possible due to the lack of high frequency measurement or empirical models for grass height. Depending on the growth stage of the plants, linear interpolation may induce overestimation at short grass after harvest due to the plants' recovery and underestimation at relatively long grass when plant growth is reaching the maxima.

Annual  $R_{eco}$ , GPP and NEE budgets were calculated by summing these hourly fluxes. Model errors and extrapolation errors are the most important sources of uncertainty in the gap-filling of annual CO<sub>2</sub> budgets (Beetz et al., 2013). Only model errors were estimated, since extrapolation errors were partly related to, and therefore discussed by, the selection of different extrapolation methods (Weideveld et al., 2021). A Monte Carlo simulation was included in each gap-filling run for model error estimation (Beetz et al., 2013; Leiber-Sauheitl et al., 2014; Hoffmann et al., 2015; Berger et al., 2019; Zhao et al., 2020) using R package nlstools (Baty et al., 2015). Parameter fitting of  $R_{eco}$  and GPP models was bootstrapped with 1,000 iterations. Annual  $R_{eco}$  and GPP budgets were calculated with all the bootstrapped model parameter sets, from which the standard deviation (SD) was calculated to represent the uncertainties of the estimates. Uncertainty of annual NEE budgets was subsequently calculated by combining the SDs of  $R_{eco}$  and GPP following the law of error propagation.

An independent quantitative validation of the annual budget estimates was also needed alongside the proposed model performance and uncertainty assessments, in order to evaluate the accuracy of the gap-filled CO<sub>2</sub> budgets. However, a direct validation was not possible in absence of a known true value of annual CO<sub>2</sub> budgets. Therefore, only an indirect validation was performed using the positive correlations between GPP and plant biomass presented in previous studies (Otieno et al., 2009; Hirota et al., 2010; Weideveld et al., 2021). Derived annual GPP budgets were linearly correlated with C-export per year and method Tier as a quality check of the estimates by examining the significance of the regression.

## 2.5 Applicability Demonstration

Our Tier list framework was developed mainly in consideration of the drought effect during our measured period that caused large variances in the fluxes data. Meanwhile, the ever-growing number of chamber-based flux measurements set up on global peatlands are performed under influence from various conditions other than drought events. For example, differences in equipment, operational techniques, environmental and weather conditions, etc. Our framework and insights on method selection also need to be tested under other types of variations or data gaps. Therefore, the framework was further demonstrated and evaluated on an unpublished CO<sub>2</sub> flux dataset from the fifth farm location over 2018 and 2019. The fifth farm location was close to the other four main locations in Friesland, with similar soil type and management regime. The farm followed the same experimental setup as the other four farms, with a control site and a treatment site installed with SSI. At this location, the SSI treatment was enhanced by installing a pressure well connected to the drainage ditch. Water level inside the well could be raised by a pump to provide increased inflow pressure, therefore keeping the groundwater level stable throughout the year (van den Akker et al., 2019). Measurement procedures were in line with the previous experiments. The measurement frequency, however, was significantly lower than in the other locations, with in total less than ten campaigns: once per month during the growing season (April–September) and twice during the non-growing season (in October and November/December) (Supplementary Table S2). Parameter fitting of gap-filling models followed the four methodological Tiers. Drought index was not used as a parameter here, since the drought effect was not as pronounced as in the four main locations due to extra irrigation in 2018. Grass height was used instead of the drought index in the R<sub>eco</sub> model from the Tier two method. Model performances and the gap-filled annual budgets were evaluated and compared. Budget estimates under data scarcity with large gaps to fill could further test the applicability of our framework on different datasets and evaluate the strengths and limitations of each Tier.

## 2.6 Statistics

The effect of gap-filling methodology on annual budget estimation and detection of treatment effects were investigated. Correlation of model performance ratings against the Tier position of gap-filling methodologies was tested by a simple

linear regression. Linear mixed-effects models were fitted using R package *lme4* (Bates et al., 2015) with gap-filled CO<sub>2</sub> fluxes (R<sub>eco</sub>, GPP and NEE) as dependent variables; year, treatment, their interaction and gap-filling methodology as fixed effects; and farm location as random effect. Type III analysis of variance tables of the linear mixed-effects models were computed with Satterthwaite's method using the *anova* function from the R basic package *stats*. The post-hoc Tukey's HSD test was used with R package *emmeans* (Lenth et al., 2020) to further detect significant differences between gap-filling methodologies. To test whether selection of different gap-filling methodology would generate a treatment effect, linear mixed-effects models were also fitted separately for all gap-filling methodologies with annual NEE as dependent variable, year, treatment, and their interaction as independent variables, and farm location as random effect. All data was processed and analyzed using R version 4.0.2 (R Core Team, 2020).

## 3 RESULTS AND DISCUSSION

### 3.1 Model Performances and Annual Budget Estimates

The model performances under different gap-filling strategies improved significantly ( $p < 0.001$ ) with higher complexity (Figure 2, Supplementary Table S3). However, such improvement did not lead to systematic differences among annual CO<sub>2</sub> budget estimates from the four Tiers (Figure 3). In general, all gap-filling strategies resulted in CO<sub>2</sub> emissions situated in the upper range of emissions from productive grasslands on organic soils (Grønlund et al., 2008; Tiemeyer et al., 2016, 2020). Large variances can be observed between the gap-filled annual budgets (Supplementary Table S4) and daily fluxes (Supplementary Figure S2) resulting from different methods. The basic empirical models from Tier one were not suitable for annual parameter estimates (Figure 2) due to limited explanatory power regarding the environmental and temporal variations. Gap-filled daily fluxes showed mild fluctuations without reflections on rapid changing conditions such as harvest. This resulted in significantly larger annual GPP estimates from the Tier one method in 2017 ( $p < 0.001$ , Figure 3). Influence from environmental changes can be accounted for by higher Tier methodologies with either inclusion of additional variables or season-/campaign-specific modeling. For example, inclusion of grass height and the temperature function in Tier two substantially improved GPP estimates in all aspects, which is in close agreement with other studies stressing the importance of accounting for plant growth and harvest (Eickenscheidt et al., 2015; Huth et al., 2017; Kandel et al., 2013). This, however, could lead to drastic fluctuations and contradicting trends in the daily fluxes (Supplementary Figure S2). The lower soil respiration (Davidson et al., 1998) and photosynthetic CO<sub>2</sub> uptake (Fu et al., 2020; Koebsch et al., 2020) under desiccation stress may have been oversimplified by the drought index proposed in our study, leading to unrealistic peaks and dips of the daily fluxes in Tier two and three. Tier three seasonal gap-filling substantially improved the

model performances by circumventing the lack of good predictors for the drought period that altered important drivers of CO<sub>2</sub> fluxes. However, it is more prone to influences of individual high  $R_{eco}$  measurements under abrupt environmental changes, such as rain-induced soil respiration pulses (Lee et al., 2004; Ma et al., 2012). Such data “outliers” may have confounded the models when fitted seasonally, leading to less representative temperature-respiration relationships, and may have resulted in the significantly higher  $R_{eco}$  from Tier three comparing to Tier four in 2017 ( $p < 0.05$ , **Figure 3**). Tier four campaign-wise model fitting further reduced model errors (**Figure 2**). The ability of the Tier four campaign-wise method to reflect environmental changes without complicated parameterization demonstrated its robustness and reliability when applied with sufficient measurement frequency. However, it is subject to over-extrapolation, since a narrow measurement range of temperature from a single campaign could introduce bias when extrapolated outside of that range (Hoffmann et al., 2015; Huth et al., 2017). Pooling of all gap-filling results over locations and treatment sites showed an absence of consistently significant differences (**Figure 3**) in spite of the above-mentioned variances. This implies a strong influence from divergence among years and locations. Gap-filling method selection should therefore be considered case-specifically in light of characteristics of the dataset, such as the time scale and frequency of the measurements and abrupt or abnormal environmental changes.

### 3.2 Sensitivity of Treatment Effect to the Choice of Gap-Filling Method

Despite the seemingly large differences between CO<sub>2</sub> budget estimates of treatment and control plots observed in individual farms (**Supplementary Table S4**), we did not find any significant treatment effect when pooling the data of the four locations (**Table 2**). The differences found in individual locations could be due to random variations in the site-specific biotic and/or abiotic processes between treatment and control plots, such as differences in vegetation growth, microbial activities, and GWT fluctuations. These processes could be highly variable due to the complexity of *in-situ* environmental conditions. Statistical results from the pooled data were less likely to be affected by such random effects. Therefore, testing of treatment effects from field trials requires a combination of multiple locations and a longer timespan (e.g., Maljanen et al., 2007; Elsgaard et al., 2012) to avoid confounding factors from site or year differences. Annual budget estimates from a single location are more consistent in representing the magnitude of CO<sub>2</sub> emissions.

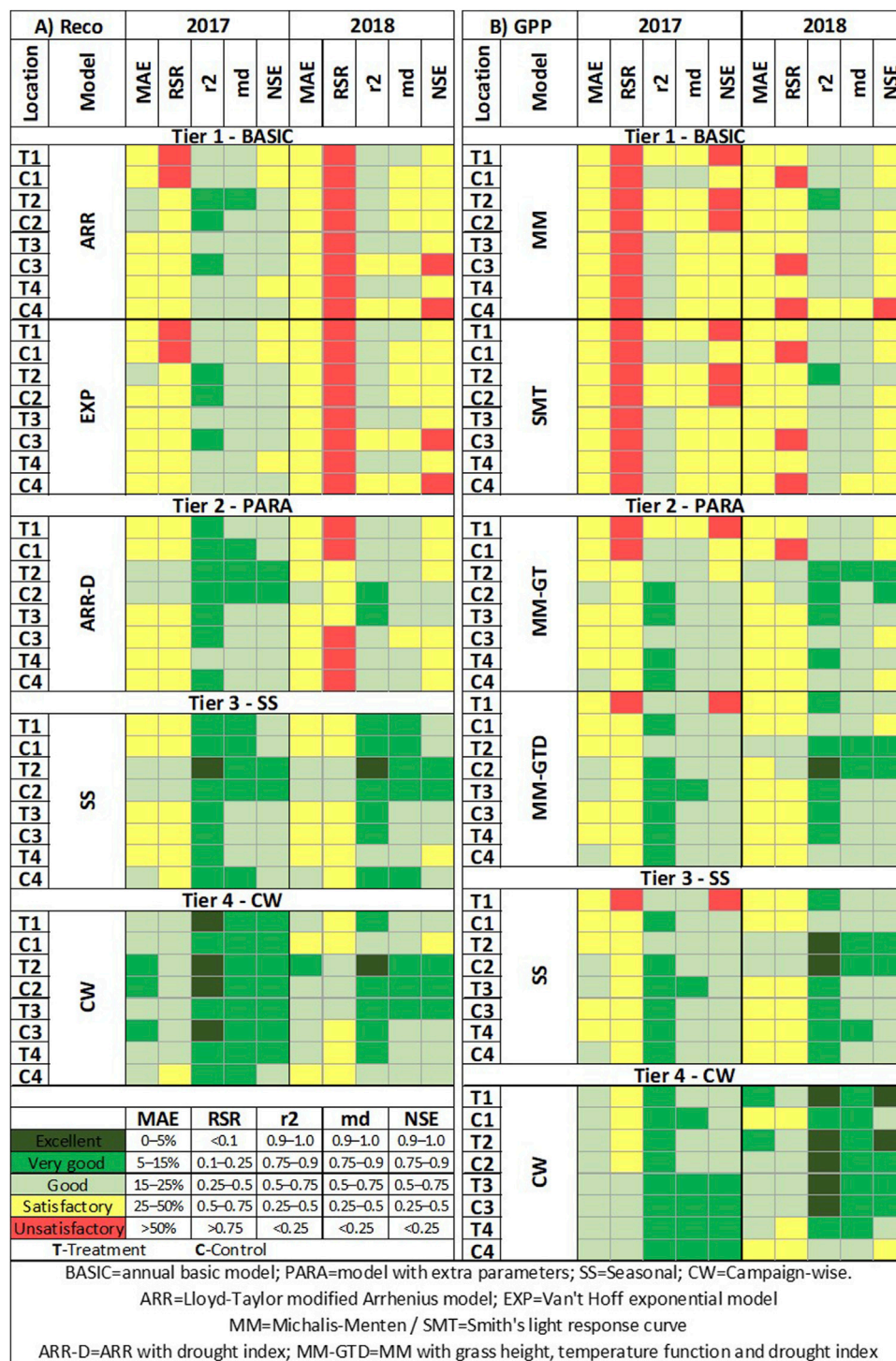
### 3.3 Applicability Demonstration: Gap-Filling Under Data Scarcity

Parameter fitting and gap-filling for the dataset from the fifth farm location was carried out for demonstration purposes, following the methodological Tier list. The low frequency of the measurement campaigns (<10 per year) in this dataset

insufficiently captured the temporal dynamics in CO<sub>2</sub> fluxes. As a result, Tier four campaign-wise gap-filling, although being the most commonly used standard approach, led to high uncertainties and poor fit of gap-filling model parameters (**Table 3**). Tiers containing models with lower temporal complexity at annual or seasonal levels were proven more applicable, as GPP modeling using Tier one (Michaelis-Menten function) and Tier two (Michaelis-Menten function with grass height) resulted in smaller uncertainties of budget estimates (**Table 3**). However, annual  $R_{eco}$  modeling methodologies from Tier one and two (Arrhenius function and with drought index) resulted in poor or even unsatisfactory performances (**Table 3**), mainly due to the large variances in the raw flux data. The best model performances were achieved by the Tier three seasonal method (**Table 3**). Meanwhile, gap-filled daily fluxes (**Figure 4**) occasionally showed large fluctuations despite the satisfactory error statistics. For example,  $R_{eco}$  and GPP fluxes from Tiers one, two and four showed potential overestimations due to low representativeness of the dataset in the winter season. Extreme peaks and dips can be observed in the  $R_{eco}$  fluxes, especially from the Tier four campaign-wise method, showing strong effects of individual high and low measurements when extrapolated over a prolonged time period (Huth et al., 2017). The extremely low  $R_{eco}$  fluxes observed in summer 2018 from Tier two method can be imputed to the low explanatory power of the drought index leading to unrealistic outputs from the model. The satisfactory model error statistics achieved by Tier three and four methods (**Table 3**) demonstrated the potential of generating annual budget estimates even from scarce data. However, large uncertainties should be acknowledged given the varying behavior of the models throughout the year (**Figure 4**). It is therefore necessary to test multiple gap-filling methods when the quality and quantity of raw flux data is limited. The resulting annual budget estimates should be interpreted with caution, merely as an indication for the order of magnitude of the emissions.

### 3.4 Validation of the Annual Budget Estimates

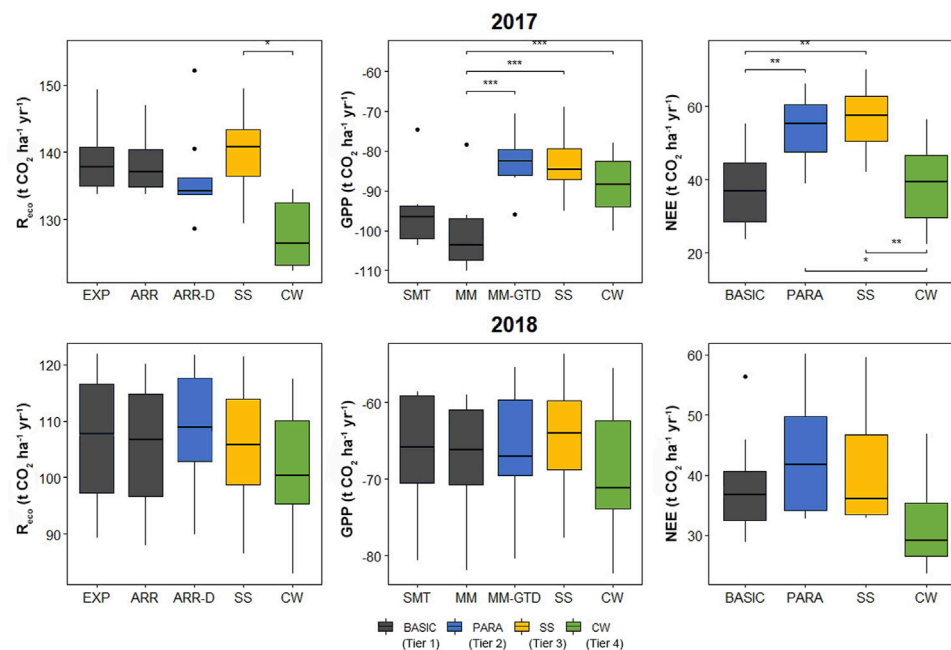
Given the lack of known true values of carbon budgets for locations in this study, independent validation of the derived CO<sub>2</sub> exchange was not possible. Nonetheless, an indirect cross-validation of derived annual GPP budgets with C-export via biomass harvest was performed (**Figure 5**). A similar validation for  $R_{eco}$  was not feasible in our analysis due to lack of comparable environmental datasets. In general, Annual GPP showed strong correlation with C-export when pooling data from all five locations and 3 years from 2017 to 2019 ( $p < 0.001$ ,  $R^2 = 0.42$ ). GPP estimates in 2018 ( $p < 0.001$ ,  $R^2 = 0.52$ ) and 2019 ( $p = 0.007$ ,  $R^2 = 0.69$ ) were roughly in agreement with the general trend. Previous meta-analysis from Tiemeyer et al. (2016) gave average values of GPP and C-export from nutrient-rich deep-drained grassland on organic soils overlapping the range of our estimates (**Figure 5**), also indicating realistic estimation of the GPP values. However, GPP estimates in 2017 showed poor correlation with C-export values ( $p = 0.598$ ,  $R^2 \sim 0$ ) and strong



**FIGURE 2 |** Heatmap of model performance indicators per farm and treatment site following the four Tiers of the gap-filling guiding framework. **(A)** Reco, and **(B)** GPP. Statistical quality criteria were adopted from Moriasi et al. (2007) as used by Hoffmann et al. (2015): MAE = mean absolute error, RSR = root mean square error (RMSE)-observations standard deviation ratio,  $r^2$  = coefficient of determination, md = modified index of agreement, NSE = Nash-Sutcliffe model efficiency.

deviation to the general trend, especially with results from the Tier one method. This is in accordance with the significant overestimation of Tier one GPP values identified (Section 3.1,

Figure 3), and is reflected in the Tier one daily fluxes (Supplementary Figure S2) that failed to represent changes of CO<sub>2</sub> exchange due to plant biomass growth and removal.



**FIGURE 3** | Gap-filled annual  $R_{eco}$ , GPP and NEE budgets from different model selections and combinations in both years. The box indicates the median and the upper/lower quartiles. The whiskers represent the maximum and minimum values. Filled points are the outliers. The asterisks between boxes indicate significant differences between models based on linear mixed-effects (LME) models (\* $p < 0.05$ ; \*\* $p < 0.01$ ; \*\*\* $p < 0.001$ ).

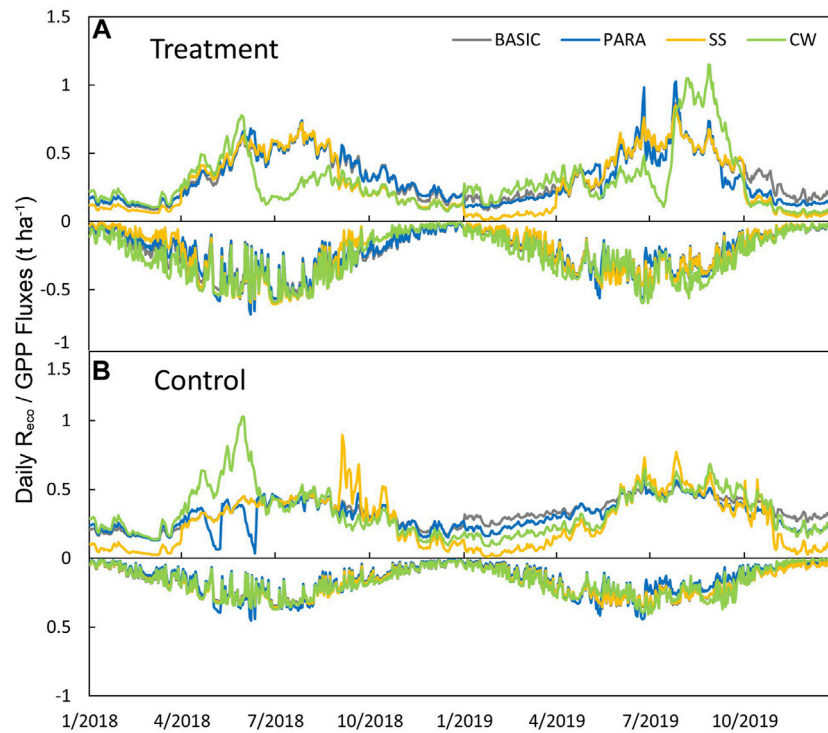
**TABLE 3** | Annual CO<sub>2</sub> budgets of the fifth farm location as a demonstration of the framework applicability. Data are CO<sub>2</sub> budget estimates in  $t\ ha^{-1}\ yr^{-1}$  ( $\pm$ SD). C-export was translated from grass yield in  $t\ CO_2\ eq\ ha^{-1}\ yr^{-1}$ .

Year		2018		2019	
Treatment		SSI	Control	SSI	Control
Reco	Tier 1—BASIC	118.2 ( $\pm$ 10.1)	107.2 ( $\pm$ 7.4)	124.2 ( $\pm$ 6.5)	136.6 ( $\pm$ 9.7)
	Tier 2—PARA	121.8 ( $\pm$ 10)	103.8 ( $\pm$ 6.9)	111.2 ( $\pm$ 4.4)	121.1 ( $\pm$ 9.6)
	Tier 3—SS	105.9 ( $\pm$ 4.8)	96.3 ( $\pm$ 4.2)	100.4 ( $\pm$ 3.5)	95 ( $\pm$ 5.4)
	Tier 4—CW	91 ( $\pm$ 13.2)	124.5 ( $\pm$ 7.1)	116.8 ( $\pm$ 16.3)	118.1 ( $\pm$ 20.1)
GPP	Tier 1—BASIC	-80.5 ( $\pm$ 4.5)	-61.7 ( $\pm$ 3.5)	-77.2 ( $\pm$ 2.6)	-63.6 ( $\pm$ 2.6)
	Tier 2—PARA	-72.3 ( $\pm$ 3.2)	-57.6 ( $\pm$ 4.1)	-72.2 ( $\pm$ 2)	-53.9 ( $\pm$ 2.2)
	Tier 3—SS	-75.4 ( $\pm$ 4.6)	-61.1 ( $\pm$ 3.3)	-76.3 ( $\pm$ 2.4)	-63.7 ( $\pm$ 3)
	Tier 4—CW	-78.6 ( $\pm$ 17.9)	-62.2 ( $\pm$ 35.3)	-89.1 ( $\pm$ 13.5)	-62.8 ( $\pm$ 11.1)
NEE	Tier 1—BASIC	37.6 ( $\pm$ 11.1)	45.5 ( $\pm$ 8.2)	47 ( $\pm$ 7)	73 ( $\pm$ 10.1)
	Tier 2—PARA	49.5 ( $\pm$ 10.5)	46.3 ( $\pm$ 8.1)	39 ( $\pm$ 4.8)	67.2 ( $\pm$ 9.8)
	Tier 3—SS	30.5 ( $\pm$ 6.7)	35.2 ( $\pm$ 5.3)	24.1 ( $\pm$ 4.2)	31.2 ( $\pm$ 6.2)
	Tier 4—CW	12.4 ( $\pm$ 22.2)	62.2 ( $\pm$ 36)	27.7 ( $\pm$ 21.1)	55.3 ( $\pm$ 22.9)
C-export		16.2	12.1	18.0	10.7

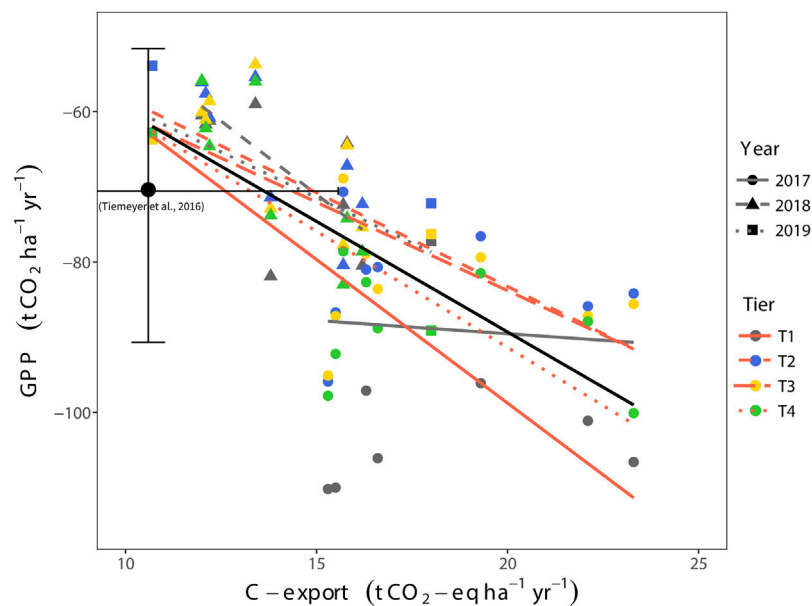
Tier 1—BASIC = annual basic model; Tier 2—PARA = model with extra parameters; Tier 3—SS = seasonal; Tier 4—CW = Campaign-wise. Colour of the cells represents model performances, following legend of **Figure 2** (red—unsatisfactory, yellow—satisfactory, light green—good, dark green—very good), adopted from Moriasi et al. (2007) as used in Hoffmann et al. (2015).

Accuracy of GPP estimates in 2017 should therefore be given low confidence. Within-day timing and frequency of the measurements (Huth et al., 2017; Gana et al., 2018; Järveoja et al., 2020) could also be a cause of this low accuracy. Our midday measurements at a fixed timeframe in 2017 resulted in poor coverage of different PAR ranges. Meanwhile, results from the four Tiers all showed strong correlation with C-export ( $p < 0.01$ ,  $R^2 = 0.38\text{--}0.43$ ) when tested separately, including the Tier one

method that also produced GPP values in good agreement with the GPP~C-export correlation in 2018 and 2019 (**Figure 5**). Therefore, the general feasibility of all four method Tiers can be concluded. However, Tiers one and two methods are more prone to bias when analyzing raw flux datasets with poor representativeness for the environmental conditions and management events, leading to potentially large variations in the GPP estimates.



**FIGURE 4** | Gap-filled daily summed CO<sub>2</sub> fluxes (R<sub>eco</sub> and GPP are depicted as the positive and negative values, respectively) from different models at **(A)** treatment and **(B)** control site of the demonstration location 5.



**FIGURE 5** | Indirect validation by comparing derived annual GPP with C-export per method Tier and year. The black solid line is the result of general linear regression of the entire dataset ( $p < 0.001$ ,  $R^2 = 0.42$ ). Grey lines are regression lines per year (2017,  $p = 0.598$ ,  $R^2 = 0$ ; 2018,  $p < 0.001$ ,  $R^2 = 0.52$ ; 2019,  $p = 0.007$ ,  $R^2 = 0.69$ ). Red lines are regression lines per method Tier (Tier one,  $p = 0.002$ ,  $R^2 = 0.42$ ; Tier two,  $p = 0.002$ ,  $R^2 = 0.43$ ; Tier three,  $p = 0.002$ ,  $R^2 = 0.42$ ; Tier four,  $p < 0.001$ ,  $R^2 = 0.38$ ). Black point with error bars represents average values of GPP and C-export from nutrient-rich deep-drained grassland adopted from Tiemeyer et al. (2016).

Better estimates of carbon pools including plant biomass could serve as a valid data source for indirect cross-validation. For example, a process-based growth model for plant biomass could

better correlate with the derived GPP values by avoiding uncertainties introduced by the harvest practice. However, such models are normally parameterized only for mineral soils

and requires extensive growth data for local calibration (e.g., Barrett et al., 2005). Long-term carbon fluxes monitoring can also be cross-validated with soil carbon pool. Hoffmann et al. (2017) validated chamber-derived net ecosystem carbon balance by resampling of soil organic carbon. Net carbon losses could be proxied by monitoring soil subsidence (Couwenberg and Hooijer, 2013), while such estimated emissions are highly uncertain due to the complicated processes involved in soil surface changes including the oscillation of peat soil (Fritz et al., 2008).

It is still challenging to sufficiently validate chamber-based annual budgets estimates given the limitations of the above-mentioned indirect validation approaches. Paired comparison of the discrete manual chamber fluxes with continuous flux measurements from eddy-covariance and automatic chamber techniques could potentially enable independent validation of the gap-filling methods and budget estimates. Lucas-Moffat et al. (2018) presented highly correlated fluxes between manual chamber and eddy-covariance fluxes from a cropland. Meanwhile, Cappoci and Vargas, (2022) discovered up to 60% underestimation of annual CO<sub>2</sub> efflux by manual chamber compared to automatic chamber in a tidal marsh. More continuous measurements with higher resolution in long term are needed for the improvement of the validation and therefore the refinement of the gap-filling methods. An ongoing year-round automatic chamber measurement including farm locations of this study (Erkens, 2020) could provide opportunities for robust cross-validation of the gap-filling approaches in the near future. However, not without acknowledgement of the specific shortcomings in each method. For example, while manual chamber provides low temporal resolution and lack of night-time fluxes; eddy-covariance measurements have a variable footprint and insufficient energy closure; automatic chambers could lead to heating up to the vegetation and upper soil layer, and are subject to disturbance of the precipitation/evapotranspiration process. Therefore, our statistical comparison provides insights for the selection of available gap-filling methods to meet the growing number of chamber measurements as well as the need to derive more annual carbon balances in drained peatlands. Despite the fact that a “best” approach could not be identified.

## 4 CONCLUSION AND IMPLICATION

In this study, we summarized the most commonly-used empirical models of  $R_{eco}$  and GPP for gap-filling manual chamber-based CO<sub>2</sub> flux into a framework of four Tiers with increasing model complexity. Model performance of the methods from the four Tiers were systematically compared in terms of error statistics. The annual CO<sub>2</sub> exchange was in the same order of magnitude with values from literature on similar ecosystems. Detection of treatment effects requires large number of independent observations (locations) and longer period of time (years) to reduce its sensitivity to random variances. Indirect validation of GPP estimates showed good agreement with the GPP~C-export correlation, except for the year 2017. However, without independent validations using high-resolution long-term continuous flux measurements, the true precision of the methods cannot be discussed but are better suited to determine only the magnitude

of the annual CO<sub>2</sub> budgets. Nonetheless, specific recommendation could be given for each Tier supporting the selection of suitable methods:

1) Tier one annual basic gap-filling is feasible when higher model complexity is not possible due to deficiency of data required for model input or a low number of measurements. However, Tier one models are not likely to provide robust parameter fitting in most cases, because the variance in CO<sub>2</sub> fluxes cannot be sufficiently explained by the limited number of explanatory variables in the models. 2) Tier two methodology introduces higher structural complexity with additional parameterization but remains temporally simple with annual parameter fitting. Robustness of such models depends on the explanatory power of the included variables as well as the representativeness and frequency of the flux measurements. However, the number of variables should be limited to avoid overfitting. 3) Tier three seasonal gap-filling has a moderate overall complexity. It is a potential solution in situations where representativeness of data is an issue, such as with low measurement frequency. The definition of the seasons used to cluster the data is essential when accounting for the unexplained temporal variation in CO<sub>2</sub> fluxes. 4) Tier four campaign-wise gap-filling represents the highest temporal complexity by fitting simple relations per measurement campaign. It is the most commonly used procedure in chamber-based CO<sub>2</sub> fluxes studies, and the most reliable way of gap-filling when data is adequately available. However, the risk of over-extrapolation should be considered in case the range in temperature or PAR is limited in single measurement campaigns.

Besides in the gap-filling of CO<sub>2</sub> fluxes from drained temperate peatlands, similar empirical models of  $R_{eco}$  and GPP have been applied also on cropland (e.g., Struck et al., 2020), forest (e.g., Zhao et al., 2020), and tropical peatlands (e.g., Hirano et al., 2014; Gana et al., 2018) with consideration of influences of temperature, groundwater table and plant phenology. The Tier system following an increased model structural and temporal complexity proposed in this study is potentially applicable to these other ecosystems. For example, CO<sub>2</sub> and CH<sub>4</sub> fluxes from waterbodies can show clear correlations with temperature and water chemistry indicators, and display seasonal differences (Peacock et al., 2021). All in all, the Tier system can provide opportunities in the modeling of various greenhouse gasses in a multitude of ecosystems, though empirical relationships and independent environmental variables should be considered.

## DATA AVAILABILITY STATEMENT

The raw data, intermediate results, and R scripts that support the findings of this study are openly available on the DANS platform at <https://doi.org/10.17026/dans-xtq-ajzs>.

## AUTHOR CONTRIBUTIONS

WL designed the methodology, performed the formal analysis and drafted the manuscript. CF conceived and supervised the study. WL and SW collected and processed the data. All authors

contributed to the review and editing of the manuscript and approved the final version.

## FUNDING

WL is supported by the China Scholarship Council (201706350201). The work of MV is funded by NWO-Veni grant 202.053. MB and CF received funding through PEATWISE (NWO ALW-GAS No.4). This research was supported by Interreg-NWE Carbon Connects.

## ACKNOWLEDGMENTS

We would like to thank all technical staff, students and volunteers who helped in the field and in the laboratory, as well as the

landowners who granted access to the measurement sites. Specifically, we are grateful for the help of Sebastian Krosse, Paul van der Ven, staff from the General Instrumentation and Roy Peters for the chemical analyses. We appreciate Reinder Nouta from Wetterskip Fryslân for insightful discussions on the flux data. We acknowledge Peter Cruisen for his assistance in fieldwork and analyses. We sincerely thank the editor and reviewers for their critical remarks that helped improving the manuscript.

## SUPPLEMENTARY MATERIAL

The Supplementary Material for this article can be found online at: <https://www.frontiersin.org/articles/10.3389/fenvs.2022.803746/full#supplementary-material>

## REFERENCES

- Barrett, P. D., Laidlaw, A. S., and Mayne, C. S. (2005). GrazeGro: A European Herbage Growth Model to Predict Pasture Production in Perennial Ryegrass Swards for Decision Support. *Eur. J. Agron.* 23 (1), 37–56. doi:10.1016/j.eja.2004.09.006
- Bates, D., Mächler, M., Bolker, B., and Walker, S. (2015). Fitting Linear Mixed-Effects Models Using lme4. *J. Stat. Soft.* 67. doi:10.18637/jss.v067.i01
- Baty, F., Ritz, C., Charles, S., Brutsche, M., Flandrois, J.-P., and Delignette-Muller, M.-L. (2015). A Toolbox for Nonlinear Regression in R: The Packagelstools. *J. Stat. Soft.* 66, 1–21. doi:10.18637/jss.v066.i05
- Beetz, S., Liebersbach, H., Glatzel, S., Jurasinski, G., Buczko, U., and Höper, H. (2013). Effects of Land Use Intensity on the Full Greenhouse Gas Balance in an Atlantic Peat Bog. *Biogeosciences* 10, 1067–1082. doi:10.5194/bg-10-1067-2013
- Berger, S., Braeckvelt, E., Blodau, C., Burger, M., Goebel, M., Klemm, O., et al. (2019). A 1-year Greenhouse Gas Budget of a Peatland Exposed to Long-Term Nutrient Infiltration and Altered Hydrology: High Carbon Uptake and Methane Emission. *Environ. Monit. Assess.* 191. doi:10.1007/s10661-019-7639-1
- Campbell, D. I., Smith, J., Goodrich, J. P., Wall, A. M., and Schipper, L. A. (2014). Year-round Growing Conditions Explains Large CO<sub>2</sub> Sink Strength in a New Zealand Raised Peat Bog. *Agric. For. Meteorology* 192–193, 59–68. doi:10.1016/j.agrformet.2014.03.003
- Capocci, M., and Vargas, R. (2022). Diel and Seasonal Patterns of Soil CO<sub>2</sub> Efflux in a Temperate Tidal Marsh. *Sci. Total Environ.* 802, 149715. doi:10.1016/j.scitotenv.2021.149715
- Couwenberg, J., and Hooijer, A. (2013). Towards Robust Subsidence-Based Soil Carbon Emission Factors for Peat Soils in South-East Asia, with Special Reference to Oil palm Plantations. *Mires Peat* 12 (1).
- Davidson, E. A., Belk, E., and Boone, R. D. (1998). Soil Water Content and Temperature as Independent or Confounded Factors Controlling Soil Respiration in a Temperate Mixed Hardwood forest. *Glob. Change Biol.* 4, 217–227. doi:10.1046/j.1365-2486.1998.00128.x
- Eickenscheidt, T., Heinichen, J., and Drösler, M. (2015). The Greenhouse Gas Balance of a Drained Fen Peatland Is Mainly Controlled by Land-Use rather Than Soil Organic Carbon Content. *Biogeosciences* 12, 5161–5184. doi:10.5194/bg-12-5161-2015
- Elsgaard, L., Görres, C.-M., Hoffmann, C. C., Blicher-Mathiesen, G., Schelde, K., and Petersen, S. O. (2012). Net Ecosystem Exchange of CO<sub>2</sub> and Carbon Balance for Eight Temperate Organic Soils under Agricultural Management. *Agric. Ecosyst. Environ.* 162, 52–67. doi:10.1016/j.agee.2012.09.001
- Erkens, G., and Boonman, J. (2020). A New National Research Programme on Greenhouse Gas Emissions from lowland Peat Meadows in The Netherlands. *EGU Gen. Assembly*, EGU2020–11169. doi:10.5194/egusphere-egu2020-11169
- Fritz, C., Campbell, D. I., and Schipper, L. A. (2008). Oscillating Peat Surface Levels in a Restiad Peatland, New Zealand-magnitude and Spatiotemporal Variability. *Hydrol. Process.* 22, 3264–3274. doi:10.1002/hyp.6912
- Fu, Z., Ciais, P., Bastos, A., Stoy, P. C., Yang, H., Green, J. K., et al. (2020). Sensitivity of Gross Primary Productivity to Climatic Drivers During the Summer Drought of 2018 in Europe. *Phil. Trans. R. Soc. B* 375, 20190747. doi:10.1098/rstb.2019.0747
- Gana, C., Nouvellon, Y., Marron, N., Stape, J. L., and Epron, D. (2018). Sampling and Interpolation Strategies Derived from the Analysis of Continuous Soil CO<sub>2</sub> Flux. *J. Plant Nutr. Soil Sci.* 181 (1), 12–20. doi:10.1002/jpln.201600133
- Gronlund, A., Hauge, A., Hovde, A., and Rasse, D. P. (2008). Carbon Loss Estimates From Cultivated Peat Soils in Norway: A Comparison of Three Methods. *Nutr. Cycl. Agroecosystems* 81 (2), 157–167. doi:10.1007/s10705-008-9171-5
- Günther, A., Huth, V., Jurasinski, G., and Glatzel, S. (2015). The Effect of Biomass Harvesting on Greenhouse Gas Emissions from a Rewetted Temperate Fen. *GCB Bioenergy* 7, 1092–1106. doi:10.1111/gcbb.12214
- Heng, L. (2021). in *Measuring Emission of Agricultural Greenhouse Gases and Developing Mitigation Options Using Nuclear and Related Techniques*. Editors M. Zaman, L. Heng, and C. Müller (Cham: Springer International Publishing). doi:10.1007/978-3-030-55396-8
- Hirano, T., Kusin, K., Limin, S., and Osaki, M. (2014). Carbon Dioxide Emissions through Oxidative Peat Decomposition on a Burnt Tropical Peatland. *Glob. Change Biol.* 20 (2), 555–565. doi:10.1111/gcb.12296
- Hirota, M., Zhang, P., Gu, S., Shen, H., Kuriyama, T., Li, Y., et al. (2010). Small-scale Variation in Ecosystem CO<sub>2</sub> Fluxes in an alpine Meadow Depends on Plant Biomass and Species Richness. *J. Plant Res.* 123, 531–541. doi:10.1007/s10265-010-0315-8
- Hoffmann, M., Jurisch, N., Albiac Borraz, E., Hagemann, U., Drösler, M., Sommer, M., et al. (2015). Automated Modeling of Ecosystem CO<sub>2</sub> Fluxes Based on Periodic Closed Chamber Measurements: A Standardized Conceptual and Practical Approach. *Agric. For. Meteorology* 200, 30–45. doi:10.1016/j.agrformet.2014.09.005
- Hoffmann, M., Jurisch, N., Garcia Alba, J., Albiac Borraz, E., Schmidt, M., Huth, V., et al. (2017). Detecting Small-Scale Spatial Heterogeneity and Temporal Dynamics of Soil Organic Carbon (SOC) Stocks: a Comparison between Automatic Chamber-Derived C Budgets and Repeated Soil Inventories. *Biogeosciences* 14 (4), 1003–1019. doi:10.5194/bg-14-1003-2017
- Hoyt, A. M., Gandois, L., Eri, J., Kai, F. M., Harvey, C. F., and Cobb, A. R. (2019). CO<sub>2</sub> Emissions from an Undrained Tropical Peatland: Interacting Influences of Temperature, Shading and Water Table Depth. *Glob. Change Biol.* 25, 2885–2899. doi:10.1111/gcb.14702
- Huth, V., Vaidya, S., Hoffmann, M., Jurisch, N., Günther, A., Gundlach, L., et al. (2017). Divergent NEE Balances from Manual-chamber CO<sub>2</sub> Fluxes Linked to Different Measurement and Gap-filling Strategies: A Source for Uncertainty of Estimated Terrestrial C Sources and Sinks? *J. Plant Nutr. Soil Sci.* 180, 302–315. doi:10.1002/jpln.201600493

- Intergovernmental Panel on Climate Change (IPCC) (2019). 2019 Refinement to the 2006 IPCC Guidelines for National Greenhouse Gas Inventories. Available at: <https://www.ipcc-nggip.iges.or.jp/public/2019rf/index.html> (Accessed on October 22, 2021).
- Järveoja, J., Peichl, M., Maddison, M., Soosaar, K., Vellak, K., Karofeld, E., et al. (2016). Impact of Water Table Level on Annual Carbon and Greenhouse Gas Balances of a Restored Peat Extraction Area. *Biogeosciences* 13, 2637–2651. doi:10.5194/bg-13-2637-2016
- Järveoja, J., Nilsson, M. B., Crill, P. M., and Peichl, M. (2020). Bimodal Diel Pattern in Peatland Ecosystem Respiration Rebutts Uniform Temperature Response. *Nat. Commun.* 11, 1–9. doi:10.1038/s41467-020-18027-1
- Jassey, V. E. J., and Signarbieux, C. (2019). Effects of Climate Warming on Sphagnum Photosynthesis in Peatlands Depend on Peat Moisture and Species-specific Anatomical Traits. *Glob. Change Biol.* 25, 3859–3870. doi:10.1111/gcb.14788
- Joosten, H. (2010). The Global Peatland CO<sub>2</sub> Picture. Peatland Status and Drainage Related Emissions in All Countries of the World. *Wetl. Int.* 36. Available at: <http://scholar.google.com/scholar?hl=en&btnG=Search&q=intitle:The+Global+Peatland+CO+2+Picture+Peatland+status+and+drainage+related+emissions+in+all+countries+of+the+world#0>.
- Juszczak, R., Humphreys, E., Acosta, M., Michalak-Galczevska, M., Kayzer, D., and Olejnik, J. (2013). Ecosystem Respiration in a Heterogeneous Temperate Peatland and its Sensitivity to Peat Temperature and Water Table Depth. *Plant Soil* 366, 505–520. doi:10.1007/s11104-012-1441-y
- Kandel, T. P., Elsgaard, L., and Lærke, P. E. (2013). Measurement and Modelling of CO<sub>2</sub> flux from a Drained Fen Peatland Cultivated with Reed Canary Grass and spring Barley. *GCB Bioenergy* 5, 548–561. doi:10.1111/gcb.12020
- Karki, S., Kandel, T. P., Elsgaard, L., Labouriau, R., and Lærke, P. E. (2019). Annual CO<sub>2</sub> Fluxes from a Cultivated Fen with Perennial Grasses during Two Initial Years of Rewetting. *Mires Peat* 25, 1–22. doi:10.19189/MaP.2017.DW.322
- Koebisch, F., Gottschalk, P., Beyer, F., Wille, C., Jurasinski, G., and Sachs, T. (2020). The Impact of Occasional Drought Periods on Vegetation Spread and Greenhouse Gas Exchange in Rewetted Fens. *Phil. Trans. R. Soc. B* 375, 20190685. doi:10.1098/rstb.2019.0685
- Lee, X., Wu, H.-J., Sigler, J., Oishi, C., and Siccama, T. (2004). Rapid and Transient Response of Soil Respiration to Rain. *Glob. Chang. Biol.* 10, 1017–1026. doi:10.1111/j.1529-8817.2003.00787.x
- Leiber-Sauheitl, K., Fuß, R., Voigt, C., and Freibauer, A. (2014). High CO<sub>2</sub> Fluxes from Grassland on Histic Gleysol along Soil Carbon and Drainage Gradients. *Biogeosciences* 11, 749–761. doi:10.5194/bg-11-749-2014
- Leifeld, J., and Menichetti, L. (2018). The Underappreciated Potential of Peatlands in Global Climate Change Mitigation Strategies. *Nat. Commun.* 9. doi:10.1038/s41467-018-03406-6
- Leifeld, J., Wüst-Galley, C., and Page, S. (2019). Intact and Managed Peatland Soils as a Source and Sink of GHGs from 1850 to 2100. *Nat. Clim. Chang.* 9, 945–947. doi:10.1038/s41558-019-0615-5
- Lenth, R., Buurkner, P., Herve, M., Love, J., Riebl, H., and Singmann, H. (2020). Emmeans: Estimated Marginal Means, Aka Least-Squares Means. R package version 1.5.1. Available at: <https://cran.r-project.org/package=emmeans>.
- Lloyd, J., and Taylor, J. A. (1994). On the Temperature Dependence of Soil Respiration. *Funct. Ecol.* 8, 315–323. doi:10.2307/2389824
- Lucas-Moffat, A. M., Huth, V., Augustin, J., Brümmer, C., Herbst, M., and Kutsch, W. L. (2018). Towards Pairing Plot and Field Scale Measurements in Managed Ecosystems: Using Eddy Covariance to Cross-Validate CO<sub>2</sub> Fluxes Modeled from Manual Chamber Campaigns. *Agric. For. Meteorology* 256–257, 362–378. doi:10.1016/j.agrformet.2018.01.023
- Ma, S., Baldocchi, D. D., Hatala, J. A., Detto, M., and Curiel Yuste, J. (2012). Are Rain-Induced Ecosystem Respiration Pulses Enhanced by Legacies of Antecedent Photodegradation in Semi-arid Environments? *Agric. For. Meteorology* 154–155, 203–213. doi:10.1016/j.agrformet.2011.11.007
- Maljanen, M., Hytönen, J., Mäkiranta, P., Alm, J., Minkinen, K., Laine, J., et al. (2007). Greenhouse Gas Emissions from Cultivated and Abandoned Organic Croplands in Finland. *Boreal Environ. Res.* 12, 133–140.
- Michaelis, L., and Menten, M. L. (1913). Die Kinetik der Invertinwirkung. *Biochemische Z.* 49, 333–369.
- Moriasi, D. N., Arnold, J. G., Van Liew, M. W., Bingner, R. L., Harmel, R. D., and Veith, T. L. (2007). Model Evaluation Guidelines for Systematic Quantification of Accuracy in Watershed Simulations. *Trans. ASABE* 50, 885–900. doi:10.13031/2013.23153
- Munson, S. M., Benton, T. J., Lauenroth, W. K., and Burke, I. C. (2010). Soil Carbon Flux Following Pulse Precipitation Events in the Shortgrass Steppe. *Ecol. Res.* 25, 205–211. doi:10.1007/s11284-009-0651-0
- Otieno, D. O., Wartinger, M., Nishiwaki, A., Hussain, M. Z., Muhr, J., Borken, W., et al. (2009). Responses of CO<sub>2</sub> Exchange and Primary Production of the Ecosystem Components to Environmental Changes in a Mountain Peatland. *Ecosystems* 12, 590–603. doi:10.1007/s10021-009-9245-5
- Parish, F., Sirin, A., Charman, D., Joosten, H., Minayeva, T., Silvius, M., et al. (2008). *Assessment on Peatlands, Biodiversity and Climate Change: Main Report*. Wageningen: Global Environment Centre, Kuala Lumpur and Wetlands International.
- Payero, J. O., Neale, C. M. U., and Wright, J. L. (2004). Comparison of Eleven Vegetation Indices for Estimating Plant Height of Alfalfa and Grass. *Appl. Eng. Agric.* 20, 385–393. doi:10.13031/2013.16057
- Peacock, M., Audet, J., Bastviken, D., Cook, S., Evans, C. D., Grinham, A., et al. (2021). Small Artificial Waterbodies Are Widespread and Persistent Emitters of Methane and Carbon Dioxide. *Glob. Change Biol.* 27 (20), 5109–5123. doi:10.1111/GCB.15762
- Peichl, M., Gažovič, M., Vermeij, I., De Goede, E., Sonnentag, O., Limpens, J., et al. (2018). Peatland Vegetation Composition and Phenology Drive the Seasonal Trajectory of Maximum Gross Primary Production. *Sci. Rep.* 8, 1–11. doi:10.1038/s41598-018-26147-4
- Querner, E. P., Jansen, P. C., van den Akker, J. J. H., and Kwakernaak, C. (2012). Analysing Water Level Strategies to Reduce Soil Subsidence in Dutch Peat Meadows. *J. Hydrol.* 446–447, 59–69. doi:10.1016/j.jhydrol.2012.04.029
- R Core Team (2020). *R: A Language and Environment for Statistical Computing*. <https://www.r-project.org/>: R Foundation for Statistical Computing, Vienna, Austria. Available at: <https://www.r-project.org/>.
- Renou-Wilson, F., Müller, C., Moser, G., and Wilson, D. (2016). To Graze or Not to Graze? Four Years Greenhouse Gas Balances and Vegetation Composition from a Drained and a Rewetted Organic Soil under Grassland. *Agric. Ecosyst. Environ.* 222, 156–170. doi:10.1016/j.agee.2016.02.011
- Shen, Z.-X., Yun-Long, L., and Gang, F. (2015). Response of Soil Respiration to Short-Term Experimental Warming and Precipitation Pulses Over the Growing Season in an Alpine Meadow on the Northern Tibet. *Appl. Soil Ecol.* 90, 35–40. doi:10.1016/j.apsoil.2015.01.015
- Stagge, J. H., Tallaksen, L. M., Gudmundsson, L., Van Loon, A. F., and Stahl, K. (2015). Candidate Distributions for Climatological Drought Indices (SPI and SPEI). *Int. J. Climatol.* 35, 4027–4040. doi:10.1002/joc.4267
- Struck, I. J. A., Taube, F., Hoffmann, M., Kluß, C., Herrmann, A., Loges, R., et al. (2020). Full Greenhouse Gas Balance of Silage maize Cultivation Following Grassland: Are No-Tillage Practices Favourable under Highly Productive Soil Conditions? *Soil Tillage Res.* 200, 104615. doi:10.1016/j.still.2020.104615
- Tiemeyer, B., Albiac Borraz, E., Augustin, J., Bechtold, M., Beetz, S., Beyer, C., et al. (2016). High Emissions of Greenhouse Gases from Grasslands on Peat and Other Organic Soils. *Glob. Change Biol.* 22, 4134–4149. doi:10.1111/gcb.13303
- Tiemeyer, B., Freibauer, A., Borraz, E. A., Augustin, J., Bechtold, M., Beetz, S., et al. (2020). A New Methodology for Organic Soils in National Greenhouse Gas Inventories: Data Synthesis, Derivation and Application. *Ecol. Indicators* 109, 105838. doi:10.1016/j.ecolind.2019.105838
- van den Akker, J., Alkemade, H., Van den Berg, M., Bijman, M., Bosma, N., Erkens, G., et al. (2019). Factsheet onderwater- en drukdrainage: Veelgestelde vragen over onderwaterdrainage en drukdrainage (Underwater and pressured drainage factsheet). Available at: <https://edepot.wur.nl/547024> (Accessed September 28, 2021).
- van den Akker, J., Kuikman, P., De Vries, F., Hoving, I., Pleijter, M., Hendriks, R., et al. (2010). “Emission of CO<sub>2</sub> from Agricultural Peat Soils in the Netherlands and Ways to Limit This Emission,” in Proceedings of the 13th International Peat Congress. After Wise Use – The Future of Peatlands, 8–13 June 2008 (Tullamore, Ireland: Oral Presentations), 645–648. Available at: <https://edepot.wur.nl/159747>.
- Waddington, J. M., and Roulet, N. T. (2000). Carbon Balance of a Boreal Patterned Peatland. *Glob. Chang. Biol.* 6, 87–97. doi:10.1046/j.1365-2486.2000.00283.x
- Weideveld, S. T. J., Liu, W., van den Berg, M., Lamers, L. P. M., and Fritz, C. (2021). Conventional Subsoil Irrigation Techniques Do Not Lower Carbon Emissions

- from Drained Peat Meadows. *Biogeosciences* 18, 3881–3902. doi:10.5194/bg-18-3881-2021
- Wilson, D., Blain, D., Couwenberg, J., Evans, C. D., Murdiyarso, D., Page, S. E., et al. (2016a). Greenhouse Gas Emission Factors Associated with Rewetting of Organic Soils. *Mires Peat* 17, 1–28. doi:10.19189/MaP.2016.OMB.222
- Wilson, D., Farrell, C. A., Fallon, D., Moser, G., Müller, C., and Renou-Wilson, F. (2016b). Multiyear Greenhouse Gas Balances at a Rewetted Temperate Peatland. *Glob. Change Biol.* 22, 4080–4095. doi:10.1111/gcb.13325
- Yamori, W., Hikosaka, K., and Way, D. A. (2014). Temperature Response of Photosynthesis in C3, C4, and CAM Plants: Temperature Acclimation and Temperature Adaptation. *Photosynth. Res.* 119, 101–117. doi:10.1007/s11120-013-9874-6
- Yu, Z., Loisel, J., Brosseau, D. P., Beilman, D. W., and Hunt, S. J. (2010). Global Peatland Dynamics Since the Last Glacial Maximum. *Geophys. Res. Lett.* 37, a–n. doi:10.1029/2010GL043584
- Zeileis, A., and Grothendieck, G. (2005). zoo: S3 Infrastructure for Regular and Irregular Time Series. *J. Stat. Softw.* 14. doi:10.18637/jss.v014.i06
- Zhao, J., Lange, H., and Meissner, H. (2020). Gap-filling Continuously-Measured Soil Respiration Data: A Highlight of Time-Series-Based Methods. *Agric. For. Meteorology* 285–286, 107912. doi:10.1016/j.agrformet.2020.107912
- Conflict of Interest:** The authors declare that the research was conducted in the absence of any commercial or financial relationships that could be construed as a potential conflict of interest.
- Publisher's Note:** All claims expressed in this article are solely those of the authors and do not necessarily represent those of their affiliated organizations, or those of the publisher, the editors and the reviewers. Any product that may be evaluated in this article, or claim that may be made by its manufacturer, is not guaranteed or endorsed by the publisher.

Copyright © 2022 Liu, Fritz, Weideveld, Aben, van den Berg and Velthuis. This is an open-access article distributed under the terms of the Creative Commons Attribution License (CC BY). The use, distribution or reproduction in other forums is permitted, provided the original author(s) and the copyright owner(s) are credited and that the original publication in this journal is cited, in accordance with accepted academic practice. No use, distribution or reproduction is permitted which does not comply with these terms.



# Soil Structural Quality and Relationships With Root Properties in Single and Integrated Farming Systems

Karina Maria Vieira Cavaleri-Polizeli<sup>1\*</sup>, Feliciano Canequetela Marcolino<sup>1</sup>,  
Cássio Antonio Tormena<sup>2</sup>, Thomas Keller<sup>3,4</sup> and Anibal de Moraes<sup>1</sup>

<sup>1</sup>Federal University of Paraná, Curitiba, Brazil, <sup>2</sup>State University of Maringá, Maringá, Brazil, <sup>3</sup>Swedish University of Agricultural Sciences, Uppsala, Sweden, <sup>4</sup>Agroscope (Switzerland), Zürich, Switzerland

## OPEN ACCESS

### Edited by:

Miriam Muñoz-Rojas,  
University of New South Wales,  
Australia

### Reviewed by:

Jagdish Chander Dagar,  
Indian Council of Agricultural Research  
(ICAR), India  
Maria Martínez-Mena,  
Spanish National Research Council  
(CSIC), Spain

### \*Correspondence:

Karina Maria Vieira Cavaleri-Polizeli  
karina.cavaleri@ufpr.br

### Specialty section:

This article was submitted to  
Soil Processes,  
a section of the journal  
Frontiers in Environmental Science

**Received:** 21 March 2022

**Accepted:** 23 May 2022

**Published:** 04 July 2022

### Citation:

Cavaleri-Polizeli KMV, Marcolino FC,  
Tormena CA, Keller T and Moraes Ad  
(2022) Soil Structural Quality and  
Relationships With Root Properties in  
Single and Integrated  
Farming Systems.  
Front. Environ. Sci. 10:901302.  
doi: 10.3389/fenvs.2022.901302

Single farming systems (SFS) such as monocultures may negatively affect soil structural quality. This study tested the hypothesis that integrated farming systems (IFS), i.e., the combination of cropping and forestry and/or livestock farming, improves soil structural quality, root development and soil organic carbon. An experimental area was set up in 2012 at the Canguiri experimental farm belonging to the Federal University of Paraná, Southern Brazil. The soils are predominantly Ferralsols. The experimental treatments representing different farming systems, organized in a random block design with three replicates, were: Forestry (F), Conventional Crop Production (C), Livestock (L), and integrated Crop-Forestry (CF), Crop-Livestock (CL), Livestock-Forestry (LF), and Crop-Livestock-Forestry (CLF). *In situ* measurements and sampling were carried out in the 0–0.3 m layer during summer 2019/20, and included soil penetration resistance (PR), soil structural quality based on visual evaluation of soil structure (Sq<sub>VESS</sub> scores), root length (RL), root volume (RV) and soil organic carbon content (SOC). Soil structural quality, penetration resistance, root length and volume, and SOC varied between farming systems, but no significant differences were found between single (C, L, F) and integrated farming systems (CF, CL, LF, CLF). The single system Forestry (F) and the integrated systems including forestry (LF, CF, CLF) tended to have higher Sq<sub>VESS</sub> scores, i.e. poorer soil structural quality, and higher PR, which we associate with the generally drier soil conditions that are due to higher soil water uptake and higher interception and reduce the frequency of wetting-drying cycles. Roots were concentrated in the shallow soil layer (0–0.1 m depth), and this was especially pronounced in the Crop (C) single farming system. Based on the measured values, our results suggest an acceptable soil structural quality in all farming systems. Our data revealed strong, significant relationships between soil structural quality, penetration resistance, root growth and SOC, demonstrating that improvements in soil structure results in lower soil penetration resistance, higher root volumes and higher SOC, and vice versa. Soil PR was positively correlated with Sq<sub>VESS</sub> ( $R^2 = 0.84$ ), indicating that better soil structural quality resulted in lower soil mechanical resistance. This, in turn, increased root length and volume, which increases carbon input to soil and therefore increases SOC in the long run.

**Keywords:** soil conservation, root growth, soil structural quality, single farming systems, integrated farming systems

# 1 INTRODUCTION

The Sustainable Development Goals (SDGs) proposed by the United Nations (UN) aim to achieve a better quality of life in a sustainable way for all. To achieve the SDGs, it is necessary to adopt soil management to improve the health of agroecosystems (Keesstra et al., 2016). In Brazil, agriculture has been intensified through the use of a set of technologies since the green revolution in the 1950s. Considerable effort has been done to develop genuinely sustainable approaches to agriculture, including crop breeding for sustainability (Meena et al., 2020; Brooker et al., 2021). Agricultural practices with techniques that combine food production with little impact on other ecosystem functions ensure soil conservation and agricultural sustainability (Rahman et al., 2017).

No-tillage have been widely adopted in Brazil, and it is often combined with other conservation practices such as crop rotation (Derpsch, 2021; FEBRAPDP, 2021). No-tillage has become an important practice to achieve sustainable agricultural production systems, especially when it is practiced in combination with crop rotation and permanent crop residues on the soil surface (Derpsch et al., 2010; Bonetti et al., 2015; Bonetti et al., 2018). Currently, in Brazil, no-tillage is practiced on more than 33 million hectares (SIDRA/IBGE, 2021), which is about one sixth of the total global area under no-tillage (Kassam, et al., 2020). The “planting green technique” refers to no-till planting of primary crops into standing cover crops (Duiker et al., 2017). Few studies have reported on the use of no-tillage under the “planting green technique,” probably because this is a relatively new practice that is still under evaluation (Duiker et al., 2017), but has shown several benefits, e.g. greater amounts of mulch in the crop that reduce weed pressure.

Although single farming systems are most common in Brazilian farms, integrated farming systems are becoming more and more popular in Brazil. They are referred as agricultural systems that integrate livestock, forestry, and crop production (Soni et al., 2014), aiming at producing various products such as meat, milk, wool, grains, and biomass, and adopting mixed-farming, crop rotation and intercropping production systems (Moraes et al., 2014). These systems have been adopted both by small and large farms in Brazil (Bendahan et al., 2018). Despite the challenges for its (re-)integration in some regions (Schut et al., 2021), such systems have several benefits (Sharma et al., 2019). No-tillage is one of the pillars of integrated farming systems, being adopted in more than 65% of these systems (Valani et al., 2020), but few studies have analyzed soil and water conservation under integrated farming systems (Moraes et al., 2014).

Integrated farming systems have been adopted in the following configurations: integrated crop-livestock-forestry (CLF), integrated crop-forestry (CF), crop-livestock (CL), and livestock-forestry (LF). According to Zhang et al. (2019), the adoption of crop-livestock has a positive effect on soil quality, mainly due to the incorporation of organic matter. They indicated that moderate grazing stimulates the regrowth of forage plants and root growth leading to the formation of macro aggregates, thus improving soil structure, infiltration, and water availability.

Soil compaction caused by animal trampling can be controlled or minimized through adequate animal stocking (Bonetti et al., 2018).

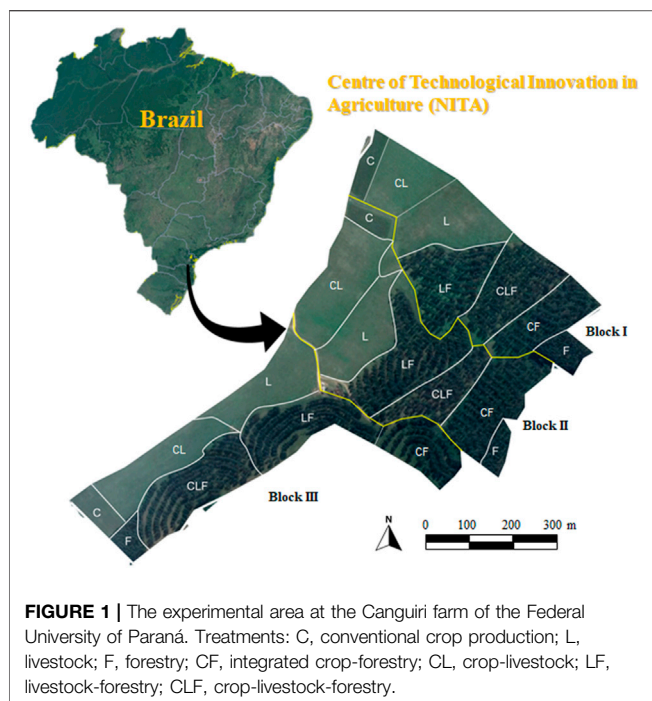
Soil structure affects root penetration, the amount of available water to plants, and other key soil properties and processes. According to Flávio Neto et al., 2015, degraded soils can be recovered using *Brachiaria* (syn. *Urochloa* spp) as forage grass in integrated farming systems. Soil structure can be evaluated through different approaches including visual methods. The visual evaluation of soil structure (VESS) method has been frequently used to assess soil structural quality (Pulido-Moncada et al., 2014; Tormena et al., 2016; Cherubin et al., 2017; Tuchtenhagen et al., 2018; Franco et al., 2019; Paiva et al., 2020; Çelik et al., 2020; Mutuku et al., 2021). The VESS method is applied globally, as it is an easy method that allows soil structure assessment directly on-farm. The VESS is a semi-quantitative method, and includes several aspects of structure and rooting to infer about the soil structural quality through assigned scores (Guimarães et al., 2017). Another important aspect of soil structure is the soil penetration resistance. Colombi et al. (2018) demonstrated that the interactive effects between soil penetration resistance, root architecture, and plant water uptake determine water accessibility by roots and ultimately affect crop yield. Popoya et al. (2016) noticed an increase in root tortuosity and reduced root elongation due to an increase in soil penetration resistance, which has been recently confirmed by Moraes and Gusmão (2021). The assessment of soil structural quality and root properties in integrated farming systems is needed to evaluate its adoption as a sustainability strategy for agricultural production.

In our study, integrated and single pesticide-free farming systems were evaluated in terms of soil structural quality and root growth. The aims of our study were: 1) to measure soil penetration resistance and VESS as indicators of soil structural quality; 2) to determine root properties and soil organic carbon down to 0.30 m depth, and; 3) to explore relationships between soil organic carbon, root growth properties and soil structural quality measured by VESS and penetrometer resistance.

## 2 MATERIAL AND METHODS

### 2.1 Experimental Area

The study was carried out at the Agricultural Technological Innovation Center (NITA) at the Canguiri experimental farm, belonging to the Federal University of Paraná (UFPR), Pinhais municipality, Paraná state, Southern Brazil (25°24′03″ S, 49°07′10″ W). The regional climate is humid-temperate (Cfb), with a mean annual rainfall and temperature of 1,602 mm and 17°C, respectively (Alvares et al., 2013). Rainfall and temperature data during the study period are presented in **Supplementary Figure S1**. The soils are identified as Ferralsols, with minor occurrence of Cambisols (WRB/FAO), differing mainly by the B horizon depth, or “Latossolo Vermelho and Cambissolo Háplico” according to Brazilian soil classification system (EMBRAPA, 2018). Soil texture is clayey with an average of 519 g kg<sup>-1</sup> clay, 112 g kg<sup>-1</sup> silt, and 369 g kg<sup>-1</sup> sand.



The NITA is located in an environmental preservation area (Figure 1) according to Brasil (2000), on the banks of the river Iraí, which supplies water to the city of Curitiba and the metropolitan region. Therefore, the area must be managed pesticide free. Until 2011, the area was also used for training and testing of agricultural machinery traffic, which led to soil physical degradation (soil loss by erosion and compacted patches), as shown in Supplementary Figure S2. Before the implementation of the experimental area in 2012, maize (*Zea mays*) was grown under conventional tillage. The soil was chisel ploughed down to 0.40 m depth and subsequently harrowed (<0.20 m). After that, the experimental area received between 8 and 10 ton ha<sup>-1</sup> sewage sludge treated by the N-VIRO<sup>®</sup> process for acidity correction as described by Kruchelski et al. (2021). Then, the area was cultivated with black oat (*Avena strigosa*) as a cover crop, which was fertilized with 100 kg ha<sup>-1</sup> of P<sub>2</sub>O<sub>5</sub>. Soil chemical attributes evaluated in 2013 were: soil organic carbon (SOC) = 20 g kg<sup>-1</sup>, pH = 5.2, a CEC of 13 cmol<sub>c</sub> kg<sup>-1</sup> and 60% for base saturation.

The experiment was established in 2012 in a randomized block design with three replicates, with three single farming systems (SFS), namely Forestry (F), Crop (C), Livestock (L), and four integrated farming systems (IFS) treatments including Crop-Forestry (CF), Crop-Livestock (CL), Livestock-Forestry (LF), and Crop-Livestock-Forestry (CLF). The plots varied in size between 0.2 and 1 ha<sup>-1</sup> (areas without livestock) and >1 ha<sup>-1</sup> for areas with livestock (Figure 1).

Soil fertilization has been done on the whole area by broadcasting 180 kg ha<sup>-1</sup> N of urea; 45 kg ha<sup>-1</sup> of P<sub>2</sub>O<sub>5</sub> (natural phosphate) and 120 kg ha<sup>-1</sup> of K<sub>2</sub>O (potassium chloride). Sowing has been done by a no-tillage seeder using the “planting green” technique without herbicides for desiccation, in all systems except in Forestry. In treatment C, crop succession has been carried out using black oat as a cover

crop and maize as a cash crop. For L, black oat is cropped for the winter pasture and guinea grass cv. aries [*Megathyrus maximus* (Jacq.) B. K. Simon and S. W. L. Jacobs cv. aries] as a summer pasture. Grazing is by animals, predominantly of Angus breed, since 2015, for around 10 months per year. There are three fixed test animals per plot and a variable number of regulatory animals, with an average of 1.6 animal unit (AU) per hectare (AU ha<sup>-1</sup>). In system F, eucalyptus (*Eucalyptus benthamii*) was planted in 2013, with seedlings of seminal origin, using fertilization of 16 g of N pit<sup>-1</sup>, 40 g of K<sub>2</sub>O pit<sup>-1</sup>, and 40 g of P<sub>2</sub>O<sub>5</sub> pit<sup>-1</sup>, under a spatial arrangement of 3 m × 2 m, with a final density of 1,667 trees ha<sup>-1</sup>. The CLF, CF, and LF systems are in an alley-cropping spatial design with the seedlings planted at single rows, following the contour lines, at 14 m × 2 m spacing, obtaining 357 trees ha<sup>-1</sup> and occupying about 14.3% of the area of the integrated systems. Details about forest component can be found in Kruchelski et al. (2021). In LF, the animal component followed the stocking rate adjustments described in system L, while the CF treatment had in the first 3 years black oats cultivated in winter, and sunflower (*Helianthus annuus*) varieties Aguará 4 and Aguará and maize hybrids 2B655HX, 30F53VYHR-early and P2866H-super early in summer. From 2015/2016 onwards, only maize is cultivated in the summer. The CL started with the pasture components, until the winter of 2015, but without grazing, and from then on, grazing with animals was started until the summer of 2016. Then, the first crop cycle was established, with black oats as a cover crop in winter, followed by maize in the summer of 2017, as described in treatment C, in a ley farming arrangement. The CLF integrated system followed the same arrangement as the LF.

In treatments with crops, between 2017 and 2019/2020, maize was harvested for the evaluation of yield. The machines used for the mechanized operations were: a New Holland tractor, model TL 75 E 4 × 4 (~3,880 kg mass); a New Holland harvester, model TC 59 (~10,300 kg mass) for the harvest in 2016/17 crop season. The implements used were a Marchesan Tatu seeder (~2,595 kg mass), a Baldan mower (~1,000 kg mass) used to control weeds, and a Marchesan Tatu fertilizer and limestone distributor (800 kg mass).

## 2.2 Soil and Roots Sampling, and *in situ* Measurements

Soil and root sampling were performed randomly at four locations within each plot, in summer 2019/20, a period with expected high amounts of plant roots for C-cash crop and L-pasture. Four undisturbed soil core samples were taken with a cup auger (Ratuchne et al., 2017) in the 0.0–0.10, 0.10–0.20, and 0.20–0.30 m layers depth, totaling 252 samples (4 samples × 3 soil layers × 7 farming systems × 3 experimental blocks). Disturbed soil samples were taken to determine soil water content, soil texture, and total soil organic carbon (SOC). Three soil penetration resistance (PR) measurements were taken near the sampling points at soil moisture close to field capacity, using a Falker<sup>®</sup> electronic penetrometer down to 0.30 m depth and a mean PR value was calculated for each studied layer.

The visual evaluation of the soil structure was carried out following the method proposed by Ball et al. (2007) and Guimarães et al. (2011). The scores identified in each soil layer were weighted and paired

within the three depth layers (0–0.1, 0.1–0.2 and 0.2–0.3 m depth) to proceed with the correlation's studies. Structural quality ( $Sq_{VESS}$ ) reflect values between “good” structural quality ( $Sq_1$ ) and “poor” structural quality ( $Sq_5$ ).

## 2.3 Soil and Roots Laboratory Measurements

Undisturbed soil samples were manually disaggregated in a plastic tray, and washed by water into a set of sieves with 2.0, 1.0, and 0.5 mm of mesh size. This procedure was standardized in 10 replication and, after washing, the roots were placed in 50 ml pots containing 70% alcohol and stored at a temperature of 2°C. Subsequently, the roots were scanned using the WinRhizo® software, to obtain the following properties: root length (RL), and root volume (RV). After being scanned, the roots were weighed and taken to the oven between 45 and 65°C until reaching constant weight. Then, the dry mass of roots (RDM) was obtained. For soil texture, the Bouyoucos hydrometer method was used (Gee and Or, 2002), and for SOC the colorimetric method according to Quaggio and van Raij, 1979.

## 2.4 Statistical Analysis

All data were submitted to the test of homogeneity of variance (Bartlett) and normality (Shapiro-Wilk). Those data that did not reach the normality assumptions were submitted to the BoxCox transformation (Box and Cox, 1964). Then, the data were submitted to analysis of variance (ANOVA) and the means were compared by Tukey test ( $p < 0.05$ ). To quantify the correlation between the studied properties, the root properties, SOC, PR, and VESS were submitted to Spearman correlation ( $p < 0.05$ ). Regression analyses were performed to determine the relationships between properties. Statistical analyzes were performed in the R® software environment (Team R. Core, 2020).

## 3 RESULTS


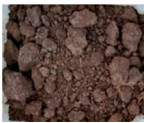





The  $Sq_{VESS}$  scores and PR varied between the studied farming systems, but most differences were not statistically significant

(**Table 1**). For both PR and VESS, forestry (F) had the highest mean values, with PR = 2.2 MPa and  $Sq = 3.1$ , respectively.  $Sq_{VESS}$  of F was statistically different from Crop (C). The integrated farming systems showed no significant difference in structural quality ( $Sq_{VESS} = 2.7$ ; 2.4; 2.5; and 2.8, for LF, CL, CF, and CLF, respectively) compared with SFS ( $Sq_{VESS} = 2.2$ ; 2.5; and 3.1, for C, L, and F, respectively). SOC was around 40 g kg<sup>-1</sup> at 0–0.30 m depth, with no statistical difference ( $p > 0.05$ ) between farming systems.

Average values of root length, root volume and root dry matter are shown in **Table 2**. Root length (but not root volume) was statistically different between farming systems, for 0–0.10 and 0.10–0.20 m layers. Root length was significantly lower in CF than in Crop at the 0–0.10 m of depth, while for the 0.10–0.20 m layer, root length in Forestry was lower than in L. No significant differences were found among the other treatments, in both soil layers. In the 0.20–0.30 m layer, no significant differences among farming systems were found for root properties. Roots were mostly concentrated at the 0–0.10 m depth, and root lengths and root volumes decreased with depth, as shown in **Table 2**.

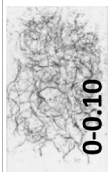


The root properties (root length, root volume) and SOC were negatively correlated (Spearman) with  $Sq_{VESS}$  ( $r_s = -0.57$ ,  $-0.62$ , and  $-0.62$ , respectively), and PR ( $r_s = -0.64$ ,  $-0.63$ , and  $-0.63$ , respectively). A positive relationship between  $Sq_{VESS}$  and PR ( $r_s = 0.81$ ) was found. Root properties and SOC was more strongly related to soil penetration resistance than  $Sq_{VESS}$ . **Figure 2** shows a nonlinear relationship between root properties and SOC, and between  $Sq_{VESS}$  and PR. Our data show that for values of  $Sq_{VESS}$  between 3.0 and 4.0 (i.e., moderate to poor soil structural quality), root lengths and root volumes were low, with values of RL < 5 m and RV < 0.35 cm<sup>3</sup>, respectively (**Figures 2A,C**). Root length and volume were low for PR values between 1.7 and 2.2 MPa (**Figures 2B,D**). Based on the regression curves (**Figures 2A–D**), it was possible to estimate the influence of soil penetration resistance on root properties. PR values around 4 MPa were associated with a reduction in root length and root volume of around 75%. Similarly, at 75% reduction in root length and volume, respectively, was associated with values of  $Sq_{VESS}$  larger than 3. In addition, there is a negative relationship between SOC for both  $Sq_{VESS}$  and PR (**Figures 2E,F**).

**TABLE 1** | Mean values of soil penetration resistance (PR), soil structural quality scores from visual evaluation of soil structure (VESS), and total organic carbon content (SOC) for different farming systems, at 0–0.30 m depth.

	Crop	Livestock	Forestry	LF	CL	CF	CLF
							
VESS	2.2 c	2.5 abc	3.1 a	2.7 abc	2.4 abc	2.5 abc	2.8 ab
PR (MPa)	1.2 b	1.3 b	2.2 a	1.5 b	1.2 b	1.6 b	1.5 b
SOC (g kg <sup>-1</sup> )	41.13 <sup>NS</sup>	43.58	41.38	42.36	39.83	38.75	44.95

<sup>NS</sup>: Not significant; Means followed by the same letters in the same row do not significantly differ based on Tukey test ( $p < 0.05$ ). LF, Integrated livestock-forestry; CL, crop-livestock; CF, crop-forestry; CLF, crop-livestock-forestry.

**TABLE 2 |** Mean values of root length (RL), root volume (RV), and root dry matter (RDM) for different farming systems.

2D Image/Layer (m)	Root Property	Crop	Livestock	Forestry	LF	CL	CF	CLF
 <b>0-0.10</b>	RL (cm)	1696 a	1480 ab	922 ab	1479 ab	1348 ab	822 b	1226 ab
	RV (cm <sup>3</sup> )	1.69 NS	1.32	1.06	1.23	0.97	1.15	1.09
	RDM (Mg ha <sup>-1</sup> )	1.42 NS	1.59	1.13	1.31	1.33	1.65	2.14
 <b>0.10-0.20</b>	RL (cm)	345 ab	856 a	262 b	831 ab	656 ab	328 ab	573 ab
	RV (cm <sup>3</sup> )	0.40 NS	0.53	0.34	0.42	0.35	0.32	0.39
	RDM (Mg ha <sup>-1</sup> )	0.39 NS	0.54	0.96	0.96	0.34	0.31	1.15
 <b>0.20-0.30</b>	RL (cm)	272 NS	530	257	526	451	371	497
	RV (cm <sup>3</sup> )	0.24 NS	0.24	0.24	0.25	0.22	0.33	0.29
	RDM (Mg ha <sup>-1</sup> )	0.23 NS	0.19	0.41	0.25	0.17	0.45	0.46

NS, Not significant; Means followed by the same letters in the same row do not significantly differ based on Tukey test ( $p < 0.05$ ), Integrated livestock-forestry (LF), crop-livestock (CL), crop-forestry (CF), and crop-livestock-forestry (CLF).

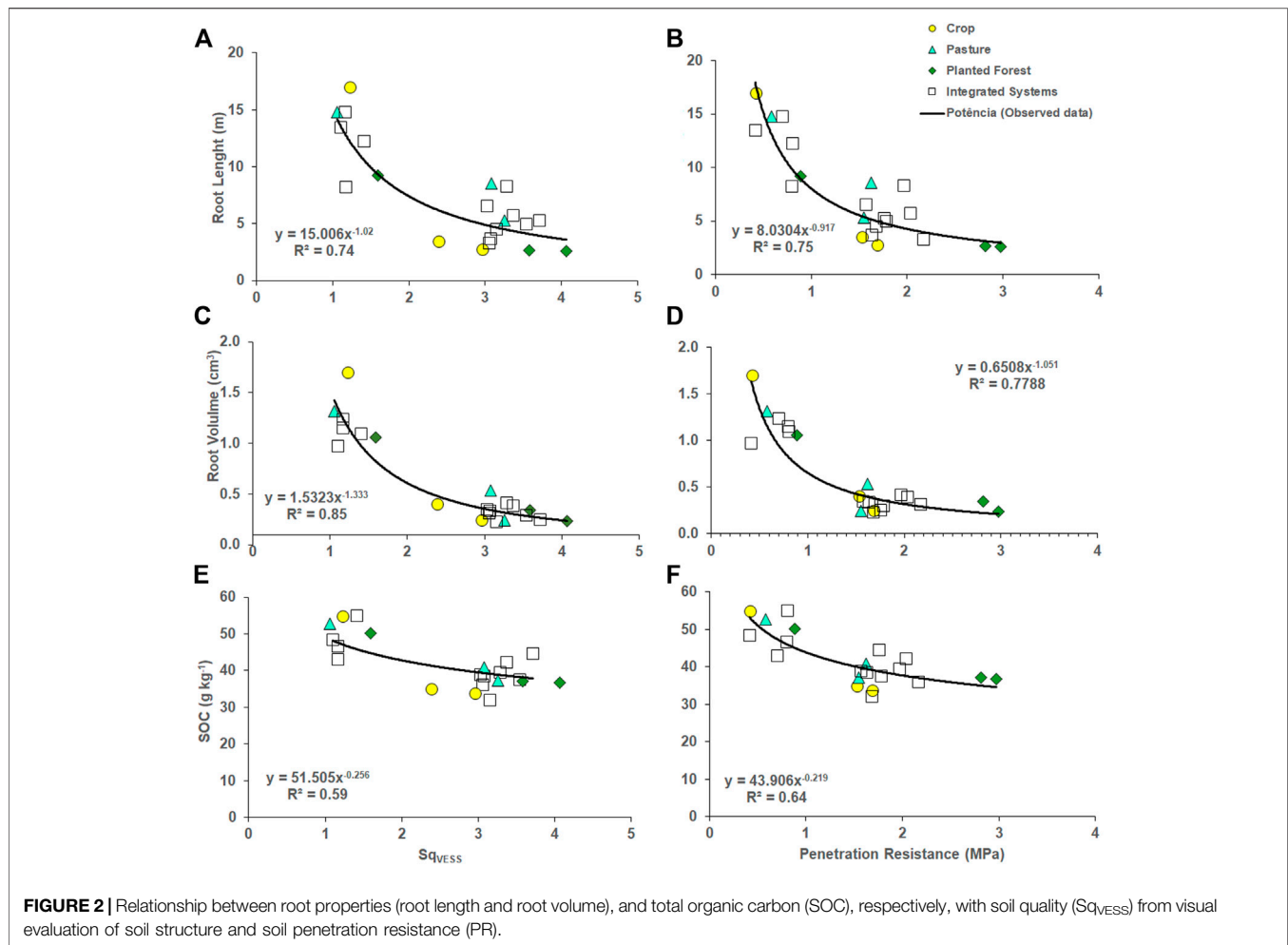
## 4 DISCUSSION

### 4.1 Soil Structural Quality Based on Visual Evaluation of Soil Structure

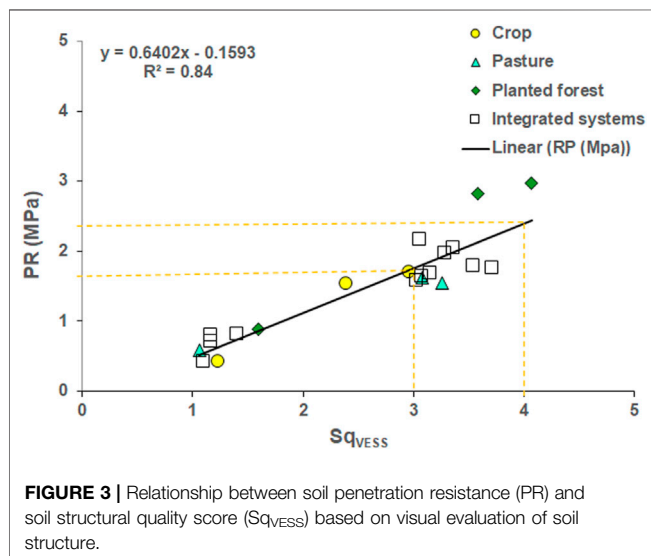
Soil structural quality presented distinct  $Sq_{VESS}$  between farming systems. Farming system Forestry (F) had rounded and sub-angular aggregates with few visible pores and only a few fine roots compared to the other systems, which resulted in the highest  $Sq_{VESS}$  ( $Sq = 3.1$ ). For the single farming systems, C and L had small and rounded aggregates, which resulted in lower  $Sq_{VESS}$ ; however, with exception of F, the soil structural quality for single farming systems was not significantly different than for integrated farming systems. Despite the statistical differences found, all studied farming systems had acceptable soil structure, with  $Sq_{VESS} < 3$  (Guimarães et al., 2011), except for the F system with  $Sq_{VESS} = 3.1$  indicating moderate soil structural quality (Ball et al., 2017). The higher  $Sq_{VESS}$  and higher soil penetration resistance for forestry treatment might be explained by drier soil conditions at the 0–0.25 m of depth ( $\sim 0.27 \text{ kg kg}^{-1}$ ) compared to the other treatments ( $\sim 0.35 \text{ kg kg}^{-1}$ ). According to Madani et al. (2018), evapotranspiration is higher in forests than grassland. In addition, rainfall data at the period of sampling (Supplementary Figure S1) indicates higher interception by trees compared with grassland, leading to a lower soil water content. Drier soil is characterized by higher soil cohesion, and this increases soil penetration resistance and decreases root development.

Several studies indicate that both systems, i.e., single and integrated farming systems, may provide suitable physical quality for plant development. Tuchtenhagen et al. (2018) found values for  $Sq_{VESS}$  of 2.5, 1.9, and 3.1, respectively, for cropping under no-tillage, native grassland, and crop-livestock, which is close to the scores found in our study. These authors mentioned that undisturbed soil surface, vegetation cover, and crop residues resulting from crop successions increased root biomass and SOC at the surface layers, contributing to the improvement in soil structure. In our study, no-tillage, the management with low machinery traffic intensity, adequate animal trampling ( $< 2 \text{ AU}$ ), proper fertilization, and large amounts of residues provided by winter and summer grasses had positive effects on soil structure. According to Carvalho et al. (2018) and Salton et al. (2014), proper pasture management encourages pasture regrowth and greater root growth, increasing inputs of organic matter into the soil. We highlight that root exudates stimulate the activity of soil microorganisms, leading to the formation of biopores that are important for air and water fluxes and preferentially used by new roots.

Single farming system F had the highest  $Sq_{VESS}$ , indicating moderate soil structural quality (Ball et al., 2017). Soil structural quality in this system could be improved by small changes in the management, e.g. by using plants with strong root systems (Guimarães et al., 2011). Introduction of intercropping species that can meet such conditions, with strong root systems, may be an option, such as pinto peanut (*Arachis pintoi*). However, eucalyptus must be at least 2 years old to avoid competition between species. When  $Sq_{VESS}$  approaches 4.0, it may be a warning sign that calls for a direct intervention with changes in management (Ball et al., 2007, 2017). In our case, high scores may be due to previous soil management in the studied area,



which had a history of excessive machinery traffic and disturbance (Dominschek et al., 2018; **Supplementary Figure S2**). Our results suggest that soil structure is recovering more



slowly in F, probably due to a lack of grasses in the F system, and because less water arrives on the soil surface due to interception from trees (**Supplementary Figure S1**). The  $Sq_{VESS}$  results obtained in C ( $Sq = 2.2$ ), CL ( $Sq = 2.4$ ), and CLF ( $Sq = 2.8$ ) are close to the results found by Demétrio et al., 2022 that indicate that no-tillage system and cattle trampling increase  $Sq_{VESS}$  when compared to native forest ( $Sq = 1.53$ ). For L, and LF,  $Sq_{VESS}$  were 2.5, and 2.7, respectively (**Table 1**), indicating that despite cattle trampling causing some negative alterations to soil structure, these IFS maintained adequate soil structural quality for plant development. According to Abdalla et al. (2018), the grass root system under low trampling pressure and rotational grazing is stimulated by compensatory growth due to herbivores, increasing new root growth and carbon input into the soil.

## 4.2 Soil Resistance to Soil Penetration Resistance in the Farming Systems

The highest mean value of PR was found in the F system (2.2 MPa), which corroborates with the  $Sq_{VESS}$  results. All integrated systems as well as C and L presented mean values of PR that are non-limiting for root plants. According to Morais et al. (2020) and Rosseti and Centurion (2017), PR values between

2.0 and 3.0 MPa do not cause a decrease in crop yield under no-tillage. Thus, our findings indicate that these farming systems preserve soil structural quality that is adequate for root development and yield. The efficiency of IFS in recovering soil structure has been reported by Polanía-Hincapié et al. (2021). Besides having found high PR values (3.8 MPa) in silvopasture farming system on a degraded Ferralsol, they observed soil structural improvements in comparison with its initial state. Similarly, Flávio Neto et al., 2015 reported that degraded soils can be recovered by pastures in IFS. We measured an increase in PR with soil depth. The increase was especially pronounced in the F system, which we attribute to the generally drier soil conditions (Supplementary Figure S1) and less heterogeneity of plant species cultivated. Consequently, roots are less exposed to ideal soil water conditions, affecting both plant growth and development as well as soil resilience.

### 4.3 Soil Organic Carbon

The SOC was  $\geq 39 \text{ g kg}^{-1}$  for all farming systems at the depth of 0–0.30 m. SOC  $> 20 \text{ g kg}^{-1}$  is considered very high for Paraná state, Brazil (Pauletti and Motta, 2019). According to Wiesmeier et al. (2019), climate is the major factor driving soil organic carbon storage at regional to global scales, while at regional or sub-regional scale, other factors such as vegetation, microorganisms/fauna, parent material, texture, and land-use and soil management play a role too. The experimental area is in a temperate summer climate (Cfb, second Köppen classification), the soil has a clayey texture, and management is pesticide free with minimum soil disturbance, and crop diversity is high in integrated farming systems. The combination of these factors likely results in enhanced soil organic carbon (Salton et al., 2014). Moreover, pesticide-free farming systems affect positively the biological functions of microorganisms and chemical processes (Meena et al., 2020). Data of SOC found in our study (Table 1) show that SOC has increased since the beginning of the experiment in 2013, where mean values did not surpass  $30 \text{ g kg}^{-1}$  at a depth of 0–0.20 m (Dominschek et al., 2018). Our data suggest that all farming systems studied, which include specific and conservative management practices, favored positively SOC content, with positive impacts on soil structural quality. No-tillage is considered a key practice for soil carbon sequestration, and for preventing structural and physical soil degradation (Calonego et al., 2017; Vizioli et al., 2021), and when adopted in IFS, no-tillage could minimize the risk of soil and environmental degradation (Ray et al., 2020).

### 4.4 Root Properties

Root length, root volume, and root dry matter are presented in Table 2, indicating that roots were concentrated in the surface layer (0–0.10 m). Although non-significant, root dry matter was higher in the CLF system, probably due to *Eucalyptus* root morphology, being thicker than grasses, and due to the combination of crop and livestock. The C and L systems had a greater volume of roots down to 0.20 m of depth, while F and the integrated systems had smaller amounts of roots at this depth. In the L farming system, there is an influence of cattle that stimulate regrowth and root growth as they feed (Bonetti et al., 2018), and deposit feces and urine, increasing

SOC and keeping the soil more biologically active. For C, the specific management with reduced machinery traffic and fertilization provides a suitable environment for root development, which was detected by the highest root length mean value, which was also the only root parameter that indicated significant differences between farming systems. Our data indicate good management strategy of all farming systems, considering the fact that root length can be related with soil hydraulic properties (Shi et al., 2021), contributing to better soil water storage capacity and water and gas fluxes capacity. Vanhees et al. (2021), studying maize roots in compacted and non-compacted soils, showed that the ability of roots to grow to depth through compacted soil is not dependent on the amount of roots but on the favorable conditions provided by biopores. The production of roots in cropping systems stimulates biological soil activity, which positively affects soil structure and soil physical quality (Gamboa et al., 2020). Fine roots of the grasses have been shown to provide improvements to soil hydraulic properties, aggregate stability, and soil porosity (Hao et al., 2020; Chen et al., 2021; Shi et al., 2021).

### 4.5 Relationships Between Soil Structure, Root Properties and Soil Organic Carbon

Root length, root volume, and SOC are linked to soil structural quality, as shown in Figure 2, as well as by Spearman correlations ( $r_s$ ). The negative relationship between soil structural quality and SOC has been reported by several authors (Pulido-Moncada et al., 2014; Tuchtenhagen et al., 2018; Cherubin et al., 2019; Mutuku et al., 2021). Likewise, positive correlation between  $Sq_{VESS}$  and PR have been reported (Castioni et al., 2018; Cherubin et al., 2019). Here, we demonstrate how soil structure, root growth and soil organic carbon are linked. Based on the regression models found in this study, root length and root volume were reduced by about 75% for  $Sq_{VESS} = 4$  and  $PR = 3 \text{ MPa}$ , compared with soil that had  $Sq_{VESS} = 1$  and  $PR = 0.5 \text{ MPa}$ . These results corroborate with critical values for root development indicated in the literature (Taylor et al., 1966; Ehlers et al., 1983; Bengough et al., 2011; Colombi et al., 2018). Values of  $Sq_{VESS} > 3.0$  indicate soil structural degradation, which require improvements of the current soil management practices.

Previous studies suggest that biopores are important as they can facilitate root growth (Cavalieri et al., 2009; Vanhees et al., 2021). A strong decrease in root length and volume under the highest PR values were found. This soils were associated with lower levels of soil organic carbon, evidencing the importance of carbon inputs from roots into the soil. Coblinski et al. (2019) studied the same experimental area, and showed that soil bulk density, porosity, soil water availability, as well SOC influence soil structural quality. According to Colombi et al. (2018), interactions between root architecture, plant water uptake, soil moisture, and soil penetration resistance are little studied. Our data of  $Sq_{VESS}$  and PR were obtained in moist soil, at a water content close to field capacity, but PR increases when soil dries, especially so in compacted soil, which reduces root development. Colombi et al. (2018) mention that water limiting crop yields may result from limiting water accessibility by roots (and not limited

water availability), which is largely caused by high soil penetration resistance that decreases root growth and ultimately crop productivity. We observed that the pesticide-free management along with adequate fertilizer use have provided sufficient root development for the species grown at our site. This is supported by the satisfactory yields in the different systems as shown by Kruchelski et al. (2021). Moreover, Dominschek et al. (2021) indicated that the management applied in the experimental area is an economically viable and efficient non-chemical strategy to manage weeds and produce grains. Forage yield and beef production also presented good results (Campos, 2019; Cavaliere-Polizeli et al., 2021).

A positive relationship between PR and VESS (Figure 3) was also observed in other studies (Cherubin et al., 2017; Castioni et al., 2018; Tuchtenhagen et al., 2018; Çelik et al., 2020). Soil structural quality is classified as firm for values of  $3.0 < \text{Sq}_{\text{VESS}} < 4.0$ , which corresponded to values of  $1.76 < \text{PR} < 2.40$  MPa (close to field capacity). However, PR is dependent on soil moisture, which can vary within days, weeks and seasons, and consequently, vary the conditions for root growth and development. However, critical PR values, such as more than 3.5 MPa, probably might be easily found, when soil remains dry for a considerable period. Ehlers et al. (1983) estimated that relative elongation rate of oats roots ceases at 4.9 MPa, which is very close to our finding (4.5 MPa) where root length was reduced by 75%. The strong correlation between VESS and PR suggests that VESS can be used to detect possible harmful conditions related to critical PR values for root growth.

The negative correlations between root properties and PR,  $\text{Sq}_{\text{VESS}}$ , and SOC, clearly show the importance of roots for soil structural quality. However, the results obtained in this study confirmed only partially the hypothesis that IFS promotes better soil structural quality compared to SFS. Management systems that favor improvement and conservation of soil physical properties are key for the environmental sustainability of agricultural production (Tuchtenhagen et al., 2018). Not all the studied integrated farming systems showed better performance for roots, for example, crop-forestry (CF) was less effective to stimulate root growth. Ray et al. (2020) pointed out that the adoption of IFS instead of SFS could enhance farm productivity, crop diversity, employment opportunity, and annual income for overall improvement of livelihood through efficient utilization of natural resources. However, the results for CF indicate that it is not enough just to integrate systems, but that the choice of crops and management have an influence on the success of such cropping strategies.

## 5 CONCLUSION

In general, both single farming systems (SFS) and integrated farming systems (IFS) presented adequate soil structural quality. The single Forestry system and integrated systems including forestry tended to have poorer soil structural quality and higher soil penetration resistance, but still adequate, which was associated with the generally drier soil conditions. Thus, our data could not support the hypothesis that integrated farming systems

promote soil structural quality. However, the similarity between SFS (C and L) and IFS in providing good soil structural quality is probably due to the specific conditions of the study (pesticide-free in combination with mineral fertilizers, and no-till using the planting green technique). We found strong relationships between scores of soil structural quality ( $\text{Sq}_{\text{VESS}}$ ), soil mechanical resistance (PR), SOC and root properties. Root length and volume were reduced by about 75% for  $\text{Sq}_{\text{VESS}} = 4$  and  $\text{PR} = 4$  MPa. These data demonstrate the positive feedbacks between soil structure, root growth and soil carbon input.

## DATA AVAILABILITY STATEMENT

The raw data supporting the conclusion of this article will be made available by the authors, without undue reservation.

## AUTHOR CONTRIBUTIONS

KC-P contributed to the conception, design of the study and wrote all sections of the manuscript. FM and KC-P organized the database, performed the statistical analysis, and wrote the first draft of the manuscript. CT wrote sections of the manuscript. AM contributed with experiment conception since the beginning, and read. KC-P, CT, and TK contributed to manuscript revision, read, and approved the submitted version.

## FUNDING

This study was financially supported by Coordination for Higher Education in Brazil (CAPES) with a scholarship to FM, and by the National Council for Scientific and Technological Development (Processo: Chamada Pública: 420140/2016-6 Universal 01/2016) through funding research to AM.

## ACKNOWLEDGMENTS

The authors thank all graduate and undergraduate students involved in the experiment during the years, taking care of animals, plants, and soils.

## SUPPLEMENTARY MATERIAL

The Supplementary Material for this article can be found online at: <https://www.frontiersin.org/articles/10.3389/fenvs.2022.901302/full#supplementary-material>

**Supplementary Figure S1** | Monthly mean rainfall and temperature for the study period.

**Supplementary Figure S2** | Experimental area in 2011, one year before initiation of experiments, with signs of degradation. Arrows: **red** indicate soil loss by erosion, **yellow** indicate intensive traffic, and **black** indicate soil covering by plants, some signs of soil degradation. Image from Google Earth.

## REFERENCES

- Abdalla, M., Hastings, A., Chadwick, D. R., Jones, D. L., Evans, C. D., Jones, M. B., et al. (2018). Critical Review of the Impacts of Grazing Intensity on Soil Organic Carbon Storage and Other Soil Quality Indicators in Extensively Managed Grasslands. *Agric. Ecosyst. Environ.* 253, 62–81. doi:10.1016/j.agee.2017.10.023
- Alvares, C. A., Stape, J. L., sentelhas, P. C., de Moraes Gonçalves, J. L., and Sparovek, G. (2013). Köppen's Climate Classification Map for Brazil. *Meteorol. Z.* 22 (6), 711–728. doi:10.1127/0941-2948/2013/0507
- Ball, B. C., Batey, T., and Munkholm, L. J. (2007). Field Assessment of Soil Structural Quality - a Development of the Peerkamp Test. *Soil Use Manag.* 23 (4), 329–337. doi:10.1111/j.1475-2743.2007.00102.x
- Ball, B. C., Guimarães, R. M. L., Cloy, J. M., Hargreaves, P. R., Shepherd, T. G., and McKenzie, B. M. (2017). Visual Soil Evaluation: a Summary of Some Applications and Potential Developments for Agriculture. *Soil Tillage Res.* 173, 114–124. doi:10.1016/j.still.2016.07.006
- Bendahan, A. B., Pocard-Chapuis, R., De Medeiros, R. D., Costa, N. L., and Tourrand, J. F. (2018). Management and Labour in an Integrated Crop-Livestock-Forestry System in Roraima, Brazilian Amazonia. *Cah. Agric.* 27. doi:10.1051/cagri/2018014
- Bengough, A. G., McKenzie, B. M., Hallett, P. D., and Valentine, T. A. (2011). Root Elongation, Water Stress, and Mechanical Impedance: a Review of Limiting Stresses and Beneficial Root Tip Traits. *J. Exp. Bot.* 62, 59–68. doi:10.1093/jxb/erq350
- Bonetti, J. d. A., Paulino, H. B., Souza, E. D. d., Carneiro, M. A. C., and Caetano, J. O. (2018). Soil Physical and Biological Properties in an Integrated Crop-Livestock System in the Brazilian Cerrado. *Pesq. Agropec. Bras.* 53 (1), 1239–1247. doi:10.1590/S0100-204X2018001100006
- Bonetti, J. d. A., Paulino, H. B., Souza, E. D. d., Carneiro, M. A. C., and Silva, G. N. d. (2015). Influência Do sistema integrado de produção agropecuária no solo e na produtividade de soja e braquiária. *Pesqui. Agropecu. Trop.* 45, 104–112. doi:10.1590/1983-40632015v45n2p625
- Box, G. E. P., and Cox, D. R. (1964). An Analysis of Transformations. *J. R. Stat. Soc. Ser. B Methodol.* 26, 211–252. doi:10.1111/j.2517-6161.1964.tb00544.x
- Brasil (2000). Decreto estadual No 2200, 12DE junho de 2000. Regulamento ao zoneamento ecológico-econômico da área de proteção ambiental do irai. Curitiba: PR.
- Brooker, R. W., George, T. S., Homulle, Z., Karley, A. J., Newton, A. C., Pakeman, R. J., et al. (2021). Facilitation and Biodiversity-Ecosystem Function Relationships in Crop Production Systems and Their Role in Sustainable Farming. *J. Ecol.* 109, 2054–2067. doi:10.1111/1365-2745.13592
- Calonego, J. C., Raphael, J. P. A., Rigon, J. P. G., Oliveira Neto, L. d., and Rosolem, C. A. (2017). Soil Compaction Management and Soybean Yields with Cover Crops under No-Till and Occasional Chiseling. *Eur. J. Agron.* 85, 31–37. doi:10.1016/j.eja.2017.02.001
- Campos (2019). *Produção de bovinos de corte, características de pasto e comportamento ingestivo em sistemas integrados de produção agropecuária*. Brazil: Thesis, Curitiba, PR.
- Carvalho, P. C. d. F., Peterson, C. A., Nunes, P. A. d. A., Martins, A. P., de Souza Filho, W., Bertolazi, V. T., et al. (2018). Animal Production and Soil Characteristics from Integrated Crop-Livestock Systems: toward Sustainable Intensification. *J. animal Sci.* 96 (8), 3513–3525. doi:10.1093/jas/sky085
- Castioni, G. A., Cherubin, M. R., Menandro, I. M. S., Sanches, G. M., Bordonal, R. d. O., Barbosa, I. C., et al. (2018). Soil Physical Quality Response to Sugarcane Straw Removal in Brazil: a Multi-Approach Assessment. *Soil Tillage Res.* 184, 301–309. doi:10.1016/j.still.2018.08.007
- Cavaleri, K. M. V., da Silva, a. P., Tormena, C. A., Leão, T. P., Dexter, A. R., and Håkansson, I. (2009). Long-term Effects of No-Tillage on Dynamic Soil Physical Properties in a Rhodic Ferrasol in Paraná, Brazil. *Soil Tillage Res.* 103 (1), 158–164. doi:10.1016/j.still.2008.10.014
- Cavaleri-Polizeli, K. M. V., Calábria, Z. K. P., Keller, T., Dominczeski, R. L., Kruchelski, S., Campos, B. M., et al. (2021). "Pesticide-free Farming Systems: Effects on Soil Quality and Yield," in *Proceedings in Eurosoil 2021*.
- Çelik, I., Günel, H., Acar, M., Acir, N., Bereket-Barut, Z., and Budak, M. (2020). Evaluating the Long-term Effects of Tillage Systems on Soil Structural Quality Using Visual Assessment and Classical Methods. *Soil Use Manag.* 36 (2), 223–239. doi:10.1111/sum.12554
- Chen, J., Wu, Z., Zhao, T., Yang, H., Long, Q., and He, Y. (2021). Rotation Crop Root Performance and its Effect on Soil Hydraulic Properties in a Clayey Ustisol. *Soil Tillage Res.* 213, 105136. doi:10.1016/j.still.2021.105136
- Cherubin, M. R., Chavarro-Bermeo, J. P., and Silva-Olaya, A. M. (2019). Agroforestry Systems Improve Soil Physical Quality in Northwestern Colombian Amazon. *Agroforest Syst.* 93, 1741–1753. doi:10.1007/s10457-018-0282-y
- Cherubin, M. R., Franco, A. L. C., Guimarães, R. M. L., Tormena, C. A., Cerri, C. E. P., Karlen, D. L., et al. (2017). Assessing Soil Structural Quality under Brazilian Sugarcane Expansion Areas Using Visual Evaluation of Soil Structure (VESS). *Soil Tillage Res.* 173, 64–74. doi:10.1016/j.still.2016.05.004
- Coblinski, J. A., Favaretto, N., Goularte, G. D., Dieckow, J., Moraes, A. d., and Souza, L. C. d. P. (2019). Water, Soil and Nutrients Losses by Runoff at Hillslope Scale in Agricultural and Pasture Production in Southern Brazil. *Jas* 11 (6), 160. doi:10.5539/jas.v11n6p160
- Colombi, T., Torres, L. C., Walter, A., and Keller, T. (2018). Feedbacks between Soil Penetration Resistance, Root Architecture and Water Uptake Limit Water Accessibility and Crop Growth - A Vicious Circle. *Sci. Total Environ.* 626, 1026–1035. doi:10.1016/j.scitotenv.2018.01.129
- de Moraes, A., Carvalho, P. C. d. F., Anghinoni, I., Lústosa, S. B. C., Costa, S. E. V. G. d. A., and Kunrath, T. R. (2014). Integrated Crop-Livestock Systems in the Brazilian Subtropics. *Eur. J. Agron.* 57, 4–9. doi:10.1016/j.eja.2013.10.004
- Demétrio, W., Cavaleri-Polizeli, K. M. V., Guimarães, R. M. L., Ferreira, S. A., Parron, L. M., and Brown, G. G. (2022). Macrofauna Communities and Their Relationship with Soil Structural Quality in Different Land Use Systems. *Soil Res.* SR21157. doi:10.1071/SR21157
- Derpsch, R., Friedrich, T., Kassam, A., and Li, H. W. (2010). Current Status of Adoption of No-Till Farming in the World and Some of its Main Benefits. *Int. J. Agric. Biol. Eng.* 3, 1. doi:10.3965/j.issn.1934-6344.2010.01.001-025
- Derpsch, R. 2021. No-Tillage, Sustainable Agriculture in the New Millennium. Available at: <http://www.roCf-derpsch.com/en/no-till/> (Access november 22 2021).
- Dominczek, R., Barroso, A. A. M., Lang, C. R., de Moraes, A., Sulc, R. M., and Schuster, M. Z. (2021). Crop Rotations with Temporary Grassland Shifts Weed Patterns and Allows Herbicide-free Management without Crop Yield Loss. *J. Clean. Prod.* 306, 127140. doi:10.1016/j.jclepro.2021.127140
- Dominczek, R., Kruchelski, S., Deiss, L., Portugal, R., Denardin, L. G., Martins, A., et al. (2018). Sistemas integrados de produção agropecuária na promoção da intensificação sustentável. Available at: [www.aliancasipa.org/wp-content/uploads/2018/12/Boletim-NITA.pdf](http://www.aliancasipa.org/wp-content/uploads/2018/12/Boletim-NITA.pdf).
- Duiker, S. W., Myers, J. C., and Blasure, L. C. (2017). "Soil Health in Field and Forage Crop Production," in *Department of Agriculture, Natural Resources Conservation Service. Penn State Cooperative Extension* (Washington, D.C., United States. Available at: <https://extension.psu.edu/soil-health-in-field-and-forage-crop-production>.
- Ehlers, W., Kopke, U., Hesse, F., and Bohm, W. (1983). Penetration Resistance and Root Growth of Oats in Tilled and Untilled Loess Soil. *Soil Tillage Res.* 3, 261–275. doi:10.1016/0167-1987(83)90027-2
- EMBRAPA (2018). Sistema brasileiro de classificação de solos. Brasília: Embrapa Solos. Available at: [www.embrapa.br/busca-de-publicacoes/-/publicacao/1107206/sistema-brasileiro-de-classificacao-de-solos](http://www.embrapa.br/busca-de-publicacoes/-/publicacao/1107206/sistema-brasileiro-de-classificacao-de-solos).
- FEBRAPDP (2021). O Que É Sistema Plantio Direto? Available at: [febrapdp.org.br/sistema-plantio-direto-o-que-e](http://febrapdp.org.br/sistema-plantio-direto-o-que-e). (Access novembro 22, 2021).
- Flávio Neto, J., Severiano, E. D. C., Costa, K. A. D. P., Junnyor, W. S. G., Gonçalves, W. G., and Andrade, R. (2015). Biological Soil Loosening by Grasses from Genus *Brachiaria* in Crop-Livestock Integration. *Acta Sci. Agron.* 37 (3), 375–383. doi:10.4025/actasciagron.v37i3.19392
- Franco, H. H. S., Guimarães, R. M. L., Tormena, C. A., Cherubin, M. R., and Favilla, H. S. (2019). Global Applications of the Visual Evaluation of Soil Structure Method: A Systematic Review and Meta-Analysis. *Soil Tillage Res.* 190, 61–69. doi:10.1016/j.still.2019.01.002
- Gamboa, C. H., Vezzani, F. M., Kaschuk, G., Favaretto, N., Cobos, J. Y. G., and Da Costa, G. A. (2020). Soil-root Dynamics in Maize-Beans-Eggplant Intercropping System under Organic Management in a Subtropical Region. *J. Soil Sci. Plant Nutr.* 20 (3), 1480–1490. doi:10.1007/s42729-020-00227-9
- Gee, G. W., and Or, D. (2002). "Bulk Density and Linear Extensibility," in *Methods of Soil Analysis*. Editors J. H. Dane and G. C. Topp (Madison: Soil Science Society of America), 201–227.

- Guimarães, R. M. L., Ball, B. C., and Tormena, C. A. (2011). Improvements in the Visual Evaluation of Soil Structure. *Soil Use Manag.* 27 (3), 395–403. doi:10.1111/j.1475-2743.2011.00354.x
- Guimarães, R. M. L., Lamandé, M., Munkholm, L. J., Ball, B. C., and Keller, T. (2017). Opportunities and Future Directions for Visual Soil Evaluation Methods in Soil Structure Research. *Soil Tillage Res.* 173, 104–113. doi:10.1016/j.still.2017.01.016
- Hao, H.-x., Wei, Y.-j., Cao, D.-n., Guo, Z.-l., and Shi, Z.-h. (2020). Vegetation Restoration and Fine Roots Promote Soil Infiltrability in Heavy-Textured Soils. *Soil Tillage Res.* 198, 104542. doi:10.1016/j.still.2019.104542
- Kassam, A., Derpsch, R., Derpsch, R., and Friedrich, T. (2020). Development of Conservation Agriculture Systems Globally. *Adv. Conservation Agric.* 1, 31–86. doi:10.19103/AS.2019.0048.02
- Keesstra, S. D., Bouma, J., Wallinga, J., Tittonell, P., Smith, P., Cerdà, A., et al. (2016). The Significance of Soils and Soil Science towards Realization of the United Nations Sustainable Development Goals. *Soil* 2, 111–128. doi:10.5194/soil-2-111-2016
- Kruchelski, S., Trauttmüller, J. W., Deiss, L., Trevisan, R., Cubbage, F., Porfirio-da-Silva, V., et al. (2021). Eucalyptus benthamii Maiden et Cambage growth and wood density in integrated crop-livestock systems. *Agroforest Syst.* 95, 1577–1588. doi:10.1007/s10457-021-00672-0
- Madani, E. M., Jansson, P. E., and Babelon, I. (2018). Differences in Water Balance between Grassland and Forest Watersheds Using Long-Term Data, Derived Using the CoupModel. *Hydrol. Res.* 49, 72–89. doi:10.2166/nh.2017.154
- Meena, R., Kumar, S., Datta, R., Lal, R., Vijayakumar, V., Brtnicky, M., et al. (2020). Impact of Agrochemicals on Soil Microbiota and Management: A Review. *Land* 9, 34. doi:10.3390/land9020034
- Moraes, M. T. d., and Gusmão, A. G. (2021). How Do Water, Compaction and Heat Stresses Affect Soybean Root Elongation? A Review. *Rhizosphere* 19, 100403. doi:10.1016/j.rhisph.2021.100403
- Morais, M. C., Siqueira-Neto, M., Guerra, H. P., Satiro, L. S., Soltangheisi, A., Cerri, C. E. P., et al. (2020). Trade-Offs between Sugarcane Straw Removal and Soil Organic Matter in Brazil. *Sustainability* 12 (22), 9363. doi:10.3390/su12229363
- Mutuku, E. A., Vanlauwe, B., Roobroeck, D., Boeckx, P., and Cornelis, W. M. (2021). Visual Soil Examination and Evaluation in the Sub-humid and Semi-arid Regions of Kenya. *Soil Tillage Res.* 213, 105135. doi:10.1016/j.still.2021.105135
- Paiva, I. A. d., Rita, Y. L., and Cavaliéri-Polizeli, K. M. (2020). Knowledge and Use of Visual Soil Structure Assessment Methods in Brazil - A Survey. *Soil Tillage Res.* 204, 104704. doi:10.1016/j.still.2020.104704
- Pauletti, V., and Motta, A. C. V. (2019). *Manual de Adubação e Calagem para o Estado do Paraná*. 2.ed. Curitiba: NEPAR-SBSC.
- Polanía-Hincapié, K. L., Olaya-Montes, A., Cherubin, M. R., Herrera-Valencia, W., Ortiz-Moreno, F. A., and Silva-Olaya, A. M. (2021). Soil Physical Quality Responses to Silvopastoral Implementation in Colombian Amazon. *Geoderma* 386, 114900. doi:10.1016/j.geoderma.2020.114900
- Popova, L., Van Dusschoten, D., nagel, K. A., Fiorani, F., and Mazzolai, B. (2016). Plant Root Tortuosity: an Indicator of Root Path Formation in Soil with Different Composition and Density. *Ann. Bot.* 118 (4), 685–698. doi:10.1093/aob/mcw057
- Pulido Moncada, M., Gabriels, D., Lobo, D., Rey, J. C., and Cornelis, W. M. (2014). Visual Field Assessment of Soil Structural Quality in Tropical Soils. *Soil Tillage Res.* 139, 8–18. doi:10.1016/j.still.2014.01.002
- Quaggio, J. A., and van Raij, B. (1979). Comparação de métodos rápidos para a determinação da matéria orgânica em solos. *R. Bras. Ci. Solo* 3, 184–187.
- Rahman, S. A., Jacobsen, J. B., Healey, J. R., Roshetko, J. M., and Sunderland, T. (2017). Finding Alternatives to Swidden Agriculture: Does Agroforestry Improve Livelihood Options and Reduce Pressure on Existing Forest? *Agroforest Syst.* 91 (1), 185–199. doi:10.1007/s10457-016-9912-4
- Ratuchne, L. C., Koehler, H. S., Koehler, H. S., Sanquetta, C. R., and Schamne, P. A. (2017). Comparison of Sampling Methods for the Evaluation of the Root System of Sugarcane. *Rev. Ciencias Agrícolas* 34 (1), 7–16. doi:10.22267/rcia.173401.59
- Ray, S. K., Chatterjee, D., Rajkhowa, D. J., Baishya, S. K., Hazarika, S., and Paul, S. (2020). Effects of Integrated Farming System and Rainwater Harvesting on Livelihood Improvement in North-Eastern Region of India Compared to Traditional Shifting Cultivation: Evidence from an Action Research. *Agroforest Syst.* 94, 451–464. doi:10.1007/s10457-019-00406-3
- Rossetti, K. V., and Centurion, J. F. (2017). Least Limiting Water Range in Oxisols under Different Levels of Machine Traffic. *Commun. Sci.* 8 (2), 337–346. doi:10.14295/cs.v8i2.2423
- Salton, J. C., Mercante, F. M., Tomazi, M., Zanatta, J. A., Concenço, G., Silva, W. M., et al. (2014). Integrated Crop-Livestock System in Tropical Brazil: Toward a Sustainable Production System. *Agric. Ecosyst. Environ.* 190, 70–79. doi:10.1016/j.agee.2013.09.023
- Schut, A. G. T., Cooledge, E. C., Moraine, M., van de Ven, G. W. J., Jones, D. L., and Chadwick, D. R. (2021). Reintegration of Crop-Livestock Systems in Europe: An Overview. *Front. Agr. Sci. Eng.* 8 (1), 111–129. doi:10.15302/j-fase-2020373
- Sharma, P. K., Dwivedi, S., Arora, R. K., Bhagat, V., Kour, C., and Sharma, M. (2019). Efficiency under Integrated Farming Systems – A Review. *Agro Econ. - Int. J.* 6 (2), 47–52. doi:10.30954/2394-8159.02.2019.1
- Shi, X., Qin, T., Yan, D., Tian, F., and Wang, H. (2021). A Meta-Analysis on Effects of Root Development on Soil Hydraulic Properties. *Geoderma* 403, 115363. doi:10.1016/j.geoderma.2021.115363
- SIDRA/IBGE (2021). Instituto Brasileiro de Geografia e Estatística. *Censo Agropecuário 2017 result. Defin. - Rio J.* 8, 1–105. Available at: sidra.ibge.gov.br/Tabela/6856#resultado (Access November 22th, 2021).
- Soni, R. P., Katoch, M., Katoch, M., and Ladolia, R. (2014). Integrated Farming Systems - A Review. *Iosrjavs* 7 (10), 36–42. doi:10.9790/2380-071013642
- Taylor, H. M., Roberson, G. M., and Parker, J. J., Jr. (1966). Soil Strength-Root Penetration Relations for Medium- to Coarse-Textured Soil Materials. *Soil Sci.* 102, 18–22. doi:10.1097/00010694-196607000-00002
- Team, R. Core (2020). *R: A Language and Environment for Statistical Computing*. Tormena, C. A., Karlen, D. L., Logsdon, S., and Cherubin, M. R. (2016). Visual Soil Structure Effects of Tillage and Corn Stover Harvest in Iowa. *Soil Sci. Soc. Am. J.* 80 (3), 720–726. doi:10.2136/sssaj2015.12.0425
- Tuchenhagen, I. K., Lima, C. L. R. d., Bamberg, A. L., Guimarães, R. M. L., and Mansonia, P.-M. (2018). Visual Evaluation of the Soil Structure under Different Management Systems in Lowlands in Southern Brazil. *Rev. Bras. Ciênc. Solo* 42, e0170270. doi:10.1590/18069657rbcs20170270
- Valani, G. P., Martini, A. F., Silva, L. F. S., Bovi, R. C., and Cooper, M. (2020). Soil Quality Assessments in Integrated Crop-Livestock-Forest Systems: A Review. *Soil Use Manage* 37, 22–36. doi:10.1111/sum.12667
- Vanhees, D. J., Loades, K. W., Bengough, A. G., Mooney, S. J., and Lynch, J. P. (2021). The Ability of Maize Roots to Grow through Compacted Soil Is Not Dependent on the Amount of Roots Formed. *Field Crops Res.* 264, 108013. doi:10.1016/j.fcr.2020.108013
- Vizioli, B., Cavaliéri-Polizeli, K. M. V., Tormena, C. A., and Barth, G. (2021). Effects of Long-Term Tillage Systems on Soil Physical Quality and Crop Yield in a Brazilian Ferralsol. *Soil Tillage Res.* 209, 104935. doi:10.1016/j.still.2021.104935
- Wiesmeier, M., Urbanski, L., hobley, E., Lang, B., von Lützw, M., Marin-Spiotta, E., et al. (2019). Soil Organic Carbon Storage as a Key Function of Soils - A Review of Drivers and Indicators at Various Scales. *Geoderma* 333, 149–162. doi:10.1016/j.geoderma.2018.07.026

**Conflict of Interest:** The authors declare that the research was conducted in the absence of any commercial or financial relationships that could be construed as a potential conflict of interest.

**Publisher's Note:** All claims expressed in this article are solely those of the authors and do not necessarily represent those of their affiliated organizations, or those of the publisher, the editors and the reviewers. Any product that may be evaluated in this article, or claim that may be made by its manufacturer, is not guaranteed or endorsed by the publisher.

Copyright © 2022 Cavaliéri-Polizeli, Marcolino, Tormena, Keller and Moraes. This is an open-access article distributed under the terms of the Creative Commons Attribution License (CC BY). The use, distribution or reproduction in other forums is permitted, provided the original author(s) and the copyright owner(s) are credited and that the original publication in this journal is cited, in accordance with accepted academic practice. No use, distribution or reproduction is permitted which does not comply with these terms.



## OPEN ACCESS

EDITED BY  
Fabio Masi,  
IRIDRA Srl, Italy

REVIEWED BY  
Calogero Schillaci,  
Joint Research Centre, Italy

\*CORRESPONDENCE  
Lucy Crockford,  
lcrockford@harper-adams.ac.uk

SPECIALTY SECTION  
This article was submitted to Soil  
Processes,  
a section of the journal  
Frontiers in Environmental Science

RECEIVED 23 June 2022  
ACCEPTED 15 September 2022  
PUBLISHED 31 October 2022

CITATION  
Crockford L (2022), Achieving cleaner  
water for UN sustainable development  
goal 6 with natural processes:  
Challenges and the future.  
*Front. Environ. Sci.* 10:976687.  
doi: 10.3389/fenvs.2022.976687

COPYRIGHT  
© 2022 Crockford. This is an open-  
access article distributed under the  
terms of the [Creative Commons  
Attribution License \(CC BY\)](#). The use,  
distribution or reproduction in other  
forums is permitted, provided the  
original author(s) and the copyright  
owner(s) are credited and that the  
original publication in this journal is  
cited, in accordance with accepted  
academic practice. No use, distribution  
or reproduction is permitted which does  
not comply with these terms.

# Achieving cleaner water for UN sustainable development goal 6 with natural processes: Challenges and the future

Lucy Crockford\*

Agriculture and Environment Department, Soil and Water Management Centre, Harper Adams University, Newport, Shropshire, United Kingdom

UN Sustainable Development Goal 6 aims to achieve clean water for all. Access to clean water is a basic human right but can be costly and challenging. Using natural processes to provide cleaner water for treatment is a cost effective, and often beneficial to other ecosystem services, method. Unfortunately, there are a number of barriers to the implementation of natural processes for cleaner water such as the difficulty of funding these nature-based solutions which is linked to the requirement of accurate valuation. Once funded, partnership with land practitioners is important to ensure that detrimental impacts are not experienced elsewhere and to ensure that these natural processes such as ponds and constructed wetlands are maintained and managed appropriately. The future in the United Kingdom and Europe, in general, is optimistic despite the large funding gap for nature-based solutions overall. Green finance, essentially a loan or investment to support environmentally-friendly activities, has been developed to funnel money towards sustainable investments with an environmental focus, and the percentage of world wealth spent on such investments has increased.

## KEYWORDS

sustainability, water, nature-based, partnership, ecosystems

## 1 Introduction

Achieving the UN Sustainable Development Goals (SDGs) by 2030 requires adoption by various stakeholders and as such now underpins much activity in industry (e.g., Zimon et al., 2020), special interest groups (e.g., Delabre et al., 2020), government (e.g., Musekiwa and Mandiyanike, 2017), and educational institutions (Giangrande et al., 2019) across the world. In response to this challenge, the 4-yearly conference EUROSoil was convened online in August 2021 with sessions covering a wide base of topics developed around each UN SDG. This article is contained in a special issue of the output of the topic “Sustainable Management of Soil Functions as a Basis to Avoid, Halt, and Reverse Land Degradation” and contains the primary perspectives relating to the theme of UN SDG 6 which aims to achieve clean water and sanitation for all (UN, 2022). Water has always been paramount to civilization with settlements in early humanity focused on either coastal areas or where

access to clean water was possible such as rivers and lakes. Estuaries with their access to clean freshwater and transport links *via* seas and oceans still harbor a number of the most influential cities across the world. Indeed, water could be thought of as the bloodstream of the natural world (Moss, 2018), providing hydration, nutrients, connection, waste management and income for those with access to substantial resources. Clean water therefore means different things to different people and we see a large disparity between the needs of clean water and sanitation in developing countries in contrast with those in developed.

Provision of safe and affordable drinking water for all is the first and probably the most basic target humanity faces. There have been some gains in this area with the proportion of people with access to clean and safe drinking water rising from 81% in 2000 to 89% in 2015 (UN, 2018). However, this still leaves 844 million people without access to basic water services and 2.1 billion people who live without clean water on their premises which is accessible and free from contamination (UN, 2018). Furthermore, the UN SDG 6 aims to provide access to sanitation and good hygiene, specifically removing the practice of open defecation. In 2015, 4.5 billion people lacked a safely managed sanitation system; where there may be a sanitation system in place but it is below the standard to ensure good hygiene and prevention of health problems (UN, 2018). Climate change adds a further pressure to these absent or poorly functioning systems, the consequences of such rather impactfully shown in the Oscar winning film “Parasite.”

While water provision in developed countries is relatively well monitored, along with developing countries, maintaining (or improving) the quality of the water continues to be challenging (Brockwell et al., 2021). The loss of pristine sites due to emerging pollutants such as new pesticides and biocides (Cheng et al., 2021), pervasive invasive species disrupting the balance of these fragile ecosystems (Mooney and Cleland, 2001), loss of soil from land increasing turbidity (Sherriff et al., 2015), along with an increased frequency of extreme low flows exacerbating any water treatment failures (Shore et al., 2017) is a concerning and difficult challenge to manage and address. The final three objectives of UN SDG 6 relate to water quality and the protection and restoration of the ecosystems that rely on it. These final objectives presume that the original objectives of clean water and sanitation have been achieved and focus largely on the ecology of water bodies. Importantly, the SDG identifies an integrated approach to water management as a key objective and thus forms the basis of this perspectives paper. An integrated approach requires a contribution from all stakeholders to maximize the natural processes that lead to cleaner water, yet various barriers remain, preventing the success in achieving this SDG. Therefore, this article presents some perspectives on economical, social and behavioral barriers with consideration on how they may be overcome.

## 2 Natural processes for cleaner water

The long-standing challenges of addressing the pollution from point and diffuse sources have been the focus of many research articles and commentary (e.g., Albek, 2003; Dai, 2014; Grimvall and Stålnacke, 1996; Jarvie et al., 2010; Zinabu et al., 2018; and Wells et al., 2020). Both sources have their characteristics and methods of management and yet our pollution problems continue and the objectives of the Water Framework Directive (WFD) in the EU and national objectives in other countries have not been met in their entirety, receiving some criticism. For example, Bouleau and Pont (2015) identified challenges around nomenclature and ecological objectives of the WFD while Huesker and Moss (2015) identified the complexities caused by different strategies by different stakeholders across scales. The criticism of the WFD has largely been levelled at the inconsistency of application (Bouleau and Pont, 2015) along with the divergent activities of different interested parties with their own interests (Huesker and Moss, 2015). In recent times we have had the added challenge of emerging pollutants such as new (and existing) pesticides (De Castro-Catala et al., 2015) and micro (and macro) plastics (van Emmerik and Schwarz, 2020). No longer are water managers concerned solely with eutrophication of natural waters but also how to remove pollutants that are hazardous to human health such as metaldehyde, which are costly and require a variety of approaches (Rolph et al., 2019).

Loss of soil from land yields numerous water quality challenges from increased turbidity to increases in particulate and dissolved pollutants (heavy metals, POPs *etc.*) and nutrients. Natural processes that address these challenges and lead to cleaner water are not a new concept, neither is this article the first time that they have been championed, e.g., Beierkuhnlein (2021) and Bredemeier (2011), but what is clear is that for these processes to have an impact they need to be implemented across a landscape and be supported both technically and financially. The realized success of installed measures is also dependent on the quality of the influent water which is controlled by land management techniques upstream. The processes themselves can be relatively small and inexpensive, to include swales, trenches and drains that hold water for periods of time (alleviating flooding in some cases). Or they can be large such as ponds which have a higher processing power, or more engineered such as constructed wetlands with advanced water treatment the main objective. Controlling water flow, retaining water and allowing settlement contributes to the removal of particulate pollutants (Johannesson et al., 2011) and further reduces the opportunity of legacy impacts in the future (Jarvie et al., 2014).

The treatment of dissolved pollutants requires a more complex approach than simply settlement. For example, riparian zones may be used to process the nitrate rich groundwaters by allowing plant uptake and the anaerobic conversion to N<sub>2</sub> gas (Ranalli and Macalady, 2010). Therefore,

it is not sufficient to install a water feature without also considering how different pollutants will be removed and importantly how these changes may be measured. In a small study located along a stretch of installed leaky debris dams, dissolved nutrients were found to be unaffected by the installed measures although, encouragingly, there was some accumulation of particulate pollutants (Crockford, L. 2020, anecdotal observation). Therefore, these measures should be considered along a continuum of water management across the catchment requiring planning and collaborative activities between stakeholders. The increase in frequency of a catchment-based approach to landscape management with Catchment Sensitive Farming in the United Kingdom (CaBA, 2022a) and Water Co-Governance in the EU (CaBA, 2022b) has led to varying success of addressing deteriorating water quality due to numerous challenges. While this perspective paper focuses largely on the United Kingdom and EU going forward, the obstacles this continent is facing is replicated worldwide to varying degrees.

## 3 The challenges

### 3.1 Valuation of natural processes

A continuing challenge across the United Kingdom, the EU and further afield is providing a valuation of these processes that provide cleaner water (Eric et al., 2022). Not only are the overt processes requiring valuation but general land management techniques that reduce water losses and soil movement such as no-till farming, contour farming and improving soil structure require recognition of the time, labour, and energy savings that they provide. The simple change from arable and pasture farming into agro-forestry can have impressive changes to water retention (Vaughan, 2019). Trees intercept and evaporate a significant proportion of rainfall, and as root depth increases soil structure improves, infiltration rates increase and overland flow decreases, so that surface runoff from up slopes can be captured, infiltrated and potentially treated. A small study across four land uses (arable, pasture, 1960 woodland, and 2010 woodland) investigated not only the change of land use to forestry but the longitudinal changes observed as the forest matures (Vaughan, 2019), which should be reflected in their value (Bredemeier, 2011). Consistently higher volumes of water were infiltrated in the woodlands with the slightly older woodland showing better water drainage than the younger. While initial drainage in the arable land use was high, it quickly reduced showing how soil wetting changes over time in relation to soil management (Vaughan, 2019).

The value of wetlands in the landscape continues to be explored with meta-analysis by Eric et al. (2022) showing that the existing income level of a country influences the level of provisioning and regulating of that ecosystem service, i.e., the existing wealth of a country determines whether the wetlands are

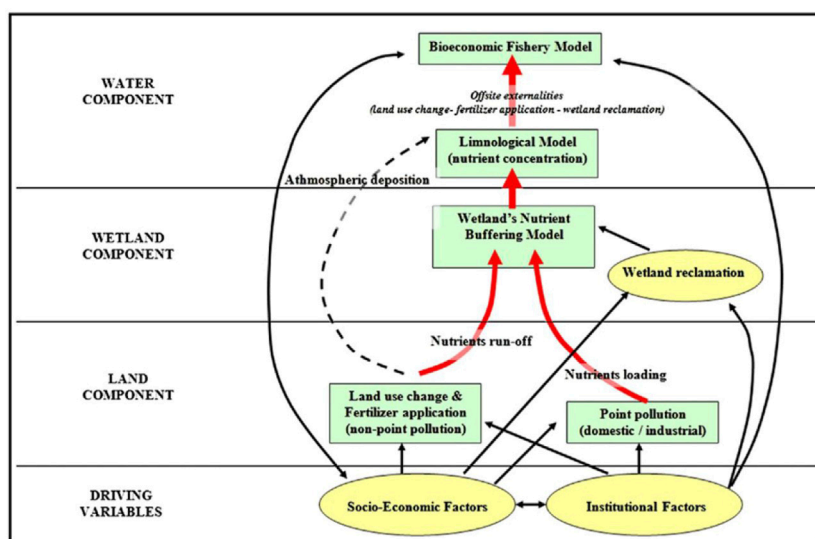
protected and thus improving their ecosystem service. Additionally, the agricultural total factor productivity index (how efficient the farming systems are) had a positive influence on the regulating value of wetlands while negatively influencing the provisioning, which was the converse to that expected (Eric et al., 2022). There was a suggestion that the income level of the country may have affected the results where there was a large proportion of high-income countries in the regulating model compared to provisioning. This in itself shows that ecosystem services vary across income thresholds and provides another complexity to the valuation of these processes. Measures of wetlands' contribution to water quality improvement may also be measured abstractly by, for example, the improvement in fishing of downstream water bodies (Simonić and Perrings, 2011), increasing the disconnection between the process and required outcome. Figure 1 shows the various levels and components of such a model.

### 3.2 Funding changing behaviors

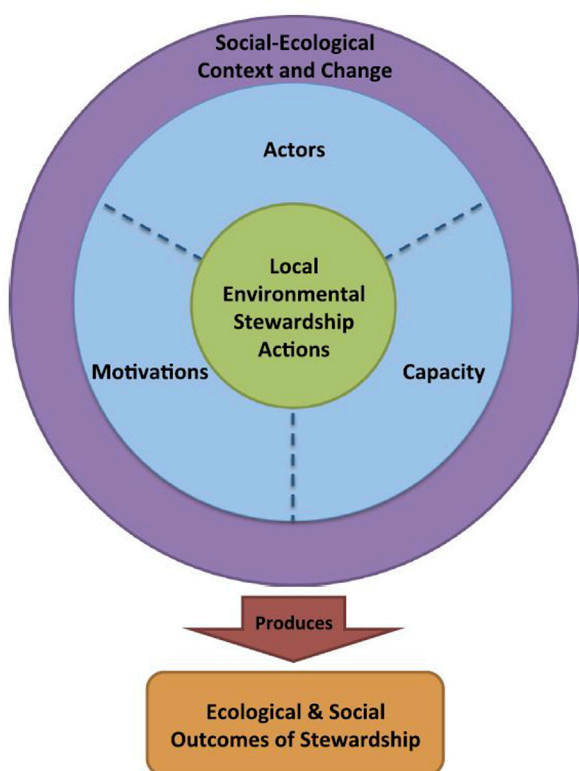
The Common Agricultural Policy provided income to farmers ensuring that the EU had a secure source of food (EC, 2022). As the impact of intensive farming resulted in reduced water quality there were many measures implemented to encourage farmers to reduce their nutrient losses from land, such as the Higher Level Stewardships in the United Kingdom. Many of these schemes received criticism (e.g., Hole, 2015) and as financial resources tighten, in the United Kingdom at least, there has been a shift from the “carrot approach,” i.e., funding farmers to farm more environmentally friendly (sometimes with poor results e.g., Brambilla and Pedrini, 2013) to the “stick approach” where legislation requires farmers to farm with lower impacts but providing no funding for lost earnings. As Figure 2 shows, stewardship has many facets, not just funding, to be considered for it to be a success (Bennett et al., 2018). The fact remains though, with real valuation of a more sustainable farming approach, there is the opportunity to appropriately quantify the value of these natural processes and ultimately their improvement on water quality (and water retention). Numerous pilot schemes on farms have been used to provide these much-needed figures to provide confidence in more sustainable farming techniques. Indeed, the planning process in the United Kingdom now requires developers to consider the biodiversity net gain of their plans (DEFRA, 2019) opening the opportunity for funding of sustainable farming and integrated water management techniques.

### 3.3 Land ownership and security

While valuing these natural processes is important, appropriate land management and advisory of such is



**FIGURE 1**  
Logical framework of a valuation model, adapted from [Simonit and Perrings \(2011\)](#).



**FIGURE 2**  
A conceptual framework for local environmental stewardship, adapted from [Bennett et al. \(2018\)](#).

required for integrated catchment management to be a success. However, land ownership can in some cases hinder the implementation of new techniques as the land may be rented rather than owned. Even land practitioners who are in a long-term rental agreement may have some hesitancy in changing behaviors firmly engrained in their practice or lack the capital to invest in new equipment/methods. In a small study of land practitioners, there was a belief that practitioners may either embrace environmentally friendly farming to ensure they continue to have a viable tenancy or reject these new measures because they require a longer-term investment ([Exelby, 2019](#)). The return on investment of conservation farming techniques, such as no-till, can take many years to yield ([Pittelkow et al., 2015](#)) and sometimes only if a holistic view of the technique is considered (e.g., reduced fertilizer and pesticide costs, reduced irrigation costs, decrease in labour, and reduced wear and tear on machinery). In fact, in the short term, conservation agriculture may prove deficit-inducing ([Afshar et al., 2022](#)) and require increased use of herbicide ([Laukkanen and Nauges, 2011](#)) as well as the capital investment. There can also be some variability on the improvement expected on the environment such as reduction in soil erosion ([Malone and Polyakov, 2020](#)). However, the measures embraced by conservation agriculture have been shown to have positive impacts on reducing soil erosion in the long term and have other important impacts such as reducing the losses of greenhouse gases which also need to be considered when striving to achieve the UN SDGs in their entirety ([Lal, 2020](#)).

## 4 The future

### 4.1 Funding

Funds flowing into nature-based solutions (NBSs) summed USD\$133 billion globally in 2021 (UN, 2021) which is a large amount of money until it is compared to the world wealth of USD\$431 trillion (Williams, 2021). The proportion of capital allocated to supporting measures to ultimately address a number of the UN SDGs is tiny but is improving. The use of Green Finance has seen an increase in sustainable investment bonds having an environmental focus with increases in funds dedicated to addressing climate change. Unfortunately, investment in NBS needs to increase triple fold by 2030 and four-fold by 2050 to meet the world targets on biodiversity, climate change and land degradation (UN, 2021). The question remains how can environmentalists get funders to care? By providing real valuation of the contribution that natural processes make to global society. This currently is in the form of natural capital where valuation of the benefits of these measures is developing as the links to wider improved environmental quality become stronger.

### 4.2 Partnership

One of the objectives of EUROSoil 2021 was to explore the importance of partnership between those in environmental research and those working the land. A special workshop aimed to investigate the methods that these two entities may work together going forward. What became clear was the success of the relationship between researchers and land practitioners is vital in our quest to meet the UN SDG 6 of cleaner water. The absence of practitioners in research was recently discussed by Bouma (2022), a long-standing researcher in the sector, and a call made for the serious involvement of farmers to achieve the UN SDGs. While researchers in soil are generally keen to work with the land practitioners, providing the opportunity for this collaborative work needs to come from the land sector themselves. Recent research in the Wupper sub-basin in Germany, by Huesker and Moss (2015), identified very different motivations for engaging with the implementation of the measures to meet the Water Framework Directive. Agricultural stakeholders were found to be particularly powerful and lobbied successfully at national and local levels to ensure that farming's interests (primarily food production) were protected. While local interest groups felt their views were considered but really the direction of the planning in the sub-basin was controlled by those with more expertise such as agriculture and the water board

(Huesker and Moss, 2015). The roles that different stakeholders play and the methods to interact with them is an area worthy of further exploration to ensure that cleaning water passively through natural processes may be achieved.

The future is relatively hopeful however. The piece by Bouma (2022) extolled the value of real engagement with land practitioners and the need for real world data for which to base our decisions going forward. Thankfully there are encouraging activities across the United Kingdom and Europe with farmers groups now actively engaging with research and efforts made to trial new methods with supportive frameworks to reduce the initial outlay of changing equipment and governmental initiatives aimed at increasing no-till farming (e.g., Jones, 2021). Grassroot based networking and conference events are also becoming popular such as GroundsWell while established farmers networking are now acknowledging the need for an environmental focus with specialist groups established such as Biodiversity, Agriculture, Soil, and Environment (BASE) in France, the United Kingdom and Ireland.

## 5 Conclusion

Ultimately, the future must hold the achieving of all of the SDG 6 objectives. This paper has focused largely on the use of integrated management and of natural processes to produce cleaner water from land and the barriers that these holistic endeavors must break. However, the objectives of SDG 6 are strongly interlinked. The objective to ensure integrated management is developed across the world could be considered a mechanism towards meeting the earlier objectives of SDG 6. With cleaner natural waters we can reduce the financial burden of cleaning water for drinking as well as improving the natural environment for ecosystem protection and enhancement.

All of these objectives require funding and partnership both of which are improving but appear to still be in their infancy. Large increases in funds allocated to environmentally sustainable measures are vital if the world is to meet the climate change crisis along with the biodiversity and social crises. Some advancement has been made with increasing funds allocated to environmentally focused sustainability but remains only a small proportion of global wealth.

Along with funding we also need "buy in" both financially and professionally from land practitioners in the quest for cleaner water using natural processes. Stakeholder engagement remains paramount to the success of these measures, once they have been financed, with continuing maintenance and ownership still a consideration. What is

clear is cleaner water will be possible when the practitioner is involved.

## Data availability statement

The original contributions presented in the study are included in the article/Supplementary Material, further inquiries can be directed to the corresponding author.

## Author contributions

This article has been solely prepared by LC.

## Acknowledgments

Thank you to Jörg Luster of the Swiss Federal Institute for Forest, Snow and Landscape Research at Wald, Schnee und

Landschaft (WSL), Switzerland, for comments on an early draft of this perspective paper.

## Conflict of interest

The authors declare that the research was conducted in the absence of any commercial or financial relationships that could be construed as a potential conflict of interest.

## Publisher's note

All claims expressed in this article are solely those of the authors and do not necessarily represent those of their affiliated organizations, or those of the publisher, the editors and the reviewers. Any product that may be evaluated in this article, or claim that may be made by its manufacturer, is not guaranteed or endorsed by the publisher.

## References

- Afshar, R. K., Cabot, P., Ippolito, J. A., Dekamin, M., Reed, B., Doyle, H., et al. (2022). Corn productivity and soil characteristic alterations following transition from conventional to conservation tillage. *Soil Tillage Res.* 220, 105351. doi:10.1016/j.still.2022.105351
- Albek, E. (2003). Estimation of point and diffuse contaminant loads to streams by non-parametric regression analysis of monitoring data. *Water Air Soil Pollut.* 147(1), 229–243. doi:10.1023/a:1024592815576
- Beierkuhnlein, C. (2021). Nature-based solutions must be realized - not just proclaimed - in face of climatic extremes. *Erdkunde* 75 (3), 225–244. doi:10.3112/erdkunde.2021.03.06
- Bennett, N. J., Whitty, T. S., Finkbeiner, E., Pittman, J., Bassett, H., Gelcich, S., et al. (2018). Environmental stewardship: A conceptual review and analytical framework. *Environ. Manage.* 61 (4), 597–614. doi:10.1007/s00267-017-0993-2
- Bouleau, G., and Pont, D. (2015). Did you say reference conditions? Ecological and socio-economic perspectives on the European water framework directive. *Environ. Sci. Policy* 47, 32–41. doi:10.1016/j.envsci.2014.10.012
- Bouma, J. (2022). How about the role of farmers and of pragmatic approaches when aiming for sustainable development by 2030? - Bouma - 2022 -. *Eur. J. Soil Sci.* 73 (1). doi:10.1111/ejss.13166
- Brambilla, M., and Pedrini, P. (2013). The introduction of subsidies for grassland conservation in the Italian Alps coincided with population decline in a threatened grassland species, the Corncrake *Crex crex*. *Bird. Study* 60 (3), 404–408. doi:10.1080/00063657.2013.811464
- Bredemeier, M. (2011). Forest, climate and water issues in Europe. *Ecohydrology*, 4(2), 159–167. doi:10.1002/eco.203
- Brockwell, E., Elofsson, K., Marbuah, G., and Nordmark, S. (2021). Spatial analysis of water quality and income in Europe. *Water Resour. Econ.* 35, 100182. doi:10.1016/j.wre.2021.100182
- CaBA (2022b). "Water Co-Governance," in *Catchment Based Approach*. Retrieved 20/06/2022 from. Available at: <https://catchmentbasedapproach.org/learn/water-co-governance/>.
- CaBA (2022a). *Catchment sensitive farming*. Retrieved 20/06/2022 from. Available at: <https://catchmentbasedapproach.org/learn/catchment-sensitive-farming/>.
- Cheng, Y. X., Chen, J., Wu, D., Liu, Y. S., Yang, Y. Q., He, L. X., et al. (2021). Highly enhanced biodegradation of pharmaceutical and personal care products in a novel tidal flow constructed wetland with baffle and plants. *Water Res.* 193, 116870. Article 116870. doi:10.1016/j.watres.2021.116870
- Dai, L. (2014). Something old, something new, something borrowed and something Blue<br>Tackling diffuse water pollution from agriculture in China: Drawing inspiration from the European union. *Utrecht Law Rev.* 10 (2), 136–154. doi:10.18352/ulr.274
- De Castro-Catala, N., Munoz, I., Armendariz, L., Campos, B., Barcelo, D., Lopez-Doval, J., et al. (2015). Invertebrate community responses to emerging water pollutants in Iberian river basins. *Sci. Total Environ.* 503, 142–150. doi:10.1016/j.scitotenv.2014.06.110
- DEFRA (2019). *Net gain: Summary of responses and government response Crown Copyright*.
- Delabre, I., Alexander, A., and Rodrigues, C. (2020). Strategies for tropical forest protection and sustainable supply chains: Challenges and opportunities for alignment with the UN sustainable development goals. *Sustain. Sci.* 15 (6), 1637–1651. doi:10.1007/s11625-019-00747-z
- EC (2022). *The Common agricultural policy at a glance*. European Commission Retrieved 20/06/2022 from. Available at: [https://ec.europa.eu/info/food-farming-fisheries/key-policies/common-agricultural-policy/cap-glance\\_en](https://ec.europa.eu/info/food-farming-fisheries/key-policies/common-agricultural-policy/cap-glance_en).
- Eric, A., Chrystal, M.-P., Erik, A., Kenneth, B., and Robert, C. (2022). Evaluating ecosystem services for agricultural wetlands: A systematic review and meta-analysis. *Wetl. Ecol. Manag.* doi:10.1007/s11273-022-09857-5
- Eurosoil (2022). *Eurosoil 2021; 20th anniversary*. Available at: <https://eurosoil-congress.com/>.
- Exelby, E. (2019). *An analysis of farming in england without subsidy: A challenge or an opportunity? [MSc rural and estate management thesis] edmond*. Shropshire, UK: Harper Adams University.
- Giangrande, N., White, R. M., East, M., Jackson, R., Clarke, T., Coste, M. S., et al. (2019). A competency framework to assess and activate education for sustainable development: Addressing the UN sustainable development goals 4.7 challenge. *Sustainability* 11 (10), 2832. Article 2832. doi:10.3390/su11102832
- Grimvall, A., and Stålnacke, P. E. R. (1996). Statistical methods for the source apportionment of riverine loads of pollutants. *Environmetrics*, 7(2), 201–213. doi:10.1002/(sici)1099-095x(199603)7:2<201::aid-env205>3.0.co;2-r
- Hole, M. (2015). Managing for nature: A farmer's view on wildlife schemes. *ECOS - A Rev. Conservation* 36 (3/4), 26–28.
- Hüesker, F., and Moss, T. (2015). The politics of multi-scalar action in river basin management: Implementing the EU Water Framework Directive (WFD). *Land Use Policy*, 42, 38–47. doi:10.1016/j.landusepol.2014.07.003

- Jarvie, H. P., Sharpley, A. N., Spears, B., Buda, A. R., May, L., and Kleinman, P. J. A. (2014). Water quality remediation faces unprecedented challenges from "Legacy Phosphorus". *Environ. Sci. Technol.*, 47, 8997–8998. doi:10.1021/es403160a
- Jarvie, H. P., Withers, P. J. A., Bowes, M. J., Palmer-Felgate, E. J., Harper, D. M., Wasia, K., et al. (2010). Streamwater phosphorus and nitrogen across a gradient in rural-agricultural land use intensity. *Agric. Ecosyst. Environ.*, 135(4), 238–252. doi:10.1016/j.agee.2009.10.002
- Johannesson, K., Andersson, J., and Tonderski, K. (2011). Efficiency of a constructed wetland for retention of sediment-associated phosphorus. *Hydrobiologia* 674, 179–190. doi:10.1007/s10750-011-0728-y
- Jones, G. (2021). "Future farming blog," in *The farming investment fund: An overview - future farming*. Available at: <https://defrafarming.blog.gov.uk/2021/03/30/the-farming-investment-fund-an-overview/>.
- Lal, R. (2020). Managing soils for resolving the conflict between agriculture and nature: The hard talk. *Eur. J. Soil Sci.* 71 (1), 1–9. doi:10.1111/ejss.12857
- Laukkanen, M., and Nauges, C. (2011). Environmental and production cost impacts of no-till in Finland: Estimates from observed behavior. *Land Econ.* 87 (3), 508–527. doi:10.3368/le.87.3.508
- Malone, M., and Polyakov, V. (2020). A physical and social analysis of how variations in no-till conservation practices lead to inaccurate sediment runoff estimations in agricultural watersheds. *Prog. Phys. Geogr. Earth Environ.* 44 (2), 151–167. doi:10.1177/0309133319873115
- Mooney, H. A., and Cleland, E. E. (2001). The evolutionary impact of invasive species. *Proc. Natl. Acad. Sci. U. S. A.* 98 (10), 5446–5451. doi:10.1073/pnas.091093398
- Moss, B. (2018). *Ecology of freshwaters: Earth's bloodstream*. New Jersey, USA: John Wiley & Sons.
- Musekiwa, N., and Mandiyanike, D. (2017). Botswana development vision and localisation of UN Sustainable Development Goals. *Commonw. J. Local Gov.* (20), 135–145. doi:10.5130/cjlg.v0i20.6469
- Pittelkow, C. M., Linquist, B. A., Lundy, M. E., Liang, X., van Groenigen, K. J., Lee, J., et al. (2015). When does no-till yield more? A global meta-analysis. *Field Crops Res.*, 183, 156–168. doi:10.1016/j.fcr.2015.07.020
- Ranalli, A. J., and Macalady, D. L. (2010). The importance of the riparian zone and in-stream processes in nitrate attenuation in undisturbed and agricultural watersheds – a review of the scientific literature. *J. Hydrol. X.*, 389(3), 406–415. doi:10.1016/j.jhydrol.2010.05.045
- Rolph, C. A., Villa, R., Jefferson, B., Brookes, A., Choya, A., Icton, G., et al. (2019). From full-scale biofilters to bioreactors: Engineering biological metaldehyde removal. *Sci. Total Environ.* 685, 410–418. doi:10.1016/j.scitotenv.2019.05.304
- Sherriff, S. C., Rowan, J. S., Melland, A. R., Jordan, P., Fenton, O., and Ó hUallacháin, D. (2015). Investigating suspended sediment dynamics in contrasting agricultural catchments using *ex situ* turbidity-based suspended sediment monitoring. *Hydrol. Earth Syst. Sci.* 19 (8), 3349–3363. doi:10.5194/hess-19-3349-2015
- Shore, M., Murphy, S., Mellander, P.-E., Shortle, G., Melland, A. R., Crockford, L., et al. (2017). Influence of stormflow and baseflow phosphorus pressures on stream ecology in agricultural catchments. *Sci. Total Environ.*, 590–591, 469–483. doi:10.1016/j.scitotenv.2017.02.100
- Simonit, S., and Perrings, C. (2011). Sustainability and the value of the 'regulating' services: Wetlands and water quality in Lake Victoria. *Ecol. Econ.*, 70(6), 1189–1199. doi:10.1016/j.ecolecon.2011.01.017
- UN (2021). *State of finance for nature*. Available at: <http://www.unep.org/resources/state-finance-nature>.
- UN (2018). *Sustainable development goal 6, synthesis report 2018 on water and sanitation - executive summary*.
- UN (2022). *The 17 Goals | sustainable development*. Available at: <https://sdgs.un.org/goals>.
- van Emmerik, T., and Schwarz, A. (2020). Plastic debris in rivers. *WIREs Water* 7 (1). Article e1398. doi:10.1002/wat2.1398
- Vaughan, T. (2019). *How do forests infiltrate water compared to other land uses in the UK and what effect does this have on flooding*. Shropshire, UK: Harper Adams University. [BSc (hons) countryside management, thesis] edmond.
- Wells, J., Labadz, J. C., Smith, A., and Islam, M. M. (2020). Barriers to the uptake and implementation of natural flood management: A social-ecological analysis. *J. Flood Risk Manag.* 13. Article UNSP e12561. doi:10.1111/jfr3.12561
- Williams, O., A. (2021). *World's wealth hits half A quadrillion dollars*. New Jersey, USA: Forbes.
- Zimon, D., Tyan, J., and Sroufe, R. (2020). Drivers of sustainable supply chain management: Practices to alignment with UN sustainable development goals. *Int. J. Qual. Res.* 14 (1), 219–236. doi:10.24874/ijqr14.01-14
- Zinabu, E., Kelderman, P., van der Kwast, J., and Irvine, K. (2018). Evaluating the effect of diffuse and point source nutrient transfers on water quality in the Kombolcha River Basin, an industrializing Ethiopian catchment. *Land Degrad. Dev.* 29 (10), 3366–3378. doi:10.1002/ldr.3096

# Frontiers in Environmental Science

Explores the anthropogenic impact on our natural world

An innovative journal that advances knowledge of the natural world and its intersections with human society. It supports the formulation of policies that lead to a more inhabitable and sustainable world.

## Discover the latest Research Topics

[See more →](#)

### Frontiers

Avenue du Tribunal-Fédéral 34  
1005 Lausanne, Switzerland  
[frontiersin.org](https://frontiersin.org)

### Contact us

+41 (0)21 510 17 00  
[frontiersin.org/about/contact](https://frontiersin.org/about/contact)

